QUANTITATIVE SYSTEMS TOXICOLOGY MODELING FOR NEURONAL ADVERSE OUTCOME

Deepika

UNIVERSITAT ROVIRA i VIRGILI

Quantitative Systems Toxicology Modeling for Neuronal Adverse Outcome

DEEPIKA

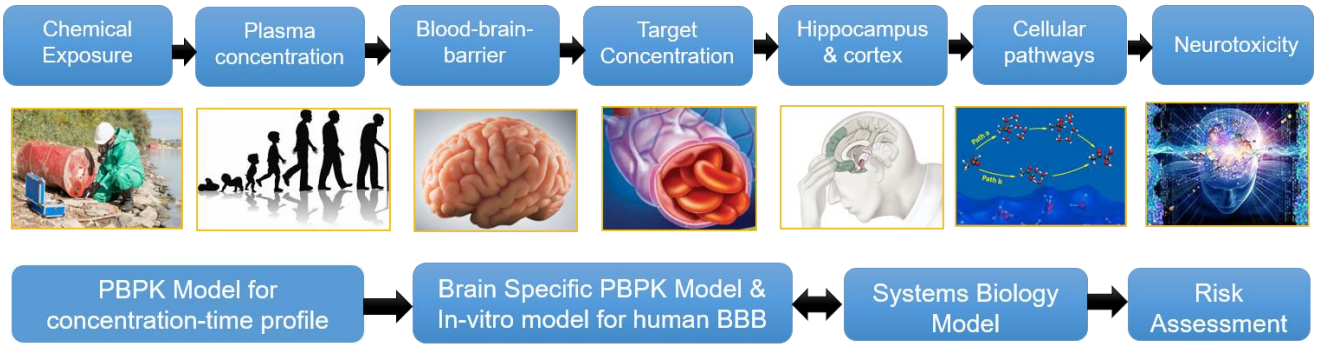

DOCTORAL THESIS
2022

UNIVERSITAT ROVIRA I VIRGILI
QUANTITATIVE SYSTEMS TOXICOLOGY MODELING FOR NEURONAL ADVERSE OUTCOME
Deepika

Deepika Deepika

Quantitative Systems Toxicology Modeling for Neuronal Adverse Outcome

DOCTORAL THESIS

Supervised by

Dr. Vikas Kumar

Dr. Raju Prasad Sharma

Dr. Marta Schuhmacher

Department of Chemical Engineering

UNIVERSITAT ROVIRA I VIRGILI

Tarragona, 2022

UNIVERSITAT ROVIRA I VIRGILI
QUANTITATIVE SYSTEMS TOXICOLOGY MODELING FOR NEURONAL ADVERSE OUTCOME
Deepika

UNIVERSITAT
ROVIRA i VIRGILI

FAIG CONSTAR que aquest treball, titulat "**Quantitative Systems toxicology modeling for Neuronal adverse outcome"** que presenta **Deepika Deepika** per a l´ obtenció del títol de Doctor, ha estat realizat sota la meva direccio al Department d´ Enginyeria Quimica d´ aquesta Universitat.

HAGO CONSTAR que el presente trabajo, titulado "**Quantitative Systems toxicology modeling for Neuronal adverse outcome"** que presenta **Deepika Deepika** para la obtención del título de Doctor, ha sido realizado bajo mi direccion en el Departmento de Ingeneria Quimico de esta univerisdad.

I STATE that the present study "**Quantitative Systems toxicology modeling for Neuronal adverse outcome**", presented by **Deepika Deepika** for the award of the degree of Doctor, has been carried out under my supervision at the Department of Chemical Engineering of this university.

Tarragona, 23rd June 2022

El/s director/s de la tesis doctoral

El/los director/es de la tesis doctoral

Doctoral Thesis Supervisor/s

Vikas Kumar

Raju Prasad Sharma

Marta Schuhmacher Ansuategui

Marta Schuhmacher Ansuategui - DNI 25134306K (AUT)

Firmado digitalmente por Marta Schuhmacher Ansuategui - DNI 25134306K (AUT)
Fecha: 2022.06.24 08:38:53 +02'00'

Supervisors

Dr. Vikas Kumar
Researcher
Department of Chemical Engineering
Universitat Rovira I Virgili (URV)
Tarragona (Spain)

Dr. Raju Prasad Sharma
Researcher
Department of Chemical Engineering
Universitat Rovira I Virgili (URV)
Tarragona (Spain)

Dr. Marta Schuhmacher Ansuategui
Professor
Department of Chemical Engineering
Universitat Rovira I Virgili (URV)
Tarragona (Spain)

Acknowledgment

I would like to express my sincere thanks to my supervisor, Prof. Marta Schuhmacher for guiding me through the tough journey of the Ph.D. She inspired me to think from broader perspective and provided courage during tough moments of life. My special thanks to co-supervisor Dr. Vikas Kumar, who has always provided me technical guidance and emotional support. Last but not the least, I would like to thank and express my gratitude to my other co-supervisor Dr. Raju Prasad Sharma. It was his continuous guidance and feedback, and emotional support for three-years that provided me hope throughout my degree to aspire for better.

My sincere thanks to Dr. Jordi Blanco Pérez and Dr. Roser Esplugas Borràs for helping me during the in-vitro studies and genomic analysis. I am very grateful to Dr. Motserrat Mari Marcos who has helped me with managerial and administrative work throughout Ph.D. I would also like to thank Núria Juanpere Mitjana, without her support it would have been difficult to understand administration od doctoral school. I would also like to thank other members from Tecnatox like Mengmei Ni, Saurav Kumar, Lara Dronjak, Oscar Sabuz Vidal, Jordina Balaguer Trias, Nuria Gayà, Montse Marquès Bueno, Dr. Joaquim Rovira, Nora Exposito Lorenzo, Dr. Neus González, Dr. Jordi Sierra, Marta Herrero, Anabel Díez, Dr. Maria Teresa Colomina, David Mateo, and Elena Sánchez-Resino for their support in working time.

I would take this opportunity to thank my friends Satyam Shukla, Deepak Parajuli, Deepa Upadhayay, Srishti Goyal, and Indrajeet who are like a family to me in Tarragona for helping me in last three years. My special thanks to Vinayak Gunderao Padmaji who helped me by discussing my Ph.D. project over time and provided guidance for improving the coding. I would like to thank my other friends from Tarragona, Sarika Kumari, Sachin, Chen, Ranga, Aanchal, Deepanshu, Jitesh, Anand and Ankur for spending time with me. I would also like to thank Ashish Rawat, Sarita Kumari for their support during my Ph.D. My special thanks to my best friend from Indian Institute of Technology, Banaras Hindu University, Kanchan, Payal, Shilpkala, Sreenu, and Vinay. I would also like to thank associate professor and a friend: Dr. Rajkumar from IIT Dhanbad who supported me emotionally over last three years.

My special thanks to my family especially my father Mr. Karmvir Singh who always inspired me to study and build my career. I would also like to show gratitude towards my brother Paramjeet Ahlawat, Pavan Ahuja, my sister Pooja Malik, my grandmother burfo devi and my bua Balakumari. At last special thanks to my boyfriend Naga Adithya Chandra Pandurangi who has always supported me during my Ph.D. His support helped me to stay in foreign and continue my studies despite various obstacles. It would never have been possible without you.

Thanks to all who helped me during my Ph.D. journey. These few words on a page cannot define the role all of my closed ones have played during these three years, but still I take the initiative to thank them for being a part of my life.

UNIVERSITAT ROVIRA I VIRGILI
QUANTITATIVE SYSTEMS TOXICOLOGY MODELING FOR NEURONAL ADVERSE OUTCOME
Deepika

I dedicate my thesis to my father **Mr. Karmvir Singh**, my sister **Mrs. Pooja Malik**, my brother **Mr. Paramjeet Ahlawat** and my friend **Naga Adithya Chandra Pandurangi**.

UNIVERSITAT ROVIRA I VIRGILI
QUANTITATIVE SYSTEMS TOXICOLOGY MODELING FOR NEURONAL ADVERSE OUTCOME
Deepika

Abbreviations

PFOS= Perfluorooctanesulfonic acid

PFOA= Perfluorooctanoic acid

BPA= Bisphenol A

EFSA= European Food Safety Authority

USEPA= United States Environmental Protection Agency

PBPK= Physiologically Based Pharmacokinetic Model

OPFRs= Organophosphate Flame Retardants

TDCIPP= tris (1,3-dichloro-2-propyl) phosphate

TCIPP= tris (1-chloro-2-propyl) phosphate

TCEP= tris (2-chloroethyl) phosphate

OPs= Organophosphates

BBB= Blood-Brain Barrier

PMT= Permethrin

CFT= Cyfluthrin

CPF= Chlorpyrifos

WHO= World Health Organization

OECD= Organization for economic co-operation and Development

SB= Systems Biology

ROS= Reactive Oxygen Species

IVIVE= In-vitro to in-vivo extrapolation

Contents

UNIVERSITAT ROVIRA I VIRGILI
QUANTITATIVE SYSTEMS TOXICOLOGY MODELING FOR NEURONAL ADVERSE OUTCOME
Deepika

Summary

Many environmental chemicals have been classified as neurotoxins due to their ability to alter the function of the nervous system by damaging neuronal cells which transmit signal in the body. These neurotoxins either directly or indirectly interfere with the normal process by either accelerating the rate of nerve cell degradation or increasing oxidative stress in the brain. Almost 200 chemicals have been identified as potential human neurotoxicants while other 1000 were shown neurotoxic in animals. It suggests that neurotoxicity may vary in animals and human due to metabolism, species-specific changes and other anatomical and physiological differences. Proper in-silico approaches are required to reduce the uncertainty regarding experimental data for human health risk assessment. Physiologically Based Pharmacokinetic Model (PBPK) are mathematical models that can be used for assessing risk of chemical substance in human including sensitive population (pediatrics, geriatrics) with involvement of complex ADME process. In-vitro data is often integrated in PBPK through IVIVE (in-vitro to in-vivo extrapolation) approach especially for liver metabolism using human cell lines. Such kind of approach reduce the usage of animals for studying chemical toxicity in human. PBPK provides the concentration-time curve for the chemical and metabolite in the organs including brain. But brain is a complex organ and presence of various tissues in the brain makes it difficult to use a generalized PBPK Model. Organ-specific PBPK including blood-brain barrier (BBB), cerebrospinal fluid (CSF), and the central nervous system (CNS) can be developed for evaluating neurotoxic risk from the environmental chemicals. Since BBB is composed of the tight and adherens junctions, and can undergo passive diffusion as well as active transport, permeability data for the chemical is must to model it. This points towards the need for in-vitro study for checking permeability of the chemicals and integrating it in the brain-specific PBPK Model. Such kind of framework fulfil the goal of REACH by reducing the animal usage. The target concentration predicted in the brain by PBPK can be further used for systems toxicology model. Chemical in the brain produce oxidative stress leading to reduction in healthy mitochondrion and ultimately the neuronal cell death. Such kind of phenomenon can be modeled using mechanistic oxidative stress cell-specific model. The main goal of this thesis was to develop a approach for improved risk assessment especially neurotoxicity in human through integrating in-silico model with the in-vitro data.

Chapter 1 focused on integrative translation approach required to predict the neurotoxicity using in-vitro, in-vivo, and epidemiological data with in-silico model. The review provided the overall generalized idea about the research which has been carried out in last 14 years in the field of neurotoxicology for the environmental chemicals like Poly- and perfluoroalkyl substances (PFAS), Flame retardants (FRs), polychlorinated biphenyl (PCBs), and Bisphenol A (BPA). Extensive experimental dataset is available in the literature but in-silico models for predicting neurotoxicity are quite few. We found that there is crucial need to develop a PBPK model specific to the brain and integrate them with the systems toxicology for predicting neurotoxicity in human.

Short-acting environmental chemicals like organophosphate flame retardants (OPFRs) are being increasing used in Europe after banning of brominated flame retardant (BFRs) as plasticizer in construction and for extinguishing fires. Till date no PBPK Model for OPFRs is available to assess the toxicokinetic in several organs and evaluate neurotoxicity. In chapter 2a, PBPK model for three OPFRs (TDCIPP, TCIPP and TCEP) was developed and validated with the rat data considering several approaches to improve the prediction. Further the model was used for its application in neurotoxicity based on predicted concentration in brain with IVIVE. Further the PBPK model for pediatric BPA was developed in chapter 2b, to include sex-based difference for pediatric population (children ages 6-12 years) and include ontogeny specific information rather than allometric scaling for assessing risk using PBPK model.

Mostly generalized PBPK model are being developed by scientists all over the world considering adult human (male) for risk assessment. Compounds like Perfluorooctanesulfonic acid (PFOS) have high bioaccumulation potential and being detected in the human across the entire lifespan due to continuous exposure and longer half-life (3-5 years). In chapter 3a, age-dependent PBPK model was developed for human lifetime to improve the risk assessment for pediatric and geriatric population. Chapter 3b involves developing a framework for risk assessment of PFAS (PFOS and PFOA) utilizing experimental studies and age-dependent PBPK Model. PBPK model was used to improve the policymaking especially comparing the exposure level predicted by reverse dosimetry with TDI/RfD set by EFSA/EPA.

For predicting neurotoxicity using PBPK, simply knowing the concentration in brain is not enough. Brain is a complex structure and is protected from chemical exposure through tight junction of BBB. Often the data is very limited with regard to human BBB which makes it difficult to develop brain-specific PBPK. In-vitro study was conducted using human brain cell lines to evaluate permeation potential and gene expression at tight junction for different environmental chemicals. In chapter 4a, apparent permeability coefficient was calculated for CPF, PMT and CFT and compared with the in-vivo data using IVIVC.

Chapter 5a consist of calculating apparent permeability coefficient for PFOS and PFOA using BBB human cell lines. The data from 5a was used as input for developing PBPK Model using IVIVE. Brain PBPK Model was developed for PFOS and PFOA using permeability limited approach for brain integrated with perfusion limited approach for whole body. Concentration in specific compartment of the brain like hippocampus, cortex was predicted to associate it with neurotoxic risk. Further the hippocampus concentration was used as input for systems toxicology model to evaluate neurotoxic risk in chapter 5b. In-silico model right from chemical exposure to neurotoxic risk was modeled using integrated translational approach

Resumen

Muchas sustancias químicas ambientales se han clasificado como neurotoxinas debido a su capacidad para alterar la función del sistema nervioso al dañar las células neuronales que transmiten señales en el cuerpo. Estas neurotoxinas interfieren directa o indirectamente con el proceso normal, ya sea acelerando la tasa de degradación de las células nerviosas o aumentando el estrés oxidativo en el cerebro. Casi 200 productos químicos han sido identificados como posibles neurotóxicos para humanos, mientras que otros 1000 han demostrado ser neurotóxicos en animales (Grandjean y Landrigan 2006). (USEPA 2021) . Sugiere que la neurotoxicidad puede variar en animales y humanos debido al metabolismo, cambios específicos de especie y otras diferencias anatómicas y fisiológicas. Se requieren enfoques in-silico adecuados para reducir la incertidumbre con respecto a los datos experimentales para la evaluación de riesgos para la salud humana. El modelo farmacocinético basado en la fisiología (PBPK) son modelos matemáticos que se pueden usar para evaluar el riesgo de sustancias químicas en humanos, incluida la población sensible (pediatría, geriatría) con la participación del proceso ADME complejo. Los datos in vitro a menudo se integran en PBPK a través del enfoque IVIVE (extrapolación in vitro a in vivo), especialmente para el metabolismo hepático utilizando líneas celulares humanas. Este tipo de enfoque reduce el uso de animales para estudiar la toxicidad química en humanos. PBPK proporciona la curva de concentración-tiempo para la sustancia química y el metabolito en los órganos, incluido el cerebro. Pero el cerebro es un órgano complejo y la presencia de varios tejidos en el cerebro dificulta el uso de un modelo PBPK generalizado. La PBPK específica de órganos, incluida la barrera hematoencefálica (BBB), el líquido cefalorraquídeo (LCR) y el sistema nervioso central (SNC), se puede desarrollar para evaluar el riesgo neurotóxico de los productos químicos ambientales. Dado que BBB se compone de uniones estrechas y adherentes, y puede sufrir difusión pasiva y transporte activo, los datos de permeabilidad para productos químicos son necesarios para modelarlo. Esto apunta a la necesidad de un estudio in vitro para comprobar la permeabilidad de los productos químicos e integrarla en el modelo PBPK específico del cerebro. Este tipo de marco cumple con el objetivo de REACH al reducir el uso de animales. La concentración objetivo predicha en el cerebro por PBPK se puede usar más para el modelo de toxicología de sistemas. Las sustancias químicas en el cerebro producen estrés oxidativo que conduce a la reducción de mitocondrias sanas y, en última instancia, a la muerte de las células neuronales. Este tipo de fenómeno se puede modelar utilizando un modelo específico de células de estrés oxidativo mecanicista. El objetivo principal de esta tesis fue desarrollar un marco para la evaluación de riesgos, especialmente la neurotoxicidad en humanos, mediante la integración del modelo in-silico con los datos in-vitro.

El Capítulo 1 se centró en el enfoque de traducción integradora necesario para predecir la neurotoxicidad utilizando datos epidemiológicos in vitro e in vivo con un modelo in-silico. La revisión proporcionó una idea generalizada general sobre la investigación que se ha llevado a cabo en los últimos 14 años en el campo de la neurotoxicología para los productos químicos ambientales como las sustancias poli y perfluoroalquiladas (PFAS), los retardantes de llama

(FR), los bifenilos policlorados (PCB), y Bisfenol A (BPA). Hay un extenso conjunto de datos experimentales disponible en la literatura, pero los modelos in-silico para predecir la neurotoxicidad son muy pocos. Descubrimos que existe una necesidad crucial de desarrollar un modelo PBPK específico para el cerebro e integrarlo con la toxicología de sistemas para predecir la neurotoxicidad en humanos.

Los productos químicos ambientales de acción corta, como los retardantes de llama organofosforados (OPFR), se utilizan cada vez más en Europa después de la prohibición del retardante de llama bromado (BFR) como plastificante en la construcción y para extinguir incendios. Hasta la fecha, no se dispone de ningún modelo PBPK para OPFR para evaluar la toxicocinética en varios órganos y evaluar la neurotoxicidad. En el capítulo 2a, se desarrolló y validó el modelo PBPK para tres OPFR (TDCIPP, TCIPP y TCEP) con los datos de rata considerando varios enfoques para mejorar la predicción. Además, el modelo se utilizó para su aplicación en neurotoxicidad en función de la concentración predicha en el cerebro con IVIVE. Además, el modelo PBPK para BPA pediátrico se desarrolló en el capítulo 2b, para incluir diferencias basadas en el sexo para la población pediátrica (niños de 6 a 12 años) e incluir información específica de ontogenia en lugar de escalas alométricas para evaluar el riesgo utilizando el modelo PBPK. (bisfenol A: BPA).

La mayoría de los modelos PBPK generalizados están siendo desarrollados por científicos de todo el mundo considerando humanos adultos (hombres) para la evaluación de riesgos. Los compuestos como el ácido perfluorooctanosulfónico (PFOS) tienen un alto potencial de bioacumulación y se detectan en los seres humanos durante toda la vida debido a la exposición continua y una vida media más larga (3-5 años). En el capítulo 3a, se desarrolló un modelo PBPK dependiente de la edad para la vida humana a fin de mejorar la evaluación de riesgos para la población pediátrica y geriátrica. El Capítulo 3b implica el desarrollo de un marco para la evaluación de riesgos de PFAS (PFOS y PFOA) utilizando estudios experimentales y un modelo PBPK dependiente de la edad. El modelo PBPK se utilizó para mejorar la formulación de políticas, especialmente comparando el nivel de exposición predicho por dosimetría inversa con TDI/RfD establecido por EFSA/EPA.

Para predecir la neurotoxicidad usando PBPK, simplemente conocer la concentración en el cerebro no es suficiente. El cerebro es una estructura compleja y está protegido de la exposición química a través de la estrecha unión de BBB. A menudo, los datos son muy limitados con respecto a BBB humano, lo que dificulta el desarrollo de PBPK específico del cerebro. Se llevó a cabo un estudio in vitro utilizando líneas celulares de cerebro humano para evaluar el potencial de permeación y la expresión génica en la unión estrecha para diferentes sustancias químicas ambientales. En el capítulo 4a, se calculó el coeficiente de permeabilidad aparente para CPF, PMT y CFT y se comparó con los datos in vivo usando IVIVC.

El Capítulo 5a consiste en calcular el coeficiente de permeabilidad aparente para PFOS y PFOA utilizando líneas celulares humanas BBB. Los datos de 5a se usaron como entrada para desarrollar el modelo PBPK usando IVIVE. Brain PBPK Model se desarrolló para PFOS y PFOA utilizando un enfoque de permeabilidad limitada para el cerebro integrado con un enfoque de perfusión limitada para todo el cuerpo. Se predijo que la concentración en un compartimento específico del cerebro, como el hipocampo, la corteza lo asociaría con un

riesgo neurotóxico. Además, la concentración del hipocampo se utilizó como entrada para el modelo de toxicología de sistemas para evaluar el riesgo neurotóxico en el capítulo 5b . El modelo in-silico desde la exposición química hasta el riesgo neurotóxico se modeló utilizando un enfoque traslacional integrado.

Resum

Molts productes químics ambientals s'han classificat com a neurotoxines a causa de la seva capacitat d'alterar la funció del sistema nerviós danyant les cèl·lules neuronals que transmeten el senyal al cos. Aquestes neurotoxines interfereixen directament o indirectament amb el procés normal, ja sigui accelerant la taxa de degradació de les cèl·lules nervioses o augmentant l'estrès oxidatiu al cervell. Gairebé 200 substàncies químiques s'han identificat com a possibles neurotòxics humans, mentre que altres 1000 es van mostrar neurotòxiques en animals. Suggereix que la neurotoxicitat pot variar en animals i humans a causa del metabolisme, els canvis específics de l'espècie i altres diferències anatòmiques i fisiològiques. Es requereixen enfocaments in-silico adequats per reduir la incertesa sobre les dades experimentals per a l'avaluació del risc per a la salut humana. El model farmacocinètic de base fisiològica (PBPK) són models matemàtics que es poden utilitzar per avaluar el risc de substàncies químiques en humans, inclosa la població sensible (pediatria, geriatria) amb la implicació del procés ADME complex. Les dades in vitro sovint s'integren a PBPK mitjançant l'enfocament IVIVE (extrapolació in vitro a in vivo), especialment per al metabolisme hepàtic mitjançant línies cel·lulars humanes. Aquest tipus d'enfocament redueix l'ús d'animals per estudiar la toxicitat química en humans. PBPK proporciona la corba de concentració-temps de la substància química i el metabòlit als òrgans, inclòs el cervell. Però el cervell és un òrgan complex i la presència de diversos teixits al cervell dificulta l'ús d'un model PBPK generalitzat. Es poden desenvolupar PBPK específics d'òrgans, inclosa la barrera hematoencefàlica (BBB), el líquid cefaloraquidi (LCR) i el sistema nerviós central (SNC), per avaluar el risc neurotòxic dels productes químics ambientals. Atès que la BBB es compon d'unions estretes i adherides, i pot patir difusió passiva i transport actiu, les dades de permeabilitat de la substància química cal modelar-la. Això apunta a la necessitat d'estudis in vitro per comprovar la permeabilitat de les substàncies químiques i integrar-la en el model PBPK específic del cervell. Aquest tipus de marc compleix l'objectiu de REACH reduint l'ús d'animals. La concentració objectiu prevista al cervell per PBPK es pot utilitzar encara més per al model de toxicologia de sistemes. Els productes químics al cervell produeixen estrès oxidatiu que condueixen a la reducció dels mitocondris sans i, finalment, a la mort de les cèl·lules neuronals. Aquest tipus de fenomen es pot modelar mitjançant un model específic de cèl·lules d'estrès oxidatiu mecanicista. L'objectiu principal d'aquesta tesi era desenvolupar un marc per a l'avaluació de riscos, especialment la neurotoxicitat en humans mitjançant la integració del model in-silico amb les dades in vitro.

El capítol 1 es va centrar en l'enfocament de traducció integrador necessari per predir la neurotoxicitat mitjançant dades epidemiològiques in vitro, in vivo amb model in-silico. La revisió va proporcionar la idea general generalitzada sobre la investigació que s'ha dut a terme en els darrers 14 anys en el camp de la neurotoxicologia per a les substàncies químiques ambientals com les substàncies poli- i perfluoroalquil (PFAS), retardants de flama (FRs), bifenil policlorat (PCB), i Bisfenol A (BPA). Hi ha un ampli conjunt de dades experimentals disponible a la literatura, però els models in-silico per predir la neurotoxicitat són força pocs. Hem trobat

que hi ha una necessitat crucial de desenvolupar un model PBPK específic per al cervell i integrar-los amb la toxicologia dels sistemes per predir la neurotoxicitat en humans.

Els productes químics ambientals d'acció curta com els retardants de flama organofosforats (OPFR) s'estan utilitzant cada cop més a Europa després de la prohibició dels retardants de flama bromats (BFR) com a plastificant en la construcció i per a l'extinció d'incendis. Fins a la data no hi ha cap model PBPK per a OPFR disponible per avaluar la toxicocinètica en diversos òrgans i avaluar la neurotoxicitat. Al capítol 2a, es va desenvolupar i validar el model PBPK per a tres OPFR (TDCIPP, TCIPP i TCEP) amb les dades de rata tenint en compte diversos enfocaments per millorar la predicció. A més, el model es va utilitzar per a la seva aplicació en neurotoxicitat basada en la concentració prevista al cervell amb IVIVE. A més, el model PBPK per al BPA pediàtric es va desenvolupar al capítol 2b, per incloure la diferència basada en el sexe per a la població pediàtrica (nens de 6 a 12 anys) i incloure informació específica d'ontogènia en lloc d'una escala alomètrica per avaluar el risc mitjançant el model PBPK.

Científics d'arreu del món estan desenvolupant un model PBPK majoritàriament generalitzat que consideren l'home adult (mascle) per a l'avaluació del risc. Compostos com l'àcid perfluorooctansulfònic (PFOS) tenen un alt potencial de bioacumulació i es detecten en l'ésser humà durant tota la vida útil a causa de l'exposició contínua i la vida mitjana més llarga (3-5 anys). Al capítol 3a, es va desenvolupar un model de PBPK depenent de l'edat per a la vida humana per millorar l'avaluació del risc per a la població pediàtrica i geriàtrica. El capítol 3b implica desenvolupar un marc per a l'avaluació del risc de PFAS (PFOS i PFOA) utilitzant estudis experimentals i un model PBPK depenent de l'edat. El model PBPK es va utilitzar per millorar l'elaboració de polítiques, especialment comparant el nivell d'exposició previst per la dosimetria inversa amb el TDI/RfD establert per l'EFSA/EPA.

Per predir la neurotoxicitat mitjançant PBPK, no n'hi ha prou amb conèixer la concentració al cervell. El cervell és una estructura complexa i està protegit de l'exposició química a través d'una estreta unió de BBB. Sovint, les dades són molt limitades pel que fa a la BBB humana, cosa que dificulta el desenvolupament de PBPK específica del cervell. Es va realitzar un estudi in vitro utilitzant línies cel·lulars del cervell humà per avaluar el potencial de permeació i l'expressió gènica a la unió estreta de diferents productes químics ambientals. Al capítol 4a, es va calcular el coeficient de permeabilitat aparent per a CPF, PMT i CFT i es va comparar amb les dades in vivo mitjançant IVIVC.

El capítol 5a consisteix a calcular el coeficient de permeabilitat aparent per a PFOS i PFOA mitjançant línies cel·lulars humanes BBB. Les dades de 5a es van utilitzar com a entrada per desenvolupar el model PBPK mitjançant IVIVE. El model PBPK del cervell es va desenvolupar per a PFOS i PFOA mitjançant un enfocament limitat de permeabilitat per al cervell integrat amb un enfocament limitat de perfusió per a tot el cos. La concentració en un compartiment específic del cervell com l'hipocamp, es va predir que l'escorça l'associaria amb un risc neurotòxic. A més, la concentració de l'hipocamp es va utilitzar com a entrada per al model de toxicologia de sistemes per avaluar el risc neurotòxic al capítol 5b . El model in-silico des de l'exposició química al risc neurotòxic es va modelar mitjançant un enfocament translacional integrat.

UNIVERSITAT ROVIRA I VIRGILI
QUANTITATIVE SYSTEMS TOXICOLOGY MODELING FOR NEURONAL ADVERSE OUTCOME
Deepika

Introduction

Human beings are getting exposed to environmental chemicals either through occupational or through dietary and environmental exposure (Ho et al. 2022). There are thousands of chemicals in the market but the information about their adverse effect on human is limited. Different types of chemicals like pesticides, insecticides, bisphenol A, phthalates, dioxins, polychlorinated biphenyls, flame retardants and per- and polyfluoroalkyl substances are some of the environmental chemicals currently studied for toxicity in Europe. There is growing evidence that exposure to these environmental chemicals is contributing to numerous ailments like obesity, reproductive diseases (Sutton et al. 2012), diabetes (Kuo et al. 2013), cancer (Cohen and Jefferies 2019; Santaliz Casiano et al. 2022) and neurotoxicity (Deepika et al. 2020; Lauretta et al. 2019; Masuo and Ishido 2011). Numerous regulatory bodies like EFSA (European food safety authority), US EPA (Environmental Protection Agency) and the non-government organizations has focused on reporting about their adverse effect in human using in-vitro and in-vivo experimental data. Biological experimental methods for detecting toxic endpoints are laborious and time consuming. Additionally, the use of in-vitro or in-vivo data calls for conducting inter-species extrapolations to understand human risk. Sometime chemicals do not follow the linear dose response relationship often making it difficult to extrapolate. However, epidemiological studies provide better evidence related to human health effects and allow for studying realistic exposure. The concentration in serum or urine can often be used to calculate daily intakes with high confidence using in-silico models. In-silico models like Physiologically Based Pharmacokinetic Model (PBPK), Pharmacodynamic Model (PD), and systems biology model (SB) helps in quantifying the risk and evaluate mechanistic pathways related to toxicity (Deepika et al. 2020). Further thousands of chemicals are entering the market every day and it is not possible to conduct the in-vitro, in-vivo and epidemiological studies. For fulfilling the gaps in research of chemicals, quantitative systems toxicology (QST) models can be a bridge to integrate all the experimental data and evaluate human toxicity like neurotoxicity.

1. Toxicokinetic of EDCs in human brain

Neurotoxicity is one of the major human toxicity and has attracted attention of research in last decade. Some compounds have also been classified as neurotoxins by several governmental agency like EPA (Environmental Protection Agency) through Toxcast (US EPA 2016), EFSA (European food and safety authority) (Masjosthusmann et al. 2018) and nation agency like German Occupational Safety Supervision agency (Breuer 2010). Considering every year thousands of chemicals enter in market, it is rather difficult to carry neurotoxic studies for each chemical. With 3R principle by REACH (Nicolotti et al. 2014) and existing deficiency in the experimental approaches, it is rather imperative to look for the integrative computational models which along with limited experimental data can fulfil the gap (Jiang et al. 2020). For environmental chemicals to affect the brain, it has to cross the Blood-brain barrier (BBB) which consists of tight junction preventing the entry of xenobiotics inside brain. Besides tight junction, efflux transporters like ABCB1 (p-glycoprotein), ABCG2 (Breast Cancer Resistant Protein) can limit the accumulation of xenobiotics inside brain. The research about chemicals as the substrate for active transport or not is still not quite evident, however some studies with peripheral organs, whole organism, cell lines demonstrate some chemicals as

substrate for efflux transporter (Denuzière and Ghersi-Egea 2022). For instance, BPA was found to be overexpressing ABCG2 or ABCB1 at 40 nM in MDCK cells (Dankers et al. 2013). In-vitro studies with EDCs can provide evidence for their BBB permeability in human and further mechanism related to toxicokinetic in brain. The data generated from in-vitro study can be further incorporated with in-silico model to predict neurotoxicity and reducing the usage of animals.

2. BBB Permeation using in-vitro Models

In-vitro model for studying BBB permeation of xenobiotics is utilized extensively by scientific community all over the globe. BBB restricts entry of molecule primarily due to complex tight junctions and expression pattern of solute carriers and ABC-type efflux transporters (Helms et al. 2015). Capillaries of BBB consist of several cell type with complex structures with endothelial cells constituting the capillary wall and thus the actual barrier (Helms et al. 2015). Endothelial cells are being surrounded by pericytes (approx. 30% coverage) which in turn is surrounded by basement membrane and astrocytes. From early 1970s, efforts to isolate brain capillaries and generate cell culture of BCEC have been carried out (Mršulja et al. 1976). Overtime, several in-vitro models both from non-cerebral origin and cerebral originals were developed. Different type of epithelial or endothelial cells from non-cerebral origin like MDCK (Madin-Darby canine kidney), human umbilical endothelial cells (HUVEC) are being used for studying different aspects of BBB but they cannot be considered as real BBB models (Wilhelm et al. 2011). BBB models of cerebral endothelial cells like b-end 3-5 of murine origin, HCMEC/D3 (Human Capillary Microvascular endothelial cell lines), co-culture of endothelial with glial cells or pericytes have been developed (Neuhaus 2020; Wilhelm et al. 2011). HCMEC/D3 is one of the best characterized human cell line which can retain BBB characteristic like junctional protein and efflux transporter expression (Neuhaus 2020; Weksler et al. 2005). In these models, the barrier function and permeability potential are often measured with the apparent permeability (Papp) and TEER for drugs and chemicals, this data can be used for building PBPK Models.

3. PBPK Models and Brain IVIVE

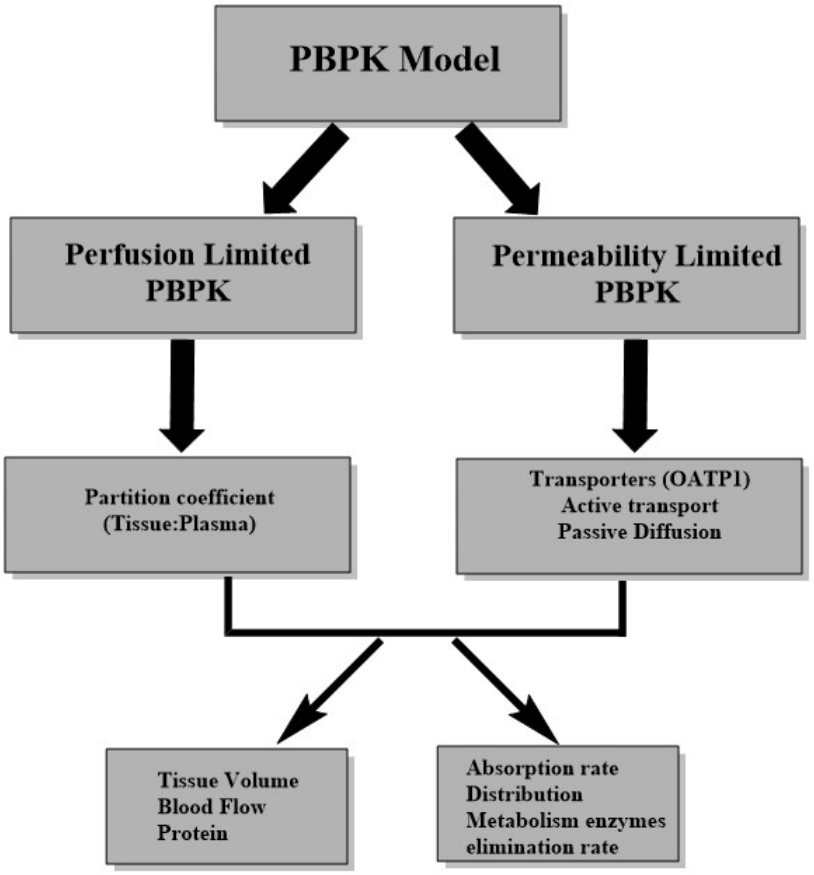

Figure 1: Types of PBPK Model and representation of physiological and biochemical parameters required for developing PBPK

PBPK Model is a computational modeling approach incorporating blood flow, tissue volume of organs and biochemical properties to achieve the mechanistic representation of xenobiotics in biological system (Kuepfer et al. 2016). These models provide the quantitative characterization of concentration-time profiles in specific site of action apart from plasma which may be difficult to measure experimentally (Fig 1). PBPK Model typically consist of liver, lung, kidney, brain, gut, stomach, small intestine, bone marrow, adipose tissue and rest of body. Organs are linked to each other by blood flow, tissue-plasma partition coefficient, permeability coefficient and organ volume (Kovar et al. 2020). There are two types of PBPK model most commonly used: perfusion limited and permeability limited PBPK. In perfusion rate limited model, blood flow to the tissues become the limiting process. The major assumption being at steady state, total chemical concentration in circulation is in equilibrium with the total chemical concentration in tissue determined by Kp values whereas fu (fraction unbound) concentration are equal (Jones and Rowland-Yeo 2013). In this typically a highly perfused tissue reaches steady state faster than less perfused tissue. Permeability across cell membrane is the rate limiting step in permeability limited model with tissue being divided into extracellular and intracellular space. In this model, the time to reach equilibrium is dependent on chemical specific permeability rather than blood flow which was used to calculate permeability rate constant. This models also consider active transport which can be

modeled by incorporating uptake parameters and can lead to variation of free concentration in the intracellular or extracellular space.

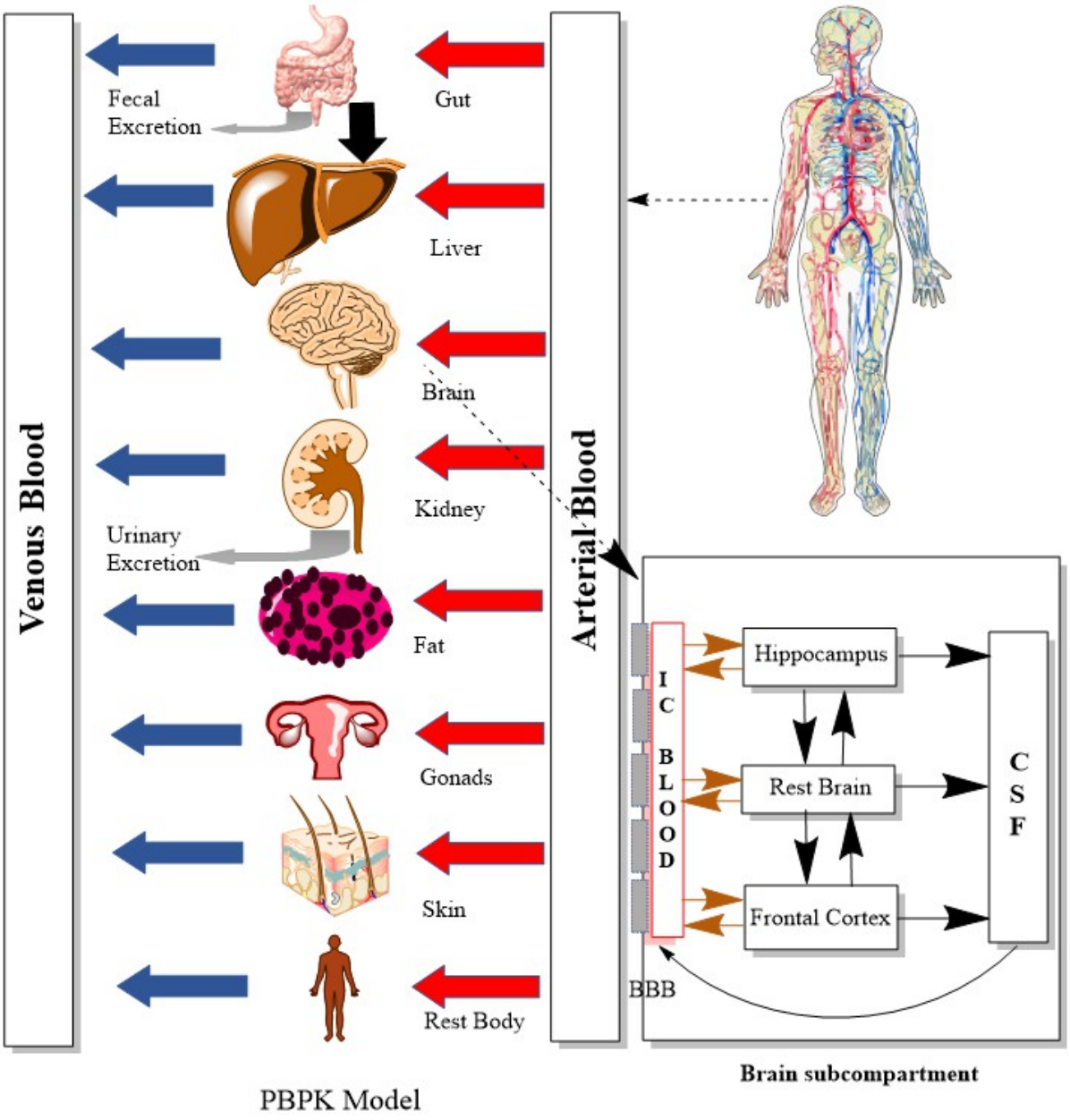

Figure 2: Overall structure for the PBPK Model. IC refers to intracranial blood, CSF: cerebrospinal fluid, BBB: blood-brain barrier.

4. Parameters for developing PBPK Model

For developing the PBPK Model, information about anatomical and physiological structure and biochemical parameters are required. Physiological parameters are species-specific and mainly include cardiac output, organ weight and blood flow to the organs (Lin et al. 2020). Accurate species-specific and variability within and between species for physiological parameters are essential for successful development, validation and extrapolation of PBPK model. Several authors have comprehensively compiled physiological literature base for

several species like human, rats, monkeys and dogs (Brown et al. 1997; Davies and Morris 1993; Valentin 2002).

Biochemical parameters are chemical-specific mainly focused on the properties related to absorption, distribution, metabolism and excretion (ADME) of a chemical. Absorption of the chemical is mainly defined by absorption rate constant (k_a). First order absorption rate constant can be predicted using in-vitro or in-vivo data (Yim et al. 2020). Absorption determines how fast the chemical is available to reach from gut to liver (in case of oral dose), hence affecting the bioavailability (Lin and Wong 2017). Other parameters like fraction unbound (fu) is chemical-specific but sometime depend on the organism also. This parameter affects the chemical distribution and clearance from body since only free fraction is available for absorption, diffusion and metabolism. Fraction unbound can vary based on the age as it is dependent on plasma proteins: serum albumin or α-acid glycoprotein. Serum albumin tend to be lesser in pediatric and geriatric than adults, this should be considered while building PBPK Model for specific age groups. Proper scaling for the fu for the sensitive population is shown in equation 1. Here, fu_x represents the fraction unbound in specific population (pediatric/geriatric), OSF is age dependent ontogeny scaling factor calculated based on human serum albumin/α-acid glycoprotein levels (Deepika et al. 2021; McNamara and Alcorn 2002; Meistelman et al. 1990).

$$fu_x = \frac{1}{1 + OSF * \frac{(1 - fu_{adult})}{fu_{adult}}} \qquad equation\ 1$$

Distribution of chemical to different organ is the key determinant factor that affects the concentration-time course behavior of the chemical at target region. Distribution is often characterized by tissue: plasma partition coefficient (PC) in perfusion limited PBPK model. Partition coefficient can generally be calculated by concentration of chemical in particular tissue divided by concentration in the plasma/blood or sometime concentration is replaced by AUC (area under curve) (eq 2). In case of non-availability of experimental data, the PC can be calculated by several algorithms available for environmental chemicals and drugs (Poulin and Krishnan 1995, 1996; Poulin and Theil 2000; Rodgers and Rowland 2006; Schmitt 2008). These algorithms are basically dependent on parameters like octanol/water partition coefficient, lipophilicity, binding constant, fraction unbound, plasma/albumin ratio, neutral lipid content, neutral and acidic phospholipids and water fraction in the tissue (Peyret et al. 2010; Schmitt 2008).

$$PC = \frac{C_{tissue}}{C_{plasma/blood}} \ or \ \frac{AUC_{tissue}}{AUC_{plasma/blood}} \qquad eq.2$$

One of the important aspects in developing PBPK Model is the parameter required to demonstrate metabolism of the chemical in gut, or the liver. IVIVE approach is extensively used for liver metabolism to predict in-vivo clearance from in-vitro metabolic data. IVIVE approach for hepatic metabolic clearance has improved over the years and has almost completely replaced the animal study for parameterizing the model in metabolic aspect (Chen et al. 2012). Metabolism is calculated using V_{max} (maximum metabolism rate) and K_m (concentration of substrate required to achieve 50% V_{max}) as shown in eq. 3. d(Amet)/dt refers

to metabolic amount with time, Corgan refers to concentration of chemical in the organ and fu represents fraction unbound in the organ. Vmax obtained from the in-vitro is scaled to in-vivo accounting for microsomal protein content (MPPGL), liver weight (V_{liver}) and body weight (BW) using eq. 4. Similar approach is used for calculating the metabolism in gut.

$$\frac{d(Amet)}{dt} = \frac{V_{max} * C_{organ} * f_u}{K_m + C_{organ} * f_u} \qquad \text{eq. 3}$$

$$V_{max\ (liver)} = \frac{V_{max\ (in-vitro)} * MPPGL * V_{liver}}{BW^{0.75}} \qquad \text{eq. 4}$$

The last parameter required for PBPK is excretion of the compound which is mostly by urine, feces or exhaled air. Compounds which are majorly eliminated by urine like PFAS chemicals, glomerular filtration rate (GFR) present in kidney become the key determinant factor. Sometime the chemical keeps on reabsorbing by the renal transporter in the filtrate compartment back to plasma through a saturable process rather than eliminating from urine. This type of mechanism has been detected in PFAS chemical one of the main reason for their longer elimination half-life (Deepika et al. 2021) (Fàbrega et al. 2014). In some chemicals, enterohepatic recirculation is observed where the metabolite keeps on circulating from liver to gut and so on (Malik et al. 2016). This leads to delayed elimination and alter the pharmacokinetic and pharmacodynamic of the compound. All these mechanistic phenomena need to be incorporated in the PBPK model. Excretion of chemical is often explained by first order or zero order elimination kinetic. In first order elimination, the kinetic is concentration-dependent process whereas zero order elimination is independent of the concentration (Borowy CS 2021). This PK parameter also need to be considered for PBPK Model.

After incorporating all physiological and biochemical parameters in the PBPK Model, the route of exposure is determined. Route of exposure determines the bioavailability of chemical in many cases and hence the toxicokinetic. Most common and prominent route of exposure is oral via dietary intake, drinking water, and dust ingestion in human for most of the chemicals. However, some chemicals like bisphenols and phthalates also have high dermal exposure through printing receipts, cosmetics etc. By considering all the parameters and input (dosing) for PBPK, concentration-time profile is predicted to understand toxicological profile in different organs. However, sometimes the risk can vary based on specific individuals due to their genotype and phenotype.

With newer discoveries and extensive research database available, science is moving towards personalized and individualized medicine. In clinical science, currently PBPK Models are being embedded through drug development to evaluate patient risk factor like drug-drug interaction, drug dosing, improved drug absorption, effect of fasting and pH and late stage drug development. Further their use is being extended to prescribe correct amount of dose to different age patients, based on sex variation, pathology and much more (Hartmanshenn et al. 2016). But, unfortunately in environmental science still most PBPK models are generalized and consider the adult physiology and biochemical parameters for assessing risk. However, in recent years some efforts are being made to specialize the PBPK model (e.g., pregnancy PBPK, pediatric PBPK) for only specific compounds (Karrer et al. 2018; Sharma et al. 2018) but still we need to make them more personalized and individualized. In my thesis

effort has been made to develop PBPK model considering sensitive population groups like pediatric, geriatric etc. Further, we tried to compare the toxicokinetic based on sex to further improve the risk assessment approach. It may be possible that for some environmental chemicals, females may behave differently than males as there are intrinsic difference in physiology like body weight, blood flow as well as differences in the absorption from gut, transporters, metabolic enzymes, and elimination (Hartmanshenn et al. 2016).

We always rely on keeping the in-silico model as simplistic as possible but sometimes to evaluate the risk in a particular organ or tissue, it is required to build organ-specific PBPK Model. The complexity of brain with presence of BBB, transporters and several compartments within brain often points towards developing brain specific PBPK which can be used for predicting neurotoxicological risk. Brain PBPK model with inclusion of hippocampus, frontal cortex, CSF etc. provides opportunity to predict the chemical concentration at the target site (Fig 2). Development of brain specific PBPK model requires the permeability limited compartments where the membrane permeability become the rate limiting factor rather than blood flow. Also, human data cannot be available for brain and conservative approach for species scaling cannot be applied since brain is too complex (Ball et al. 2012). So, brain PBPK model are a good in-silico approach for predicting brain toxicokinetic with inclusion of mechanistic IVIVE by using in-vitro data (Ball et al. 2013; Gaohua et al. 2016). The regional concentration predicted in brain can further act an input for systems toxicology model for regional risk assessment.

5. Systems Biology Model

Systems biology model involves the computational and mathematical modeling for understanding the dynamics and structure of biological system (Kremling 2013; Mayer et al. 2012; Sasidharakurup and Diwakar 2020). This would help in understanding the neurological risk developing from chemical exposure at the cellular and biochemical level. Modeling the neurological signalling pathway helps in evaluating experimentally relevant relationship between proteins and related perturbations that can help connect critical factors statistically relevant as common signalling mechanism. Deciphering the balance of oxidative stress and harmful process after chemical exposure is particularly interesting to understand the neuronal death and toxicity. After chemical exposure to neurons,

Considering the input dose equivalent to brain concentration while using systems biology model may not be correct approach since kinetic of the chemical can affect dynamics and hence the risk. Integration of PBPK model with systems biology model to predict neuronal damage can improve the translational framework for risk assessment.

UNIVERSITAT ROVIRA I VIRGILI
QUANTITATIVE SYSTEMS TOXICOLOGY MODELING FOR NEURONAL ADVERSE OUTCOME
Deepika

Hypothesis and Objectives

UNIVERSITAT ROVIRA I VIRGILI
QUANTITATIVE SYSTEMS TOXICOLOGY MODELING FOR NEURONAL ADVERSE OUTCOME
Deepika

Hypothesis

The number of environmental chemicals present in U.S. and Europe market are around 75,000-140,000 with exposure to human directly or indirectly (Johnson et al. 2020) (Egeghy et al. 2012). Among them almost 200 chemicals are known to cause human neurotoxicity while other 1000 have shown animal neurotoxicity. However, for vast majority of chemicals, the information related to their mechanistic kinetics and dynamics for neurotoxicity is still missing. An additional challenge is that it is often difficult to measure the toxicity in particular organ in human through non-invasive methods. Therefore, computational predictive methods designed for human can help in overcoming these challenges, hence improving human risk assessment. But, most of the time computational methods are based on conventional approach where the basic assumption is that the risk is similar among sex and several age groups. This is the major drawback of risk assessment where the risk is underestimated in sensitive population. Sex-specific as well as age-specific computational models (PBPK) considering the sensitive population are increasingly useful for improved risk assessment. Several researchers have pointed out that metabolism of chemical might vary in specific gender, for instance higher percentage of glucuronide are found in men´s urine with females having higher percentage of sulfate conjugates (Kortenkamp et al. 2022). Further, the pediatric and geriatric population may experience adverse effects due to their physiology whereas such effects may not be evident in adults. Considering this age-difference is must while calculating the risk for a specific end-point. In-silico models like PBPK have advanced overtime, now the in-vitro as well as in-vivo data is being utilized for building these models. For instance, parameters related to liver metabolism are always extrapolated from in-vitro data using IVIVE and incorporated into PBPK. But still other parameters are being calculated from in-vivo data. Improved in-vitro models like caco-2 intestinal permeability, BBB permeability assays can help in further reducing the in-vivo data usage in these models. BBB permeability assay with human cell lines can provide the permeability coefficient as well as the active transport and passive diffusion which can be integrated in PBPK reducing the animal usage. Such kind of approach strengthen the 3R principle and reduce the reliability on in-vivo data for risk assessment.

Brain is quite complex organs with presence of BBB, CSF, multiple transporters and several sub-parts responsible for different functions. Compartmental models are not adequate to describe the permeability of chemical and metabolite and further transport inside several parts of brain. Organ-specific PBPK Model are required for mechanistic and quantitative prediction of chemical toxicokinetic inside brain. Further, integrating the results from PBPK with systems biology models will facilitate better insights into mechanism of neurotoxicity thus improving human risk assessment. Systems biology model can serve to broaden the perspective of cell physiology under chemical induced stress by exploring the alteration in proteins and other biomarkers. In addition, integrating both models can capture the chemical exposure, organ concentration, protein alteration and toxicity in brain which can help in building new AOPs. Such kind of framework reduce the animal usage, enhance the in-vitro data incorporation in the computational model and improve the human risk assessment.

Objective

The objective of my thesis is to develop an in-silico approach integrating environmental exposure, target concentration and toxicity at cellular level for improved risk assessment. Age-based PBPK model was developed to evaluate the toxicokinetic in pediatric, adult, and geriatric. In-vitro study was conducted to collect data for specific PBPK Model. The results from in-vitro and PBPK were used as input in systems biology model to evaluate mechanistic pathways happening in brain leading to cell death and ultimately neurotoxicity.

Specific Objectives

- Assess the life stage development of long acting chemical (PFOS) in the human body.
- Risk Assessment by developing Pediatric and sex-specific PBPK model for small acting chemical (BPA) and comparison with adult model.
- PBPK model for organophosphate flame retardant to understand toxicokinetic and hence the risk.
- Conducting in-vitro kinetic study for checking the BBB permeation potential of pesticides and IVIVC focused on reducing animal usage.
- Developing Brain specific PBPK model for PFOS and PFOA using IVIVE through in-vitro experimental data.
- Integrating brain PBPK model to ROS SB Model for understanding mechanistic pathways related to neurotoxicity and hence proposing AOP.

Chapter 1

Deepika Deepika, Raju Prasad Sharma, Marta Schuhmacher & Vikas Kumar (2020) An integrative translational framework for chemical induced neurotoxicity – a systematic review, Critical Reviews in Toxicology, 50:5, 424-438, DOI: 10.1080/10408444.2020.1763253.

UNIVERSITAT ROVIRA I VIRGILI
QUANTITATIVE SYSTEMS TOXICOLOGY MODELING FOR NEURONAL ADVERSE OUTCOME
Deepika

An Integrative Translational Framework for Chemical Induced Neurotoxicity- A Systematic Review

Abstract

Many chemicals in day-to-day and industrial usage have the ability to cross the blood-brain barrier and develop neurotoxicity in human beings. There are numerous *in vitro*, *in vivo*, epidemiological and *in silico* studies developed to test the neurotoxicity of such chemicals. This systematic review summarized the endpoints and biochemical markers generated from *in vitro* models, organism-based models, human studies and *in silico* tools and how they are used to translate the data for risk assessment of neurotoxic chemicals. Increased evidence about different biomarkers through genomics and proteomics has developed data related to microRNAs, translocator proteins, acidic proteins and basic proteins facilitating some understanding about the molecular mechanism of neurotoxicity. Fluid based biomarkers such as those found in serum, plasma and urine from human studies act as indirect endpoints for neurotoxicity. Meanwhile, with improvement in knowledge of molecular mechanism and different biomarkers, there is a potential to develop a translational platform that can integrate the biological data from different studies mechanistically and thereby translated across intra and interspecies for neurotoxicity assessment. Further, this review proposed an integrative translational framework combining experimental and *in silico* studies like toxicokinetic models and integrative systems biology to assess the chemicals for neurotoxicity. This framework can be used to predict the inherent risk of neurotoxicity and extend to such chemicals where less experimental data exists.

Keywords: *in vitro*, *in vivo*, epidemiology, *in silico*, translation, neurotoxicity

Abbreviations

ATSDR	Agency for Toxic Substances and Disease Registry	MTT	3-(4,5-dimethylthiazol-2-yl)-2,5-diphenyl tetrazolium bromide
AOPs	Adverse Outcome Pathways	NO	Nitric Oxide
BPA	Bisphenol A	NHANES	National Health and Nutrition Examination Survey
BSID	Bayley Scales of Infant Development	PBPK	Physiologically Based Pharmacokinetic Modelling
BRIEF	Behavior Rating Inventory of Executive Function 2	PCBs	Polychlorinated biphenyls
CGMP	Cyclic Guanosine Monophosphate	PD	Pharmacodynamics
CNS	Central Nervous System	PFAS	Polyfluoroalkyl substances
EDCs	Endocrine Disruptor Compounds	PFOS	Perfluoro octane sulfonic acid
EEA	European Environment Agency	POD	Point of Departure
EFSA	European Food Safety Authority	PFOA	Perfluoro octanoic acid
EPA	Environmental Protection Agency	QIVIVE	Quantitative *In Vitro* to *In Vivo* Extrapolation
EU-OSHA	European Union information agency for occupational safety and health	QSAR	Quantitative Structure Activity Relationship
FRs	Flame Retardants	ROS	Reactive Oxygen Species
GSMN	Genome Scale Metabolic Network	REACH	Registration, Evaluation, Authorisation and Restriction of Chemicals
IVIVE	*In Vitro* to *In Vivo* Extrapolation	SB	Systems Biology
KEs	Key Events	TUNEL	Terminal deoxynucleotidyl transferase dUTP nick end labelling
LDH	Lactate Dehydrogenase	VMWM	Virtual Water Maze test
LTD	long-term Depression	WHO	World Health Organization
LTP	long-term Potentiation		

1. Introduction

Chemicals have been produced to serve numerous purposes, starting from its usage in common household items to industrial products. Many of these substances are released in the environment and accumulate inside living organisms to harmful concentration (Fonnum and Mariussen 2009). Exposure of these chemicals to living beings have been linked to several adverse outcomes as demonstrated through *in vitro*, *in vivo*, epidemiological and *in silico* studies (Coecke et al. 2006; Asimakopoulos et al. 2016; Tsatsakis et al. 2017). Most of the environmental chemicals are lipophilic in nature and knowledge that they can cross blood-brain barrier raise the concern about harmful effect on the nervous system especially leading to neurotoxicity (Weiss 2000; Fonnum and Mariussen 2009; Maffini and Neltner 2015; Philips et al. 2018). Exposure of these chemicals in the early phase of life might be critical, where the developing human brain undergoes a series of changes critically depending on the particular sequence of processes occurring at the right time and right place (Rice and Barone 2000; Grandjean and Landrigan 2006; Fritsche et al. 2018; Li et al. 2019). There are several regulatory agencies (NHANES, EEA, EPA, EU-OSHA, WHO, ATSDR & EFSA) that keep track of these chemicals related hazardous effects on human health. However, looking into the number of facts for instance; a large number of chemicals released into environment, occupational exposure, individual susceptibility, concurrent exposure of multiple chemicals, and complex human nervous system, it is very challenging to apply research finding (*in vitro*, *in vivo*, epidemiology and *in silico* studies) to quantifying the effects of these chemicals on the human nervous system (Cowell et al. 2018). To unmet these challenges, the area of integrated translational toxicology has been proposed (Vodovotz et al. 2008; Drolet and Lorenzi 2011; Mumtaz et al. 2012; Hughes et al. 2013; Sedman et al. 2016; Phillips and Bogdanffy 2017).

Translational toxicology is a broader concept and different authors define it in different ways. *In vitro* models translate or evaluate the toxicological profile of chemicals on the human nervous system through different endpoints, biomarkers and mechanistic pathways (Hartung and Daston 2009; Breznan et al. 2016; Goldberg et al. 2018). *In vivo* has been defined as a field where preclinical findings from animal models are used for assessing behavioral and sensory perturbations and mode of action for better extrapolation to the human nervous system (Bruch et al. 2015; Coecke et al. 2006; Huang et al. 2016; Hughes et al. 2013; Kerb et al. 2017). Epidemiological study involves evaluating distribution and determinants of health-related events in a specific population to predict the effect of chemicals on humans (Shah et al. 2016). Understanding about human nervous system is increasing but still the process of translating fundamental knowledge from *in vitro*, *in vivo* and epidemiological toxicological data to quantification of a toxicity in human is challenging (Bornstein and Licinio 2011; Boberg et al. 2019). As the human brain is a continuously changing organ forming new synapses to store new information and such a way develops a complex network in response to interaction between genetic and environmental factors (Roberts et al. 2015). Also despite similarity in neurodevelopmental processes in mammals, interspecies differences exist leading to species specific features and differences in cognition and behaviour (Silbereis et al. 2016).

Advances in computational toxicology have led to different *in silico* tools like cheminformatics, toxicokinetics, toxicodynamics, systems biology and toxicogenomics for assessing neuronal risk in different species. Also, the need for in silico approaches has been suggested by a panel of experts for an alternative to experimental testing (Laroche et al. 2018). Different guidelines like REACH, IATA and ITS, focus on integrated analysis of existing information with new information generated from in silico tools (Vinken 2019) (Benfenati et

al. 2011). Toxicological and biomedical research on nervous system from many decades has led to lot of scientific data which includes information on mechanisms by which neurotoxicants can alter signaling pathways and how such alterations can lead to adverse impacts on the human biological system (Bal-Price et al. 2017).

The main objective of this review was to conduct a systematic search for *in vitro*, *in vivo*, epidemiological and *in silico* studies being conducted in neurotoxicological research and to propose a framework for translational neurotoxicity. To examine the translation in neurotoxicity a systematic study for a specific group of chemicals (FRs, PFOS, PFOA, PCB, BPA and Phthalates) were conducted in this manuscript. In addition, the framework for integrative translation was proposed to transform the results for prediction of neurotoxicity in human species (Figure 1) for risk assessment. This review emphasize how the integration of experimental data (*in vitro*, *in vivo* and epidemiological studies) with *in silico* tools is important to translate the data and also for predicting the adverse effects on human nervous system (Auffray et al. 2003;Vodovotz et al. 2008; Adcock et al. 2010; Drolet and Lorenzi 2011; Kerb et al. 2017; Linne 2018). It will also help in understanding the mechanism and long-term effect of neurotoxicants on anatomical, physiological and cognitive functions of nervous system.

2. Methods

2.1 Data Search

A Systematic approach was used for searching database Scopus and PubMed with different keywords as mentioned in SI (Refer Table 1 in annexure). Different search strings were designed to search from these databases in order to identify all the relevant publications for a certain group of chemicals. Research articles from 2006 to Feb 2019 were included in this review. Timespan was used to limit the search results to a reasonable amount. We did not restrict the search by language. Review articles and duplicated studies were overlooked (Figure 1).

2.2 Inclusion Criteria

In vitro: We included 2D (e.g. embryonic cell lines), 3D cell lines (e.g. human pluripotent stem cells), cultures and co-cultures. Electrochemical cell chips were excluded.

In vivo: It includes rats, mice, zebrafish, Marine Medaka, nematodes and Caenorhabditis elegans (C. elegans).

Epidemiology: It includes human (pregnant females, males, elderly and children).

In silico: It includes PBPK, PD, PK, IVIVE, QIVIVE, SB, GSMN and QSAR.

2.3 Chemical Exposure

The exposure of our interest is some of the organic chemicals like flame retardants (FRs), Perfluoro octane sulfonic acid (PFOS), Perfluoro octanoic acid (PFOA), Polychlorinated biphenyls (PCBs), Bisphenol A (BPA) and Phthalates. These chemicals have proven neurotoxic effects. This review will include these neurotoxic chemicals and exclude other chemicals.

2.4 Outcomes

Studies which represent the translation of data to assess neurotoxicity by various means like endpoints, biomarkers, mechanism of action and neurobehavioral assessments were considered for this review. Research of the results was screened for significance in

neurotoxicity (Figure 1). For the different endpoints obtained by *in vitro*, *in vivo* and epidemiological studies, the percentage has been calculated to demonstrate about the significance of performed test for neurotoxicity. In order to calculate the percentage, an average number of times the particular test conducted was divided by total number of articles included in the review for a particular section.

2.5 Publication Types

Multiple publications based on the same study population were considered individually. Articles that do not contain original data like meta-analysis, reviews, conference abstracts were not considered for the study. Studies containing irrelevant population, irrelevant exposure or irrelevant outcome were excluded. Data mining from grey literature was not performed (Figure 1).

2.6 Publications Included

For *in vitro*; Out of total articles published, 53 articles were taken for the systematic study after eliminating duplicates and other publication bias. For *in vivo*; 22 articles were included for systematic study. For epidemiology; 15 articles were taken, and for *in silico*, 6 articles were taken for the review.

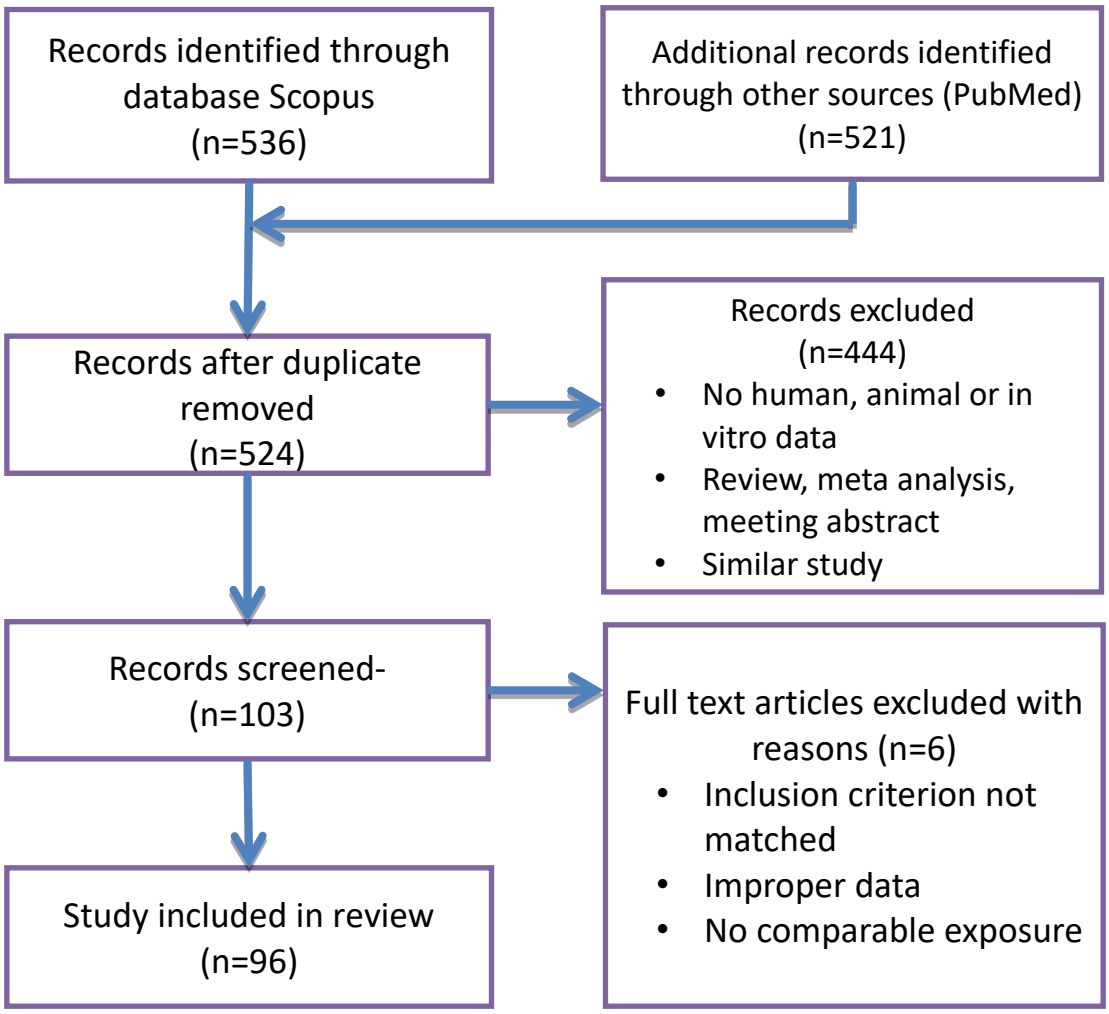

Figure 1: Diagram summarizing the research from pilot systematic review. It includes total articles searched using different database and keywords, reasons for excluding the articles and total number of review articles included for this systematic review.

3. Results

3.1 Translational *In Vitro*

This section focuses on various *in vitro* methods and the approaches that are being used to understand and quantify the chemical-induced neuronal toxicity (Refer Table 2 in annexure), hereby we called these as translational approaches. Results are summarized in Figure 2. To discuss the literature finding in a systematic way, we have categorized it as follows: 1) Preliminary screening test i.e. identification and characterization of the neurotoxicants, and 2) Molecular level-screening test i.e. to identify the mechanisms, adverse pathways and endpoint biomarkers. *In vitro* publications include different endpoints for neurotoxicity as shown in Figure 2 & Figure 3.

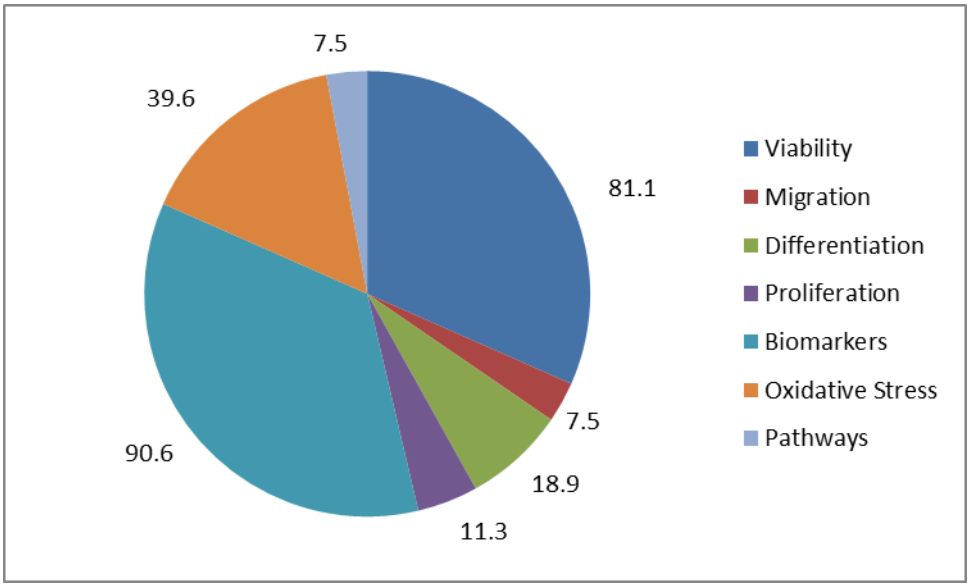

Figure 2: Diagram represents percentage distribution of various tests performed in vitro for inspecting the influence of chemicals on nervous system. Primary tests include cell viability, differentiation, migration and proliferation. Molecular level tests comprise of oxidative stress, pathways and biomarkers for assessing neurotoxicity by different chemicals.

Preliminary Screening for neurotoxicity involves cell viability (81.1%), differentiation (18.9%), migration (7.5%) and proliferation (11.3%) (Figure 3). These are key cellular processes critical to neuronal development. *In vitro* cellbased cytotoxicity assays like LDH, MTT assay and high content analysis approach is used for quantification of neurites to measure cell viability (Wilson et al. 2014). Out of 53 articles, 43 articles included cell viability as the test for neurotoxicity (Reistad et al. 2006; Lyng et al. 2007; Yoot et al. 2007; Costa et al. 2007, 2016; Giordano et al. 2008; Le et al. 2008; Slotkin et al. 2008, 2017; Dingemans et al. 2009; Giordano et al. 2009; Götz et al. 2009; Ndountse and Chan 2009; Rodrigo et al. 2009; Fan et al. 2010; Tagliaferri et al., 2010; Dishaw et al. 2011; Tofighi et al. 2011; Chen et al. 2011, 2017; Al-Mousa and Michelangeli 2012; Ziemińska et al. 2012; Fanelli et al. 2012; Jiang et al. 2012; Hendriks et al. 2012, 2014; T. Li et al., 2013; Gassmann et al. 2014; Ishido and Suzuki 2014; Xu et al. 2014; Wu et al. 2014, 2016; Yin et al. 2015, 2018b, 2018a; Szychowski and Wójtowicz 2016; Hirsch et al. 2017; Li et al. 2017; Sethi et al. 2017; Canzoniero et al. 2017; Cho et al. 2018; Sirenko et al. 2019; Wójtowicz et al. 2019). In ten articles, authors have measured neurite outgrowth to check the neuronal differentiation (Tofighi et al. 2011; Chen et al. 2011, 2017; T. Li et al., 2013; Wu et al. 2014; Xu et al. 2014; Yin et al. 2015, 2018a, 2018b; Sethi et al. 2017). Various authors have observed cell migration in different cell culture like neural crest cell (Hirsch et al. 2017), stem cells (Ishido and Suzuki 2014), human neural progenitor cells (Götz et al. 2009) and hippocampal neuron glial co-culture (Sethi et al. 2017). Cell proliferation has also been studied as the marker of neurotoxicity (Costa et al. 2007; Götz et al. 2009; Li et al., 2013; Ishido and Suzuki 2014; Tofighi et al. 2011; Wu et al. 2016).

Molecular level screening comprises of the mechanism of action, cellular and molecular pathway responsible for causing change in the neuronal cell through functional toxicity assays. Oxidative stress (39.6%) and signaling pathways (7.5%) (Figure 2) are being extensively studied through *in vitro* models and considered important key events (KEs) (Bal-Price et al.

2015). Neurons have high glucose metabolic demand which make oxidative stress as one of key factor leading to neuronal cell death (Gartlon et al. 2006). Increase in ROS (Reistad et al. 2006; Giordano et al. 2008; Tagliaferri et al., 2010; Liu et al. 2011; Al-Mousa and Michelangeli 2012; Ziemińska et al. 2012; Jiang et al. 2012; Hendriks et al. 2012, 2014; Wu et al. 2014; Costa et al. 2016; Cho et al. 2018; Yin et al. 2018b, 2018a; Wójtowicz et al. 2019), change in mitochondrial membrane permeability (MMP) (Al-Mousa and Michelangeli 2012; Ziemińska et al. 2012; Sirenko et al. 2019), ATP levels (Hirsch et al. 2017), lipid peroxidation (Giordano et al. 2008; Slotkin et al. 2008; Tagliaferri et al., 2010; Costa et al. 2016) and GSH levels (Lyng and Seegal 2008; Giordano et al. 2008, 2009) are mechanistic endpoints (Figure 3) being studied which cause oxidative stress (Gartlon et al. 2006). Also, NO CGMP pathway; lead to hippocampal LTP and LTD impairing learning capabilities (Rodrigo et al. 2009; Chen et al. 2018), NOTCH and WNT signaling pathway; affect HES1 & HES5 which results in delayed neurogenesis (Tofighi et al. 2011) and phosphorylated extracellular signal-regulated kinase (Perk)1/2 pathway; for neuronal impairment (Fan et al. 2010) has been extensively reported as the endpoint for human nervous system toxicity.

Increasing evidence with time support the utility of certain biomarkers (90.6%) like alteration in protein levels (Lyng et al. 2007; Ndountse and Chan 2009; Chen et al. 2011; Dishaw et al. 2011; Al-Mousa and Michelangeli 2012; Fanelli et al. 2012; Jiang et al. 2012; T. Li et al., 2013; Canzoniero et al. 2017; Slotkin et al. 2017; Cho et al. 2018; Sethi et al. 2018; Yin et al. 2018a), neurotransmitters including GABA and glutamate (Lyng and Seegal 2008; Giordano et al. 2008; Dingemans et al. 2009; Costa et al. 2016; Chen et al. 2018), synaptic markers (Fanelli et al. 2012; Lesiak et al. 2014) and change in enzymatic activity (Reistad et al. 2006; Slotkin et al. 2008; Dishaw et al. 2011; Wójtowicz et al. 2019) as indicators of neuronal damages and important key events for AOPs (Bal-Price et al. 2015; Roberts et al. 2015). Neurotoxicity of a chemical can be often determined by presence of particular membrane receptors (Ndountse and Chan 2009; Lesiak et al. 2014; Chen et al. 2017; Sethi et al. 2018) and gene expression (Chen et al. 2011; Dishaw et al. 2011; Warita et al. 2013; Lesiak et al. 2014; Sirenko et al. 2019) which affect the molecular target/pathways. Calcium Homeostasis has a pivotal role in inter and intra neuronal processes like neurodevelopment, neuronal function, gene transcription (Carrasco and Hidalgo 2006), neurotransmission (Westerink 2008), neurodegeneration and dopaminergic cell survival. Changes in calcium (Reistad et al. 2006; Dingemans et al. 2009; Götz et al. 2009; Rodrigo et al. 2009; Liu et al. 2011; Tofighi et al. 2011; Al-Mousa and Michelangeli 2012; Ziemińska et al. 2012; Langeveld et al. 2012; Hendriks et al. 2012, 2014; Gassmann et al. 2014; Costa et al. 2016; Yin et al. 2018a; Sirenko et al. 2019) is considered an important KEs. Different end-points and biomarkers from *in vitro* neurotoxicity were identified as common KEs with high predictivity for neuronal damage. AOPs development for neurotoxicity are one-step forward for translation of results to human species. Further, data is needed to demonstrate and validate the results properly.

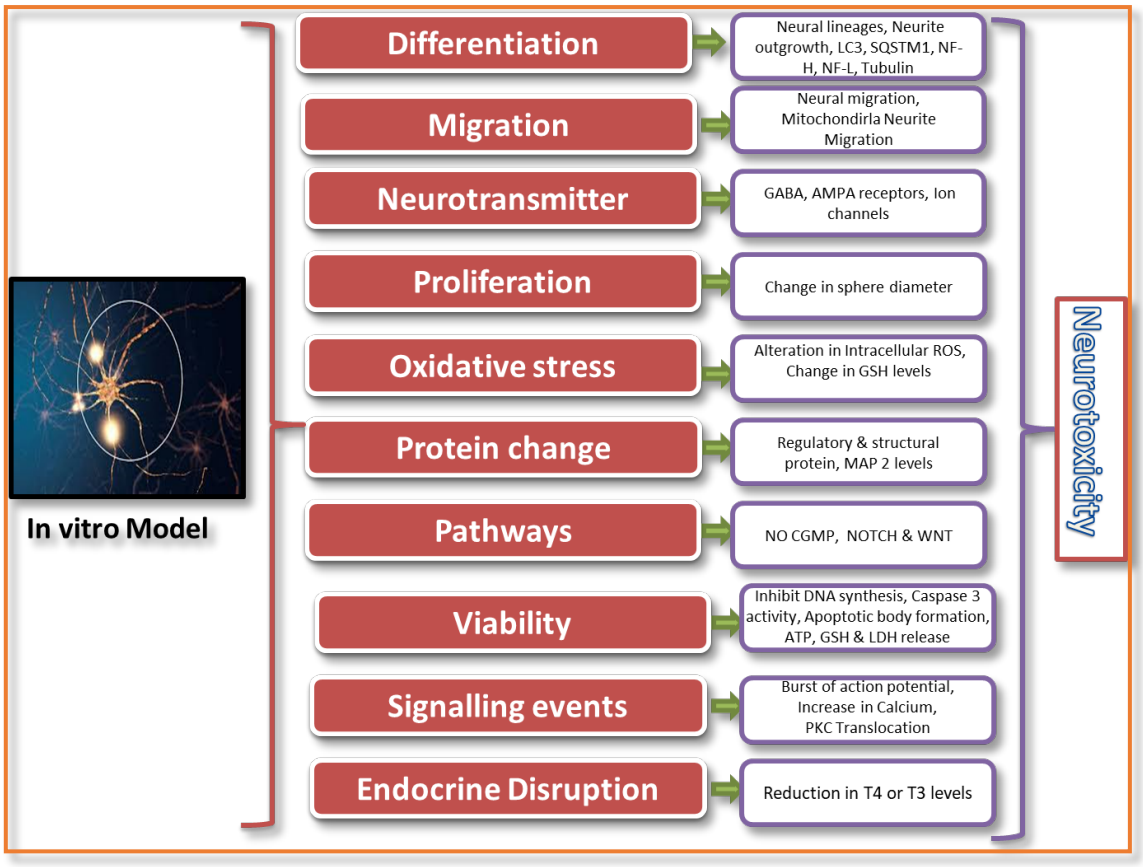

Figure 3: Mechanistic Pathways and endpoints for *in vitro* chemical testing. It provides a summary of key processes involved in neurotoxicity caused by different chemicals.
Abbreviations: LC3- Microtubule-associated protein 1 light chain 3, SQSTM1- Sequestosome1, NF-H- Neurofilament heavy Chain, NF-L- Neurofilament Light Chain, GABA- Gamma-Aminobutyric Acid, AMPA- α-amino-3-hydroxy-5-methyl-4-isoxazolepropionic acid, ROS- Reactive Oxygen Species, MAP2- Microtubule-associated protein 2, NO CGMP- Nitric Oxide Cyclic Guanosine Monophosphate, GSH-Glutathione, LDH- Lactate dehydrogenase, T4- Tetra iodothyronine, T3- Triiodothyronine PKC- Protein Kinase C, DNA- Deoxyribonucleic Acid.

3.2 Translational *In Vivo*

This section will encompass various *in vivo* tests and the translational approaches to understand and quantify the chemical induced neuronal toxicity (Figure 4) (Refer Table 3 in annexure). Here we will be discussing neurobehavioral assays (phenotypic biomarkers), histopathology test and identification of cellular and molecular biomarkers (Figure 5).

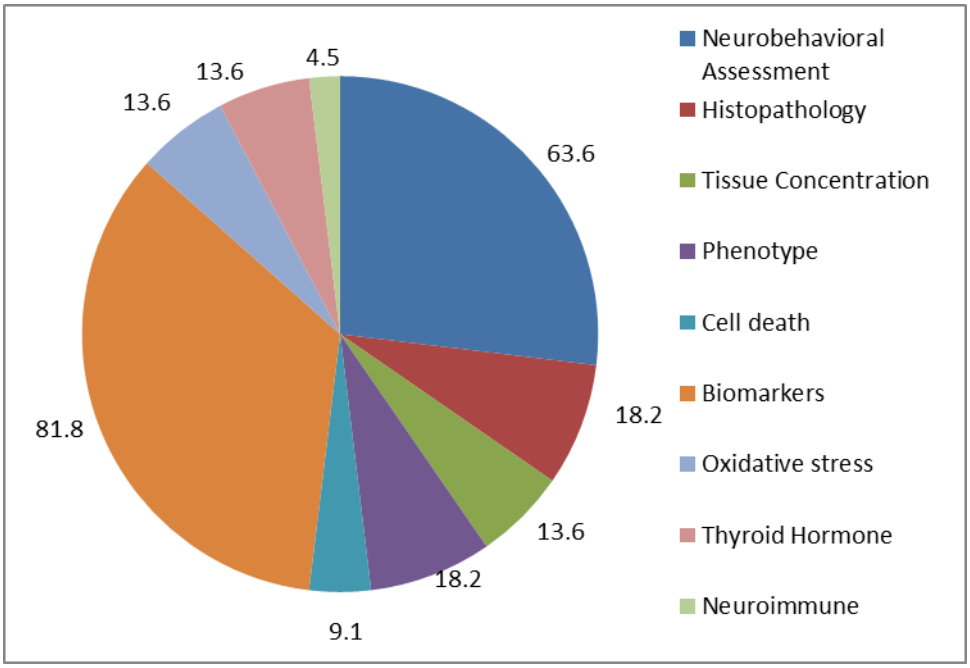

Figure 4: *In vivo* studies for identifying chemicals induced neurotoxicity. It includes different neurological endpoints, biomarkers and pathways for identifying toxicity.

In vivo models like zebrafish, nematodes, Caenorhabditis elegans, rats and mice have been used to evaluate neuronal behavior after chemical exposure (van der Merwe et al. 2019). These models offer chemical safety reference and are one-step closer to translate the effects on the human nervous system. Mostly neurobehavioral assessment (63.6%) has been used as a close proxy to check neurological disturbances or damage (Figure 5) (Dingemans et al. 2007; Vitalone et al. 2008; Boix et al. 2010; Kim and Pessah 2011; Tseng et al. 2013; Lee et al. 2014; Ma et al. 2015; Moser et al. 2015; Liu et al. 2018; Yang et al. 2018; Zhang et al. 2018, 2016; Zhu et al. 2018).

Neuroscientists conduct basic tests in animals to detect changes in brain morphology which includes phenotypic characters such as organ weight and growth (18.2%) (Malkiewicz et al. 2006; Moser et al. 2015; Vitalone et al. 2008; Yang et al. 2018), histopathological study (18.2%) (Ma et al. 2015; Liu et al. 2018; Yang et al. 2018; Zhang et al. 2018) and target tissue concentration of the chemical (13.6%) (Vitalone et al. 2008; Ruan et al. 2009; Lee et al. 2014). Hormonal activities e.g. thyroid hormones play an important role in brain growth during foetal and early phases of life. Unbalances in these hormones level has an impact on brain development, cell number, cell migration and synaptogenesis as studied by Moser et al. (2015), Wang et al (2015) and Zhu et al (2018). Cell death research in recent years has led to the development of certain gold techniques like TUNEL and other mechanisms for identifying neuronal cell death (9.1%) (Yang and Lein 2010; Zhang et al. 2018) (Figure 5).

Concerning to the effect of chemicals on the nervous system, some authors have explored the principal mechanism behind neurotoxicity through different biomarkers (81.8%) (Figure 5). Firstly, neurotransmission as an important mechanism how neuron conducts message and the impact on this can be known by measuring neurotransmitters as a biomarker (Boix et al. 2010; Dingemans et al. 2007; Gee et al. 2011; Lei et al. 2017; Moser et al. 2015; Pham-Lake et al. 2017; Wang et al. 2015; Zhang et al. 2018; Zhu et al. 2018). Secondly, neurochannels

balance ionic concentration inside and outside of the cell through voltage-gated calcium channels and calcium could be a biomarker to study the ion channel mechanism (Mochida 2000; Dingemans et al. 2007). Altered neurotransmitters like GABA, glutamate and dopamine can cause impairment in frontal cortex thereby affecting learning and memory (Bradner et al. 2013). Also, ROS (13.6%) production due to oxidative stress leads to an effect on the nervous system (Tseng et al. 2013; Ma et al. 2015; Wang et al. 2015). Lately, advancement is being made in recognizing the patterns of response in genes (transcriptome) (Basha et al. 2006; Malkiewicz et al. 2006; Tseng et al. 2013;Wang et al. 2015; Liu et al. 2018; Yang et al. 2018; Zhang et al. 2018; Zhu et al. 2018) and proteins (proteomics) (Basha et al. 2006; Malkiewicz et al. 2006; Dingemans et al. 2007; Boix et al. 2010; Yang and Lein 2010; Morris et al. 2012; Lee et al. 2014; Ma et al. 2015; Wang et al. 2015; Lei et al. 2017) that might be predictive of neuronal effects. Study on effect of immune cells (4.5%) on the nervous system measuring subsets of T cells from spleen, myelin basic protein level, serum markers and T cells infiltration in brain region has evaluated by Morris et al. (2012) (Figure 5).

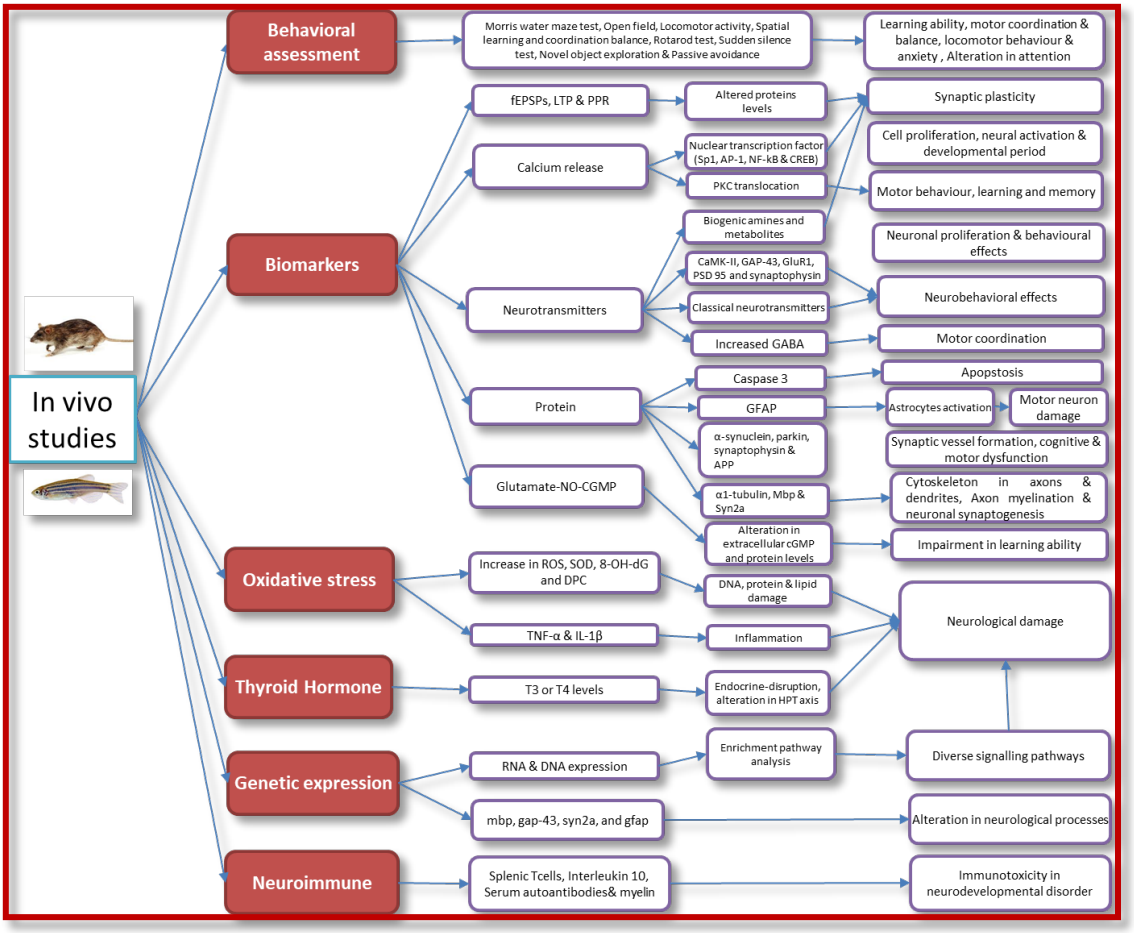

Figure 5: End points, biomarkers and mechanistic pathways for in vivo neurotoxicity. Behavioral assessment act as qualitative test for neuronal damage. Biomarkers, oxidative stress, thyroid hormones, genetic expression (transcriptome) and immune system provide mechanistic pathways for damage.

Abbreviations: LTP- Long term potentiation, PKC- Protein Kinase C, TH- Thyroid Hormone, AP1- Activator protein, Sp1 – Specificity protein, NF-KB – Nuclear factor Kappa-B, CREB- Camp Responsive Element Modulator, LTP- Long

term Potentiation, fEPSPs- Field Excitatory Postsynaptic Potentials, Classical neurotransmitters - acetylcholine, glutamate, c-aminobutyric acid, glycine, dopamine, norepinephrine, epinephrine, serotonin, aspartic acid, and taurine, SOD- superoxide dismutase, 8-OH-dG- 8-hydroxy- 2-deoxyguanosine, DPC - DNA-protein crosslinks, GFAP- glial fibrillary acidic protein, Caspase-3- cysteine-aspartic acid protease 3, ROS- reactive oxygen species, DPC- DNA-protein crosslinks, TNF-a - tumor necrosis factor alpha, IL-1β- interleukin-1 beta, Syn2a-synapsin Iia, Mbp- Myelin basic protein, gap-43- growth associated protein 43, HPT- hypothalamic–pituitary–thyroid.

3.3 Translational Epidemiology

This section includes epidemiology studies and the translational approaches to understand the chemical induced neuronal toxicity (Figure 6) (Refer Table 4 in annexure). Here we will be discussing neurobehavioral assays-based scoring, questionnaire survey, biomonitoring assays and statistical tools to interpret the results for the risk assessment (Figure 7).

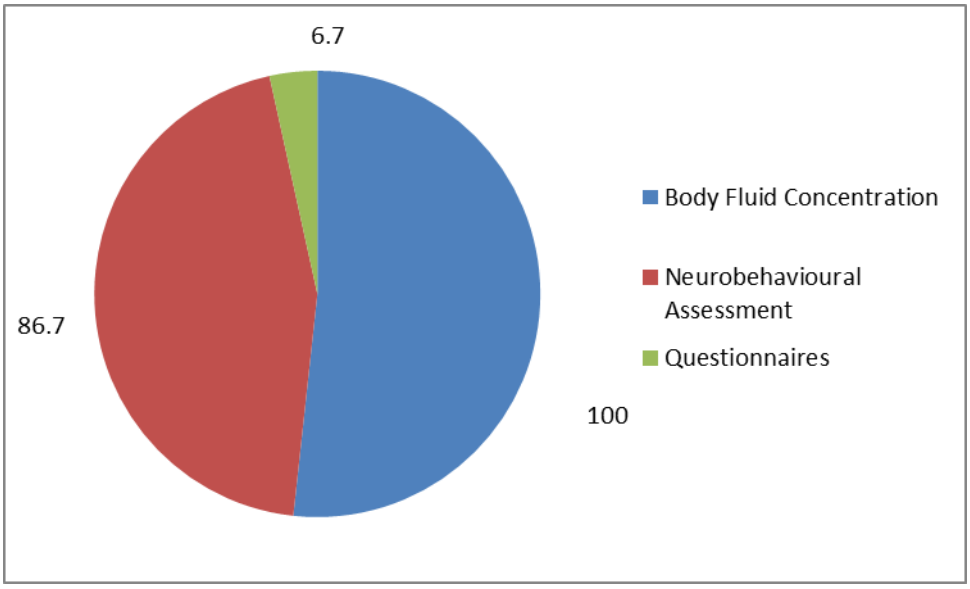

Figure 6: Endpoints for epidemiological studies to assess impact of chemicals on human nervous system. Body fluid concentration includes maternal cord and serum, urine, breast milk and CSF fluid for detecting concertation of chemicals and metabolites inside human body.

Epidemiological studies are widely recognized and different authors have estimated the neuronal risk via statistical analysis of various endpoints and exposure assessment (Chiu 2017). Studies confirm the complex interaction between neurodevelopmental changes and exposure to environmental toxicants (Al Aïn et al. 2017). Neurobehavioral assessment is for providing insight into functional integrity of brain and predictive of neurodevelopment of different brain regions (Craciunoiu and Holsti 2017; Eeles et al. 2017). Out of fifteen articles, thirteen studies evaluated the performance through neurobehavioral assessment (86.7%) to analyze the development of brain (Park et al. 2010; Chen et al. 2013, 2016; Adgent et al. 2014; Bellinger et al. 2016; Shin et al. 2016; Goudarzi et al. 2016; Braun et al. 2017; Doherty et al. 2017; Gaum et al. 2017; Shrestha et al. 2017; Vuong et al. 2018a, 2018b). These assessments evaluated various aspects like reading abilities, intelligence, behavior, cognitive and motor skills to develop a causal link between chemical exposure and the development of human brain. Exposure to the general population has been studied by all the authors (100%) measuring the concentration of chemicals in serum, breast milk, blood, cerebrospinal fluid,

lipid and urine in pregnant female, fetus, children and adults (Park et al. 2010; Chen et al. 2013, 2016; Adgent et al. 2014; Bellinger et al. 2016; Shin et al. 2016; Goudarzi et al. 2016; Lien et al. 2016; Braun et al. 2017; Doherty et al. 2017; Gaum et al. 2017; Shrestha et al. 2017; Vinceti et al. 2017; Vuong et al. 2018a, 2018b). Goudarzi et al. (2016) have done a self-administered questionnaire survey (6.7%) to understand information about smoking, weight, economic status and other social factors to observe impact on the human nervous system.

Different kind of regression models were applied to evaluate the effect of explanatory variables like exposure, risk factor etc. on the response variable (neuronal damage, development of nervous system) (Park et al. 2010; Chen et al. 2013, 2016; Adgent et al. 2014; Bellinger et al. 2016; Goudarzi et al. 2016; Braun et al. 2017; Doherty et al. 2017; Gaum et al. 2017; Vinceti et al. 2017; Vuong et al. 2018). Goudarzi et al. (2016) & Shin et al. (2016) used Spearman rank correlation coefficient, the Mann–Whitney U-test, and the Kruskal–Wallis test to analyze the correlation between chemical concentration and BSIDII scores individually with participant's characteristics. For accommodating multiple comparison Hsu-Dunnet method was used to compare the least square means of BSIDII (Goudarzi et al. 2016). Vuong et al. (2018) applied multiple informant model to generate odd ratio and confidence intervals to analyze the correlation between In-transformed childhood PFAS concentration and BRIEF score. Bellinger et al. (2016) calculated Pearson correlation coefficient between log 10 creatinine standardized urinary phthalate metabolite and then used a linear mixed model to estimate the difference in VMWM performance between girls and boys. Authors are able to translate the data from epidemiological studies using end-points and statistical tools and come up with conclusions but still criticism lies where study on a larger scale is required or sometimes researchers are unable to come up with a clear conclusion.

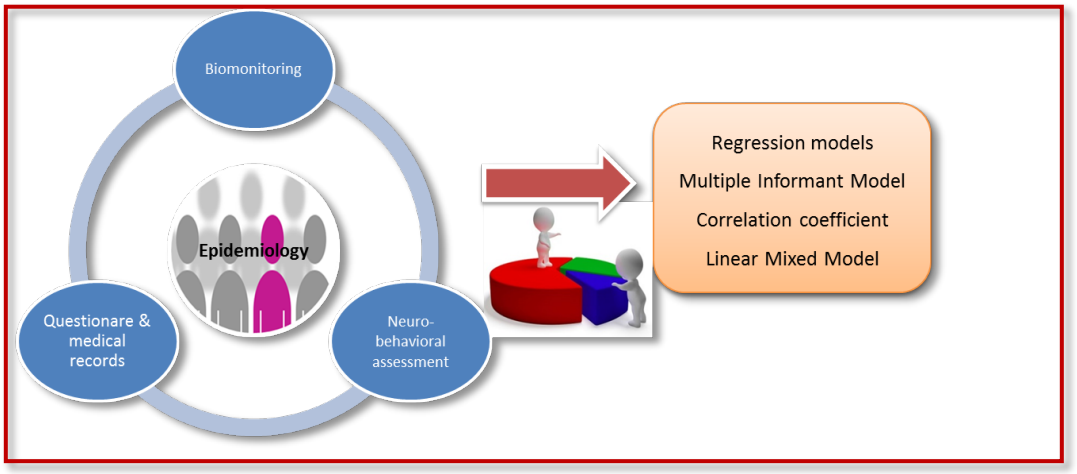

Figure 7: End-points and statistical tools for translating effect of chemicals to further assess risk.

3.4 Translational *In Silico*

With advancement in computational modeling, different *in silico* tools are available to assess the potential of chemicals to initiate adverse effects on the nervous system based on structure, physicochemical and biological properties. The examples include cheminformatics model like Quantitative Structure Activity Relationship (QSAR) and Structure Activity

Relationship (SAR) for predicting activity of compound based on structure. Also, toxicokinetics, toxicodynamic and toxicogenomic models like PBPK, IVIVE, QIVIVE, PD, SB and GSMN are available to determine concentration range relevant to realistic exposure and extrapolation of health risk for chemicals on human species from *in vitro* and other species (Coecke et al. 2006; Gartlon et al. 2006; Li et al. 2019).

Search was conducted with different keywords (Refer Table 1 in annexure) to see *in silico* tools for neurotoxicity but only 6 articles were found (Refer Table 5 in annexure). In four articles, QSAR with *in vitro* data was used to investigate the neurotoxicity (Rayne and Forest 2010; Stenberg et al. 2011; Holland et al. 2017; Pradeep et al. 2019). Stenberg et al. (2011) used *in vitro* screening coupled with QSAR to investigate the toxicity and classify PCBs in two groups based on structure activity relationship and toxicity. They used QSAR modeling to recognize the chemical properties, which can describe potency of non-dioxin like PCBs, and to predict the activities of different congeners of PCBs on nervous system. Holland et al. (2017) assessed the ryanodine receptor activity of 14 untested PCB congeners for evaluating QSAR predictability. *In vitro* assay was done to support the QSAR findings. In another article by Gascon et al (2013), epidemiology study was performed to validate the PBPK model. They conducted epidemiological study to evaluate neurotoxicity of persistent organic pollutant in Spanish children through breastfeeding exposure to validate the results from PBPK model for postnatal exposure assessment. In addition, Sharma et al. (2017) showed one example of integrated approach. Authors used PBPK/PD model to understand dynamics and steady state behavior of cellular response under perturbed condition. They developed PBPK/PD coupled transduction signalling linking miRNA- mRNA-BDNF-cell survivability to evaluate the PFOS induced neurotoxicity. Authors showed BDNF as a biomarker linking environmental exposure and neuronal adverse outcomes and taken *in vitro* data to assess neuronal cell survivability.

4. Integrated Approach for Translating data

Regulatory authorities across the world have made considerable progress towards developing pragmatic frameworks to deal with combined exposure for chemicals to assess risk. The National Research Council (NRC) of the National Academies of Science published a report of its vision of toxicity testing in the 21st century proposing the current toxicity testing paradigm that depends upon whole-animal tests to be replaced with a strategy based upon *in vitro* tests, *in silico* models and evaluations of toxicity at the human population level (Bushnell et al. 2010). Programs like Integrated testing strategy (ITS) and Integrated Approach to Testing and Assessment (IATA) focus on combining information from testing and non-testing methods and aims on prioritizing chemicals using hypothesis (Tollefsen et al. 2014; Vinken 2019). REACH guidelines accept *in silico/in chemico/in vitro* tools for skin sensitization prediction apart from *in vivo* and further propose integrated strategy (European Chemicals Agency 2006). This is strong proof that *in silico* methods can be used for toxicity prediction and are future of the toxicity testing.

Current *in silico* models are QSAR, toxicokinetics, pharmacodynamics, systems biology and genome scale models. QSAR are first-level models for predicting the activity of compound based on structure, which can be used for screening of thousands of chemicals. Rayne and

Forest 2010 and Pradeep et al. 2019 used QSAR to screen PCBs and further used *in vitro* data for validation. The second level are toxicokinetics models which take information on absorption, distribution, metabolism and excretion, therefore can be used to understand the concentration of particular chemical in different organs and also to extrapolate dose taking into account biological differences (Martínez et al. 2018; Sharma et al. 2018). Ramoju et al. 2017 developed PBPK model for estimating manganese (Mn) concentration in different parts of the human brain through different routes. They used exposure data from eight epidemiological studies and in conjunction with severity scores, a tissue dose-response relationship was developed. Croom et al. 2015 used *in vitro* data and PBPK modelling to perform IVIVE for Lindane neurotoxicity in humans. Third level is pharmcodynamic and systems biology model which can use data from toxicokinetics and experiments to further understand mechanistic approach and toxicity pathways at molecular and cellular level. Kolodkin et al 2019 applied ROS model with altered proteins and antioxidants levels for disease like Parkinson. Audouze et al. 2018 developed a network-based model by integrative systems biology approach to examine the developmental neurotoxicity by larvicidal pyriproxyfen. Last and advanced stage is toxicogenomics (genome scale model) for utilizing gene expression which is a step forward for proactive predictive, personalized and preventive toxicology (P4). GSMN models are still not available widely for brain-specific pathologies but with increased omics data, there lies an opportunity for computational investigation of brain networks (Sertbas and Ulgen 2018).

Objective of our manuscript was to propose an integrative translational framework where collected data and all information available can be coupled to predict the neuronal adverse effects. We propose a framework that incorporate the four levels of *in silico* model gene specific functions (GSMN), molecular & cellular mechanism (SB & PD), quantitative kinetic modeling (PBPK, QIVIVE) and QSAR along with experimental data for different organs and exposure scenario to understand neuronal homeostasis, plasticity, learning and neurotoxicity (Figure 8). Such approach can be used to study dynamical function of the brain at various levels and explore mechanistic pathways for both healthy and unhealthy nervous system. This can provide a clear picture about nervous system function and adverse outcome pathways (Geschwind and Konopka 2009). With lots of data available (*in vitro*, *in vivo*, epidemiology, genetic, transcriptomic, metabolomics, proteomic), *in silico* models can be validated and integrated for future hazard and risk assessment in Neurotoxicology (Figure 8).

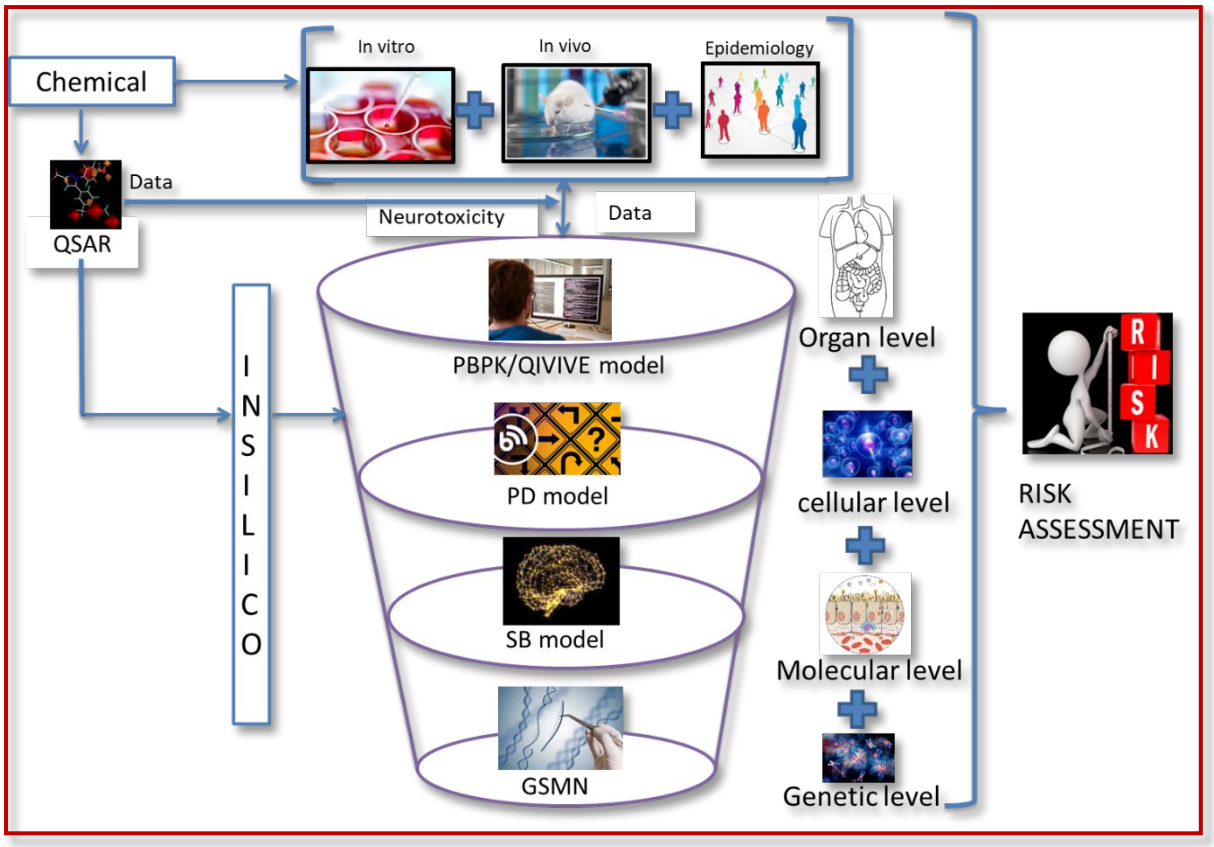

Figure 8: Integrated Translational approach for neuronal risk Assessment. This approach consists of utilizing data from *in vitro*, *in vivo* and epidemiology studies to validate *in silico* model. This model will further act as a tool for translation and prediction of risk to human species.

5. Discussion & Path Forward

Translating the data for chemicals through *in vitro*, *in vivo*, epidemiology and *in silico* studies is very critical for human risk assessment. This review was to broadly understand how authors are translating the data in neuroscience to predict the toxicity and discuss about the integrated approach for neurotoxicology. Research has yielded a lot of scientific literature on neurotoxicity, which contains information about various chemicals, mechanism by which chemicals affect neuronal development and toxicity pathways. *In vitro* studies are conducted from a long time and traditional cytotoxicity test is considered as early markers for neuronal damage. Other tests like oxidative stress, biomarkers and pathways are common in both animal model and *in vitro* studies. Various authors have indicated the involvement of oxidative stress (ROS) in a number of neurodegenerative states due to neurotoxic chemicals. ROS is widely known to damage biomacromolecules like lipid, proteins, sugar and polynucleotides and lead to the formation of secondary products which are as much damaging as the initial ROS (Sayre et al. 2008). Both *in vitro* and *in vivo* studies check the ROS formation as indicator for neurotoxicity. Different biomarkers have been studied in animals and *in vitro* models to observe physiological and morphological changes in neuronal cells and tissues resulting from chemical exposure (Roberts et al. 2015). This indicates that *in vivo* studies can be replaced by *in vitro* model for checking chemical-induced neurotoxicity.

Behavioral alterations from *in vivo* studies and mechanistic pathways from *in vitro* models demonstrate that neurotoxic chemicals may impair neural development, synaptic plasticity and brain organ growth. However, are these studies enough for human risk assessment taking into account these are indirect measures of neuronal damage and are dose-dependent? Are we extrapolating dose correctly from *in vivo* animal studies to humans based on anatomical and physiological differences? Such findings arise the awareness for necessity of human exposure assessment for further confirmation of the risk. Epidemiological studies are conducted for selected neurotoxicants. These studies have investigated the causal association between chemical exposure and neurobehavioral assessment through significant statistical tools. In epidemiology, most of the time exposure effect is assessed by observational data and there is a possibility that exposure-response association may be biased. Nevertheless, large sample size, multiple end-points and further investigation is needed to get the confidence for neuronal damages. Also, signs and symptoms in the human brain tend to be non-specific and variable upon environment and exposure (Grandjean et al. 1996).

The fact that a particular chemical is causing neurotoxicity is not enough for risk assessment. As we are being exposed to a number of chemicals every day, chronic toxicity evaluation for each chemical to set reference dose and regulatory limits like daily acceptable intake, occupational exposure limit and derived no-effect level using *in vivo* study is not feasible (Tsatsakis et al. 2016). Human real-life scenario for chemical exposure is totally different due to low dose exposure of chemicals for humans and mixture of chemicals (Tsatsakis et al. 2019). It is not feasible to conduct epidemiological studies for testing every chemical in human biological fluids. Recognizing the need for a paradigm shift of current approaches to risk assessment, regulatory guidelines have changed. Regulatory toxicology is shifting from decision making based on animal models to biological pathways, *in silico* and mechanistic approaches that lead to the understanding of cellular, molecular, organism and population-based dynamics. A key driver for this change is computational tools and the *in vitro* studies that are less time consuming and cost-efficient for toxicity prediction (NRC 2007).

Authors have used *in silico* tools like cheminformatics and toxicokinetics models with available experimental data to validate their results. QSAR has been widely used to screen chemicals and determine priority in which they need to be tested (Holland et al. 2017; Stenberg et al. 2011). With *in vitro* and *in vivo* data available for validation of these QSAR findings, the limitations of QSAR approach can be improved. PBPK model along with *in vitro* and epidemiological data was used for predicting effect of chemicals on the brain (Gascon et al. 2013; Sharma et al. 2017). Toxicodynamics and toxicogenomic models are rare for neurotoxicity for a selected group of chemicals. Very few articles for the brain *in silico* modeling raises obvious question. Are we utilizing the available data properly to assess the human nervous system risk? Is there a need for an integrated testing strategy or a framework for risk assessment? The answer is that *in silico*, models can be used as stepwise strategy for screening of chemicals. For instance, QSAR is used to identify the possible biological activities for thousands of chemicals and classify them based on structure and activity reducing the *in vivo* and *in vitro* tests (Chen et al. 2014). Toxicokinetics and toxicodynamics models, can be developed for identifying the target tissue dosimetry and dynamic response in the brain region following different exposure. For instance, the PBPK/PD model was developed for an

organophosphorus insecticide to quantitatively compare dosimetry and receptor response in rats and humans in blood components and the brain (Timchalk 2002). Toxicogenomics model or diagnosing toxicity based on altered gene expression connected to toxic outcomes (Burczynski 2000). Such strategy is in line with European Union recommendations like the new REACH system for chemical regulation (Chen et al. 2014; Liu et al. 2007). Such computational models can be developed to utilize different datasets (*in vitro*, *in vivo* and epidemiological) for validation and prediction of risk (Figure 8). *In vitro* data can provide mechanistic understanding and *in vivo* data for pathways and better understanding on neuronal damage. Epidemiology studies gives clear understanding about adverse effects in humans and different levels of *in silico* model can use above data in a fruitful manner to predict the neurotoxicity. The proposed integrated framework utilizing all available data in a constructive manner will help in screening thousands of chemicals with less effort and reduced cost. This integrated framework requires collaborative efforts from different fields to validate and evaluate the performance to assess human risk from neurotoxic chemicals.

However, some gaps exist in this framework like dose variation in animal, human and *in vitro* studies, limited data availability, species to species variation, extrapolation of results from adult to mother and children, human brain complexity, etc. Data availability for chemicals on different compartments of human brain region is one of the major challenges for developing and validating the *in silico* models need for an integrated approach. Another is a different dose of chemical used for *in vitro* and *in vivo* studies and short exposure time which do not reflect the real-life scenario for the toxicity of chemicals (Zhang et al. 2019). Lack of data for different age groups and complex brain anatomy and physiology also poses a major challenge for predicting neurotoxicity. However, risk from these gaps can be minimized by further utilizing other tools available in the integrated modeling in which output of experiment data can be used as initial input for *in silico* models. For instance, data obtained from *in vitro* can be used in the predictive chemistry approach (read across) for predicting the hazard of neurotoxic chemicals where endpoint data is lacking by linking to structurally similar chemicals (Roncaglioni et al. 2013). Quantitative *in vitro* to *in vivo* extrapolation can be used to accurately link concentration of chemicals that induce *in vitro* response to *in vivo* exposure levels (Yoon et al. 2012). Combination of *in silico* and *in vitro* parameters with PBPK and QIVIVE can be used to predict the human exposure conditions that would produce the toxic concentration inside brain regions (Yoon et al. 2012).

Nevertheless, further research on computational models and integrated framework will make the strategy more robust and strengthen the confidence for predicting toxicity. New scientific fields like integrated systems biology for toxicity assessment, combining data sets from different origin, elucidation of mechanisms and three dimensional *in silico* will provide novel possibilities to model neurotoxicity (Roncaglioni et al. 2013). Then, it may be possible to conduct human risk assessment of specific chemical classes with more clear and precise data. Therefore, the integrated translational framework must be tested with different set of chemicals for assessing its performance and detecting the gaps.

6. Conclusion

After reviewing all the endpoints, biomarkers and pathways used for translation through *in vitro*, *in vivo*, epidemiological and *in silico* studies, it provides a clear picture of extensive datasets available with us. In addition, it provides an idea of different tests being used for assessing the neurotoxicity of chemicals. The proposed integrated approach utilizes the available experimental dataset along with *in silico* model for translation of results to human neurotoxicity. To date, only minor fraction of chemicals available has been screened for neurotoxicity. Therefore, there is a crucial need for addressing the lack of neurotoxicity data and the proposed solution for this is to develop an integrated approach utilizing in silico models like QSAR and PBPK. This integrated approach can be used for screening and evaluating the toxicity of thousands of chemicals with unknown neurotoxic potential.

Acknowledgment

This study was financially supported by Marie Skłodowska-Curie “Neurosome Project” under the grant agreement No. 766251. V. Kumar has received funds from Health Department of Catalonia Government trough "Pla Estratègic de Recerca i Innovació en salut" (PERIS 2016-2020). This publication reflects only the authors' views. The Community and other funding organizations are not liable for any use made of the information contained therein.

References

Adcock IM, Chung KF, Auffray C, Pison C, Sterk PJ, Djukanovic R. 2010. An Integrative Systems Biology Approach to Understanding Pulmonary Diseases. Chest 137:1410–1416; doi:10.1378/chest.09-1850.

Adgent MA, Hoffman K, Goldman BD, Sjödin A, Daniels JL. 2014. Brominated flame retardants in breast milk and behavioural and cognitive development at 36 months. Paediatr Perinat Epidemiol 28:48–57; doi:10.1111/ppe.12078.

Al-Mousa F, Michelangeli F. 2012. Some commonly used brominated flame retardants cause ca 2+-atpase inhibition, beta-amyloid peptide release and apoptosis in sh-sy5y neuronal cells. PLoS One 7:3–10; doi:10.1371/journal.pone.0033059.

Al Aïn S, Perry RE, Nuñez B, Kayser K, Hochman C, Brehman E, et al. 2017. Neurobehavioral assessment of maternal odor in developing rat pups: implications for social buffering. Soc Neurosci 12:32–49; doi:10.1080/17470919.2016.1159605.

Asimakopoulos AG, Xue J, De Carvalho BP, Iyer A, Abualnaja KO, Yaghmoor SS, et al. 2016. Urinary biomarkers of exposure to 57 xenobiotics and its association with oxidative stress in a population in Jeddah, Saudi Arabia. Environ Res 150:573–581; doi:10.1016/j.envres.2015.11.029.

Audouze K, Taboureau O, Grandjean P. 2018. A systems biology approach to predictive developmental neurotoxicity of a larvicide used in the prevention of Zika virus transmission. Toxicol Appl Pharmacol 354:56–63; doi:10.1016/j.taap.2018.02.014.

Auffray C, Imbeaud S, Roux-Rouquié M, Hood L. 2003. From functional genomics to systems biology: Concepts and practices. Comptes Rendus - Biol 326:879–892; doi:10.1016/j.crvi.2003.09.033.

Bal-Price A, Crofton KM, Sachana M, Shafer TJ, Behl M, Forsby A, et al. 2015. Putative adverse outcome pathways relevant to neurotoxicity. Crit Rev Toxicol 45:83–91; doi:10.3109/10408444.2014.981331.

Bal-Price A, Lein PJ, Keil KP, Sethi S, Shafer T, Barenys M, et al. 2017. Developing and applying the adverse outcome pathway concept for understanding and predicting neurotoxicity. Neurotoxicology 59:240–255; doi:10.1016/j.neuro.2016.05.010.

Basha MR, Braddy NS, Zawia NH, Kodavanti PRS. 2006. Ontogenetic alterations in prototypical transcription factors in the rat cerebellum and hippocampus following perinatal exposure to a commercial PCB mixture. Neurotoxicology 27:118–124; doi:10.1016/j.neuro.2005.07.006.

Bellinger DC, Wright RO, Yolton K, Braun JM, Lanphear BP, Hauser R, et al. 2016. Prenatal phthalate, triclosan, and bisphenol A exposures and child visual-spatial abilities. Neurotoxicology 58:75–83; doi:10.1016/j.neuro.2016.11.009.

Benfenati E, Diaza RG, Cassano A, Pardoe S, Gini G, Mays C, et al. 2011. The acceptance of in silico models for REACH: Requirements, barriers, and perspectives. Chem Cent J 5:58; doi:10.1186/1752-153X-5-58.

Boberg J, Dybdahl M, Petersen A, Hass U, Svingen T, Vinggaard AM. 2019. A pragmatic

approach for human risk assessment of chemical mixtures. Curr Opin Toxicol 15:1–7; doi:10.1016/j.cotox.2018.11.004.

Boix J, Cauli O, Felipo V. 2010. Developmental exposure to polychlorinated biphenyls 52, 138 or 180 affects differentially learning or motor coordination in adult rats. mechanisms involved. Neuroscience 167:994–1003; doi:10.1016/j.neuroscience.2010.02.068.

Bornstein SR, Licinio J. 2011. Improving the efficacy of translational medicine by optimally integrating health care, academia and industry. Nat Med 17:1567–1569; doi:10.1038/nm.2583.

Bradner JM, Suragh TA, Caudle WM. 2013. Alterations to the circuitry of the frontal cortex following exposure to the polybrominated diphenyl ether mixture, DE-71. Toxicology 312:48–55; doi:10.1016/j.tox.2013.07.015.

Braun JM, Yolton K, Stacy SL, Erar B, Papandonatos GD, Bellinger DC, et al. 2017. Prenatal environmental chemical exposures and longitudinal patterns of child neurobehavior. Neurotoxicology 62:192–199; doi:10.1016/j.neuro.2017.07.027.

Breznan D, Karthikeyan S, Phaneuf M, Kumarathasan P, Cakmak S, Denison MS, et al. 2016. Development of an integrated approach for comparison of in vitro and in vivo responses to particulate matter. Part Fibre Toxicol 13:1–24; doi:10.1186/S12989-016-0152-6.

Bruch J, McCunney RJ, Levy L, Morfeld P, Muranko HJ, Chaudhuri I, et al. 2015. Translational toxicology in setting occupational exposure limits for dusts and hazard classification – a critical evaluation of a recent approach to translate dust overload findings from rats to humans. Part Fibre Toxicol 12; doi:10.1186/s12989-015-0079-3.

Burczynski ME. 2000. Toxicogenomics-Based Discrimination of Toxic Mechanism in HepG2 Human Hepatoma Cells. Toxicol Sci 58:399–415; doi:10.1093/toxsci/58.2.399.

Bushnell PJ, Kavlock RJ, Crofton KM, Weiss B, Rice DC. 2010. Behavioral toxicology in the 21st century: Challenges and opportunities for behavioral scientists. Summary of a symposium presented at the annual meeting of the Neurobehavioral Teratology Society, June, 2009. Neurotoxicol Teratol 32:313–328; doi:10.1016/j.ntt.2010.02.002.

Canzoniero LMT, Di Renzo G, Molinaro P, Montuori P, Mascolo L, Formisano L, et al. 2017. The neurotoxicant PCB-95 by increasing the neuronal transcriptional repressor REST down-regulates caspase-8 and increases Ripk1, Ripk3 and MLKL expression determining necroptotic neuronal death. Biochem Pharmacol 142:229–241; doi:10.1016/j.bcp.2017.06.135.

Carrasco MA, Hidalgo C. 2006. Calcium microdomains and gene expression in neurons and skeletal muscle cells. Cell Calcium 40:575–583; doi:10.1016/j.ceca.2006.08.021.

Chen A, Webster GM, Calafat AM, Lanphear BP, Zhang H, Dietrich KN, et al. 2016. Prenatal PBDE and PCB Exposures and Reading, Cognition, and Externalizing Behavior in Children. Environ Health Perspect 125:746–752; doi:10.1289/ehp478.

Chen H, Streifel KM, Singh V, Yang D, Mangini L, Wulff H, et al. 2017. BDE-47 and BDE-49 inhibit axonal growth in primary rat hippocampal neuron-glia co-cultures via ryanodine receptor-dependent mechanisms. Toxicol Sci 156:375–386; doi:10.1093/toxsci/kfw259.

Chen J, Li X, Li X, Chen D. 2018. The environmental pollutant BDE-209 regulates NO/cGMP signaling through activation of NMDA receptors in neurons. Environ Sci Pollut Res 25:3397–3407; doi:10.1007/s11356-017-0651-5.

Chen MH, Ha EH, Liao HF, Jeng SF, Su YN, Wen TW, et al. 2013. Perfluorinated compound levels in cord blood and neurodevelopment at 2 years of age. Epidemiology 24:800–808; doi:10.1097/EDE.0b013e3182a6dd46.

Chen T, Yang W, Li Y, Chen X, Xu S. 2011. Mono-(2-ethylhexyl) phthalate impairs neurodevelopment: Inhibition of proliferation and promotion of differentiation in PC12 cells. Toxicol Lett 201:34–41; doi:10.1016/j.toxlet.2010.12.002.

Chen Y, Cheng F, Sun L, Li W, Liu G, Tang Y. 2014. Computational models to predict endocrine-disrupting chemical binding with androgen or oestrogen receptors. Ecotoxicol Environ Saf 110:280–287; doi:10.1016/j.ecoenv.2014.08.026.

Chiu WA. 2017. Chemical risk assessment and translation to socio-economic assessments. Env/Wkp(2017)4; doi:10.1787/a930054b-en.

Cho JH, Kim AH, Lee S, Lee Y, Lee WJ, Chang SC, et al. 2018. Sensitive neurotoxicity assessment of bisphenol A using double immunocytochemistry of DCX and MAP2. Arch Pharm Res 41:1098–1107; doi:10.1007/s12272-018-1077-4.

Coecke S, Eskes C, Gartlon J, Kinsner A, Price A, Van Vliet E, et al. 2006. The value of alternative testing for neurotoxicity in the context of regulatory needs. Environ Toxicol Pharmacol 21:153–167; doi:10.1016/j.etap.2005.07.006.

Costa LG, Fattori V, Giordano G, Vitalone A. 2007. An in vitro approach to assess the toxicity of certain food contaminants: Methylmercury and polychlorinated biphenyls. Toxicology 237:65–76; doi:10.1016/j.tox.2007.05.003.

Costa LG, Tagliaferri S, Roqué PJ, Pellacani C. 2016. Role of glutamate receptors in tetrabrominated diphenyl ether (BDE-47) neurotoxicity in mouse cerebellar granule neurons. Toxicol Lett 241:159–166; doi:10.1016/j.toxlet.2015.11.026.

Cowell WJ, Sjödin A, Jones R, Wang Y, Wang S, Herbstman JB. 2018. Determinants of prenatal exposure to polybrominated diphenyl ethers (PBDEs) among urban, minority infants born between 1998 and 2006. Environ Pollut 233:774–781; doi:10.1016/j.envpol.2017.10.068.

Craciunoiu O, Holsti L. 2017. A Systematic Review of the Predictive Validity of Neurobehavioral Assessments During the Preterm Period. Phys Occup Ther Pediatr 37:292–307; doi:10.1080/01942638.2016.1185501.

Croom EL, Shafer TJ, Evans M V., Mundy WR, Eklund CR, Johnstone AFM, et al. 2015. Improving in vitro to in vivo extrapolation by incorporating toxicokinetic measurements: A case study of lindane-induced neurotoxicity. Toxicol Appl Pharmacol 283:9–19; doi:10.1016/j.taap.2014.11.006.

Dingemans MML, Heusinkveld HJ, De Groot A, Bergman Å, Van den Berg M, Westerink RHS. 2009. Hexabromocyclododecane inhibits depolarization-induced increase in intracellular calcium levels and neurotransmitter release in PC12 cells. Toxicol Sci 107:490–497; doi:10.1093/toxsci/kfn249.

Dingemans MML, Ramakers GMJ, Gardoni F, van Kleef RGDM, Bergman Å, Di Luca M, et al. 2007. Neonatal exposure to brominated flame retardant BDE-47 reduces long-term potentiation and postsynaptic protein levels in mouse hippocampus. Environ Health Perspect 115:865–870; doi:10.1289/ehp.9860.

Doherty BT, Engel SM, Buckley JP, Silva MJ, Calafat AM, Wolff MS. 2017. Prenatal phthalate biomarker concentrations and performance on the Bayley Scales of Infant Development-II in a population of young urban children. Environ Res 152:51–58; doi:10.1016/j.envres.2016.09.021.

Drolet BC, Lorenzi NM. 2011. Translational research: Understanding the continuum from bench to bedside. Transl Res 157:1–5; doi:10.1016/j.trsl.2010.10.002.

Eeles AL, Olsen JE, Walsh JM, McInnes EK, Molesworth CML, Cheong JLY, et al. 2017. Reliability of Neurobehavioral Assessments from Birth to Term Equivalent Age in Preterm and Term Born Infants. Phys Occup Ther Pediatr 37:108–119; doi:10.3109/01942638.2015.1135845.

European Chemicals Agency. 2006. *Guidance on information requirements and chemical safety assessment Chapter R.16: Environmental Exposure Estimation*.

Fan CY, Besas J, Kodavanti PRS. 2010. Changes in mitogen-activated protein kinase in cerebellar granule neurons by polybrominated diphenyl ethers and polychlorinated biphenyls. Toxicol Appl Pharmacol 245:1–8; doi:10.1016/j.taap.2010.02.008.

Fanelli R, De Paola M, Brunelli L, Felipo V, Airoldi L, Pastorelli R, et al. 2012. Insight into the neuroproteomics effects of the food-contaminant non-dioxin like polychlorinated biphenyls. J Proteomics 75:2417–2430; doi:10.1016/j.jprot.2012.02.023.

Fonnum F, Mariussen E. 2009. Mechanisms involved in the neurotoxic effects of environmental toxicants such as polychlorinated biphenyls and brominated flame retardants. J Neurochem 111:1327–1347; doi:10.1111/j.1471-4159.2009.06427.x.

Fritsche E, Grandjean P, Crofton KM, Aschner M, Goldberg A, Heinonen T, et al. 2018. Consensus statement on the need for innovation, transition and implementation of developmental neurotoxicity (DNT) testing for regulatory purposes. Toxicol Appl Pharmacol 354:3–6; doi:10.1016/j.taap.2018.02.004.

Gartlon J, Kinsner A, Bal-Price A, Coecke S, Clothier RH. 2006. Evaluation of a proposed in vitro test strategy using neuronal and non-neuronal cell systems for detecting neurotoxicity. Toxicol Vitr 20:1569–1581; doi:10.1016/j.tiv.2006.07.009.

Gascon M, Verner MA, Guxens M, Grimalt JO, Forns J, Ibarluzea J, et al. 2013. Evaluating the neurotoxic effects of lactational exposure to persistent organic pollutants (POPs) in Spanish children. Neurotoxicology 34:9–15; doi:10.1016/j.neuro.2012.10.006.

Gaum PM, Gube M, Schettgen T, Putschögl FM, Kraus T, Fimm B, et al. 2017. Polychlorinated biphenyls and depression: Cross-sectional and longitudinal investigation of a dopamine-related Neurochemical path in the German HELPcB surveillance program. Environ Heal A Glob Access Sci Source 16:106; doi:10.1186/s12940-017-0316-3.

Gee JR, Moser VC, McDanie KL, Herr DW. 2011. Neurochemical changes following a single dose of polybrominated diphenyl ether 47 in mice. Drug Chem Toxicol 34:213–219;

doi:10.3109/01480545.2010.536768.

Geschwind DH, Konopka G. 2009. Neuroscience in the era of functional genomics and systems biology. Nature 461:908–915; doi:10.1038/nature08537.

Giordano G, Kavanagh TJ, Costa LG. 2009. Mouse cerebellar astrocytes protect cerebellar granule neurons against toxicity of the polybrominated diphenyl ether (PBDE) mixture DE-71. Neurotoxicology 30:326–329; doi:10.1016/j.neuro.2008.12.009.

Giordano G, Kavanagh TJ, Costa LG. 2008. Neurotoxicity of a polybrominated diphenyl ether mixture (DE-71) in mouse neurons and astrocytes is modulated by intracellular glutathione levels. Toxicol Appl Pharmacol 232:161–168; doi:10.1016/j.taap.2008.06.018.

Goldberg A, Schmuck G, Solecki R, Heinonen T, Fritsche E, Grandjean P, et al. 2018. Consensus statement on the need for innovation, transition and implementation of developmental neurotoxicity (DNT) testing for regulatory purposes. Toxicol Appl Pharmacol 354:3–6; doi:10.1016/j.taap.2018.02.004.

Götz C, Scanlan TS, Gassmann K, Fritsche E, Abel J, Moors M, et al. 2009. Polybrominated Diphenyl Ethers Induce Developmental Neurotoxicity in a Human in Vitro Model: Evidence for Endocrine Disruption . Environ Health Perspect 118:572–578; doi:10.1289/ehp.0901435.

Goudarzi H, Nakajima S, Ikeno T, Sasaki S, Kobayashi S, Miyashita C, et al. 2016. Prenatal exposure to perfluorinated chemicals and neurodevelopment in early infancy: The Hokkaido Study. Sci Total Environ 541:1002–1010; doi:10.1016/j.scitotenv.2015.10.017.

Grandjean P, Landrigan P. 2006. Developmental neurotoxicity of industrial chemicals. Lancet 368:2167–2178; doi:10.1016/S0140-6736(06)69665-7.

Grandjean P, White RF, Weihe P. 1996. Neurobehavioral Epidemiology: Application in Risk Assessment. Environ Health Perspect 104:397; doi:10.2307/3432660.

Hartung T, Daston G. 2009. Are in vitro tests suitable for regulatory use? Toxicol Sci 111:233–237; doi:10.1093/toxsci/kfp149.

Hendriks HS, Meijer M, Muilwijk M, Van Den Berg M, Westerink RHS. 2014. A comparison of the in vitro cyto- and neurotoxicity of brominated and halogen-free flame retardants: Prioritization in search for safe(r) alternatives. Arch Toxicol 88:857–869; doi:10.1007/s00204-013-1187-1.

Hendriks HS, Van kleef RGDM, Van den berg M, Westerink RHS. 2012. Multiple novel modes of action involved in the in vitro neurotoxic effects of tetrabromobisphenol-A. Toxicol Sci 128:235–246; doi:10.1093/toxsci/kfs136.

Hirsch C, Striegl B, Mathes S, Adlhart C, Edelmann M, Bono E, et al. 2017. Multiparameter toxicity assessment of novel DOPO-derived organophosphorus flame retardants. Arch Toxicol 91:407–425; doi:10.1007/s00204-016-1680-4.

Holland EB, Feng W, Zheng J, Dong Y, Li X, Lehmler HJ, et al. 2017. An extended structure-Activity relationship of nondioxin-like PCBs evaluates and supports modeling predictions and identifies picomolar potency of PCB 202 towards ryanodine receptors. Toxicol Sci

155:170–181; doi:10.1093/toxsci/kfw189.

Huang R, Xia M, Sakamuru S, Zhao J, Shahane SA, Attene-Ramos M, et al. 2016. Modelling the Tox21 10 K chemical profiles for in vivo toxicity prediction and mechanism characterization. Nat Commun 7:1–10; doi:10.1038/ncomms10425.

Hughes C, Waters M, Allen D, Obasanjo I. 2013. Translational toxicology: a developmental focus for integrated research strategies. BMC Pharmacol Toxicol 14:1; doi:10.1186/2050-6511-14-51.

Ishido M, Suzuki J. 2014. Classification of phthalates based on an in vitro neurosphere assay using rat mesencephalic neural stem cells. J Toxicol Sci 39:25–32; doi:10.2131/jts.39.25.

Jiang C, Zhang S, Liu H, Zeng Q, Xia T, Chen Y, et al. 2012. The role of the IRE1 pathway in PBDE-47-induced toxicity in human neuroblastoma SH-SY5Y cells in vitro. Toxicol Lett 211:325–333; doi:10.1016/j.toxlet.2012.04.009.

Kerb R, Igel S, Erhart W, Brosch M, Lippert J, Schuppert A, et al. 2017. Translational learning from clinical studies predicts drug pharmacokinetics across patient populations. npj Syst Biol Appl 3:1–10; doi:10.1038/s41540-017-0012-5.

Kim KH, Pessah IN. 2011. Perinatal exposure to environmental polychlorinated biphenyls sensitizes hippocampus to excitotoxicity ex vivo. Neurotoxicology 32:981–985; doi:10.1016/j.neuro.2011.04.004.

Langeveld WT, Meijer M, Westerink RHS. 2012. Differential effects of 20 non-dioxin-like PCBs on basal and depolarization-evoked intracellular calcium levels in PC12 cells. Toxicol Sci 126:487–496; doi:10.1093/toxsci/kfr346.

Laroche C, Aggarwal M, Bender H, Benndorf P, Birk B, Crozier J, et al. 2018. Finding synergies for 3Rs – Toxicokinetics and read-across: Report from an EPAA partners' Forum. Regul Toxicol Pharmacol 99:5–21; doi:10.1016/j.yrtph.2018.08.006.

Le HH, Carlson EM, Chua JP, Belcher SM. 2008. Bisphenol A is released from polycarbonate drinking bottles and mimics the neurotoxic actions of estrogen in developing cerebellar neurons. Toxicol Lett 176:149–156; doi:10.1016/j.toxlet.2007.11.001.

Lee I, Leonards PEG, Koolen LAE, Viberg H, Hendriks HS, Westerink RHS, et al. 2014. Effects of neonatal exposure to the flame retardant tetrabromobisphenol-A, aluminum diethylphosphinate or zinc stannate on long-term potentiation and synaptic protein levels in mice. Arch Toxicol 89:2345–2354; doi:10.1007/s00204-014-1366-8.

Lei ENY, Yau MS, Yeung CC, Murphy MB, Wong KL, Lam MHW. 2017. Profiling of Selected Functional Metabolites in the Central Nervous System of Marine Medaka (Oryzias melastigma) for Environmental Neurotoxicological Assessments. Arch Environ Contam Toxicol 72:269–280; doi:10.1007/s00244-016-0342-0.

Lesiak A, Zhu M, Chen H, Appleyard SM, Impey S, Lein PJ, et al. 2014. The Environmental Neurotoxicant PCB 95 Promotes Synaptogenesis via Ryanodine Receptor-Dependent miR132 Upregulation. J Neurosci 34:717–725; doi:10.1523/JNEUROSCI.2884-13.2014.

Li J, Settivari R, LeBaron MJ, Marty MS. 2019. An industry perspective: A streamlined screening strategy using alternative models for chemical assessment of developmental

neurotoxicity. Neurotoxicology 73:17–30; doi:10.1016/j.neuro.2019.02.010.

Li R, Zhou P, Guo Y, Zhou B. 2017. The involvement of autophagy and cytoskeletal regulation in TDCIPP-induced SH-SY5Y cell differentiation. Neurotoxicology 62:14–23; doi:10.1016/j.neuro.2017.05.002.

Lien GW, Huang CC, Shiu JS, Chen MH, Hsieh WS, Guo YL, et al. 2016. Perfluoroalkyl substances in cord blood and attention deficit/hyperactivity disorder symptoms in seven-year-old children. Chemosphere 156:118–127; doi:10.1016/j.chemosphere.2016.04.102.

Linne M-L. 2018. Neuroinformatics and Computational Modelling as Complementary Tools for Neurotoxicology Studies. Basic Clin Pharmacol Toxicol 123:56–61; doi:10.1111/bcpt.13075.

Liu H, Papa E, Walker JD, Gramatica P. 2007. In silico screening of estrogen-like chemicals based on different nonlinear classification models. J Mol Graph Model 26:135–144; doi:10.1016/j.jmgm.2007.01.003.

Liu QS, Liu N, Sun Z, Zhou Q, Jiang G. 2018. Intranasal administration of tetrabromobisphenol A bis(2-hydroxyethyl ether) induces neurobehavioral changes in neonatal Sprague Dawley rats. J Environ Sci (China) 63:76–86; doi:10.1016/j.jes.2017.05.036.

Liu X, Jin Y, Liu W, Wang F, Hao S. 2011. Possible mechanism of perfluorooctane sulfonate and perfluorooctanoate on the release of calcium ion from calcium stores in primary cultures of rat hippocampal neurons. Toxicol Vitr 25:1294–1301; doi:10.1016/j.tiv.2011.04.016.

Ma P, Liu X, Wu J, Yan B, Zhang Y, Lu Y, et al. 2015. Cognitive deficits and anxiety induced by diisononyl phthalate in mice and the neuroprotective effects of melatonin. Sci Rep 5:1–14; doi:10.1038/srep14676.

Maffini M V., Neltner TG. 2015. Brain drain: The cost of neglected responsibilities in evaluating cumulative effects of environmental chemicals. J Epidemiol Community Health 69:496–499; doi:10.1136/jech-2014-203980.

Malkiewicz K, Mohammed R, Folkesson R, Winblad B, Szutowski M, Benedikz E. 2006. Polychlorinated biphenyls alter expression of α-synuclein, synaptophysin and parkin in the rat brain. Toxicol Lett 161:152–158; doi:10.1016/j.toxlet.2005.08.010.

Martínez MA, Rovira J, Prasad Sharma R, Nadal M, Schuhmacher M, Kumar V. 2018. Comparing dietary and non-dietary source contribution of BPA and DEHP to prenatal exposure: A Catalonia (Spain) case study. Environ Res 166:25–34; doi:10.1016/j.envres.2018.05.008.

Mochida S. 2000. Protein–protein interactions in neurotransmitter release. Neurosci Res 36:175–182; doi:10.1016/S0168-0102(99)00128-5.

Morris E, Wood A, DeWitt JC, Franklin JN, Bryan I, Hu Q. 2012. Does developmental exposure to perflurooctanoic acid (PFOA) induce immunopathologies commonly observed in neurodevelopmental disorders? Neurotoxicology 33:1491–1498; doi:10.1016/j.neuro.2012.10.016.

Moser VC, Phillips PM, Hedge JM, McDaniel KL. 2015. Neurotoxicological and thyroid evaluations of rats developmentally exposed to tris(1,3-dichloro-2-propyl)phosphate

(TDCIPP) and tris(2-chloro-2-ethyl)phosphate (TCEP). Neurotoxicol Teratol 52:236–247; doi:10.1016/j.ntt.2015.08.004.

Mumtaz MM, Ray M, Crowell SR, Keys D, Fisher J, Ruiz P. 2012. Translational research to develop a human pbpk models tool kit-volatile organic compounds (VOCS). J Toxicol Environ Heal - Part A Curr Issues 75:6–24; doi:10.1080/15287394.2012.625546.

Park HY, Hertz-Picciotto I, Sovcikova E, Kocan A, Drobna B, Trnovec T. 2010. Neurodevelopmental toxicity of prenatal polychlorinated biphenyls (PCBs) by chemical structure and activity: A birth cohort study. Environ Heal A Glob Access Sci Source 9:1–13; doi:10.1186/1476-069X-9-51.

Pham-Lake C, Aronoff EB, Camp CR, Vester A, Peters SJ, Caudle WM. 2017. Impairment in the mesohippocampal dopamine circuit following exposure to the brominated flame retardant, HBCDD. Environ Toxicol Pharmacol 50:167–174; doi:10.1016/j.etap.2017.02.003.

Philips EM, Jaddoe VWV, Asimakopoulos AG, Kannan K, Steegers EAP, Santos S, et al. 2018. Bisphenol and phthalate concentrations and its determinants among pregnant women in a population-based cohort in the Netherlands, 2004–5. Environ Res 161:562–572; doi:10.1016/j.envres.2017.11.051.

Phillips JA, Bogdanffy MS. 2017. Editorial overview: Translational biomarker concepts and practices for toxicological assessment. Curr Opin Toxicol 4:i–iii; doi:10.1016/j.cotox.2017.08.003.

Pradeep P, Carlson LM, Judson R, Lehmann GM, Patlewicz G. 2019. Integrating data gap filling techniques: A case study predicting TEFs for neurotoxicity TEQs to facilitate the hazard assessment of polychlorinated biphenyls. Regul Toxicol Pharmacol 101:12–23; doi:10.1016/j.yrtph.2018.10.013.

Ramoju SP, Mattison DR, Milton B, McGough D, Shilnikova N, Clewell HJ, et al. 2017. The application of PBPK models in estimating human brain tissue manganese concentrations. Neurotoxicology 58:226–237; doi:10.1016/j.neuro.2016.12.001.

Rayne S, Forest K. 2010. Quantitative structure-activity relationship (QSAR) studies for predicting activation of the ryanodine receptor type 1 channel complex (RyR1) by polychlorinated biphenyl (PCB) congeners. J Environ Sci Heal - Part A Toxic/Hazardous Subst Environ Eng 45:355–362; doi:10.1080/10934520903467980.

Reistad T, Fonnum F, Mariussen E. 2006. Neurotoxicity of the pentabrominated diphenyl ether mixture, DE-71, and hexabromocyclododecane (HBCD) in rat cerebellar granule cells in vitro. Arch Toxicol 80:785–796; doi:10.1007/s00204-006-0099-8.

Rice D, Barone S. 2000. Critical periods of vulnerability for the developing nervous system: Evidence from humans and animal models. Environ Health Perspect 108:511–533; doi:10.1289/ehp.00108s3511.

Roberts RA, Aschner M, Calligaro D, Guilarte TR, Hanig JP, Herr DW, et al. 2015. Translational biomarkers of neurotoxicity: A health and environmental sciences institute perspective on the way forward. Toxicol Sci 148:332–340; doi:10.1093/toxsci/kfv188.

Rodrigo R, Felipo V, Montoliu C, Piedrafita B, Llansola M. 2009. Polychlorinated Biphenyls PCB

153 and PCB 126 Impair the Glutamate–Nitric Oxide–cGMP Pathway in Cerebellar Neurons in Culture by Different Mechanisms. Neurotox Res 16:97–105; doi:10.1007/s12640-009-9055-8.

Roncaglioni A, Toropov AA, Toropova AP, Benfenati E. 2013. In silico methods to predict drug toxicity. Curr Opin Pharmacol 13:802–806; doi:10.1016/j.coph.2013.06.001.

Ruan D-Y, Wang M, Chen L, Tao Y, Xing T, Chen J. 2009. Effects of Decabrominated Diphenyl Ether (PBDE 209) Exposure at Different Developmental Periods on Synaptic Plasticity in the Dentate Gyrus of Adult Rats In Vivo. Toxicol Sci 110:401–410; doi:10.1093/toxsci/kfp114.

Sayre LM, Perry G, Smith MA. 2008. Oxidative stress and neurotoxicity. Chem Res Toxicol 21:172–188; doi:10.1021/tx700210j.

Sedman E, Rossetti L, Ogden J, Trusheim M, Gross D, Osterwalder B, et al. 2016. Translational Medicine Guide transforms drug development processes: the recent Merck experience. Drug Discov Today 21:517–526; doi:10.1016/j.drudis.2016.01.003.

Sertbas M, Ulgen KO. 2018. Unlocking human brain metabolism by genome-scale and multiomics metabolic models: Relevance for neurology research, health, and disease. Omi A J Integr Biol 22:455–467; doi:10.1089/omi.2018.0088.

Sethi S, Keil KP, Lein PJ. 2018. 3,3’-Dichlorobiphenyl (PCB 11) promotes dendritic arborization in primary rat cortical neurons via a CREB-dependent mechanism. Arch Toxicol 92:3337–3345; doi:10.1007/s00204-018-2307-8.

Sethi S, Keil KP, Lein PJ. 2017. Species and Sex Differences in the Morphogenic Response of Primary Rodent Neurons to 3,3’-Dichlorobiphenyl (PCB 11). Toxics 6:4; doi:10.3390/toxics6010004.

Shah R, Pico AR, Freedman JE. 2016. Translational Epidemiology: Entering a Brave New World of Team Science. Circ Res 119:1060–1062; doi:10.1161/CIRCRESAHA.116.309881.

Sharma RP, Schuhmacher M, Kumar V. 2017. Developing integrated PBPK/PD coupled mechanistic pathway model (miRNA-BDNF): An approach towards system toxicology. Toxicol Lett 280:79–91; doi:10.1016/j.toxlet.2017.08.003.

Sharma RP, Schuhmacher M, Kumar V. 2018. The development of a pregnancy PBPK Model for Bisphenol A and its evaluation with the available biomonitoring data. Sci Total Environ 624:55–68; doi:10.1016/j.scitotenv.2017.12.023.

Shin MY, Lee S, Kim HJ, Lee JJ, Choi G, Choi S, et al. 2016. Polybrominated diphenyl ethers in maternal serum, breast milk, umbilical cord serum, and house dust in a South Korean birth panel of mother-neonate pairs. Int J Environ Res Public Health 13:767; doi:10.3390/ijerph13080767.

Shrestha S, Bloom MS, Yucel R, Seegal RF, Rej R, McCaffrey RJ, et al. 2017. Perfluoroalkyl substances, thyroid hormones, and neuropsychological status in older adults. Int J Hyg Environ Health 220:679–685; doi:10.1016/j.ijheh.2016.12.013.

Silbereis JC, Pochareddy S, Zhu Y, Li M, Sestan N. 2016. The Cellular and Molecular Landscapes of the Developing Human Central Nervous System. Neuron 89:248;

doi:10.1016/j.neuron.2015.12.008.

Sirenko O, Parham F, Dea S, Sodhi N, Biesmans S, Mora-Castilla S, et al. 2019. Functional and Mechanistic Neurotoxicity Profiling Using Human iPSC-Derived Neural 3D Cultures. Toxicol Sci 167:58–76; doi:10.1093/toxsci/kfy218.

Slotkin TA, MacKillop EA, Meinick RL, Thayer KA, Seidler FJ. 2008. Developmental neurotoxicity of perfluorinated chemicals modeled in vitro. Environ Health Perspect 116:716–722; doi:10.1289/ehp.11253.

Slotkin TA, Skavicus S, Stapleton HM, Seidler FJ. 2017. Brominated and organophosphate flame retardants target different neurodevelopmental stages, characterized with embryonic neural stem cells and neuronotypic PC12 cells. Toxicology 390:32–42; doi:10.1016/j.tox.2017.08.009.

Stenberg M, Hamers T, Machala M, Fonnum F, Stenius U, Lauy AA, et al. 2011. Multivariate toxicity profiles and QSAR modeling of non-dioxin-like PCBs - An investigation of in vitro screening data from ultra-pure congeners. Chemosphere 85:1423–1429; doi:10.1016/j.chemosphere.2011.08.019.

Szychowski KA, Wójtowicz AK. 2016. TBBPA causes neurotoxic and the apoptotic responses in cultured mouse hippocampal neurons in vitro. Pharmacol Reports 68:20–26; doi:10.1016/j.pharep.2015.06.005.

Timchalk C. 2002. A Physiologically Based Pharmacokinetic and Pharmacodynamic (PBPK/PD) Model for the Organophosphate Insecticide Chlorpyrifos in Rats and Humans. Toxicol Sci 66:34–53; doi:10.1093/toxsci/66.1.34.

Tofighi R, Wan Ibrahim WN, Rebellato P, Andersson PL, Uhlén P, Ceccatelli S. 2011. Non-dioxin-like polychlorinated biphenyls interfere with neuronal differentiation of embryonic neural stem cells. Toxicol Sci 124:192–201; doi:10.1093/toxsci/kfr221.

Tollefsen KE, Scholz S, Cronin MT, Edwards SW, de Knecht J, Crofton K, et al. 2014. Applying Adverse Outcome Pathways (AOPs) to support Integrated Approaches to Testing and Assessment (IATA). Regul Toxicol Pharmacol 70:629–640; doi:10.1016/j.yrtph.2014.09.009.

Tsatsakis A, Goumenou M, Liesivuori J, Dekant W, Hernández AF. 2019. Toxicology for real-life risk simulation – Editorial preface to this special issue. Toxicol Lett 309:33–34; doi:10.1016/j.toxlet.2018.12.003.

Tsatsakis AM, Docea AO, Tsitsimpikou C. 2016. New challenges in risk assessment of chemicals when simulating real exposure scenarios; simultaneous multi-chemicals' low dose exposure. Food Chem Toxicol 96:174–176; doi:10.1016/j.fct.2016.08.011.

Tsatsakis AM, Kouretas D, Tzatzarakis MN, Stivaktakis P, Tsarouhas K, Golokhvast KS, et al. 2017. Simulating real-life exposures to uncover possible risks to human health: A proposed consensus for a novel methodological approach. Hum Exp Toxicol 36:554–564; doi:10.1177/0960327116681652.

Tseng IL, Yang YF, Yu CW, Li WH, Liao VHC. 2013. Phthalates induce neurotoxicity affecting locomotor and thermotactic behaviors and AFD neurons through oxidative stress in Caenorhabditis elegans. PLoS One 8; doi:10.1371/journal.pone.0082657.

van der Merwe J, van der Veeken L, Ferraris S, Gsell W, Himmelreich U, Toelen J, et al. 2019. Early neuropathological and neurobehavioral consequences of preterm birth in a rabbit model. Sci Rep 9:1–11; doi:10.1038/s41598-019-39922-8.

Vinceti M, Violi F, Tzatzarakis M, Mandrioli J, Malagoli C, Hatch EE, et al. 2017. Pesticides, polychlorinated biphenyls and polycyclic aromatic hydrocarbons in cerebrospinal fluid of amyotrophic lateral sclerosis patients: a case-control study. Environ Res 155:261–267; doi:10.1016/j.envres.2017.02.025.

Vinken M. 2019. Omics-based input and output in the development and use of adverse outcome pathways. Curr Opin Toxicol 18:8–12; doi:10.1016/j.cotox.2019.02.006.

Vitalone A, Catalani A, Chiodi V, Cinque C, Fattori V, Goldoni M, et al. 2008. Neurobehavioral assessment of rats exposed to low doses of PCB126 and methyl mercury during development. Environ Toxicol Pharmacol 25:103–113; doi:10.1016/j.etap.2007.09.006.

Vodovotz Y, Csete M, Bartels J, Chang S, An G. 2008. Translational systems biology of inflammation. PLoS Comput Biol 4; doi:10.1371/journal.pcbi.1000014.

Vuong AM, Yolton K, Wang Z, Xie C, Webster GM, Ye X, et al. 2018. Childhood perfluoroalkyl substance exposure and executive function in children at 8 years. Environ Int 119:212–219; doi:10.1016/j.envint.2018.06.028.

Wang Q, Lai NLS, Wang X, Guo Y, Lam PKS, Lam JCW, et al. 2015. Bioconcentration and transfer of the organophorous flame retardant 1,3-dichloro-2-propyl phosphate causes thyroid endocrine disruption and developmental neurotoxicity in zebrafish larvae. Environ Sci Technol 49:5123–5132; doi:10.1021/acs.est.5b00558.

Warita K, Mitsuhashi T, Ohta K ichi, Suzuki S, Hoshi N, Miki T, et al. 2013. In vitro evaluation of gene expression changes for gonadotropin-releasing hormone 1, brain-derived neurotrophic factor and neurotrophic tyrosine kinase, receptor, type 2, in response to bisphenol A treatment. Congenit Anom (Kyoto) 53:42–45; doi:10.1111/j.1741-4520.2012.00381.x.

Weiss B. 2000. Vulnerability of children and the developing brain to neurotoxic hazards. Environ Health Perspect 108:375–381; doi:10.2307/3454523.

Westerink R. 2008. Targeting Exocytosis: Ins and Outs of the Modulation of Quantal Dopamine Release. CNS Neurol Disord - Drug Targets 5:57–77; doi:10.2174/187152706784111597.

Wilson MS, Graham JR, Ball AJ. 2014. Multiparametric High Content Analysis for assessment of neurotoxicity in differentiated neuronal cell lines and human embryonic stem cell-derived neurons. Neurotoxicology 42:33–48; doi:10.1016/j.neuro.2014.03.013.

Wójtowicz AK, Sitarz-Głownia AM, Szczęsna M, Szychowski KA. 2019. The Action of Di-(2-Ethylhexyl) Phthalate (DEHP) in Mouse Cerebral Cells Involves an Impairment in Aryl Hydrocarbon Receptor (AhR) Signaling. Neurotox Res 35:183–195; doi:10.1007/s12640-018-9946-7.

Wu X, Majumder A, Webb R, Stice SL. 2016. High content imaging quantification of multiple in vitro human neurogenesis events after neurotoxin exposure. BMC Pharmacol Toxicol 17:1–15; doi:10.1186/s40360-016-0107-4.

Wu Y, Li K, Zuo H, Yuan Y, Sun Y, Yang X. 2014. Primary neuronal-astrocytic co-culture platform for neurotoxicity assessment of di-(2-ethylhexyl) phthalate. J Environ Sci (China) 26:1145–1153; doi:10.1016/S1001-0742(13)60504-5.

Xu X, Lu Y, Zhang G, Chen L, Tian D, Shen X, et al. 2014. Bisphenol A promotes dendritic morphogenesis of hippocampal neurons through estrogen receptor-mediated ERK1/2 signal pathway. Chemosphere 96:129–137; doi:10.1016/j.chemosphere.2013.09.063.

Yang D, Lein PJ. 2010. Polychlorinated biphenyls increase apoptosis in the developing rat brain. Curr Neurobiol 1: 70–76.

Yang W, Zhao F, Fang Y, Li L, Li C, Ta N. 2018. 1H-nuclear magnetic resonance metabolomics revealing the intrinsic relationships between neurochemical alterations and neurobehavioral and neuropathological abnormalities in rats exposed to tris(2-chloroethyl)phosphate. Chemosphere 200:649–659; doi:10.1016/j.chemosphere.2018.02.056.

Yin N, Liang S, Liang S, Yang R, Hu B, Qin Z, et al. 2018a. TBBPA and Its Alternatives Disturb the Early Stages of Neural Development by Interfering with the NOTCH and WNT Pathways. Environ Sci Technol 52:5459–5468; doi:10.1021/acs.est.8b00414.

Yin N, Yang R, Liang S, Liang S, Hu B, Ruan T, et al. 2018b. Evaluation of the early developmental neural toxicity of F-53B, as compared to PFOS, with an in vitro mouse stem cell differentiation model. Chemosphere 204:109–118; doi:10.1016/j.chemosphere.2018.04.011.

Yin N, Yao X, Qin Z, Wang YL, Faiola F. 2015. Assessment of Bisphenol A (BPA) neurotoxicity in vitro with mouse embryonic stem cells. J Environ Sci (China) 36:181–187; doi:10.1016/j.jes.2015.06.004.

Yoon M, Campbell JL, Andersen ME, Clewell HJ. 2012. Quantitative in vitro to in vivo extrapolation of cell-based toxicity assay results. Crit Rev Toxicol 42:633–652; doi:10.3109/10408444.2012.692115.

Yoot ML, Min JS, Jae WL, Yong KL, Tae MK, Nam SY, et al. 2007. Estrogen receptor independent neurotoxic mechanism of bisphenol A, an environmental estrogen. J Vet Sci 8: 27–38.

Zhang D, Zhou S, Lu X, Jin M, Zhang Y, Zhao H. 2018. Neurological responses of embryo-larval zebrafish to short-term sediment exposure to decabromodiphenylethane, J Zhejiang Univ B 19:400–408; doi:10.1631/jzus.b1800033.

Zhang Q, Liu W, Niu Q, Wang Y, Zhao H, Zhang H, et al. 2016. Effects of perfluorooctane sulfonate and its alternatives on long-term potentiation in the hippocampus CA1 region of adult rats in vivo. Toxicol Res (Camb) 5:539–546; doi:10.1039/c5tx00184f.

Zhang Y, Wei L, Wang Y, Zhang Y, Wang L, Chang W. 2019. Neurotoxic effects of perfluoroalkyl acids : neurobehavioral deficit and its molecular mechanism. Toxicol Lett 305:65–72; doi:10.1016/j.toxlet.2019.01.012.

Zhu B, Zhao G, Yang L, Zhou B. 2018. Tetrabromobisphenol A caused neurodevelopmental toxicity via disrupting thyroid hormones in zebrafish larvae. Chemosphere 197:353–361; doi:10.1016/j.chemosphere.2018.01.080.

Ziemińska E, Stafiej A, Toczyłowska B, Łazarewicz JW. 2012. Synergistic neurotoxicity of oxygen-glucose deprivation and tetrabromobisphenol A in vitro: Role of oxidative stress. Pharmacol Reports 64:1166–1178; doi:10.1016/S1734-1140(12)70913-1.

Chapter 2a

Deepika Deepika, Raju Prasad Sharma, Marta Schuhmacher, Vikas Kumar, Development of Physiologically Based Pharmacokinetic Model (PBPK) for three Organophosphate Flame Retardants (TDCIPP, TCIPP, TCEP) in rat (In preparation).

Chapter 2b

Deepika Deepika, Raju Prasad Sharma, Marta Schuhmacher, Amrit Kaur Sakhi, Cathrine Thomsen, Leda Chatzi, Marina Vafeiadi, Joane Quentin,Remy Slama, Regina Grazuleviciene, Sandra Andrušaitytė, Dagmar Waiblinger, John Wright, Tiffany C Yang, Jose Urquiza, Martine Vrijheid, Maribel Casas, Vikas Kumar, Unravelling sex-specific BPA toxicokinetics in children using a pediatric PBPK model (Under Revision).

UNIVERSITAT ROVIRA I VIRGILI
QUANTITATIVE SYSTEMS TOXICOLOGY MODELING FOR NEURONAL ADVERSE OUTCOME
Deepika

Development of Physiologically Based Pharmacokinetic Model (PBPK) for three Organophosphate Flame Retardants (TDCIPP, TCIPP, TCEP) in rat

Abstract

Tris(1,3-dichloro-2-propyl) phosphate (TDCIPP), Tris (1-chloro-2-propyl) phosphate (TCIPP) and tris (2-chloroethyl) phosphate (TCEP) are 3 widely used organophosphate flame retardants (OPFRs) being frequently detected in human bodily fluids. Although OPFRs are being detected in human beings, currently the toxicological effect from its exposure is not clearly understood. A PBPK model could help in improving the understanding about toxicity of OPFRs. For this, a seven compartment physiologically based pharmacokinetic model (PBPK) was developed and validated in rats to understand their toxicokinetic. Several assumptions were considered while developing the model for fitting the data. Four type of scenario for PBPK Model was built: 1) Inclusion of enterohepatic recirculation (EHR), 2) Time dependent EHR, 3) Biphasic clearance, and 4) Inclusion of separate unbound fraction for adipose tissue and brain. Model was optimized through Bayesian framework (Markov Chain Monte Carlo (MCMC) along with visual fitting to fit the toxicokinetic data. Goodness-of-fit and AIC score was calculated for each individual model to find the optimal model that fit best the individual chemicals data. Then, both the uncertainty and sensitivity analysis were conducted for the best model for all three OPFRs. The model was able to predict the concentration of OPFRs in several organs like plasma, urine, kidney etc within 1-2-fold of experimental data. The model predicted that the slow elimination of OPFRs from adipose tissue and brain especially at late time points, showed their potential to accumulate upon the daily exposure. This further warrant to investigate whether these chemicals follow the similar kinetics in human, which could lead to a greater risk to human health. Further, this PBPK model can be used as a basis for further extrapolating to predict the toxicokinetic or to predict total daily intake of these compounds in human.

Highlights

Multi-compartment PBPK model for 3 flame retardants, Tris(2-chloroethyl) phosphate (TCEP), Tris(1-chloro-2-propyl) phosphate (TClPP), Tris(1,3-dichloro-2-propyl) phosphate (or isopropyl) (TDClPP) was developed for the first time.

In-vitro kinetic data was utilized in PBPK for predicting in-vivo data.

Independent multiple data sets were used for validated the model and EHR was included.

1. Introduction

Organophosphate flame retardants (OPFRs) contain alkyl chain or aryl group with organic ester of phosphoric acid with or without a halogen group. Flame retardant like PBDE (Polybrominated Diethyl Ether) has been phased out of USA and banned in Europe due to human health concerns (Hogberg et al. 2021). As a replacement of brominated flame retardants (BFRs), the use of OPFRs has increased as plasticizers in construction and for fire safety standard in recent years (Blum et al. 2019). OPFRs are the second most widely used FR (Flame Retardant) in Europe after aluminium trihydroxide with approximate consumption of 89640 metric tons almost double of BFRs (Chupeau et al. 2020).

Several studies showed OPFRs association with various adversity such as neurotoxicity, endocrine disruption, carcinogenicity, and developmental toxicity (Hoffman et al. 2014; Yang et al. 2019, 2022). Human are exposed to OPFRs through dietary intake, inhalation and ingestion of indoor dust (Hou et al. 2016; Wang et al. 2020a). Numerous studies detected OPFRs in both the indoor and outdoor environments (dust, furniture and ambient air) (Bajard et al. 2019; Esplugas et al. 2022; Zhang et al. 2016). A study conducted in Sweden suggested phosphorus flame retardants (PFR), daily per capita from food range from 406-3266 ng/day equivalent to 6-49 ng/Kg BW/day (Poma et al. 2017). This result suggested human dietary intake to PFR is equally important to dust ingestion. Further in recent years, European Commission banned the uses of organohalogen chemicals in electronic displays and stands (Schreder 2019) (EUROPEAN COMMISSION BANS HARMFUL CLASS OF FLAME RETARDANTS IN TVS - NEW MEASURES MAKE APPLIANCES MORE SUSTAINABLE), which forced the manufacturers to explore the potential of using OPFRs as a replacement substitute. As a result, use of OPFR is continuously increasing and being a persistent organic pollutant, it bioaccumulates (Hou et al. 2016).

Human biomonitoring studies detected OPFRs and their metabolites in various biological samples such as blood, urine (Wang et al. 2020b), hair and milk (Chupeau et al. 2020). OPFRs are ubiquitous in environment, which makes it crucial to understand their toxicokinetic in living beings. As per our knowledge, currently there is no PBPK Model developed to understand their disposition. There are a few experimental data available with kinetic study in rats and mice (Lynn et al. 1981; MINEGISHI et al. 1988; Nomeir et al. 1981; Zhu et al. 2020). For instance Minegishi et al., compared the PK of several OPFRs in rats after exposure through oral route (MINEGISHI et al. 1988). Study by Lynn et al. and Chapman et al. reported TDCIPP disposition in rats after IV exposure (Chapman et al. 1991; Lynn et al. 1981). In general for OPFRs, almost all parent compound get metabolized quickly to the metabolites but their elimination is relatively slow in living beings (Lynn et al. 1981; Nomeir et al. 1981). Nomeir et al. conducted a biliary excretion study and pointed out that radioactive TDCIPP was excreted in bile within 4 hour while the feces excretion was over the course of 10 days (Nomeir et al. 1981). This indicates that the compound excreted in bile undergoes the enterohepatic recirculation (EHR). Such kind of phenomenon can be captured by PBPK Model by integrating in-vitro metabolism data, and available mechanistic evidence along with physiology, biochemical and physicochemical properties (McNally et al. 2021).

The objective of this work was to develop and validate the PBPK model for three OPFRs in rat to understand the biology influencing the distribution of these compounds in organs like brain, adipose tissue, liver etc. For this, perfusion limited PBPK model was developed for understanding the toxicokinetic inside living being. In-vitro to in-vivo extrapolation (IVIVE) and animal data was used to develop the PBPK Model. In this model, the major assumption was that time required to reach steady state can be evaluated by blood flow, tissue volume and the partition coefficient of tissue with respect to plasma. Sensitivity analysis was conducted to find the physiological and biochemical parameters affecting the output. Developed PBPK model can be used further for the human risk assessment by cross-species extrapolation. Further, this model can help in pointing out the existing gaps in the data of OPFRs which can be fulfilled using in-vitro studies.

2. Methodology

2.1 Building of the PBPK Model

A PBPK model was developed comprising of the seven compartments i.e., gut, liver, brain, kidney, fat, plasma and the rest of body along with their major metabolites: TDCIPP to bis(1,3-dichloro-2-propyl) phosphate (BDCIPP), TCIPP to bis(1-chloropropyl) phosphate (BCIPP) and TCEP to bis(2-chloroethyl) hydrogen phosphate (BCEP) respectively (Figure and Fig 2). PBPK was built for oral administration with the gut as a site of absorption. A chemical exchange between the organs and blood is restricted by flow rather than permeation also called as perfusion limited model. The fundamental assumption for this kind of model is that equilibrium between plasma and organs chemical concentration is instantaneous. Another assumption in this model is that almost all the chemical is getting metabolized to the metabolites. Based on the literature data, enterohepatic recirculation (EHR) was introduced in perfusion limited PBPK model to capture the data trend. To further improve the prediction of model, a new mechanistic hypothesis was introduced and thus a new model. Consequently, several model versions were designed representing different biological mechanisms to best explain the chemical kinetics (explained below). All developed models and equations were provided in the supplementary file.

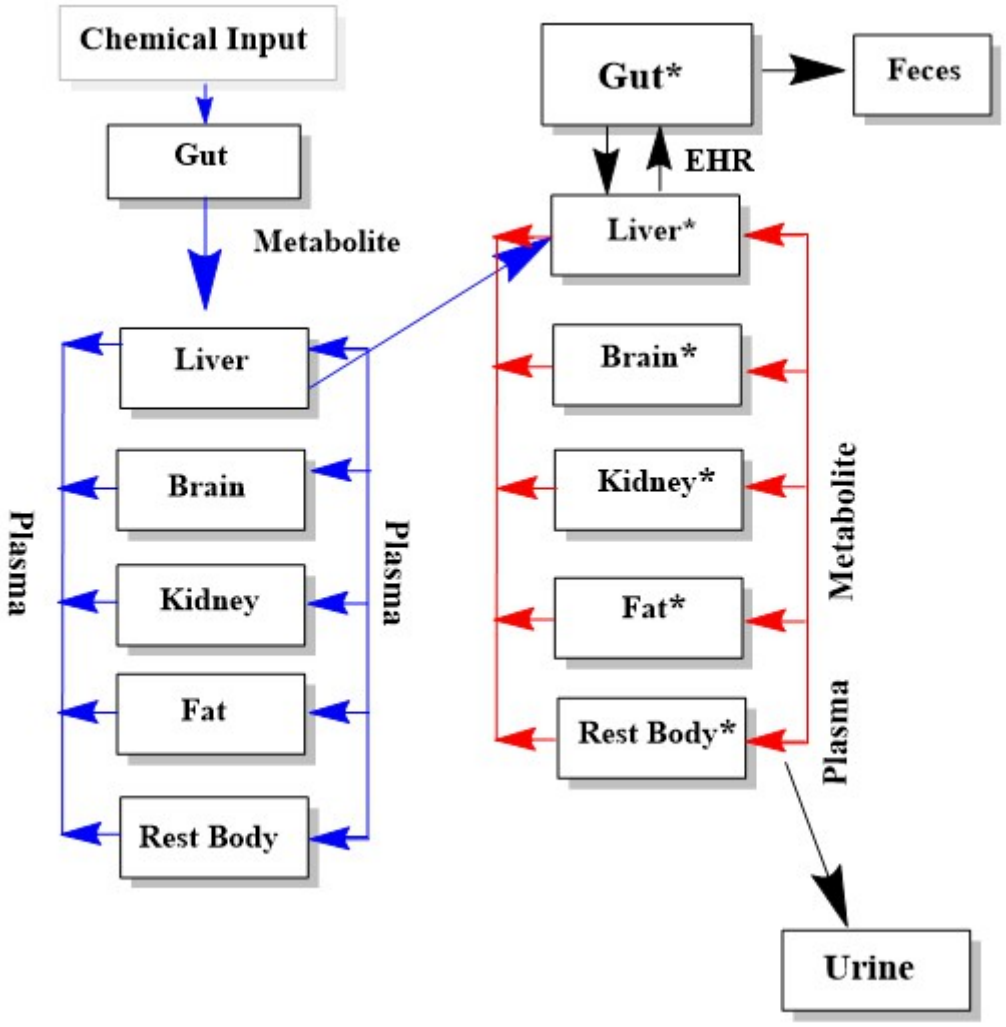

Figure 1: PBPK Model for three OPFRs with seven compartments. Enterohepatic recirculation (EHR) of the metabolite was included in the model. * represents the respective metabolite getting circulated inside human body. Metabolite is getting excreted from feces through gut and from urine through plasma. Almost all the parent compound is getting metabolized to metabolites.

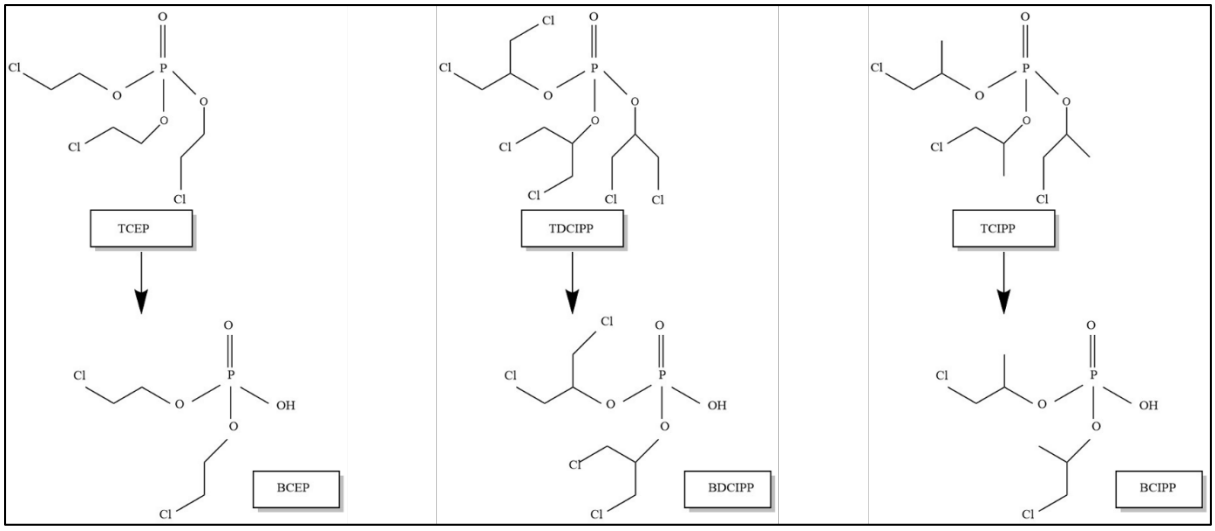

Figure 2: Chemical Structure of parent compound and its metabolites being considered for the PBPK Model, Tris(2-chloroethyl) phosphate (TCEP), Tris(1-chloro-2-propyl) phosphate (TCIPP), and Tris(1,3-dichloro-2-propyl) phosphate (or isopropyl) (TDCIPP). For this model, we considered that metabolism is only happening in liver and major metabolites are being formed: bis(2-chloroethyl) hydrogen phosphate (BCEP), bis(1,3-dichloro-2-propyl) phosphate (BDCIPP), and bis(1-chloropropyl) phosphate (BCIPP).

Scenario 1 and 2: Perfusion Limited PBPK Model with EHR and time dependent EHR

Perfusion limited PBPK Model was built for explaining the pharmacokinetic of chemical inside rat. Eq. 1 is the fundamental equation applies to all the compartments except chemical eliminating organs such as liver, kidney and gut includes additional clearance equation. For more details about equations, see Supplementary file.

$$\frac{dC_i}{dt} = \frac{Q_i * C_p - \frac{C_i}{Ki:p}}{V_i} \qquad \text{Eq. 1}$$

Here, C_i refers to the concentration in the particular compartment i (ug/L), $Q_i$represents blood flow in i_{th} compartment, Cp represents concentration in plasma, Ki:p denotes partition coefficient of i_{th} compartment in relation to plasma and Vi is the volume of the i_{th} compartment.

Several versions of the model were built to explain particular scenario. In the first version of model (scenario 1), enterohepatic recirculation (EHR) (Figure) process was included based on kinetic data that showed the biliary excretion of OPFRs and slow elimination in urine (Nomeir et al. 1981). In the experimental data, a secondary peak was observed resulting in slow elimination from 20 hours after dose administration (Nomeir et al. 1981). The EHR process was modelled considering the metabolite only since the OPFRs undergo very fast metabolism. For instance, in case of TDCIPP, within 5 min of dose administration the metabolite started appearing in all the organs and after 30 min, the parent compound was not detected (Lynn et al. 1981). Uptake of the OPFR was done from gut to liver, in liver it undergoes metabolism. Metabolite from liver to gut was modeled as first order uptake process where the metabolite

was available for reabsorption. Data on the reabsorption rate and uptake has been provided in the supplementary file.

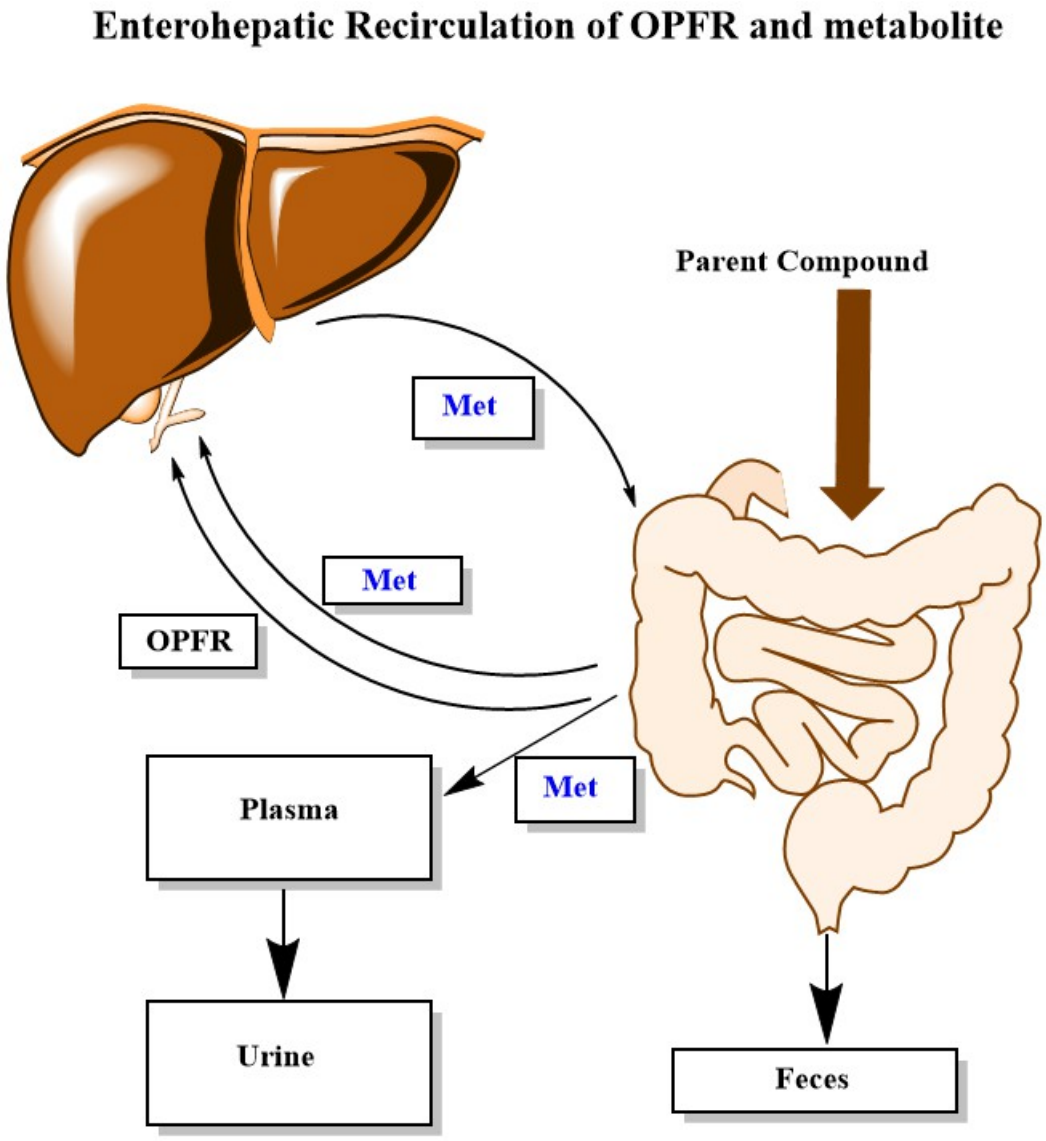

Figure 3: Enterohepatic Recirculation (EHR) between gut and liver for OPFRs. Parent compound is getting transformed into metabolite in liver and then the respective metabolite is getting circulated from liver to gut and gut to liver. Transformation of parent compound to metabolite is very quick in OPFRs. Elimination of the metabolite is partially from feces and urine for all OPFRs except TCEP where only urinary elimination is present.

In scenario 2, the model was further adapted to include EHR as a function of time as the model was not able to explain few datapoints. Thus, the model was extended to capture the delay in elimination and also to make it close to physiological reality since extent of biliary emptying depends on the food, digestion in GIT and quantity of fat in the meal (Roberts et al. 2002). Model was based on lag-time intervals with separate rate constant for EHR (EHR_1, EHR_2) and absorption (kgut_1, kgut_2) after particular time point to better capture data trends (eq. 2).

$$Aorg = [t \leq 20?\,(kgut\_1 * Ag\_1 + Qorg * (cpl * fu - corg * (fu/k\_org\_pl)) + (RAM - EHR\_1 * Aorg) : t > 20?\,(kgut\_2 * Ag\_1 + Qorg * (cpl * fu - corg * (fu/k\_org\_pl)) + (RAM - EHR\_2 * Aorg)] \quad \text{eq. 2}$$

Where Aorg, refers to amount of OPFRs in the organ and Ag_1 for gut (µmol), Qorg refers to blood flow in organ, cpl is concentration of chemical in plasma and corg for plasma (µmol/L), fu is fraction unbound for plasma, k_org_plasma is partition coefficient for organ with plasma, and RAM refers to micheles menten kinetic which is equal to korgan mentioned below.

Scenario 2: Biphasic clearance

To capture the late time points kinetics in plasma and other organs, perfusion limited model was updated with both the time dependent EHR and a biphasic clearance. It was assumed that initially the chemical can eliminate very fast afterward it can become very slow. So, we have implemented first order elimination followed by zero order elimination as a function of time in excretion compartments (urine and feces). In zero order elimination, the amount eliminated will be mostly dependent on time rather than chemical present whereas in first order, it depends on maximum plasma concentration (Borowy CS 2022). To capture the elimination after a certain time period the elimination rate constant was decreased as shown in eq. 3.

$$Ael = [t <= 20?\,(kel * cpl) : t > 20?\,(kel\_1 * cpl)] \quad \text{eq. 3}$$

Where Ael refers to amount of chemical in eliminating organ (µmol), kel refers to elimination rate, cpl is concentration in plasma (µmol/L) and kel_1 is elimination rate after 20 hours of dosing. This elimination rate was decreased by 10% after 20 hours to keep the elimination steady.

Scenario 3: Independent fraction unbound for Adipose and Brain tissue

The physicochemical properties of OPFRs for instance, Log Ko/w for the OPFRs (TDCIPP: 3.65, TCIPP: 2.59, TCEP: 1.78) demonstrates their lipid affinity. Similarly, a study on brominated flame retardant like HBCDD, a close analogue of FRs showed its binding to lipoproteins like low density lipoproteins (LDL), high density lipoproteins (HDL) and chylomicrons (CLC) (Emond et al. 2021). This shows that we need to include their specific binding activity to a particular organ. Also, being lipophilic these compounds may also easily cross the BBB but might not have the same influx and efflux rate, assuming transporter might play a certain role. As per Lipinski rule of five, compound with mol wt.<500 KDa, Log P<5, no more than 10 hydrogen bond acceptor and no more than 5 hydrogen bond donor can be a good moiety for BBB permeation. OPFRs followed all the properties stating that it may be a good substrate for BBB permeation. Based on all evidences, a separate fraction unbound was considered for certain compartments like adipose and brain shown in eq. 4.

$$Aorg = Qorg * (cpl * fu) - corg * (fu\_1/K\_org\_pl) \quad \text{eq. 4}$$

Where Aorg refers to amount of chemical in organ (nm), Qorg refers to blood flow in organ, cpl is concentration of chemical in plasma (nm/gm), fu is fraction unbound for plasma, fu_1

is fraction unbound for the particular organ, corg is concentration of chemical in specific organ and K_org_plasma is partition coefficient for organ with plasma.

2.2 Optimization of the parameters

Parameterization of the PBPK model includes physiological and biochemical parameters for the rat. All physiological parameters related to organ volumes and blood flows to respective organs were adopted from several articles published by authors as shown in Table 1 (Supplementary file) (Brown et al. 1997; Merrill et al. 2003; Sharma et al. 2020). Biochemical parameters such as partition coefficient was calculated based on Minigeshi experimental study (MINEGISHI et al. 1988). To calculate the partition coefficient, first the AUC of different organs and plasma was determined using trapezoidal method. Then the partition coefficient for several organs was calculated using eq. 5 where Ki:p refers to partition coefficient of the organ with respect to plasma, AUC is the area under curve.

$$Ki{:}p = \frac{AUC_{Organ\,(0:24hours)}}{AUC_{Plasma\,(0:24hours)}} \qquad \text{Eq. 5}$$

Absorption from gut to liver was defined by first order rate constant. Separate fraction unbound was considered for the chemical and its metabolite which was available for distribution, metabolism and excretion from the human body. Metabolism was determined by Michaelis-Menten equation with parameters like Vmax (maximum reaction velocity at the saturable substrate concentration) and Km (concentration at which reaction occurs at half-maximum rate) given in eq. 6. Vmax was scaled from pmol/min/mg protein to in-vivo per kg BW (eq. 7). MPPGL refers to microsomal protein per gram of the liver, V_{liver} represents volume of liver in L (Table 1 in supp file), and BW refers to body weight in Kg. Metabolic equations were included in separate compartment responsible for metabolism of chemical (Figure). Almost similar chemical structure of three chemicals depicts that they might have similar kind of metabolic profile. All three was considered as possible substrates of glutathione S-transferases (GSTs) since GSTs react primarily with electrophilic functions or substituents in the molecule (Van den Eede et al. 2013). For TCEP, in terms of relative abundance, BCEP was the major metabolite (Van den Eede et al. 2013) in human liver. BDCIPP diester was major metabolite measured followed by glutathione conjugate in TDCIPP (Van den Eede et al. 2013). However, in case of TCIPP, TCIPP-M2 was the major metabolite, however BCIPP was also detected (Van den Eede et al. 2013). The major metabolite was considered for the model except for TCIPP we considered BCIPP since in human biomonitoring studies, most researcher quantify BCIPP. Study by Eede et al. where the author calculated Vmax and Km for TCIPP in human liver microsomes was taken (Van den Eede et al. 2016). For the plasma, the value was found very low, so the major metabolite (BCIPP) was being formed in liver. Similar assumption was considered for PBPK and due to limited availability of data, similar kind of distribution was assumed for other 2 OPFRs (Table1).

$$k_{Organ} = \frac{V_{max} * C_{organ} * f_u}{k_m + C_{organ} * f_u} \qquad \text{Eq. 6}$$

$$V_{max} = V_{max} * MPPGG * V_{liver}/BW^{0.25} \qquad \text{Eq. 7}$$

Excretion was explained by urinary and fecal route which accounts for major elimination for all three chemicals. However, for TCEP only urinary elimination was considered since it accounts for 90% of excretion. Several parameters were optimized by Markov Chain Monte Carlo (MCMC) Bayesian analysis for fitting the toxicokinetic due to lack of experimental data. Distribution set for initial optimization has been provided in supplementary file. After initial optimization, convergence for the parameters was not so optimal, however it narrowed down the range for optimization. Value from initial optimization was considered for further refinement of several parameters by visually fitting within margin of errors of dataset for increasing the model goodness of fit (U. S. Environmental Protection Agency 2006). All biochemical parameters calculated and fitted were provided in Table.

Table 1: Biochemical parameters for TDCIPP, TCIPP and TCEP. Monte Carlo (MC) was done to capture uncertainty and log normal was used for distributing the parameter. Log normal in MCSim takes the two real number as parameter: 1) geometric mean (exponential of mean in log-space) and geometric standard deviation (exponential of SD in log-space strictly superior to 1) (Bois 2009).

Parameters	Values (TDCIPP), Distribution	Values (TCIPP), Distribution	Values (TCEP), Distribution
BW (Kg)	0.15	0.15	0.15
MW (g/mol)	430.9	327.6	285.5
Log P (octanol/water)	3.65	2.59	1.44
Liver: Plasma	0.30 (LN 1.1) [a]	0.38 (LN 1.1) [a]	0.45 (LN 1.1) [a]
Brain: Plasma	0.13 (LN 1.1)	0.9 (LN 1.1) [a]	0.702 (LN 1.1)
Kidney: Plasma	1.31 (LN 1.1)	5.25 (LN 1.1)	6.31 (LN 1.1) [a]
Fat: Plasma	0.794 (LN 1.1) [a]	0.8 (LN 1.1)	2.09 (LN 1.1) [a]
Absorption Rate Constant^0 (kgut)	0.098 (LN 1.1)	0.083 (LN 1.1)	0.5 (LN 1.1)
Absorption Rate Constant^1 (kgut_1)	0.099 (LN 1.1)	0.5 (LN 1.1)	0.5 (LN 1.1)
Enterohepatic recirculation (EHR_1)	3.01 (LN 1.1)	0.8 (LN 1.1)	18.99 (LN 1.1)
Fraction unbound (Fu)	0.001 (LN 1.1)	0.035 (LN 1.1)	0.010 (LN 1.1)
Fraction unbound for metabolite (fu_1)	0.019 (LN 1.1)	0.015 (LN 1.1)	0.035 (LN 1.2)
Bound fraction for lipoprotein (fu_adp)	0.5 (LN 1.1)	0.5 (LN 1.1)	0.035 (LN 1.3)
Bound fraction inside brain (fu_br)	0.55 (LN 1.1)	0.09 (LN 1.1)	0.015 (LN 1.1)
Vmax_liver_c[b] (µmol/hr/BW$^{0.25}$)	1509.11	1509.11	1509.11
Km_liver (µM)	96.1[a]	96.1 [a]	96.1 [a]
Clearance rate (Cl)	0.040 (LN 1.1)	0.18 (LN 1.1)	0.98 (LN 1*)
Fecal elimination rate (kfeces_c)	0.045 (LN 1.1)	0.065 (LN 1.1)	-

[a]Parameters for partition coefficient were calculated based on data. Other parameters were optimized based on the experimental data. b represents Vmax for major metabolite assumed to be similar.

2.3 Model Validation with experimental animal studies

OPFRs kinetics study in rats performed by Minegishi et al. was used for the development of the model and the data were extracted from the graph plots using webPlot digitizer (MINEGISHI et al. 1988). Author measured the chemical concentrations at 3, 6, 12, 24, 72, and 168 hours after a single dose of 50 µmol/kg administered orally to the group of five rats for all three OPFRs. For TDCIPP, Lynn et al. administered a IV dose of ^{14}C-TDCPP (10.04 µCi, sp. act. 12.5 mCi/mmol) and estimated the distribution, metabolism and elimination in rats in all the organs measured at 0.08, 0.5, 8, 24, and 120 hours (Lynn et al. 1981). Extracted data from this study was used to further validate the TDCIPP model. In another study for TDCIPP by Noemir et al., 2 µmol/Kg dose (0.867 mg/kg) was administered through the oral route and chemical concentrations was measured in all organs till 10 days (Nomeir et al. 1981). Noemir et al. in his article has clearly stated that the absorption of TDCIPP is so rapid that after absorption from the dermal route or the gastrointestinal tract (GIT), the tissue distribution is similar to the IV dose except for lungs. Another point worth mentioning is that all the parent compound gets metabolized quickly to the metabolites. The author checked after administering by both oral and IV route and found the tissue/blood distribution to be same after 24 hours (Nomeir et al. 1981). Further, he checked for dermal administration and tissue blood ratio was similar as anticipated by oral and IV. Considering this, we have kept administration route which is oral similar for all our simulations.

2.4 Model evaluation and Sensitivity Analysis

For each scenario, individual model was built, there were total of 4 model for each chemical (16 model in total). Goodness of fit was plotted for each model for comparing the simulating and observed data. R (correlation coefficient) and p value was calculated for each organ using Pearson correlation coefficient (PCC). Further, to select the best model out of four, Akaike information criterion (AIC) was performed using the following eq..

$$Residual = \sum W\ X\ \left(C_i - C_{aj}\right)^2 \qquad \text{Eq. 8}$$

Where, W is the weighting factor, ∑the sum, C_i is the observed concentration and C_{aj} is the adjusted concentration

$$AIC = n\ X\ In\ Residual\ +\ 2P \qquad \text{Eq. 9}$$

Where, n represents the number of data points, and P is the number of pharmacokinetic parameters.

A normalized sensitivity analysis (SA) was done to evaluate impact of input parameters on plasma Area under Curve ($AUC_{0\text{-}t}$). AUC was used since OPFRs have longer half-life and calculating AUC can give better estimate of the sensitivity. A single parameter was changed to 2% of their original value while all others were kept constant to evaluate the influence on output. SA was performed at the dose used for validation of the model (50 mg/Kg BW). The following eq. 10 was used to calculate the SA.

$$SA = \frac{\left(AUC_{increase} - AUC_{original}\right) / AUC_{original}}{\left(Param_{increase} - Param_{Original}\right) / Param_{Original}} \qquad \text{Eq. 10}$$

Here, AUC refers to area under curve and param refers to the physiological and biochemical parameters included in the analysis.

2.5 Computing Software

Coding and simulation were performed with MCSIM (Bois 2009) integrated with R studio (Version 4.1.2) (Team 2015). For data analysis, Rstudio has been used with package like ggplot2, ggscatter, ggpubr, and AICcmodavg for carrying out activities like plotting, correlation coefficient, and AIC score.

3. Results

3.1 Model Scenarios and their evaluation

Concentration-time plot was generated for all four scenarios (EHR, time-dependent EHR, biphasic clearance and separate fu for brain and adipose) for three OPFRs (total 12 plots). For TDCIPP, the observed cumulative urine data points were below the median while for feces, data points were above the median in scenario 2, 3 and 4 (Figure 1, 2, 3 in supp file) whereas scenario 1 accurately predicted the cumulative urine and feces. Scenario 4 for TDCIPP was only able to capture the brain and adipose tissue maximum concentration (Cmax) within 2.5 and 97.5 percentile (Fig 3 in supp file). For TCIPP, in scenario 1 the observed cumulative urine was at 2.5 percentile whereas cumulative feces was above the median (Fig 6 in supp file). Fig 7, 8 (supp file) and 5 showed the improved prediction for cumulative urine in scenario 2, 3 and 4. Scenario 1, 2 and 3 for TCIPP were able to capture the Cmax for adipose tissue (Fig 6, 7 and 8 in supp file) whereas scenario 4 was not able to capture the Cmax (Fig 5). For TCEP, scenario 1, 2 and 3 underpredicts the concentration in adipose tissue whereas the prediction improved for scenario 4. Scenario 3 (Fig 11 supp file) and 4 (Fig 6) were able to predict the cumulative urine whereas scenario 1 and 2 were overpredicting (Fig 9 and 10 supp file). Overall, different scenarios considered for developing the PBPK model improved the prediction for one or another organ. The developed model with all four different scenarios was able to predict chemical concentrations up to 20 hours (Fig 1,2,3,6,7,8,9,10,11 in supp file and fig 4,5,6). However, time points beyond 20 h (last time points), not all the scenario, but particular scenario for a particular chemical was only able to match closely the data points. Through visual comparison, it was difficult to understand which scenario is predicting better than the other.

3.2 Best Model based on AIC Scores

PBPK model was simulated upon oral administration of 50 µmol/Kg and the results were compared to the rat data published by Minegishi et al. (1988). The best fit scenario was calculated based on AIC score considering the time points beyond the 20 h (supp file). For instance, in case of TDCIPP, the scenario 1 best predicted the concentration in all the organs based on AIC_c score (Table 1 supp file). The AIC_c score was good for scenario 4 in case of TCIPP and TCEP. Here, only the best fit scenario was shown, rest others were provided in the supplementary file. Overall, the best model predicted concentrations in different organs (liver, brain, kidney, fat, blood, urine and feces) were within 2-3 folds of the experimental data. The model was able to predict very well the major elimination organ i.e., liver and kidney. The highest concentration is being detected in liver and kidney for all the OPFRs. At the same dose, the maximum plasma concentration (Cmax) was highest in TDCIPP followed

by TCEP and TCIPP. Both the data and simulation result showed that OPFRs concentrations in all the organs declined by more than half of their Cmax after 24 hours of dosing for all OPFRs (Figure , 5, 6) except for brain and adipose tissue this decline was very slow. TDCIPP concentration was quite high (brain and adipose tissue) compared to the other two OPFRs at 168 h. This trend correlates with the log $K_{o/w}$ which is highest for TDCIPP followed by TCIPP and TCEP, hence the higher lipid affinity and brain permeability. The urinary elimination followed the following order: TCEP>TCIPP>TDCIPP whereas the feces elimination: TDCIPP>TCIPP>TCEP. In TCEP, feces elimination was less than 6%, so it was not included in the model.

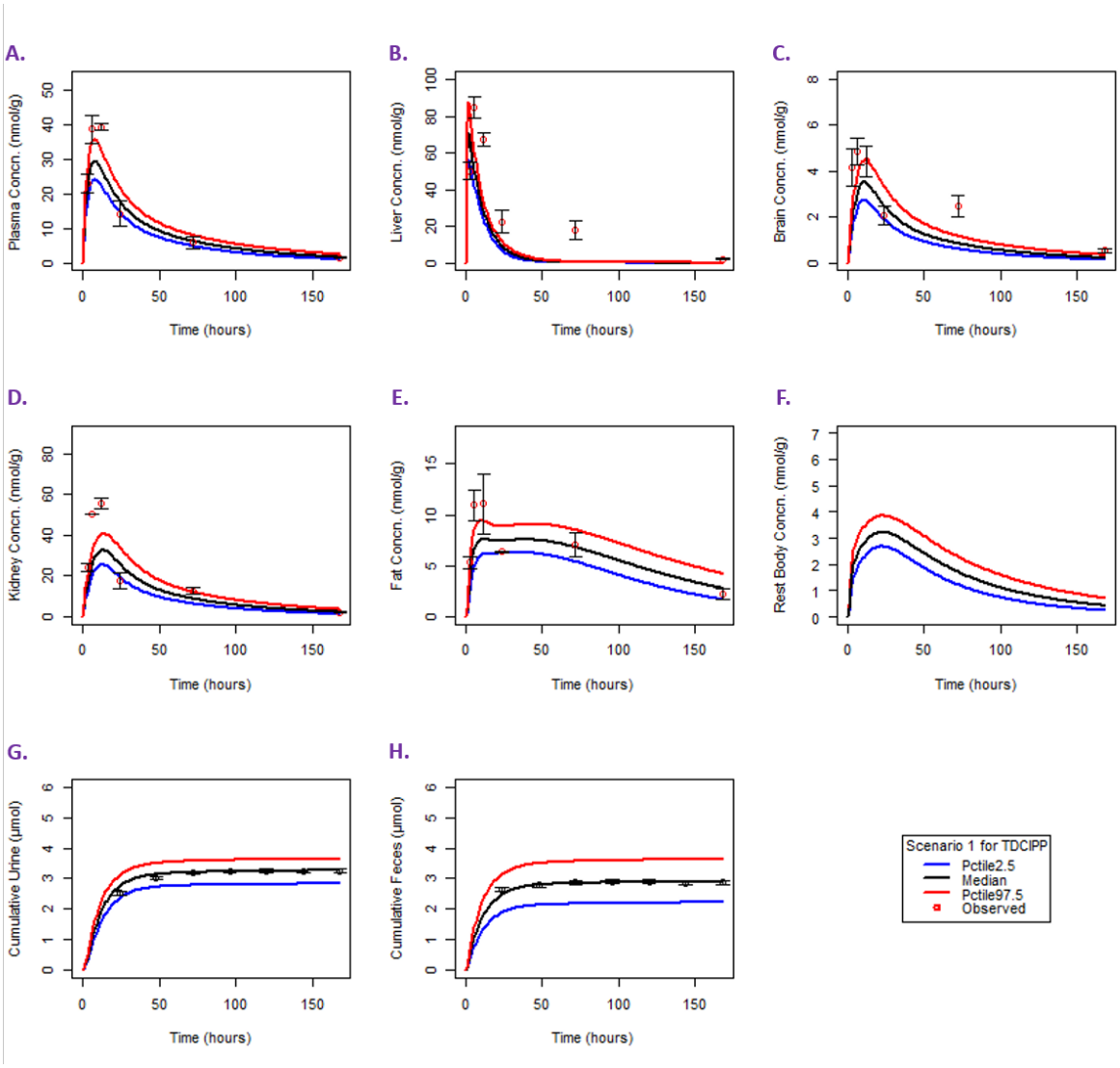

Figure 4: Concentration-time curves for TDCIPP in plasma (A), liver (B), brain (C), kidney (D), fat (E), rest body (F), urine (G) and feces (H). The Y-axis showed the chemical concentrations (nmol/g) or amount (µmol) and the X-axis showed the time in hrs. The solid lines correspond to the model simulation i.e., red (97.5th percentile), black (median), and blue (2.5th percentile), and the red dots (mean) with black bars (Standard deviations) represent the experimental value (MINEGISHI et al. 1988) with the best fit model (scenario 4).

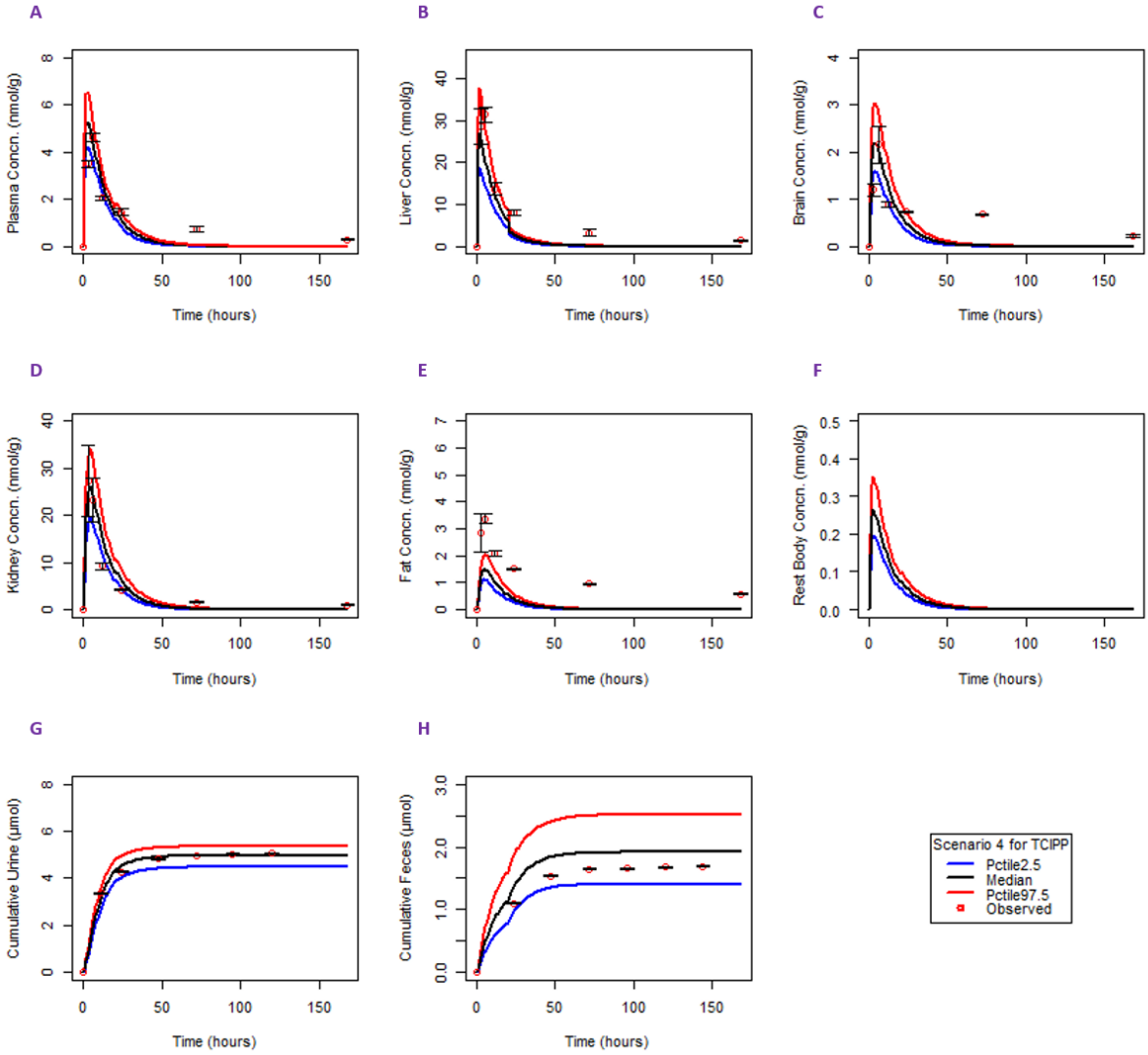

Figure 5: Concentration-time curves for TCIPP in plasma (A), liver (B), brain (C), kidney (D), fat (E), rest body (F), urine (G) and feces (H). The Y-axis showed the chemical concentrations (nmol/g) or amount (µmol) and the X-axis showed the time in hrs. The solid lines correspond to the model simulation i.e., red (97.5th percentile), black (median), and blue (2.5th percentile), and the red dots (mean) with black bars (Standard deviations) represent the experimental value (MINEGISHI et al. 1988) with the best fit model (scenario 4).

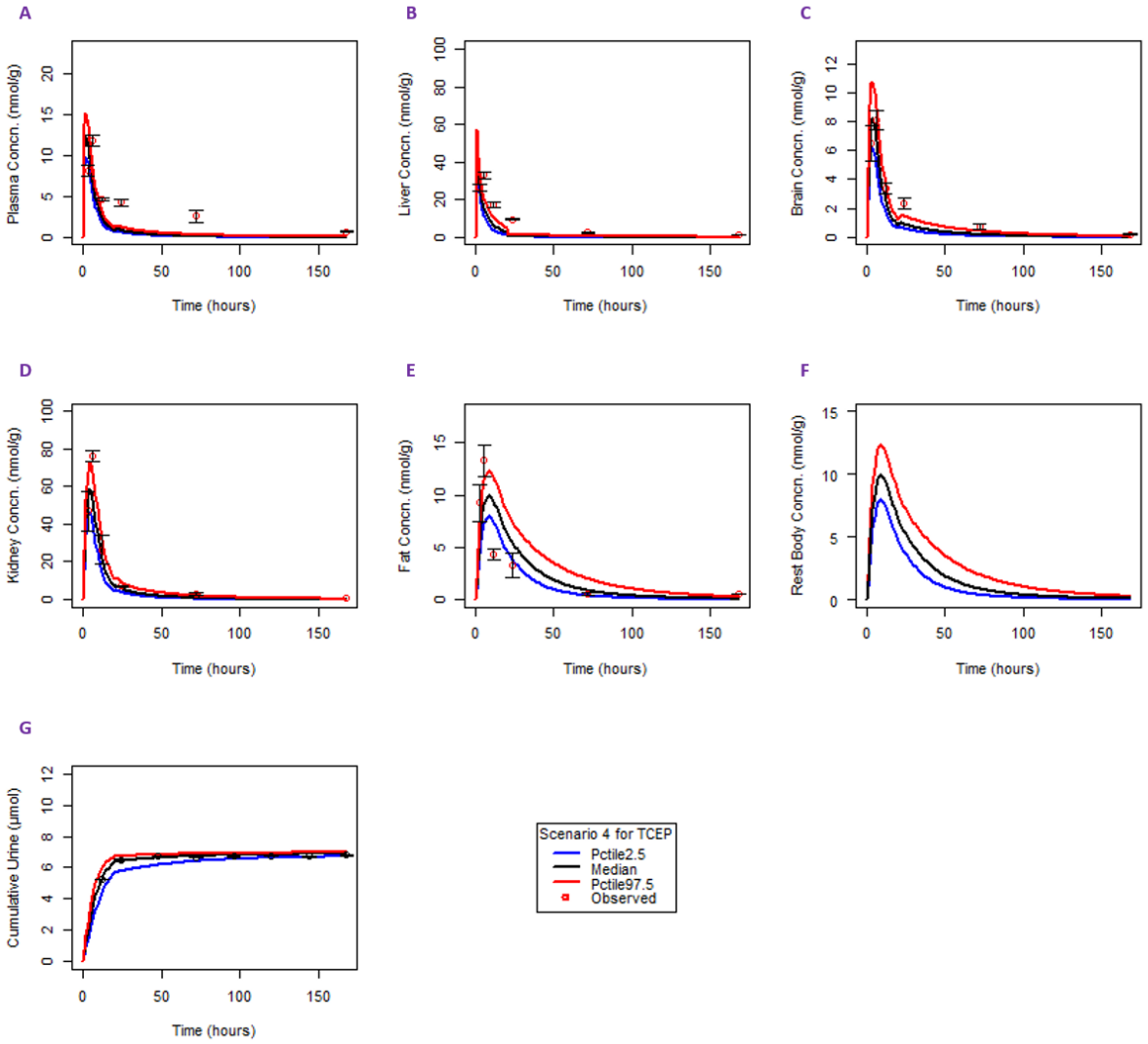

Figure 6: Concentration-time curves for TCEP in plasma (A), liver (B), brain (C), kidney (D), fat (E), rest body (F), urine (G). The Y-axis showed the chemical concentrations (nmol/g) or amount (µmol) and the X-axis showed the time in hrs. The solid lines correspond to the model simulation i.e., red (97.5th percentile), black (median), and blue (2.5th percentile), and the red dots (mean) with black bars (Standard deviations) represent the experimental value (MINEGISHI et al. 1988) with the best fit model (scenario 4).

The best TDCIPP model with the same parameters was used to predict the another set of experimental data upon oral administration of 2 µg/Kg BW (Nomeir et al. 1981). The model was able to explain almost all the time points (Fig. 7) (Fig 4 supp file). However, the chemical concentrations over time in kidney, urine, and feces are 1-2-fold outside the median model predictions which falls within the World Health Organization PBPK precision criterion (on Chemical Safety and for the Sound Management of Chemicals 2010). In case of urine, the experimental data was at 97.5 and for feces, it was at 2.5 percentile. Another independent experimental dataset from Lynn et al. was compared with the simulated data for TDCIPP till 120 hour (Figure 8) (Lynn et al. 1981). The model was able to explain the concentration-time profile for organs like plasma, liver, kidney, urine and feces. But, the plot for adipose tissue and fat was not explained by this model (Fig 5 supp file). In case of urine, our model

underpredicted but it was within two-fold of the experimental data. The model overpredicted the feces but it was at the border of 2.5 percentile (Fig 8).

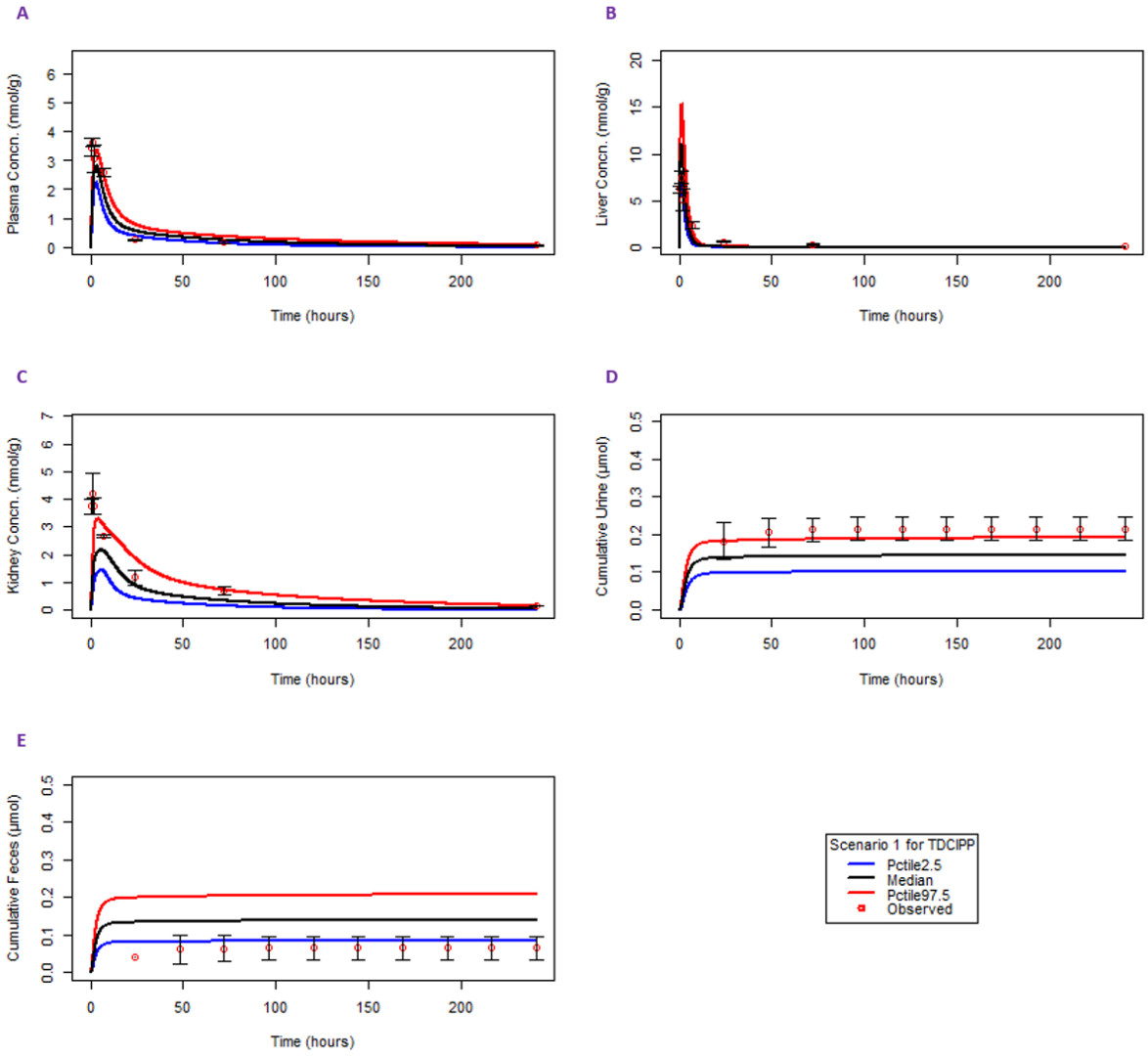

Figure 7: Simulated vs experimental TDCIPP concentration-time curves of different organs i.e., plasma (A), liver (B), kidney (C), urine (D) and feces (E). The Y-axis showed the chemical concentrations (nmol/g) or amount (µmol) and the X-axis showed the time in hrs. The solid lines corresponds to the model simulation i.e., red (97.5th percentile), black (median), and blue (2.5th percentile), and the red dots (mean) with black bars (Standard deviations) represent the experimental value (Nomeir et al. 1981) with the best fit model (scenario 1).

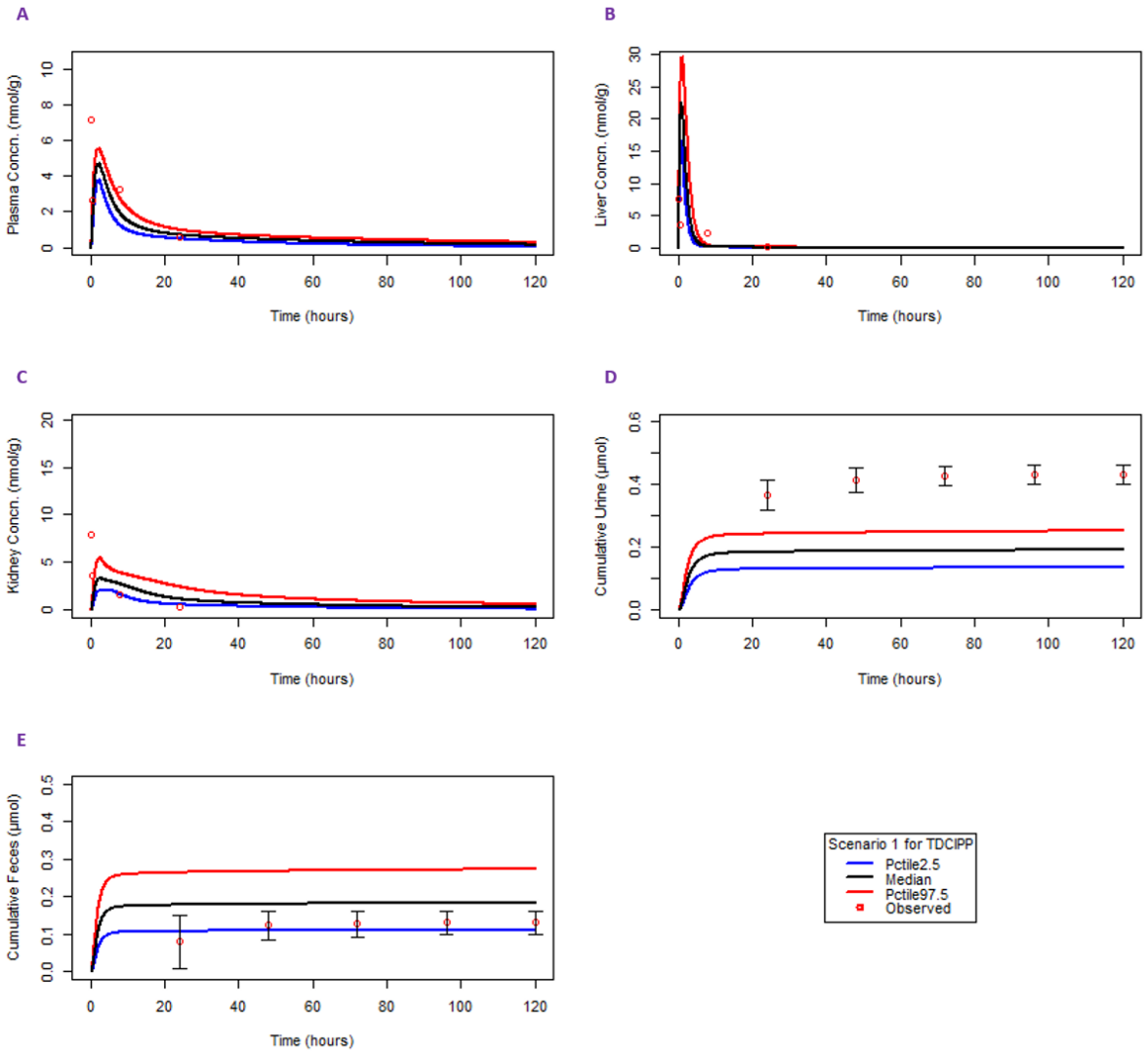

Figure 8: Concentration-time curves for TDCIPP of plasma (A), liver (B), kidney (C), urine (D) and feces (E). The Y-axis showed the chemical concentrations (nmol/g) or amount (µmol) and the X-axis showed the time in hrs. The solid lines corresponds to the model simulation i.e., red (97.5th percentile), black (median), and blue (2.5th percentile), and the red dots (mean) with black bars (Standard deviations) represent the experimental value (Lynn et al. 1981) with the best fit model (scenario 1).

3.3 Goodness of Fit

PBPK Model was able to adequately describe the concentration-time profile for all organs as depicted by the goodness-of-fit plot. Correlation coefficient for all organs was above 0.7 based on PCC for the best scenario model (Fig in annex). In Figure 9, correlation coefficient was above 0.95 for plasma, urine and feces for TDCIPP. For other organs, correlation coefficient was 0.75-0.85 (Figure 9). For TCIPP, correlation coefficient was above 0.9 for all the organs except feces where it was 0.87 (Figure 10). Figure 11 represent correlation coefficient for TCEP, and it was above 0.9 for all organs except plasma and fat where it was 0.8 and 0.63 respectively. Correlation coefficient was also calculated for other scenarios and it has been provided in the supplementary file.

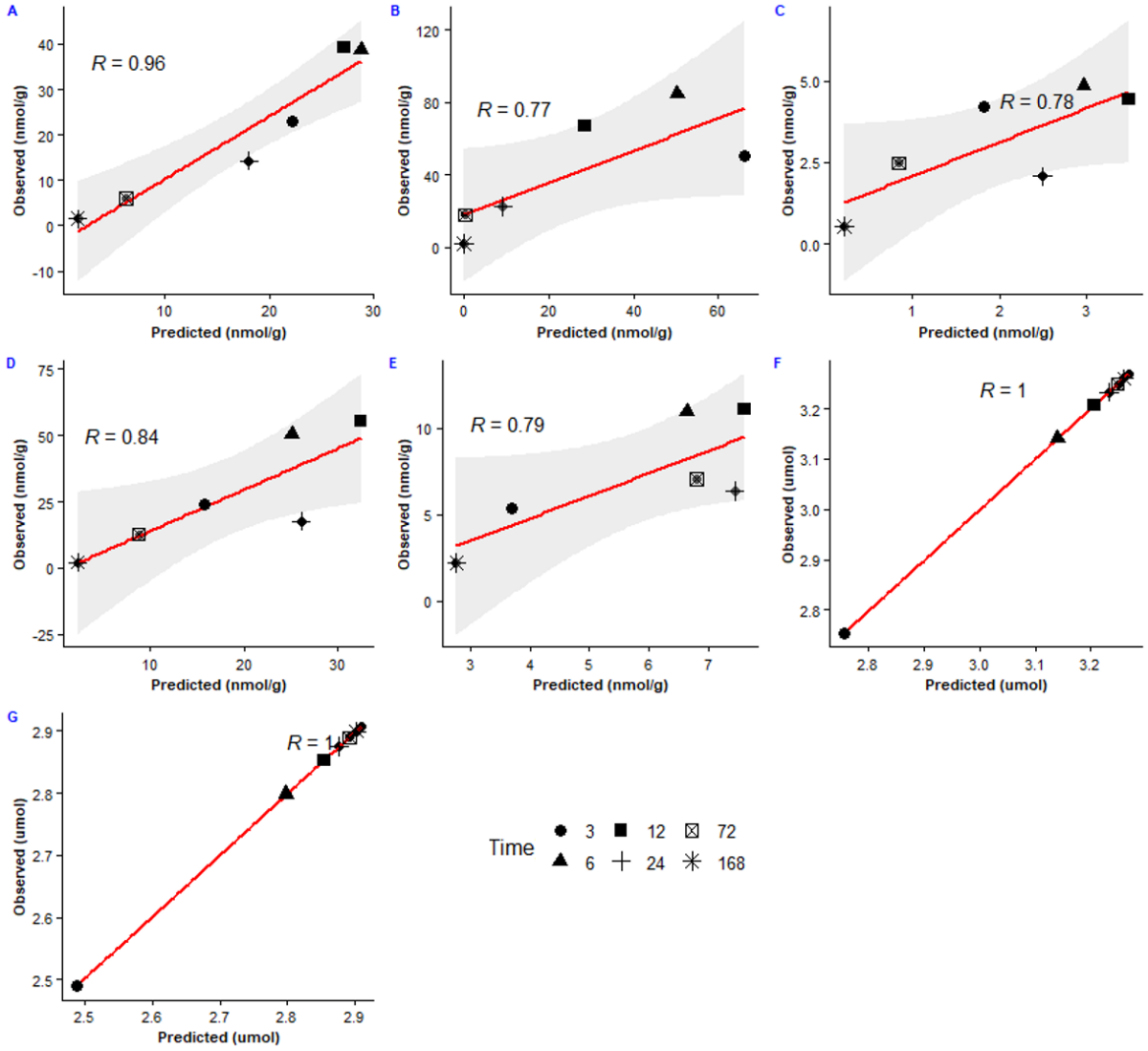

Figure 9: Goodness-of-fit plot for TDCIPP for several organs at various time point from 3 to 168 hours. R (correlation coefficient) was above 70% for all the organs using Pearson correlation coefficient (PCC). A represents plasma, B: Liver, C: Brain, D: Kidney, E: Fat, F: Urine and G: Feces.

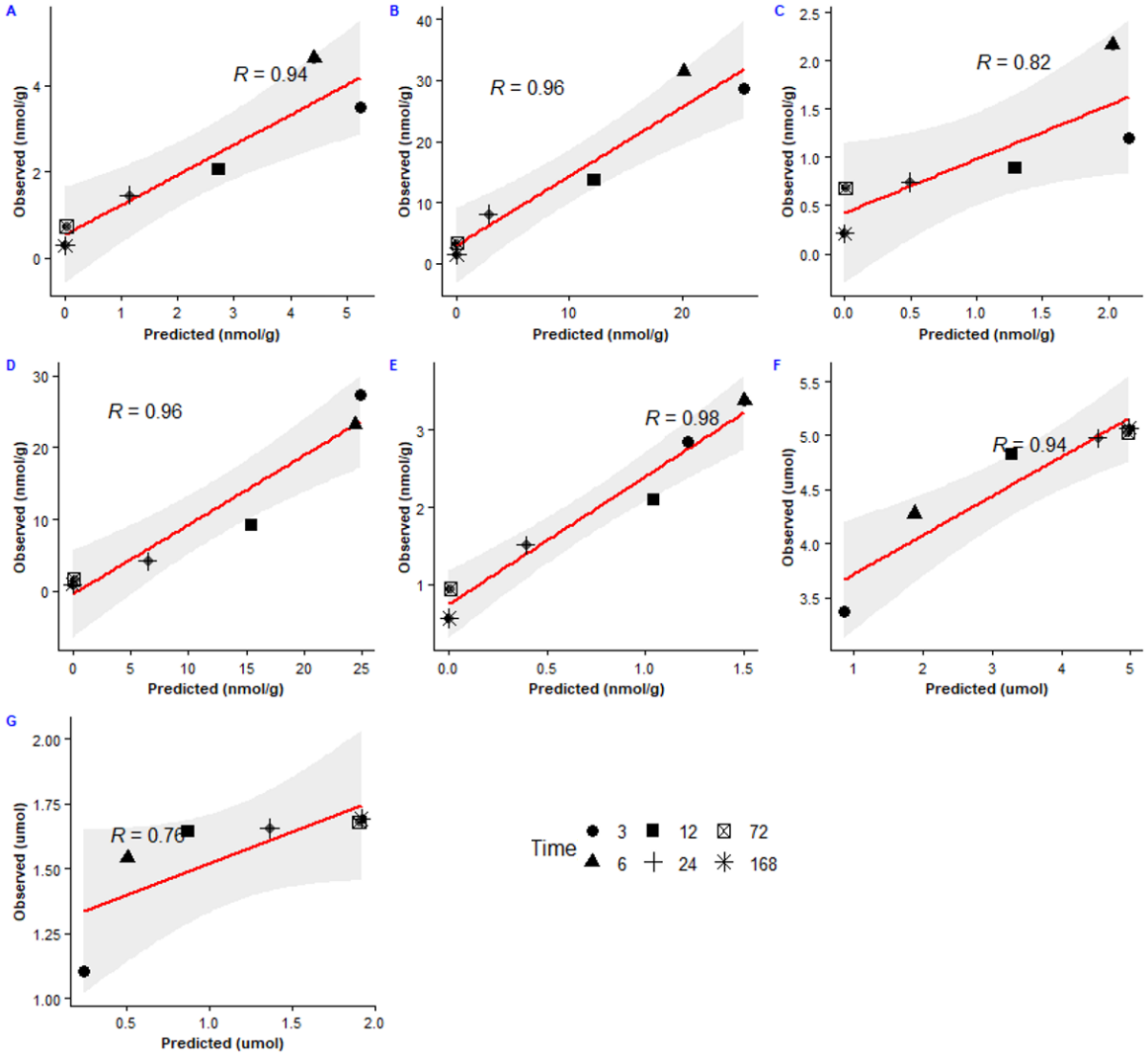

Figure 30: Goodness-of-fit plot for TCIPP for several organs at various time point from 3 to 168 hours. R (correlation coefficient) was above 85% for all the organs using Pearson correlation coefficient (PCC). A represents plasma, B: Liver, C: Brain, D: Kidney, E: Fat, F: Urine and G: Feces.

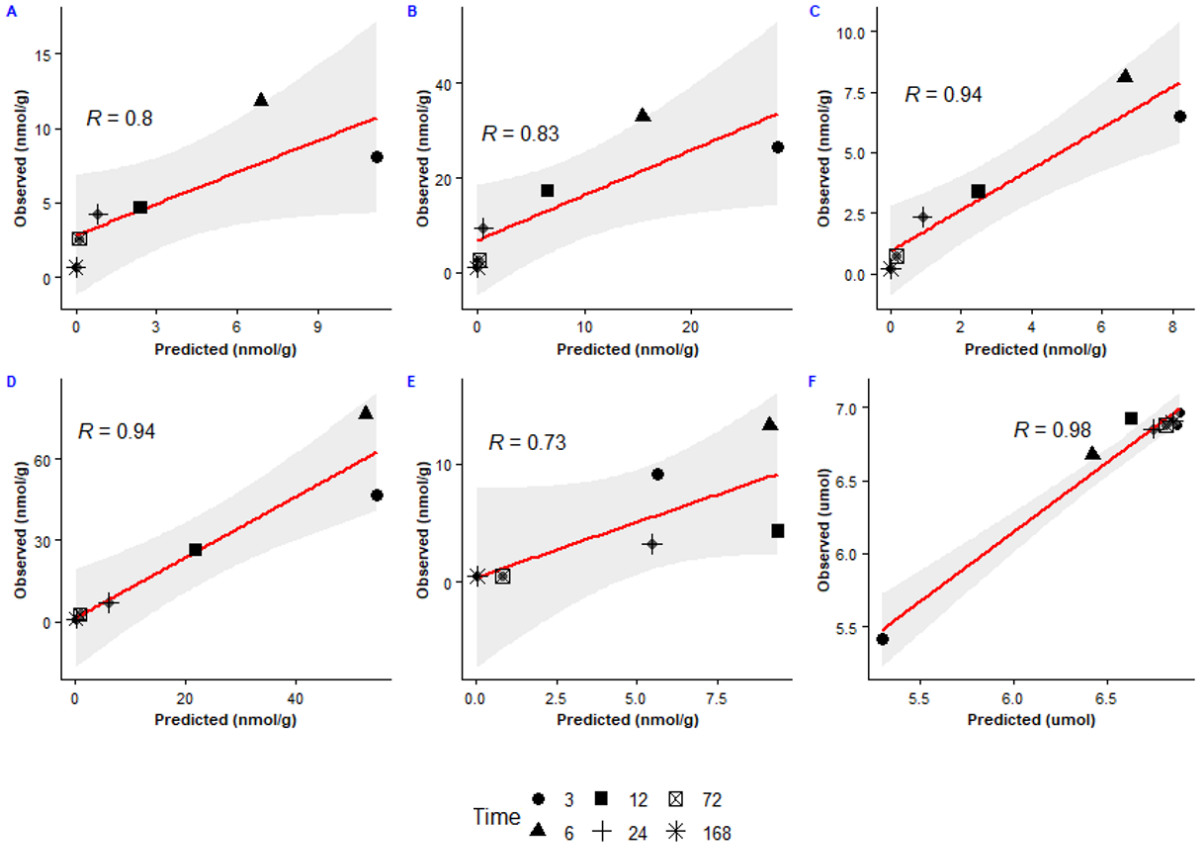

Figure 11: Goodness-of-fit plot for TCEP for several organs at various time point from 3 to 168 hours. R (correlation coefficient) was above 70% for all the organs using Pearson correlation coefficient (PCC). A represents plasma, B: Liver, C: Brain, D: Kidney, E: Fat, and F: Urine.

3.4 Sensitivity Analysis

SA was performed for all the parameters used for developing PBPK and the result has been summarized in Figure , Figure , Figure . As expected, that plasma AUC is having negative correlation towards renal clearance (Cl) in case of TDCIPP (Figure) followed by EHR (kehr_1) and liver partition coefficient (K_liver_plasma). Decrease in renal clearance will lead to increase in plasma AUC as more compound will be getting circulated in the body. Later finding suggest that decreasing the EHR rate and liver blood flow means more plasma levels as less compounds will be distributed in the liver and gut, thus less fecal elimination. Interestingly, metabolic rate constant (Kmliver_bcipp) and body weight (BW) has a positive correlation with the plasma levels. In case of TCIPP, body weight has a profound positive effect on the plasma followed by negative effect from K_liver_plasma and Cl (Figure) similar to TDCIPP. TCEP also show the same pattern towards BW, K_liver_plasma and Cl. Surprisingly, for TCEP fu has the major impact than other parameters (Figure). Decreasing the fu leads to increase in plasma concentration. Vmax (positive) and Km (negative) has the opposite impact for all OPFRs. It suggests that the distribution of both these parameters could improve the plasma concentration profile. For our case, the calculated Km was used for the model.

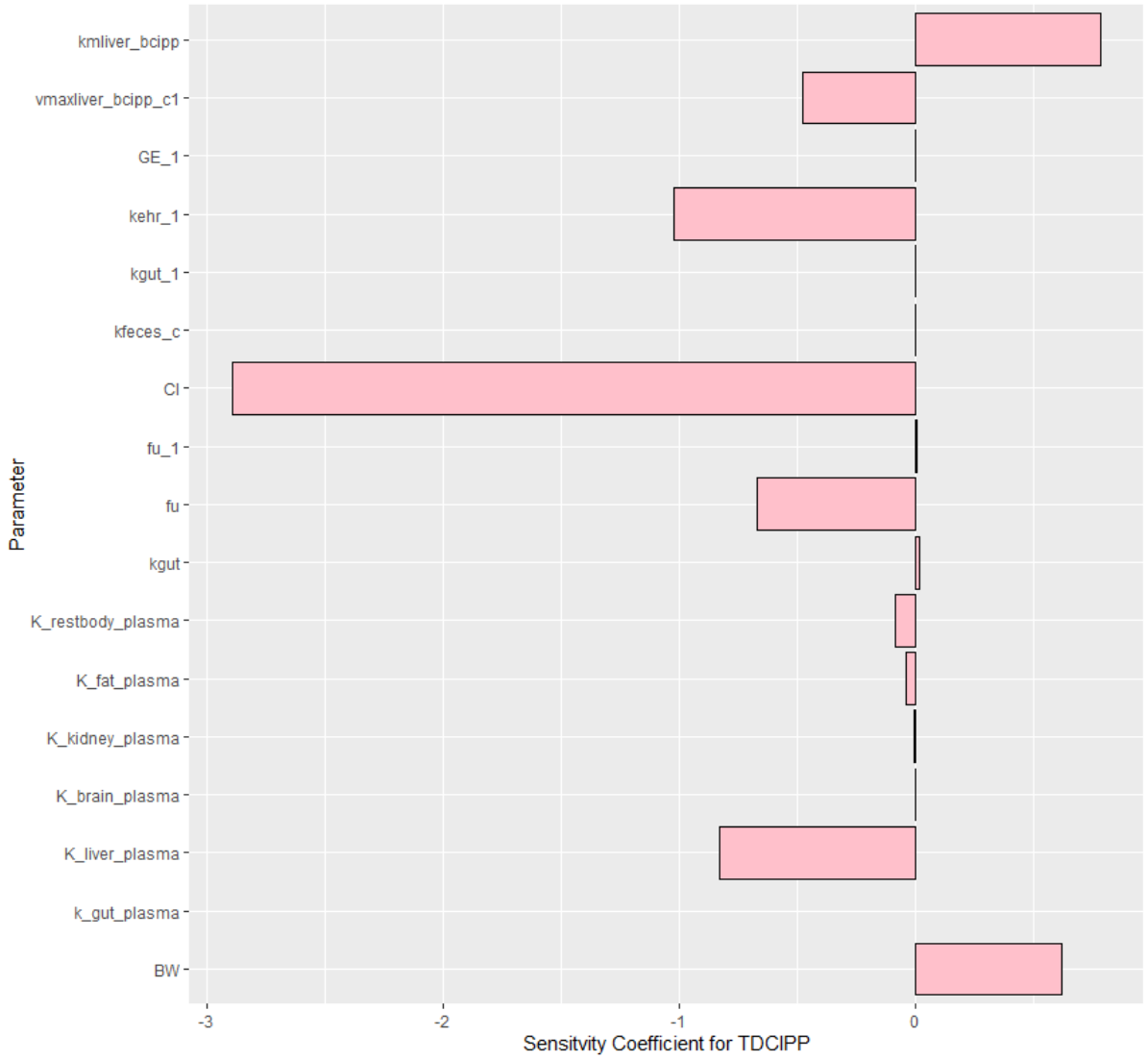

Figure 12: Sensitivity coefficient for TDCIPP. Physiological and biochemical parameters were used for calculating the change in output (plasma AUC) at the dose of 50 µmol/Kg.

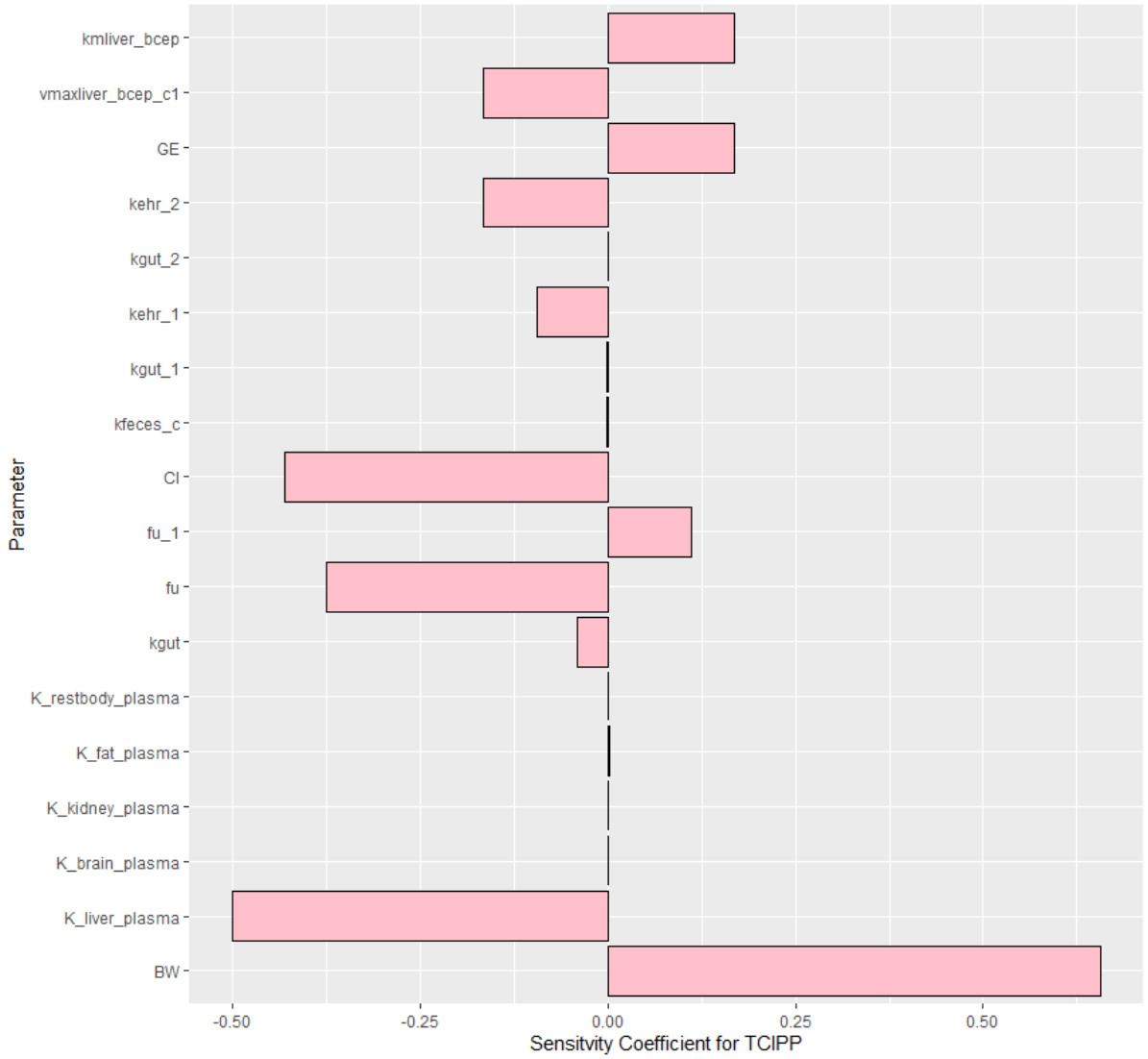

Figure 13: Sensitivity coefficient for TCIPP. Physiological and biochemical parameters were used for calculating the change in output (plasma AUC) at the dose of 50 µmol/Kg.

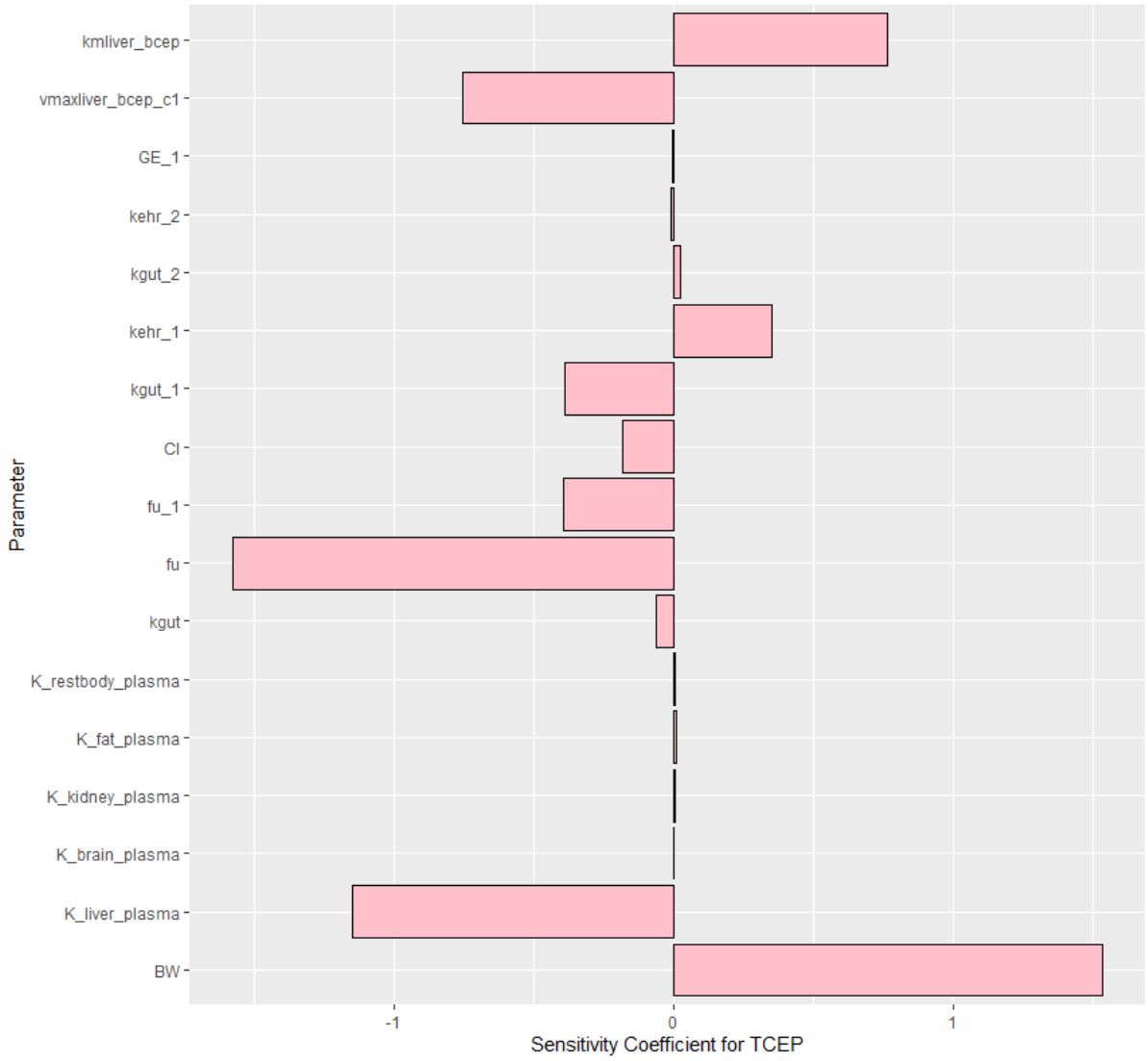

Figure 14: Sensitivity analysis for TCEP. Physiological and biochemical parameters were used for calculating the change in output (plasma AUC) at the dose of 50 µmol/Kg.

4. Discussion

For evaluating the pharmacokinetics of xenobiotics in various organs and tissues, PBPK model serve as an important tool. They can be used to comprehend the relationship between exposure and its effect on the body. In this paper, a PBPK Model for rat was developed to gain insight about tissue disposition properties of three OPFRs. Using a dose of 50 µmol/Kg, we found that perfusion limited kinetic model can explain the concentration-time profile in rat up to a time point. After 24 hours, the perfusion limited PBPK model was not able to explain the disposition in several organs. To improve this, several scenarios like EHR rate, biphasic clearance, separate fu for brain and adipose were considered to slow down the elimination of chemical from the body. This model serves as a framework about how to improve the perfusion limited model and also focus on the prospective that sometime alone perfusion limited PBPK is not enough.

The disposition of all three OPFRs was quite extensive in liver and kidney both being the metabolizing and elimination site. In contrast, the concentration in brain was lower than all

other organs but still, a good quantity of OPFRs was being detected in the brain (TCEP>TDCIPP>TCIPP). All of these molecules follow Lipinski rule of five; a molecular weight less than 500 (TDCIPP: 430.5, TCIPP: 327.6, TCEP: 285.5 g/mol), log P less than 5 (3.65, 2.6, 1.3), hydrogen bond donor 0 (all OPFRs), and hydrogen bond acceptor less than 10 (4 for all), making them a good candidate for permeating the blood-brain-barrier (Neidle 2012). Another major point was that rather than influx, efflux from the brain was quite slow (can be infer based on the elimination phase of concentration time course) for all three OPFRs. It could be due to these compounds bind with specific proteins inside the brain tissue extensively. This type of phenomenon can be explained by permeability rate limited model; however, we considered a separate fu to capture this in our perfusion model which improve the model prediction (fig). The result indicated kinetic related neurotoxic potential of these compounds. As zebrafish study showed that the slow efflux of OPFRs might responsible for their neurotoxic effect. For instance, Li et al. demonstrated that exposure to TDCIPP induce autophagy and potentially down-regulate the expression of neurodevelopmental genes and protein biomarkers (α-1 tubulin, syn 2a, mbp etc.) in zebrafish larvae (Li et al. 2018). It was observed that these compounds metabolize very fast inside the rat, and further mechanistic pathway for neurotoxic potential of metabolites need to be investigated.

Another key point from the simulation was that all OPFRs residence time is longer in the adipose tissue than all other organs. This can be implicated partially to the lipophilicity of these chemicals as their log ko/w correlated with the adipose tissue distribution. However, partition coefficient for adipose tissue was not high for any of three OPFRs but the disposition in the tissue is quite slow. Even adjusting partition coefficient in our model did not result in a good fit (data not shown). Dobrev et al. explained this kind of phenomenon with hexamethyldisiloxane, a class of FRs, which accumulated inside lipoprotein and deep fat, acting as a reservoir (Dobrev et al. 2003). Compounds like chlorodecane (CDC) and dichlorophenyltrichloroethane (DDT) also showed similar trend with lymphatic and lipoprotein sequestration (Soine et al. 1982). Being chemical congener, it is highly likely that OPFRs would also follow the similar mechanism. Keeping separate fu (scenario 4) leads to a good fit of result indicates that there is a difference in the rate by which chemical enters to the fat compartment than it leaves the compartment. Either addition of deep adipose tissue as a sub compartment or permeability limited model can improve the model fitting apart from the approach that we have used here.

Different scenarios considered for building the model improved the prediction accuracy of the model as shown by AIC_c score. For TCEP and TCIPP, scenario 4 where we included time dependent EHR, biphasic clearance and separate fu was the best fit model. Regarding time dependent EHR, it may be possible that other oxidative metabolite was generated after a particular time or the binding sites were saturated leading to variation in EHR rates for these chemicals. Such kind of phenomenon has been observed with several compounds like immunosuppressant mycophenolate mefotil, cholestyramine and valproic acid (VPA) (Roberts et al. 2002). In VPA, the author demonstrated that active enterohepatic recycling (ER) and attenuation of ER at certain time can explain the overshoot of VPA in brain (Padowski and Pollack 2012). Separate fu and biphasic clearance was required since both of the chemicals showed extremely slow elimination after a particular time point which was difficult

to model through perfusion limited model without adding further rate constants. Interestingly for TDCIPP, scenario 1 which is inclusion of EHR was able to explain the data. Based on the experimental data point and simulation plots, it was observed that TDCIPP follows a linear kinetics, there is no saturation observed at particular time point. This can be one of the reasons that biphasic clearance and separate fu was not required. Considering these scenarios for building the PBPK model opens the door for conducting further experiments to understand toxicokinetic of OPFR.

The developed PBPK model was robust enough to predict the dynamic distribution of OPFRs in all the rat tissues; the median value predicted by the model was within two times the experimental data. The uncertainty was included in the model for biochemical parameters and multiple iterations were run to capture the observed concentration within predicted intervals. As per commonly applied criterion for PBPK, the observed and predicted concentration can be within two folds for general compounds (Shebley et al. 2018) observed in out model with data from Minigeshi et al. (MINEGISHI et al. 1988). In case of two independent data sets for TDCIPP, the model was able to explain all the organs except brain and adipose tissue. Since the model has been optimized for higher dose, additional rate constant might need to be introduced for the low dose 24 times lower). Another reason might be that influx rate for adipose and brain in case of extremely low dose can be higher or inclusion of influx and efflux rate can better explain. The model is underestimating the concentration by 3-4-fold only at the starting time points, at later time points the model is able to explain the kinetics. But further data is required to understand the reason behind this. Also, this may be explained by permeability limited model, so the further improvement in the model can be integrating perfusion limited PBPK with permeability limited for specific organs.

SA performed for PBPK model was based on 2% change in the physiological and biochemical parameter after single exposure and measuring the plasma AUC till 168-hour post exposure. Physiological parameter like body weight and blood flow to liver from plasma is highly related to variation in AUC suggesting the importance of physiological parameters. Regarding biochemical parameters, clearance (urine elimination rate constant) and fu has the major impact on plasma AUC. Free fraction can play an important role in limiting the elimination of compound from the living body.

5. Discussion on the model and Conclusion

PBPK models are currently used for exposure, kinetics, inter-species and toxicological risk assessment. Current model serves as an important starting point for extrapolation to other species and understanding the toxicokinetic in human beings. In this model, the metabolic parameters were taken from in-vitro study and based on IVIVE they were incorporated in the PBPK model. Further, the developed model was evaluated at several doses where experimental data were available. For instance, model was able to explain the kinetics data at both high and low dose TDCIPP, showing the model reliability. The metabolite has been included and major compartments of living beings were taken extending the usage of this model to understand the kinetics of OPFRs in several species. Several scenarios of this model provide understanding about the approach on how to improve such kinds of model.

Experimental data was quite limited for developing the PBPK model, several parameters were optimized rather than calculated. There is a future scope of improving this model by integrating organ specific permeation limited model with perfusion limited. In addition, for other BFRs like HBCDD, lymphatic circulation has been introduced for slowing down the elimination of chemicals (Emond et al. 2021), it may be possible that the same has been happening in OPFRs. Currently, there is no experimental evidence for this, so it was not included in this model. As an additional step of model validation and reducing uncertainty, the chemical and all the minor metabolites can be measured in several organs, for now we have considered major metabolite only. The results from this model are quite promising for applying in field of risk assessment for OPFRs. To date, no PBPK model for three OPFRs has been developed for predicting the chemical kinetics in several tissues and organs. This model can be further extrapolated to predict the OPFRs kinetics in human as a prototype model and can further optimized on availability of experimental data in near future. This can be used for reconstructed exposure based on urine or plasma data to understand how much human population is being exposed on daily basis with OPFRs by several routes. Some of the important understanding from this model is the slow efflux from brain, OPFRs getting accumulated in adipose tissue for longer time and the role of EHR for explaining the longer half-life in rats.

Declaration of Competing Interest

The author declare that they have no known competing financial interest or personal relationship that could have appeared to influence the work reported in this paper.

Acknowledgments

This study was financially supported by Marie Skłodowska-Curie “Neurosome project” under grant agreement no. 766251 funded by European Union as well as FlameRisk project under grant agreement number RTI2018-095466-B-I00 funded by the Spanish Ministry of Science, Innovation and Universities. This publication reflects only the author views. The community and other funding organizations are not liable for any use made of the information contained.

Credit Author Statement

D. Deepika: Methodology, Investigation, Writing-original draft; R.P. Sharma: Methodology, Review and Supervision; M. Schuhmacher: Funding acquisition, Review and Supervision; and Vikas Kumar: Funding acquisition, Methodology, Review and Supervision.

References

Bajard L, Melymuk L, Blaha L. 2019. Prioritization of hazards of novel flame retardants using the mechanistic toxicology information from ToxCast and Adverse Outcome Pathways. Environ Sci Eur 31:14; doi:10.1186/s12302-019-0195-z.

Blum A, Behl M, Birnbaum LS, Diamond ML, Phillips A, Singla V, et al. 2019. Organophosphate Ester Flame Retardants: Are They a Regrettable Substitution for Polybrominated Diphenyl Ethers? Environ Sci Technol Lett 6:638–649; doi:10.1021/acs.estlett.9b00582.

Bois FY. 2009. GNU MCSim: Bayesian statistical inference for SBML-coded systems biology models. Bioinformatics 25:1453–1454; doi:10.1093/bioinformatics/btp162.

Borowy CS AJP. 2022. Zero and First Order Kinetics. StatPearls [Internet] Treasure Isl StatPearls Publ. Available: https://www.ncbi.nlm.nih.gov/books/NBK499866/.

Brown RP, Delp MD, Lindstedt SL, Rhomberg LR, Beliles RP. 1997. Physiological Parameter Values for Physiologically Based Pharmacokinetic Models. Toxicol Ind Health 13:407–484; doi:10.1177/074823379701300401.

Chapman DE, Michener SR, Powis G. 1991. Metabolism of the flame retardant plasticizer tris(2-chloroethyl)phosphate by human and rat liver preparations. Toxicol Sci 17:215–224; doi:10.1093/toxsci/17.2.215.

Chupeau Z, Bonvallot N, Mercier F, Le Bot B, Chevrier C, Glorennec P. 2020. Organophosphorus Flame Retardants: A Global Review of Indoor Contamination and Human Exposure in Europe and Epidemiological Evidence. Int J Environ Res Public Health 17:6713; doi:10.3390/ijerph17186713.

Dobrev ID, Reddy MB, Plotzke KP, Varaprath S, McNett DA, Durham J, et al. 2003. Closed-Chamber Inhalation Pharmacokinetic Studies with Hexamethyldisiloxane in the Rat. Inhal Toxicol 15:589–617; doi:10.1080/08958370390205083.

Emond C, DeVito MJ, Birnbaum LS. 2021. A PBPK model describing the pharmacokinetics of γ-HBCD exposure in mice. Toxicol Appl Pharmacol 428:115678; doi:10.1016/j.taap.2021.115678.

Esplugas R, Rovira J, Mari M, Fernández-Arribas J, Eljarrat E, Domingo JL, et al. 2022. Emerging and legacy flame retardants in indoor air and dust samples of Tarragona Province (Catalonia, Spain). Sci Total Environ 806:150494; doi:10.1016/j.scitotenv.2021.150494.

EUROPEAN COMMISSION BANS HARMFUL CLASS OF FLAME RETARDANTS IN TVS - NEW MEASURES MAKE APPLIANCES MORE SUSTAINABLE. 02 Mar 2020. Available: https://ergo-project.eu/european-commission-bans-harmful-class-of-flame-retardants-in-tvs-new-measures-make-appliances-more-sustainable/.

Hoffman K, Daniels JL, Stapleton HM. 2014. Urinary metabolites of organophosphate flame retardants and their variability in pregnant women. Environ Int 63:169–172; doi:10.1016/j.envint.2013.11.013.

Hogberg HT, de Cássia da Silveira E Sá R, Kleensang A, Bouhifd M, Cemiloglu Ulker O, Smirnova L, et al. 2021. Organophosphorus flame retardants are developmental neurotoxicants in a rat primary brainsphere in vitro model. Arch Toxicol 95:207–228; doi:10.1007/s00204-020-02903-2.

Hou R, Xu Y, Wang Z. 2016. Review of OPFRs in animals and humans: Absorption, bioaccumulation, metabolism, and internal exposure research. Chemosphere 153:78–90; doi:10.1016/j.chemosphere.2016.03.003.

Li R, Zhang L, Shi Q, Guo Y, Zhang W, Zhou B. 2018. A protective role of autophagy in TDCIPP-induced

developmental neurotoxicity in zebrafish larvae. Aquat Toxicol 199:46–54; doi:10.1016/j.aquatox.2018.03.016.

Lynn RK, Wong K, Garvie-Gould C, Kennish JM. 1981. Disposition of the flame retardant, tris(1,3-dichloro-2-propyl) phosphate, in the rat. Drug Metab Dispos 9: 434–441.

McNally K, Sams C, Hogg A, Lumen A, Loizou G. 2021. Development, Testing, Parameterisation and Calibration of a Human PBPK Model for the Plasticiser, Di-(2-propylheptyl) Phthalate (DPHP) Using in Silico, in vitro and Human Biomonitoring Data. Front Pharmacol 12; doi:10.3389/fphar.2021.692442.

Merrill EA, Clewell RA, Gearhart JM, Robinson PJ, Sterner TR, Yu KO, et al. 2003. PBPK predictions of perchlorate distribution and its effect on thyroid uptake of radioiodide in the male rat. Toxicol Sci 73:256–269; doi:10.1093/toxsci/kfg080.

MINEGISHI K, KUREBAYASHI H, NAMBARU S, MORIMOTO K, TAKAHASHI T, YAMAHA T. 1988. Comparative studies on absorption, distribution, and excretion of flame retardants halogenated alkyl phosphate in rats. Eisei kagaku 34:102–114; doi:10.1248/jhs1956.34.102.

Neidle S. 2012. Design Principles for Quadruplex-binding Small Molecules. In: *Therapeutic Applications of Quadruplex Nucleic Acids* (S. Neidle, ed). Elsevier:Boston. 151–174.

Nomeir AA, Kato S, Matthews HB. 1981. The metabolism and disposition of tris(1,3-dichloro-2-propyl) phosphate (fyrol FR-2) in the rat. Toxicol Appl Pharmacol 57:401–413; doi:10.1016/0041-008X(81)90238-6.

on Chemical Safety IP, for the Sound Management of Chemicals I-OP. 2010. Characterization and application of physiologically based phamacokinetic models in risk assessment. iv, 92 p.

Padowski JM, Pollack GM. 2012. Influence of Enterohepatic Recycling on the Time Course of Brain-to-Blood Partitioning of Valproic Acid in Rats. Drug Metab Dispos 40:1846–1853; doi:10.1124/dmd.112.045500.

Poma G, Glynn A, Malarvannan G, Covaci A, Darnerud PO. 2017. Dietary intake of phosphorus flame retardants (PFRs) using Swedish food market basket estimations. Food Chem Toxicol 100:1–7; doi:10.1016/j.fct.2016.12.011.

Roberts MS, Magnusson BM, Burczynski FJ, Weiss M. 2002. Enterohepatic Circulation. Clin Pharmacokinet 41:751–790; doi:10.2165/00003088-200241100-00005.

Schreder E. 2019. Europe bans most harmful class of flame retardants in TVs. Safer Chem Heal Fam. Available: https://saferchemicals.org/2019/10/01/europe-bans-most-harmful-class-of-flame-retardants-in-tvs/.

Sharma RP, Kumar V, Schuhmacher M, Kolodkin A, Westerhoff H V. 2020. Development and evaluation of a harmonized whole body physiologically based pharmacokinetic (PBPK) model for flutamide in rats and its extrapolation to humans. Environ Res 182:108948; doi:10.1016/j.envres.2019.108948.

Shebley M, Sandhu P, Emami Riedmaier A, Jamei M, Narayanan R, Patel A, et al. 2018. Physiologically Based Pharmacokinetic Model Qualification and Reporting Procedures for Regulatory Submissions: A Consortium Perspective. Clin Pharmacol Ther 104:88–110; doi:10.1002/cpt.1013.

Soine PJ, Blanke R V, Guzelian PS, Schwartz CC. 1982. Preferential binding of chlordecone to the protein and high density lipoprotein fractions of plasma from humans and other species. J Toxicol Environ Health 9:107–118; doi:10.1080/15287398209530146.

Team Rs. 2015. RStudio: Integrated Development Environment for R [Internet]. Boston, MA. Available:

http://www.rstudio.com/.

U. S. Environmental Protection Agency. 2006. Approaches for the Application of Physiologically Based Pharmacokinetic (PBPK) Models and Supporting Data in Risk Assessment. Epa/600/R-05/043F.

Van den Eede N, Maho W, Erratico C, Neels H, Covaci A. 2013. First insights in the metabolism of phosphate flame retardants and plasticizers using human liver fractions. Toxicol Lett 223:9–15; doi:10.1016/j.toxlet.2013.08.012.

Van den Eede N, Tomy G, Tao F, Halldorson T, Harrad S, Neels H, et al. 2016. Kinetics of tris (1-chloro-2-propyl) phosphate (TCIPP) metabolism in human liver microsomes and serum. Chemosphere 144:1299–1305; doi:10.1016/j.chemosphere.2015.09.049.

Wang C, Chen Z, Lu Y, Wang L, Zhang Y, Zhu X, et al. 2020a. Neurotoxicity and related mechanisms of flame retardant TCEP exposure in mice. Toxicol Mech Methods 30:490–496; doi:10.1080/15376516.2020.1765060.

Wang X, Shan G, Zhu L. 2020b. Estimation of internal human daily intakes of organophosphate esters using one-compartment toxicokinetic model in the whole blood from Hebei Province, China. Environ Res 186:109493; doi:10.1016/j.envres.2020.109493.

Yang J, Zhao Y, Li M, Du M, Li X, Li Y. 2019. A review of a class of emerging contaminants: The classification, distribution, intensity of consumption, synthesis routes, environmental effects and expectation of pollution abatement to organophosphate flame retardants (opfrs). Int J Mol Sci 20:2874; doi:10.3390/ijms20122874.

Yang Y, Chen P, Ma S, Lu S, Yu Y, An T. 2022. A critical review of human internal exposure and the health risks of organophosphate ester flame retardants and their metabolites. Crit Rev Environ Sci Technol 52:1528–1560; doi:10.1080/10643389.2020.1859307.

Zhang X, Zou W, Mu L, Chen Y, Ren C, Hu X, et al. 2016. Rice ingestion is a major pathway for human exposure to organophosphate flame retardants (OPFRs) in China. J Hazard Mater 318:686–693; doi:10.1016/j.jhazmat.2016.07.055.

Zhu T, Zheng X-B, Yan X, Tang B, Zheng J, Luo X-J, et al. 2020. In vivo distribution and biotransformation of Tris (1,3-dichloro-2-propyl) phosphate in mice. Environ Pollut 263:114595; doi:10.1016/j.envpol.2020.114595.

Unravelling sex-specific BPA toxicokinetics in children using a pediatric PBPK model

Abstract

Bisphenol A (BPA) is a widely known endocrine disruptor (ED) found in many children's products such as toys, feeding utensils, and teething rings. Recent epidemiology association studies have shown postnatal BPA exposure resulted in developing various diseases such as diabetes, obesity, and neurodegeneration, etc., later in their lives. However, little is known about its sex-specific metabolism and consequently, its internal exposure. The aim of this study was to develop a sex-specific pediatric physiologically based pharmacokinetic model (PBPK) for BPA to compare their toxicokinetic differences. First, the published adult PBPK model was re-validated and then this model was interpolated extended to incorporate pediatric sex-based physiological and biochemical parameters. We have used both the classical body weight and the ontogeny-based scaling approach to interpolate the metabolic process. Then the various pharmacokinetic attributes of models with the mentioned two scaling approaches were compared with the adult model. Further, sex-specific PBPK model with an ontogeny scaling approach was preferred to evaluate the pharmacokinetic differences. Moreover, this model was used to reconstruct the BPA exposure from two cohorts (Helix and PBAT Cohort) comprising 7 EU countries. The half-life of BPA was predicted to be 1.5 higher in girls than boys at similar exposure levels. Our model estimated the BPA exposure of pediatrics approximately 1500 times higher than the recent tolerable daily intake (TDI) set by European Food Safety Authority (EFSA) i.e., 0.04 ng/Kg BW/ day. Our model demonstrated feasibility of extending the adult PBPK to sex specific pediatric, thereby improving the sex-based health risk assessment.

Keywords: Bisphenol A; Pediatric PBPK; Pharmacokinetic; Sex-specific risk; children cohort; endocrine disruptor

1. Introduction

Humans are being exposed to bisphenol A (BPA) through plastic food, beverage containers, thermal receipts, medical devices, canned food, and sealant with detectable levels in urine all across the globe (Harley et al. 2013; Braun and Hauser 2011; Bushnik et al. 2010). Several human studies have reported BPA exposure associated with adverse health outcomes particularly at their early age (Nalbantoğlu et al. 2021; Healy et al. 2015; Eng et al. 2013). Since BPA has endocrinological activity and can mimic hormones like estrogen, dysregulating hormone-regulated pathways, thereby affecting normal growth and development (Ohore and Zhang 2019). BPA exposure during childhood is associated with altered neurodevelopment (Roen et al. 2015), obesity, precocious diabetes, asthma, immunity impairment, and metabolic diseases among other disorders (Deepika et al. 2020; Ohore and Zhang 2019; Braun and Hauser 2011).

BPA has a short half-life (approximately 4-6 hours) in adult humans (Sasso et al. 2020; Völkel et al. 2005; Tsukioka et al. 2004). BPA is metabolized into two major metabolites such as BPA glucuronide (BPAG) and BPA sulfates (BPAS) in the liver and intestine (Karrer et al. 2018). The formation of BPAG is majorly regulated by UGT2B15, a uridine diphosphate glucuronosyltransferases enzyme (UGTs),, and BPAS is controlled by SULT1A1, a sulfotransferase enzyme (SULT), (Neumann et al. 2016). The levels of these hepatic enzymes are different for children than adults, leading to variations in the extent of the metabolism process (Karrer et al. 2018). In addition, the pediatric population is more susceptible to BPA exposure and its associated health risk than adults (Bushnik et al. 2010; Lv et al. 2016; Shelby 2008; Stahlhut et al. 2009). Moreover, several studies have shown the sex-related differences associated to BPA exposure and its adverse effects (Kim et al. 2003; Takeuchi and Tsutsumi 2002). For example, in utero BPA exposure was associated with alteration in the timing of pubertal development (Kasper-Sonnenberg et al. 2017; Miao et al. 2017) and neurotoxicity like autism spectrum disorder in girls only (Hansen et al. 2021). Toxicokinetic differences can exist based on sex due to metabolic differences (enzyme abundance), absorption kinetics (lower body-weight, low blood flow, less plasma volumes), and physiological changes (Schwartz 2003). A study by Caporossi and Papaleo (2015) investigated about different impact of BPA in males and females and concluded that in toxicology, the gender differences for BPA should be assessed. The variations in toxicokinetic, sex-differences and exposure can be explored further using a physiologically based pharmacokinetic model (PBPK). The tolerable daily intake (TDI) for BPA has been determined by EFSA (European Food Safety Authority) based on adverse effects on immune system. EFSA has reduced the BPA TDI from 4 µg/kg BW/day (temporary-TDI) in 2015 to 0.04 nanogram (ng) per kilogram body weight (BW) taking into account BPA adverse effects and uncertainty factors (Bisphenol A: EFSA draft opinion proposes lowering the tolerable daily intake 2021). Nevertheless, the question remains whether the TDI should be same for the adult and pediatric populations. Another debatable aspect is should we include a separate TDI based on sex. To resolve such issues, PBPK model can be utilized incorporating the age and sex.

PBPK model has been widely used for dosimetry risk assessment and is recommended for toxicity testing in the field of pharmaceuticals and the environment (Sharma et al. 2017; Wagner et al. 2015). PBPK model for BPA in monkeys, adults (Fisher et al. 2011; Teeguarden

et al. 2005), pregnant females (Sharma et al. 2018), and generic model from infants to 25 years (Karrer et al. 2018) have been developed. However, to the best of our knowledge, no PBPK model for BPA is currently available that captures the pharmacokinetics and sex differences in children of growing age and evaluates the health risk. In this work, we have modified and refined an adult PBPK model developed by Sharma et al. (2018). The aim of this work was to first extrapolate the adult model for the pediatric population based on ontogeny and body-weight scaling. Anatomical and physiological changes were incorporated based on an earlier paper published by our group (Deepika et al. 2021). Further, changes in the biochemical parameters (absorption, distribution and elimination) and sex were incorporated for improving the sex-specific prediction property of the PBPK model. Secondly, a dosimetry risk assessment was conducted to evaluate exposure in boys and girls. Thirdly, the model was used to compare the changes in pharmacokinetic properties for BPA in children (both boys and girls) with adults suggesting the need for the pediatric PBPK model to improve risk assessment.

2. Methodology

2.1 Overall methodological concept

The present study aims to evaluate the pharmacokinetic and sex-specific differences in children compared to adults and highlight the risk associated with BPA exposure. This study includes the validation of an adult PBPK model. It was followed by interpolation of the adult PBPK model to develop a pediatric (boys) PBPK model with two approaches (body-weight and ontogeny-scaling) and comparison with the adult model. Then pediatric PBPK model for further refined for girls, and pharmacokinetics like Area under Curve (AUC), bioavailability (F), Mean Residence Time (MRT), and half-life ($t_{1/2}$) were compared in boys and girls. At last, exposure was reconstructed using data from two child cohorts. A schematic diagram and workflow for the development and evaluation of the Pediatric PBPK model have been presented in Figure 1.

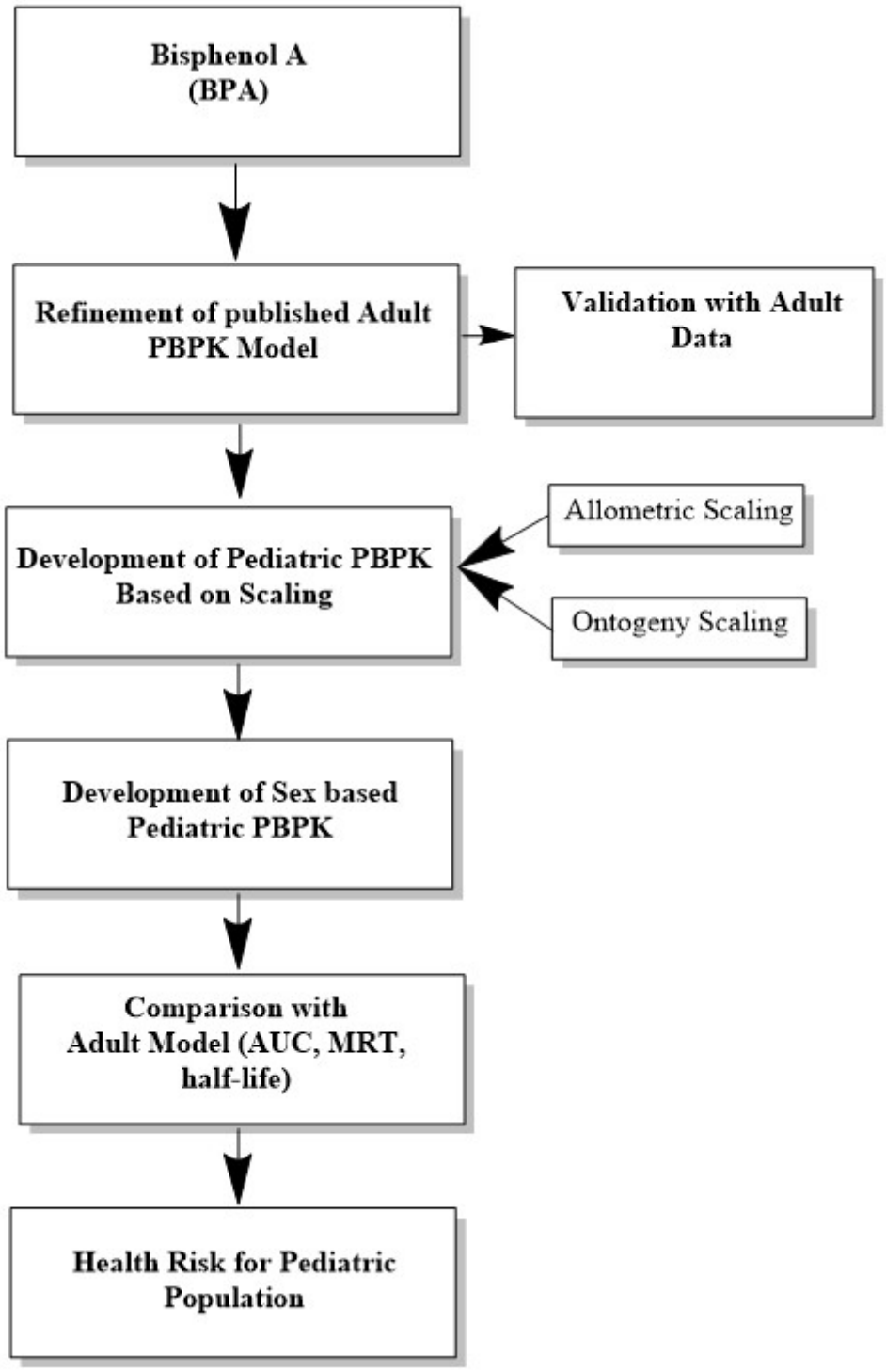

Figure 1: Workflow for development and evaluation of the Pediatric PBPK model. The pediatric PBPK Model is composed of physiological parameters (organ volume and blood flow) and biochemical parameters (A: Absorption, D: Distribution, M: Metabolism and E: Elimination). Scaling of biochemical parameters can be performed by allometric scaling (body-weight specific) and ontogeny scaling (enzymatic change specific). For sex based PBPK, only ontogeny scaling was used. PK (pharmacokinetic parameters) like AUC (area under curve), half-life and MRT (mean residence time) can be calculated and compared with adults and based on sex. Pediatric PBPK model serves as framework for risk assessment from chemicals like Bisphenol A (BPA) in boys and girls.

2.2 Adult and Pediatric PBPK Model

The pediatric PBPK model with eight compartments was adapted from Sharma et al. (2018) (Figure 2). It consists of the following compartments: gut, liver, brain, adipose tissue, kidney, skin, gonads, and rest of the body for describing the kinetics of free BPA and its metabolites (BPAG & BPAS). Biochemical parameters have been mentioned in Table 1 (mentioned below) and Table 2 (supp file). Initially adapted adult PBPK model was refined by including dynamic physiological equations published by our group (Deepika et al. 2021). These equations are provided in the supplementary file. Then this model was validated with the the human data from Thayer et al. (2015). the human experimental study involved administration of a single oral dose of 100 µg/kg BW/day of deuterated BPA (d6-BPA) to 12 healthy volunteers. Blood and urine samples were analysed for free BPA and its metabolites. The human adult PBPK model predictions were compared with the plasma data from the human study (Thayer et al. 2015). After validating the adult model, the same model was adapted for the pediatric population (age 6 to 12 years), incorporating dynamic physiological and biochemical changes for children described in section 2.3. Only oral exposure was considered in this model. The model was coded in R program 1.3.1093 with MCSIM version 6.2.0 (Bois 2009).

Table 1: Partition Coefficient for tissue to plasma and other parameters and their statistical distribution used in PBPK Model for BPA. LN means log normal, first value in bracket is the mean and second value is standard deviation in LN space. Partition coefficient was taken similar for adult and children.

Parameter	**Value (Distribution)**	**Reference**
Molecular Weight (g/mol)	228.29	(Sharma et al. 2018)
GEC (hr^{-1})	3.5	(Sharma et al. 2018)
Vmax gluC*	707537	(Sharma et al. 2018)
Vmax SulfC*	11657	(Sharma et al. 2018)
$SF_{UGT2B15}$	0.67	(Ladumor et al. 2019)**
$SF_{SULT1A1}$**	1.25	(Ladumor et al. 2019)**
Liver: Plasma	LN (0.73, 1.1)	(Doerge et al. 2011; Fisher et al. 2011; Karrer et al. 2018; Sharma et al. 2018)
Brain: Plasma	LN (2.8, 1.1)	(Doerge et al. 2011; Fisher et al. 2011; Karrer et al. 2018; Sharma et al. 2018)
Kidney: Plasma	LN (0.858, 1.1)	(Csanády et al. 2002; Doerge et al. 2011; Fisher et al. 2011; Karrer et al. 2018; Sharma et al. 2018)
Adipose Tissue: Plasma	LN (5.0, 1.1)	(Doerge et al. 2011; Fisher et al. 2011; Karrer et al. 2018; Sharma et al. 2018)
Skin: Plasma	LN (5.7, 1.1)	(Doerge et al. 2011; Fisher et al. 2011; Karrer et al. 2018; Sharma et al. 2018)
Gonads: Plasma	LN (2.6, 1.1)	(Sharma et al. 2018)

* Vmax gluC represents glucuronidation of BPA in liver (nm/h/BW) and Vmax SulfC represents sulfation of BPA in liver (nm/h/BW). ** SF represents scaling factor calculated in children based on ontogeny changes by Ladumor et al. (2019).

2.3 Model physiology and biochemical parameterization

Dynamic growth was considered for all the organs based on the children's body-weight, height, and surface area. The equations were taken from our previously published paper (also provided in supp file), for the detail information on equations, please refer to the original

article published by Deepika et al. For biochemical changes, the partition coefficient for liver, fat, brain, skin, and kidney is provided in Table 1 and was obtained from Sharma et al. (Sharma et al. 2018) and the study of different authors (Csanády et al. 2002; Doerge et al. 2011; Fisher et al. 2011). The elimination of BPA follows rapid metabolism in the liver and intestine and subsequently urinary excretion. BPA undergoes biotransformation by phase II enzymes that include glucuronidation by UDP-glucuronyl transferase UGT2B15 and sulfation by SULT1A1 in human beings. The rate of reaction for glucuronidation and sulfation was derived using the in-vitro to in-vivo extrapolation (IVIVE) scaling approach for adults based on eq. 1. In eq. 1, MPPGL refers to microsomal protein per gm of the liver. The scaling approach is based on Michaelis-Menten kinetic provided in eq. 2. In eq. 2, *V* represents the measured velocity of enzyme-catalyzed reaction, S represents substrate concentration, V_{max} represents maximum reaction velocity per whole body-weight (nM/hr), and K_m (nM) is Michaelis Menten constant. Based on eq. 2, Vmax values for glucuronidation and sulfation have been calculated as provided in Table 1. Further detail about scaling can be found in the paper by Sharma et al. (Sharma et al. 2018).

$$Vmax_{(liver)} = \frac{\left(Vmax_{(in-vitro)} * MPPGL * Vliver\right)}{BW^{0.75}} \qquad eq.1$$

$$V = \frac{V_{max}[S]}{K_m + [S]} \qquad eq.2$$

To interpolate the metabolic process in children from the adult, allometric (eq. 3), which takes into account children's body-weight, and ontogeny (eq.4), which takes into account an enzyme abundance scaling, were used. Based on the observation reported by Ladumor et al. (2019) that in children a higher fractional contribution of sulfation process over glucuronidation in metabolizing BPA was considered (Ladumor et al. 2019). In the ontogeny-based model, we integrated this information by using a scaling factor ($SF_{children}$) for individual enzymes calculated by Ladumor et al. (2019), which was 1.25 for SULT1A1 and 0.67 for UGT2B15 for children using eq. 4. It was calculated based on selective quantitative proteomic analysis of UGTs in the human liver samples from 137 pediatric and 37 adult samples and studying SULT1A1 by a robust LC-MS/MS proteomics methodology by Ladumor et al. (2019).

$$Adjusted\ V_{max1} = V_{maxadult} * BW^{0.75} \qquad eq.3$$

$$Adjusted\ V_{max2} = V_{maxadult} * SF_{children} \qquad eq.4$$

Here, Adjusted Vmax2 is Vmax of children based on ontogeny scaling (nM/hr), $V_{maxadult}$ refers to maximum rate of reaction in adults (nM/hr) and $SF_{children}$ refers to scaling factor based on age depended enzyme abundance.

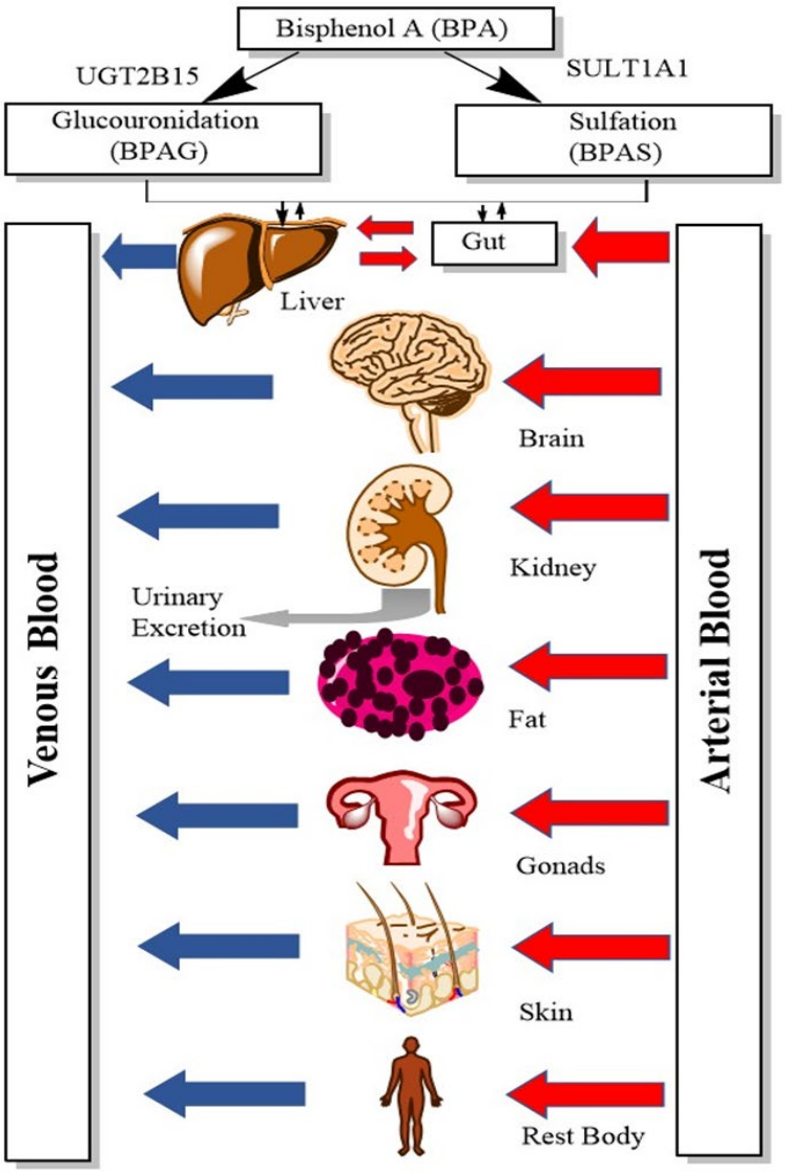

Figure 2: Physiologically Based Pharmacokinetic (PBPK) Model for Bisphenol A (BPA) in human. Two types of liver and gut enzymes are involved in metabolism of BPA: Isoform of UGT2B15 responsible for glucuronidation (BPAG) and SULT1A1 for sulfation (BPAS). Metabolisms are rapidly excreted in urine from human body. UGT stands for uridine diphosphate-glucouronosyl transferase, SULT for sulfotransferase.

2.4 Pharmacokinetic analysis for pediatric PBPK

The pediatric PBPK model was used to compare the simulated pharmacokinetic parameters in adults and children from both the scaling techniques. Predicted plasma concentration-time data was used to calculate the maximum concentration (Cmax, nM), $t_{1/2}$ (hr), and $AUC_{0\text{-}24}$ using trapezoidal rule (eq. five). The half-life was calculated using elimination rate constant (K_{el}, hr^{-1}) based on eq. 6. Bioavailability (F) is the percentage of free BPA that actually reaches the systemic circulation and is calculated based on eq. 7. Mean Residence time (MRT, hr) was defined by the average time a molecule stays in the body. When the chemical follows first-order kinetics, MRT is defined by eq. 8. In eq. 8, AUMC represents (Area under the first

moment curve), c represents the concentration of chemical in the plasma, and *t* represents the time.

Formula	**Eq. Num.**
$AUC_{0-24} = \int_{t1}^{t2} C * dt$	$eq.5$
$t_{1/2} = \frac{In(2)}{K_{el}}$	$eq.6$
$F = \frac{AUC_{oral}}{Dose_{oral}} * \frac{Dose_{IV}}{AUC_{IV}}$	$eq.7$
$MRT = \frac{AUMC}{AUC} = \frac{t * c(t)}{c(t)}$	$eq.8$

AUC: area under curve, t: time, c: concentration, t1/2: half-life, In: logarithmic, Kel: elimination constant, AUCoral: area under curve from oral exposure, AUCIV: area under curve from intravenous exposure, DoseIV: intravenous dose, MRT: mean residence time, and AUMC: area under first moment time curve.

2.5 Ontogeny based Pediatric PBPK Model based on Sex

After developing the pediatric PBPK Model for boys, the same model was further refined for girls. The physiological parameters were changed based on published equations by our group (Deepika et al. 2021) (mentioned in supp file). In biochemical parameters, only metabolic parameters were changed keeping rest of the parameters similar to the previous adult model. The metabolic sex differences present in girls, can be understood by changes in Phase II metabolism, especially UGTs and SULTs. For instance, a study by Gallagher et al. took human liver specimens (n=103) and analyzed mRNA expression of seven UGT2B genes in males and females. Some UGT genes like UGT2B7, UGT2B15, and UGT2B17 were expressed more in men with UGT2B4, UGT2B10, UGT2B11, and UGT2B28 expressed significantly in females. UGT2B7 and UGT2B15 are mainly responsible for the glucuronidation of BPA in human beings (Gallagher et al. 2010). For SULT enzymes, the SULT1A1 expression varies among sexes and also by season as studied by several authors (Nowell and Falany 2006; Marazziti et al. 1998). Based on literature evidence, it was observed that glucuronidation could be higher in boys and sulfation in girls (Gallagher et al. 2010; Kim et al. 2003; Kurebayashi 2003; Neumann et al. 2016). Taking this assumption into account, metabolic parameters were optimized (Table 2 supp. File). Further, pharmacokinetic parameters (Bioavailability, MRT and half-life) were calculated similarly as mentioned before in section 2.4. These pharmacokinetic parameters calculated by ontogeny-based girls PBPK model was compared with ontogeny-based boys PBPK model.

2.6 Exposure reconstruction using child cohorts and Sensitivity analysis

Reverse dosimetry computes the external exposure from internal organ/plasma concentration or biomarker level in urine (Lin et al. 2020). In this study, the PBPK model was used to reconstruct daily exposure from two cohorts. The HELIX (Human Early-Life Exposome,

http://www.projecthelix.eu/es) cohorts include 6 population-based birth cohorts in Europe (Spain, France, Greece, UK, Norway, and Lithuania). Details about this cohort can be found here (Maitre et al. 2018; Magnus et al. 2016; Vrijheid 2013). From this cohort, the data of children were used for the present study, which was collected from 1999-2010. Measured BPA concentrations were extracted for 1357 children (753 boys and 604 girls) at 6-11 years of age after excluding outliers. Total BPA (conjugated and free) was determined in a pool of equal amounts of two spot urine samples collected at bedtime and in the morning. Creatinine concentration was measured for all urinary samples to conduct adjustment with respect to urinary dilutions. Details of the analytical procedure can be found elsewhere (Tamayo-Uria et al. 2019; Haug et al. 2018). BPA urinary concentrations, and the child's weight and height measured using regularly calibrated instruments (Maitre et al. 2018), were considered for reverse dosimetry in the PBPK Model. The other cohort used was the Austrian PBAT cohort in which data was collected from 2010-2012, that is part of the Human Biomonitoring for EU (HBM4EU) project. Aggregate data from this cohort was available for boys and girls aged 6-10 years (n=253, 138 boys and 115 girls) and was downloaded from the website and further used for reconstructing the exposure from total BPA (HBM4EU 2021).

For calculating cumulative urine, eq. 9 was considered which include spot urine, spot creatinine, and total urinary creatinine (Table 3 Supp file). Value for total urinary creatinine was obtained from the article published by Remer et al. (2002) in which the author has calculated the values based on sex, body weight and height of children. Reconstructed exposure (ng/kg bw/day) was calculated using Markov Chain Monte Carlo (MCMC) simulation with 10,000 iterations were done. Individual simulation was run for each children considering their specific BW, height, sex information, and cohorts' urine concentration (total number of participants: 1359). Oral dose was considered as a parameter to be estimated by the model and it was randomly distributed using uniform distribution and cohorts´ BPA urine concentration was used as a likelihood parameter that follows a normal distribution with 10 percent variation and rest other parameters were not distributed. Then, individual simulation was run and from the individual output, which is the reconstructed exposure, median, 5^{th} and 95^{th} percentiles value was calculated separately for boys and girls in case of Helix cohort. For the PBAT cohort, since there was no individual data, the variation in urinary creatinine was taken for capturing the distribution. The reconstructed exposure for both boys and girls was compared with TDI set by EFSA for BPA. MCMC simulation was performed using the MCSim version 6.2.0. Correlation between data (experimental data point) and predicted was checked by calculation r^2 for all the individual simulations.

$$Cumulative\ Urine = \frac{Spot\ Urine}{Spot\ Creatinine} * Total\ Urinary\ Creatinine \qquad eq.9$$

At last, we performed the sensitivity analysis for both boys and girls PBPK model using the R package FME. FME package allows to run the complex model containing ODE (ordinary differential equation), producing output as a function of input parameter (Soetaert and Petzoldt 2010). This package allows for varying the parameter by 1% up and down, keeping all other parameters constant. In FME, the sensitivity matrix contains dimensionless sensitivity of the parameter to the model output whose $(i,j)^{th}$ element $S_{i,j}$ contains:

$$\frac{\partial y_i}{\partial \Theta_j} = \frac{w\Theta_j}{wy_i} \qquad \text{eq. 10}$$

Here, y_i is the output variable, Θ_j is the parameter, wy_i is the scaling of variable y_i which is usually equal to its value and $w\Theta_j$ is thr scaling of variable j which is usually equal to parameter value. Also, the parameters can be ranked based on importance of the parameter for the output variable. The higher is the absolute sensitivity value, the higher will be the ranking.

3. Results

3.1 Age dynamic based Adult PBPK Model showed good accuracy

The refined adult PBPK model predictions of free BPA and its metabolite concentration in plasma were compared with the 12 healthy volunteers plasma data of single oral administration obtained from Thayer et al. (2015) shown in Supp Figure 9. The adult model contains age-based dynamic physiological parameters to improve the prediction. The predictive accuracy of the model was calculated through Pearson correlation which showed that the simulated data fits well with the observed data, within a 2-fold deviation from observed values with r value ≥0.95 and p value less than 0.05 (Supp file, Figure 8).

3.2 A ontogeny scaling based Pediatric PBPK model showed the critical differences in pharmacokinetic characteristics vs classical body-weight scaling

Pharmacokinetic parameters were calculated and compared among the adult PBPK and the two different pediatric PBPK models: 1) the classical body-weight scaling and 2) the ontogeny scaling. Plasma concentration of free BPA in children with ontogeny scaling was found to be comparatively higher than in adults and body-weight-based scaling for the same amount of exposure (Figure 10 in supplementary file). However, BPAG plasma concentration were almost similar between adult and two pediatric models but BPAS plasma concentration was significantly higher in children with ontogeny-based scaling than the body-weight based scaling and adult PBPK model (supplementary figure 10). Figure 3 showed pharmacokinetic parameters like AUC, $t_{1/2}$, bioavailability, and MRT for free BPA for different organs. The trend followed for half-life was adult> pediatric PBPK with ontogeny scaling> pediatric PBPK with body-weight scaling. An increased terminal half-life was seen in gonads compared to other organs for both children and adults ($t_{1/2}$=7-10 hours in gonads, $t_{1/2}$=4.5-5.1 hour for plasma) (Figure 3 A). The AUC for classical body-weight scaling was quite the opposite trend than ontogeny in comparison to adult for all organs (Fig. 3B): in case of plasma, the AUC for ontogeny based pediatric model was approximately 17% higher, and the classical body-weight-based model was approximately 13% lower than the adult model (Figure 3B). Bioavailability was also high in children with ontogeny scaling followed by body-weight and adult model (Figure 3C), but mean residence time was highest in adults compared to children (Figure 3C). Overall, the pediatric PBPK model based on ontogeny showed the critical differences in pharmacokinetic of short-acting chemical (BPA), which could not have been explained by simply considering the body-weight-based scaling.

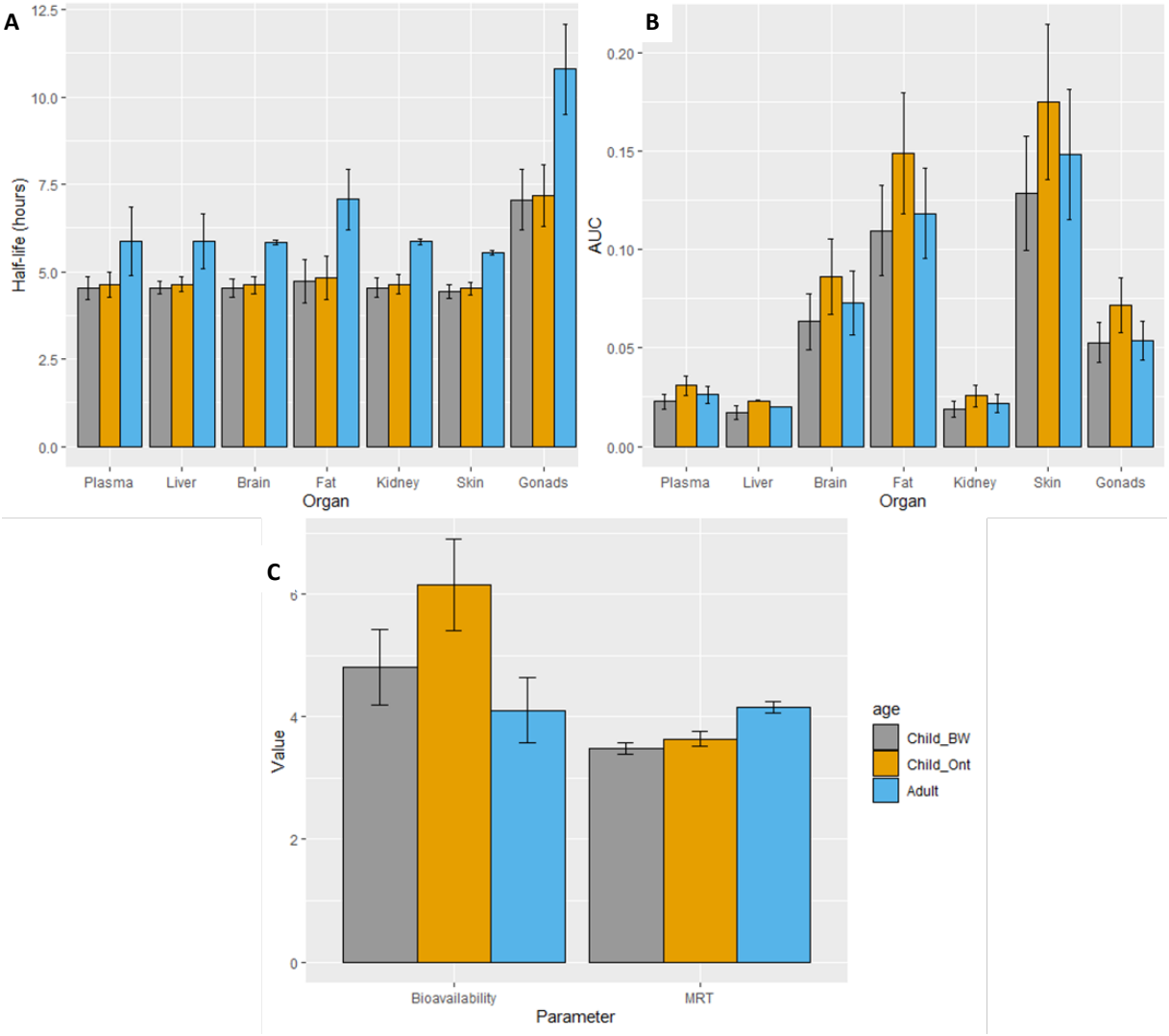

Figure 3: Comparison for different pharmacokinetic parameters in children (based on body-weight and ontogeny scaling) and adults at the dose of 1 µg/Kg BW/day. 3A. represents half-life ($t_{1/2}$) for different organs, B. represents area under curve (AUC) for 7 organs (plasma, liver, brain, fat, kidney, skin and gonads), and C. represents bioavailability (F) and mean residence time (MRT) for free BPA in children and adult. Bioavailability (F) is in % and MRT is in hours in Figure 3C.

3.3 Impact of sex difference on Pharmacokinetics characteristic

Further, the ontogeny-based PBPK model for boys and girl (UGT, SULT, and physiology changes) was taken for sex-specific differences in pharmacokinetics for similar exposure. Plasma concentration of free BPA was slightly higher in boys than girls. Glucuronidation of BPA was slightly higher in boys than girls, however sulfation was comparatively more in girls (Supplementary figure 11). Free BPA half-life was found to be higher in girls than boys (girls, $t_{1/2}$=6.7 hours vs. boys, $t_{1/2}$= 4.61 hours) in plasma and all other organs (Figure 4). Half-life in gonads was significantly higher, followed by adipose tissue than the other organs. The trend followed by half-life was gonads>fat>liver>plasma>kidney>brain>skin. The mean residence time was higher in girls which was also reflected while calculating half-life, but bioavailability was found to be more in boys (Supplementary figure 12).

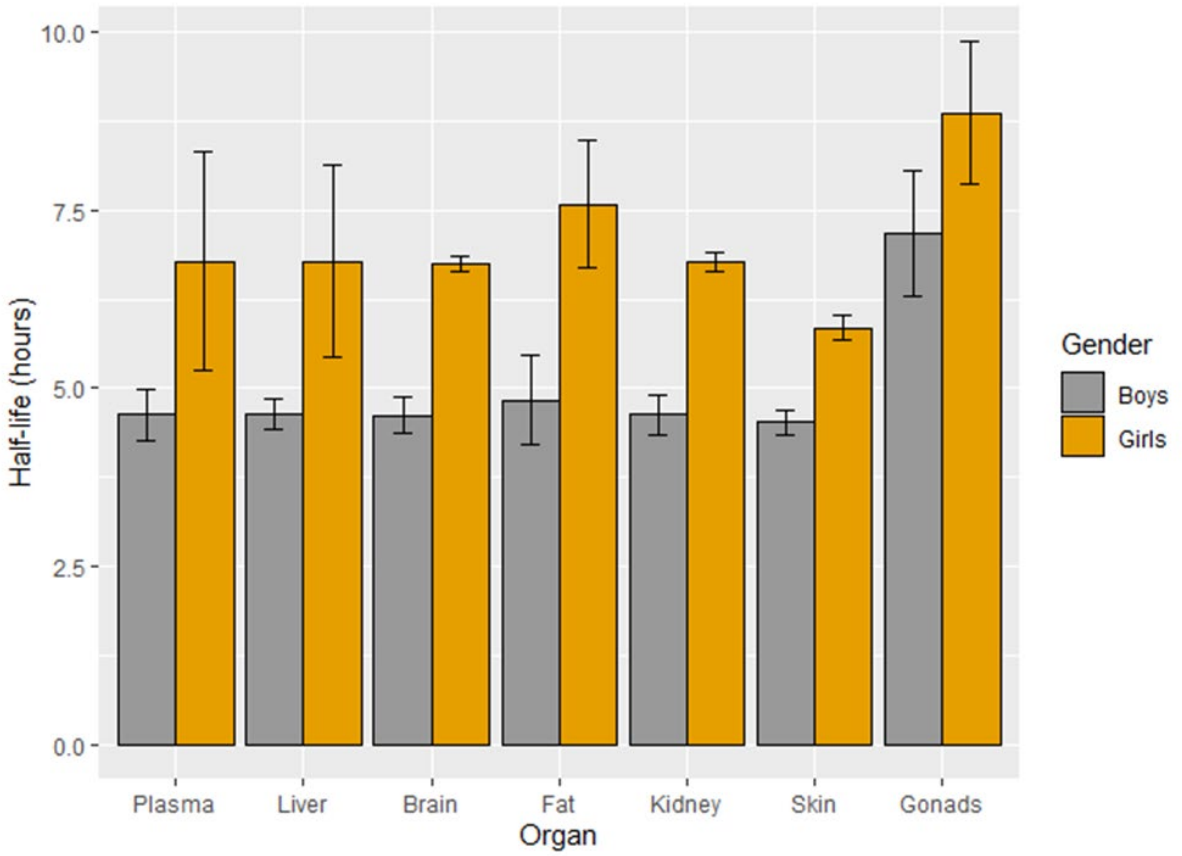

Figure 4: Half-life for boys and girls based on ontogeny scaling PBPK Model at the dose of 1 µg/Kg BW/day.

3.4 Daily exposure in boys and girls: reverse dosimetry and sensitive parameters

The ontogeny-based PBPK model for both boys and girls was used for calculating daily exposure from total BPA. Figure 5 represents the daily dose calculated from the HELIX and the PBAT cohorts for different countries in Europe using the pediatric PBPK model. The percentile shown for Helix cohort is the distribution of the data, and for the PBAT cohort, the percentile is due to variation in total urinary creatinine since it was aggregated data. Exposure was found to be a little higher in girls than boys for all seven countries. The daily intake was lowest in France (girls: 0.039, boys: 0.034 ug/kg BW/day) and highest in Austria (girls: 0.244, boys: 0.221 ug/kg BW/day). Daily intake estimates for all the cohorts were in the range of 0.0131-0.294 (P5:P95) with a median of 0.0727 µg/Kg BW/day. The P95 value was approx. thirteen times lower than the temporary total daily intake (t-TDI) set by EFSA in 2015, which was 4 µg/kg BW/day (EFSA Panel on Food Contact Materials Flavourings and Processing Aids (CEF) 2015). In 2021, EFSA drastically decreased the TDI for BPA to 0.04 ng/Kg BW/day recently opened for comments. Now, median value of daily intake is comparatively 1500 times higher than recent TDI established by EFSA (Bisphenol A: EFSA draft opinion proposes lowering the tolerable daily intake 2021). Correlation was checked by calculating the r2, which was found to be 0.95 (Figure 14, Supp file). Correlation was between urinary concentration cohort data (experimental) and the urinary concentration calculated by the model after reconstructed exposure (Simulated).

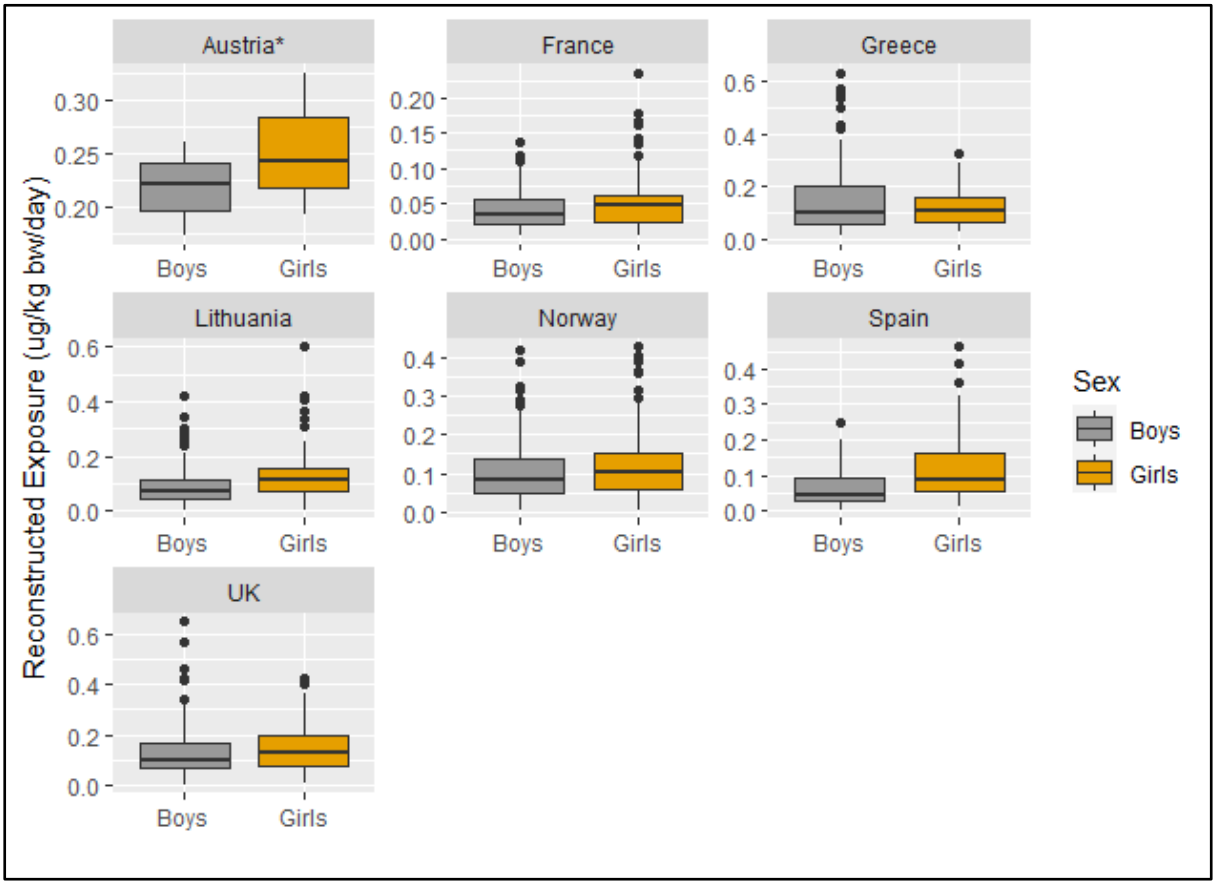

Figure 5: Reconstructed exposure for boys and girls for two different cohorts (HBM4EU and Helix Cohort). Data from Austria is from PBAT cohort from HBM4EU and for rest other countries, it is from Helix cohort. Upper whisker represents P95 and lower whisker represents P5 confidence interval. For Helix cohort, the percentiles is from combining the individual output results. *represents the aggregated data downloaded from HBM4EU website and the distribution represent changes in creatinine levels. X-axis represents country and y-axis represents daily intake levels (µg/kg BW/day) for boys and girls.

Sensitivity analysis has been carried out for all the biochemical parameters used for developing the pediatric PBPK Model for both boys and girls. Table 5 (Supp file) represents the statistics of parameter sensitivity results along with ranking. Ranking for sensitivity varies in boys and girls for many parameters like conjugation, fat and gonads partition coefficient and much more (Table 5). Figure 6 represents the mean sensitivity coefficient for boys and girls respectively. Glucuronidation has major impact in case of boys but lesser in girls with the opposite trend showing for sulfation for both Vmax and Km. Liver_plasma partition coefficient is highly sensitive for both sex with a sensitivity coefficient of -1 suggesting that 10% increase in the partition may reduce the plasma concentration by 10%. Fat_plasma partition coefficient is more sensitive in boys than girls. The mean sensitivity coefficient of Vmax is negative, and Km is positive for both sex, implicating both the parameters have opposite impact on the output plasma concentration.

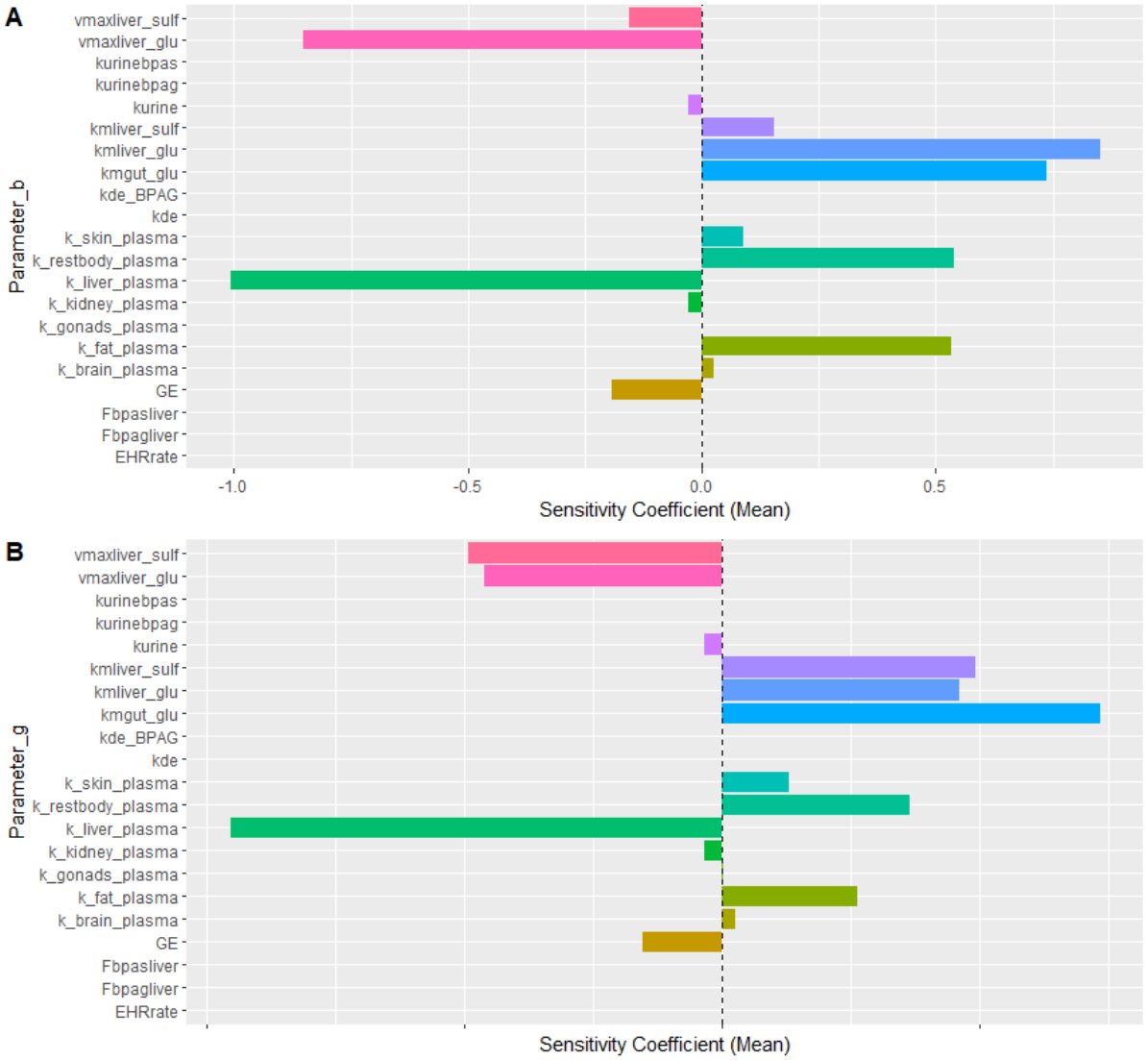

Figure 6: Sensitivity Coefficient for boys and girls. A) Sensitivity plot for boys, B) Sensitivity plot for girls. All the biochemical parameter used for developing PBPK Model has been used for the sensitivity analysis. Analysis has been done with FME Package.

4. Discussion

This study was the first to investigate the pharmacokinetic differences between pediatric population taking into account gender differences with different scaling approaches and adults using the PBPK model for BPA. The workflow presented in Figure 1 ensures developing of the pediatric PBPK model based on adult models considering 2 approaches: 1) body-weight scaling and 2) ontogeny Scaling. In the present study, data from two different cohort studies was taken and used to estimate daily exposure for boys and girls. Overall, the pediatric PBPK model with ontogeny scaling greatly improves the understanding of toxicokinetic and risk assessment for short-acting molecules like BPA based on sex and age.

The adult model was validated and then extrapolated for the pediatric population following the classical approach of building PBPK. Overall, BPA metabolizes and eliminates faster in adults as increased levels of BPAS and BPAG were seen. Individual adult PBPK simulations showed not much difference in plasma time profile of free BPA, indicating physiological

parameters have little impact on BPA elimination. However, for two subjects, the data did not fit well which could be explained by enzymatic polymorphism leading to high variability of glucuronidation and sulfation metabolic processes (Skledar et al. 2015; Hanioka et al. 2008). It can be overcome by optimizing the excretion rate for metabolites for those individuals, but this was outside the scope of this paper.

In the pediatric PBPK model, AUC for plasma and all other organs was higher in ontogeny-based scaling representing the underestimation of risk from short-acting chemicals in the case of children with body weight-based scaling. A higher AUC of free BPA indicates higher systemic exposure to the chemical and comparatively lower metabolism. As mentioned already in the methodology that glucuronidation is lower in children, and sulfation is comparatively higher in children than adults, but the important point is glucuronidation is the major metabolic pathway for BPA (Karrer et al. 2018), which may be responsible for higher AUC in children. Overall, the model indicated that the body-weight scaling approach might lead to an underestimation of the risk.

Estimated half-life was found to be higher in gonads followed by adipose tissue and then other organs for both pediatric and adult model. This estimation could be correlated with other research finding that showed gonads are highly sensitive to BPA exposure which is known to be an endocrine disruptor. It suggests the potential of BPA to interact with developing female and male reproductive systems in children. This finding is in accordance with literature where Ferguson et al. demonstrated association between BPA exposure and increased sex hormone-binding globulin (SBHG) levels and reduced free and total testosterone levels in boys (8-14 years) along with several other studies finding links between BPA exposure and varying onset of puberty (Berger et al. 2018; Braun and Hauser 2011; Ferguson et al. 2014; Forner-Piquer et al. 2020; Santangeli et al. 2016). In all the organs, decreased half-life in children than in adults suggests slower elimination capabilities meaning free BPA stays in the body for a longer time. This trend was also captured for mean residence time, emphasizing on the importance of calculating MRT. Nevertheless, bioavailability and AUC were higher in children with ontogeny scaling than adults. Higher AUC and higher bioavailability mean more chemical is present in systemic circulation and hence more risk. The possible reason for increased bioavailability may be due to decreased extent of metabolic capabilities in the liver and intestine in children than adults which was also seen in case of the infant PBPK model for BPA (Karrer et al. 2018). This points towards the question: Should we set a separate TDI for children than adults as children may be more susceptible to risk? However, further research is needed in this area to come to conclusion.

Sex differences in growing children were represented on the basis of PK parameters with half-life ($t_{1/2}$), bioavailability, mean residence time and plasma concentration-time curve. Model simulated that plasma concentration, and bioavailability was higher in boys than girls based on ontogeny-scaling PBPK model which has been reported by other authors in case of adult. The sex-related differences in BPA can be due to differences in androgen-related activity as several authors have reported higher levels in serum BPA in males (fetus and adult ones) compared with females even at equal exposure (Caporossi and Papaleo 2015). On the contrary, the model predicts mean residence time and elimination half-life (1.25-2 times) higher in girls than boys in almost all the organs, which may be due to decreased clearance.

This trend has been captured by ontogeny specific pediatric PBPK Model. Boys show higher elimination of free BPA since BPA is majorly metabolized by UGT2B15 enzyme, which is higher in boys than girls. This model prediction is in-line with literature evidence, for instance the drugs like oxazepam, and acetaminophen which are highly metabolized by the UGT enzymes have found to have a longer half-life in females than males (Court et al. 2004; Greenblatt et al. 1980; Wojcicki et al. 1979). Another important point is that girls have relatively more body fat than boys, so they may store more lipophilic chemicals, and boys have higher rate of clearance than girls, so the half-life can be higher in girls for lipophilic chemicals like BPA (Caporossi and Papaleo 2015). However, further experimental studies are needed to understand the sex differences in detail. The trend for half-life was noticed in case of girls was: gonads > adipose tissue > kidney > brain > liver > plasma > skin. The model predicted a higher half-life in gonads which coincides with literature findings demonstrating BPA exposure associated with variation in puberty onset in girls (Berger et al. 2018), highlighting the advantage of such a model in tissue dosimetry based risk assessment. For instance, BPA being a structural analogue of estrogen, it interacts with estrogen receptor and its prolonged presence in reproductive organs may disrupt normal estrogen related biology inside human especially affecting reproduction growth (Teeguarden et al. 2013).

Most biomonitoring studies have reported higher BPA levels in urine samples than adults with increased levels in the children at school- age (Abraham and Chakraborty 2019; Covaci et al. 2015). Study by Covaci et al. has shown 5 out of 6 countries in Europe with having more than 87% population exposed to BPA above the limit of quantification (LOQ) and children with higher exposure than adults (Covaci et al. 2015). Exposure reconstruction through model for these two cohorts showed that exposure is slightly higher in girls than boys for most countries. One possible reason behind this higher exposure can be that girls are getting more exposed than boys through everyday use products. A recent study by Robles-Aguilera et al. et al. (2021) showed sex-related differences in exposure concluding that a higher risk of dietary exposure in boys was not from BPA but other analogues, but the girls aged under 14 years were at higher risk for increased BPA dietary exposure, especially overweight and obese girls. A critical finding from the pediatric PBPK model is that even with similar exposure in boys and girls, the risk can be higher in girls due to slower elimination in younger girls than boys. The study by Sonnenberg et al. have reported pre-pubertal exposure with phthalates and BPA associated with pubertal timing in girls (mean age: 8.8 years) observed in 472 subjects with no association for boys (Kasper-Sonnenberg et al. 2017). An important outcome of developing ontogeny and sex-specific pediatric models is to better understand the toxicity, metabolic pathway and exposure in children of growing age.

At last, the reconstructed exposure by the PBPK model for children was compared with the t-TDI established by EFSA in 2015 for BPA (4 µg/Kg BW/day) and it was found to be lower than the t-TDI (EFSA Panel on Food Contact Materials Flavourings and Processing Aids (CEF) 2015). It points towards that there may not be any risk or adverse effects involved with the exposure of BPA in human beings. This may not be true. Several epidemiological studies published over the years showed positive associations between BPA exposure and health outcome in children (Healy et al. 2015). But, recent drastic lowering of TDI by EFSA in 2021 (0.04 ng/Kg BW/day) which is open for comments, reconstructed exposure by PBPK is approximately 1500

times higher in children pointing towards multiple health concerns ranging from immune effects to neurotoxicity (Bisphenol A: EFSA draft opinion proposes lowering the tolerable daily intake 2021). Further, pediatric PBPK Model can be combined with toxicodynamic to understand the signaling mechanism involving estrogen, aryl hydrocarbon and thyroid hormone receptors (Sharma et al. 2017). This could help towards improving the understanding towards adverse effects involved with BPA exposure taking into account toxicokinetic for children.

Interpolation of the pediatric PBPK model from an adult is the most widely used and preferred approach by scientists and regulatory bodies based on allometric scaling. In this model, we tried to incorporate ontogeny-specific metabolic parameters to improve the model. However, a detailed kinetic study in pediatric population or in-vitro study is required to further refine the model for ADME parameters. This is the first model to incorporate sex-specific differences in children for BPA and highlights the need of considering this while building regulatory guidelines. But, more data on sex-specific differences and adverse effects is required to increase the confidence in the PBPK Model. This model also aids in calculating the external dosimetry taking into account all the dietary and non-dietary exposure, which is often difficult to calculate during experimental studies. The model can predict aggregate exposure which may be from multiple sources. However, the limitation being difficulty in predicting route of intake (oral, dermal, inhalational or sublingual exposure). Further refinement of the model by including separate exposure sources and dermal compartments can help overcome some of the limitations. Overall, the pediatric PBPK model help provides a framework to integrate sex differences and consider pediatric population for risk assessment in case of such short-acting chemicals. Also, toxicologists should take into account sex-related differences while developing research protocols since boys and girls can have quite different effects on the health even with the same exposure.

5. Conclusion

In summary, the BPA pediatric PBPK model was developed for dosimetry assessment and predicting tissue concentration-time profile in plasma and other organs. With the same exposure, the ontogeny-based pediatric PBPK model, showed children could be at higher risk than adults (higher AUC and higher bioavailability in all the organs), which could not be explained by classical body-weight scaling. Half-life and MRT were found to be higher in girls than boys in all the organs suggesting free BPA stays in girls' body longer than in boys at the same exposure. Further, the reconstructed daily exposure was found to be higher than the recently established TDI by EFSA and daily exposure was found to be higher in girls than boys. This indicates that sex- differences must be included in the experimental and modeling studies. However, for an improved understanding of sex-related differences, especially hepatic and intestinal metabolism, more in-vivo experiments need to be conducted which can be helpful for increasing the confidence in sex-based risk. Overall, this study presents an example of how ontogeny based pediatric PBPK model can improve the risk assessment in children as well as in boys and girls, leaving behind the traditional approach. Also, it is one step forward towards incorporating sex-specific differences in the PBPK model improving the translation of risk.

Acknowledgment

This study was financially supported by Marie Skłodowska-Curie “Neurosome Project” under the grant agreement No. 766251, the European Community funded H2020 HBM4EU project under Grant Agreements no. 733032, and the Instituto de Salud Carlos III (PI17/01194), and the European Community’s Seventh Framework Programme (FP7/2007-206) under grant agreement no 308333 (HELIX project). Maribel Casas holds a Miguel Servet fellowship (CP16/00128) funded by Instituto de Salud Carlos III and co-funded by European Social Fund “Investing in your future". We acknowledge support from the Spanish Ministry of Science and Innovation through the “Centro de Excelencia Severo Ochoa 2019-2023” Program (2018-000806-S), and support from the Generalitat de Catalunya through the CERCA Program. This publication reflects only the authors' views. The Community and other funding organizations are not liable for any use made of the information contained therein. Born in Bradford is only possible because of the enthusiasm and commitment of the children and parents in Born in Bradford. We are grateful to all participants, health professionals and researchers who have made Born in Bradford happen. BiB receives core infrastructure funding from the Wellcome Trust (WT101597MA) and a joint grant from the UK Medical Research Council (MRC) and Economic and Social Science Research Council (ESRC) (MR/N024397/1). This study has received support from European Research Council under the European Union's Seventh Framework Programme (FP7/2007-2013) / ERC grant agreement no 669545 and National Institute for Health Research Applied Research Collaboration Yorkshire and Humber (NIHR200166). The Norwegian Mother, Father and Child Cohort Study is supported by the Norwegian Ministry of Health and Care Services and the Ministry of Education and Research. We are grateful to all the participating families in Norway who take part in this on-going cohort study. The views expressed are those of the author(s), and not necessarily those of the NHS, the NIHR or the Department of Health and Social Care. Jose Urquiza is supported by Spanish regional program PERIS (Ref.: SLT017/20/000119), granted by Departament de Salut de la Generalitat de Catalunya.

CRediT author statement

Deepika Deepika: Conceptualization, Methodology, Data analysis and simulation, and writing; Raju Prasad Sharma: Supervision, Conceptualization, Methodology, writing, review and revision, Marta Schuhmacher: Supervision, Review and revision, Amrit Kaur Sakhi: Provided Cohort Data and reviewing, Cathrine Thomsen: Provided Cohort Data and reviewing, Leda Chatzi: Provided Cohort Data and reviewing, Marina Vafeiadi: Provided Cohort Data and reviewing, Remy Slama: Provided Cohort Data and reviewing, Joane Quentin: Provided Cohort Data and reviewing, Sandra Andrušaitytė: Provided Cohort Data and reviewing, Regina Grazuleviciene: Provided Cohort Data and reviewing, Tiffany C Yang: Provided Cohort Data and reviewing, John Wright: Provided Cohort Data and reviewing, Dagmar Waiblinger: Provided Cohort Data and reviewing, Martine Vrijheid: Provided Cohort Data and reviewing, Jose Urquiza: Provided Cohort Data and reviewing, Maribel Casas: Provided Cohort Data, Writing, Review and revision, Vikas Kumar: Supervision, Conceptualization, Methodology, Data analysis and simulation, writing, review and revision.

Reference

Abraham A, Chakraborty P. 2019. A review on sources and health impacts of bisphenol A. Rev Environ Health 1–10; doi:10.1515/reveh-2019-0034.

Berger K, Eskenazi B, Kogut K, Parra K, Lustig RH, Greenspan LC, et al. 2018. Association of Prenatal Urinary Concentrations of Phthalates and Bisphenol A and Pubertal Timing in Boys and Girls. Environ Health Perspect 126:097004; doi:10.1289/EHP3424.

Bisphenol A: EFSA draft opinion proposes lowering the tolerable daily intake. 2021. Available: https://www.efsa.europa.eu/en/news/bisphenol-efsa-draft-opinion-proposes-lowering-tolerable-daily-intake.

Bois FY. 2009. GNU MCSim: Bayesian statistical inference for SBML-coded systems biology models. Bioinformatics 25:1453–1454; doi:10.1093/bioinformatics/btp162.

Braun JM, Hauser R. 2011. Bisphenol A and children's health. Curr Opin Pediatr 23:233–239; doi:10.1097/MOP.0b013e3283445675.

Bushnik T, Haines D, Levallois P, Levesque J, Van Oostdam J, Viau C. 2010. Lead and bisphenol A concentrations in the Canadian population. Heal reports 21: 7—18.

Caporossi L, Papaleo B. 2015. Exposure to bisphenol A and gender differences: from rodents to humans evidences and hypothesis about the health effects. J Xenobiotics 5:15–19; doi:10.4081/xeno.2015.5264.

Court MH, Hao Q, Krishnaswamy S, Bekaii-Saab T, Al-Rohaimi A, Von Moltke LL, et al. 2004. UDP-glucuronosyltransferase (UGT) 2B15 pharmacogenetics: UGT2B15 D85Y genotype and gender are major determinants of oxazepam glucuronidation by human liver. J Pharmacol Exp Ther 310:656–665; doi:10.1124/jpet.104.067660.

Covaci A, Hond E Den, Geens T, Govarts E, Koppen G, Frederiksen H, et al. 2015. Urinary BPA measurements in children and mothers from six European member states: Overall results and determinants of exposure. Environ Res 141:77–85; doi:10.1016/j.envres.2014.08.008.

Csanády GA, Oberste-Frielinghaus HR, Semder B, Baur C, Schneider KT, Filser JG. 2002. Distribution and unspecific protein binding of the xenoestrogens bisphenol A and daidzein. Arch Toxicol 76:299–305; doi:10.1007/s00204-002-0339-5.

Deepika D, Sharma RP, Schuhmacher M, Kumar V. 2020. An integrative translational framework for chemical induced neurotoxicity–a systematic review. Crit Rev Toxicol 50:424–438; doi:10.1080/10408444.2020.1763253.

Deepika D, Sharma RP, Schuhmacher M, Kumar V. 2021. Risk Assessment of Perfluorooctane Sulfonate (PFOS) using Dynamic Age Dependent Physiologically based Pharmacokinetic Model (PBPK) across Human Lifetime. Environ Res 199:111287; doi:10.1016/j.envres.2021.111287.

Doerge DR, Twaddle NC, Vanlandingham M, Brown RP, Fisher JW. 2011. Distribution of bisphenol A into tissues of adult, neonatal, and fetal Sprague–Dawley rats. Toxicol Appl Pharmacol 255:261–270; doi:10.1016/j.taap.2011.07.009.

EFSA Panel on Food Contact Materials Flavourings and Processing Aids (CEF) E. 2015. Scientific Opinion on the risks to public health related to the presence of bisphenol A (BPA) in foodstuffs. EFSA J 13:3978; doi:https://doi.org/10.2903/j.efsa.2015.3978.

Eng DS, Lee JM, Gebremariam A, Meeker JD, Peterson K, Padmanabhan V. 2013. Bisphenol A and Chronic Disease Risk Factors in US Children. Pediatrics 132:e637–e645; doi:10.1542/peds.2013-0106.

Ferguson KK, Peterson KE, Lee JM, Mercado-García A, Blank-Goldenberg C, Téllez-Rojo MM, et al. 2014. Prenatal and peripubertal phthalates and bisphenol A in relation to sex hormones and puberty in boys. Reprod Toxicol 47:70–76; doi:10.1016/j.reprotox.2014.06.002.

Fisher JW, Twaddle NC, Vanlandingham M, Doerge DR. 2011. Pharmacokinetic modeling: Prediction and evaluation of route dependent dosimetry of bisphenol A in monkeys with extrapolation to humans. Toxicol Appl Pharmacol 257:122–136; doi:10.1016/j.taap.2011.08.026.

Forner-Piquer I, Beato S, Piscitelli F, Santangeli S, Di Marzo V, Habibi HR, et al. 2020. Effects of BPA on zebrafish gonads: Focus on the endocannabinoid system. Environ Pollut 264:114710; doi:10.1016/j.envpol.2020.114710.

Gallagher CJ, Balliet RM, Sun D, Chen G, Lazarus P. 2010. Sex differences in UDP-glucuronosyltransferase 2B17 expression and activity. Drug Metab Dispos 38:2204–2209; doi:10.1124/dmd.110.035345.

Greenblatt DJ, Divoll M, Harmatz JS, Shader RI. 1980. Oxazepam kinetics: effects of age and sex. J Pharmacol Exp Ther 215: 86–91.

Hanioka N, Naito T, Narimatsu S. 2008. Human UDP-glucuronosyltransferase isoforms involved in bisphenol A glucuronidation. Chemosphere 74:33–36; doi:10.1016/j.chemosphere.2008.09.053.

Hansen JB, Bilenberg N, Timmermann CAG, Jensen RC, Frederiksen H, Andersson A-M, et al. 2021. Prenatal exposure to bisphenol A and autistic- and ADHD-related symptoms in children aged 2 and5 years from the Odense Child Cohort. Environ Heal 20:24; doi:10.1186/s12940-021-00709-y.

Harley KG, Gunier RB, Kogut K, Johnson C, Bradman A, Calafat AM, et al. 2013. Prenatal and early childhood bisphenol A concentrations and behavior in school-aged children. Environ Res 126:43–50; doi:10.1016/j.envres.2013.06.004.

Haug LS, Sakhi AK, Cequier E, Casas M, Maitre L, Basagana X, et al. 2018. In-utero and childhood chemical exposome in six European mother-child cohorts. Environ Int 121:751–763; doi:10.1016/j.envint.2018.09.056.

HBM4EU. 2021. HBM4EU - science and policy for a healthy future. Available: https://www.hbm4eu.eu/deliverables/.

Healy BF, English KR, Jagals P, Sly PD. 2015. Bisphenol A exposure pathways in early childhood: Reviewing the need for improved risk assessment models. J Expo Sci Environ Epidemiol 25:544–556; doi:10.1038/jes.2015.49.

Karrer C, Roiss T, von Goetz N, Skledar DG, Mašič LP, Hungerbühler K. 2018. Physiologically based pharmacokinetic (PBPK) modeling of the bisphenols BPA, BPS, BPF, and BPAF with new experimental metabolic parameters: Comparing the pharmacokinetic behavior of BPA with its substitutes. Environ Health Perspect 126:077002; doi:10.1289/EHP2739.

Kasper-Sonnenberg M, Wittsiepe J, Wald K, Koch HM, Wilhelm M. 2017. Pre-pubertal exposure with phthalates and bisphenol A and pubertal development. PLoS One 12:1–18; doi:10.1371/journal.pone.0187922.

Kim Y-H, Kim C-S, Park S, Han SY, Pyo M-Y, Yang M. 2003. Gender differences in the levels of bisphenol A metabolites in urine. Biochem Biophys Res Commun 312:441–448; doi:10.1016/j.bbrc.2003.10.135.

Kurebayashi H. 2003. Disposition of a Low Dose of 14C-Bisphenol A in Male Rats and Its Main Biliary Excretion as BPA Glucuronide. Toxicol Sci 73:17–25; doi:10.1093/toxsci/kfg040.

Ladumor MK, Bhatt DK, Gaedigk A, Sharma S, Thakur A, Pearce RE, et al. 2019. Ontogeny of hepatic sulfotransferases and prediction of age-dependent fractional contribution of sulfation in acetaminophen metabolism. Drug Metab Dispos 47:818–831; doi:10.1124/dmd.119.086462.

Lin YJ, Hsiao JL, Hsu HT. 2020. Integration of biomonitoring data and reverse dosimetry modeling to assess population risks of arsenic-induced chronic kidney disease and urinary cancer. Ecotoxicol Environ Saf 206:111212; doi:10.1016/j.ecoenv.2020.111212.

Lv Y, Rui C, Dai Y, Pang Q, Li Y, Fan R, et al. 2016. Exposure of children to BPA through dust and the association of urinary BPA and triclosan with oxidative stress in Guangzhou, China. Environ Sci Process Impacts 18:1492–1499; doi:10.1039/c6em00472e.

Magnus P, Birke C, Vejrup K, Haugan A, Alsaker E, Daltveit AK, et al. 2016. Cohort Profile Update: The Norwegian Mother and Child Cohort Study (MoBa). Int J Epidemiol 45:382–388; doi:10.1093/ije/dyw029.

Maitre L, de Bont J, Casas M, Robinson O, Aasvang GM, Agier L, et al. 2018. Human Early Life Exposome (HELIX) study: a European population-based exposome cohort. BMJ Open 8:e021311; doi:10.1136/bmjopen-2017-021311.

Marazziti D, Palego L, Rossi A, Cassano GB. 1998. Gender-Related Seasonality of Human Platelet Phenolsulfotransferase Activity. Neuropsychobiology 38:1–5; doi:10.1159/000026509.

Miao M, Wang Z, Liu X, Liang H, Zhou Z, Tan H, et al. 2017. Urinary bisphenol A and pubertal development in Chinese school-aged girls: a cross-sectional study. Environ Heal 16:80; doi:10.1186/s12940-017-0290-9.

Nalbantoğlu A, Çelikkol A, Samancı N, Günaydın NC, Nalbantoğlu B. 2021. Bisphenol A as a risk factor for allergic rhinitis in children. Hum Exp Toxicol 40:395–402; doi:10.1177/0960327120958105.

Neumann E, Mehboob H, Ramírez J, Mirkov S, Zhang M, Liu W. 2016. Age-Dependent Hepatic UDP-Glucuronosyltransferase Gene Expression and Activity in Children. Front Pharmacol 7:1–7; doi:10.3389/fphar.2016.00437.

Nowell S, Falany CN. 2006. Pharmacogenetics of human cytosolic sulfotransferases. Oncogene 25:1673–1678; doi:10.1038/sj.onc.1209376.

Ohore OE, Zhang S. 2019. Endocrine disrupting effects of bisphenol A exposure and recent advances on its removal by water treatment systems. A review. Sci African 5:e00135; doi:10.1016/j.sciaf.2019.e00135.

Remer T, Neubert A, Maser-Gluth C. 2002. Anthropometry-based reference values for 24-h urinary creatinine excretion during growth and their use in endocrine and nutritional research. Am J Clin Nutr 75:561–569; doi:https://doi.org/10.1093/ajcn/75.3.561.

Robles-Aguilera V, Gálvez-Ontiveros Y, Rodrigo L, Salcedo-Bellido I, Aguilera M, Zafra-Gómez A, et al. 2021. Factors associated with exposure to dietary bisphenols in adolescents. Nutrients 13:1553; doi:10.3390/nu13051553.

Roen EL, Wang Y, Calafat AM, Wang S, Margolis A, Herbstman J, et al. 2015. Bisphenol A exposure and behavioral problems among inner city children at 7–9 years of age. Environ Res 142:739–745; doi:10.1016/j.envres.2015.01.014.

Santangeli S, Maradonna F, Gioacchini G, Cobellis G, Piccinetti CC, Dalla Valle L, et al. 2016. BPA-Induced Deregulation Of Epigenetic Patterns: Effects On Female Zebrafish Reproduction. Sci Rep 6:21982; doi:10.1038/srep21982.

Sasso AF, Pirow R, Andra SS, Church R, Nachman RM, Linke S, et al. 2020. Pharmacokinetics of bisphenol A in humans following dermal administration. Environ Int 144:106031; doi:10.1016/j.envint.2020.106031.

Schwartz JB. 2003. The influence of sex on pharmacokinetics. Clin Pharmacokinet 42:107–121; doi:10.2165/00003088-200342020-00001.

Sharma RP, Schuhmacher M, Kumar V. 2017. Developing integrated PBPK/PD coupled mechanistic pathway model (miRNA-BDNF): An approach towards system toxicology. Toxicol Lett 280:79–91; doi:10.1016/j.toxlet.2017.08.003.

Sharma RP, Schuhmacher M, Kumar V. 2018. The development of a pregnancy PBPK Model for Bisphenol A and its evaluation with the available biomonitoring data. Sci Total Environ 624:55–68; doi:10.1016/j.scitotenv.2017.12.023.

Shelby MD. 2008. NTP-CERHR monograph on the potential human reproductive and developmental effects of bisphenol A. NTP CERHR MON v, vii–ix, 1-64 passim.

Skledar DG, Troberg J, Lavdas J, Mašič LP, Finel M. 2015. Differences in the glucuronidation of bisphenols F and S between two homologous human UGT enzymes, 1A9 and 1A10. Xenobiotica 45:511–519; doi:10.3109/00498254.2014.999140.

Soetaert K, Petzoldt T. 2010. Inverse modelling, sensitivity and monte carlo analysis in R using package FME. J Stat Softw 33:1–28; doi:10.18637/jss.v033.i03.

Stahlhut RW, Welshons W V., Swan SH. 2009. Bisphenol A Data in NHANES Suggest Longer than Expected Half-Life, Substantial Nonfood Exposure, or Both. Environ Health Perspect 117:784–789; doi:10.1289/ehp.0800376.

Takeuchi T, Tsutsumi O. 2002. Serum bisphenol a concentrations showed gender differences,

possibly linked to androgen levels. Biochem Biophys Res Commun 291:76–78; doi:10.1006/bbrc.2002.6407.

Tamayo-Uria I, Maitre L, Thomsen C, Nieuwenhuijsen MJ, Chatzi L, Siroux V, et al. 2019. The early-life exposome: Description and patterns in six European countries. Environ Int 123:189–200; doi:10.1016/j.envint.2018.11.067.

Teeguarden J, Hanson-Drury S, Fisher JW, Doerge DR. 2013. Are typical human serum BPA concentrations measurable and sufficient to be estrogenic in the general population? Food Chem Toxicol 62:949–963; doi:10.1016/j.fct.2013.08.001.

Teeguarden JG, Waechter JM, Clewell HJ, Covington TR, Barton HA. 2005. Evaluation of oral and intravenous route pharmacokinetics, plasma protein binding, and uterine tissue dose metrics of bisphenol A: a physiologically based pharmacokinetic approach. Toxicol Sci 85:823–38; doi:10.1093/toxsci/kfi135.

Thayer KA, Doerge DR, Hunt D, Schurman SH, Twaddle NC, Churchwell MI, et al. 2015. Pharmacokinetics of bisphenol A in humans following a single oral administration. Environ Int 83:107–115; doi:10.1016/j.envint.2015.06.008.

Tsukioka T, Terasawa J, Sato S, Hatayama Y, Makino T, Nakazawa H. 2004. Development of Analytical Method for Determining Trace Amounts of BPA in Urine Samples and Estimation of Exposure to BPA. J Environ Chem 14:57–63; doi:10.5985/jec.14.57.

Völkel W V., Bittner N, Dekant W. 2005. Quantitation of bisphenol A and bisphenol A glucuronide in biological samples by high performance liquid chromatography-tandem mass spectrometry. Drug Metab Dispos 33:1748–1757; doi:10.1124/dmd.105.005454.

Vrijheid M. 2013. The Human Early Life Exposome (HELIX): Project Rationale and Design. ISEE Conf Abstr 2013:5849; doi:10.1289/isee.2013.s-2-32-05.

Wagner C, Zhao P, Pan Y, Hsu V, Grillo J, Huang SM, et al. 2015. Application of physiologically based pharmacokinetic (PBPK) modeling to support dose selection: Report of an FDA public workshop on PBPK. CPT Pharmacometrics Syst Pharmacol 4:226–230; doi:10.1002/psp4.33.

Wojcicki J, Gawronska-Szklarz B, Kazimierczyk J, Baskiewicz Z, Raczyński A. 1979. Comparative pharmacokinetics of paracetamol in men and women considering follicular and luteal phases. Arzneimittel-Forschung/Drug Res 29: 350–352.

UNIVERSITAT ROVIRA I VIRGILI
QUANTITATIVE SYSTEMS TOXICOLOGY MODELING FOR NEURONAL ADVERSE OUTCOME
Deepika

Chapter 3a

Deepika Deepika, Raju Prasad Sharma, Marta Schuhmacher, Vikas Kumar, Risk Assessment of Perfluorooctane Sulfonate (PFOS) using Dynamic Age Dependent Physiologically based Pharmacokinetic Model (PBPK) across Human Lifetime, Environmental Research, Volume 199, 2021, 111287.

Chapter 3b

Deepika Deepika, Joaquim Rovira, Óscar Sabuz, Jordina Balaguer, Marta Schuhmacher, José L. Domingo, Vikas Kumar, Framework for risk assessment of PFAS utilizing experimental studies and in-silico models, Environmental Research, Volume 208, 2022, 112722.

UNIVERSITAT ROVIRA I VIRGILI
QUANTITATIVE SYSTEMS TOXICOLOGY MODELING FOR NEURONAL ADVERSE OUTCOME
Deepika

Risk Assessment of Perfluorooctane Sulfonate (PFOS) using Dynamic Age Dependent Physiologically based Pharmacokinetic Model (PBPK) across human lifetime

Abstract

The widespread use of Perfluorooctane sulfonate (PFOS) in everyday life, its long half-life, and the lipophilicity that makes it easily accumulate in the body, raises the question of its safe exposure among different population groups. There are currently enough epidemiological studies showing evidence of PFOS exposure and its associated adverse effects on humans. Moreover, it is already known that physiological changes along with age e.g. organ volume, renal blood flow, cardiac output and albumin concentrations affect chemicals body burden. Human biomonitoring cohort studies have reported PFOS concentrations in blood and autopsy tissue data with PFOS present in sensitive organs across all human lifespan. However, to interpret such biomonitoring data in the context of chemical risk assessment, it is necessary to have a mechanistic framework that explains show the physiological changes across age affects the concentration of chemical inside different tissues of the human body. PBPK model is widely and successfully used in the field of risk assessment. The objective of this manuscript is to develop a dynamic age-dependent PBPK model as an extension of the previously published adult PFOS model and utilize this model to predict and compare the PFOS tissue distribution and plasma concentration across different age groups. Different cohort study data were used for exposure dose reconstruction and evaluation of time-dependent concentration in sensitive organs. Predicted plasma concentration followed trends observed in biomonitoring data and model predictions showed the increased disposition of PFOS in the geriatric population. PFOS model is sensitive to parameters governing renal resorption and elimination across all ages, which is related to PFOS half-life in humans. This model provides an effective framework for improving the quantitative risk assessment of PFOS throughout the human lifetime, particularly in susceptible age groups. The dynamic age-dependent PBPK model provides a step forward for developing such kind of dynamic model for other perfluoroalkyl substances.

Keywords: PFOS, PBPK model, age-dependent, Dynamic, pediatrics, geriatrics, adult

1. Introduction

PFOS (perfluoro octane sulfonate) is a fluorinated organic compound having a sulfonated functional group and eight carbon backbone with a wide variety of use in industrial and consumer applications (Abraham et al. 2020; Roberts et al. 2016; Tan et al. 2008). It is widely used in consumer products like furniture, household cleaners, clothing, and due to its resistance to environmental and metabolic degradation, it was also categorized as persistent organic pollutants (POPs) in 2009 under the Stockholm Convention (Chou and Lin 2019; Domazet et al. 2020; Dourson et al. 2019; Roberts et al. 2016; Zhang et al. 2011a). Due to its high bioaccumulation potential, PFOS is detected in many human tissues and biological samples in both occupational and non-occupation people across the human lifespan. Because of its widespread persistence in the environment, human exposure to this emerging pollutant occurs through multiple pathways and multiple sources, including the food chain, dust ingestion, air inhalation, and municipal drinking water (Augustsson et al. 2021; Ericson et al. 2009a; Grandjean et al. 2017; Rovira et al. 2019a; Tian et al. 2016). Biomonitoring studies have found that dietary intake is the major exposure pathway for PFOS followed by other sources of exposure like drinking water and dust ingestion (Černá et al. 2020; Domingo and Nadal, 2019; Ehresman et al. 2007; Rovira et al. 2019). Different cohort studies have reported variation in exposure pathways based on different variables like age groups, gender, and body weight. For instance, Ericson et al showed that children ages 4-8 years showed the highest daily intake values and geriatric people (>65 years old) corresponded to the lowest daily intake (Ericson et al. 2009). Another study by Zhang et al. showed estimated daily intake on a bodyweight basis for PFOS to be higher in toddlers than in adolescent groups (Zhang et al. 2011). However, in most of these studies, only dietary intake has been considered and the source of other exposure has not been characterized. Exposure in different age groups especially pediatric can be via multiple pathways apart from dietary intake like ingestion of house dust, contact with specific consumer products etc. leading to high body weight normalized estimated daily intakes (Winkens et al. 2017). There are no experimental studies that have measured the exposure associated with direct contact of consumer products in the pediatric population or external exposure by indoor environment after breastfeeding till adulthood. The limited data regarding multiple exposure pathways for the pediatric and other populations need for pharmacokinetic models for reconstructed exposure and assess the risk in different organs considering the variation in kinetics and toxicological activity of PFOS with changes in physiological and biochemical parameters.

In recent years tremendous research has been done on kinetics and toxicity study for PFOS in the human, in-vitro and in-vivo (Butenhoff et al. 2012; Cui et al. 2009; Li et al. 2017; Loccisano et al. 2012; Luebker et al. 2005; Tan et al. 2008; Yu et al. 2009; Zeng et al. 2019). Pharmacokinetic studies from humans and animal data demonstrated that PFOS is readily absorbed and distributed inside the human body after binding to plasma proteins (Thibodeaux et al. 2003). Human serum albumin (HSA) is considered the most abundant protein in plasma. HSA is the main carrier for PFOS in human beings with a binding ratio of 1:1 (Luo et al. 2012). Plasma proteins like HSA and alpha 1 acid glycoprotein tend to be less in children than in adults which may account for varying unbound fractions in children (Edginton et al. 2006). In the case of the geriatric population, HSA declines by almost 1.5% in each age

decade leading to hypoalbuminemia in some patients (Mene-Afejuku et al. 2019; Stader et al. 2019). This shows the need for the proper scaling of absorption and distribution factors in the different age groups. In relation to the elimination, PFOS studies carried out in adults showed a biological half-life of approx. between 3.1-7.4 years. In a study conducted with retired production workers, a half-life of up to 8-9 years was reported (Conway et al. 2018; Olsen et al. 2007; Thibodeaux et al. 2003). One explanation for the long-half life in humans may be due to saturable resorption from kidneys and enterohepatic recycling of PFOS. In the case of pediatric & geriatric populations, PFOS clearance may vary leading to different elimination half-life. The clearance mechanism is immature from birth to several months until the adult clearance is achieved (Hayton 2000). This question becomes more prominent in renally eliminated chemicals with a long biological half-life (PFOS, PFOA, etc.). Extrapolation for renal clearance from adults to pediatric and geriatric should be approached taking into account the half-life, the fraction unbound for specific chemicals, and the variation in glomerular filtration rate. Also, some other physiological factors like body weight, height, body mass index (BMI) play a major role in the kinetics of the xenobiotics. Interspecies, gender, physiological and age-wise difference in toxicokinetic makes the risk assessment challenging which can only be addressed through the aid of the PBPK model. PBPK model can be a valuable tool for risk assessment in PFOS and other related compounds to address the concerns of age-related sensitivity across the human lifespan. PBPK model for PFOS has been developed for rats, monkeys, and humans (adult, pregnant female and fetus, lactation) (Chou and Lin 2019, 2020; Fàbrega et al. 2014, 2016; Loccisano et al. 2011, 2013). Different authors developed the PFOS pregnancy PBPK model for estimating risk in the maternal and fetal population (Loccisano et al. 2013; Rovira et al. 2019). However, to date, there is not a PBPK model for PFOS that considers the risk assessment across the human lifespan (from pediatrics, adults to the geriatric population). Although for different chemicals, PBPK models have been developed for different life stages, it does not exist for the whole lifespan. For instance, Sharma et al. has developed dynamic pregnancy PBPK for BPA to predict the toxicokinetic profile of BPA in the fetus during gestational growth (Sharma et al. 2018). Song et al. developed an age-specific PBPK model for pyrethroids in rats for risk assessment in early age population (Song et al. 2019). Recently, Mallick et al. (2019) has developed a whole life-stage PBPK model for evaluating age-related differences in internal target tissue exposure and pharmacokinetics for pyrethroids in humans (Mallick et al. 2019). The widespread use, bioaccumulative nature, and observed health effects in humans for PFOS by epidemiologists call for the dynamic age-dependent PBPK model for assessing risk across the human life span. This PBPK model, which includes the entire lifespan, can be used to assess individual risk, or for a specific age group (with their anthropometric, physiological, and pharmacokinetic parameters). This can help to assess risk in a high-risk population (Loccisano et al. 2013; Zheng et al. 2019).

The objective of this manuscript is to develop and evaluate a dynamic age-dependent PBPK model to understand pharmacokinetic and assess the potential risk across different age groups (Figure 1). Age kinetic equations were developed considering the changes in the organ's physiology, and biochemical parameters were scaled to incorporate them in the PBPK model. Already published adult model and autopsy tissue data across age groups from Spain was used for validation. Biomonitoring data from three countries (China, Norway, and

Australia) was used for model evaluation. Sensitivity analysis was performed to assess the impact of uncertainty/variability in anthropometric, physiological and biochemical parameters with the context of changes in the accumulation of PFOS in different organs across age. The use of dynamic age-dependent PBPK may aid in understanding how the physiological changes along the age affect the tissue distribution of this compound in pediatrics, adult and geriatrics, thus improving the life stage-specific risk assessment for PFOS. It also helps in defining the reconstructed exposure in a sensitive population (pediatrics and geriatrics). Further, this model can be extended to other PFAS chemicals and examine the specific risks (neurotoxicity, reproductive effects, etc.) in the population based on the pharmacokinetic (Sharma et al. 2017).

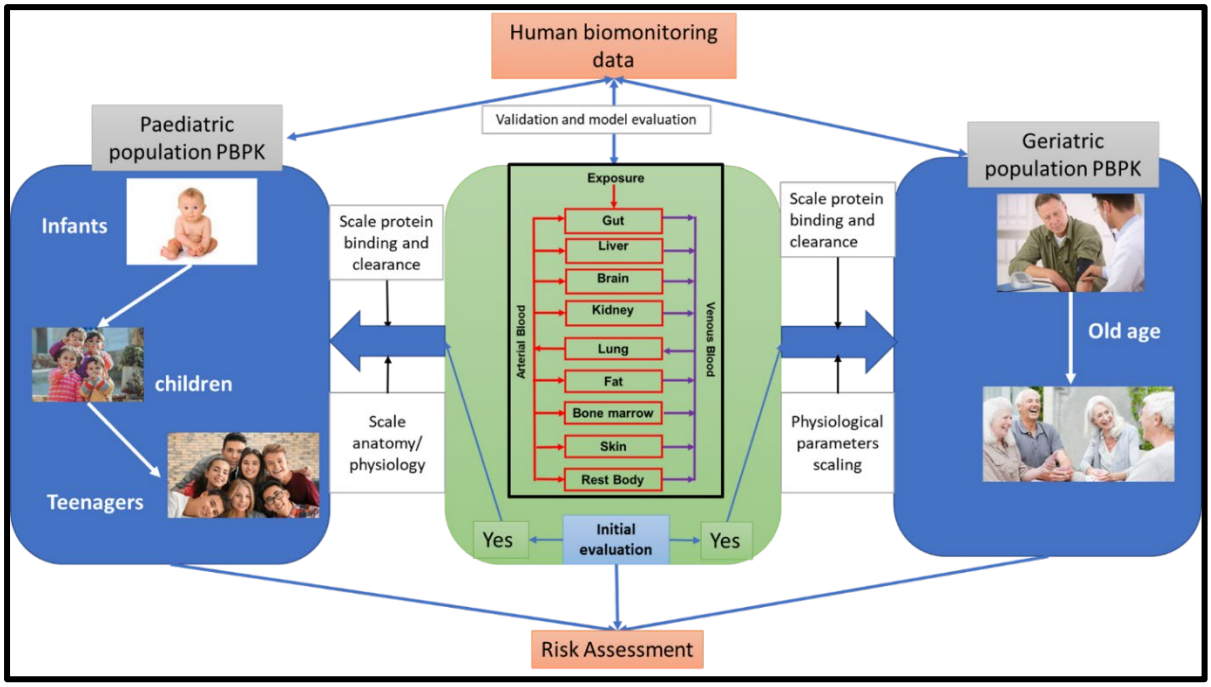

Figure 1: Model building framework for dynamic age dependent PBPK model. Already published adult model was evaluated and extended to pediatric and aged people. Physiological and biochemical parameters were scaled using different approaches for prediction of risk across human lifespan.

2. Methods

2.1 PBPK Model Structure

The structure of proposed dynamic age-dependent PBPK model is shown in Figure 1. Previously developed adult model for PFOS has been described in earlier published papers (Fàbrega et al. 2014, 2016; Rovira et al. 2019). The structural changes made to the model were addition of bone marrow and skin as two new compartments. This model was further extended to incorporate physiological and physicochemical parameters for the pediatric & geriatric population along with dynamic age growth. This model includes the pediatric, teenagers, adult, and geriatric module together with demography (height, weight, body surface area), physiology (organ volume, organ blood flow, cardiac output), and biochemistry (unbound fractions, renal elimination) for simulation of PK profile across different age groups. From four different countries i.e. China, Australia, Spain & Norway biomonitoring data were

used to check the performance of the model. The model was built and analyzed in MCSIM version 5.6.6 (Bois 2009) along with the R studio.

2.2 Age-Dependent Scaling (Parameterization of the model)

Physiological Parameters

Age-specific human anatomical and physiological parameters; like height, body weight, organ weight (or volumes), cardiac output, and blood flows were scaled across human lifetime considering the available human biomonitoring data (Clewell et al. 2004; Haddad et al. 2001; Mallick et al. 2019; Ogiu et al. 1997; Stader et al. 2019; Valentin and Streffer 2002). Changes in body weight and height along with age were incorporated to generate equations for organ growth in pediatrics, adults, and geriatric population from 0 to 90 years. Based on the trends observed in the data, the linear regression equations, polynomial equations of second, third, or fourth degree were considered. These regression equations were made in R studio which included the variability for 0 to 90 years and distribution was done for 1000 virtual population (Table 1 in Supplementary file). Observed data from ICRP 89, Stader et al., and Hermanussen et al. was used to verify the simulated data from different regression equations for organ volume (Haddad et al. 2001; Heinemann et al. 1999; Hermanussen et al. 2012; Johnson et al. 2005; Mallick et al. 2019; Noda et al. 1997; Stader et al. 2019; Valentin and Streffer 2002; Ogiu et al. 1997; Dekaban and Sadowsky 1978).

Data on cardiac output were taken from ICRP 89 and Stader et al. which collected data from 12 studies with 645 subjects (Valentin and Streffer 2002; Stader et al. 2019). The surface area was calculated using equations from Du Bois et al. corresponding to body weight and height for both males and females (D. Du Bois and E. Du Bois 1989). Due to lack of data for blood flow and unavailability of standard equations in different organs in children, allometric scaling was done considering the adult blood flow of 25 years from ICRP 89 as the standard value. For validating and verifying the physiological equations, data from several authors were taken to make a robust equation with incorporated variability (supplementary file 1) (Clewell et al. 2004; Haddad et al. 2001; Johnson et al. 2005; Ogiu et al. 1997; Price et al. 2003; Stader et al. 2019; Valentin and Streffer 2002).

Physicochemical Parameters

Tissue: plasma partition coefficient parameters for dynamic age-dependent PBPK model were taken from the earlier published model (Fàbrega et al. 2016). Other parameters like fraction unbound, elimination rate constant & renal resorption were calculated based on available data or scaled using the standard approach. In this model, the fraction absorbed from stomach to liver is considered as one. All the values of parameters were reported in Table 1.

Unbound Fraction

Plasma protein binding levels are lower in children and geriatrics than in adults especially newborn and old age. For PFOS, the binding affinity is higher for HSA than any other plasma protein. Fraction Unbound for PFOS was calculated based on equation 1 for all age groups considering the variation in their albumin levels (McNamara and Alcorn 2002). Unbound fraction was calculated based on the binding characteristic of PFOS in adults and ontogeny for binding protein factor as shown in eq. 1.

$$fu_{child} = \frac{1}{1+OSF*\frac{(1-fu_{adult})}{fu_{adult}}} \quad \text{eq. 1}$$

Here, fu_{child} represents unbound fraction of PFOS in child, fu_{adult} represents unbound fraction in adults, OSF is age dependent ontogeny scaling factor calculated based on human serum albumin levels (McNamara and Alcorn 2002; Meistelman et al. 1990; Zheng et al. 2019).

Renal Resorption

Long half-lives of PFOS suggest that renal resorption is the main driving factor that has been considered by resorption maximum (Tm) and affinity constant (Kt) in the model. Values of Tm and Kt for adults were taken from an already published adult model (Table 1) (Fàbrega et al. 2014, 2016; Rovira et al. 2019). Scaling up these parameters in the pediatric and geriatric population is somewhat complicated due to the lack of renal data in these population groups; therefore, dynamic allometric scaling was used. For renal resorption, the value of adult resorption maximum constant (Tmc) was used and the scaling was done with respect to the fraction of BW in different age groups (BW_{AG}) and adult body weight (BW_{adult}) (eq. 2). Value of urinary elimination rate constant (KurineC) was taken from adult model to calculate urinary elimination rate and then scaled based on $BW^{-0.25}$ (eq. 3).

$$Tm = Tmc * (\frac{BW_{AG}}{BW_{adult}})^{0.75} \quad \text{Eq. 2}$$

$$Kurine = KurineC*(BW)^{-0.25} \quad \text{Eq. 3}$$

Table 1: Compound-specific parameter value for PFOS PBPK Model

Parameters	Values	Reference
Molecular weight (g/mol)	500.13	(PubChem Compound Summary for CID 74483, Perfluorooctanesulfonic acid)
Unbound fraction in plasma (fu, age<=3)	0.031	(McNamara and Alcorn 2002; Meistelman et al. 1990; Zheng et al. 2019)
Unbound fraction in plasma (fu, age<=10)	0.027	(McNamara and Alcorn 2002; Meistelman et al. 1990; Zheng et al. 2019)
Unbound fraction in plasma (fu, age<=71)	0.025	(Meistelman et al. 1990); b (Zheng et al. 2019); c (McNamara and Alcorn 2002); d (Fàbrega et al. 2016); e (Rovira et al. 2019)
Unbound fraction in plasma (fu, age<=89)	0.026	(McNamara and Alcorn 2002; Meistelman et al. 1990; Zheng et al. 2019)
Unbound fraction in plasma (fu, age>=90)	0.028	(McNamara and Alcorn 2002; Meistelman et al. 1990; Zheng et al. 2019)

Tmc*	3.5-5.5	(Fàbrega et al. 2016; Rovira et al. 2019)
Tissue: Plasma partition coefficient		
Liver	2.56	(Fàbrega et al. 2016; Loccisano et al. 2013; Rovira et al. 2019)
Gut	0.05	(Fàbrega et al. 2016; Loccisano et al. 2013; Rovira et al. 2019)
Brain	0.35	(Fàbrega et al. 2016; Loccisano et al. 2013; Rovira et al. 2019)
Kidney	1.21	(Fàbrega et al. 2016; Loccisano et al. 2013; Rovira et al. 2019)
Adipose Tissue	0.32	(Fàbrega et al. 2016; Loccisano et al. 2013; Rovira et al. 2019)
Lung	8.70	(Fàbrega et al. 2016; Loccisano et al. 2013; Rovira et al. 2019)
Bone marrow	17.94	(Fàbrega et al. 2016; Loccisano et al. 2013; Rovira et al. 2019)
Skin	0.11	(Fàbrega et al. 2016; Loccisano et al. 2013; Rovira et al. 2019)

*Tmc refers to resorption maximum constant (ug/h/$kg^{0.75}$)

2.3 Adult Model Simulation

Firstly, the dynamic age-dependent PBPK model was evaluated at the adult age as a reference by doing simulation from 25-35 years, and results were verified against the data obtained by simulating the same age group using the already published model (Fàbrega et al. 2014, 2016; Rovira et al. 2019). Model predictions were evaluated using the Pearson correlation test. It provided the correlation coefficient to establish the relationship (goodness of fit) for results from both the models using a statistical level of significance (p-value). Statistical analysis and data processing were done in R studio using a correlation package (corr) (Makowski et al. 2020).

2.4 Exposure Reconstruction

Very limited experimental or modeling studies have measured or estimated external exposure in pediatric and geriatric populations considering the different exposure routes. Dynamic PBPK model was used to estimate the external exposure for different age groups through internal plasma concentration from human biomonitoring data. The daily intakes were estimated for different age groups using the Bayesian framework and a uniform prior distribution using Markov Chain Monte Carlo (MCMC) distribution. Bayesian framework along with MCMC distribution helps in optimizing the model and evaluating the uncertainty and variability of model parameters (Chou and Lin 2020). For the autopsy data in different organs from Perez et al., the liver data was used for reconstructed exposure using MCMC distribution. Reconstructed exposure was needed as there was no available data about daily exposure from multiple pathways in different age groups. Then the reconstructed exposure was used to simulate the concentration of chemicals in other organs (brain, kidney, lungs, and liver) at specific ages. Different biomonitoring studies from three countries were available with the reported concentration in plasma, serum, or blood at varying ages (Haug et al. 2009;

Kärrman et al. 2006; Zhang et al. 2010). Raw data was not available from these studies and reported data was with wide age groups. In order to cover all the exposure range for observed biomonitoring plasma samples, which could be due to random sample at any specific year or variability in the subjects, the dynamic distribution for external exposure was simulated.

2.5 Biomonitoring Data and Model Simulation

For evaluating accumulation of PFOS in different body compartments with age, human biomonitoring data of PFOS in autopsy tissues of liver, brain, lung, and kidney from subjects who had been living in Spain (Tarragona, Catalonia) was used (Pérez et al. 2013a). Samples were collected in 2008 within the first 24 hours of the death of the patient and 21 PFAS were analyzed in 99 samples. Subject ages ranged from 28 to 86 years. This data was used for model evaluation covering different age groups. Another biomonitoring Data from China contains 245 human blood samples with age-related differences (Zhang et al. 2010). PFC concentrations were characterized in human blood from infants, toddlers, children, and adolescents in China (Table 1 in supplementary file). Another study by Haug et al. analyzed serum samples at different years (from 1976 to 2007) in Norwegian residents covering age groups (0 to 59 years) (Haug et al. 2009). An Australian study by Karrman et al. (2006) reported pooled serum samples from 3802 Australian residents with people from 5 different age groups (0-80 years). Serum samples were collected from rural and urban regions of Australia. Data was divided into pools for each specific region with 2 pools in each stratum (Table 1 in supplementary file).

Different model simulations were carried out to obtain the plasma concentration as a function of age and these data were compared with the biomonitoring results. Monte Carlo simulation was performed taking into account the parameter distribution representing interindividual variations. Agreement of the model results with biomonitoring data was examined graphically and statistically using the correlation plot with the Pearson correlation coefficient.

2.6 Sensitivity Analysis

Global sensitivity analysis (GSA) was performed on the dynamic age-dependent model across ages through the pksensi R package. A global sensitivity analysis was performed instead of local sensitivity analysis because it allows all input factors to be varied simultaneously and quantifies the importance of model input and their interaction with respect to model output. The analysis was performed considering the system at a steady state similar to the realistic scenario. Variance-based GSA method is based on the Sobol sensitivity index (SI) and calculates the sensitivity with the effect of specific parameters on organs (Hsieh et al. 2018a, 2018b). All the parameters were varied 1% to compute the effect on model output (plasma, liver, kidney, bone marrow, lung, and fat compartment). Sometimes, due to smaller sample size, SI is not stable showing high variability, random phase shift approach was used for replicating samples across random points to test the robustness and convergence of the sensitivity index. If the model is built under $y=f(x_i)$, the sampling scheme can be described as

$$x_i = \frac{1}{2} + \frac{1}{\pi}\arcsin(\sin(w_i s + \phi_i)) \quad \text{(Hsieh et al. 2018a)} \qquad \text{Eq. 4}$$

Where x_i refers to the nominal value of the i_{th} parameter, w_i is a vector giving the set of frequencies, one frequency for each parameter, and s is a random phase-shift coefficient

ranged from 0 to 2 one frequency for each parameter, and φ_i is a random phase-shift coefficient ranged from 0 to 2 π. Extended Fourier amplitude sensitivity testing (eFAST), a variance-based sensitivity analysis method helps in determining influential parameters by randomly generating the sequence. Further, heat map visualization was performed to distinguish between influential and non-influential parameters with a cut-off point. If the cut-off is more than 0.1, it was considered as a highly influential parameter and less than 0.05 was considered as non-influential parameters indicating these parameters would not contribute to a major change in the output. Results were analyzed to detect sensitive parameters at different age groups (Figure 1,2 & 3 in supplementary file).

3. Results

Variations in anthropometric and physiological parameters across the human lifetime are shown in Table 2 in the supplementary file. The equations cover the physiological growth of a complete human lifetime along with variability in parameters. Initially, dynamic age-dependent PBPK model at adult age was compared with the results from the published PBPK model at the same age. Then this model was used to simulate organ concentration over a human lifetime and validated with autopsy data. Further, the model was used to simulate plasma concentration across a human lifetime and evaluated with data from 3 different cohorts. Across age groups, sensitive parameters were evaluated for the sensitivity of different organs with PFOS exposure.

3.1 Adult Model Evaluation

To evaluate the dynamic age-dependent PBPK model, first, this model was run at an adult age for plasma concentration. For comparison, results from an already published adult model from Fàbrega et al. was used to evaluate the plasma concentration with the same exposure level (Fàbrega et al. 2014, 2016). Concentration in plasma from the dynamic adult model was in good agreement with the concentration in plasma from the published model (Figure 12 in Supplementary file). The relationship (goodness of fit) between results from concentration in plasma from both models using linear regression (Pearson correlation coefficient) showed a good correlation with p-value less than 0.001 and correlation coefficient approximately equal to 1.

3.2 Model Predictions for Autopsy Data

Next, we evaluated the dynamic age-dependent PBPK model across different age groups by simulating PFOS tissue distribution with the autopsy data of the population living in Tarragona. First, individual exposure was reconstructed utilizing the liver PFOS concentration and then the estimated reconstructed exposure was used to predict the concentration in different organs (brain, kidney, liver, lungs) (Figure 2). As indicated in figure 2, simulation results were within the range of autopsy data in liver, brain, and kidney except for the lung. In kidney few data points were outside the simulated range but within 2-fold of simulated concentration. However, in the lungs, the model overpredicted the results in comparison to autopsy data which may be due to variation in partition coefficient. From autopsy data, it is noticed that PFOS accumulation is lowest in the brain from age 20 to 85 years and the same trend can be seen in the simulation results from PBPK (Figure 2).

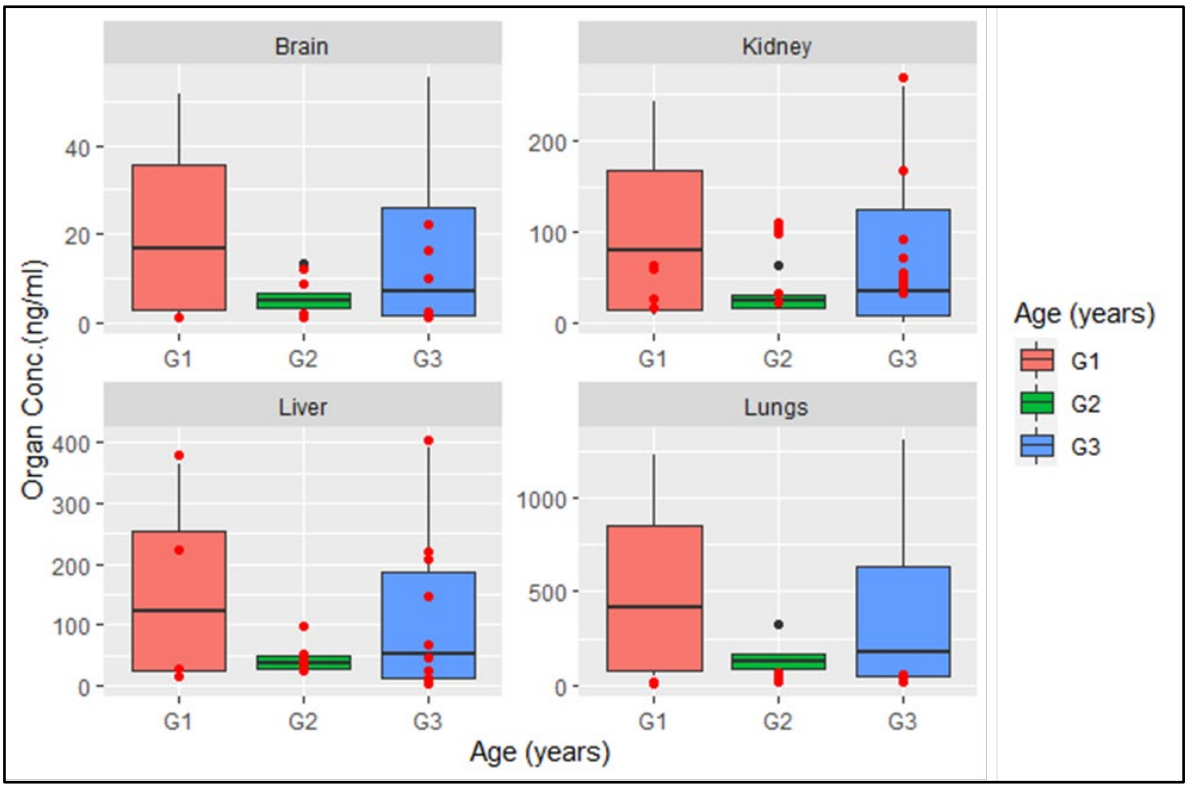

Figure 2: PFOS concentrations in brain, kidney, liver and lungs of human at different ages simulated individually using PBPK model. G1 refers to the age group 25-35 years, G2 for 36-60 years and G3 for 61-86 years. Red dot represents the autopsy data obtained from postmortem samples of different human tissues in Tarragona region (Catalonia, Spain). Upper whiskers shows the percentile 95 and lower whisker presents the percentile 5 of the simulated organ concentration. More detailed description about the data can be obtained from (Pérez et al. 2013b).

3.3 Model Evaluation using Different Cohorts

Dynamic age-dependent PBPK model was used to simulate plasma concentration over the human lifespan and biomonitoring data from the different cohort was used for comparing the results. Figure 3 compares the observed and predicted plasma concentration from China (ages ranging from 0 to 90 years). The PFOS biomonitoring data from Zhang et al. for different age groups showed that the concentrations increase slightly with age. This same trend was observed in simulated data (Zhang et al. 2010). Figure 4 represents the plasma concentration of the Norwegian population from 1976 to 2007. To capture the downfall trend after 2000, dynamic exposure was used considering the reduction in daily exposure. This was due to the phase-out of PFOS production in many countries and reduced emission in European countries after 2000 (Nøst et al. 2014a; Sun et al. 2020). Comparison of model-predicted plasma PFOS concentration versus Australian biomonitoring data from 2007-2008 (range from 0 to 85 years) was in good agreement for all pools based on region and age groups (Figure 5). Simulated results from this study indicate that PFOS accumulation increase with age. Similar results were obtained from a biomonitoring study by Kärrman et al. (2006) with elevated PFOS accumulation at age <16 years and > 60 years. The reason behind this may be elimination, chemical half-life with age, physiological factors and exposure to the chemical (Kärrman et al. 2006).

To better illustrate the plasma concentration, a goodness-of-fit plot was used for predicted and observed plasma concentration as shown in Figure 6. This figure shows that most of the predicted concentrations fall within the two-fold error range of observed concentrations which meets the WHO model precision criteria (Project and No 2010). Thus, based on these studies, we can validate that the developed PBPK model can reasonably predict the concentration of PFOS inside human body for different age groups.

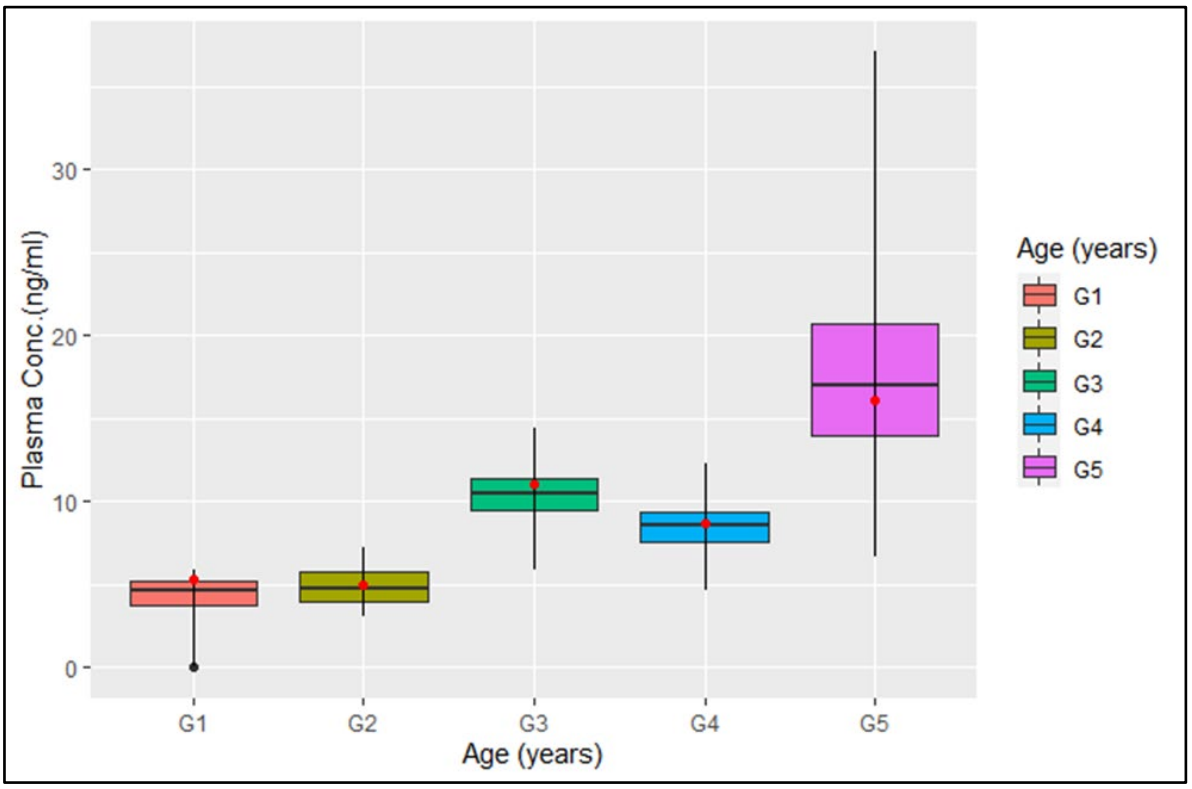

Figure 3: Time course concentration of PFOS in plasma with age in infants (G1: 0-1 years), toddlers (G2: 1-5 years), children (G3: 5-10 years), adolescents (G4: 10-18 years) and adults (G5:18 to 90 years). Biomonitoring data was from China from year 2009 across all age group (0 to 90 years) presented by red circles. Upper whisker represents 95 percentile and lower whisker represents 5 percentiles of PFOS distribution in plasma.

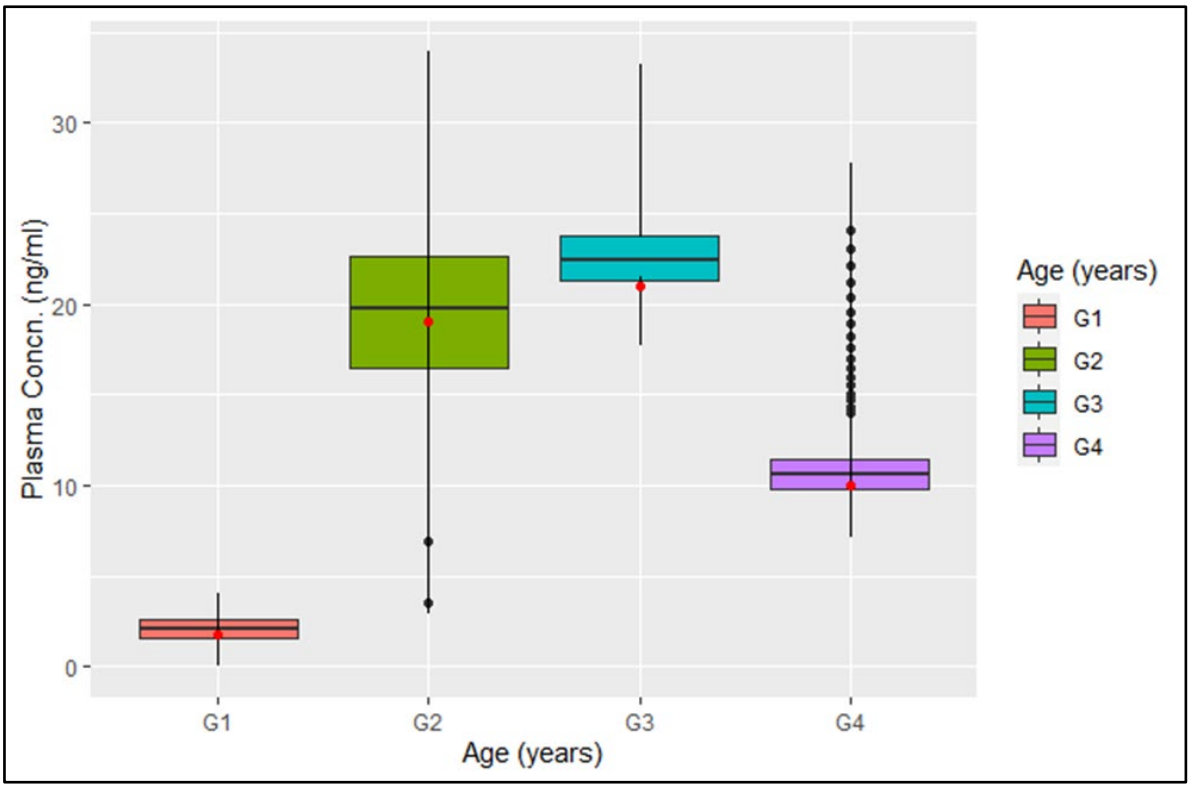

Figure 4: Concentration of PFOS (ng/ml) in plasma sample of Norwegian population. G1 represents age 0 to 4 years, G2 for 5 to 14 years, G3 for 15 to 24 years and G4 for 25-59 years. Red dot represents biomonitoring data from 1976 to 2007 covering population from 0 to 59 years.

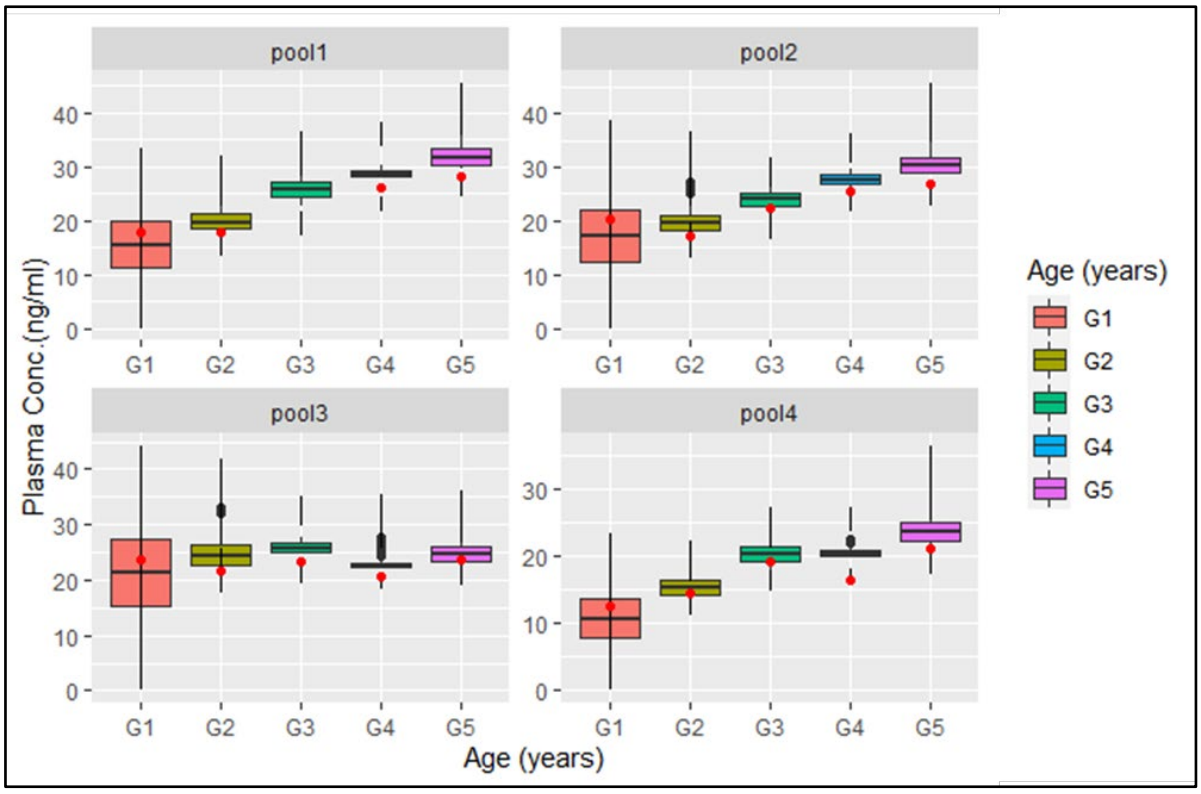

Figure 5: Concentration of PFOS in Australian population with each pool having serum samples divided based on age and region. G1 refers to 0-16 years, G2 for 16 to30 years, G3: 31 to 45 years, G4: 46 to 60 years, G6: 61 to 80 years and red dot represents biomonitoring data in specific age groups. Pool 1 and pool 2 represents the rural region where pool 3 and pool 4 represents the urban region.

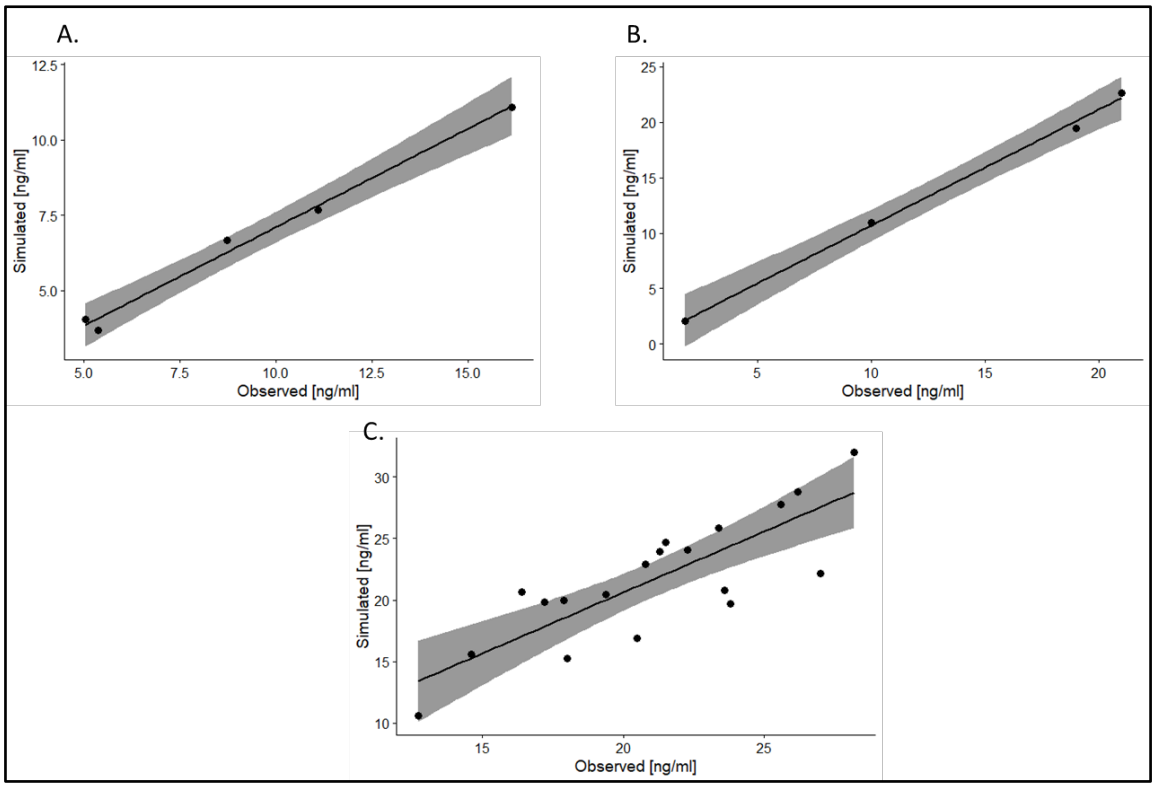

Figure 6: Comparison of simulated (y-axis) and observed (x-axis) plasma concentration with goodness of model fit with correlation plot from 3 different cohorts. In the plot, A represents biomonitoring data from China, B represents the biomonitoring data from Norway and C represents biomonitoring data from Australia.

3.4 Sensitivity Analysis

A global sensitivity analysis was performed for a total of 33 anthropometric, physiological and biochemical parameters to determine the most influential parameters for concentrations of PFOS in 5 organs (plasma, fat, liver, kidney and bone marrow) in the human (Figure 1, 2, 3 in supplementary file). Results of the GSA were based on a 1% variation in parameter values. The results indicated that in the physiological parameters, body weight, bone marrow volume, liver volume, blood flow to the kidney, GFR were most sensitive across all ages (Figure 2 in supplementary file). Other physiological parameters were reported to have low sensitivity and showed variation with age (Figure 7). Another sensitivity analysis was carried out for partition coefficient across all ages for 5 compartments (Figure 1). Partitioning for liver and bone marrow is highly sensitive across all ages (Figure 1 in supplementary file). The sensitivity analysis for biochemical parameters (Figure 3 in supplementary file) in which affinity constant, renal reabsorption, and fraction unbound are the highly sensitive parameter for all age groups. The sensitivity of some parameters changing with age shows that the risk factor changes with the age. This behavior has also been noted in autopsy data from Tarragona where accumulation in different organs changes with age. As renal clearance decreases with age, the half-life of these chemicals in the human body may increase more in geriatrics than adults.

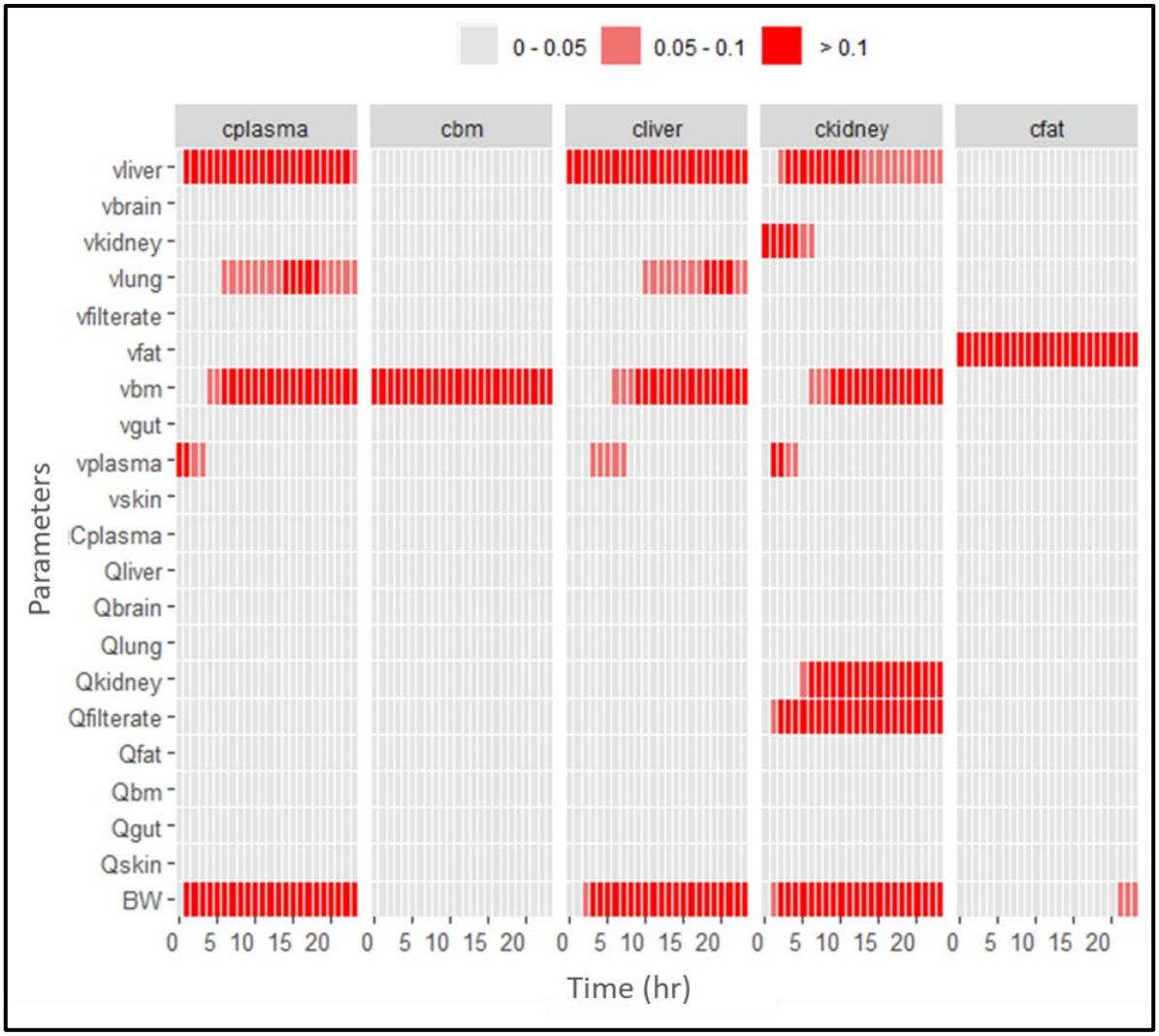

Figure 7: Heat map representing sensitive physiological parameters to the different body organs at adult age.

Here, cplasma refers to concentration in plasma, cbm refers to concentration in bone marrow, cliver refers to concentration in liver, ckidney to concentration in kidney and cfat to concentration in adipose tissue, vliver- volume of liver, vbrain- volume of brain, vkidney- volume of kidney, vlung- volume of lungs, vfiltrate- filtrate compartment volume, vfat- volume of adipose tissue, vbm- volume of bone marrow, vgut- volume of gut, vplasma- volume of plasma, vskin- volume of skin, QCplasma – cardiac output, Qliver- liver blood flow, Qbrain- brain blood flow, Qlung- lung blood flow, Qkidney- kidney blood flow, Qfilterate- glomerular filtration rate, Qfat- adipose tissue blood flow, Qbm- bone marrow blood flow, Qgut- gut blood flow, Qskin- skin blood flow and BW- Body weight.

4. Discussion

Adult PBPK model for PFOS had been developed by several researchers (Brochot et al. 2019; Chou and Lin 2020; Fàbrega et al. 2014; Loccisano et al. 2012, 2013; Rovira et al. 2019) for describing the kinetics of PFOS in human but risk varies across human lifespan raising the need for robust dynamic age-dependent PBPK model. For PFOS risk assessment, a dynamic age-specific PBPK model was developed incorporating physiological and biochemical changes with age and their impact on the disposition of chemicals inside the human body. This is the first dynamic age-specific PBPK model for PFOS and provides a framework for understanding PFOS behavior in pediatrics, adults, and geriatric populations. The analysis was performed with the Monte Carlo simulation technique considering the uncertainty and variability of the

anthropometric, physiological, and biochemical model parameters. This model was used for reconstructed exposure and to provide estimates in sensitive populations with high susceptibility to risk. Limited data are available on internal dose in human and this PBPK model serves as an important tool for improving the accuracy of quantitative risk assessment of chemicals like PFOS in sensitive population.

4.1 Biochemical Parameters

Biochemical parameters are hybrid parameters that represent both the physiology and the chemical characteristics, thus these parameters become very important to investigate for the age-specific dynamic model taking into account both the uncertainty and variability. Free fraction is generally determined mostly by the level of the albumin which varies depending on the age group and this was emulated in the current model based on Edginton et al. 2006. (Forsthuber et al. 2020). As the level of albumin determine the extent of PFOS binding to plasma proteins and hence affecting the kinetics of PFOS as only the unbound fraction is subjected to clearance (Mallick et al. 2019). Renal clearance of PFOS is also being impacted by reabsorption from the proximal tubule back to the renal blood and this process follows saturation kinetics (Loccisano et al. 2012). This process could be responsible for varying plasma half-life of PFOS in young population and other sensitive age groups. Being the dynamically scaled age-dependent PBPK model, the clearance and reabsorption process were made dynamic based on the two biochemical parameters i.e. transporter maximum (Tmc) (refer equation 2) and affinity constant (Kt). Both the dynamic changes in binding and elimination accounts for describing the pharmacokinetics of PFOS with age, hence giving a better perspective of quantitative risk assessment.

4.2 Model Evaluation

Initially, the adult PBPK model was validated with the published model from Fabrega et al. (Fàbrega et al. 2014). The agreement between the predicted and observed concentration of PFOS in adult human plasma was good with an R-square value of more than 0.95. Next, the biomonitoring data from the Tarragona autopsy study was used for validating the model which include PFOS concentrations in various organs i.e. liver, kidney, brain, and lungs. First, the reconstructed external exposure was estimated utilizing the liver concentration data for various age groups separately (20 to 85 years) and then the estimated exposure was used to simulate the individual internal exposure for kidney, lungs, and brain along with the liver. The simulated data from the Tarragona autopsy study was in good correlation with the observed results from the dynamic PBPK model all within a factor of 2 (Figure 2). In Fabrega et al., study, simulated concentrations were much less than experimental data, but the dynamic PBPK model developed was able to capture the biomonitoring data. However, in the case of lung tissue, the model overpredicted the concentration compared to the autopsy results. This indicates there might be some additional mechanisms or it could be just the volume of distribution for lungs is different. This could compensate easily by recalibrating the partition coefficient between lungs to plasma. To confirm this further a detailed inhalational PBPK model along with some control experimental data might be required.

Reconstructed exposure was used for simulating plasma concentration with 3 independent cohorts from different countries. In China, the data covered all the age groups from 0 to 90

years and the trend shown by biomonitoring data was comparatively increased concentration of PFOS with age. Simulated data also showed the increased PFOS concentration in plasma with old age. The possible reason behind this could be PFOS is a long-acting chemical and as with the age, the organs like bone marrow and adipose tissue matures leading to higher disposition inside the body. Also, a positive correlation of PFOS with age may be due to increased dietary intake including seafood and fish having high PFOS levels in China (Zhang et al. 2010). In another study by Gulkowska et al. PFOS has been detected in all the seafood samples with a higher concentration in fish and crab (Gulkowska et al. 2006). However, in the case of the geriatric population, the dietary intake is low but decreased kidney elimination, reduced GFR capacity, decreased bone marrow volume, and increase in adipose tissue, leading to deposition of this lipophilic chemical inside human tissues. In general, accumulative, lipophilic nature and continuous exposure of PFOS may be responsible for an increase in PFOS concentration with age. Even in sensitivity analysis, the blood flow to the kidney, GFR, and volume of bone marrow and adipose tissue were parameters highly sensitive for PFOS. Gracia et al. (2018) showed the ability of PFOS to accumulate in adipocyte cells almost comparable to reference compounds (cationic amphiphilic drugs). Another study by Xu et al. showed that PFOS promotes adipogenesis and lipid accumulation by Nrf2 signaling activation and PPAR alpha induction leading to adverse effects (Xu et al. 2016). These studies indicate that the sensitivity of adipose tissue towards PFOS could be linked with both its kinetic and dynamic aspects. Further experimental studies need to be done for explaining the sensitivity and accumulation potential of PFOS in the geriatric population. Another study by Kärrman et al. has shown that PFOS disposition increase from 16 to 60 years in the rural and urban population which is in sync with biomonitoring results from Zhang et al. suggesting that the geriatric population is more susceptible to PFOS risk as compared to adults (Kärrman et al. 2006; Zhang et al. 2010) (Figure 5). Also, comparatively, higher reconstructed exposure and plasma concentration in children with age group 5-10 years was observed. This is in line with the other study where it has been showed that children's outdoor PFOS exposure involves more dust particles, dermal contact with PFOS or PFOS treated products, and multiple other sources, this may be responsible for comparatively higher plasma concentration in children (Winkens et al. 2017). In case of infant age (0-1), exposure from the mother is present by breastfeeding and other contacts which can lead to increased PFOS in plasma compared to other groups as has been seen in figure 3 (Liew et al. 2018). Another study from Haug et al. was used for model evaluation where they had pooled data for PFOS serum from 1976 to 2007 in different age groups from 0 to 59 years. Simulated and observed plasma concentration showed a drastic decrease in the 2007-year age group (Figure 4) due to dynamic exposure. The possible reason for this decline may be due to i) after 2000, major producers like 3M announced the phase-out production of perfluoro compounds and ii) PFOS inclusion in the Stockholm convention in 2009. These global efforts and strict adherence to POPs regulations have led to reduced exposure of PFOS in the Norwegian population (Nøst et al. 2014).

4.3 Sensitivity Analysis

To analyze the influential parameters across age, a global sensitivity analysis was performed for all physiological and biochemical parameters. The sensitivity analysis results suggest that

the free fraction (fu), transporter maximum constant (Tmc), and affinity constant (Kt) are influential biochemical parameters at all ages. Several studies for PFOS by different authors have reported these parameters as the most influential which are consistent with our findings (Chou and Lin 2019; Fàbrega et al. 2016). Tmc and Kt affect the renal reabsorption process thus lowering the renal clearance causing PFOS to accumulate inside the human body. The free fraction of PFOS is available to move and potential to accumulate and eliminate respectively in and from the different organs. Physiological parameters such as liver and bone marrow volume, kidney blood flow, GFR, and partition coefficient for liver, bone marrow, and kidney are highly sensitive across the human lifespan. These results support the finding of previously published studies that the kidney is the main organ for elimination in PFOS and contributes to predicted PFOS concentration in plasma and other organs (Chou and Lin 2020; Loccisano et al. 2013; Tan et al. 2008). Liver volume is shown to be sensitive for all the organs as the liver is the primary highly exposed organ that receives the xenobiotics, via portal vein from the intestine before it gets distributed to plasma and then other organs (Figure 2 in supplementary file). Exposure of PFOS to liver is higher in the human body from childhood and it starts accumulating in the organ. Even in Tarragona autopsy data (Figure 2), the liver showed the highest accumulation across ages. The volume of bone marrow is more sensitive during childhood than adult. This may be due to immature bone marrow during early life stages. Also, the PFOS exposure is higher in bone marrow due to a higher partition coefficient. Kidney plays an important part in the elimination of PFOS making it a sensitive parameter especially for renal resorption which is affected by GFR. Autopsy data from Tarragona showed PFOS concentration in the kidney with an increased level in the geriatric population as compared to adults.

4.4 Dosimetry and Risk Assessment

One application of this dynamic age-dependent PBPK model is to estimate the human daily exposure from observed plasma/blood/serum concentration from biomonitoring studies. Because in a real-life scenario, it is very difficult to accurately estimate the contribution from various sources (diet, dust, water, soil, indoor exposure, and other sources), the currently developed PBPK model serves as an excellent tool for finding exposure at different age groups. For PFOS, the estimated reconstructed exposure varied from $1.4e^{-5}$ to $1.25e^{-4}$ ug/g body weight per day (Table S3 in supplementary file). The higher exposure was noticed in children than teenagers and adults in all the 3 cohorts which may be due to higher relative uptake by food consumption and hand-to-mouth transfer from carpets and dust ingestion (Trudel et al. 2008). Another reason behind high exposure can be the changes in physiology (varied distribution and elimination capabilities) in children than adults. The high exposure indicates that children may be more susceptible to health effects than adults from exposure to PFOS as they are in the development stage. The exposure in the geriatric population is less than in other age groups, still it poses a major challenge. With age, the kidney loses its nephrons and a corresponding decrease in GFR leading to decreased capability for the elimination of xenobiotics. Also, epidemiological studies have linked PFOS exposure to lower eGFR and chronic kidney disease further increasing the risk even with relatively lower exposure.

Due to variation in toxicokinetic across the human lifespan, higher external exposure may result in different internal dosimetry in humans. The varied concentration of PFOS in different organs increase the risk for toxicity in sensitive population. Currently, there are many mechanisms of actions (MOA) being evaluated by different researchers linked to toxicity in the liver, kidney, adipose tissue, and other organs (hepatocellular hypertrophy, liver, and kidney cancer, decreased triglyceride levels, increased cholesterol levels and decreased GFR) (Deepika et al. 2020; Huang et al. 2020). Continuous exposure to PFOS inside the human body like kidney and liver for longer times pauses risk to sensitive population (Figure 2) and gives insights into the association of PFOS with liver damage and kidney cancer (Saikat et al. 2013; Sunderland et al. 2019). A study by Gong et al. showed PFOS exposure increases kidney injury by impaired metabolism of purines and amino acids and increased oxidative stress in rat mesangial cells (Gong et al. 2019). Also, different epidemiological studies point towards associations between PFAS exposure and lower kidney functions. PFAS exposure alters different pathways like the peroxisome proliferator-activated receptor (PPAR) pathway, NF-E2 related factor 2 pathway, oxidative stress pathway, and increased endothelial permeability through actin filament modeling linking PFAS to kidney disease. PFOS was linked to liver toxicity by interfering with mitochondrial beta-oxidation of fatty acids and affecting the transcriptional activity of PPAR alpha in the liver (Martin et al. 2007; Wan et al. 2012; Wang et al. 2014). Such kind of associations can be explained indirectly by a dynamic PBPK model across ages through a simulated concentration in the liver, kidney, and other sensitive organs. Further, the dynamic age-dependent PBPK model can be linked to the pharmacodynamic and systems biology model to explain the effects of toxicity through mechanistic pathways at cellular and molecular levels.

5. Conclusion

The present study provided a dynamic age-dependent PBPK model for PFOS in different age groups from pediatrics, adult to geriatrics. By incorporating physiological and physicochemical parameters at different age groups, the model can describe the kinetics of PFOS in sensitive populations and different organs where biomonitoring data are limited or difficult to measure. The simulated results show that the geriatric populations have relatively higher PFOS concentration even with lower exposure than children making them more prone to risk. The presence of PFOS in different organs with age points towards adverse effects and increased vulnerability to PFOS linked adverse outcomes. The dynamic age-dependent PBPK model can be used to support risk assessment in a susceptible population like pediatrics and geriatric population and can be used to assess the exposure at different age groups. Further, this framework can be extended to predict the risk for the coming generation by introducing exposure for the next generation through pregnancy and lactation.

Acknowledgment

This study was financially supported by Marie Skłodowska-Curie “Neurosome Project” under the grant agreement No. 766251 as well as by the European Community funded H2020 HBM4EU project under Grant Agreements no. 733032. This publication reflects only the authors' views. The Community and other funding organizations are not liable for any use made of the information contained therein.

Reference

Abraham K, Mielke H, Fromme H, Völkel W, Menzel J, Peiser M, et al. 2020. Internal exposure to perfluoroalkyl substances (PFASs) and biological markers in 101 healthy 1-year-old children: associations between levels of perfluorooctanoic acid (PFOA) and vaccine response. Arch Toxicol 94:2131–2147; doi:10.1007/s00204-020-02715-4.

Augustsson A, Lennqvist T, Osbeck CMG, Tibblin P, Glynn A, Nguyen MA, et al. 2021. Consumption of freshwater fish: A variable but significant risk factor for PFOS exposure. Environ Res 192:110284; doi:10.1016/j.envres.2020.110284.

Bois FY. 2009. GNU MCSim: Bayesian statistical inference for SBML-coded systems biology models. Bioinformatics 25:1453–1454; doi:10.1093/bioinformatics/btp162.

Brochot C, Casas M, Manzano-Salgado C, Zeman FA, Schettgen T, Vrijheid M, et al. 2019. Prediction of maternal and foetal exposures to perfluoroalkyl compounds in a Spanish birth cohort using toxicokinetic modelling. Toxicol Appl Pharmacol 379:114640; doi:10.1016/j.taap.2019.114640.

Butenhoff JL, Chang S-C, Olsen GW, Thomford PJ. 2012. Chronic dietary toxicity and carcinogenicity study with potassium perfluorooctanesulfonate in Sprague Dawley rats. Toxicology 293:1–15; doi:10.1016/j.tox.2012.01.003.

Černá M, Grafnetterová AP, Dvořáková D, Pulkrabová J, Malý M, Janoš T, et al. 2020. Biomonitoring of PFOA, PFOS and PFNA in human milk from Czech Republic, time trends and estimation of infant's daily intake. Environ Res 188; doi:10.1016/j.envres.2020.109763.

Chou W-C, Lin Z. 2019. Bayesian evaluation of a physiologically based pharmacokinetic (PBPK) model for perfluorooctane sulfonate (PFOS) to characterize the interspecies uncertainty between mice, rats, monkeys, and humans: Development and performance verification. Environ Int 129:408–422; doi:10.1016/j.envint.2019.03.058.

Chou WC, Lin Z. 2020. Probabilistic human health risk assessment of perfluorooctane sulfonate (PFOS) by integrating in vitro, in vivo toxicity, and human epidemiological studies using a Bayesian-based dose-response assessment coupled with physiologically based pharmacokinetic . Environ Int 137:105581; doi:10.1016/j.envint.2020.105581.

Clewell HJ, Gentry PR, Covington TR, Sarangapani R, Teeguarden JG. 2004. Evaluation of the Potential Impact of Age- and Gender-Specific Pharmacokinetic Differences on Tissue Dosimetry 2Current address: Novartis Pharmaceuticals, East Hanover, NJ 07936. Toxicol Sci 79:381–393; doi:10.1093/toxsci/kfh109.

Conway B, Badders A, Costacou T, Arthur J, Innes K. 2018. Perfluoroalkyl substances and kidney function in chronic kidney disease, anemia, and diabetes. Diabetes, Metab Syndr Obes Targets Ther Volume 11:707–716; doi:10.2147/DMSO.S173809.

Cui L, Zhou QF, Liao CY, Fu JJ, Jiang G Bin. 2009. Studies on the toxicological effects of PFOA and PFOS on rats using histological observation and chemical analysis. Arch Environ Contam Toxicol 56:338–349; doi:10.1007/s00244-008-9194-6.

Deepika D, Sharma RP, Schuhmacher M, Kumar V. 2020. An integrative translational

framework for chemical induced neurotoxicity–a systematic review. Crit Rev Toxicol 50:424–438; doi:10.1080/10408444.2020.1763253.

Domazet SL, Jensen TK, Wedderkopp N, Nielsen F, Andersen LB, Grøntved A. 2020. Exposure to perfluoroalkylated substances (PFAS) in relation to fitness, physical activity, and adipokine levels in childhood: The european youth heart study. Environ Res 191; doi:10.1016/j.envres.2020.110110.

Dourson ML, Gadagbui B, Onyema C, McGinnis PM, York RG. 2019. Data derived Extrapolation Factors for developmental toxicity: A preliminary research case study with perfluorooctanoate (PFOA). Regul Toxicol Pharmacol 108:104446; doi:10.1016/j.yrtph.2019.104446.

Du Bois D, Du Bois EF. 1989. A formula to estimate the approximate surface area if height and weight be known. 1916. Nutrition 5: 303–11; discussion 312-3.

Edginton AN, Schmitt W, Voith B, Willmann S. 2006. A Mechanistic Approach for the Scaling of Clearance in Children. Clin Pharmacokinet 45:683–704; doi:10.2165/00003088-200645070-00004.

Ehresman DJ, Froehlich JW, Olsen GW, Chang S-C, Butenhoff JL. 2007. Comparison of human whole blood, plasma, and serum matrices for the determination of perfluorooctanesulfonate (PFOS), perfluorooctanoate (PFOA), and other fluorochemicals. Environ Res 103:176–184; doi:10.1016/j.envres.2006.06.008.

Ericson I, Domingo JL, Nadal M, Bigas E, Llebaria X, van Bavel B, et al. 2009a. Levels of Perfluorinated Chemicals in Municipal Drinking Water from Catalonia, Spain: Public Health Implications. Arch Environ Contam Toxicol 57:631–638; doi:10.1007/s00244-009-9375-y.

Ericson I, Domingo JL, Nadal M, Bigas E, Llebaria X, van Bavel B, et al. 2009b. Levels of Perfluorinated Chemicals in Municipal Drinking Water from Catalonia, Spain: Public Health Implications. Arch Environ Contam Toxicol 57:631–638; doi:10.1007/s00244-009-9375-y.

Fàbrega F, Kumar V, Schuhmacher M, Domingo JL, Nadal M. 2014. PBPK modeling for PFOS and PFOA: Validation with human experimental data. Toxicol Lett 230:244–251; doi:10.1016/j.toxlet.2014.01.007.

Fàbrega F, Nadal M, Schuhmacher M, Domingo JL, Kumar V. 2016a. Influence of the uncertainty in the validation of PBPK models: A case-study for PFOS and PFOA. Regul Toxicol Pharmacol 77:230–239; doi:10.1016/j.yrtph.2016.03.009.

Fàbrega F, Nadal M, Schuhmacher M, Domingo JL, Kumar V. 2016b. Influence of the uncertainty in the validation of PBPK models: A case-study for PFOS and PFOA. Regul Toxicol Pharmacol 77:230–239; doi:10.1016/j.yrtph.2016.03.009.

Forsthuber M, Kaiser AM, Granitzer S, Hassl I, Hengstschläger M, Stangl H, et al. 2020. Albumin is the major carrier protein for PFOS, PFOA, PFHxS, PFNA and PFDA in human plasma. Environ Int 137:105324; doi:10.1016/j.envint.2019.105324.

Gong X, Yang C, Hong Y, Chung ACK, Cai Z. 2019. PFOA and PFOS promote diabetic renal injury in vitro by impairing the metabolisms of amino acids and purines. Sci Total Environ

676:72–86; doi:10.1016/j.scitotenv.2019.04.208.

Grandjean P, Heilmann C, Weihe P, Nielsen F, Mogensen UB, Timmermann A, et al. 2017. Estimated exposures to perfluorinated compounds in infancy predict attenuated vaccine antibody concentrations at age 5-years. J Immunotoxicol 14:188–195; doi:10.1080/1547691X.2017.1360968.

Gulkowska A, Jiang Q, So MK, Taniyasu S, Lam PKS, Yamashita N. 2006. Persistent perfluorinated acids in seafood collected from two cities of China. Environ Sci Technol 40:3736–3741; doi:10.1021/es060286t.

Haddad S, Restieri C, Krishnan K. 2001. Characterization of age-related changes in body weight and organ weights from birth to adolescence in humans. J Toxicol Environ Health A 64:453–464; doi:10.1080/152873901753215911.

Haug LS, Thomsen C, Becher G. 2009a. Time trends and the influence of age and gender on serum concentrations of perfluorinated compounds in archived human samples. Environ Sci Technol 43:2131–2136; doi:10.1021/es802827u.

Haug LS, Thomsen C, Becher G. 2009b. Time trends and the influence of age and gender on serum concentrations of perfluorinated compounds in archived human samples. Environ Sci Technol 43:2131–2136; doi:10.1021/es802827u.

Hayton WL. 2000. Maturation and growth of renal function: Dosing renally cleared drugs in children. AAPS PharmSci 2:22–28; doi:10.1208/ps020103.

Heinemann A, Wischhusen F, Puschel K, Rogiers X. 1999. Standard liver volume in the Caucasian population. Liver Transplant Surg 5:366–368; doi:10.1002/lt.500050516.

Hsieh N, Reisfeld B, Chiu WA. 2018a. pksensi : an R package to apply sensitivity analysis in pharmacokinetic modeling. SoftwareX 2:80521; doi:10.1016/j.softx.2020.100609.

Hsieh NH, Reisfeld B, Bois FY, Chiu WA. 2018b. Applying a global sensitivity analysis workflow to improve the computational efficiencies in physiologically-based pharmacokinetic modeling. Front Pharmacol 9:1–17; doi:10.3389/fphar.2018.00588.

Huang H, Yu K, Zeng X, Chen Q, Liu Q, Zhao Y, et al. 2020. Association between prenatal exposure to perfluoroalkyl substances and respiratory tract infections in preschool children. Environ Res 191:110156; doi:10.1016/j.envres.2020.110156.

Johnson TN, Tucker GT, Tanner MS, Rostami-Hodjegan A. 2005. Changes in liver volume from birth to adulthood: A meta-analysis. Liver Transplant 11:1481–1493; doi:10.1002/lt.20519.

Kärrman A, Mueller JF, van Bavel B, Harden F, Toms L-ML, Lindström G. 2006a. Levels of 12 Perfluorinated Chemicals in Pooled Australian Serum, Collected 2002−2003, in Relation to Age, Gender, and Region. Environ Sci Technol 40:3742–3748; doi:10.1021/es060301u.

Kärrman A, Mueller JF, van Bavel B, Harden F, Toms L-ML, Lindström G. 2006b. Levels of 12 Perfluorinated Chemicals in Pooled Australian Serum, Collected 2002−2003, in Relation to Age, Gender, and Region. Environ Sci Technol 40:3742–3748; doi:10.1021/es060301u.

Li Z, Liu Q, Liu C, Li C, Li Y, Li S, et al. 2017. Evaluation of PFOS-mediated neurotoxicity in rat

primary neurons and astrocytes cultured separately or in co-culture. Toxicol Vitr 38:77–90; doi:10.1016/j.tiv.2016.11.002.

Liew Z, Goudarzi H, Oulhote Y. 2018. Developmental Exposures to Perfluoroalkyl Substances (PFASs): An Update of Associated Health Outcomes. Curr Environ Heal reports 5:1–19; doi:10.1007/s40572-018-0173-4.

Loccisano AE, Campbell JL, Andersen ME, Clewell HJ. 2011. Evaluation and prediction of pharmacokinetics of PFOA and PFOS in the monkey and human using a PBPK model. Regul Toxicol Pharmacol 59:157–175; doi:10.1016/j.yrtph.2010.12.004.

Loccisano AE, Campbell JL, Butenhoff JL, Andersen ME, Clewell HJ. 2012. Comparison and evaluation of pharmacokinetics of PFOA and PFOS in the adult rat using a physiologically based pharmacokinetic model. Reprod Toxicol 33:452–467; doi:10.1016/j.reprotox.2011.04.006.

Loccisano AE, Longnecker MP, Campbell JL, Andersen ME, Clewell HJ. 2013a. Development of Pbpk Models for Pfoa and Pfos for Human Pregnancy and Lactation Life Stages. J Toxicol Environ Heal Part A 76:25–57; doi:10.1080/15287394.2012.722523.

Loccisano AE, Longnecker MP, Campbell JL, Andersen ME, Clewell HJ. 2013b. Development of Pbpk Models for Pfoa and Pfos for Human Pregnancy and Lactation Life Stages. J Toxicol Environ Heal Part A 76:25–57; doi:10.1080/15287394.2012.722523.

Luebker DJ, York RG, Hansen KJ, Moore JA, Butenhoff JL. 2005. Neonatal mortality from in utero exposure to perfluorooctanesulfonate (PFOS) in Sprague-Dawley rats: Dose-response, and biochemical and pharamacokinetic parameters. Toxicology 215:149–169; doi:10.1016/j.tox.2005.07.019.

Luo Z, Shi X, Hu Q, Zhao B, Huang M. 2012. Structural Evidence of Perfluorooctane Sulfonate Transport by Human Serum Albumin. Chem Res Toxicol 25:990–992; doi:10.1021/tx300112p.

Makowski D, Ben-Shachar M, Patil I, Lüdecke D. 2020. Methods and Algorithms for Correlation Analysis in R. J Open Source Softw 5:2306; doi:10.21105/joss.02306.

Mallick P, Moreau M, Song G, Efremenko AY, Pendse SN, Creek MR, et al. 2019. Development and Application of a Life-Stage Physiologically-Based Pharmacokinetic (PBPK) Model to the Assessment of Internal Dose of Pyrethroids in Humans. Toxicol Sci 173:86–99; doi:10.1093/toxsci/kfz211.

Martin MT, Brennan RJ, Hu W, Ayanoglu E, Lau C, Ren H, et al. 2007. Toxicogenomic Study of Triazole Fungicides and Perfluoroalkyl Acids in Rat Livers Predicts Toxicity and Categorizes Chemicals Based on Mechanisms of Toxicity. Toxicol Sci 97:595–613; doi:10.1093/toxsci/kfm065.

McNamara PJ, Alcorn J. 2002. Protein binding predictions in infants. AAPS PharmSci 4:19–26; doi:10.1208/ps040104.

Meistelman C, Benhamou D, Barre J, Levron J-C, Mahe V, Mazoit X, et al. 1990. Effects of Age on Plasma Protein Binding of Sufentanil. Anesthesiology 72:470–473; doi:10.1097/00000542-199003000-00013.

Mene-Afejuku TO, Moisa EA, Akinlonu A, Dumancas C, Veranyan S, Perez JA, et al. 2019. The relevance of serum albumin among elderly patients with acute decompensated heart failure. J Geriatr Cardiol 16:522–528; doi:10.11909/j.issn.1671-5411.2019.07.005.

Noda T, Todani T, Watanabe Y, Yamamoto S. 1997. Liver volume in children measured by computed tomography. Pediatr Radiol 27:250–252; doi:10.1007/s002470050114.

Nøst TH, Vestergren R, Berg V, Nieboer E, Odland JØ, Sandanger TM. 2014a. Repeated measurements of per- and polyfluoroalkyl substances (PFASs) from 1979 to 2007 in males from Northern Norway: Assessing time trends, compound correlations and relations to age/birth cohort. Environ Int 67:43–53; doi:10.1016/j.envint.2014.02.011.

Nøst TH, Vestergren R, Berg V, Nieboer E, Odland JØ, Sandanger TM. 2014b. Repeated measurements of per- and polyfluoroalkyl substances (PFASs) from 1979 to 2007 in males from Northern Norway: Assessing time trends, compound correlations and relations to age/birth cohort. Environ Int 67:43–53; doi:10.1016/j.envint.2014.02.011.

Ogiu N, Nakamura Y, Ijiri I, Hiraiwa K, Ogiu T. 1997. A statistical analysis of the internal organ weights of normal Japanese people. Health Phys 72:368–383; doi:10.1097/00004032-199703000-00004.

Olsen GW, Burris JM, Ehresman DJ, Froehlich JW, Seacat AM, Butenhoff JL, et al. 2007. Half-Life of Serum Elimination of Perfluorooctanesulfonate,Perfluorohexanesulfonate, and Perfluorooctanoate in Retired Fluorochemical Production Workers. Environ Health Perspect 115:1298–1305; doi:10.1289/ehp.10009.

Pérez F, Nadal M, Navarro-Ortega A, Fàbrega F, Domingo JL, Barceló D, et al. 2013a. Accumulation of perfluoroalkyl substances in human tissues. Environ Int 59:354–362; doi:10.1016/j.envint.2013.06.004.

Pérez F, Nadal M, Navarro-Ortega A, Fàbrega F, Domingo JL, Barceló D, et al. 2013b. Accumulation of perfluoroalkyl substances in human tissues. Environ Int 59:354–362; doi:10.1016/j.envint.2013.06.004.

Price PS, Conolly RB, Chaisson CF, Gross EA, Young JS, Mathis ET, et al. 2003. Modeling Interindividual Variation in Physiological Factors Used in PBPK Models of Humans. Crit Rev Toxicol 33:469–503; doi:10.1080/10408440390242324.

Project H, No D. 2010. Characterization and Application of Physiologically Based Pharmacokinetic Models. Ipcs - Who.

PubChem Compound Summary for CID 74483, Perfluorooctanesulfonic acid. Natl Cent Biotechnol Inf. Available: https://pubchem.ncbi.nlm.nih.gov/compound/Perfluorooctanesulfonic-acid.

Roberts M, Grice J, Hungerford N, Liang X, Liu X. 2016. A Critical Review of Pharmacokinetic Modelling of PFOS and PFOA to Assist in Establishing HGBVs for these Chemicals.

Rovira J, Martinez MA, Sharma RP, Espuis T, Nadal M, Kumar V, et al. 2019a. Prenatal exposure to PFOS and PFOA in a pregnant women cohort of Catalonia, Spain. Environ Res 175:384–392; doi:10.1016/j.envres.2019.05.040.

Rovira J, Martínez MÁ, Sharma RP, Espuis T, Nadal M, Kumar V, et al. 2019b. Prenatal exposure

to PFOS and PFOA in a pregnant women cohort of Catalonia, Spain. Environ Res 175:384–392; doi:10.1016/j.envres.2019.05.040.

Saikat S, Kreis I, Davies B, Bridgman S, Kamanyire R. 2013. The impact of PFOS on health in the general population: A review. Environ Sci Process Impacts 15:329–335; doi:10.1039/c2em30698k.

Sanchez Garcia D, Sjödin M, Hellstrandh M, Norinder U, Nikiforova V, Lindberg J, et al. 2018. Cellular accumulation and lipid binding of perfluorinated alkylated substances (PFASs) – A comparison with lysosomotropic drugs. Chem Biol Interact 281:1–10; doi:10.1016/j.cbi.2017.12.021.

Sharma RP, Schuhmacher M, Kumar V. 2018. The development of a pregnancy PBPK Model for Bisphenol A and its evaluation with the available biomonitoring data. Sci Total Environ 624:55–68; doi:10.1016/j.scitotenv.2017.12.023.

Song G, Moreau M, Efremenko A, Lake BG, Wu H, Bruckner J V., et al. 2019. Evaluation of age-related pyrethroid pharmacokinetic differences in rats: Physiologically-based pharmacokinetic model development using in vitro data and in vitro to in vivo extrapolation. Toxicol Sci 169:365–379; doi:10.1093/toxsci/kfz042.

Stader F, Siccardi M, Battegay M, Kinvig H, Penny MA, Marzolini C. 2019. Repository Describing an Aging Population to Inform Physiologically Based Pharmacokinetic Models Considering Anatomical, Physiological, and Biological Age-Dependent Changes. Clin Pharmacokinet 58:483–501; doi:10.1007/s40262-018-0709-7.

Sun J, Letcher RJ, Eens M, Covaci A, Fernie KJ. 2020. Perfluoroalkyl acids and sulfonamides and dietary, biological and ecological associations in peregrine falcons from the Laurentian Great Lakes Basin, Canada. Environ Res 191:110151; doi:10.1016/j.envres.2020.110151.

Sunderland EM, Hu XC, Dassuncao C, Tokranov AK, Wagner CC, Allen JG. 2019. A review of the pathways of human exposure to poly- and perfluoroalkyl substances (PFASs) and present understanding of health effects. J Expo Sci Environ Epidemiol 29:131–147; doi:10.1038/s41370-018-0094-1.

Tan Y-M, Clewell HJ, Andersen ME. 2008. Time dependencies in perfluorooctylacids disposition in rat and monkeys: A kinetic analysis. Toxicol Lett 177:38–47; doi:10.1016/j.toxlet.2007.12.007.

Thibodeaux JR, Hanson RG, Rogers JM, Grey BE, Barbee BD, Richards JH, et al. 2003. Exposure to perfluorooctane sulfonate during pregnancy in rat and mouse. I: Maternal and prenatal evaluations. Toxicol Sci 74:369–381; doi:10.1093/toxsci/kfg121.

Tian Z, Kim SK, Shoeib M, Oh JE, Park JE. 2016. Human exposure to per- and polyfluoroalkyl substances (PFASs) via house dust in Korea: Implication to exposure pathway. Sci Total Environ 553:266–275; doi:10.1016/j.scitotenv.2016.02.087.

Trudel D, Horowitz L, Wormuth M, Scheringer M, Cousins IT, Hungerbühler K. 2008. Estimating consumer exposure to PFOS and PFOA. Risk Anal 28:251–269; doi:10.1111/j.1539-6924.2008.01017.x.

Valentin J, Streffer C. 2002. Basic anatomical and physiological data for use in radiological

protection: Reference values - ICRP Publication 89. Ann ICRP 32:1–277; doi:10.1016/S0146-6453(03)00002-2.

Wan HT, Zhao YG, Wei X, Hui KY, Giesy JP, Wong CKC. 2012. PFOS-induced hepatic steatosis, the mechanistic actions on β-oxidation and lipid transport. Biochim Biophys Acta - Gen Subj 1820:1092–1101; doi:10.1016/j.bbagen.2012.03.010.

Wang L, Wang Y, Liang Y, Li J, Liu Y, Zhang J, et al. 2014. PFOS induced lipid metabolism disturbances in BALB/c mice through inhibition of low density lipoproteins excretion. Sci Rep 4:4582; doi:10.1038/srep04582.

Winkens K, Vestergren R, Berger U, Cousins IT. 2017. Early life exposure to per- and polyfluoroalkyl substances (PFASs): A critical review. Emerg Contam 3:55–68; doi:10.1016/j.emcon.2017.05.001.

Xu J, Shimpi P, Armstrong L, Salter D, Slitt AL. 2016. PFOS induces adipogenesis and glucose uptake in association with activation of Nrf2 signaling pathway. Toxicol Appl Pharmacol 290:21–30; doi:10.1016/j.taap.2015.11.002.

Yu W-G, Liu W, Jin Y-H, Liu X-H, Wang F-Q, Liu L, et al. 2009. Prenatal and Postnatal Impact of Perfluorooctane Sulfonate (PFOS) on Rat Development: A Cross-Foster Study on Chemical Burden and Thyroid Hormone System. Environ Sci Technol 43:8416–8422; doi:10.1021/es901602d.

Zeng Z, Song B, Xiao R, Zeng G, Gong J, Chen M, et al. 2019. Assessing the human health risks of perfluorooctane sulfonate by in vivo and in vitro studies. Environ Int 126:598–610; doi:10.1016/j.envint.2019.03.002.

Zhang T, Sun H, Lin Y, Wang L, Zhang X, Liu Y, et al. 2011a. Perfluorinated Compounds in Human Blood, Water, Edible Freshwater Fish, and Seafood in China: Daily Intake and Regional Differences in Human Exposures. J Agric Food Chem 59:11168–11176; doi:10.1021/jf2007216.

Zhang T, Sun H, Lin Y, Wang L, Zhang X, Liu Y, et al. 2011b. Perfluorinated Compounds in Human Blood, Water, Edible Freshwater Fish, and Seafood in China: Daily Intake and Regional Differences in Human Exposures. J Agric Food Chem 59:11168–11176; doi:10.1021/jf2007216.

Zhang T, Wu Q, Sun HW, Zhang XZ, Yun SH, Kannan K. 2010a. Perfluorinated compounds in whole blood samples from infants, children, and adults in China. Environ Sci Technol 44:4341–4347; doi:10.1021/es1002132.

Zhang T, Wu Q, Sun HW, Zhang XZ, Yun SH, Kannan K. 2010b. Perfluorinated compounds in whole blood samples from infants, children, and adults in China. Environ Sci Technol 44:4341–4347; doi:10.1021/es1002132.

Zheng L, Xu M, Tang S wei, Song H xin, Jiang X hua, Wang L. 2019. Physiologically Based Pharmacokinetic Modeling of Oxycodone in Children to Support Pediatric Dosing Optimization. Pharm Res 36:171; doi:10.1007/s11095-019-2708-2.

Framework for Risk Assessment of PFAS utilizing experimental studies and in-silico models

Abstract

Perfluoroalkyl substances (PFAS), especially PFOS and PFOA, are two widely used synthetic chemicals that can impact human health based on evidence from animal and epidemiologic studies. In this paper, we have reviewed and summarized the influence of PFAS exposure on health, pointing the quality of evidence, and applied translational techniques to integrate evidence for PFAS policy making. This is the first review where highly referred articles on PFAS used for policymaking by several regulatory agencies were collected and evaluated based on the review guidelines developed by the US National Toxicology Program´s Office of Health Assessment and Translation (OHAT) review guidelines. Several limitations were observed, including co-exposure to multiple chemicals and limited measurement of primary and secondary outcomes related to specific toxicity. However, data from all the studies provided a moderate to strong level of confidence for link between PFAS exposure and different adverse outcomes. Secondly, for translating the risk to humans, an in-silico model and scaling approach was utilized. Physiologically based pharmacokinetic model (PBPK) was used to calculate the human equivalent dose (HED) from two widely accepted studies and compared with tolerable daily intakes (TDIs) established by various regulatory agencies. Inter-species dose extrapolation was done to compare with human the relevance of dosing scenarios used in animals. Overall, a framework for translation of risk was proposed based on the conclusions of this review with the goal of improving policymaking. The current paper can improve the methodological protocols for PFAS experimental studies and encourage the utilization of in-silico models for translating risk.

Keywords: Perfluorinated compounds; PFAS; PFOA; PFOS; Health effects; Human biomonitoring; Systematic analysis; Toxicokinetic model; Translational in silico models; Regulatory limits

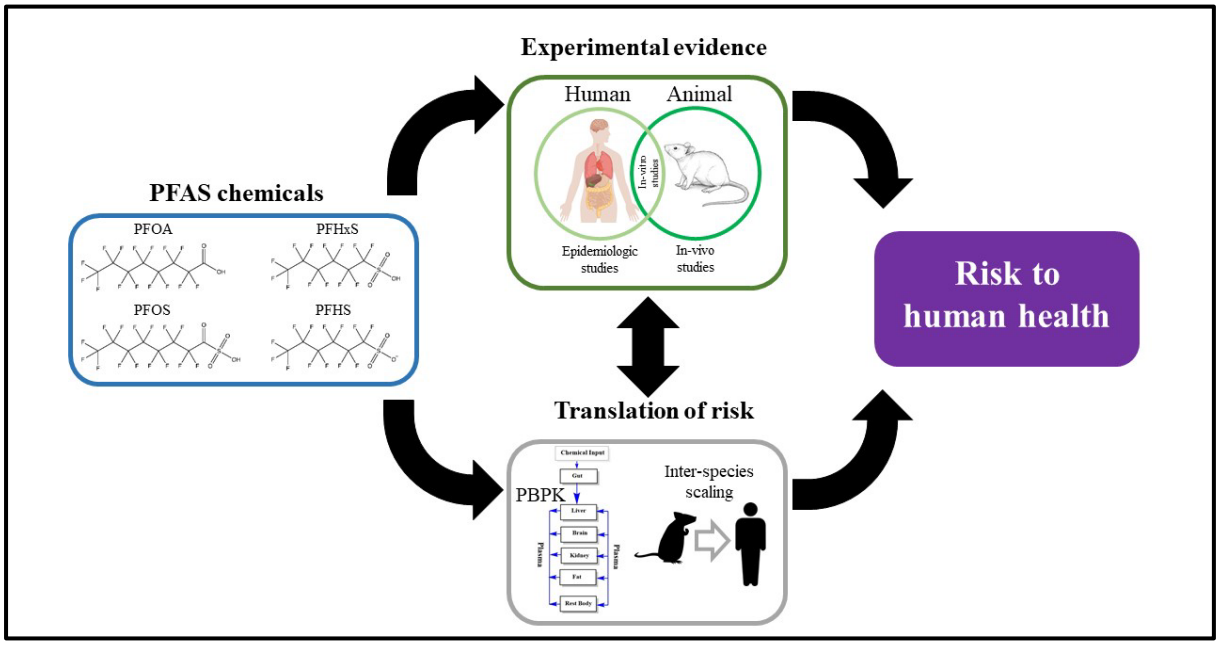

Graphical abstract: Framework for PFAS and health risk assessment

Abbreviations

ADME	Absorption, distribution, metabolism, and excretion	MCMC	Markov Chain Monte Carlo
ADONA	4,8-dioxa-3H-perfluorononanoate	MRL	Minimal Risk Level
ALT	Alanine aminotransferase	NAM	New approach methodologies
AOP	Adverse Outcome Pathway	NHANES	National Health and Nutrition Examination Survey
ATSDR	Agency for toxic substances and Registry	NOAEC	Comparable no observed adverse effect concentration
AUC	Area under the curve	NOAEL	No observed adverse effect level
BMDL	Benchmark dose (lower confidence limit)	OHAT	Office of Health Assessment and Translation
Cmax	Peak serum concentration	PBPK	Physiologically based pharmacokinetic modelling
CRP	C-reactive protein	PCBs	Polychlorinated Biphenyls
CONTAM	Contaminants in the Food Chain	PFAS	Per- and polyfluoroalkyl substances
DDEF	Data derived extrapolation factors	PFBS	Perfluorobutanesulfonic acid
DDEs	Dichlorodiphenyldichloroethylenes	PFDA	Perfluorodecanoic acid
EFSA	European food safety authority	PFDoDA	Perfluorododecanoic acid
FSANZ	Food Standards Australia New Zealand	PFHxA	Perfluorohexanoic acid
GFR	Glomerular filtration rate	PFHxS	Perfluorohexanesulfonic acid
GSH	Glutathione	PFNA	Perfluorononanoic acid
HC	Health Canada	PFOA	Perfluorooctanoic acid
HDL	High-density lipoprotein	PFOS	Perfluorooctane sulfonate
HED	Human equivalent dose	QSAR	Quantitative structure-activity relationship
IATA	Integrated Approaches to Testing and Assessment	RfD	Reference dose
IQR	Interquartile range	TDI	Tolerable daily intake
LC-MS	Liquid chromatography- mass spectrometry	TWI	Total weekly intake
LOAEL	Lowest observed adverse effect level	USEPA	United States Environment Protection Agency
MAC	Maximum acceptable concentration		

1. Introduction

Per- and polyfluoroalkyl substances (PFAS) are a class of synthetic organic substances with perfluoroalkyl moieties that are highly resistant to environmental and metabolic degradation. Most PFAS are either non-degradable or transform into other stable PFAS metabolites (Pelch et al. 2019). Under EU chemicals regulation, they are classified as very persistent substances (Schrenk et al. 2020). PFAS are widely used in consumer products such as furniture, household cleaners, and clothing. Due to their resistance to environmental and metabolic degradation, many of these chemicals are increasingly found in the environment, as well as the human body, all over the globe (Wang et al. 2017). Among all PFAS, perfluorooctane sulfonate (PFOS) and perfluorooctanoic acid (PFOA) have been the most widely studied, due to their toxic effects on living beings and their common use in consumer and industrial applications (Chang et al. 2016). Regulatory agencies, for example the European Food Safety Authority (EFSA), the United States Environmental Protection Agency (USEPA), and the Agency for Toxic Substances and Registry (ATSDR), consider PFAS a public health concern, having established the tolerable daily intake (TDI) or reference dose (RfD) based on developmental toxicity and other toxic endpoints (Schrenk et al. 2020; USEPA 2016) Our current understanding about effects of PFAS's is based on studies focused on a relatively small number of compounds. Little is known about the properties and behaviors of most PFAS's, either as individual chemicals, or as the much more commonly present complex mixtures. Diversity among various PFAS based on structures, properties, accumulation potential and toxicity, leads to frequent arguments about whether all PFAS cannot be treated as a single class of chemicals (Bowman 2015). However, despite their diversity, PFAS share one common structural feature that makes them highly problematic - the presence of perfluoroalkyl moieties, resulting in their shared resistance to environmental and metabolic degradation (Cousins et al. 2020; Wang et al. 2017). It has been scientifically accepted that the diversity of these substances, in terms of properties, behavior, hazards, and risks, is a significant criterion for risk classification. Categorizing a large group of chemicals based upon single structural components has the potential to be overgeneralized and debatable.

From 2000 until today, a number of epidemiological, animal, and in-vitro studies have found links between PFAS and health effects. Developmental toxicity (Gaballah et al. 2020; Lau 2019), carcinogenicity (Singh and Hsieh 2021), weight gain (Mitro et al. 2020; Ashley-Martin et al. 2016), hormonal imbalance (Ashley-Martin et al. 2016; Tsai et al. 2015), and immunity-related effects (Abraham et al. 2020), are some of the adverse effects reported in the literature (Sunderland et al. 2019). It has been noted that some studies contain controversies, as well as lack of scientific and statistical rigor of evidence to reach stated conclusions. The most common of these include statistical bias in interpreting results, bias in the convincing calculation of half-life, which includes occupational or real-time exposure, and uncertainty of in-silico models in predicting daily intake or kinetics of such chemicals (Chang et al. 2016).

Human health effects for some PFAS exposures have also been reported from animal models. However, a longer half-life, no metabolism, and high resorption of these chemicals make extrapolation from animal models to humans complicated. For PFOA and PFOS, half-life varies among rats (PFOA: 0.08-5.68 days, PFOS: 14.5-71.13 days), mice (PFOA: NR, PFOS: 30.45-42.81 days), cynomolgus monkeys (PFOA: 19.5-32.6 days, PFOS: 110-132 days) and humans

(2-4 years, 5 years) (Schrenk et al. 2020; Knutsen et al. 2018). Considerable differences in biological half-lives among different species, as well as the proper accounting for this information in the extrapolation of dose and risk for humans, are still crucial issues. An additional major controversy lies in the varying renal clearance and resorption capability of these chemicals among different age groups (Deepika et al. 2021). Variations in the glomerular filtration capacity, protein binding, and disposition of the chemicals may lead to varied toxicokinetic and calls for differences in TDI among sensitive age groups.

Taking into account all of the above, the purpose of this study was to provide a summary of the the experimental findings including the strengths and limitations in the methodologies and results of the research studies. These studies were identified by an independent group of experts for the Center for Truth in Science (CTS). The Center selected these studies because they were among the most widely cited, or most influential studies used by policymakers, PFAS manufacturers, environmental groups, plaintiffs, attorneys, social media influencers, and the news media to express views about the potentially harmful effects of these compounds, how they should be regulated, and whether individuals and organizations damaged by exposure to these compounds should be compensated. Various studies have been used to estimate a particular “safe” dose assessment by government agencies. Some investigations have provided vital information to enable credible extrapolation between experimental animals and humans. Other studies may have produced inconsistent findings or expressed dissenting scientific claims. For example, minimal risk level (MRL) derived by ATSDR is based on the study of neurodevelopmental effects conducted by Koskela et al. (2016) in the offspring of mice that were fed a diet containing PFOA. Similarly, the human equivalent dose (HED) and the lowest observed adverse effect level (LOAEL) for PFAS were estimated by the Agency for Toxic Substances and Disease Registry (ATSDR) with the data reported by the Luebker et al. (2005) . The current analysis is aimed at determining the internal validity of each individual study based on accepted scientific standards for best practices. For this, we critically reviewed the selected scientific publications having multiple endpoints, evaluated and rated them based on confidence, and further applied the previously validated and published in-silico tool (PBPK) to assess the criterion of risk assessment for PFAS with the goal of improving policymaking. Moreover, based on immunotoxicity, the predicted daily dose was compared with those established TDI/RfD by EFSA and USEPA. In addition, scaling approaches for reducing inter-species differences were analyzed. Finally, an integrated framework for risk translation is proposed.

2. Analysis of Research Articles using the OHAT Guideline

To evaluate the quality of evidence and research protocols of the selected articles regarding PFAS, a risk-of-bias tool which was developed using OHAT guidelines was employed. It outlines a parallel approach to assess risk of bias from human, animal, and in vitro studies in order to facilitate consideration of the risk of bias across evidence streams (NTP 2015). This evaluation process was developed by consulting experts from the Cochrane Collaboration, the Grading of Recommendations Assessment, Development and Evaluation (GRADE) working group, the Collaborative Approach to Meta-Analysis and Review of Animal Experimental Studies (CAMARADES), the Systematic Review Center for Laboratory animal

Experimentation (SYRCLE), Navigation guide, and other experts, and in accordance with PRISMA guidelines.

Different types of scientific studies focused on analytical investigations, epidemiology, and kinetic assessments were included. Justification for why these specific studies were selected for PFAS are summarized in Table 1. Five of the selected articles focused on animal studies, primarily rats and mice, that evaluates chronic and acute toxicity with multiple endpoints. The four epidemiological studies were based on immunotoxicity, drinking water exposure, and half-life in humans (shown in Table 1). In total, the key health outcomes named in these articles included: immunotoxicity, carcinogenicity, bone toxicity, in-utero toxicity, two generational exposure, organ toxicity, and chronic toxicity. For the independent review by experts, a review template was developed consisting of questions related to methodology protocols, randomization procedures, statistical evaluation, publication biases, outcomes measured, consistency, and confounding (Appendix 2). The overall rating of the reviewed articles based on the aforementioned aspects were as follows: first, the risk of bias was reported; secondly, the level of evidence and confidence ratings were analyzed (supplementary file, table 3 and 4). All individual scoring was integrated in order to create a rating of confidence in the risk assessment for PFAS chemicals.

Table 2: Summary Table of the human and animal studies selected by CTS for this review.

Brief Description about why the studies were selected	**Reference**
Internal exposures to PFAS matched with biological markers and vaccine responses; the principal study used by the European Food Safety Authority (EFSA) in its recent risk assessment.	(Abraham et al. 2020)
Investigation of community exposures to PFOA and serum concentrations.	(Emmett et al. 2006)
Serum vaccine antibody concentrations monitored in children exposed to PFAS chemicals highlighted by the European Food Safety Authority (EFSA) in its recent risk assessment.	(Grandjean et al. 2012)
Study on half-life of several PFAS compounds in the serum of retired production workers that is cited by all authorities in their assessment work.	(Olsen et al. 2007)
Chronic study in rats showing Leydig cell tumors; this is the principal study used by Health Canada in its 2018 assessment.	(Butenhoff et al. 2012)
Short term gestational exposure in mice with implications for long term effects; this is the principal study used by the Agency for Toxic Substances and Disease Registry (ATSDR) in its determination of minimum risk level.	(Koskela et al. 2016)
Effects of PFOA on pregnancy in mice; this is the principal study used by U.S. Environmental Protection Agency to estimate its health advisory of 70 ppt.	(Lau et al. 2006)
Liver changes in rats associated with PFOA exposure; this is the principal studies used by Health Canada in its 2018 assessment.	(Perkins et al. 2004) and (Luebker et al. 2005)

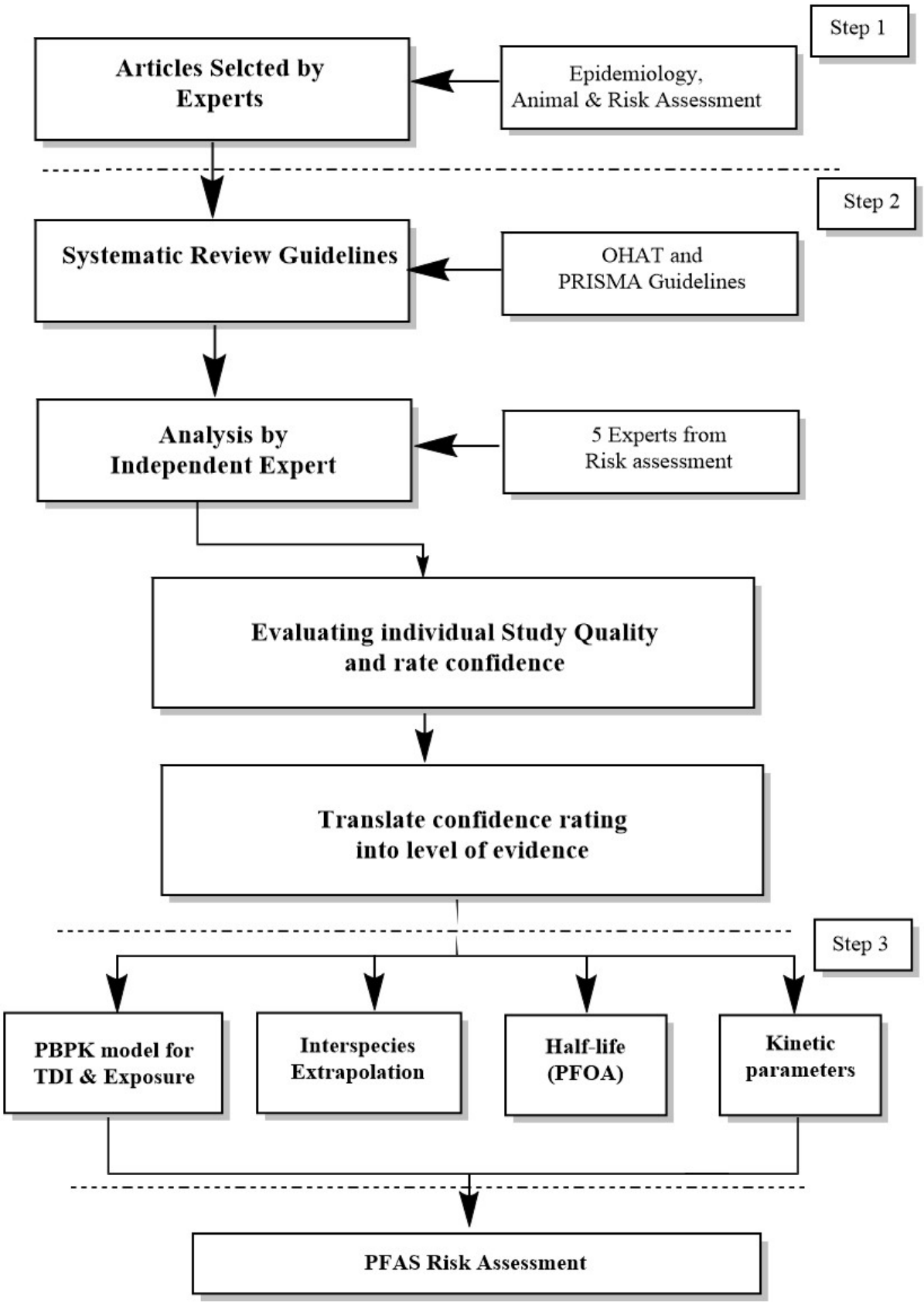

Figure 2: Framework followed for evaluating the quality of evidence in the selected studies. OHAT and Prisma guideline were used for evaluating strength and weakness in different studies followed by in-silico models and other kinetic assessment for human health.

3. Quality of Evidence and Limitation of studies

Based on the quality and the limitations we identified (Table 3 and 4 in appendix), the level of evidence for PFAS health effects in the articles were listed in Tables 1 and 2 (supplementary file appendix 1), was integrated. Also, several issues related to outcomes and methodology from the studies were identified by our independent experts mentioned below.

The first one concerns the effects of co-exposures on the human body. For instance, a similar adverse effect can be the result of multiple chemicals, especially in the case of epidemiological studies that are difficult to control. There may already be existing exposures affecting a particular toxicity endpoint, or leading to toxicokinetic interference (e.g., competing for the elimination of the chemical). Especially in the case of PFAS, the toxicity of mixed PFAS's and their interactions with each other and other classes of chemicals is currently a significant knowledge gap in the area of risk assessment (Ojo et al. 2021). Inter-individual variability should also be considered especially for end-points like immunotoxicity. Two epidemiological studies (Abraham et al. 2020; Grandjean et al. 2012) used standard immune antibody biomarkers for their immunity endpoints, but there are certain other standard biomarkers, such as leukocyte count and c-reactive protein (CRP) that need to be take into account. Although, Abraham et al. (2020) did consider the leukocyte count and other clinical biomarkers, the study by Grandjean et al. (2012) assessed only antibody levels. Another important point is the antibody level variation with time, making a single sample collection at the one-time point and with a small sample size (Abraham et al. 2020) is not guaranteed to give complete information. In one of the epidemiological studies, the participants were aware of the study and the protocols. In this case, the questionnaire given to participants might have been biased, especially if the questionnaire involved self-reported outcomes. In such cases, adverse outcomes reported by the participant may or may not hold true, if they know that they are being exposed to PFOA through drinking water (Emmett et al. 2006). There was no cross-check of the administered questionnaire mentioned by the author in the Emmett's article, being the results still used for statistical analysis (Emmett et al. 2006). Some of the included articles were published by manufacturers of PFAS. However, in each of these cases, one or more authors were from outside the sponsoring organization, indicating the chance for some more rigorous scientific review and minimization of possible bias. Considering the fact that the funding sources are manufacturers, there could be a probability of bias. This was included in the protocol, but it was not assumed initially. The methodology reported outcomes and data quality were evaluated to further report any suspected bias.

There were many strengths identified in the included studies, which increases the confidence for conducting risk assessment. In the animal studies, the primary and secondary outcomes were measured for specific endpoints. For example, in the carcinogenicity study for PFOS exposure in rats, a necropsy was done to measure weight, and a histopathology study was conducted on major organs. In addition, clinical observation, body weight, food consumption, hematology, urine analysis, etc. were conducted to determine secondary outcomes (Butenhoff et al. 2012). Complete outcome assessment improved the confidence level and helped to reduce bias. In most studies on rodents, randomization was done to select control and exposed groups, and in some cases, an automated randomization procedure was used. All exclusion criteria, including the death of animals, and results of pathology were reported

by the various authors (Butenhoff et al. 2012; Luebker et al. 2005). Feed consumption and serum levels were measured to exclude any inconsistencies. In the two epidemiological studies, PCBs, which have the potential to affect immunological results, were measured by both authors to reduce statistical bias (Abraham et al. 2020; Grandjean et al. 2012). Heavy metals, such as cadmium, lead, mercury, and DDEs were measured by Abraham et al. (2020), including all clinical outcomes. In most studies, standard statistical analyses were followed-up with multiple tests, including p values and other required methods. In most cases, significant and non-significant results were reported by authors for both human and animal studies (Abraham et al. 2020; Koskela et al. 2016; Butenhoff et al. 2012; Grandjean et al. 2012; Lau et al. 2006). In some animal studies, a large sample size was used to reduce the variability (Butenhoff et al. 2012; Lau et al. 2006; Luebker et al. 2005; Perkins et al. 2004). In the two epidemiological studies, repeated sampling of blood/serum was sometimes conducted to avoid measurement bias (Grandjean et al. 2012; Olsen et al. 2007). Most analyses of the chemicals were done by LC-MS (liquid chromatography-mass spectrometry), a standard method used for analysis. In many cases, the analyses of samples were repeated to increase the accuracy of the data.

4. Risk of bias and confidence levels in individual studies

This section focuses on the risk of bias detected in methodological protocol reported, level of evidence, shortcomings, and the significant findings from each individual study.

4.1 Animal Studies

A 2-year dietary exposure study (PFOS) by Butenhoff et al. (2012) in which different concentrations were used in male and female Sprague Dawley rats (n=720), was quite extensive. In males, total cholesterol levels decreased, while total urea levels increased with the 5 and 20 µg/g (ppm) diet. Hepatocellular carcinoma in the females and increased hepatocellular adenoma in both males (p=0.046) and females (p=0.039), was detected for the 20-ppm exposure group. In the methodology protocol and statistical analyses, a low risk of bias was detected. Randomization of the rats was done based on an automated blocking procedure. Considering the methodology and outcomes reported, the level of evidence was high for PFOS contributing to adverse effects in rats, particularly in the liver, but significant adverse effects were observed specifically in the 20-ppm group.

Koskela et al. (2016) evaluated the effects of PFOA (0.3 mg/kg/day) in-utero and during lactational exposure on the bones of female offspring of mice at 15 (n=5) and 17 (n=5) months. The methodology protocol had a low risk of bias based on specific inclusion and exclusion criteria. However, one of the major concerns with this study was the dose selection procedure and use of single dosing. Additionally, detail about randomization of both the control and exposed groups were not articulated clearly, except for the fact that one or two female offspring from the same litter were randomly selected for inclusion into the exposed group. Also, for PFOA analysis in bones, the samples were pooled, and aggregate data were presented. An inconsistency was observed in one figure that was reported in the osteoblast viability study, where the authors reported that an increase in calcium peaked at 1 and 10 µm dose and further decreased at 100 and 200 µm, compared to controls. Overall, a rating of

moderate to high level of evidence was given to this study, due to inconsistencies in some of the reported results as well as the use of aggregated data.

In the study by Lau et al. 2006, pregnant CD-1 mice and Sprague-Dawley rats were exposed to different PFOA concentrations in order to evaluate developmental toxicity. A low risk of bias was detected in methodology, as well as in statistical evaluation, as the mice were exposed to different concentrations and randomization was used to select animals. Also, exclusions were clearly reported with rationale and details. For instance, neonates in the 10 and 20 mg/kg dosing groups did not survive, while in the 40 mg/kg dosing group, no births were reported. A good sample size of rats was included in each group to reduce variability and uncertainty. This study demonstrates a high level of evidence.

PFOA exposure was related to prenatal and postnatal toxicity in mice and sex-related differences in reproductive maturity between males and females. Luebker et al. (2005) conducted a two-generation study in rats to evaluate the PFOS effects on reproduction, pregnancy, and offspring development. Different doses (0, 0.1, 0.4, 1.6, and 3.2 mg/kg) were administered before six weeks of mating and continued through gestation and lactation. A low risk of bias was detected in the methodology and statistical analyses. However, all samples went to a 3M laboratory for analysis, and were found to be accurate to ±30%. Overall, it was concluded that there was a high level of evidence that PFOS could contribute to prenatal and postnatal toxicity in mice.

A thirteen-week dietary toxicity study was conducted in male rats in order to evaluate liver effects, hormonal changes, and effects on other target organs (Perkins et al. 2004). A low risk of bias was detected in methodology and statistical evaluation. The strengths of this study were a low statistical bias due to the use of a large number of animals and a computerized randomization process with multiple dosing ranging up to 100 ppm. There was a high level of evidence that the liver is a target organ of PFOA toxicity. At 100 ppm, liver weight change, enzymatic activity, and hepatocellular hypertrophy were observed with a LOAEL of 10 ppm.

4.2 Epidemiology Studies

Abraham et al. (2020) reported that exposure to PFAS especially PFOA, in Germany had negative associations with serum levels, as well as negative immune response against three vaccine antibodies with high consistency and comparable no observed adverse effect concentrations (NOAEC). Significant associations were detected for PFOA exposure and Haemophilus influenza type B (Hib) (r=0.32), tetanus (r=0.25), and diphtheria (r=0.23) with NOAEC of -86, -54 and -53%. Mean Serum levels (ng/ml) detected in 101 healthy, one-year old, formula-fed children and breastfed children for PFOA were 3.8±1 and 16.8±6.6 respectively, being for PFOS 6.8±3.4 and 15.2±6.9 respectively. Overall, a low risk of bias was detected based on the methodology. The data had high variability but presented statistically significant results. For instance, the ranges of IgG (Hib and diphtheria) and IgG1 (tetanus) antibody levels, (Hib: 0.026-100 mg/L, Diphtheria: 0.009-4.45 IU/mL, tetanus: 0.286-191 mg/L), were quite broad. An additional point to be noted is that multivariate analysis with few exclusions and the existence of confounders in a small sample size may lead to statistical bias. However, statistical bias with respect to the variables, co-exposure, and protocol deviation was found to be quite low. In addition, based on outcomes (primary effects such as antibody

response and clinical parameters) and other factors (dose-response, magnitude of effect etc.), overall confidence was found to be high. Based on the methodology and results reported in this article, there is convincing evidence that PFOA exposure is associated with a reduced level of vaccine antibody response in children.

The association of PFOA exposure from air and water and human serum concentration levels was investigated to identify potential exposure sources for people living near production facilities in the U.S. (Emmett et al. 2006). Residential Drinking water was found to be a contamination source responsible for blood serum levels with little contribution from air exposure. There was a low risk of bias found in the methodology and statistical evaluation. However, a significant risk of bias identified in the study was the exposure characterization of a diverse population group (2-60 years) over a large exposure period. Serum levels were found to be considerably higher in the age group >60 years (approx. IQR 217-874 ng/ml) followed by the 2-5-year-old age group (approx. IQR 385-780 ng/ml) and the 51-60-year-old age group (approx. IQR 134-576 ng/ml). The use of an air dispersion model to identify areas with higher PFOA exposure from the air was one of the strong points of this study, avoiding the risk of bias from other potential sources. A high level of evidence of the association of PFOA exposure from drinking water and blood serum levels was found, but this evidence perhaps not present the complete picture, since exposure might be from additional sources.

Grandjean et al. (2012) conducted a prospective birth cohort study in the Faroe Islands, which included approximately 656 singleton births recruited from 1997-2000, and 587 who were followed up in 2008. Antibody concentration against diphtheria and tetanus was measured for children aged 5-7 years with significant results. A low risk of bias was detected in the protocol and statistical analysis. Parameters including age, sex, and vaccine schedule were considered for this study. There was still potential for a high risk of bias due to possible confounders such as co-exposure and other population confounders, which could have affected the results. The study was adjusted for some known confounders such as PCBs and duration of breastfeeding. However, it didn't consider others including co-exposure to other PFAS (there is limited ability to differentiate effects of PFOA or PFOS from other PFAS). The selected cohort population in the Faroe Islands had known exposure to PCBs, which has been shown to suppress the antibody response. However, the analysis accounting for adjustment of PCBs showed no effects on the principal outcome. Nevertheless, exposure to PCBs was monitored along with PFAS. The percentage difference in antibody concentration at 5 years of age prebooster, postbooster, and 7 years of age for year 5 (prebooster: -30.9 to 10.9, postbooster: -45.5 to 6.1 and 7 years of age (-44.3 to 4.2) in case of tetanus and for diphtheria for 5 (prebooster: -34.9 to 8.3, postbooster: -31.5 to 4.3 and 7 years of age (-45.8 to 3.3) was quite wide for PFOS. For PFOA, the difference was also quite significant. Moderate to high evidence was found for available data on PFAS, and especially on immunity, for PFOS and PFOA.

The elimination half-life was calculated for PFOS, PFHS, and PFOA from human serum in retired fluorochemical production workers based on first-order elimination (Olsen et al. 2007). There was a low risk of bias detected in this study. Calculating half-life without random sampling of participants and strict inclusion criterion were seen as a bias. Whether the 26

retirees were suffering from any disease or ailment was neither checked, nor specified, which can lead to altered elimination of these chemicals, especially when all the participants were older than 50 years of age, and likely had previous exposure. Another important question was whether the exposure source was constant or varying. The only information available from the article was that the sampled population was not working at the APFO production facility any longer. However, there could be other exposure sources such as living in a polluted area, or drinking PFOA polluted water. For calculating the half-life of these chemicals, first-order kinetics was used, taking into account that the exposure might have decreased from the initial to the second sampling. However, this decrease could have been due to reduced exposure and the ban on PFAS chemicals after the year 2000. Moderate risk of bias was detected in methodology and half-life calculation. No confounders or modifying variables were considered during calculations, especially co-exposures or disease pathology.

5. Risk Assessment for PFAS Chemicals to improve policymaking

Based on the above review, there were certain questions which emerged related to translation of risk: 1) calculating exposure level of PFOS/PFOA for plasma/serum concentration detected during immunotoxicity in children of different ages and its comparison with TDI/RfD; and 2) the dosing used for animal studies and its relevance for human risk assessment. The second part of the review focused on all the above questions for finding the gaps and improving risk assessment. A pharmacokinetic assessment was done utilizing dosimetry modeling for reconstructed exposure. Published physiologically based pharmacokinetic (PBPK) models for PFOS and PFOA were used, which simulated the Markov Chain Monte Carlo (MCMC) approach for calculating reconstructed exposure taking into account parametric uncertainty (Deepika et al. 2021; Rovira et al. 2019; Fàbrega et al. 2014). With the help of PBPK models, expected daily exposure was calculated using reverse dosimetry from the observed plasma/serum level concentration reported by Abraham et al. (2020) and Grandjean et al. (2012). Results were then compared with TDI/RfD set by EFSA and USEPA. Further, inter-species extrapolation was done to compare the dosing scenario used in the animal studies and its relevance was evaluated, with respect to the daily exposure set by regulatory agencies.

5.1 PBPK Modelling and extrapolation

In 2020, total weekly intake (TWI) was set by EFSA to 4.4 ng/kg BW/day, based on a reported decreased immune response to vaccination. Two widely cited articles, Abraham et al. (2020) and Grandjean et al. (2012), concluding that there is a decreased immune response in infants and children after PFAS exposure, were evaluated. Previously validated and published PBPK Models by our group for PFOS and PFOA (Deepika et al. 2021; Rovira et al. 2019; Fàbrega et al. 2014) were used to calculate the reconstructed exposure and to compare it with the TDI by EFSA and USEPA (appendix 3, table 5 and 6). In relation to the EFSA 2020 limit (the concentration at which immunotoxic effects are observed) the TDI is 100-1000 times lower for the minimum concentration simulated for PFOS and PFOA. Compared to the USEPA guidance value, where TDI or RfD is 0.02 µg/kg BW/day, the TDI is only 1-10 times lower than the concentration at which toxic effects were observed in children for PFOS and PFOA (Figure 3 and 4). For USEPA, considering the safety and uncertainty factors, it may be equivalent to a

toxic dose. This daily exposure found in both studies was subsequently compared with an animal dosing scenario used to determine which is the immunotoxicity dose observed in animals.

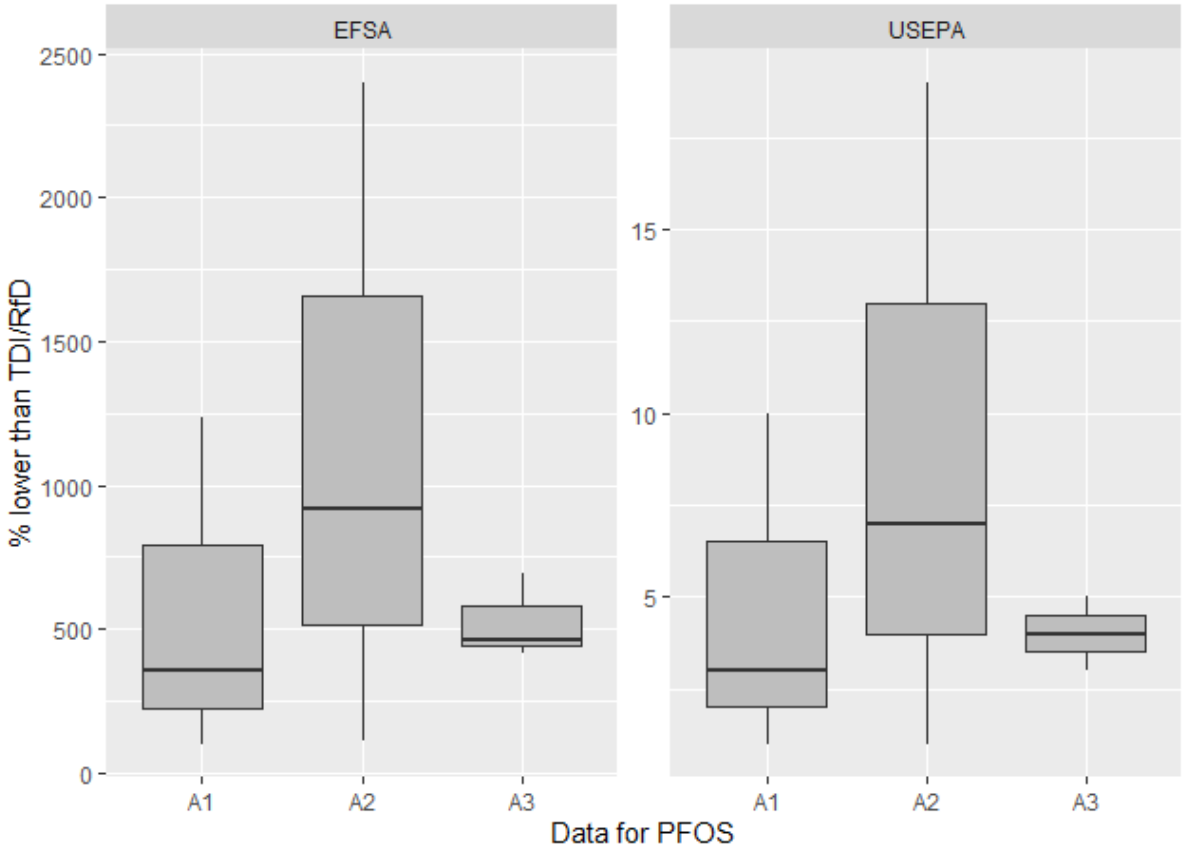

Figure 3: Comparison with the TDI or RfD set by regulatory bodies for PFOS. A1 and A2 represent the daily exposure simulated of 1-year-old children formula-fed (n=21) and breast-fed (n=80), respectively (Abraham et al. 2020). A3 represents the daily exposure simulated by PBPK for 5-year-old children (Grandjean et al. 2012).

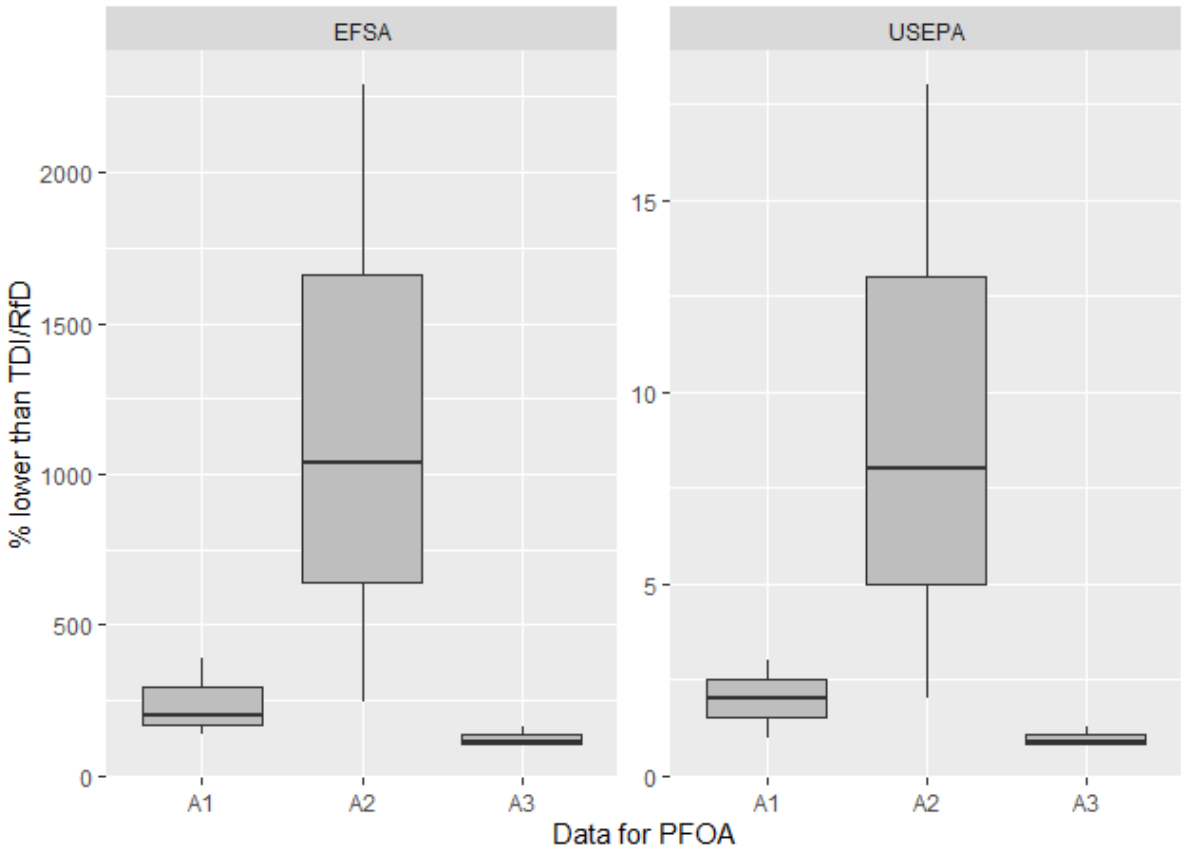

Figure 4: Comparison with the TDI and RfD sets by regulatory bodies for PFOS. A1 and A2 represent the daily exposure simulated in1-year-old children formula-fed (n=21) and breastfed (n=80) respectively (Abraham et al. 2020). A3 represents the daily exposure simulated by PBPK in 5-year-old children (Grandjean et al. 2012).

5.2 Inter-species dose extrapolation

Extrapolation of doses between species, from animals to humans, and their relevance in policy making is an important issue for toxicity assessment. Human equivalent dose (HED) scaling approaches, including allometric scaling, ontogeny scaling, pharmacokinetically guided scaling, etc., are some of the methods used. However, the most acceptable scaling method used today is allometrically based on body surface area, due to limited data availability for supporting other extrapolation methods (Nair and Jacob 2016). Five articles which were reviewed above related to animal studies (Koskela et al. 2016; Butenhoff et al. 2012; Lau et al. 2006; Luebker et al. 2005; Perkins et al. 2004) were used to evaluate dose scaling (Table 7, appendix 3). The United States' Food and Drug Administration (USFDA) formulated an interspecies dose conversion table, which was used for calculating HEDs, by multiplying or dividing NOAELs (no observed adverse effect levels) by a conversion factor. For calculating the dose, a safety factor of 10 was taken into account based on variability in extrapolation from animals to humans. There can be many reasons for variability in both species; unanticipated toxicity in human which may not be observed in animals, variation in metabolism and elimination, or increased sensitivity towards toxicity in humans compared to animals. Table 2 shows references for animal to human scaling based on BSA. A similar approach was used to calculate HED based on animal studies of PFAS.

$$HED = \frac{Animal\ dose\ in\ mg}{kg} * \left(\frac{Animal\ weight\ in\ kg}{Human\ Weight\ in\ kg}\right)^{0.33} \qquad Equation 1$$

Table 2: Animal to Human Equivalent Doses (HED) based on BSA (Adapted from USFDA).

Species	**Divide animal dose by**	**Multiply animal dose by**
Mouse	12.3	0.08
Hamster	7.4	0.13
Rat	6.2	0.16
Ferret	5.3	0.19
Guinea pig	4.6	0.22
Rabbit	3.1	0.32
Dog	1.8	0.54
Monkeys (cynomolgus, rhesus, and stumptail)	3.1	0.32
Marmoset	6.2	0.16
Squirrel Monkey	5.3	0.19
Baboon	1.8	0.54
Micro-pig	1.4	0.73
Mini-pig	1.1	0.95

When comparing the human equivalent dose to the TWI set by the EFSA after including a safety factor of 10, the dosing used in animals is approximately six to fifty-two thousand times higher than the lower dose used in the studies (Figure 1, Supplementary file). However, compared to the TDI set by USEPA, which is relatively high compared to that of the EFSA, the dosing used was between forty and four hundred times higher (Figure 1, Supplementary file). The dosing used in the animal studies is quite appropriate as per limit set by USEPA to find toxic effects and to understand risk assessment in humans. But compared to the EFSA limit, animal dosing is very high, raising a question as to whether these animal studies can be considered valid for human risk assessment. Nevertheless, critical questions remain. These include the following: Is the dose scaling with respect to body surface area relevant when the half-life of chemicals such as PFOA varies from 28 days to 1.2-8.5 years (Schrenk et al. 2020) in humans? Should we consider the pharmacokinetic phase from first order to zero order in relation to clearance and consideration of varied volume of distribution? Should species differences in glomerular filtration and the number of nephrons should be considered in allometric scaling for chemicals such as PFAS, which are not metabolized? Also, tubular secretion and high resorption of chemicals can affect scaling. Therefore, explaining chemicals with renal excretion is not amenable to allometric scaling (Nair and Jacob 2016). Thus, limited

data and variation in clearance rates reported by several authors make difficult to validate such scaling.

6. Discussion for improving risk assessment

Throughout the world, regulatory and public agencies have been setting limits for persistent chemicals or groups of chemicals such as PFAS with the objective of preventing human health and environmental risks. Over the past 20 years, a variety of health effects related to PFAS exposure have been reported. These range from decreased birth weight, adverse reproductive effects, liver toxicity, developmental toxicity, increase in cholesterol levels, altered immune and thyroid function, and cancer (Knutsen et al. 2018; Alexander et al. 2008). With new scientific strategies, including epidemiological studies, effects in animals, toxicokinetic, and observed levels in human blood, PFAS safe limits have been decreased over time from micrograms to nanograms (as discussed below). There are still fundamental gaps in the way limits that are being established using specific data and processes. Based on our review, we emphasize some of the shortcomings in existing research and introduce an improved framework for assessing risk.

The first question is about using a conventional approach to assess the toxicity of individual chemicals (PFOS, PFOA, etc.) when in fact, human beings are exposed to a complex mixture of PFAS. It is well known that co-exposure to chemicals, especially different types of PFAS may be synergistic or antagonistic. Discussions on whether PFAS should be addressed using an additive approach, relative potency framework, or toxic equivalency factor approach are ongoing. Substances could be grouped by their persistence (toxicokinetic), bioaccumulation, biological functions, or molecular initiating events, with potency factors derived from several assays, or subclassifications (structural similarity). Also, the mechanisms behind the combined effect of mixtures of PFAS have not yet been elucidated. A recent study reported that individual and binary combinations of PFAS (PFOS, PFOA, PFNA, PFHxS, and PFDA) have concentration-dependent cytotoxicity and decreased GSH levels in HepG2 cells (Ojo et al. 2021). Developing a grouping strategy to evaluate the potential health effects of a large number of PFAS, requires consideration of PFAS heterogeneity. In recent years, subclass names have been proposed (Sha et al. 2019; Wang et al. 2017). However, there are still major disagreements regarding these groupings. For example, exposure routes may be complex and biological persistence and elimination half-lives are still not predictable using in silico tools based on structure. For a large number of PFAS, traditional approaches to evaluating toxicity may not be feasible. New approach methodologies (NAM), which include a combination of in vitro high-throughput toxicity screening and in silico models, are necessary to inform further testing of PFAS (Patlewicz G. 2020).

Secondly, different population groups can have different risk profiles for these chemicals. There have been multiple pieces of evidence that point towards a higher concentration of PFAS in children and older-age populations. The C8 health project study conducted in 69,030 U.S. participants who were enrolled over 13 months (2005-2006), showed lower median PFAS (PFOS, PFOA, PFHxS, and PFNA) concentrations in women than in men. Also, the reported concentrations of PFOS and PFOA were relatively lower in adults (20-39 years of age) than in teenagers (12-19 years of age) and people over the age of 60 years (Frisbee et al. 2009).

Additionally, a great amount of uncertainty and variability in published data often makes difficult to reach clear conclusions. In most epidemiological studies, the variability is very high, which leads to inconsistent results.

Third, reporting of methodological protocols and results of epidemiological and animal studies must be consistent and follow a standardized protocol set by several regulatory bodies. Statistical bias, consideration of confounders, and multiple sampling for human biomonitoring over a specified time period, are required to increase the confidence level in the research findings. Inclusion of types and numbers of animals, computerized randomization, and descriptions of deviations from the protocol in published articles, will reduce bias in and help strengthen the evidence from animal studies. When deciding dosing levels for animals, a human-relevant dose needs to be appropriately calculated in order to further link associations with human risk assessment and help set TDI for humans. Also, sometimes uncertainty in studies with different in-vivo models and epidemiology is so high especially for endpoints like immunotoxicity that it becomes difficult to translate the results for risk assessment (Vidal et al. 2021, in press). In such cases, utilizing different computational models help in filling some gaps and improving translation of risk.

Advancements in computational toxicology and availability of experimental data is beginning to shift the focus of research on PFAS towards translation of risk from exposure scenarios to health risk assessment using in-silico tools. Translational toxicology involves the integration of pharmacokinetics, pharmacodynamics, systems biology, and adverse outcome pathways (AOPs) in order to understand the interactions among chemicals and living beings at different levels of biological organization (Kumar et al. 2020). Compared to traditional dose-response models, integrative translation toxicology implements a more complex structure, as shown in Figure 5. In-silico tools such as PBPK models, are currently being utilized to estimate daily exposure based on serum levels found in the population, together with additional evidence from epidemiology and animal studies. A large amount of data is required for translation toxicology which often becomes the limiting factor but, in such cases, semi-mechanistic model can be used. In-silico techniques including QSAR, PBPK, and read-across, help to reduce the need for experimental studies and to provide strong evidence for toxicity assessment and grouping of persistent chemicals (Deepika et al. 2020). The translational framework should combine different approaches such as in-silico, in-vitro, in-vivo, epidemiological studies, and omics techniques, for integrating results and characterizing biological and toxicological risks from xenobiotic exposure. Such kind of translational framework can help to fill some of the existing gaps, including incorporating sensitivity populations, reducing uncertainty in interspecies extrapolation, and identifying mechanisms. With more than 150 PFAS (long-chain and short-chain) currently registered, it is difficult to group them and evaluate individual and co-exposure toxicities based on current experimental and epidemiological data. The translational framework is helpful in these cases, especially for chemical hazard characterization by grouping chemicals and characterizing potency, based on in-silico and experimental data.

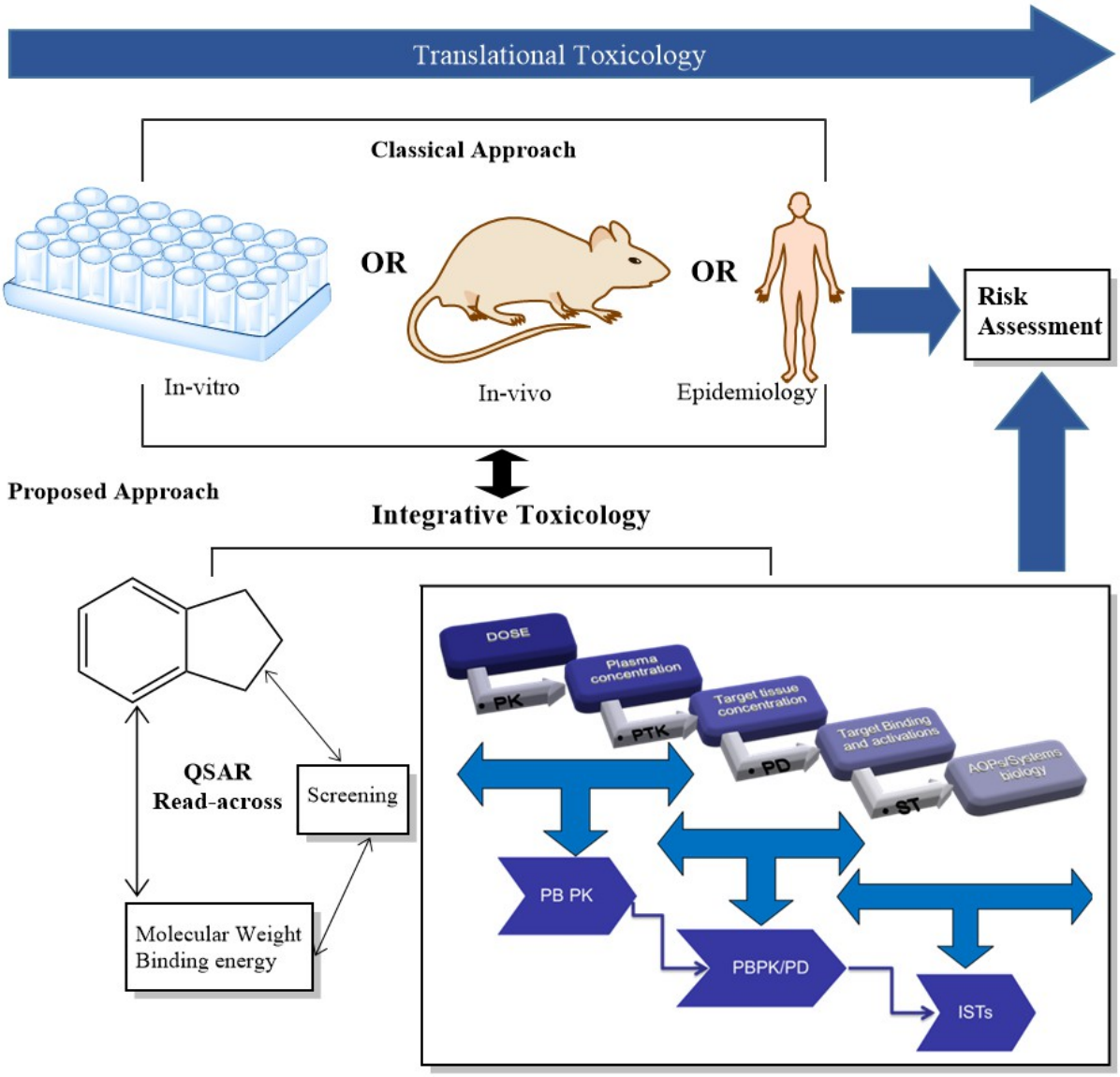

Figure 5: Proposed framework for integrational toxicology. Integrative toxicology includes incorporating both experimental studies like in-vitro, in-vivo, or epidemiological and in-silico models like PBPK, PD, QSAR, and read-across to improve human health risk assessment (Sharma 2018).

7. Conclusions and Future Actions

Like other harmful and potentially harmful chemicals, many PFAS have potential to produce a wide range of adverse health effects. Establishing health effects guidelines requires a careful review of the strength of evidence, consistency of evidence across studies, species concordance, strength of effect associations in epidemiological studies, and selection of effect/s for determining which potential impacts are either severe, or of great concern.

Two of the reviewed studies found an association between PFAS exposure and negative immune outcomes, but some inconsistency has been observed. Although recent studies have associated exposure to PFAS with adverse health outcomes, most are cross-sectional analyses. Therefore, data are insufficient to draw accurate conclusions about the association of PFAS with any specific disease. With some recent evidence of selected PFAS involvement

in immune hazards to humans, future human studies must characterize wider immune outcomes including (but not limited to) immune effects from early exposure during pregnancy and the possible role of PFAS's in initiating allergic and autoimmune processes, conditions for which a dose-response is hard to predict. More longitudinal epidemiology studies are required with additional susceptible human endpoints. In particular, prospective vaccination studies covering more varied types of vaccines and including different populations, as well as additional studies on other human immune outcomes. Epidemiological studies must also include cumulative exposures of several PFAS. Particularly, studies of the effects of PFNA and PFHxS on the immune system should be conducted.

Significant toxicokinetic differences have been observed in various animal and human studies. For example, in rodents, half-life varies from a few hours to several weeks, being in general much shorter than that in humans. For some PFAS's, interactions with various transporters involved in the reabsorption processes, occurring at the hepatic, intestinal and renal levels have been observed, which affects the elimination half-life. The half-life of PFAS has been a major controversial issue, with varying PFAS half-lives in human differing by years.

Although PBPK models for some PFAS are well developed health risk assessment, they still need to be further developed, optimized, and validated for other PFAS. Experimental evidence is needed to understand and quantify the association between PFAS and blood lipids (cholesterol levels) and the role of enterohepatic recirculation and glomerular reabsorption, including organic anion transporters.

In the case of mixture toxicity - "an additive RfD approach" compared to a "relative potency factor (RFD) approach," should be considered. However, for most PFAS, RFD values are still lacking for susceptible hazard endpoints. The development of new approaches to determining PFAS toxicity must consider tissue-specific modes of action. New approaches should rely on molecular interactions involving enzymes, storage, transport proteins, and ability to alter cell membrane fluidity within a particular organ/system. Collaborative development of new AOPs should be encouraged. However, predictive results should be biologically plausible and represent dose-effect responses across species. A greater emphasis on developing workable and effective risk assessment methods for human health, including AOPs to support regulatory processes and development of relevant policy-related strategies are clearly necessary.

Acknowledgment
This study was financially supported by the Center for Truth in Science, Glenview, Ill. (USA).

References

Abraham K, Mielke H, Fromme H, Völkel W, Menzel J, Peiser M, et al. 2020. Internal exposure to perfluoroalkyl substances (PFASs) and biological markers in 101 healthy 1-year-old children: associations between levels of perfluorooctanoic acid (PFOA) and vaccine response. Arch Toxicol 94:2131–2147; doi:10.1007/s00204-020-02715-4.

Alexander J, Auðunsson GA, Benford D, Cockburn A, Dogliotti E, Domenico A Di, et al. 2008. Perfluorooctane sulfonate (PFOS), perfluorooctanoic acid (PFOA) and their salts Scientific Opinion of the Panel on Contaminants in the Food chain. EFSA J 6:1–131; doi:10.2903/j.efsa.2008.653.

Ashley-Martin J, Dodds L, Arbuckle TE, Morisset AS, Fisher M, Bouchard MF, et al. 2016. Maternal and neonatal levels of perfluoroalkyl substances in relation to gestational weight gain. Int J Environ Res Public Health 13:1–11; doi:10.3390/ijerph13010146.

Bowman JS. 2015. Response to “Comment on ‘Fluorotechnology Is Critical to Modern Life: The FluoroCouncil Counterpoint to the Madrid Statement’”. Environ Health Perspect 123:A170-1; doi:10.1289/ehp.1510295.

Butenhoff JL, Chang S-C, Olsen GW, Thomford PJ. 2012. Chronic dietary toxicity and carcinogenicity study with potassium perfluorooctanesulfonate in Sprague Dawley rats. Toxicology 293:1–15; doi:10.1016/j.tox.2012.01.003.

Chang ET, Adami HO, Boffetta P, Wedner HJ, Mandel JS. 2016. A critical review of perfluorooctanoate and perfluorooctanesulfonate exposure and immunological health conditions in humans. Crit Rev Toxicol 46:279–331; doi:10.3109/10408444.2015.1122573.

Cousins IT, DeWitt JC, Glüge J, Goldenman G, Herzke D, Lohmann R, et al. 2020. The high persistence of PFAS is sufficient for their management as a chemical class. Environ Sci Process Impacts 22:2307–2312; doi:10.1039/D0EM00355G.

Deepika D, Sharma RP, Schuhmacher M, Kumar V. 2020. An integrative translational framework for chemical induced neurotoxicity–a systematic review. Crit Rev Toxicol 50:424–438; doi:10.1080/10408444.2020.1763253.

Deepika D, Sharma RP, Schuhmacher M, Kumar V. 2021. Risk Assessment of Perfluorooctane Sulfonate (PFOS) using Dynamic Age Dependent Physiologically based Pharmacokinetic Model (PBPK) across Human Lifetime. Environ Res 199:111287; doi:10.1016/j.envres.2021.111287.

Emmett EA, Shofer FS, Zhang H, Freeman D, Desai C, Shaw LM. 2006. Community Exposure to Perfluorooctanoate: Relationships Between Serum Concentrations and Exposure Sources. J Occup Environ Med 48:759–770; doi:10.1097/01.jom.0000232486.07658.74.

Fàbrega F, Kumar V, Schuhmacher M, Domingo JL, Nadal M. 2014. PBPK modeling for PFOS and PFOA: Validation with human experimental data. Toxicol Lett 230:244–251; doi:10.1016/j.toxlet.2014.01.007.

Food E, Authority S. 2012. Perfluoroalkylated substances in food: occurrence and dietary exposure. EFSA J 10; doi:10.2903/j.efsa.2012.2743.

Frisbee SJ, Brooks AP, Maher A, Flensborg P, Arnold S, Fletcher T, et al. 2009. The C8 health project: Design, methods, and participants. Environ Health Perspect 117:1873–1882; doi:10.1289/ehp.0800379.

G. P. 2020. A Chemical Category-Based Approach for Selecting and Screening PFAS for Toxicity and Toxicokinetic Testing.; doi:10.23645/epacomptox.11904930.v1..

Gaballah S, Swank A, Sobus JR, Howey XM, Schmid J, Catron T, et al. 2020. Evaluation of developmental toxicity, developmental neurotoxicity, and tissue dose in zebrafish exposed to genX and other PFAS. Environ Health Perspect 128:1–22; doi:10.1289/EHP5843.

Grandjean P, Andersen EW, Budtz-Jørgensen E, Nielsen F, Mølbak KR, Weihe P, et al. 2012. Serum vaccine antibody concentrations in children exposed to perfluorinated compounds. JAMA - J Am Med Assoc 307:391–397; doi:10.1001/jama.2011.2034.

Knutsen HK, Alexander J, Barregård L, Bignami M, Brüschweiler B, Ceccatelli S, et al. 2018. Risk to human health related to the presence of perfluorooctane sulfonic acid and perfluorooctanoic acid in food. EFSA J 16; doi:10.2903/j.efsa.2018.5194.

Koskela A, Finnilä MA, Korkalainen M, Spulber S, Koponen J, Håkansson H, et al. 2016. Effects of developmental exposure to perfluorooctanoic acid (PFOA) on long bone morphology and bone cell differentiation. Toxicol Appl Pharmacol 301:14–21; doi:10.1016/j.taap.2016.04.002.

Kumar V, Deepika D, Sharma RP. 2020. Chapter 4. Integrated Translation Framework for Endocrine Disruptors in the area of Computational Toxicology. In: *Challenges in Endocrine Disruptor Toxicology and Risk Assessment*. The Royal Society of Chemistry. 80–120.

Lau C. 2019. A snap-shot of reproductive and developmental toxicity of Perfluoroalkyl Substances (PFAS).

Lau C, Thibodeaux JR, Hanson RG, Narotsky MG, Rogers JM, Lindstrom AB, et al. 2006. Effects of Perfluorooctanoic Acid Exposure during Pregnancy in the Mouse. Toxicol Sci 90:510–518; doi:10.1093/toxsci/kfj105.

Luebker DJ, Case MT, York RG, Moore JA, Hansen KJ, Butenhoff JL. 2005. Two-generation reproduction and cross-foster studies of perfluorooctanesulfonate (PFOS) in rats. Toxicology 215:126–148; doi:10.1016/j.tox.2005.07.018.

Mitro SD, Sagiv SK, Rifas-Shiman SL, Calafat AM, Fleisch AF, Jaacks LM, et al. 2020. Per- and Polyfluoroalkyl Substance Exposure, Gestational Weight Gain, and Postpartum Weight Changes in Project Viva. Obesity 28:1984–1992; doi:10.1002/oby.22933.

Nair A, Jacob S. 2016. A simple practice guide for dose conversion between animals and human. J Basic Clin Pharm 7:27; doi:10.4103/0976-0105.177703.

NTP. 2015. *Handbook for conducting a literature-based health assessment using OHAT approach for systemic review and evidence integration*.

Ojo AF, Xia Q, Peng C, Ng JC. 2021. Evaluation of the individual and combined toxicity of perfluoroalkyl substances to human liver cells using biomarkers of oxidative stress.

Chemosphere 281:130808; doi:10.1016/j.chemosphere.2021.130808.

Olsen GW, Burris JM, Ehresman DJ, Froelich JW, Seacat AM, Butenhoff JL, et al. 2007. Half-life of serum elimination of perfluorooctanesulfonate, perfluorohexanesulfonate, and perfluorooctanoate in retired fluorochemical production workers. Environ Health Perspect 115:1298–1305; doi:10.1289/ehp.10009.

Pelch KE, Reade A, Wolffe TAM, Kwiatkowski CF. 2019. PFAS health effects database: Protocol for a systematic evidence map. Environ Int 130:104851; doi:10.1016/j.envint.2019.05.045.

Perkins RG, Butenhoff JL, Kennedy GL, Palazzolo MJ. 2004. 13-Week Dietary Toxicity Study of Ammonium Perfluorooctanoate (APFO) in Male Rats. Drug Chem Toxicol 27:361–378; doi:10.1081/DCT-200039773.

Rovira J, Martínez MÁ, Sharma RP, Espuis T, Nadal M, Kumar V, et al. 2019. Prenatal exposure to PFOS and PFOA in a pregnant women cohort of Catalonia, Spain. Environ Res 175:384–392; doi:10.1016/j.envres.2019.05.040.

Schrenk D, Bignami M, Bodin L, Chipman JK, del Mazo J, Grasl-Kraupp B, et al. 2020. Risk to human health related to the presence of perfluoroalkyl substances in food. EFSA J 18; doi:10.2903/j.efsa.2020.6223.

Sha B, Schymanski EL, Ruttkies C, Cousins IT, Wang Z. 2019. Exploring open cheminformatics approaches for categorizing per- And polyfluoroalkyl substances (PFASs). Environ Sci Process Impacts 21:1835–1851; doi:10.1039/c9em00321e.

Sharma RP. 2018. Integrative Systems Toxicology For Human Health.

Singh N, Hsieh CYJ. 2021. Exploring Potential Carcinogenic Activity of Per- and Polyfluorinated Alkyl Substances Utilizing High-Throughput Toxicity Screening Data. Int J Toxicol 40:355–366; doi:10.1177/10915818211010490.

Sunderland EM, Hu XC, Dassuncao C, Tokranov AK, Wagner CC, Allen JG. 2019. A review of the pathways of human exposure to poly- and perfluoroalkyl substances (PFASs) and present understanding of health effects. J Expo Sci Environ Epidemiol 29:131–147; doi:10.1038/s41370-018-0094-1.

Tsai MS, Lin CY, Lin CC, Chen MH, Hsu SHJ, Chien KL, et al. 2015. Association between perfluoroalkyl substances and reproductive hormones in adolescents and young adults. Int J Hyg Environ Health 218:437–443; doi:10.1016/j.ijheh.2015.03.008.

USEPA 2016. Health Effects Support Document for Perfluorooctanoic Acid (PFOA).

Vidal OS. 2021. EDC-induced mechanisms of Immunotoxicity: A Systematic Review. Crit Rev Toxicol; doi:10.1080/10408444.2021.2009438.

Wang Z, DeWitt JC, Higgins CP, Cousins IT. 2017. A Never-Ending Story of Per- and Polyfluoroalkyl Substances (PFASs)? Environ Sci Technol 51:2508–2518; doi:10.1021/acs.est.6b04806.

UNIVERSITAT ROVIRA I VIRGILI
QUANTITATIVE SYSTEMS TOXICOLOGY MODELING FOR NEURONAL ADVERSE OUTCOME
Deepika

Chapter 4

Deepika Deepika, Natalia Bravo, Roser Esplugas, Marco Capodiferro, Raju Prasad Sharma, Marta Schuhmacher, Joan O. Grimalt, Jordi Blanco, Vikas Kumar, Chlorpyrifos, Permethrin and Cyfluthrin effect on cell survival, permeability, and tight junction in an in-vitro model of the Human Blood-Brain Barrier (BBB) (Under Revision).

UNIVERSITAT ROVIRA I VIRGILI
QUANTITATIVE SYSTEMS TOXICOLOGY MODELING FOR NEURONAL ADVERSE OUTCOME
Deepika

Chlorpyrifos, Permethrin and Cyfluthrin effect on cell survival, permeability, and tight junction in an in-vitro model of the Human Blood-Brain Barrier (BBB)

Abstract

The blood-brain-barrier (BBB) is a structural and functional interface between plasma and the human brain. Predictive BBB in-vitro models like immortalized human capillary microvascular endothelial cells (HCMEC/D3) are required to explore the neurotoxic risk for daily exposed chemicals. The present study was focused on investigating the human BBB permeation potential of one organophosphate pesticide, chlorpyrifos (CPF), and two pyrethroids, permethrin (PMT) and cyfluthrin (CFT). HCMEC/D3 cells were exposed to the chemical and the time-dependent pass across BBB along with permeation coefficient (Papp) was calculated. Transendothelial electrical resistance (TEER) was measured for the cells to check the monolayer formation and later to check reduction in integrity after chemical exposure. Real time PCR was conducted to investigate the effect of chemicals on expression of tight and adherens junction proteins of BBB. Calculated Papp value for three chemicals was with the following order: CPF>CFT>PMT, where CPF showed a highest permeation coefficient. TEER calculation showed that the integrity decreased after CPF exposure which was in concordance with Papp value whereas for other chemicals, no change in TEER after exposure was observed. In addition, transwell study showed higher efflux ratio (ER) (>2) of CFT indicated that CFT could be a substrate for active transport. For CPF and PMT, ER was less than 2, so no active transport seems to be involved. The evaluation of the mRNA expression analysis revealed a statistically significant decrease in Occludin (OCLN) gene expression for CPF, VE-Cadherin (CDH5) for PMT and Zonula Occludens (ZO1) expression for CFT. Our study showed that CPF has the highest potential for inducing cell death, higher permeation, and capability to inducing BBB dysfunction than among the above-mentioned chemicals. Additionally, the results of permeation study could be useful to build a human PBPK model using in-vitro in-vivo extrapolation approach.

Keywords: Blood-Brain-Barrier, HCMEC/D3, Chlorpyrifos, Insecticides, Pyrethroids, Permethrin, Cyfluthrin, Permeability, Efflux Ratio

1. Introduction

Chlorpyrifos (CPF) is a widely used organophosphate pesticide (OP) for pest control in animals, plants for agriculture and public health applications (Goel et al. 2005; Li and Ehrich 2013). Several epidemiological studies revealed that general population may be getting exposed to the CPF through air, food, soil and water (Eaton et al. 2008; Oliver et al. 2000). Overtime, studies have been published focused on neurotoxic effects of CPF. For instance, CPF has been associated with neurodevelopmental disorders in infants and children (Guo et al. 2019). Further, it has been shown that CPF inhibits brain cholinesterase, a target neurotransmitter associated with behavioural disturbances in exposed rodents (Saunders et al. 2012; Whitney et al. 1995). Recently, CPF has been banned for sale in Europe due to geno- and neurotoxicity but its use still continues in many developing nations (EU-Wide ban of Chlorpyrifos and Chlorpyrifos-methyl - Eurofins Scientific). In recent years, CPF is being replaced by pyrethroids like permethrin (PMT) and cyfluthrin (CFT) (Fluegge et al. 2016; Rodríguez et al. 2018). Exposure to these insecticides may occur by dietary intake, respiratory uptake and dermal contact (Rodríguez et al. 2018). These insecticides have also shown neurotoxic effects; however their mechanism and potency might differ based on the exposure. For instance, in a comparative study for neurotoxicity, it was observed that both pyrethroids (PMT and CFT) had separate effects on sodium, chloride and calcium ion channels in brain (Breckenridge et al. 2009). Type I pyrethroid like PMT mainly acts by changing the conformation of sodium channel whereas type II pyrethroid like CFT act on chloride channel including GABA receptors (γ-aminobutyric acid) (López-Aceves et al. 2021). However, CPF mainly acts by inducing cholinergic crisis in human due to irreversible inhibition of cholinesterase, an enzyme that hydrolyse acetylcholine (ACh) (Burke et al. 2017). Similarly, the dose at which neurotoxicity is observed varies for the insecticides indicating that they might have the ability to cross the human blood-brain-barrier (BBB) at specific exposure levels.

The BBB is a network of complex tight junction formed by specialized capillary endothelial cells lining the brain microvessels whereas neighbouring cells like astrocytes and pericytes forms the neurovascular unit. However, the major interface is formed by endothelial cells preventing the transport of toxic compounds from blood to the cerebrospinal fluid (CSF) or nervous system (Abbott 2013). Transport of hydrophilic compounds across the BBB is restricted, however lipophilic or uncharged compounds can pass by passive diffusion. Nevertheless, the efflux transporters like P-GP (P glycoprotein), and BCRP (Breast cancer resistant protein) often regulates the movement of lipophilic compounds (Abbott 2013). Numerous in-vitro models of human BBB based on endothelial cells like human brain microvascular endothelial cells (HBMEC) and human pluripotent stem cells (hPSC) have been developed for studying the transport of xenobiotics. Non-endothelial cell lines like Caco-2, MDRK-MDCK, and LLC-PK1 are also used as a model for studying permeation, but they cannot replicate the complexity of human BBB (Gericke et al. 2020). Immortalized Human Microvascular Endothelial Cell lines (HCMEC/D3) are extensively used in-vitro model to study the chemical kinetics and gene expression at BBB. They form the tight junction (Weksler et al. 2013a) and hence serve as a suitable model for studying the transport kinetics of xenobiotics.

Despite previous evidences of the neurotoxicity of these insecticides, limited studies are available for assessment of their abilities to cross human BBB at different concentrations using in-vitro models. As per literature, most xenobiotics that enters the brain are less than 500 Da, neutral and lipophilic which can diffuse through brain endothelial cells (Brian Houston and Carlile 1997), still many xenobiotics do not follow this rule. Conducting animal experiments for thousands of chemicals is time-consuming, against the principles of 3R (replacement, reduction and refinement) for reducing animal experiment (Laroche et al. 2018) and interspecies differences in tight junction, proteins, specific receptor and enzymes can alter the BBB permeability (Wilhelm and Krizbai 2014). A study comparing rat and human BBB showed more than two-fold difference with P-GP, MDRP4 (multidrug resistance-associated protein 4), OAT3 (organic anion transporter 3) and L1 type amine acid (Hoshi et al. 2013). In the same study, more than two-fold difference in CLDN-5 expression was shown in human compared to rats, monkeys and marmosets in the in-vivo study (Hoshi et al. 2013). Since CLDN-5 is one of the major genes expressed at BBB and plays pivotal role in regulation of tight junction, human cell lines should be used for studies related to permeation potential. Regulatory bodies like FDA (Food and drug administration) recommends the need to conducts test for P-GP for the new molecular entities (NME) to understand the pharmacokinetics within central nervous system (CNS) and drug-drug interaction at early stage of drug discovery (Akamine et al. 2019). Such kind of in-vitro test can be used for these assays to reduce the dependence on animal models. In case of environmental chemicals, the test like P-GP assay, and transwell permeability can be conducted as initial tests to classify chemicals as CNS+ or CNS- before evaluating their neurotoxic potential using in-vitro cell lines.

The objective of this study was to investigate the toxicokinetic of CPF, PMT and CFT across human BBB using HCMEC/D3. Initially cell viability was measured to evaluate cytotoxicity of chemical. Further, Transendothelial electrical resistance (TEER) was calculated for confirming the formation of tight junction. Later, a bidirectional permeability experiment was conducted to calculate the permeation profile using Transwell assay. In-vitro results were correlated with in-vivo permeability using IVIVC (in-vitro to in-vivo correlation). Changes in mRNA (or gene) expression of several tight junction were also evaluated by RT-qPCR. In future, characterization of toxicokinetic of these chemicals could provide a basis to develop brain-physiologically based pharmacokinetic model (PBPK) using in-vitro data and decrease the uncertainty in humans risk assessment.

2. Material and Methodology

2.1 Materials

Chlorpyrifos (CPF), permethrin (PMT) and cyfluthrin (CFT) were purchased with purity of 98.0% CPF, 90.0% sum of cis+trans PMT and 95% (sum of diastereomers) from Sigma Aldrich (St. Louis, MO, USA). Immortalized human brain microvascular endothelial cell lines (HCMEC/D3) were obtained from Cederlane labs (Burlington, Canada). Endothelial cell growth medium (EGM) along with supplements was purchased from Sigma Aldrich (St. Louis, MO, USA). MTT (3-(4,5-dimethylthiazol-2-yl)-2,5-diphenyltetrazolium bromide) reagent, trypan-blue, trypsin-EDTA (ethylenediaminetetraacetic acid), HBSS (Hanks Balanced Salt Solution), HEPES (4-(2-hydroxyethyl)-1-piperazineethanesulfonic acid), DMSO (dimethyl sulfoxide) and

rat tail collagen type 1 were purchased from Sigma Aldrich (St. Louis, MO, USA). Transwell inserts (6-well and 12-well) were obtained from Sigma Aldrich and Corning (St. Louis, MO, USA).

2.2 Growth of the cells and exposure

HCMEC/D3 cell lines were cultured in endothelial cell growth medium (2% v/v) supplemented with fetal calf serum (0.02 ml/ml), endothelial cell growth supplement (0.004 ml/l), epidermal growth factor (0.1 ng/ml), basic fibroblast growth factor (1 ng/ml), heparin (90 µgm) and hydrocortisone (1 µgm/ml) at 37°C, 5% CO2 and 95% relative humidity. For ensuring BBB properties, passage used ranged from 27 to 34 (Weksler et al. 2013b). Cells were grown to 80-90% confluency for 3-5 days on T75 flask with change of medium every 2-3 days. Then trypsin-EDTA was used as dissociation buffer and cells were resuspended in EGM. Resuspended cells were counted and used for sub-culturing for further experiments. For all the experiments, cells were seeded at the density of 3-5*10^4 cells/cm^2. All the tests were carried out in triplicate.

2.3 Viability Assay

Cells were cultured in 48 well plates and incubated at different concentration for three chemicals along with DMSO (0.1% vehicle) treatment. Cells were treated with different concentrations of CPF (0, 1, 5, 10, 15, 30 and 60 µM), PMT (0, 1, 50, 100, 200, 600, and 800 µM), and CFT (0, 50, 100, 200, 600, and 800 µM) from low to high for 24 hours. Cells were cultured for 2-3 days before starting of the treatment. Cell viability was measured at 24 hours by adding 50 µl (5 mg/ml) MTT. They were kept for 4 hours in incubator for formation of formazan and then DMSO was added to dissolve the formazan. Absorbance was measured using UV-Vis spectrophotometer at 560 nm. Cell viability was calculated as percentage of absorbance in comparison to control (Eq.1).

$$Cell\ Viability = \frac{Abs_{sample}}{Abs_{control}} * 100 \qquad \text{Eq. 1}$$

2.4 Bidirectional permeability Assay and TEER Measurement

For permeability experiment, HCMEC/D3 cells were cultured on 12-well transwell inserts (0.4 µm pores, PET) with EGM medium (Figure). Transwell inserts were coated with rat tail collagen type 1 diluted in 70% ethanol and dried for minimum 3 hours before seeding the cells. Cells were grown to confluence for minimum 7-8 days with change in medium after 2-3 days until a monolayer was formed. The TEER was measured on every second day of cell growth for 7-8 days on inserts using Millicell ERS2 system for evaluating the tightness of the cell monolayers. Blank resistance was determined before starting the measurement and an electrode tip was kept in the disinfecting solution for 15 min followed by the cell culture medium (5-10 min) for equilibration. Cells were allowed to reach room temperature to avoid temperature changes affecting the resistance. The electrode was immersed so that a shorter tip was in the insert and a longer tip in the outer well. Precaution was taken so that shorter tip did not touch the surface of cells for disrupting the integrity. Inserts with collagen and without cells were considered as blank and all the measurements were done in duplicate. The TEER was calculated by the equation 2 and 3, that is

$$\text{Resistance}_{\text{cell monolayer}} = \text{Resistance}_{\text{cell}} - \text{Resistance}_{\text{blank}} \quad \text{Eq. 2}$$

$$\text{Unit area resistance}_{\text{cell monolayer}} = \text{Resistance} * \text{Effective membrane area } (\text{cm}^2) \quad \text{Eq. 3}$$

All transwell assays were performed with transport buffer (Hanks balanced salt solution with 20 mM HEPES, 25 Mm D-glucose, 1.25 mM CaCl2, and 0.5 mM MgCl2) at pH 7.4. Before starting the experiment, both sides of the inserts were prewashed with transport buffer (approximately 15 min in incubator) and then the medium was decanted. This procedure was repeated for 2 times for complete removal of EGM. After completion of washing, the inserts were transferred to a new plate before starting the experiment to avoid carryover of cell growth medium. Assays were performed in two concentrations (min, and max) with stock solution diluted in transport buffer for all chemicals. Well plates were incubated at 37°C on orbital shaker with moderate speed (100 rpm) to maintain sink conditions. Media samples (100-200 µl) were removed in determined time points: 30, 60, 120, 240 and 300 min from apical compartments to study the A>B transport; and from basolateral compartment to study the B>A transport in two separate experiment. In the similar study to calculate the efflux at 300 min, sample was withdrawn from basolateral compartment for A>B transport and apical compartment for B>A transport. Samples were maintained at -80ºC until analysis. At 300 min after chemical exposure, membrane integrity was again measured with TEER.

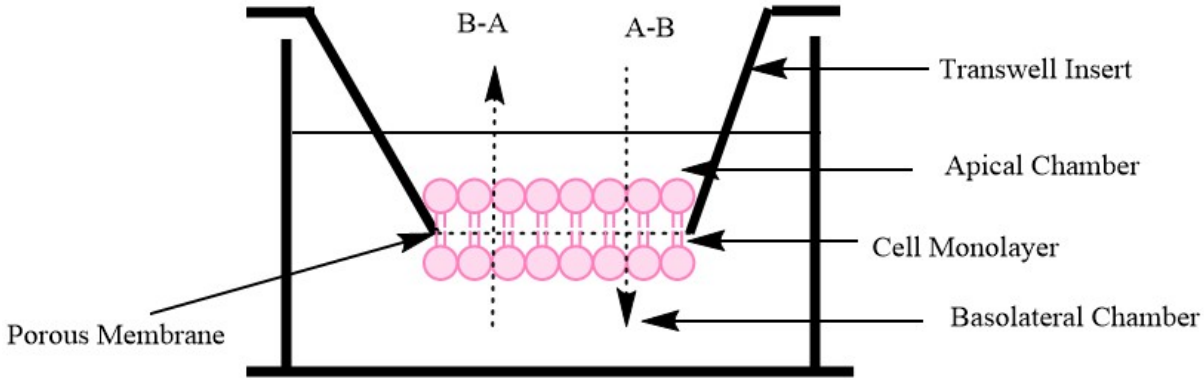

Figure 1: Bidirectional permeability study

2.5 Sample Analysis by GC-ECD

Collected media samples (200 µl) were placed into centrifuge tubes, pesticides extraction and isolation were achieved by addition of n-hexane, vortex mixing and centrifugation. The supernatant n-hexane layer was aspirated and placed into a chromatographic vial, the sample was re-extracted two more times with n-hexane. All the n-hexane extracts were combined and reduced to dryness under a very gentle stream of nitrogen. Finally, they were dissolved with 200 µL of parathion-ethyl (internal standard) in isooctane.

Organophosphate pesticide and pyrethroid were quantified by gas chromatography with electron captor detection (GC-ECD, Agilent Technologies 7890A). The instrument was equipped with a HP-5MS capillary column (60 m length, 0.25 mm internal diameter, 0.25 µm film thickness; JW Scientific) protected with a retention gap. Two microliters were injected in splitless mode. Injector and detector temperatures were 250 and 320 °C, respectively. The oven temperature program started at 90 °C, held for 2 min, then it increased to 130 °C at 15 °C/min and to 290 °C at 4 °C/min with a final holding time of 15 min. Ultrapure helium was

used as carrier gas and nitrogen was the make-up gas. Calibration straight lines used for the quantification can be found in the supplemental information (Fig 4). Limits of detection and quantification were 0.0019 and 0.0044 µM for CPF, 0.0045 and 0.0066 µM for CYF and 0.0034 and 0.0047 µM for PMT. Coefficients of variance (CV) calculated to test reproducibility ranged between 11 to 16% (CPF and PMT 11%; CYF 16%).

2.6 Transwell Data Analysis

From apical to basolateral transport (A>B transport), initially cumulative amount permeated was calculated followed by flux which is nanomolar passed per cm^2 surface area for all three chemicals to observe the increase in permeation with time. Further, the apparent permeability coefficient of endothelial monolayer was calculated ($P_{app\ A\text{-}B}$) in centimetres/sec (cm/s) that is (Eq. 4),

$$P_{app\ A-B} = \frac{V_b}{AC_{a0}} * \frac{\Delta C_b}{\Delta t} \qquad \text{Eq. 4}$$

where V_b is the volume in basolateral compartment, A is the surface area of filter membrane, C_{a0} is the initial concentration in apical compartment, $\Delta C_b/\Delta t$ concentration change over time in basolateral compartment.

The formula used for calculating permeability for basolateral to apical compartment ($P_{app\ B\text{-}A}$) was (Eq. 5),

$$P_{app\ B-A} = \frac{V_a}{AC_{b0}} * \frac{\Delta C_a}{\Delta t} \qquad \text{Eq. 5}$$

where V_a is the volume in apical compartment, C_{b0} is the initial concentration in basolateral compartment, $\Delta C_a/\Delta t$ concentration change over time in apical compartment. Efflux ratio is the inverse of uptake that is (Eq. 6),

$$Efflux\ Ratio = \frac{P_{app\ BA}}{P_{app,AB}} \qquad \text{Eq. 6}$$

The efflux ratio was set to 2, all chemicals with ratio above 2 were considered as substrate of active transporters while in those below 2, passive diffusion was considered as the major transport route (Crowe and Wright 2012; Shirasaka et al. 2006).

2.7 In-vitro to in-vivo correlation (IVIVC)

The chemicals' BBB kinetics correlation between the in vitro and in-vivo was established using IVIVC approach [21,22,23]. First, log BB (blood-brain) was calculated with already published in-vivo data [21,22,23] using the Eq. 7 that represents the ratio of chemical concentration between the brain and plasma. Second, we estimate the log of apparent permeability coefficient from our in-vitro data (Papp $_{A\text{-}B}$) that represent the ratio of intracellular chemical concentrations to media concentration. Then, the log Papp $_{A\text{-}B}$ data against the log BB was fitted using the linear regression to calculate the coefficient of determination (r^2).

$$log\ BB\ = log(\frac{C_{brain}}{C_{blood/plasma}}) \qquad \text{Eq. 7}$$

Here C_{brain} refers to the concentration in brain and $C_{blood/plasma}$ refers to the concentration quantified in blood or plasma.

For the PMT, Velez et al. calculated the AUC (area under curve) in brain and blood upon the oral administration of PMT in rats (Tornero-Velez et al. 2012). For calculating log BB, trans isomer was used by the author but in our in-vitro study, the PMT used was the mixture of cis+trans with more contribution from trans isomer (55 - 75% Trans-Isomer). For the CFT, data from rats based on oral administration of 20 mg/Kg BW was used. AUC reported by author for 0-24 hours was taken for plasma and brain. Since the published article contained AUC in several parts of the brain (hypothalamus, striatum, frontal cortex and hippocampus), cumulative AUC was taken for calculating log BB (Rodríguez et al. 2018). Study by Khokhar et al. at the dose of 0.6 µg calculated the brain and plasma concentration in rat at 4 h. BB (cbrain/cplasma) for CPF was directly extracted from the article published by Poet et al. on PBPK/PD model. The author has mentioned that this BB was used to validate multiple studies for rat. This value was taken since it has been used by multiple authors irrespective of the dose used in animal (Lowe et al. 2009; Poet et al. 2014; Timchalk et al. 2002) and further it was converted to logarithmic for equivalency to log BB (Poet et al. 2014).

2.8 RNA isolation and cDNA synthesis

The RNA was extracted from cells cultured on the transwell inserts after treatment with the chemicals for 5 h. Total RNA was extracted and isolated from cells using a speedtools Total RNA Extraction Kit (Biotools, Madrid, Spain) as per manufacture´s protocol. RNA was quantified and measured to check purity using a spectrophotometer at the UV absorbance of 260-280 nm (Nanodrop UV-Vis Spectrometer, Thermo Scientific, USA). RNA quality was evaluated by electrophoresis on a 1% denaturing agarose gel. Using 1 µg of total RNA from each sample, RNA was reverse transcribed by using the GeneAmp PCR System 2700 Thermal Cycler (Applied Biosystems™) for 60min at 42°C for reversing transcript, 5min at 95°C to inactivate the Reverse Transcriptase and an ultimate 4°C maintenance.

2.9 Real Time PCR

The expression of genes (primer showed in Table 1) involved for maintaining tight and adherens junction was evaluated (occludin: OCLN, zona occludens: ZO1, claudin 1: CLDN1, claudin 5: CLDN5, and vascular endothelial cadherins: CDH5) by quantitative RT-PCR in accordance with the manufacturer protocol using a Maxima SYBR Green/ROX qPCR Master Mix (2X) kit (ThermoFisher Scientifics, Waltham, USA). For normalized expression, housekeeping genes (GAPDH) was used. qPCR was performed using Rotor-gene Q Real-Time PCR cycler (Qiagen Inc, U.S.). Samples were tested per triplicate and negative controls (0.1% DMSO) were also run for each assay. At the end of PCR cycle, heat dissociation protocol was used to analyse the PCR product for confirming that SYBR green dye detect only a single PCR product. The threshold cycle (Ct) was calculated using Rotor-Gene Q 2.0 software for identifying fluorescent signals above noise during the early amplification cycle. The relative expression of target genes was calculated with respect to GAPDH following the $2^{-\Delta\Delta Ct}$ method and it was compared with the control (GAPDH).

Table 1: Primer sequence of tight junction genes used in the RT-PCR experiment

Primer Name	**Oligo Sequence Forward**	**Oligo Sequence Reverse**
Occludin (OCLN)	CAGGAACCGAGAGCCAGGT	ATAAACCAATCTGCTGCGTCCTA
Zona Occludens (ZO1)	CAGCCGGTCACGATCTCCT	TCCGGAGACTGCCATTGC
Claudin 1 (CLDN1)	GTTGGGCTTCATTCTCGC	CTGCACCTCATCGTCTTCC
Claudin 5 (CLDN5)	CTGCTGGTTCGCCAACATT	TGCGACACGGGCACAG
VE-Cadherin (CDH5)	ACCAGGACGCTTTCACCAT	AAAGGCTGCTGGAAAATGGG
Glyceraldehyde-3-phosphate dehydrogenase (GAPDH)	GAAGGTGAAGGTCGGAGTCAAC	CAGAGTTAAAAGCAGCCCTGGT

3 Statistical Analysis

All the experiments were performed in triplicate using cells from at least three independent batches. Data was presented as mean ± SD. Significant differences between groups were analysed using one-way analysis of variance (ANOVA) followed by Dunette test was done. Homogeneity of variance was analysed using Levene´s test. Kruskal-Walis test was conducted when variance was not homogenous. p values less than 0.05 were considered significant. The analysis was done with Graphpad Prism 9.3.1 software (Graphpad software, San Diego, CA, USA) and R studio version 2022.02.2+461 (Boston, U.S.).

3. Results

3.1 PMT, CFT and CPF significantly altered cell growth and survival

HCMEC/D3 cells were treated with different concentrations of CPF (0, 1, 5, 10, 15, 30 and 60 µM), PMT (0, 1, 50, 100, 200, 600, and 800 µM), and CFT (0, 50, 100, 200, 600, and 800 µM) for 24 hours. Results were expressed as mean ± SD in triplicate (Fig 2). In PMT, the viability decreased from 1 µM to 200 µM significantly up to 78% and then at higher concentration (600 and 800 µM), slight increase was seen but it was not significant. In case of CFT, viability decreased at 50 and 100 µM till 71% compared to control whereas after 100 µM viability increased till 800 µM to 77%. CPF showed a statistically significant decrease in viability at 1 and 5 µM upto 92%. At 30 and 60 µM, viability decreased further below 70%.

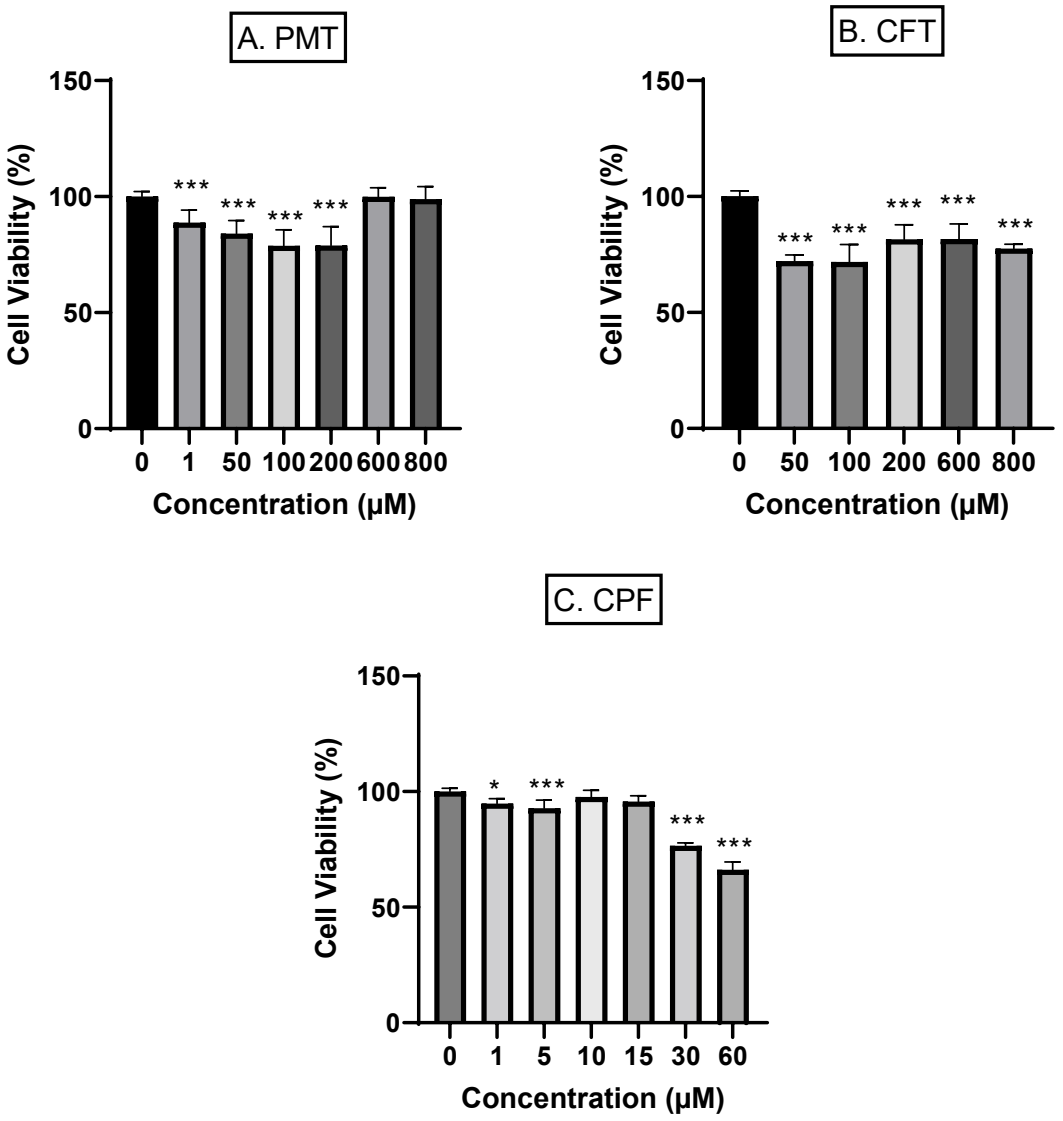

Figure 2: Cell Viability of three chemicals. A represents PMT, B represents CFT and C represents CPF. At lower concentration, cell viability decreased at 50 and 100 µM, whereas at 200 µM, cell viability increased and then again started decreasing. Data is represented as mean ± SD of at least three independent experiment. Differences relative to the control was analysed by one-way ANOVA followed by Dunnett test with p value < 0.05 as significant.

3.2 Integrity of BBB monolayer with time through TEER

The chemical transport through intercellular spaces depends on the integrity of BBB. The TEER assay was conducted to check the integrity of monolayer for simulating the same condition as human BBB. Increase in TEER was seen from day 1 to day 5 and then the constant phase was observed till 7 days (Fig 3). A decrease in electrical resistance was observed after exposure to the chemicals especially CPF but for the other pesticides, the decrease was non-significant (Fig 1 in supplementary file).

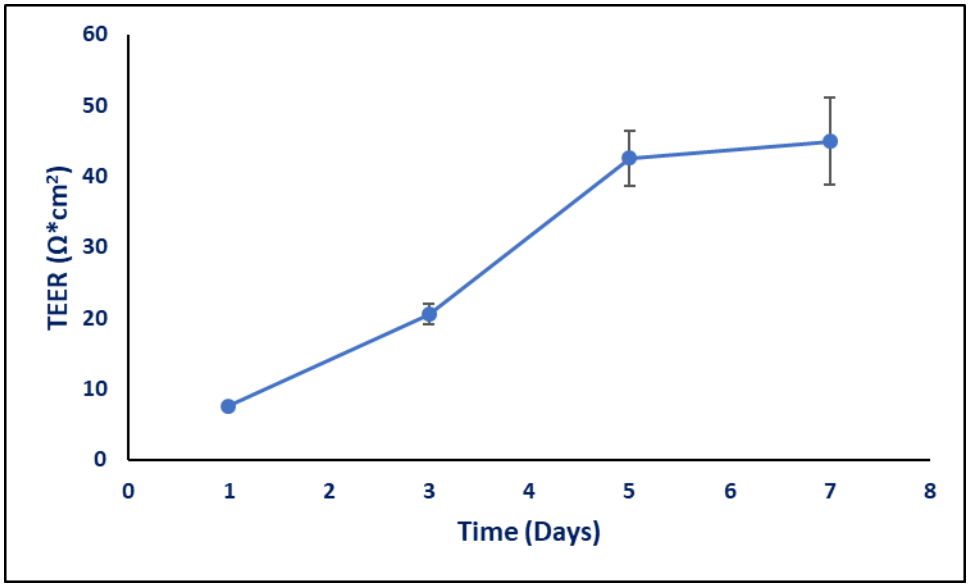

Figure 3: TEER for Transwell plate after growing the cells for 7-8 days. Resistance increased with time unless it became stable after 5 days. Data is represented as mean ± SD of at least three independent experiment.

3.3 Permeability across BBB and the role of active transport

Based on cell viability results, dosing was chosen for all three compounds with 1 dose for viability of less than 70% max dose and one above 80% viability, (PMT: 50 and 200 µM, CFT: 100 and 600 µM, CPF: 10 and 30 µM). This was done to check if concentration has some effect on permeation property especially due to cell death. The cumulative amount permeated per cm^2 remained almost similar for PMT and CFT whereas for CPF, the increase was minimal (Fig 1 in supplementary file). At 30 µM for CPF, the amount permeated was slightly more than 10 µM, but the increase was not significant (less than 1.5-fold). So, the lower concentration was used for further calculations. It was seen that cumulative amount and hence the permeability was independent of the concentration for most pesticides. The flux was in-line with the cumulative amount (Fig 2 supp file) with almost no change based on concentration for PMT and CFT and a little variation in case of CPF. $Papp_{A-B}$ and $Papp_{B-A}$ were calculated for all three compounds. Low permeability was observed for cyfluthrin and permethrin. In contrast, CPF showed high permeability (CPF>CFT>PMT; Fig 4). The efflux ratio was less than 2 for CPF (10 and 30 µM) and PMT (50 and 200 µM) but for CFT only at higher concentration (600 µM), the efflux ratio was more than 2 (Fig 5).

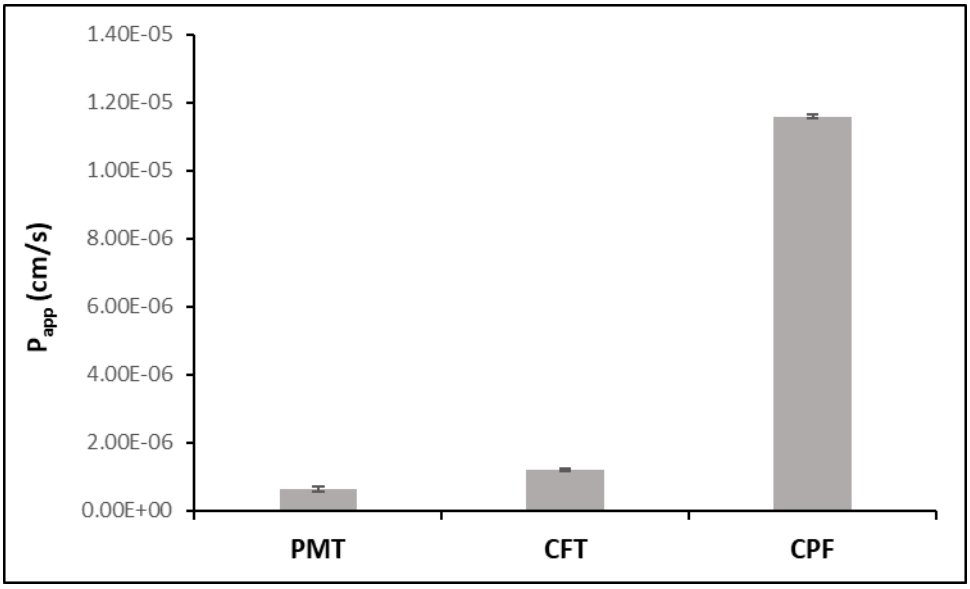

Figure 4: P_{app} for all three compounds for apical to basolateral transport. P_{app} more than 10^{-5} is considered to be highly permeable which is the case of CPF among all three pesticides. Both PMT and CFT are low permeable compounds. Data is represented as mean ± SD of at least three independent experiment.

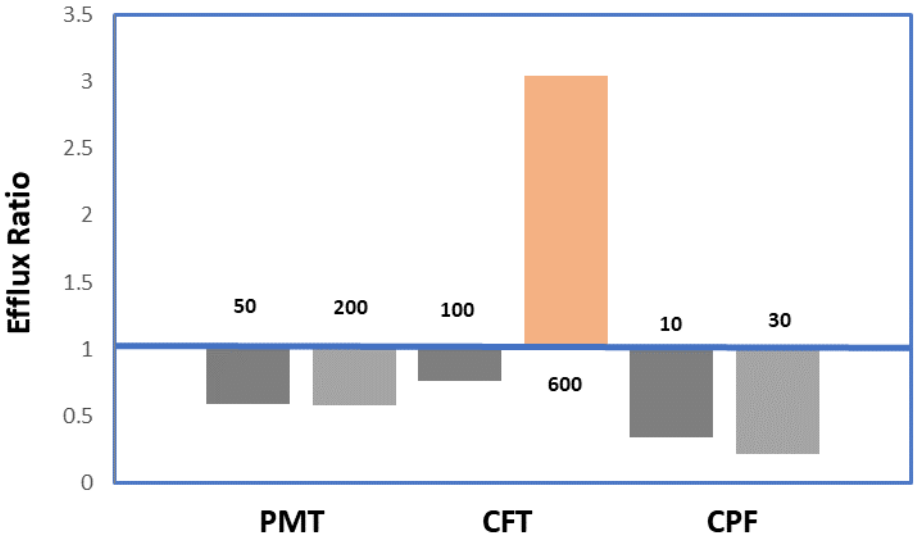

Figure 5: Efflux Ratio for several chemicals, PMT represents permethrin, CFT: Cyfluthrin and CPF: Chlorpyrifos. Bi-Permeability assay was done to identify and quantify the level of active efflux (B-A/A-B). The CFT at higher concentration with efflux ratio of more than 2 indicates that compound may be subject to active efflux. Data is represented as mean ± SD of at least three independent experiment.

3.4 Physicochemical Properties and IVIVC Evaluation

Performance of the in-vitro BBB model was compared with the in-vivo values to discriminate the ability of predicting chemical permeation. The log BB was in good correlation with the log Papp value with a correlation coefficient of 0.82 calculated using Pearson method (Fig 6). The

permeability values were then classified to determine the chemical ranking from best to worst ability for crossing the BBB. This was in opposite trend with the lipophilicity of the compound. CPF has the lowest lipophilicity, log P = 4.96, but the highest ability to cross both in-vitro and in-vivo, followed by CFT (log P = 5.95) and PMT (log P = 6.5). Thus, chemicals with log P value of less than 5 could permeate better than chemicals having log P above 5.

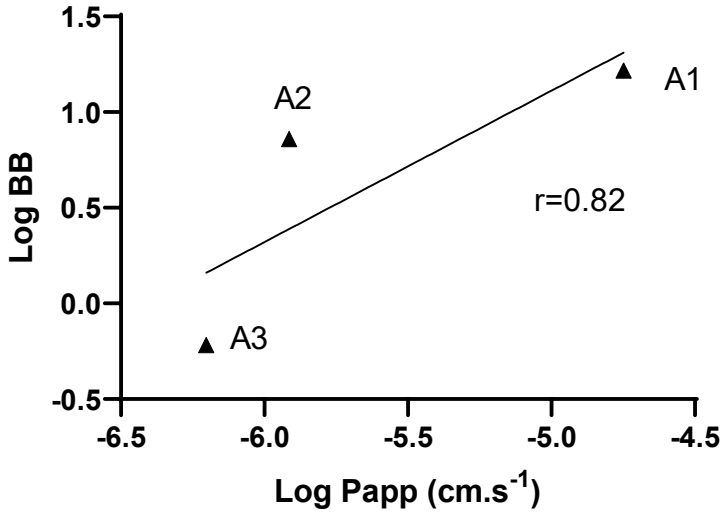

Figure 6: Linear regression plot for in-vitro Papp value with in-vivo log BB correlation (IVIVC) for 3 chemicals. Pearson correlation was used for calculating the correlation coefficient (r). A1, A2 and A3 represent the three chemicals, PMT, CFT and CPF.

3.5 Endothelial Gene Expression of tight junction present in BBB

Overall, the gene expression profiles were assessed using HCMEC/D3 cell lines after treatment for 5 hours with each pesticide. Several genes associated with the expression of TJ and adherens protein are responsible for limiting permeation of xenobiotics and contribute to high TEER value (Lochhead et al. 2020; Lopez-Ramirez et al. 2013). In the case of PMT, the significant decrease in CDH5 gene expression was observed after treatment at 50 and 200 µM (Fig 7). For the other genes, downregulation was observed but it was not statistically significant. CFT showed significant downregulation of ZO1 gene expression at both 100 and 600 µM (Fig 8). At 100 µM, downregulation of CLDN5 gene was observed but not at higher concentration. The OCLN gene was down expressed in CPF at both 10 and 30 µM (Fig 9). The other genes did not show any significant change in the expression.

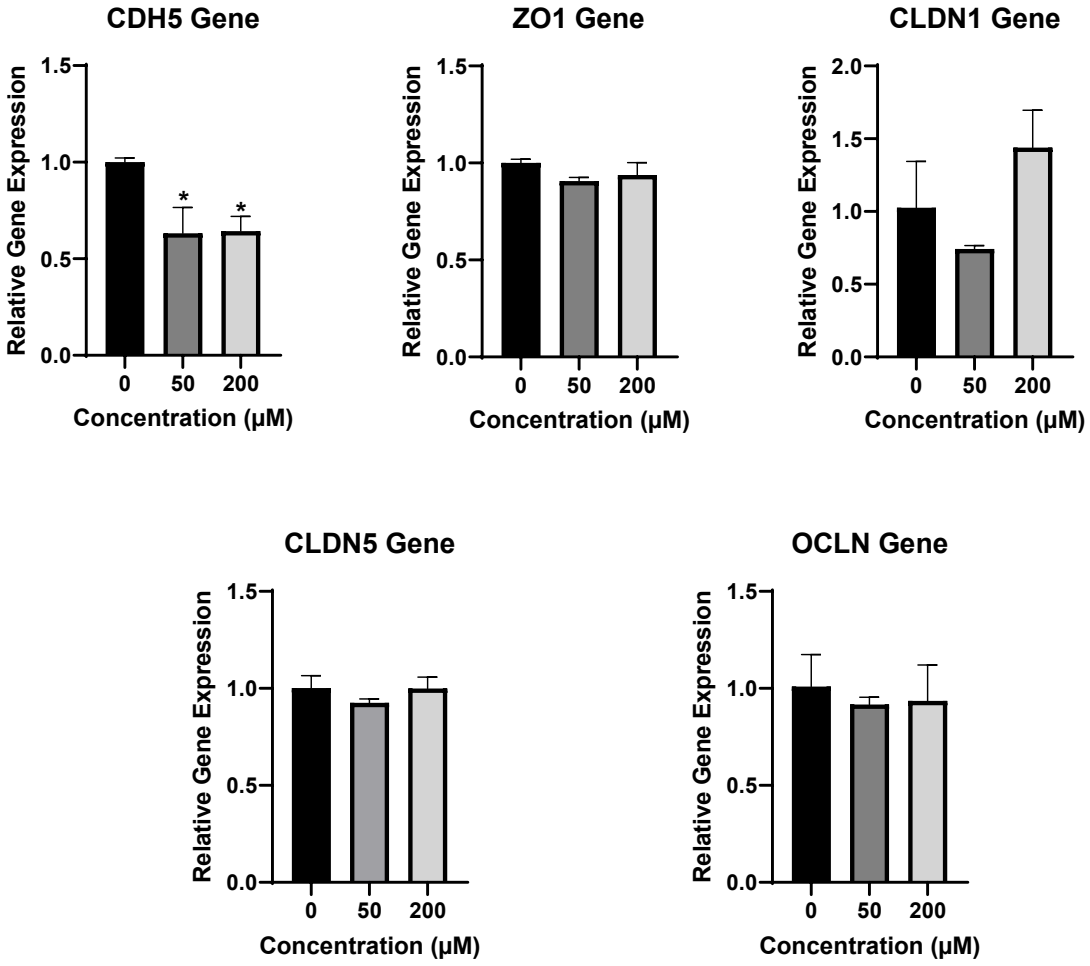

Figure 7: BBB genetic expression after exposure to permethrin. The genes represented in the figure are OCLN (occludin gene), CLDN1 (claudin 1), CDH5 (vascular endothelial cadherin), ZO1 (zona occludens), and CLDN5 (claudin-5). Data is represented as mean ± SD of three independent experiment. Differences relative to the control was analysed by one-way ANOVA followed by Dunnett test with p value < 0.05 as significant.

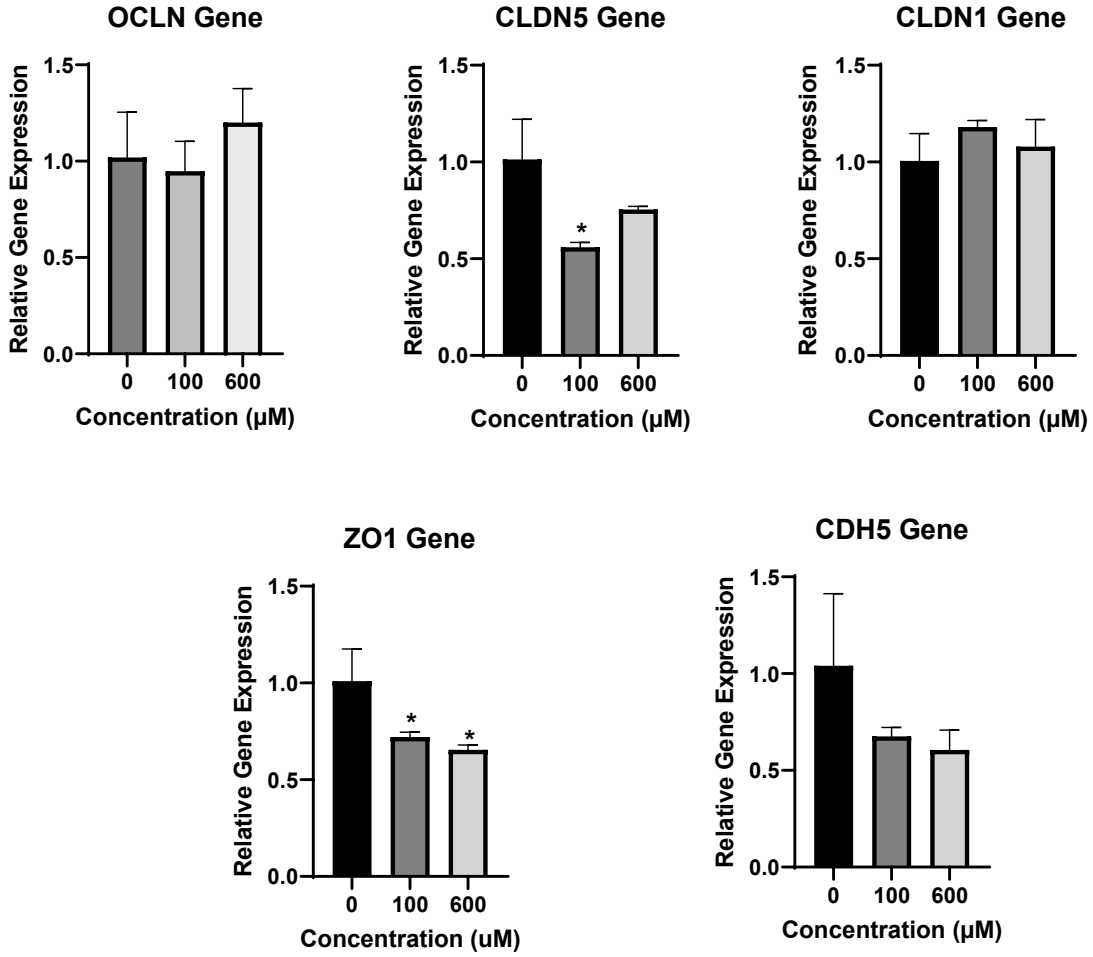

Figure 8: Genetic expression of Cyfluthrin. The genes represented in the figure are OCLN (occludin gene), CLDN1 (claudin 1), CDH5 (vascular endothelial cadherin), ZO1(zona occludens), and CLDN5 (claudin-5). Data is represented as mean ± SD of three independent experiment. Differences relative to the control was analysed by one-way ANOVA followed by Dunnett test with p value < 0.05 as significant.

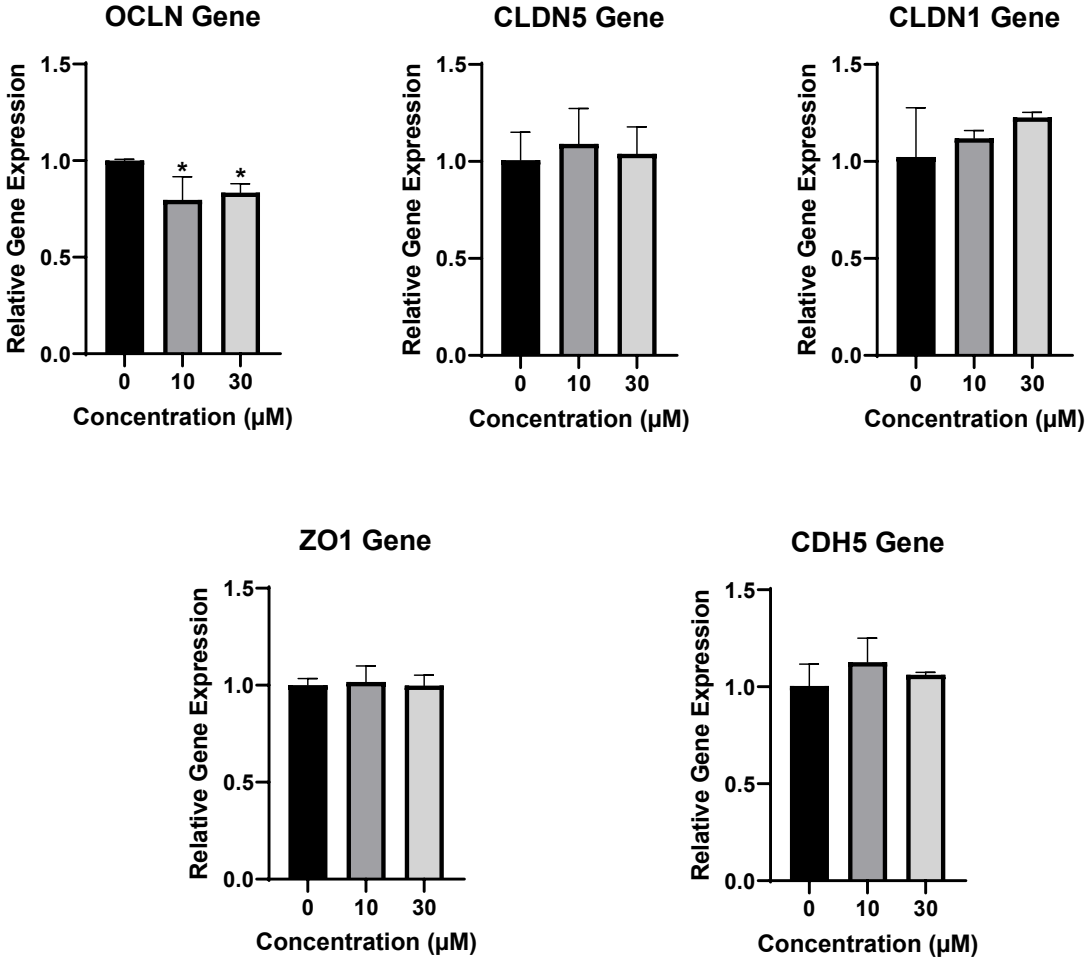

Figure 9: Genetic expression of CPF. The genes represented in the figure are OCLN (occludin gene), CLDN1 (claudin 1), CDH5 (vascular endothelial cadherin), ZO1 (zona occludens), and CLDN5 (claudin-5). Data is represented as mean ± SD of three independent experiment. Differences relative to the control was analysed by one-way ANOVA followed by Dunnett test with p value < 0.05 as significant.

4 Discussion

The present study utilizes an in-vitro model to examine the permeation of three insecticides (CPF, PMT and CFT) across the BBB. The model used consist of a HCMEC/D3 cell line which has been used in the past for similar studies (Łukasiewicz et al. 2017; Weksler et al. 2013a). CPF, PMT and CFT are neurotoxic chemicals and have been associated with neurobehavioral disturbances in humans (Bjørling-Poulsen et al. 2008; López-Aceves et al. 2021).

CPF exposure both at 10 and 30 µM had the highest potential to compromise the BBB integrity (Fig 9) and a high Papp value than the two other pesticides (Fig 4). The reason behind high permeation of the CPF can be its inherent physicochemical properties. CPF has the log P value less than 4.96 and lower molecular weight of 350.6, hydrogen bond donor count 0 and

hydrogen bond acceptor count of 5 (National Center for Biotechnology Information (2022). https://pubchem.ncbi.nlm.nih.gov/compound/Chlorpyrifos.). CPF follows all parameters for Lipinski´s rule making it good candidate for permeation. Additionally, our result on genetic expression suggest that CPF interaction with tight junction may play a pivotal role in BBB disruption. OCLN gene was down expressed significantly both at 10 and 30 µM compared to control (0.1% DMSO). OCLN is a transmembrane protein of tight junction and key structural component of BBB (Yuan et al. 2020). Many studies have indicated that disruption in OCLN gene serve as an important biomarker for BBB permeability and integrity (Yuan et al. 2020). The OCLN gene is being regulated by several signalling pathways like nuclear factor-kappa B, mitogen-activated protein kinase (MAPK), protein kinase C, RhoK, and ERK1/2 (Yuan et al. 2020). So, it might be possible that CPF might downregulate the OCLN via these pathways. This study demonstrated that OCLN down-regulation was in line with the significant reduction seen in TEER after CPF exposure (Fig 1 in supp file) and also decreased cell viability (Fig 2).

PMT was found to be a low permeable compound at the tested concentration in our experiment with human BBB cell line. PMT has a log P value of 6.5 and a molecular weight of 391.3 violating one criterion for Lipinski rule (National Center for Biotechnology Information (2022). PubChem Compound Summary for CID 40326, Permethrin.). The efflux ratio of PMT was found to be less than 2, suggesting that PMT was not a substrate for active transporter. This observation suggested capability of PMT for passive permeation only. The point worth mentioning is that literature suggest BBB penetration increase with lipophilicity upto a certain point, but very high log P might lead to decrease in permeation. The PMT might be trapped in membrane due to reduced flux and poor partitioning coupled with hydrophobic bonding of highly lipophilic compounds (Mortuza et al. 2019). In the genetic expression, significant downregulation of CDH5 gene was observed (Fig 7). CDH5 is one of the important components in vascular system and is responsible for assembly of BBB architecture and adherens Junction (AJs). CDH5 is exclusive to endothelial cells and aids in communicating with the cells of similar type. One study has established that CDH5 along with other TJs protein affect the integrity of BBB (Weber 2012). It may be possible that single downregulation of CDH5 cannot completely disrupt the BBB integrity, that's why also no significant change in TEER was observed at the tested concentrations of PMT. To further understand this, neuroinflammatory cytokines and other potential biomarkers like TNFα (Tumor necrosis factor) and IFNγ (Interferon gamma) should be measured to clarify this aspect, which indirectly concerns the maintenance of barrier integrity (Lopez-Ramirez et al. 2013). It may be possible that being a low permeable molecule for human at the selected doses, still it can affect the brain directly or indirectly as it may have high potency.

CFT was also low permeable but the permeability coefficient was more than PMT. CFT has log P value of 6.2 and molecular weight of 434.3 violating one criterion for Lipinski rule similar to PMT. In our study CFT was found to be low-medium permeable with Papp value of $1.22*10^{-6}$ ($cm.s^{-1}$) and was found to be a concentration dependent substrate for active transport (discussed below). At the tested concentration CFT did not show any alteration in the integrity (shown by no significant change in resistance). However, CFT exposure to the cells resulted in the significant downregulation of the ZO1 gene at both concentrations whereas CLDN5 was downregulated only at lower concentration (100 µM). Downregulation of CLDN5 at 100 µM

did not impacted the permeability as the cumulative amount permeated was found to be similar at both the concentrations (Fig 2 in supp file). ZO1 is considered as the support for signal transduction protein and as recognition protein for tight junction placement. A study has shown that alteration in ZO1 could result in TJ disorganization (Jiao et al. 2011). So, It may be possible that downregulation of ZO1 may have impact BBB tight junction consequently increased permeation (Jiao et al. 2011). However, the major TJ proteins directly involved in BBB are CLDN5, CLDN3 and OCLN (Luissint et al. 2012). Further studies need to be conducted to understand the activation of pathways associated with ZO1 at BBB. For instance, in a rat study seizure was associated with downregulation of ZO-1, claudins and occludin at BBB resulting in glutamate production (Lochhead et al. 2020; Rempe et al. 2018). This increased glutamate could activates the cytosolic phospholipase A2, by activation of enzyme matrix metalloproteinase (MMP)-2 and MMP9, leading further aggravation of BBB leakage (Lochhead et al. 2020; Rempe et al. 2018). Such aggravation of BBB leakage could play a role in alteration of Papp value.

Apart from passive diffusion, active transport also plays an important role in the permeation of xenobiotics. Transporter like P-GP, and Breast Cancer Resistant Protein (BCRP) play a major role in active transport at BBB. P-GP being widely studied transporter in the BBB cell lines and to understand the active transport, we calculated the efflux ratio. The efflux ratio for CPF was found to be lower than 2 suggesting that CPF may not be the substrate for active transport in our in-vitro model. This result was not in agreement with the rat study by Lanning et al. (Lanning 1996). Author demonstrated that CPF have the ability to interact and increase the expression of P-GP in several organs (Lanning 1996). The study suggested that CPF can be pumped outside the BBB, in another sense, the efflux ratio (P_{app} B-A/ P_{app} A-B) should be high. However, the differences in both results could be explained by the fact that CPF can be metabolized to CPF-oxon by CYP enzymes and that could act as a substrate for P-GP (Yang et al. 2001). Moreover, the incubation time with the chemical was 5 hours in our study which may be shorter than time required for energy mediated transport as a time-dependent transport of xenobiotic may happen which has also been observed with other chemicals (Di Leo et al. 2021). Moreover, it has been shown that efflux ratio can vary based on the concentration used for flux. For instance, a candidate drug for treating Parkinson showed varied efflux ratio with several concentration ranging from 1 to 10 µM (Liu et al. 2014). A similar kind of phenomenon was seen in case of CFT, where at a particular concentration (600 µM), efflux ratio was found to be more than 2 making it a substrate for active transport (Saaby and Brodin 2017). Overall study suggests that CPF efflux ratio could be dose and time dependent, and formation of its active metabolites. However, an in-vitro study using immortalized rat brain endothelium 4 (RBE4) cell line showed that CPF concentration did not change after blocking the P-GP using VPM (Verapamil) indicating CPF is not a substrate for P-GP (Yang et al. 2001). Further study needs to be done to understand the active transport role for CPF and its metabolite. The Papp value does not take into account the saturable nature of the transporter, so the efflux ratio can vary based on the concentration used for flux (Liu et al. 2014). In our study, the PMT was not found to be the substrate for active transport. We have not found any study in the literature where it was shown that whether or not PMT is a

substrate for active transport. This is the first study to report about active transport of PMT and this data can be valuable for understanding toxicokinetic of this chemical.

In-vitro models are valuable tools for screening of chemicals and drug compounds allowing fast screening and helps in reducing the animal usage focusing towards the goal of 3Rs (Curzer et al. 2016). The ultimate step of our study was to correlate the in-vitro results with the published in-vivo data from rat or mice. Conventional IVIVC approach was used based on linear regression between log BB and log Papp. The good correlation was observed with r value of 0.812 (Fig 6). Thus, the in-vitro model seemed to display a good prediction for pesticides. In future, the Papp data calculated in our in-vitro study could be used for building permeability limited physiologically based pharmacokinetic models (PBPK) for human considering both the A-B and B-A transport. Such kind of in-silico models utilizing the in-vitro data from human cell lines are promising to reduce animal exploitation in research. For instance, permeability limited human brain and CSF PBPK model was developed utilizing the in-vitro data for paracetamol and phenytoin (Gaohua et al. 2016).

However, our study has few limitations like plasma protein binding was not considered. It may be possible that binding of these chemicals with the albumin and plasma proteins can impact their permeation potential (Amaraneni et al. 2016). It may be possible that binding might or might not have statistically significant alteration. Chemicals like PMT, CFT and CPF are extensively oxidized and hydrolysed by the rat and human hepatic microsomal enzymes (Lanning 1996; Scollon et al. 2009). It may be possible that the metabolite could affect the BBB integrity and hence the permeation potential. Subsequent in-vitro models can be improved by including the albumin in the permeation study and checking the permeation for both chemical and metabolite.

5 Conclusion

In the present study, we calculated the Papp value both influx (A-B) and efflux (B-A) for organophosphate CPF and two pyrethroids PMT and CFT using HCMEC/D3 cell lines. The results of the present study showed that CPF have the highest potential to permeate the BBB of the three pesticides examined. This compound disrupts the tight junction independently of the concentration. This effect can lead to disturbances in the BBB tight junction as evidenced from the genetic expression, change in resistance and hence increased neurotoxicity. The efflux ratio of CFT was found to increase at higher concentration pointing towards concentration dependent active transport. In case of PMT, no active transport was observed, and this is the first study to report this data using human cell lines. Further, IVIVC pointed towards the validity of in-vitro results. Such kind of rich in-vitro data can be used in future to build brain specific PBPK model to understand the risk reducing the animal dependency.

Acknowledgment

This study was financially supported by Marie Skłodowska-Curie “Neurosome Project” under the grant agreement No. 766251. This publication reflects only the authors' views. The Community and other funding organizations are not liable for any use made of the information contained therein.

Credit Authorship

Deepika Deepika: Conceptualization, Methodology, Data Analysis, and writing; Natalia Bravo: Analysis by GC-ECD, writing about GC-ECD, and review; Roser Esplugas: Supervision, and Review; Marco Capodiferro: Writing about GC-ECD and review; Raju Prasad Sharma: Supervision and Review, Marta Schuhmacher: Supervision and Review; Joan O. Grimalt: Supervision, Analysis by GC-ECD, writing, and Review; Jordi Blanco: Supervision, Conceptualization, Data Analysis, Review and Revision, Vikas Kumar: Supervision, Conceptualization, Methodology, Data Analysis, writing, review and revision.

References

Abbott NJ. 2013. Blood–brain barrier structure and function and the challenges for CNS drug delivery. J Inherit Metab Dis 36:437–449; doi:10.1007/s10545-013-9608-0.

Akamine Y, Yasui-Furukori N, Uno T. 2019. Drug-Drug Interactions of P-gp Substrates Unrelated to CYP Metabolism. Curr Drug Metab 20:124–129; doi:10.2174/1389200219666181003142036.

Amaraneni M, Sharma A, Pang J, Muralidhara S, Cummings BS, White CA, et al. 2016. Plasma protein binding limits the blood brain barrier permeation of the pyrethroid insecticide, deltamethrin. Toxicol Lett 250–251:21–28; doi:10.1016/j.toxlet.2016.03.006.

Bjørling-Poulsen M, Andersen HR, Grandjean P. 2008. Potential developmental neurotoxicity of pesticides used in Europe. Environ Heal A Glob Access Sci Source 7:50; doi:10.1186/1476-069X-7-50.

Breckenridge CB, Holden L, Sturgess N, Weiner M, Sheets L, Sargent D, et al. 2009. Evidence for a separate mechanism of toxicity for the Type I and the Type II pyrethroid insecticides. Neurotoxicology 30:S17–S31; doi:10.1016/j.neuro.2009.09.002.

Brian Houston J, Carlile DJ. 1997. Prediction of Hepatic Clearance from Microsomes, Hepatocytes, and Liver Slices. Drug Metab Rev 29:891–922; doi:10.3109/03602539709002237.

Burke RD, Todd SW, Lumsden E, Mullins RJ, Mamczarz J, Fawcett WP, et al. 2017. Developmental neurotoxicity of the organophosphorus insecticide chlorpyrifos: from clinical findings to preclinical models and potential mechanisms. J Neurochem 142:162–177; doi:10.1111/jnc.14077.

Crowe A, Wright C. 2012. The impact of P-glycoprotein mediated efflux on absorption of 11 sedating and less-sedating antihistamines using Caco-2 monolayers. Xenobiotica 42:538–549; doi:10.3109/00498254.2011.643256.

Curzer HJ, Perry G, Wallace MC, Perry D. 2016. The Three Rs of Animal Research: What they Mean for the Institutional Animal Care and Use Committee and Why. Sci Eng Ethics 22:549–565; doi:10.1007/s11948-015-9659-8.

Di Leo N, Moscato S, Borso' M, Sestito S, Polini B, Bandini L, et al. 2021. Delivery of thyronamines (Tams) to the brain: A preliminary study. Molecules 26:1616; doi:10.3390/molecules26061616.

Eaton DL, Daroff RB, Autrup H, Bridges J, Buffler P, Costa LG, et al. 2008. Review of the Toxicology of Chlorpyrifos With an Emphasis on Human Exposure and Neurodevelopment. Crit Rev Toxicol 38:1–125; doi:10.1080/10408440802272158.

EU-Wide ban of Chlorpyrifos and Chlorpyrifos-methyl - Eurofins Scientific. Available: https://www.eurofins.de/food-analysis/food-news/food-testing-news/eu-wide-ban-of-chlorpyrifos-and-chlorpyrifos-methyl/.

Fluegge KR, Nishioka M, Wilkins JR. 2016. Effects of simultaneous prenatal exposures to organophosphate and synthetic pyrethroid insecticides on infant neurodevelopment at three months of age. J Environ toxiology public Heal 1:60–73; doi:10.5281/zenodo.218417.

Gaohua L, Neuhoff S, Johnson TN, Rostami-Hodjegan A, Jamei M. 2016. Development of a permeability-limited model of the human brain and cerebrospinal fluid (CSF) to integrate known physiological and biological knowledge: Estimating time varying CSF drug concentrations and their variability using in vitro data. Drug Metab Pharmacokinet 31:224–233; doi:10.1016/j.dmpk.2016.03.005.

Gericke B, Römermann K, Noack A, Noack S, Kronenberg J, Blasig IE, et al. 2020. A face-to-face comparison of claudin-5 transduced human brain endothelial (hCMEC/D3) cells with porcine brain endothelial cells as blood-brain barrier models for drug transport studies. Fluids Barriers CNS 17:53; doi:10.1186/s12987-020-00212-5.

Goel A, Dani V, Dhawan DK. 2005. Protective effects of zinc on lipid peroxidation, antioxidant enzymes and hepatic histoarchitecture in chlorpyrifos-induced toxicity. Chem Biol Interact 156:131–140; doi:10.1016/j.cbi.2005.08.004.

Guo J, Zhang J, Wu C, Lv S, Lu D, Qi X, et al. 2019. Associations of prenatal and childhood chlorpyrifos exposure with Neurodevelopment of 3-year-old children. Environ Pollut 251:538–546; doi:10.1016/j.envpol.2019.05.040.

Hoshi Y, Uchida Y, Tachikawa M, Inoue T, Ohtsuki S, Terasaki T. 2013. Quantitative Atlas of Blood–Brain Barrier Transporters, Receptors, and Tight Junction Proteins in Rats and Common Marmoset. J Pharm Sci 102:3343–3355; doi:https://doi.org/10.1002/jps.23575.

Jiao H, Wang Z, Liu Y, Wang P, Xue Y. 2011. Specific Role of Tight Junction Proteins Claudin-5, Occludin, and ZO-1 of the Blood–Brain Barrier in a Focal Cerebral Ischemic Insult. J Mol Neurosci 44:130–139; doi:10.1007/s12031-011-9496-4.

Lanning CL. 1996. CHLORPYRIFOS OXON INTERACTS WITH THE MAMMALIAN MULTIDRUG RESISTANCE PROTEIN, P-GLYCOPROTEIN. J Toxicol Environ Health 47:395–407; doi:10.1080/009841096161726.

Laroche C, Aggarwal M, Bender H, Benndorf P, Birk B, Crozier J, et al. 2018. Finding synergies for 3Rs – Toxicokinetics and read-across: Report from an EPAA partners' Forum. Regul Toxicol Pharmacol 99:5–21; doi:10.1016/j.yrtph.2018.08.006.

Li W, Ehrich M. 2013. Transient alterations of the blood-brain barrier tight junction and receptor potential channel gene expression by chlorpyrifos. J Appl Toxicol 33:1187–1191; doi:10.1002/jat.2762.

Liu Q, Hou J, Chen X, Liu G, Zhang D, Sun H, et al. 2014. P-glycoprotein mediated efflux limits the transport of the novel anti-Parkinson's disease candidate drug FLZ across the physiological and PD pathological in Vitro BBB models. M. Ahmad, ed PLoS One 9:e102442; doi:10.1371/journal.pone.0102442.

Lochhead JJ, Yang J, Ronaldson PT, Davis TP. 2020. Structure, Function, and Regulation of the Blood-Brain Barrier Tight Junction in Central Nervous System Disorders. Front Physiol 11; doi:10.3389/fphys.2020.00914.

López-Aceves TG, Coballase-Urrutia E, Estrada-Rojo F, Vanoye-Carlo A, Carmona-Aparicio L, Hernández ME, et al. 2021. Exposure to Sub-Lethal Doses of Permethrin Is Associated with Neurotoxicity: Changes in Bioenergetics, Redox Markers, Neuroinflammation and Morphology. Toxics 9:337; doi:10.3390/toxics9120337.

Lopez-Ramirez MA, Male DK, Wang C, Sharrack B, Wu D, Romero IA. 2013. Cytokine-induced changes in the gene expression profile of a human cerebral microvascular endothelial cell-line, hCMEC/D3. Fluids Barriers CNS 10:27; doi:10.1186/2045-8118-10-27.

Lowe ER, Poet TS, Rick DL, Marty MS, Mattsson JL, Timchalk C, et al. 2009. The Effect of Plasma Lipids on the Pharmacokinetics of Chlorpyrifos and the Impact on Interpretation of Blood Biomonitoring Data. Toxicol Sci 108:258–272; doi:10.1093/toxsci/kfp034.

Luissint A-C, Artus C, Glacial F, Ganeshamoorthy K, Couraud P-O. 2012. Tight junctions at the blood brain barrier: physiological architecture and disease-associated dysregulation. Fluids Barriers

CNS 9:23; doi:10.1186/2045-8118-9-23.

Łukasiewicz S, Błasiak E, Szczepanowicz K, Guzik K, Bzowska M, Warszyński P, et al. 2017. The interaction of clozapine loaded nanocapsules with the hCMEC/D3 cells – In vitro model of blood brain barrier. Colloids Surfaces B Biointerfaces 159:200–210; doi:10.1016/j.colsurfb.2017.07.053.

Mortuza TB, Edwards GL, White CA, Patel V, Cummings BS, Bruckner J V. 2019. Age Dependency of Blood-Brain Barrier Penetration by cis- and trans -Permethrin in the Rat. Drug Metab Dispos 47:234–237; doi:10.1124/dmd.118.084822.

National Center for Biotechnology Information (2022). PubChem Compound Summary for CID 2730, Chlorpyrifos. Retrieved May 30, 2022 from https://pubchem.ncbi.nlm.nih.gov/compound/Chlorpyrifos.

National Center for Biotechnology Information (2022). PubChem Compound Summary for CID 40326, Permethrin. Available: https://pubchem.ncbi.nlm.nih.gov/compound/Permethrin.

Oliver GR, Bolles HG, Shurdut BA. 2000. Chlorpyrifos: probabilistic assessment of exposure and risk. Neurotoxicology 21: 203—208.

Poet TS, Timchalk C, Hotchkiss JA, Bartels MJ. 2014. Chlorpyrifos PBPK/PD model for multiple routes of exposure. Xenobiotica 44:868–81; doi:10.3109/00498254.2014.918295.

Rempe RG, Hartz AMS, Soldner ELB, Sokola BS, Alluri SR, Abner EL, et al. 2018. Matrix Metalloproteinase-Mediated Blood-Brain Barrier Dysfunction in Epilepsy. J Neurosci 38:4301–4315; doi:10.1523/JNEUROSCI.2751-17.2018.

Rodríguez J-L, Ares I, Martínez M, Martínez-Larrañaga M-R, Anadón A, Martínez M-A. 2018. Bioavailability and nervous tissue distribution of pyrethroid insecticide cyfluthrin in rats. Food Chem Toxicol 118:220–226; doi:10.1016/j.fct.2018.05.012.

Saaby L, Brodin B. 2017. A Critical View on In Vitro Analysis of P-glycoprotein (P-gp) Transport Kinetics. J Pharm Sci 106:2257–2264; doi:10.1016/j.xphs.2017.04.022.

Saunders M, Magnanti BL, Correia Carreira S, Yang A, Alamo-Hernández U, Riojas-Rodriguez H, et al. 2012. Chlorpyrifos and neurodevelopmental effects: a literature review and expert elicitation on research and policy. Environ Heal 11:S5; doi:10.1186/1476-069X-11-S1-S5.

Scollon EJ, Starr JM, Godin SJ, DeVito MJ, Hughes MF. 2009. In Vitro Metabolism of Pyrethroid Pesticides by Rat and Human Hepatic Microsomes and Cytochrome P450 Isoforms. Drug Metab Dispos 37:221–228; doi:10.1124/dmd.108.022343.

Shirasaka Y, Kawasaki M, Sakane T, Omatsu H, Moriya Y, Nakamura T, et al. 2006. Induction of human P-glycoprotein in Caco-2 cells: development of a highly sensitive assay system for P-glycoprotein-mediated drug transport. Drug Metab Pharmacokinet 21:414–423; doi:10.2133/dmpk.21.414.

Timchalk C, Nolan RJ, Mendrala AL, Dittenber DA, Brzak KA, Mattsson JL. 2002. A physiologically based pharmacokinetic and pharmacodynamic (PBPK/PD) model for the organophosphate insecticide chlorpyrifos in rats and humans. Toxicol Sci 66:34–53; doi:10.1093/toxsci/66.1.34.

Tornero-Velez R, Davis J, Scollon EJ, Starr JM, Setzer RW, Goldsmith M-R, et al. 2012. A Pharmacokinetic Model of cis- and trans-Permethrin Disposition in Rats and Humans With Aggregate Exposure Application. Toxicol Sci 130:33–47; doi:10.1093/toxsci/kfs236.

Weber CR. 2012. Dynamic properties of the tight junction barrier. Ann N Y Acad Sci 1257:77–84; doi:10.1111/j.1749-6632.2012.06528.x.

Weksler B, Romero IA, Couraud PO. 2013a. The hCMEC/D3 cell line as a model of the human blood brain barrier. Fluids Barriers CNS 10:16; doi:10.1186/2045-8118-10-16.

Weksler B, Romero IA, Couraud PO. 2013b. The hCMEC/D3 cell line as a model of the human blood brain barrier. Fluids Barriers CNS 10:16; doi:10.1186/2045-8118-10-16.

Whitney KD, Seidler FJ, Slotkin TA. 1995. Developmental Neurotoxicity of Chlorpyrifos: Cellular Mechanisms. Toxicol Appl Pharmacol 134:53–62; doi:10.1006/taap.1995.1168.

Wilhelm I, Krizbai IA. 2014. In Vitro Models of the Blood–Brain Barrier for the Study of Drug Delivery to the Brain. Mol Pharm 11:1949–1963; doi:10.1021/mp500046f.

Yang J, Mutkus LA, Sumner D, Stevens JT, Eldridge JC, Strandhoy JW, et al. 2001. Transendothelial permeability of chlorpyrifos in RBE4 monolayers is modulated by astrocyte-conditioned medium. Mol Brain Res 97:43–50; doi:10.1016/S0169-328X(01)00296-0.

Yuan S, Liu K, Qi Z. 2020. Occludin regulation of blood–brain barrier and potential therapeutic target in ischemic stroke. Brain Circ 6:152; doi:10.4103/bc.bc_29_20.

UNIVERSITAT ROVIRA I VIRGILI
QUANTITATIVE SYSTEMS TOXICOLOGY MODELING FOR NEURONAL ADVERSE OUTCOME
Deepika

Chapter 5a

Deepika Deepika, Raju Prasad Sharma, Marta Schuhmacher, Joan O. Grimalt, Jordi Blanco, Vikas Kumar, Integration of in-vitro and Brain sub-compartment PBPK model for PFOS and PFOA induced neurotoxicity. (In preparation)

Chapter 5b

Deepika Deepika, Raju Prasad Sharma, Marta Schuhmacher, Vikas Kumar, Estimating neuronal risk through ROS Systems Biology Model for PFOS and PFOA (In preparation).

UNIVERSITAT ROVIRA I VIRGILI
QUANTITATIVE SYSTEMS TOXICOLOGY MODELING FOR NEURONAL ADVERSE OUTCOME
Deepika

Integration of Brain PBPK Model with in-vitro data using in-vitro to in-vivo extrapolation (IVIVE) for PFAS Chemicals to evaluate neurotoxicity

Abstract

Perfluoroalkyl substances (PFAS), especially PFOS (Perfluorooctane sulfonate) and PFOA (Perfluorooctanoic acid) are widely used in manufacturing and ubiquitously spread in the environment throughout the world. Recent studies have claimed the accumulation potential of PFOS and PFOA in the brain linked to various neurological disorders. However, the research regarding the penetration of these chemicals across the blood-brain barrier (BBB) is still lacking due to ethical concerns suggesting the need for an integrated in-vitro and in-silico framework. The objective of this study is to develop a mechanistic model describing the penetration of PFAS across human BBB utilizing the data generated from the in-vitro study and then to investigate the risk based on the brain tissue dosimetry physiologically based pharmacokinetic (PBPK) model. The in-vitro study includes quantification of PFAS permeability, it's interaction with uptake and efflux transporters proteins, and PFAS induced expression of these transporters at the transcript level using human derived in-vitro cell lines. Further, a brain-specific PBPK model is developed incorporating BBB penetration mechanism using in-vitro to in-vivo extrapolation (IVIVE) of data and dividing the brain into different sub compartments like cortex, hippocampus, CSF and rest of brain. This model is used to predict maximum concentration (Cmax), area under curve (AUC) for brain tissue regions to associate it with neurological disorders. Such mechanistic brain PBPK model combined with in-vitro study can provide quantitative estimation about pharmacokinetics of PFAS in human population. This model could improve the understanding of PFAS toxicological profile at target sites and its association with neurological disorders.

Keywords: Brain PBPK, Neurotoxicity, PFOS, PFOA, IVIVE, HCEMEC/D3, BBB

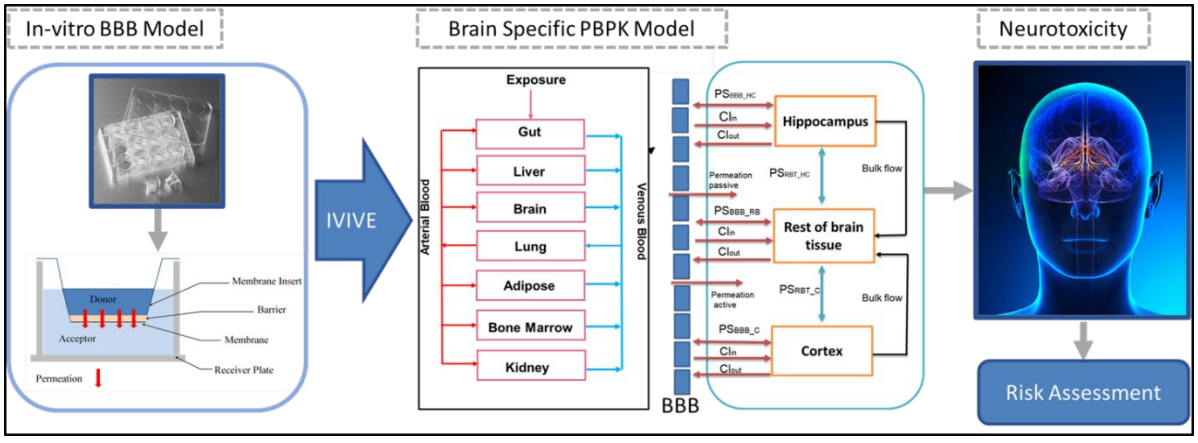

Figure 1: Integration of in-vitro transwell permeability data with mechanistic PBPK-IVIVE for evaluating neurotoxic risk assessment.

1. Introduction

Per- and polyfluoroalkyl substances (PFAS) also called as forever chemicals are extensively used in commercial and industrial application like non-stick pans, firefighting foams, semiconductors, and food packaging resulting in everyday exposure to living beings (Cao and Ng 2021; Fiedler et al. 2010; Glüge et al. 2020). PFAS is non-biodegradable and have potential for bioaccumulation due to long fluorinated carbon chain making it the perfect candidate for having negative effect on the living organism (Buck et al. 2011; Di Nisio et al. 2022). Previous studies have shown PFAS exposure implicated towards both developmental and non-developmental neurotoxicity in mice and rats (Cui et al. 2008; Johansson et al. 2008). Cholinergic system demonstrated by nicotine's hypoactive response was found to be affected during neonatal exposure to PFOS and PFOA in mice. This neurotoxic effect is similar to observed in other persistent organic pollutant (POPs) like polychlorinated biphenyls (PCBs) and polybrominated diphenyl ether (PBDEs) (Johansson et al. 2008). In another study, subchronic exposure to both PFOS and PFOA (28 days) was found to cause slight congestion followed by concomitant symptoms pointing towards neurotoxic potential (Cui et al. 2008). These studies point towards ability of these compounds to enter the brain through blood-brain-barrier (BBB) in rats which was also confirmed by another study where variation in serum corticosterone and serum leptin were observed after PFOS exposure (Austin et al. 2003). BBB transport of PFAS chemicals have been also studied in polar bears (*Ursu Maritimus*) where outer brain regions like striatum, frontal, cerebellum, occipital and temporal cortex have considerably lower concentration than inner brain regions (thalamus, hypothalamus and pons/medulla) (Greaves et al. 2013). These kinds of studies imply towards varying capabilities of PFAS to accumulate in several brain region based on blood flow, lipophilicity and other properties.

Regulatory bodies like USEPA and EFSA do not consider neurotoxic effect due to non-availability of concrete evidence in human (Fenton et al. 2021). In-vitro study using PC12 cell lines showed PFAS exposure related to effect on replication and differentiation of neurons and alteration in neurotransmitter level contributing towards developmental neurotoxicity (Slotkin et al. 2008). However, all PFAS behave differently and one single mechanism cannot explain their toxicity. This suggest that all PFAS need to be studied independently as their toxicokinetic and toxicodynamic can vary. Studying disposition of PFAS in human brain is quite tricky due to limited tools available for non-invasive techniques. But, permeability through BBB can be studied using in-vitro human BBB cell lines. Brain microvascular endothelial cell lines (HCMEC/D3) are widely used due to the ease with culturing, resemblance with BBB and a good model for studying transport mechanism with relevance to central nervous system (CNS) (Weksler et al. 2013). The result from permeability assay can be used further by scaling to human brain using in-vitro to in-vivo extrapolation technique (IVIVE).

PBPK model can be used for studying the toxicokinetic of PFAS in human brain. Several whole-body PBPK model for rat (Chou and Lin 2019; Loccisano et al. 2012), monkey (Loccisano et al. 2011) and human (Deepika et al. 2021; Fàbrega et al. 2014; Loccisano et al. 2013) has been published for both PFOS and PFOA. But till today, no brain-specific PBPK model for these chemicals is available. The varied kinetic seen in polar bears and rat implicates that among

several compartment of human brain, the risk can be different. Brain-specific PBPK model has been developed mostly for drugs like morphine, oxycodone (Ball et al. 2012), opioids (German et al. 2019), paracetamol and phenytoin (Gaohua et al. 2016) and many other drugs (Verscheijden et al. 2019; Zakaria and Badhan 2018). Overtime, the brain-specific PBPK model has moved from two compartment (brain extravascular and vascular) to multi compartments in brain like hippocampus, cortex, spinal CSF, Cranial CSF and much more. The improvement in structure of these models has led to confidence and reduce variability in predictions. In case of environmental chemicals, these models are not common even for neurotoxicants.

The objective of this work was to develop a brain-specific PBPK model consisting of 4 compartments integrating physiology and biochemical properties for PFOS and PFOA to evaluate their neurotoxic potential. The in-vitro study was done using HCMEC/D3 cell lines to understand and compare the BBB permeation of these chemicals. Data from in-vitro data was integrated in the model through IVIVE. The model was evaluated in rat to improve the prediction power and then extrapolated to human. Also, partial validation was done for human brain PBPK and toxicokinetic inside human brain was observed to associate it with neuronal risk.

2. Methodology

2.1 Development and Evaluation of full-Body PBPK Model

Adult PBPK model was developed for rat taking the template from Deepika et al. consisting of seven compartments: gut, liver, brain, kidney, bone marrow, lung, fat and rest body (Fig 1) (Deepika et al. 2021). Physiological parameters like blood flow and tissue volume for rat was obtained from literature (Deepika et al. 2022) (Sharma et al. 2020). Some biochemical parameters were considered same for human and rat while other were optimized based on Markov Chain Monte Carlo (MCMC) sampling. Developed PBPK model was evaluated by rat kinetic data extracted from published paper for PFOS (Chang et al. 2012) and PFOA (Kudo et al. 2007; Perkins et al. 2004). Oral dosing was considered for the model. Model was built in MCSIM 6.2.0 with Rstudio.

2.2 Development of Brain Model and IVIVE

Brain model was connected to full body PBPK and subdivided in several compartments like IB, HC, FT, BT, and CSF. Several assumptions were considered while developing the brain PBPK Model:

1. IB and brain are separated by permeability barrier (BBB).
2. All the compartments have constant volume and are well-stirred with no rate limiting barrier between ECF and CSF.
3. Fraction unbound (fu) was considered similar for plasma, HC, FC, CSF and brain since the data for separate fu is not available in literature for PFOS and PFOA. Only fu can cross the permeability barrier.
4. Active transport from brain was defined by Cl_{in} and Cl_{out} which was fitted due to unavailability of data.
5. Apparent permeability (Papp) in-vitro data was used for scaling to brain bi-directional passive transport (PS) using eq.1.

6. Volume and blood flow of HC, FC, BT and CSF were taken from published data in literature (Zakaria and Badhan 2018).

The brain was modeled with perfusion limited compartment along with permeability clearance from BBB which was collected using in-vitro experiment. IVIVE (in-vitro to in-vivo extrapolation) approach was used to calculate the PS for in-vivo from apparent permeability coefficient (P_{app}). Correction for endothelial surface area and brain weight was done accordingly as per eq. 1. PS_{B_bb} refers to permeability for blood to brain, $Papp_{A-B}$ refers to apical to basolateral permeability calculated using human BBB cell lines for PFOS and PFOA, brain weight is 150 $cm^2*g*brain^{-1}$ (rats), 157 $cm^2*g*brain^{-1}$ (human). Similar equation can be applied for PS_{bb_B} (permeability from brain to blood) where $Papp_{A-B}$ is replaced by $Papp_{B-A}$.

$$PS_{B\_bb} = Papp_{A-B} * Brain\ weight * Surface\ area \qquad \text{eq. 1}$$

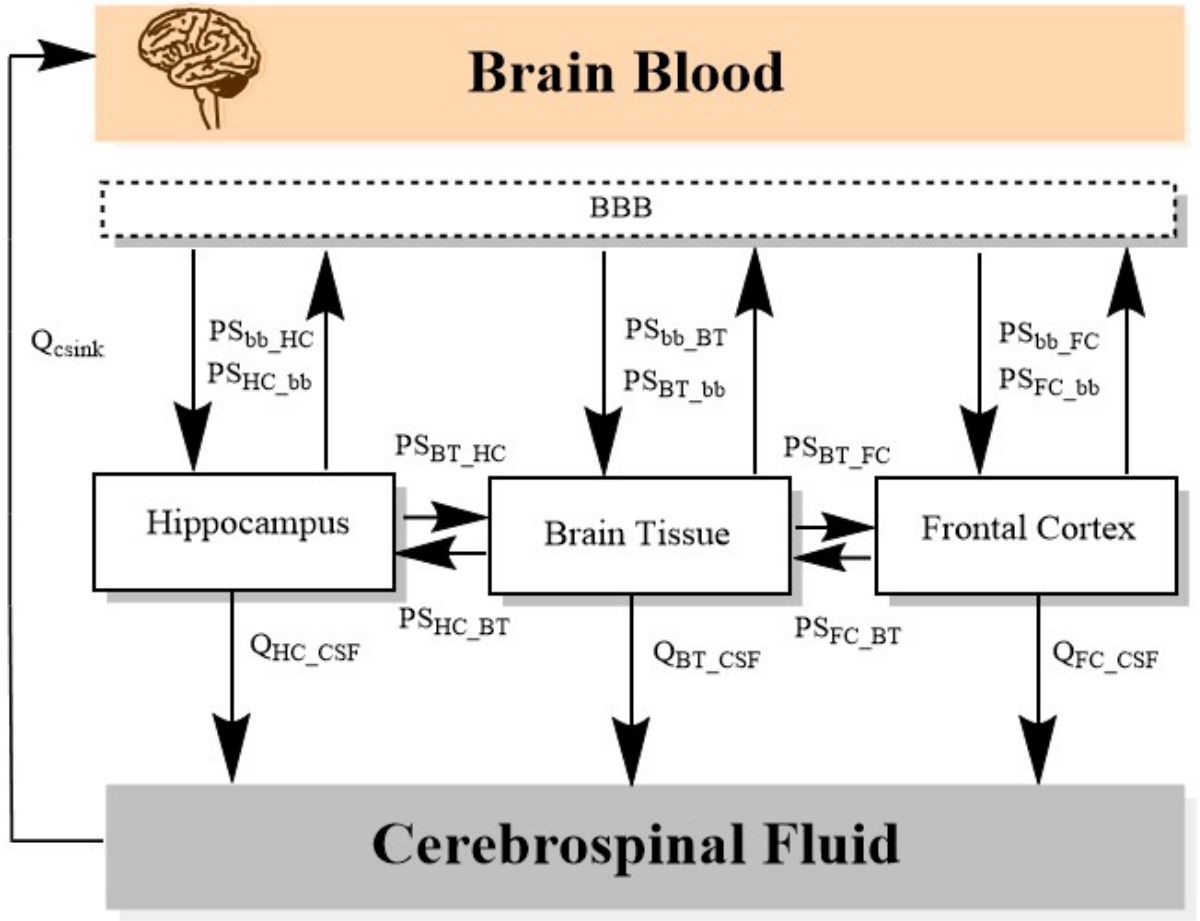

Figure 2: Brain-specific PBPK model

2.3 Evaluation of Brain PBPK Model

Study by Liu et al. evaluated the effect of sub-chronic PFOS exposure on rats at dose of 1.7, 5.0 and 15 mg/L in drinking water for 91 days (Liu et al. 2010). Adult male rats were around 140-180 g in weight and cortex and hippocampus concentration was measured at last day. Mean concentration in cortex were 0.56, 3.25 and 17.21 µg/g with dose of 1.7, 5.0 and 15 mg/L. Another study by Austin et al. exposed the adult female rats to 0,1 and 10 mg/Kg BW

for 2 weeks. At the end, PFOS concentration in hippocampus, cortex and rest of the brain were calculated at both the doses (Austin et al. 2003).

2.4 Development and evaluation of Human PBPK Model

Rat brain PBPK model was further extended to human for predicting brain pharmacokinetics. For this, human physiological parameters were used (Table 1) and biochemical parameters were kept same as rat (Table 2). However, some biochemical parameters were scaled which has been shown in Table 2. In human, brain data is only available for the brain tissue and CSF which was used to evaluate the model predictability.

PFAS penetration in CSF and plasma was studied in 233 samples using UPLC/MS/MS (Wang et al. 2018). Study was conducted in China and additionally for all the patients, albumin ratio ($Albumin_{csf}/Albumin_{serum}$) was also calculated to understand BBB disruption. Mean Data along with percentile and SD was available which was used for evaluation of the model. Another dataset from other laboratory with 7 pairs of serum and CSF with 6 males and 1 female was also considered for the model (Harada et al. 2007). Individual serum and CSF ratio were available and in general, it was observed that PFOA detected in CSF was less than PFOS. A recent study conducted for PFAS measurement in several brain regions in 5 male subjects calculated the concentration in serum as well as brain but for PFOS it was below LOD (Di Nisio et al. 2022).

Table 1: Physiological parameters for rat and human

Parameters	Rat	Human
BW (Kg)	0.20-0.30	65-75
Organ volume as a fraction of total body weight (Kg)		
Fliver	0.036	0.026
Fbrain	0.006	0.021
Flung	0.006	0.014
Fkidney	0.0073	0.004
Ffat	0.07	0.187
Fgut	0.027	0.016
Fskin	0.1903	0.0371
Fbm	0.0007	0.05
Fplasma	0.074	0.0428
Fhipp	0.062	0.062
Ffc	0.15	0.15
Frb	1.148	1.148
Fcsf	0.166	0.166
Fraction of blood flow to organ (fraction of cardiac output)		
QCC (L/hr/kg)	18.7	16
HCT	0.46	0.46
FQliver	0.174	0.257
FQlung	0.021	0.034
FQkidney	0.141	0.177
FQfat	0.07	0.052
FQgut	0.075	0.181

FQskin	0.058	0.058
FQbm	0.08	0.1
FQbrain	0.02	0.117
FQhipp_csf	1.2e-6	1.2e-6
FQcortex_csf	3e-6	3e-6
FQrb_csf	1.2e-6	1.2e-6

Table 2: Biochemical parameters for rat and human.

Parameter	Rat	Human
Molecular Weight (g/mol)	500.13	500.13
K_liver_plasma	2.67	2.67
K_gut_plasma	0.05	0.05
K_ kidney_plasma	1.26	1.26
K_ lung_plasma	9.08	9.08
K_ fat_plasma	0.33	0.33
K_ skin_plasma	0.12	0.12
K_ bm_plasma	18.73	18.73
K_ restbody_plasma	0.125	0.125
Tmc	220	6
kt	0.5	0.5
fu	0.022	0.025
kurineC	0.001	6

2.5 Uncertainty and Sensitivity Analysis

Since the parameters like CSF can vary extensively among human and rats. In the monte carlo simulation CV of 20% was applied for brain related parameters and for other biochemical parameters LN 1.1 was used to incorporate uncertainty with atleast 10000 runs per compound. This was done for both rat and human simulations. Sensitivity analysis was conducted to find the sensitive parameter affecting the AUC of the plasma and AUC of brain shown by eq. 2. The parameters were varied by 1 percent for calculating normalized sensitivity coefficient (SC).

$$SC = \frac{dC/C}{dP/P} \qquad \text{eq.2}$$

2.6 In-vitro data for brain PBPK Model

Material and Cell culture

HCMEC/D3 cells were used from passage 27 to 34 as instructed by the manufacturer and cultured using EGM medium (2% v/v) supplemented with endothelial cell growth supplement (0.004 ml/l), fetal calf serum (0.02 ml/l), basic fibroblast growth factor (1 ng/ml), epidermal growth factor (0.1 ng/ml), hydrocortisone (1 µg/ml) and heparin (90 µg). T75 flask was used

for culturing the cells up to 80-90% confluency. Dissociation buffer (Trypsin-EDTA) was used and cells were resuspended in EGM before sub-culturing at the density of 3-5*10^4 cells/cm2.

Viability Study

Cells were cultured in 48 well plate before exposing to the respective concentration of PFOS (25, 50, 75, 100, 200, and 400 µM) and PFOA (12.5, 25, 50, 100 and 200 µM) for 24 hours. MTT (5 mg/ml) was added to the well after 24 hours and kept for 4 hours in incubator for the formation of formazan crystal. DMSO was added to dissolve the formazan and then absorbance was measured using UV-Vis spectrophotometer at 560 nm. Cell viability was calculated using eq. 3.

$$Cell\ Viability = \frac{Abs_{sample}}{Abs_{control}} * 100 \qquad \text{eq.3}$$

TEER and bidirectional permeability Assay

Transwell inserts were used for carrying out bidirectional permeability assay (6-well inserts, 0.4 µm pores PET). Cells were cultured in apical compartment with approx. 1.5 ml medium in apical and 2.5 ml medium in basolateral compartment. TEER was measured after every 2-3 days using an Endohm meter followed by change of media. On experiment day, TEER was measured once again and EGM medium was decanted completely followed by washing 2-3 times with PBS. EGM medium was replaced with HBSS (hank´s balanced salt solution) followed by HEPES also called as transport buffer. Transport buffer along with chemical concentration was added to the Transwell along with control (DMSO 0.1%). At 30, 60, 120, 240 and 300 min, samples were taken from the basolateral compartment in case of A-B and apical compartment for B-A experiment. The concentration was adjusted by replacing it with transport buffer. At the end of experiment TEER was measured again to check the integrity. TEER can be calculated by the equation 4 where R refers to resistance which is resistance cell subtracted by resistance blank and EMA for effective membrane area.

$$Unit\ area\ resistance_{cell\ monolayer} = R * EMA\ (cm^2) \qquad \text{eq. 4}$$

All samples were analysed by LC-MS technique which has been mentioned in supplementary file. Apparent permeability (Papp) was calculated with the equation 5 where VD is volume of basolateral compartment for A-B or apical compartment for B-A, A: surface area of the insert, Ca0 is initial concentration in apical chamber for A-B transport, or basolateral chamber for B-A transport, ΔCb/Δt is slope for change in concentration with time. Efflux ratio was also calculated which is $Papp_{BA}$ divided by $Papp_{AB}$.

$$Papp = \frac{V_D}{A*C_{a0}} * \frac{\Delta C_b}{\Delta t} \qquad \text{eq. 5}$$

Genetic Expression by RT-PCR

RNA extraction and cDNA synthesis were done using the protocol described in previous article published by Deepika et al. (2022) and also, same has been mentioned in supplementary file. Quantitative RT-PCR was conducted for checking the genetic expression of several tight and adherens junction genes (Occludin: OCLN, Zona occludens: ZO1, claudin 5: CLDN5, claudin 1: CLDN1, and vascular endothelial cadherin: CDH5). Information related to primer and kit has

been provided in supplementary file. qPCR was performed using Rotor-gene Q Real-time PCR cycler. House-keeping gene (GAPDH) was used for normalized expression. The relative expression of target gene was calculated with the $2^{-\Delta\Delta Ct}$ method and compared with the control.

3. Results

3.1 Evaluation with Rat data

Results from simulations were compared with the observed data obtained from rat. The simulated plasma, liver concentration and urine were within two-fold of the experimental data (Fig 3). Concentration in liver was higher compared to plasma and after 15 days drop in the concentration was observed. Percent dose eliminated in urine was very low even after 80 days of single exposure at 15 mg/kg BW. Similar trend was observed for PFOA (plots in supplementary file).

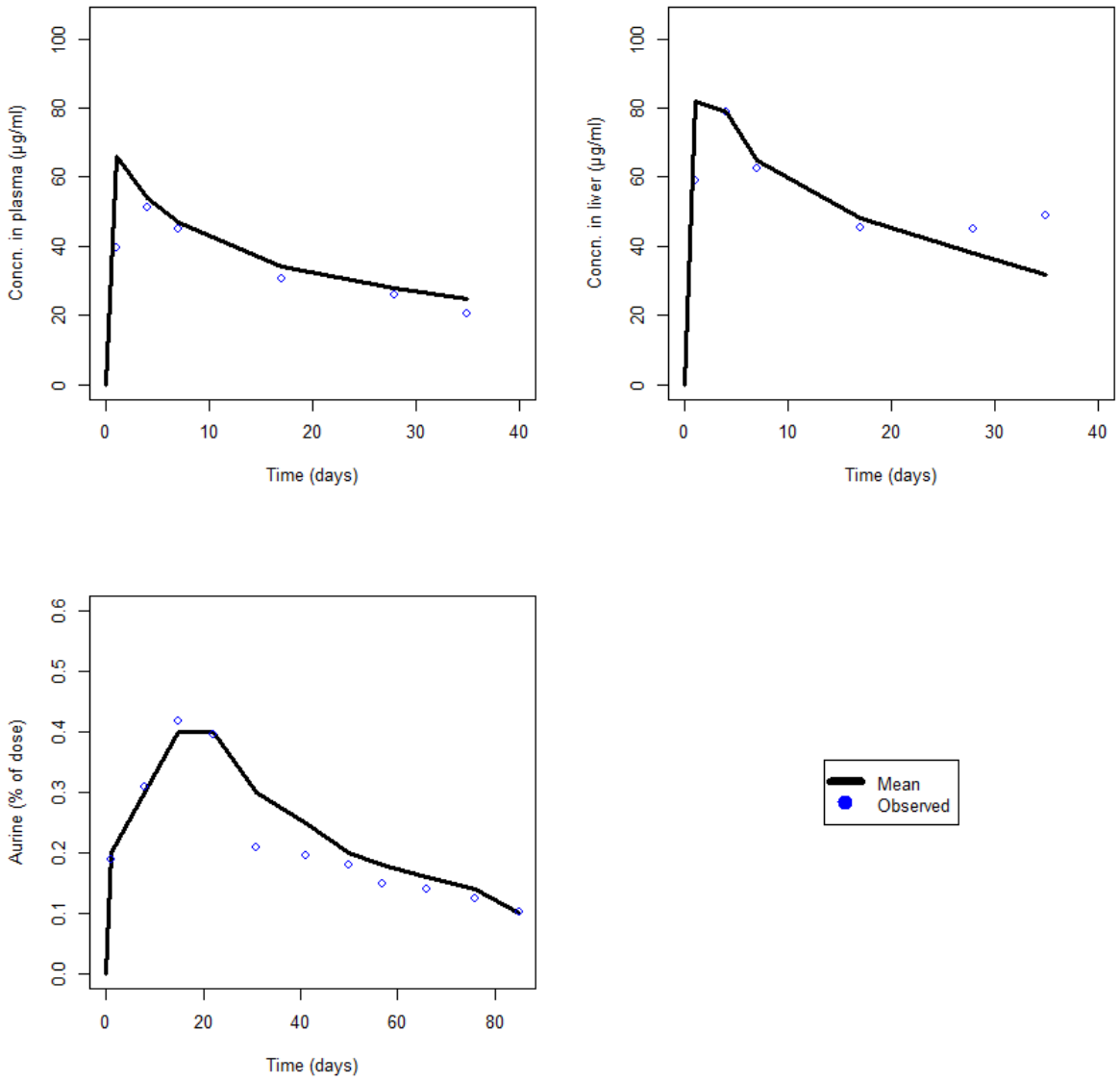

Figure 4: Observed and simulated concentration for plasma, liver and urine in rat for PFOS.

3.2 Evaluation with human data

Normal exposure concentration was used for human PFOS and PFOA. It was found that concentration in plasma and brain reached steady state after 3-5 years of exposure in both chemicals (Fig 4 and 5). Hippocampus and Cortex concentration showed a slow and steady increase being affected by influx and efflux of the chemical. PFOA showed lower disposition in both sub-compartments compared to PFOS pointing towards PFOS being high permeable and hence possess the risk for neuronal damage.

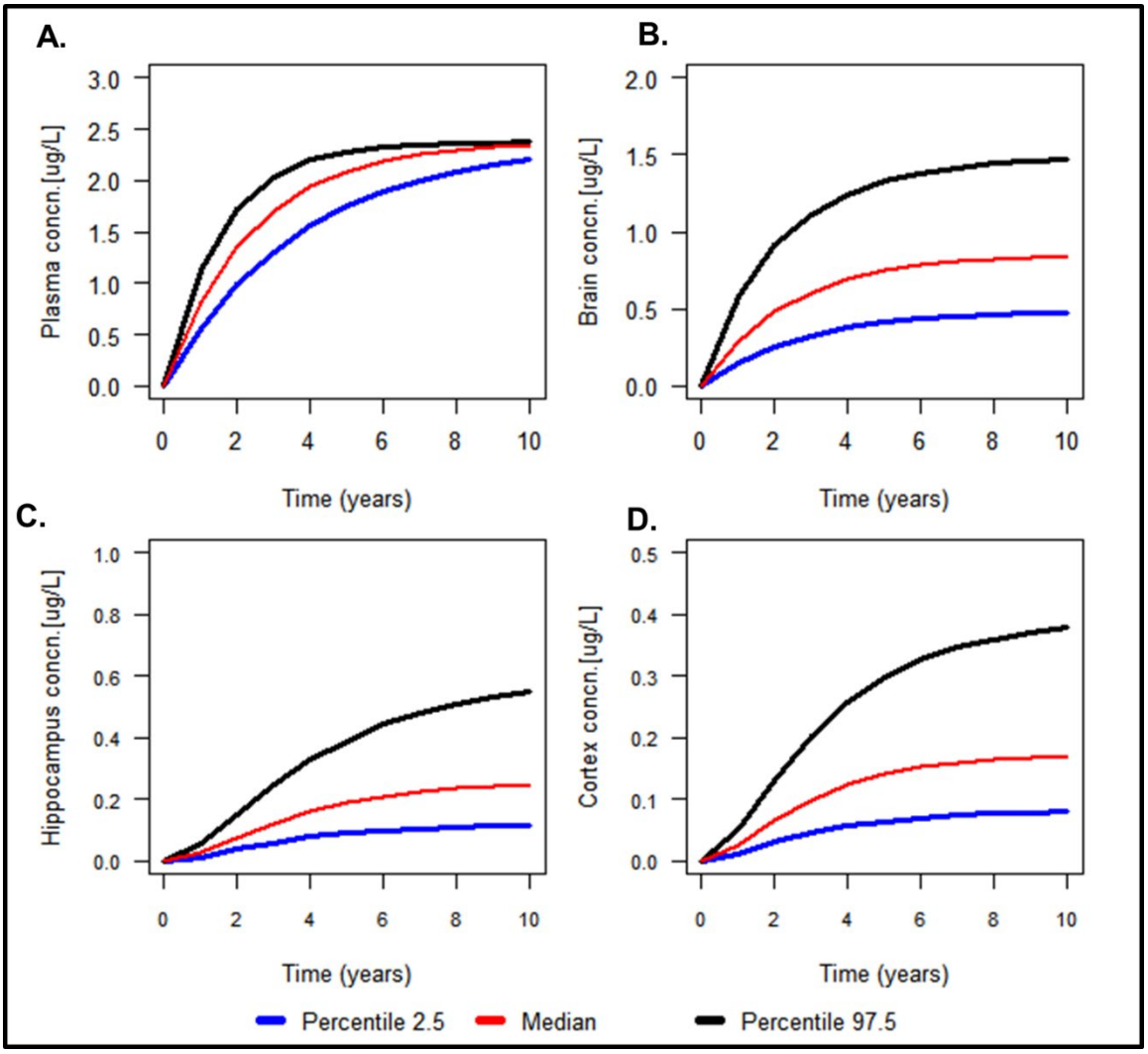

Figure 4: PFOS levels in plasma, brain, hippocampus and cortex after BPA exposure at 3.4 ng/Kg BW/day.

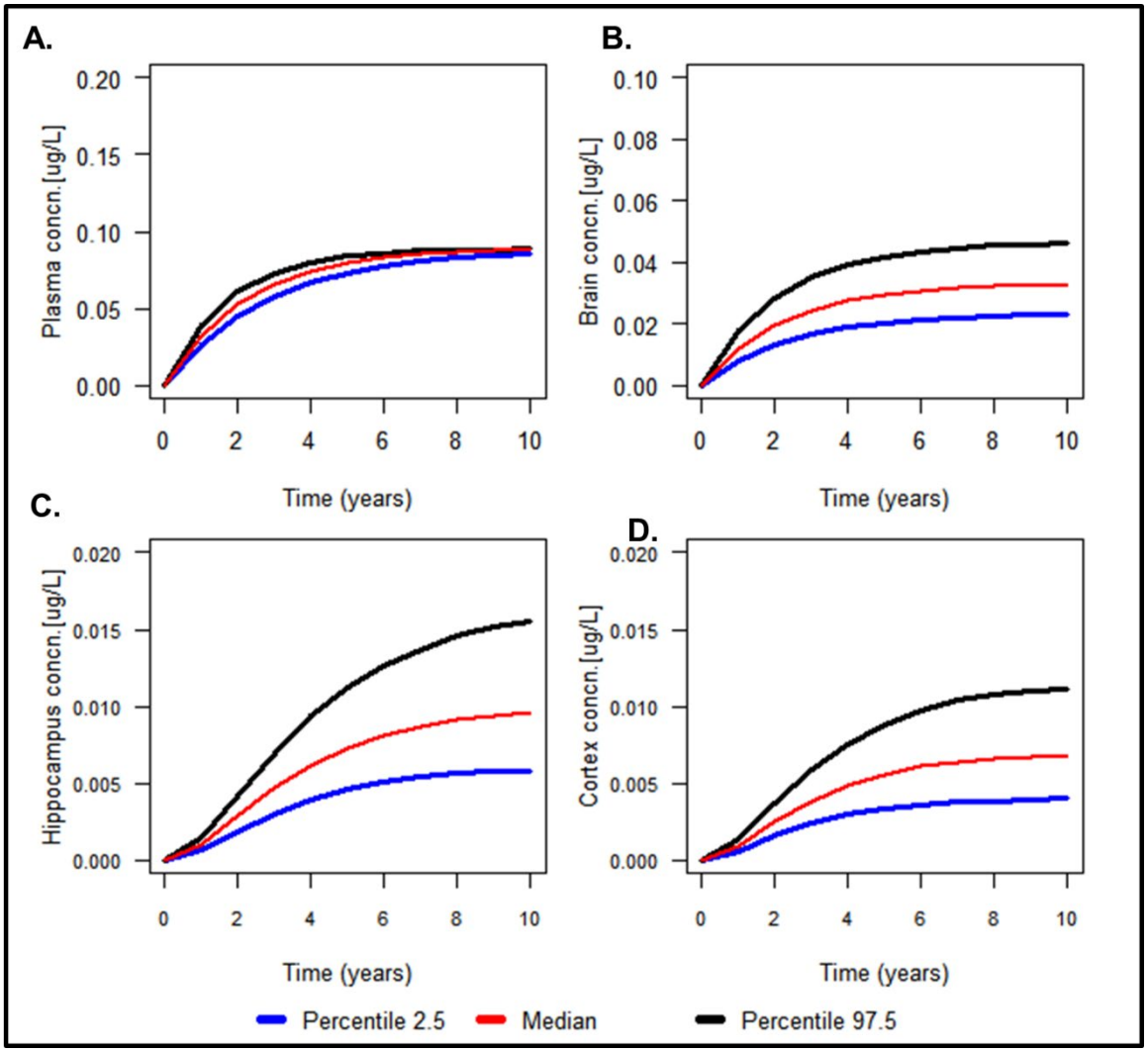

Figure 5: PFOA concentration in plasma, brain, hippocampus and cortex with normal exposure scenario (0.14 ng/kg BW/day)

3.3 Sensitivity Analysis

Liver partitioning (K_liver_plasma) was found to be the most sensitive parameter followed by restbody (K_restbody_plasma) and lung partitioning (K_lung_plasma) (Fig 6). Increase in liver_plasma would lead to decrease in the cplasma. Parameter which has positive influence are Body weight (BW), influx ($Papp_{A-B}$) and efflux ($Papp_{B-A}$) for the brain. Tmc and kt do not have major influence on the plasma. This analysis provided an overall picture about the parameters which needs to be changed for better fitting of the experimental data.

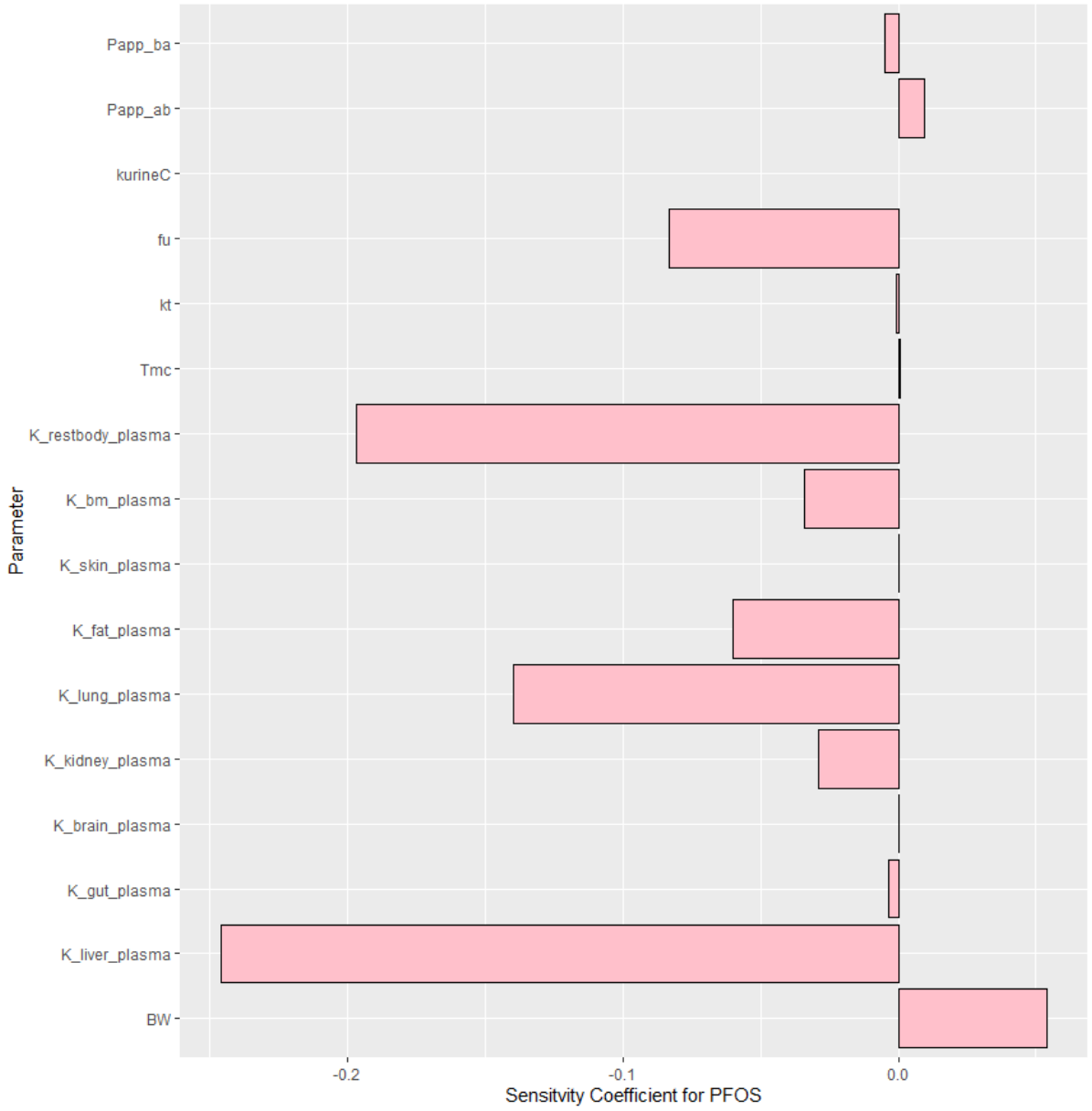

Figure 6: Sensitivity coefficient for PFOS

In-vitro results

3.4 Cell growth and Cell Viability Study

Cell viability decreased significantly from 25 to 200 µM for PFOA. At 100 µM, cell viability was around 78.5% followed by 66.8% at 200 µM (Fig 7). In case of PFOS, there was no change in viability till 50 µM. At 75 µM, viability decreased to 70.7% and then at 200 and 400 µM, viability was very low (24.5% 23.7%) (Fig 7).

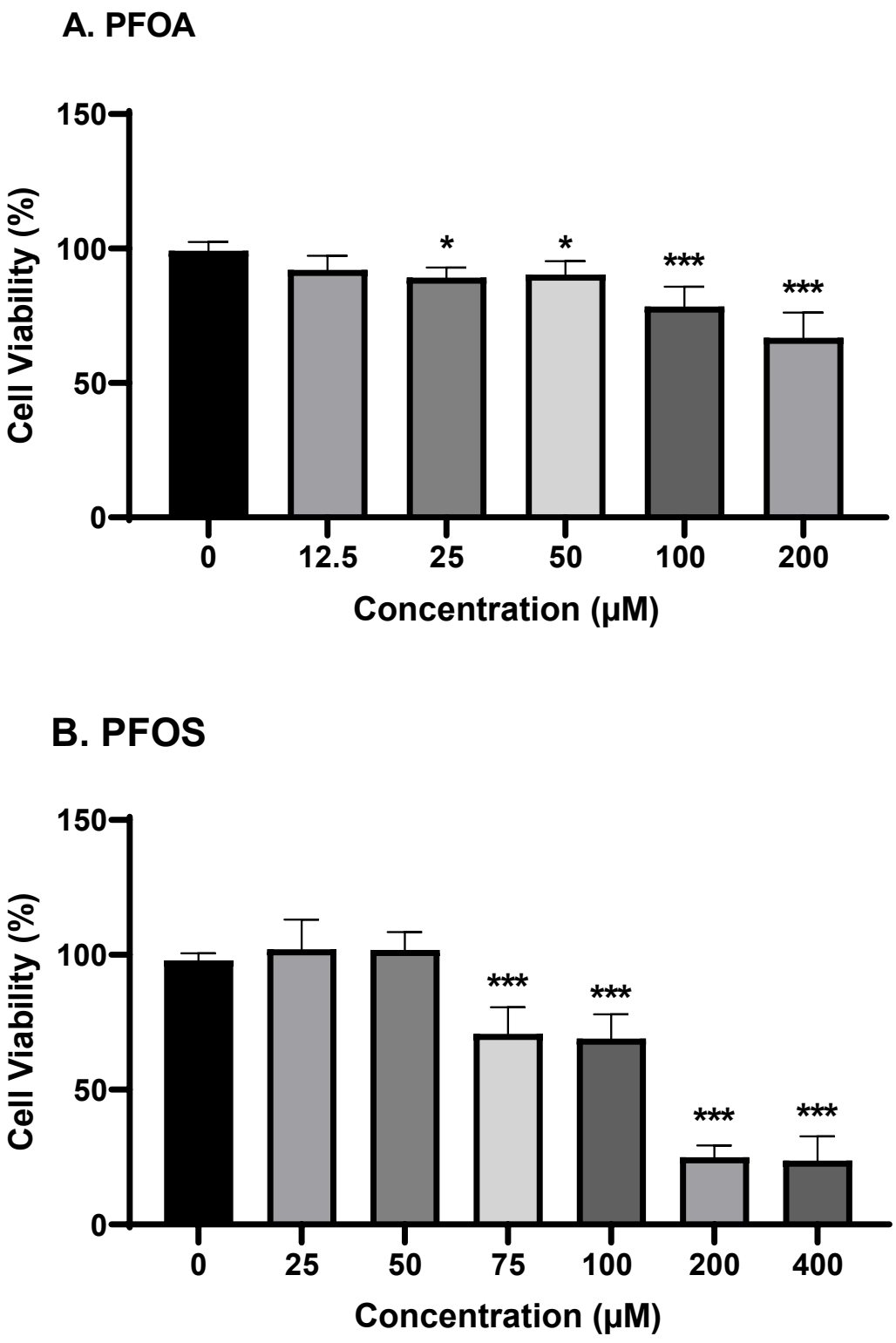

Figure 7: Cell Viability for PFOS and PFOA at several concentration. For PFOS, concentration from 25 µM to 400 µM and for PFOA from 12.5 to 200 µM were tested. The viability decreased drastically from 100 µM and reached approximately 20% at 200 and 400 µM for PFOS. For PFOA, at 200 µM the viability was approx. 60%. Data is presented as mean ± SD of at least three independent batches. One-way ANOVA was conducted for comparing differences

relative to control followed by Dunnett test. * represent p value between 0.01 and 0.05, ** represent p value between 0.01 and 0.001 and *** p value<0.001.

3.5 Integrity and Bidirectional Permeability

Before starting the experiment for permeability, TEER value was checked every 2-3 days for ensuring integrity. After 6 days of incubation, there was no further change in the TEER, and it was found to be 46.5 Ω*cm^2 (Fig 8).

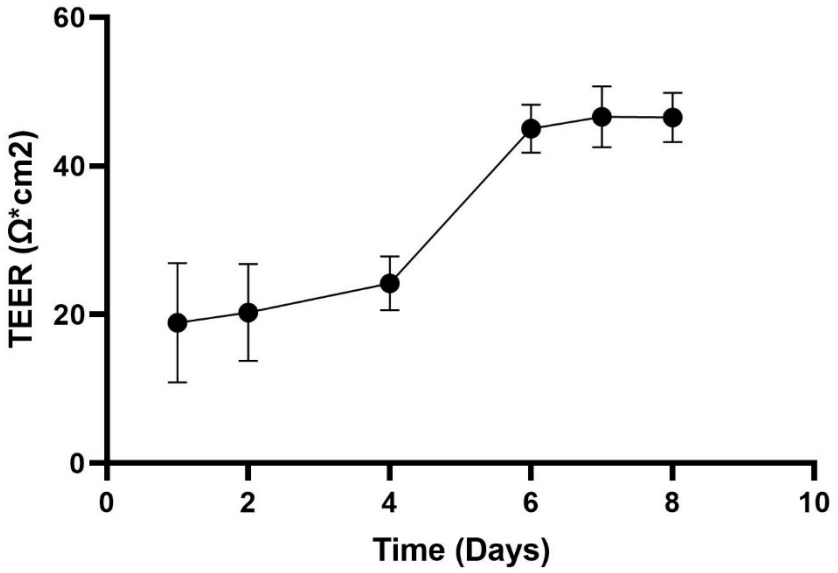

Figure 8: TEER Values for HCEMEC/D3 Cells. Data is presented as mean ± SD of at least three independent batches.

The cells were exposed at (25 and 50 µM) based on the results from cell viability. Cumulative amount permeated per cm^2 and Papp value increased slightly with increase in concentration for both PFOS and PFOA, but the change was minimal. PFOS has higher Papp $_{A-B}$ value than PFOA at the similar concentration point towards higher permeation capabilities. Both PFOS and PFOA showed the efflux ratio less than 2 but PFOA has comparatively higher efflux than PFOS (Fig 9).

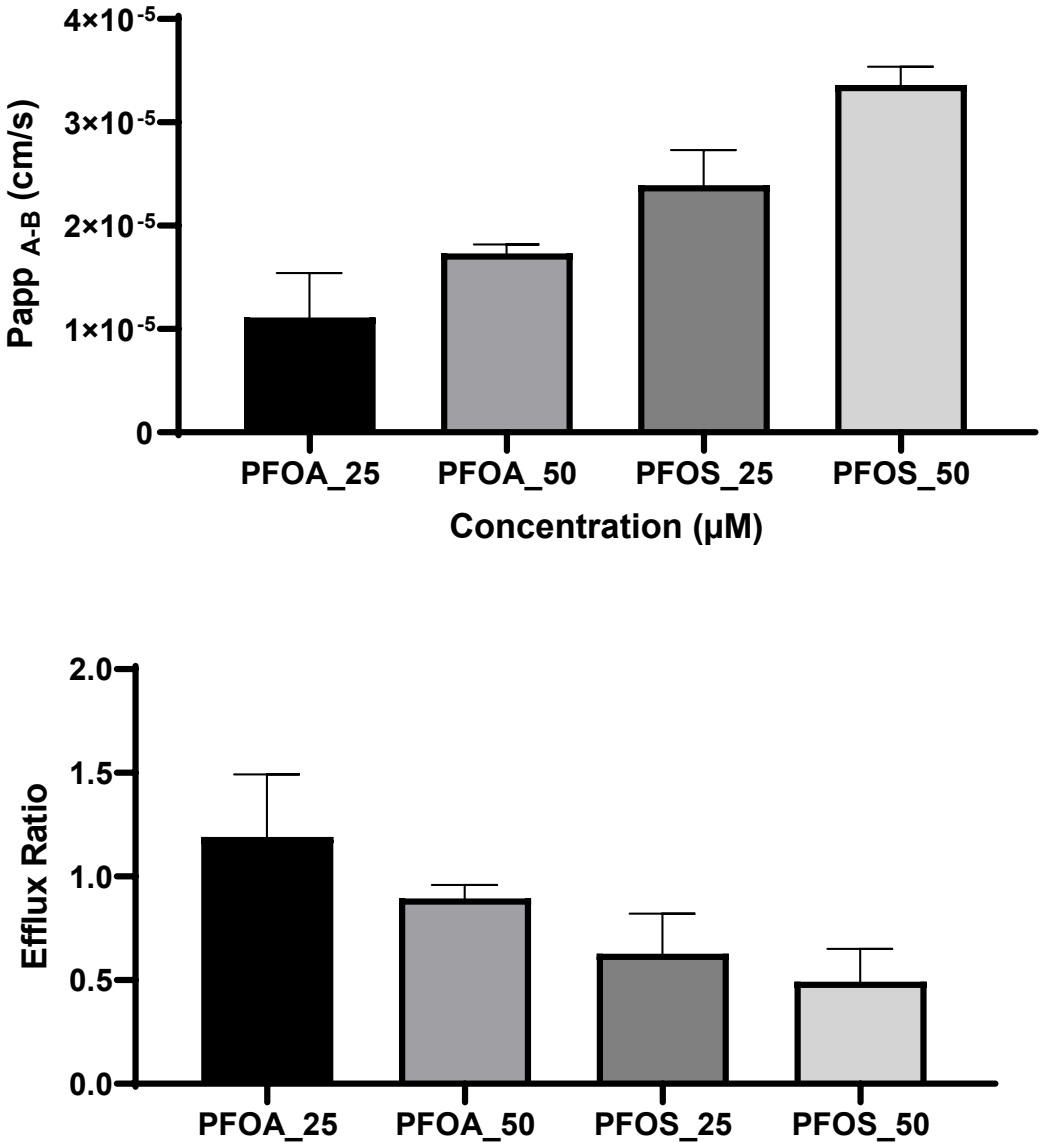

Figure 9: Bidirectional permeability and efflux ratio for both PFOS and PFOA. A represents the Papp $_{A-B}$ and Papp $_{B-A}$ with both being highly permeable. Data is presented as mean ± SD of at least three independent batches.

3.6 Gene Expression

Genetic expression was done to measure the tight and adherens junction after exposure to PFOA and PFOS. In case of PFOS, CLDN5 was down expressed whereas other genes did not show any significant alteration from control (0.1% DMSO) (Fig 10). CLDN1 was down expressed for PFOA at both the concentration (25 and 50 µM) (Fig 11).

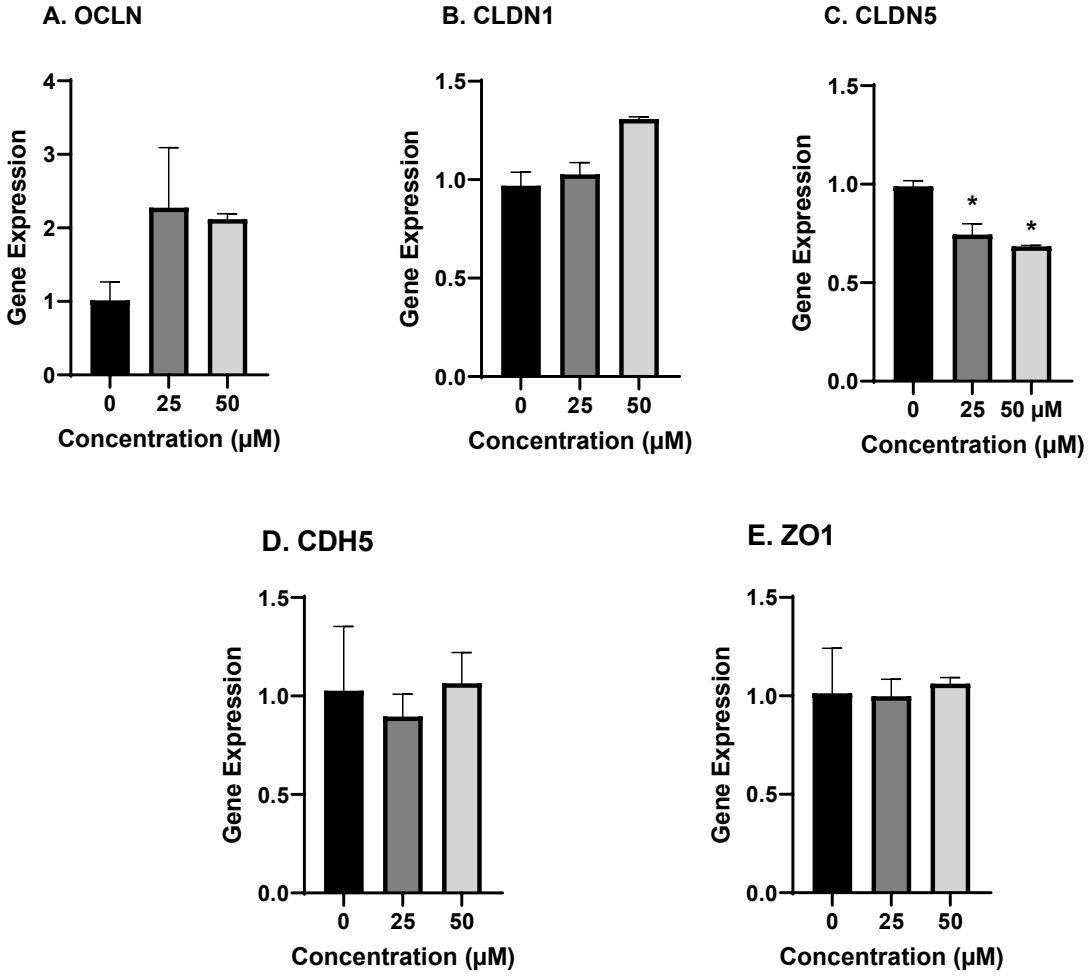

Figure 10: Genetic expression for PFOS at 25 and 50 µM. Data is presented as mean ± SD of at least three independent batches. One-way ANOVA was conducted for comparing differences relative to control followed by Dunnett test. * represent p value between 0.01 and 0.05, ** represent p value between 0.01 and 0.001 and *** represents p value<0.001.

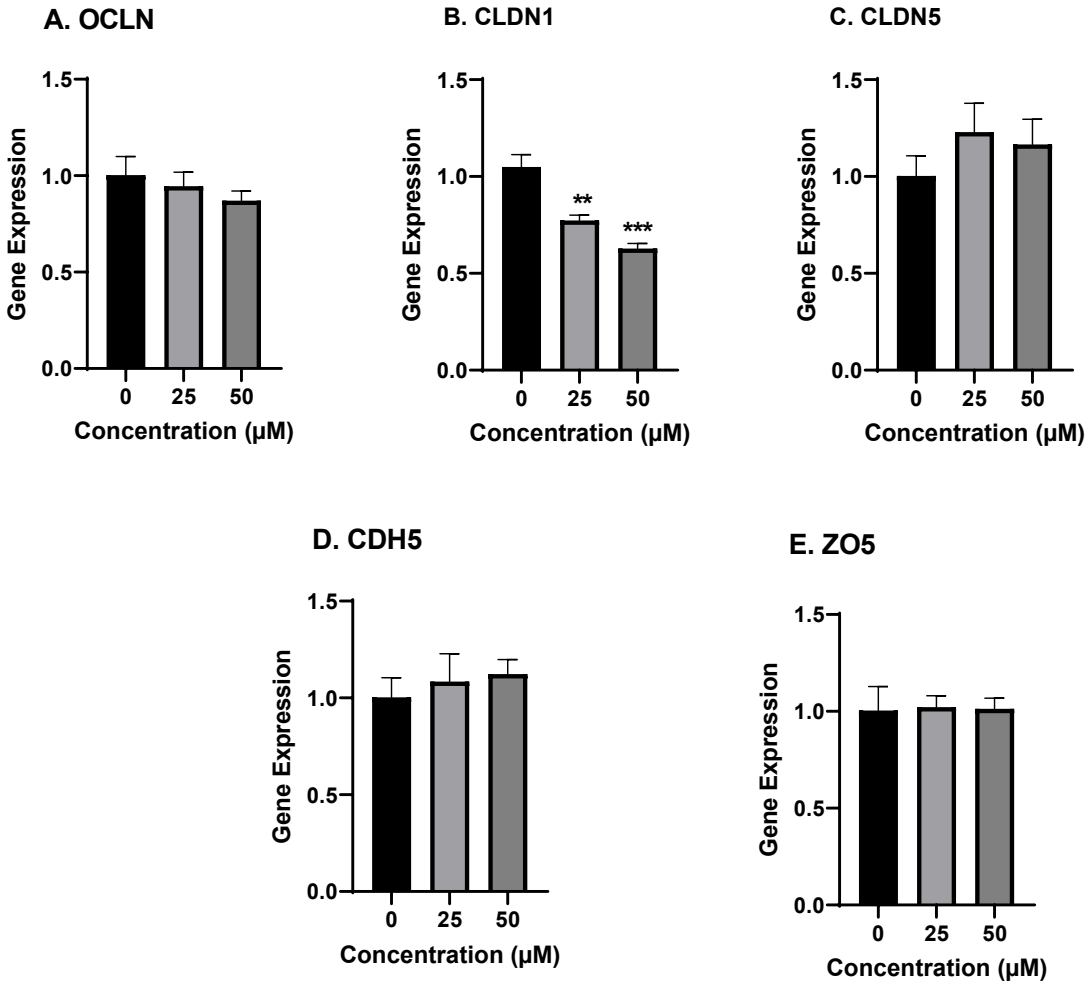

Figure 11: Genetic expression for PFOA at 25 and 50 μM. Data is presented as mean ± SD of at least three independent batches. One-way ANOVA was conducted for comparing differences relative to control followed by Dunnett test. * represent p value between 0.01 and 0.05, ** represent p value between 0.01 and 0.001 and *** represents p value<0.001.

4. Discussion and Conclusion

Brain is the most complex organ in the human body with the present of BBB (tight and adherens junction) limiting the entry of xenobiotics inside the brain. Due to ethical concern, it is not possible to quantify the concentration of chemical deposited in several parts of brain. Hence, there is a need to develop mechanistic and reliable brain PBPK model for predicting tissue kinetics. PFAS chemicals are found to be neurotoxic in several species (Foguth et al. 2019; Shi and Zhou 2010) and in-vitro studies, so it is imperative to understand their accumulation in brain (Piekarski et al. 2020) through developing brain-specific PBPK Model.

The developed PBPK model included the anatomy and physiology of the rat and human brain. Several biochemical parameters were considered similar for both organism while extrapolating based on respective bodyweight. The brain was divided in only four compartments due to availability of data, it is possible to divide them into further brain sub compartment but in such cases, parameterizing the model will be a difficult task. The in-vitro

study was conducted to calculate BBB permeation potential both influx and efflux of chemical for human. Also, gene expression showed that CLDN5 was down expressed for PFOS and CLDN1 for PFOA, but further studies are required to explore the mechanism responsible for permeation. Both were found to be highly permeable which means that they both can be neurotoxic. Study by Hoffman et al. showed both PFOS and PFOA exposure is positively correlated with attention-deficit-hyperactive-disorder (ADHD) in children (Hoffman et al. 2010). The in-vitro study showed absence of efflux transport, considering this efflux was not modeled in PBPK. The result from $Papp_{A-B}$ and $Papp_{B-A}$ was integrated in brain PBPK for both chemicals showing that chemical-related parameters can be generated using in-vitro model. Such approach also focus on one of the main application of 3Rs reducing the usage of animals for research (Strech and Dirnagl 2019).

For building this model, we used both bottom-up and top-down approach integrating in-vitro and experimental data for improving the model performance. Sensitivity analysis showed the parameters which need to be adjusted for improving the model prediction. In rat brain, cortex concentration was found to be highest compared to the other parts pointing towards the frontal cortex related toxicity. In human brain, concentration present in hippocampus was quite high suggesting that higher exposure to PFAS chemical may affect the learning and memory. PFOS and PFOA exposure was found to affect the four proteins in hippocampus (CaMKII, GAP-43, synaptophysin and tau) on PND10 (Johansson et al. 2009). These proteins are required for synaptogenesis and normal brain development.

This was the first attempt to building brain-specific PBPK mode for PFOS and PFOA. We were able to successfully predict the brain concentration in rat and human. But this model could be improved further by incorporating separate fu for brain sub-compartment. The differences in lipid/water content can contribute to variation in fu levels and also the variation in these content in white and grey matter has been reported in literature (Löhmann et al. 2010; O'Brien and Sampson 1965a, 1965b). Further in-vitro setup can be improved by adding albumin during the permeability experiment. In future, the result from brain toxicokinetic for two chemicals can be integrated in pharmacodynamic or systems biology model to predict neuronal damage/neuronal disorders. Such kind of model provide a successful framework for modeling from exposure to the cellular toxicity using mechanistic approach and improve the understanding of living cells.

Acknowledgments
This study was financially supported by Marie Skłodowska-Curie "Neurosome project" under grant agreement no. 766251. This publication reflects only the author views. The community and other funding organizations are not liable for any use made of the information contained.

References

Austin ME, Kasturi BS, Barber M, Kannan K, MohanKumar PS, MohanKumar SMJ. 2003. Neuroendocrine effects of perfluorooctane sulfonate in rats. Environ Health Perspect 111:1485–1489; doi:10.1289/ehp.6128.

Ball K, Bouzom F, Scherrmann J-M, Walther B, Declèves X. 2012. Development of a Physiologically Based Pharmacokinetic Model for the Rat Central Nervous System and Determination of an In Vitro–In Vivo Scaling Methodology for the Blood–Brain Barrier Permeability of Two Transporter Substrates, Morphine and Oxycodone. J Pharm Sci 101:4277–4292; doi:10.1002/jps.23266.

Buck RC, Franklin J, Berger U, Conder JM, Cousins IT, de Voogt P, et al. 2011. Perfluoroalkyl and polyfluoroalkyl substances in the environment: Terminology, classification, and origins. Integr Environ Assess Manag 7:513–541; doi:10.1002/ieam.258.

Cao Y, Ng C. 2021. Absorption, distribution, and toxicity of per- and polyfluoroalkyl substances (PFAS) in the brain: a review. Environ Sci Process Impacts 23:1623–1640; doi:10.1039/D1EM00228G.

Chang SC, Noker PE, Gorman GS, Gibson SJ, Hart JA, Ehresman DJ, et al. 2012. Comparative pharmacokinetics of perfluorooctanesulfonate (PFOS) in rats, mice, and monkeys. Reprod Toxicol 33:428–440; doi:10.1016/j.reprotox.2011.07.002.

Chou W-C, Lin Z. 2019. Bayesian evaluation of a physiologically based pharmacokinetic (PBPK) model for perfluorooctane sulfonate (PFOS) to characterize the interspecies uncertainty between mice, rats, monkeys, and humans: Development and performance verification. Environ Int 129:408–422; doi:10.1016/j.envint.2019.03.058.

Cui L, Zhou Q, Liao C, Fu J, Jiang G. 2008. Studies on the Toxicological Effects of PFOA and PFOS on Rats Using Histological Observation and Chemical Analysis. Arch Environ Contam Toxicol 56:338; doi:10.1007/s00244-008-9194-6.

Deepika D, Sharma RP, Schuhmacher M, Kumar V. 2021. Risk Assessment of Perfluorooctane Sulfonate (PFOS) using Dynamic Age Dependent Physiologically based Pharmacokinetic Model (PBPK) across Human Lifetime. Environ Res 199:111287; doi:10.1016/j.envres.2021.111287.

Di Nisio A, Pannella M, Vogiatzis S, Sut S, Dall'Acqua S, Rocca MS, et al. 2022. Impairment of human dopaminergic neurons at different developmental stages by perfluoro-octanoic acid (PFOA) and differential human brain areas accumulation of perfluoroalkyl chemicals. Environ Int 158:106982; doi:10.1016/j.envint.2021.106982.

Fàbrega F, Kumar V, Schuhmacher M, Domingo JL, Nadal M. 2014. PBPK modeling for PFOS and PFOA: Validation with human experimental data. Toxicol Lett 230:244–251; doi:10.1016/j.toxlet.2014.01.007.

Fenton SE, Ducatman A, Boobis A, DeWitt JC, Lau C, Ng C, et al. 2021. Per- and Polyfluoroalkyl Substance Toxicity and Human Health Review: Current State of Knowledge and Strategies for Informing Future Research. Environ Toxicol Chem 40:606–630; doi:10.1002/etc.4890.

Fiedler S, Pfister G, Schramm K-W. 2010. Poly- and perfluorinated compounds in household consumer products. Toxicol Environ Chem 92:1801–1811; doi:10.1080/02772248.2010.491482.

Foguth RM, Flynn RW, de Perre C, Iacchetta M, Lee LS, Sepúlveda MS, et al. 2019. Developmental exposure to perfluorooctane sulfonate (PFOS) and perfluorooctanoic acid (PFOA) selectively decreases brain dopamine levels in Northern leopard frogs. Toxicol Appl Pharmacol 377:114623; doi:10.1016/j.taap.2019.114623.

Gaohua L, Neuhoff S, Johnson TN, Rostami-Hodjegan A, Jamei M. 2016. Development of a

permeability-limited model of the human brain and cerebrospinal fluid (CSF) to integrate known physiological and biological knowledge: Estimating time varying CSF drug concentrations and their variability using in vitro data. Drug Metab Pharmacokinet 31:224–233; doi:10.1016/j.dmpk.2016.03.005.

German C, Pilvankar M, Przekwas A. 2019. Computational framework for predictive PBPK-PD-Tox simulations of opioids and antidotes. J Pharmacokinet Pharmacodyn 46:513–529; doi:10.1007/s10928-019-09648-1.

Glüge J, Scheringer M, Cousins IT, DeWitt JC, Goldenman G, Herzke D, et al. 2020. An overview of the uses of per- and polyfluoroalkyl substances (PFAS). Environ Sci Process Impacts 22:2345–2373; doi:10.1039/D0EM00291G.

Greaves AK, Letcher RJ, Sonne C, Dietz R. 2013. Brain region distribution and patterns of bioaccumulative perfluoroalkyl carboxylates and sulfonates in east greenland polar bears (Ursus maritimus). Environ Toxicol Chem 32:713–722; doi:10.1002/etc.2107.

Harada KH, Hashida S, Kaneko T, Takenaka K, Minata M, Inoue K, et al. 2007. Biliary excretion and cerebrospinal fluid partition of perfluorooctanoate and perfluorooctane sulfonate in humans. Environ Toxicol Pharmacol 24:134–139; doi:10.1016/j.etap.2007.04.003.

Hoffman K, Webster TF, Weisskopf MG, Weinberg J, Vieira VM. 2010. Exposure to Polyfluoroalkyl Chemicals and Attention Deficit/Hyperactivity Disorder in U.S. Children 12–15 Years of Age. Environ Health Perspect 118:1762–1767; doi:10.1289/ehp.1001898.

Johansson N, Eriksson P, Viberg H. 2009. Neonatal Exposure to PFOS and PFOA in Mice Results in Changes in Proteins which are Important for Neuronal Growth and Synaptogenesis in the Developing Brain. Toxicol Sci 108:412–418; doi:10.1093/toxsci/kfp029.

Johansson N, Fredriksson A, Eriksson P. 2008. Neonatal exposure to perfluorooctane sulfonate (PFOS) and perfluorooctanoic acid (PFOA) causes neurobehavioural defects in adult mice. Neurotoxicology 29:160–169; doi:10.1016/j.neuro.2007.10.008.

Kudo N, Sakai A, Mitsumoto A, Hibino Y, Tsuda T, Kawashima Y. 2007. Tissue Distribution and Hepatic Subcellular Distribution of Perfluorooctanoic Acid at Low Dose Are Different from Those at High Dose in Rats. Biol Pharm Bull 30:1535–1540; doi:10.1248/bpb.30.1535.

Liu X, Liu W, Jin Y, Yu W, Liu L, Yu H. 2010. Effects of subchronic perfluorooctane sulfonate exposure of rats on calcium-dependent signaling molecules in the brain tissue. Arch Toxicol 84:471–479; doi:10.1007/s00204-010-0517-9.

Loccisano AE, Campbell JL, Andersen ME, Clewell HJ. 2011. Evaluation and prediction of pharmacokinetics of PFOA and PFOS in the monkey and human using a PBPK model. Regul Toxicol Pharmacol 59:157–175; doi:10.1016/j.yrtph.2010.12.004.

Loccisano AE, Campbell JL, Butenhoff JL, Andersen ME, Clewell HJ. 2012. Comparison and evaluation of pharmacokinetics of PFOA and PFOS in the adult rat using a physiologically based pharmacokinetic model. Reprod Toxicol 33:452–467; doi:10.1016/j.reprotox.2011.04.006.

Loccisano AE, Longnecker MP, Campbell JL, Andersen ME, Clewell HJ. 2013. Development of Pbpk Models for Pfoa and Pfos for Human Pregnancy and Lactation Life Stages. J Toxicol Environ Heal Part A 76:25–57; doi:10.1080/15287394.2012.722523.

Löhmann C, Schachmann E, Dandekar T, Villmann C, Becker C-M. 2010. Developmental profiling by mass spectrometry of phosphocholine containing phospholipids in the rat nervous system reveals temporo-spatial gradients. J Neurochem 114:no-no; doi:10.1111/j.1471-4159.2010.06836.x.

O'Brien JS, Sampson EL. 1965a. Fatty acid and fatty aldehyde composition of the major brain lipids in normal human gray matter, white matter, and myelin. J Lipid Res 6:545–551; doi:10.1016/S0022-2275(20)39620-6.

O'Brien JS, Sampson EL. 1965b. Lipid composition of the normal human brain: gray matter, white matter, and myelin. J Lipid Res 6:537–544; doi:10.1016/S0022-2275(20)39619-X.

Perkins RG, Butenhoff JL, Kennedy GL, Palazzolo MJ. 2004. 13-Week Dietary Toxicity Study of Ammonium Perfluorooctanoate (APFO) in Male Rats. Drug Chem Toxicol 27:361–378; doi:10.1081/DCT-200039773.

Piekarski D, Diaz K, McNerney M. 2020. Perfluoroalkyl chemicals in neurological health and disease: Human concerns and animal models. Neurotoxicology 77:155–168; doi:10.1016/j.neuro.2020.01.001.

Sharma RP, Kumar V, Schuhmacher M, Kolodkin A, Westerhoff H V. 2020. Development and evaluation of a harmonized whole body physiologically based pharmacokinetic (PBPK) model for flutamide in rats and its extrapolation to humans. Environ Res 182:108948; doi:10.1016/j.envres.2019.108948.

Shi X, Zhou B. 2010. The Role of Nrf2 and MAPK Pathways in PFOS-Induced Oxidative Stress in Zebrafish Embryos. Toxicol Sci 115:391–400; doi:10.1093/toxsci/kfq066.

Slotkin TA, MacKillop EA, Melnick RL, Thayer KA, Seidler FJ. 2008. Developmental Neurotoxicity of Perfluorinated Chemicals Modeled in Vitro. Environ Health Perspect 116:716–722; doi:10.1289/ehp.11253.

Strech D, Dirnagl U. 2019. 3Rs missing: animal research without scientific value is unethical. BMJ Open Sci 3:bmjos-2018-000048; doi:10.1136/bmjos-2018-000048.

Verscheijden LFM, Koenderink JB, de Wildt SN, Russel FGM. 2019. Development of a physiologically-based pharmacokinetic pediatric brain model for prediction of cerebrospinal fluid drug concentrations and the influence of meningitis. J. Gallo, ed PLOS Comput Biol 15:e1007117; doi:10.1371/journal.pcbi.1007117.

Wang J, Pan Y, Cui Q, Yao B, Wang J, Dai J. 2018. Penetration of PFASs Across the Blood Cerebrospinal Fluid Barrier and Its Determinants in Humans. Environ Sci Technol 52:13553–13561; doi:10.1021/acs.est.8b04550.

Weksler B, Romero IA, Couraud PO. 2013. The hCMEC/D3 cell line as a model of the human blood brain barrier. Fluids Barriers CNS 10:16; doi:10.1186/2045-8118-10-16.

Zakaria Z, Badhan R. 2018. Development of a region-specific physiologically based pharmacokinetic brain model to assess hippocampus and frontal cortex pharmacokinetics. Pharmaceutics 10:14; doi:10.3390/pharmaceutics10010014.

Estimating neuronal risk through ROS Systems Biology Model for PFOS and PFOA

Abstract

PFOS is one of the most abundant perfluoroalkyl substances (PFASs) in environment with wide exposure to human population through contaminated food, water, consumer products and occupational exposure. Various epidemiological, in vitro and in vivo studies have found the causal link between the exposure of PFOS and neurotoxicity. Several studies have indicated that PFOS and PFOA cause oxidative damage in neurons by generating ROS like peroxide and free radicals. Consequently, ROS alters antioxidant response elements (ARE), disturb redox signalling and activation of apoptotic pathway which may increases the neuronal cell death. In-silico modelling along with high throughput in vitro assays is gaining attention to assess the environmental chemicals related human health effects. The objective of this study is to develop an integrated tool that describes both the kinetic and dynamic effects of PFOS and PFOA via coupling physiological based pharmacokinetics (PBPK) to a systems biology model of ROS effects. This integrative approach will be applied for the human, where neuronal damage in adult, and children will be investigated. A PBPK model describing pharmacokinetics of PFAS and a systems biology (SB) model describing the ROS generation was made. PBPK along with systems biology model will be used to understand the mechanistic pathway regarding PFOS induced neurotoxicity. Developed PBPK coupled ROS SB model is able to demonstrate the effects of PFOS on ROS, thus predicting effects of ROS on ARE and consequently mitochondrial damage and alteration in ATP production as a proxy for neuronal survivability.

Keywords: ROS, PFOS, PFOA, Neuronal death, oxidative stress

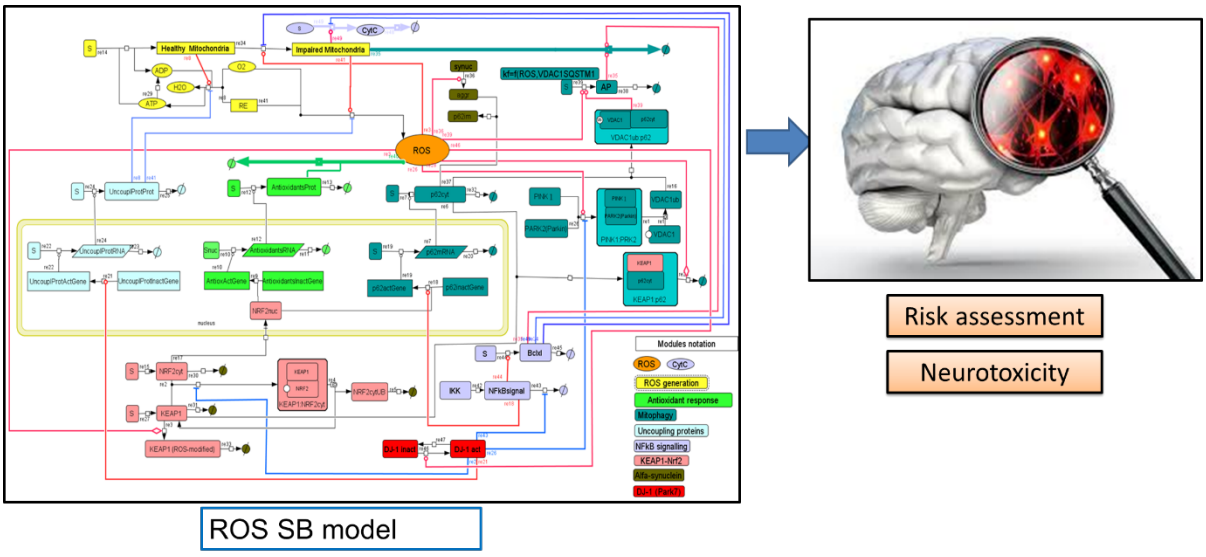

Figure 1: Oxidative stress Systems Biology Model for predicting neurotoxicity

1. Introduction

PFAS, a persistent organic pollutant (POP) distributes inside brain and can induce brain damage. Several studies have pointed towards the neurotoxic potential of PFOS and PFOA conducted in-vitro, in-vivo in zebrafish, polar beers, rats and mice. Spatial learning and memory impairment was observed after 3 months PFOS exposure to mice pointing towards adult hippocampal damage (Long et al. 2013). In another study with 28 days PFOS exposure in rats, hypothalamus-pituitary axis (HPA) was inhibited along with inhibition of Gr protein expression in amygdala and prefrontal cortex implicating towards neuroendocrine axis damage (Salgado-Freiría et al. 2018). Developmental exposure to PFOS in zebrafish caused dopaminergic deficit due to spontaneous hyperactivity supporting the association of ADHD with PFOS (Spulber et al. 2014). Higher serum PFAS concentration were associated with behavioral problems in children (7 years) in the epidemiological study (Spulber et al. 2014). In another cross-sectional study, significant association between PFAS blood level and behavioral inhibition deficit in children were detected (Gump et al. 2011). PFAS was found to be accumulated in brainstem region where dopaminergic neurons are present in brain autopsy sample of five adult in Italy (Di Nisio et al. 2022). Another in-vitro study pointed out towards alteration in surface area of neural stem cells due to PFOA and PFOS exposure suggesting that immature brain is more susceptible to neurobehavioral alterations (Pierozan and Karlsson 2021).

As PFAS are widespread in environment and human beings get major exposure through oral intake (contaminated, water and food), it is inevitable to have continuous exposure over human lifetime. PFOS (5.3 years) and PFOA (2.7 years) have larger human half-life, and they distribute in various organs including brain causing potential risk (Li et al. 2018). PFAS exposure in aging population may be the contributing factor for increasing neurodegenerative diseases like Alzheimer and Parkinson. In a study with 903 subjects aged 60 years and older, PFOA was found to be significantly associated with cognition z-score whereas no significant association was found for PFOS (Park et al. 2021). Nevertheless, the mechanism behind neurotoxicity in geriatric population is quite unclear and need to be explored further.

Oxidative stress is one of the prominent biomarkers induced by PFAS and can result in increased production of ROS (Wielsøe et al. 2015). PFOS exposure increased ROS in dopaminergic neurons along with mitochondrial dysfunction related to neuropathology in *Caenorhabditis Elegans* (Sammi et al. 2019). Similar in cerebellar granule cells, PFOS exposure increased ROS, caspase-3 activity and nucleosomal DNA fragmentation leading to apoptosis (Lee et al. 2012). Even PFOA showed similar profile in SH-SY5Y cells with 100 µM, ROS production, the metabolic signature shift, decrease in ATP related metabolites and other precursors were observed (Souders et al. 2021). All the studies point out that ROS, oxidative stress and cell death is common after PFOS and PFOA exposure. These biomarkers can be modeled using systems biology (SB) model to understand the mechanistic pathway leading to neuronal toxicity in human and animals. We did not find any work in the literature where computational model like systems biology was developed for PFAS.

The objective of this work was to build a SB model for PFOS and PFOA to predict neurotoxicity. Since we have an online model available for ROS for other drugs, the same model was

improved to add chemical related parameters. Further, we checked other factor like aging due to ROS, cell death in sensitive population like pediatric and geriatric. Integrated approach was used and results from brain-specific PBPK model was combined with SB model to improve the risk assessment.

2. Methodology

2.1 Extraction of data for PFOS and PFOA

Webplot was used to extract the data from several articles for both the compounds. Nuclear factor erythroid 2-related factor 2 (NRF2) signalling pathway was investigated using SH-SY5Y cells after PFOS exposure at 10, 50, 100 and 200 µM and 200 µM at different time points (1, 6, 12, 24, 48 h) (Sun et al. 2018). Data for putative biomarkers like ROS, antioxidant, caspase 3, Bax, Bcl-2, mitochondrial damage, cell death, and the data about effect of antioxidant N-acetyl-l-cysteine (NAC) on these biomarkers was extracted. Another independent data was present in literature for PFOA exposure to neuronal cells at the concentration of 10, 100, 250 and 500 µM for 4, 24 and 48 hours (Souders et al. 2021). Cell viability, apoptosis, cytotoxicity, ATP production, mitochondrial potential, ROS production data was extracted for PFOA.

2.2 Hypothesis and assumption for the model

The common pathway for both PFOS and PFOA was ROS production, ATP, mitochondrial damage and cell death which was considered for biochemical modeling. Already published model for ROS was taken and modified further (N. Kolodkin et al. 2020). This model consists of the signalling pathway and reactions required for predicting neuronal risk. Overall framework of the model is presented in Fig 1.

2.3 Pathway involved for PFOS induced neuronal damage

NRF2 decreased in the cytoplasm and increased in the nucleus after PFOS exposure with pronounced nuclear expression at 200 µM. The expression of heme oxygenase 1 (HO-1) (an antioxidant and transcriptional target of NRF2) depleted after PFOS exposure whereas nuclear expression of HO-1 increased pointing towards the NRF2 activation in SH-SY5Y cells. ROS was enhanced in a dose-dependent manner, but the N-acetly-l-cysteine (NAC) decreased the ROS levels. Further, apoptosis related factor like caspase-3, Bax, bcl-2 expression also increased, and cell viability decreased significantly after PFOS exposure in dose-dependent manner pointing towards neuronal risk (Sun et al. 2018).

2.4 Pathway involved for PFOA induced neuronal damage

Caspase mediated apoptosis was observed after PFOA exposure at 250 µM pointing towards toxicological risk in SH-SY5Y cells as well as PC12 cells (Slotkin et al. 2008). Oxidative stress especially increases in ROS and decreased mitochondrial membrane potential was observed after 4 h of exposure. PFOA exposure was also associated with reduced ATP levels, which was in correlation with decreased MMP and also indicator for mitochondrial dysfunction.

2.5 PBPK Model for Brain (PFOS and PFOA)

PFOS and PFOA concentration in plasma and brain was predicted using brain PBPK Model. Brain PBPK model consist of hippocampus, cortex, rest brain and CSF. Hippocampal concentration was used as the input for ROS model to evaluate neuronal damage. Concentration provided in-vitro was used as the original dose, but then reverse dosimetry

was done to find equivalent daily dose. Equivalent daily dose was compared with TDI set by EFSA. Further age-kinetic PBPK model was used and then hippocampal concentration was calculated for infants, adult and geriatric population to understand the PFAS exposure and neuronal damage, and aging.

3. Results

3.1 Change in antioxidant levels after exposure

Antioxidant HO-1 level showed a slight increase and then further a little decrease with time, but the variation was not very huge. Predicted antioxidant was within two folds of experimental datapoint (Fig 2). Concentration of PFOS was 200 µM exposed to SH-SY5Y cells for 48 hours. This shows that antioxidant levels are not changing after PFOS exposure.

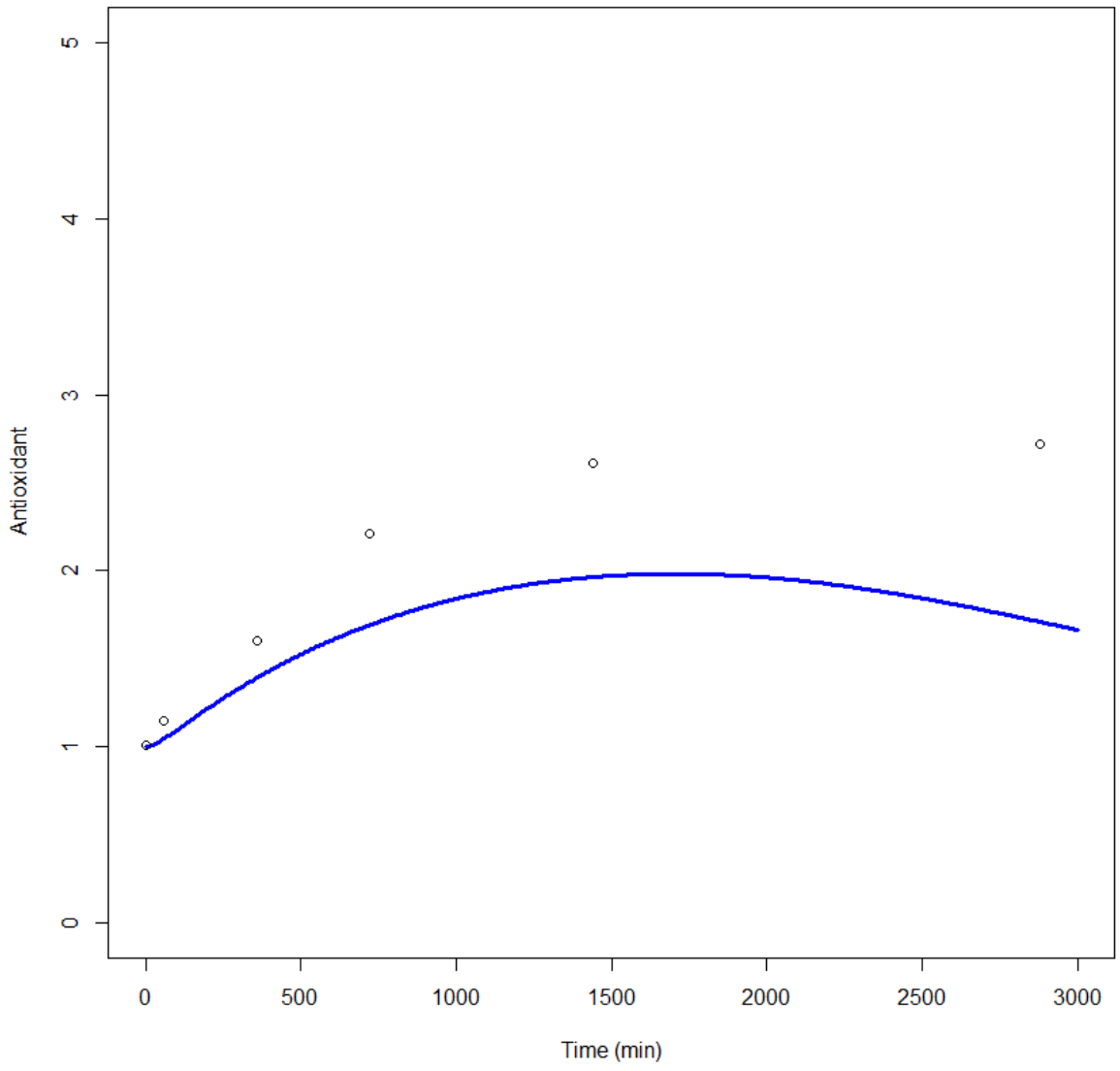

Figure 2: Antioxidant level in neurons after PFAS exposure. Blue line represents mean and dot represents the observed time point.

3.2 Depletion in ROS level with time

Oxidative stress implicated by relative ROS increased in the cell at initial time point but then it decreased later (Figure 3). Cmax for ROS was observed at initial time point (at 200 min). Predicted concentration was within two folds of observed datapoint for ROS.

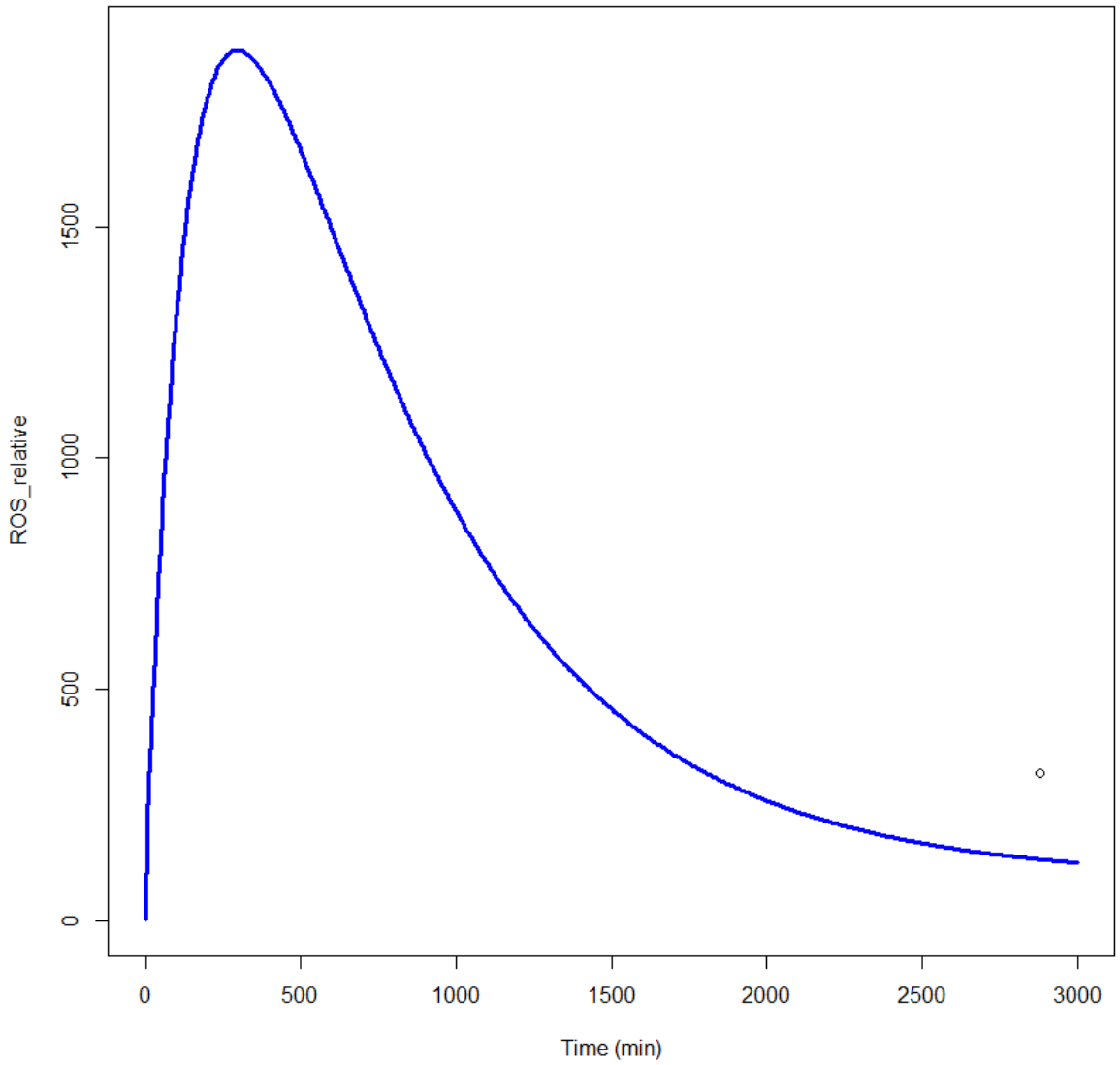

Figure 3: ROS relative expression with time after PFAS exposure. Blue line represents mean and dot represents the observed time point.

3.3 Bcl expression and neuronal cell death

Bcl2 levels did not vary much with time and it was close to one. Observed data point was very close to the predicted Bcl level. Bcl level is the indicator for neuronal cell death. However, cell death was observed at the higher concentration of PFOS i.e., 200 µM.

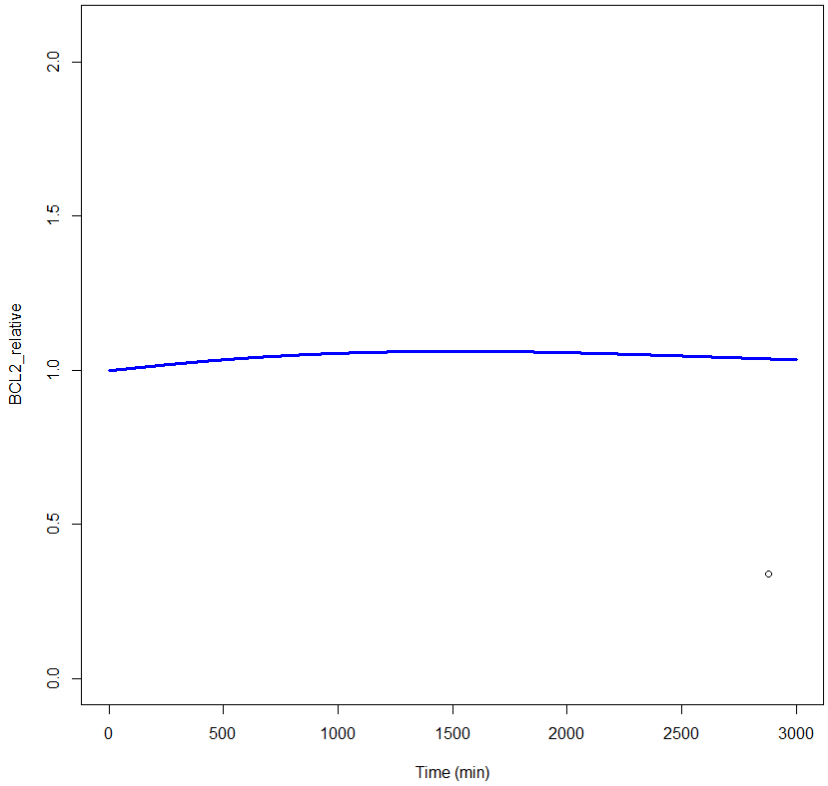

Figure 4: BCL2 relative with time after exposure to PFAS. Blue line represents mean and dot represents the observed time point.

3.4 Biomarkers with time

PFOS induced ROS, in turn there was amplified NRF2. NRF2 is the transcriptional factor which induces expression of p62, the antioxidant response element (ARE). The ARE scavenges ROS and p62 increasing the healthy mitochondria via mitopsis. ROS increase was complemented by decreased ATP and hence decreased mitochondria (Fig 5).

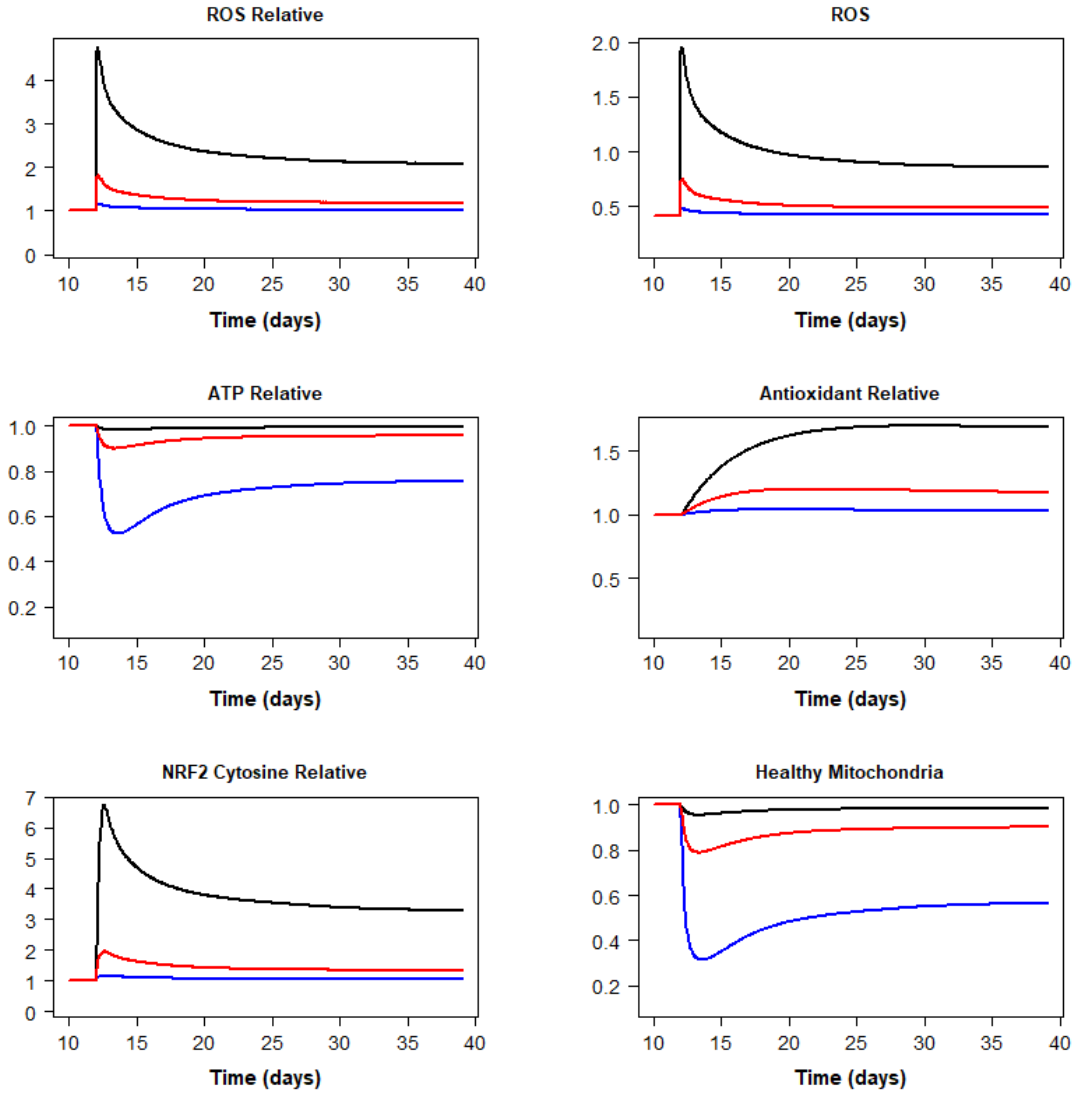

Figure 5: ROS, ROS relative, ATP relative, Antioxidant relative, NRF2 and health mitochondria after PFAS exposure. Black represents 97.5 percentile, red represents median and blue represent 2.5 percentile.

4. Discussion and Conclusion

In this paper, we used the ROS model to understand the neurotoxicity caused by PFOS and PFOA. We used the model already published in Copasi and optimized in further for environmental chemical. The model behaved differently for long acting chemical like PFAS. Model was further used with the input from PBPK model and to predict aging in adult population using age specific PBPK Model.

NRF2 is one of the major pathway and has been involved in the progression of Alzheimer and Parkinson disease (Osama et al. 2020; Zhong et al. 2022). Under normal condition, cellular abundance of NRF2 is maintained by Keap1, but during stress, Keap 1 gets inactivated stabilizing NRF2, which allows it to enter nucleus and hence bind with ARE promoting gene expression (Tonelli et al. 2018). The PFOS supress the NRF2 signalling in cytoplasm, promoting

the oxidative stress and hence may contribute to neurotoxicity or neurodegenerative disorder.

In this study, increase in ROS was observed with PFAS exposure contributing towards increased oxidative stress and hence neuronal cell death. Generally, if increased ROS is complemented by increase in antioxidant level, the ATP loss is reduced and hence cell can revive back to its normal state. But the feedback loop is not getting activated in case of PFOS, so cell death is happening. In case of AD, ROS can contribute to damage on amyloid β levels, and damaging other proteins, lipids and nutrients required for cell survival contributing to increased progression of AD (Cheignon et al. 2018).

Dysfunction of mitochondria coupled with oxidative stress is often considered for neuronal death. Mitochondrial dysfunction is associated with reduced ATP levels which is the cellular energy currency (Ebanks et al. 2020). ATP can also alter the misfolding of amyloid β which can contribute towards aging (Coskuner and Murray 2014). PBPK model helped in providing the accurate concentration present at hippocampus region which helped in improving the risk assessment. It was observed that PFAS present in hippocampus for longer time can contribute to cell death and hence learning and impairment.

In conclusion, the induction of NRF2 in nucleus by PFOS and cell death may be one of the reasons for Parkinson disease in older population. Decreased ATP levels, reduced health mitochondria and altered levels of ARE can be the leading cause for neurodegeneration and disrupt normal brain activity. Integrated PBPK Model coupled with ROS allowed to simulate the perturbations in biomarkers of ROS managing network providing a broader picture about altered cell dynamics.

Acknowledgments
This study was financially supported by Marie Skłodowska-Curie “Neurosome project” under grant agreement no. 766251. This publication reflects only the author views. The community and other funding organizations are not liable for any use made of the information contained.

Reference

Cheignon C, Tomas M, Bonnefont-Rousselot D, Faller P, Hureau C, Collin F. 2018. Oxidative stress and the amyloid beta peptide in Alzheimer's disease. Redox Biol 14:450–464; doi:10.1016/j.redox.2017.10.014.

Coskuner O, Murray IVJ. 2014. Adenosine Triphosphate (ATP) Reduces Amyloid-β Protein Misfolding in vitro. J Alzheimer's Dis 41:561–574; doi:10.3233/JAD-132300.

Di Nisio A, Pannella M, Vogiatzis S, Sut S, Dall'Acqua S, Rocca MS, et al. 2022. Impairment of human dopaminergic neurons at different developmental stages by perfluoro-octanoic acid (PFOA) and differential human brain areas accumulation of perfluoroalkyl chemicals. Environ Int 158:106982; doi:10.1016/j.envint.2021.106982.

Ebanks B, Ingram TL, Chakrabarti L. 2020. ATP synthase and Alzheimer's disease: putting a spin on the mitochondrial hypothesis. Aging (Albany NY) 12:16647–16662; doi:10.18632/aging.103867.

Gump BB, Wu Q, Dumas AK, Kannan K. 2011. Perfluorochemical (PFC) Exposure in Children: Associations with Impaired Response Inhibition. Environ Sci Technol 45:8151–8159; doi:10.1021/es103712g.

Lee H-G, Lee YJ, Yang J-H. 2012. Perfluorooctane sulfonate induces apoptosis of cerebellar granule cells via a ROS-dependent protein kinase C signaling pathway. Neurotoxicology 33:314–320; doi:10.1016/j.neuro.2012.01.017.

Li Y, Fletcher T, Mucs D, Scott K, Lindh CH, Tallving P, et al. 2018. Half-lives of PFOS, PFHxS and PFOA after end of exposure to contaminated drinking water. Occup Environ Med 75:46–51; doi:10.1136/oemed-2017-104651.

Long Y, Wang Y, Ji G, Yan L, Hu F, Gu A. 2013. Neurotoxicity of Perfluorooctane Sulfonate to Hippocampal Cells in Adult Mice. H. Wang, ed PLoS One 8:e54176; doi:10.1371/journal.pone.0054176.

N. Kolodkin A, Sharma RP, Colangelo AM, Ignatenko A, Martorana F, Jennen D, et al. 2020. ROS networks: designs, aging, Parkinson's disease and precision therapies. npj Syst Biol Appl 6:34; doi:10.1038/s41540-020-00150-w.

Osama A, Zhang J, Yao J, Yao X, Fang J. 2020. Nrf2: a dark horse in Alzheimer's disease treatment. Ageing Res Rev 64:101206; doi:10.1016/j.arr.2020.101206.

Park SK, Ding N, Han D. 2021. Perfluoroalkyl substances and cognitive function in older adults: Should we consider non-monotonic dose-responses and chronic kidney disease? Environ Res 192:110346; doi:10.1016/j.envres.2020.110346.

Pierozan P, Karlsson O. 2021. Differential susceptibility of rat primary neurons and neural stem cells to PFOS and PFOA toxicity. Toxicol Lett 349:61–68; doi:10.1016/j.toxlet.2021.06.004.

Salgado-Freiría R, López-Doval S, Lafuente A. 2018. Perfluorooctane sulfonate (PFOS) can alter the hypothalamic–pituitary–adrenal (HPA) axis activity by modifying CRF1 and glucocorticoid receptors. Toxicol Lett 295:1–9; doi:10.1016/j.toxlet.2018.05.025.

Sammi SR, Foguth RM, Nieves CS, De Perre C, Wipf P, McMurray CT, et al. 2019. Perfluorooctane Sulfonate (PFOS) Produces Dopaminergic Neuropathology in Caenorhabditis elegans. Toxicol Sci 172:417–434; doi:10.1093/toxsci/kfz191.

Slotkin TA, MacKillop EA, Melnick RL, Thayer KA, Seidler FJ. 2008. Developmental Neurotoxicity of Perfluorinated Chemicals Modeled in Vitro. Environ Health Perspect 116:716–722; doi:10.1289/ehp.11253.

Souders CL, Sanchez CL, Malphurs W, Aristizabal-Henao JJ, Bowden JA, Martyniuk CJ. 2021. Metabolic profiling in human SH-SY5Y neuronal cells exposed to perfluorooctanoic acid (PFOA). Neurotoxicology 85:160–172; doi:10.1016/j.neuro.2021.05.009.

Spulber S, Kilian P, Wan Ibrahim WN, Onishchenko N, Ulhaq M, Norrgren L, et al. 2014. PFOS Induces Behavioral Alterations, Including Spontaneous Hyperactivity That Is Corrected by Dexamfetamine in Zebrafish Larvae. F. Del Bene, ed PLoS One 9:e94227; doi:10.1371/journal.pone.0094227.

Sun P, Nie X, Chen X, Yin L, Luo J, Sun L, et al. 2018. Nrf2 Signaling Elicits a Neuroprotective Role Against PFOS-mediated Oxidative Damage and Apoptosis. Neurochem Res 43:2446–2459; doi:10.1007/s11064-018-2672-y.

Tonelli C, Chio IIC, Tuveson DA. 2018. Transcriptional Regulation by Nrf2. Antioxid Redox Signal 29:1727–1745; doi:10.1089/ars.2017.7342.

Wielsøe M, Long M, Ghisari M, Bonefeld-Jørgensen EC. 2015. Perfluoroalkylated substances (PFAS) affect oxidative stress biomarkers in vitro. Chemosphere 129:239–245; doi:10.1016/j.chemosphere.2014.10.014.

Zhong Y, Cai X, Ding L, Liao J, Liu X, Huang Y, et al. 2022. Nrf2 Inhibits the Progression of Parkinson's Disease by Upregulating AABR07032261.5 to Repress Pyroptosis. J Inflamm Res 15:669–685; doi:10.2147/JIR.S345895.

General Discussion and Conclusions

UNIVERSITAT ROVIRA I VIRGILI
QUANTITATIVE SYSTEMS TOXICOLOGY MODELING FOR NEURONAL ADVERSE OUTCOME
Deepika

General Discussion

Every year, almost thousands of environmental chemicals enters in market present in countless products used by customer, from pesticides and toys, to clothing and automobiles. Prediction about bioaccumulation, persistence and toxicity especially neurotoxicity of these chemicals for the human is the biggest challenge for regulatory bodies. In addition, several regulatory frameworks like IATA, REACH etc. in EU focus on the use of computational, and in-vitro models to reduce the use of animals for testing. Computational tools like QSAR, PBPK, helps in improving the design of in-vitro screening assays while others facilitate through improving data analysis. These models are helping in risk assessment to fill the data gap where hazard data is not available. They are particularly useful for chemical prioritisation, human risk assessment, chronic toxicity, toxicokinetic properties (ADME), and QIVIVE moving the science towards mechanism-based risk assessment approach. Overtime use of in-vitro data for parameterizing PBPK is replacing the in-vivo data. Conducting in-vitro experiments with biological relevance and producing data can be a useful approach for reducing the animal usage.

Increased in the in-vitro experiments has also led to increased data about proteins and biological markers through OMICS (proteomics, transcriptomics, metabolomics), which made it crucial to build systems biology model. SB model helps in understanding the perturbations and interactions at biological level. These models are generally based on biochemistry and biology and required deep understanding about the cell and its structure. For improved human risk assessment, SB model can be integrated with PBPK for interpreting the neurotoxicity of environmental chemicals in human. This approach can help in elucidating the mechanistic pathway and allow better understanding of chemical toxicokinetic. In this thesis, we developed the PBPK model for several environmental chemicals to capture sensitive age groups, built organ-specific PBPK model and combined with SB for assessing neurotoxicity in human utilizing in-vitro data from human BBB cell lines.

For assessing neurotoxicity, initially we developed the state of art by collecting the extensive database present in literature (chapter 1) from 2004 to 2019. Systematic study was done for several chemicals (FRs, PFOS, PFOA, PCB, BPA and phthalates) to understand the mechanism and long-term effect of neurotoxicants on nervous system. This review helped in understanding the type of in-vitro, in-vivo, and epidemiological data available for building the in-silico models. Different biomarkers, for instance ROS (oxidative stress) was found to be a common test for indicating neurotoxicity among both in-vitro and in-vivo studies. Several questions arise during the review: are we doing the inter-species dose extrapolation correctly, can in-vitro replace the in-vivo experiments and whether results from experimental studies be extended to human for risk assessment using conservative approach. Based on the available data, the framework for risk assessment was proposed: combining in-silico with in-vitro using IVIVE for improving the prediction of the human exposure, risk and brain toxicity. Further, the PBPK model can be made more species-specific to target a particular risk.

Flame retardants are being widely used as plasticizer in construction and for extinguishing fire with OPFRs replacing other traditional FRs. Recent in-vitro studies have pointed towards neurotoxicity of OPFRs but there is limited knowledge about the kinetics of these FRs in human. This was the first attempt to develop a PBPK model for OPFRs (TDCIPP, TCIPP and TCEP) in rats for risk assessment in chapter 3. Four different kind of models were developed to include several biological phenomena like EHR (scenario 1), time dependent EHR (scenario 2), biphasic clearance (scenario 3) and separate fu for brain and adipose tissue (scenario 4). EHR considered the circulation of metabolite within gut and liver which led to slowing down the elimination of chemical. MCMC approach along with visual fitting was used to optimize the biochemical parameters. AIC score was used to find the best fit model. For TCIPP and TCEP, the model with scenario 4 was the best fit but for TDCIPP, the model with scenario 1 was the best fit. Best model was evaluated with the independent animal studies conducted in different labs. This led to increase in confidence in the model predictions. It was found that OPFRs metabolize very fast with no parent chemical detected in urine or feces. The elimination from brain and adipose tissue was very slow compared to other organs. Among three chemicals, the TDCIPP concentration was high followed by TCIPP and TCEP in brain and adipose tissue correlating with the log $K_{o/w}$ (lipophilicity) of the chemical. Model was also applied for calculating equivalent HED with the in-vitro and in-vivo studies where neurotoxicity was observed to compare it with limits set by regulatory bodies. This shows the model application in neurotoxicity and risk assessment. This model can be further extrapolated in human to calculated reconstructed exposure and evaluate accumulation in different human organs.

In Chapter 2b, sex-specific PBPK model was developed for pediatric population for risk assessment of Bisphenol A. Initially we validated the model for adult bisphenol A, then the same model was extended to children. Two approaches were considered: body-weight scaling (conservative approach), and ontogeny-based scaling. Main idea behind this approach was to

capture the variation in metabolic enzymes and hence the varied toxicokinetic. IVIVE scaling approach was used for enzymatic scaling in pediatric population for both glucuronidation and sulfation. Plasma concentration was found to be higher in children with ontogeny scaling compared to adults and body-weight scaling with similar exposure. Differences in kinetics of boys and girls were compared with respect to AUC, half-life, mean residence time and bioavailability. Girls were found to have higher half-life for BPA than boys. The TDI set by EFSA was compared with the reconstructed exposure to understand whether children are at higher risk. Reconstructed exposure was 1500 times higher than recent TDI by EFSA in children pointing towards underestimation of risk. This approach helped in capturing the sex-difference with BPA and hence improve prediction for adverse effect leaving behind the traditional approach.

In chapter 3a, PBPK model was developed for PFOS which covered human lifetime. Since PFOS is a lipophilic chemical with half-life of around 3-5 years with high accumulation potential, the question was that whether the sensitive age groups are at more risk compared to adult. This was done to improve the framework for risk assessment considering pediatric and geriatric population. Physiological equations were developed for all age groups for both male and female. Biochemical parameters were modified, for instance considering the protein (serum albumin, α-acid glycoprotein) variation across age. Since PFOS do not metabolize inside the human body, kidney filtration incorporating reabsorption play a major role for elimination which was scaled considering the body weight of both adult and children/old age people. Glomerular filtration rate was varied based on the literature evidence for population. Exposure reconstruction was done using MCMC simulation to compare the variation among age groups. It was found that the exposure increased with age which might be due to disposition of the chemical inside bone marrow or adipose tissue. In old age due to reduced GFR, decreased bone marrow volume and increased adipose tissue can be responsible for the PFOS accumulation. GSA was conducted to evaluate the sensitive parameters and all the above parameters were found to be sensitive. This was the first study for PFOS where age related kinetic and dynamic was captured providing a framework for understanding risk based on age.

In the second part of the chapter (3b), similar framework was used for conducting in-silico experiment to improve PFAS policy making. Highly referred article on PFAS being used by regulatory bodies in U.S. and Europe were taken and a systematic review was conducted as per OHAT review guidelines. Further, for risk translation to human, PBPK model was used to calculate HED from studies published for immunotoxicity in children. HED was compared with TDI/RfD set by EFSA and USEPA. It was found that TDI (EFSA) was 100-1000 time lower than minimum concentration simulated for PFOS and PFOA whereas RfD (USEPA) was only 1-10 times lower than the concentration at which toxic effect were observed in children. If additional uncertainty factor has to be considered, then the TDI becomes equal to the toxic dose. Further, the PFAS dosing used for animal studies with observed toxicity was converted

to HED to understand their relevance for human risk. This was done using allometric scaling since we did not have the validated PFAS model in rat or mice. It was found that the HED calculated from animal dose is very high (six to fifty-two thousand times) compared to TWI by EFSA which suggest that the experiments conducted may not be relevant for human. But the RfD by USEPA was very close to HED calculated (forty to four hundred times) which was quite appropriate for understanding the risk. With high variation in limits set by both regulatory bodies, huge differences in comparison of the results was observed. A framework was proposed to improve the human risk assessment from PFAS chemicals consisting of recommendation for improving experiments and utilization of in-silico tools. This study provided insight and confidence about whether available experimental data for PFAS is enough for concluding the risk in human. This study was a part of project funded by Center for Truth in Science (CTS), US for improving the PFAS policymaking.

Often in-silico models need data from several in-vitro studies. The most common being liver metabolising assay where Vmax and Km is calculated and through IVIVE integrated in PBPK. Even for the brain, similar IVIVE approach can be used for calculating the permeability reducing the animal usage. In-vitro study was conducing for checking the BBB permeation potential of three OPs (CPF, PMT and CFT) using HCMEC/D3 cell lines in chapter 4. The cell death was checked to select the concentration of chemicals. Both the active transport and passive diffusion was calculated for three OPs. It was found that only CFT showed concentration dependent active transport whereas PMT and CPF were not substrates for active transport. Passive diffusion as found to be highest in CPF followed by CFT and PMT. Concentration-dependent permeation and flux was not observed. Genetic expression was checked to associate their permeation with variation in tight and adherens junction protein. In case of CPF, occludin gene was down expressed which was in correlation with the reduction in TEER observed. It was concluded that CPF being the highly permeable molecule also can alter the tight junction. IVIVC conducted with experimental in-vivo data extracted from literature showed a good correlation with the in-vitro data from our study. This implies that the data obtained from our study can be integrated in PBPK to understand the neuronal risk in human.

Similar in-vitro study for PFOS and PFOA was conducted in chapter 5a and the permeability coefficient value was calculated. PFOS was found to be highly permeable than PFOA at the similar concentration. Both were not found to be substrate for active transport, however the efflux ratio was higher for PFOA compared to PFOS. The data from the experiment was integrated in brain-specific PBPK model. IVIVE was used to extrapolate in-vitro permeability coefficient value to human permeability and rat permeability in brain considering the volume and surface area of brain. Clearance influx and efflux was included in the model to include the metabolism happening in the brain. Initially the PBPK model was developed and validated in rat for PFAS chemical. Validated rat model was then further extended to include brain specific compartment like hippocampus, frontal cortex, csf, and rest of the brain. The biochemical

parameters were calculated, and physiological parameters were taken from literature. The model was considered to be perfusion limited with permeability limited for brain. Predicted concentration-time profile in brain sub-organs was compared with the experimental value. The model was then extended to human and evaluated for brain and CSF concentration with respect to plasma. It was found that the disposition of chemical varies in different sub-organs of brain. This input can be further used to make integrated model for predicting neurotoxicity. Brain-specific PBPK model helped in understanding the toxicokinetic of PFAS compounds inside the brain. This approach pointed towards individualized risk rather than considering generalized risk. The assumption that all parts in the human brain are equal with uniform distribution is not valid anymore based on results from brain-specific PBPK since each part has their specific blood flow, specific volume and specific inherent characters.

In the last chapter of the thesis 5b, the focus was to integrate the input from PBPK model into systems biology model for evaluating neurotoxicity at the cellular level. Hippocampus brain concentration was taken as input rather than putting a generalized assumption that plasma and brain concentration are equivalent. In-vitro data was extracted from the literature using webplot and used for validating the systems biology model focused on ROS production. The effect of PFOS on NRF2 signalling, mitochondrial damages and ROS production in neuronal cells was modeled for neurodegenerative diseases. Neuronal apoptosis was observed with increased production of ROS leading to decreased cell viability. Antioxidant factor was also found to increase with increased concentration of PFOS and variation in ATP levels were observed. The alteration in neuronal biomarkers and proteins were observed with variation in cellular PFOS levels. This approach is the illustration of integrative systems toxicology comprising of IVIVE, organ specific PBPK and systems biology model which can be helpful for building AOPs in the near future. Our results pointed out towards the application of considered organ-specific risk for improving human risk assessment in the field of neurotoxicity.

UNIVERSITAT ROVIRA I VIRGILI
QUANTITATIVE SYSTEMS TOXICOLOGY MODELING FOR NEURONAL ADVERSE OUTCOME
Deepika

Conclusions

The work in the thesis provided an integrative framework for prediction of neurotoxicity in the context of risk assessment. Integrated computational models like PBPK, IVIVE and SB model along with in-vitro data provided a mechanistic view towards risk assessment for human. This thesis provided an overall strategy for human risk assessment especially in the field of neurotoxicity. Several questions were answered like can we consider a generalized risk for all the population? Should we underestimate the sex and keep on using adult male model to predict risk for both age groups? Can adult behave similar to pediatric population for different chemicals? Can we make PBPK model even with limited data by taking several biologically relevant assumptions? Should we sometime follow the same protocol as pharmaceutical research for environmental chemicals? Do we need organ-specific model for risk assessment? This thesis tried to provide answer to these wider questions taking environmental chemicals and utilizing the integrative approach. The major strong point of this thesis is to move from traditional ways of doing research to innovative ways more focused towards personalized risk. Variability and uncertainty in population with age and sex through computational models were considered. Another strong point being utilizing the IVIVE technique for integrating in-vitro data in the PBPK model. Today, researchers have completely stated utilizing the liver in-vitro data for PBPK, in similar way we will move towards using BBB data for PBPK with improved IVIVE overtime.

In future, genomic data can be integrated in the brain-specific PBPK to directly associate with the neuronal damage and calculate the equivalent HED. The policymaking can be improved if such kind of models are developed and evaluated for wider range of chemicals. Nonetheless, we provided a framework which can be further used for other chemicals. This thesis showed that girls cannot be considered equivalent to boys and thus we should not aim for a generalized risk. As pharmaceutical and biotechnological products are moving towards personalized therapy considering the specific epigenome and individual physiology, its time for environmental science to take a step towards the personalized risk.

Chapter 1 discussed about the integrative framework approach for predicting neurotoxicity of several chemicals. Extensive systematic review conducted for in-vitro, and in-vivo studies helped in pointing out that for neurotoxicity oxidative stress through generation of ROS is one of the important biomarkers. This helped in increased understanding about experimental data, generating evidences related to toxicity and building effective hypothesis for the research. It was found that limited PBPK model exist which point towards kinetics of brain being the biggest gap in the field of neurotoxicity. This review provided overall idea about the research conducted in the decade and provided new ideas about novel research in computational and in-vitro field.

In chapter 2, for the first time PBPK model for three OPFRs was developed and evaluated with the rat data. There have been few studies published related to the neurotoxicity of these chemicals but there was no PBPK model available to understand the toxicokinetic and hence the risk. This model also provided a framework about the kind of assumptions which can be made based on experimental data, for instance inclusion of biphasic clearance. The finding from the model suggested that the metabolites of OPFRs stays in the organs like brain and adipose tissue for longer compared to other organs. Also, correlation was observed with the lipophilicity and accumulation in both the organs for TDCIPP, TCIPP and TCEP. Further, the application of model in the field of neurotoxicity was shown by calculating HED for both in-vitro and in-vivo data. In chapter 2b, another PBPK model for short-acting chemical (BPA) was developed for children considering the ontogeny-based scaling. Often in the area of risk assessment, allometric scaling is quite common. This study was done to show that sometime allometric scaling is not evident to understand kinetic risk. In this model, sex-related differences were also observed. The model was made for both boys and girls and it was found that girls may be at higher risk than boys due to their varied physiology and metabolizing capabilities.

Chapter 3 was majorly focused on improving the existing PBPK model to make them more specialized and focused on specific populations. This was done to emphasize the fact that generic PBPK model need to be modified to have better understanding about human risk. Age-kinetic PBPK model considering the entire human lifespan was the first model to be built for PFOS. This model helped in exploring the kinetic variation which may be arise due to age. It covered the pediatric and geriatric population (0 to 90 years) which is often ignored during chemical risk assessment. The physiological equations generated during the model development can be used by other researchers to develop specific models for other group of chemicals. The framework used paved a path for building such kind of models for the long-acting chemicals. The model developed was used further for the immunotoxicity risk assessment in infants to predict the daily exposure. Daily exposure was compared with regulatory limits to understand the risk for children. This work was funded by center for truth in science with the objective of improving PFAS policymaking and provide recommendation to the general public about the risk.

In-vitro data should be incorporated in the PBPK model to reduce the dependence on animals. In chapter 4, BBB cell lines were used to calculate the permeability potential of three OPs. Such kind of data can be used to build brain-specific PBPK model with the utilization of IVIVE. These types of studies are very common in the field of pharmaceutical drugs where caco-2, BBB and MDCK cell lines are often taken to calculate the permeability. But, still in case of environmental chemicals it is not quite often that researchers perform these experiments. IVIVC conducted with in-vivo data also showed that the in-vitro can act as a suitable alternative. In future, this data will be used to build brain-specific PBPK model.

Similar approach as chapter 4 was used to calculate permeability for PFOS and PFOA in chapter 5. Both active transport and passive diffusion was calculated and using IVIVE the data was incorporated in the PBPK model. Brain-specific PBPK model showed that generalizing the brain compartment is the underestimation of risk. Output from PBPK was used as an input for SB model, where NRF2 pathway was evaluated for neuronal damage. ROS was increased upon the chemical exposure, leading to mitochondrial damage, decrease in ATP and neuronal apoptosis. All this pathway was modeled and the neuronal adverse effects were predicted providing road for building AOPs through quantitative systems toxicology modeling.

References

Ball K, Bouzom F, Scherrmann J-M, Walther B, Declèves X. 2012. Development of a Physiologically Based Pharmacokinetic Model for the Rat Central Nervous System and Determination of an In Vitro–In Vivo Scaling Methodology for the Blood–Brain Barrier Permeability of Two Transporter Substrates, Morphine and Oxycodone. J Pharm Sci 101:4277–4292; doi:10.1002/jps.23266.

Ball K, Bouzom F, Scherrmann J-M, Walther B, Declèves X. 2013. Physiologically Based Pharmacokinetic Modelling of Drug Penetration Across the Blood–Brain Barrier—Towards a Mechanistic IVIVE-Based Approach. AAPS J 15:913–932; doi:10.1208/s12248-013-9496-0.

Borowy CS AJ. 2021. Physiology, Zero and First Order Kinetics.

Breuer D. 2010. Analytical Performance Issues. J Occup Environ Hyg 7:D37–D42; doi:10.1080/15459621003781231.

Brown RP, Delp MD, Lindstedt SL, Rhomberg LR, Beliles RP. 1997. Physiological parameter values for physiologically based pharmacokinetic models. Toxicol Ind Health 13: 407–484.

Chen Y, Jin JY, Mukadam S, Malhi V, Kenny JR. 2012. Application of IVIVE and PBPK modeling in prospective prediction of clinical pharmacokinetics: strategy and approach during the drug discovery phase with four case studies. Biopharm Drug Dispos 33:85–98; doi:10.1002/bdd.1769.

Cohen L, Jefferies A. 2019. Environmental Exposures and Cancer: Using the Precautionary Principle. Ecancermedicalscience 13:ed91–ed91; doi:10.3332/ecancer.2019.ed91.

Dankers ACA, Roelofs MJE, Piersma AH, Sweep FCGJ, Russe FGM, van den Berg Martin M, et al. 2013. Endocrine disruptors differentially target ATP-binding cassette transporters in the blood-testis barrier and affect leydig cell testosterone secretion in vitro. Toxicol Sci 136:382–391; doi:10.1093/toxsci/kft198.

Davies B, Morris T. 1993. Physiological Parameters in Laboratory Animals and Humans. Pharm Res 10:1093–1095; doi:10.1023/A:1018943613122.

Deepika D, Sharma RP, Schuhmacher M, Kumar V. 2020. An integrative translational framework for chemical induced neurotoxicity – a systematic review. Crit Rev Toxicol 50:424–438; doi:10.1080/10408444.2020.1763253.

Deepika D, Sharma RP, Schuhmacher M, Kumar V. 2021. Risk Assessment of Perfluorooctane Sulfonate (PFOS) using Dynamic Age Dependent Physiologically based Pharmacokinetic Model (PBPK) across Human Lifetime. Environ Res 199:111287; doi:10.1016/j.envres.2021.111287.

Denuzière A, Ghersi-Egea J-F. 2022. Cerebral concentration and toxicity of endocrine disrupting chemicals: The implication of blood-brain interfaces. Neurotoxicology 91:100–118; doi:https://doi.org/10.1016/j.neuro.2022.04.004.

Fàbrega F, Kumar V, Schuhmacher M, Domingo JL, Nadal M. 2014. PBPK modeling for PFOS and PFOA: Validation with human experimental data. Toxicol Lett 230:244–251; doi:10.1016/j.toxlet.2014.01.007.

Gaohua L, Neuhoff S, Johnson TN, Rostami-Hodjegan A, Jamei M. 2016. Development of a permeability-limited model of the human brain and cerebrospinal fluid (CSF) to integrate known physiological and biological knowledge: Estimating time varying CSF drug concentrations and their variability using in vitro data. Drug Metab Pharmacokinet 31:224–233; doi:10.1016/j.dmpk.2016.03.005.

Hartmanshenn C, Scherholz M, Androulakis IP. 2016. Physiologically-based pharmacokinetic models:

approaches for enabling personalized medicine. J Pharmacokinet Pharmacodyn 43:481–504; doi:10.1007/s10928-016-9492-y.

Helms HC, Abbott NJ, Burek M, Cecchelli R, Couraud PO, Deli MA, et al. 2015. In vitro models of the blood-brain barrier: An overview of commonly used brain endothelial cell culture models and guidelines for their use. J Cereb Blood Flow Metab 36:862–890; doi:10.1177/0271678X16630991.

Ho V, Pelland-St-Pierre L, Gravel S, Bouchard MF, Verner MA, Labrèche F. 2022. Endocrine disruptors: Challenges and future directions in epidemiologic research. Environ Res 204:111969; doi:10.1016/j.envres.2021.111969.

Jiang C, Zhao P, Li W, Tang Y, Liu G. 2020. In silico prediction of chemical neurotoxicity using machine learning. Toxicol Res (Camb) 9:164–172; doi:10.1093/toxres/tfaa016.

Jones HM, Rowland-Yeo K. 2013. Basic concepts in physiologically based pharmacokinetic modeling in drug discovery and development. CPT Pharmacometrics Syst Pharmacol 2:63; doi:10.1038/psp.2013.41.

Karrer C, Roiss T, von Goetz N, Gramec Skledar D, Peterlin Mašič L, Hungerbühler K. 2018. Physiologically Based Pharmacokinetic (PBPK) Modeling of the Bisphenols BPA, BPS, BPF, and BPAF with New Experimental Metabolic Parameters: Comparing the Pharmacokinetic Behavior of BPA with Its Substitutes. Environ Health Perspect 126:077002; doi:10.1289/EHP2739.

Kovar L, Weber A, Zemlin M, Kohl Y, Bals R, Meibohm B, et al. 2020. Physiologically-Based Pharmacokinetic (PBPK) Modeling Providing Insights into Fentanyl Pharmacokinetics in Adults and Pediatric Patients. Pharmaceutics 12:908; doi:10.3390/pharmaceutics12100908.

Kremling A. 2013. Systems biology: Mathematical modeling and model analysis. Syst Biol Math Model Model Anal 12:1–362; doi:10.1080/17513758.2017.1400121.

Kuepfer L, Niederalt C, Wendl T, Schlender J-F, Willmann S, Lippert J, et al. 2016. Applied Concepts in PBPK Modeling: How to Build a PBPK/PD Model. CPT Pharmacometrics Syst Pharmacol 5:516–531; doi:10.1002/psp4.12134.

Kuo C-C, Moon K, Thayer KA, Navas-Acien A. 2013. Environmental Chemicals and Type 2 Diabetes: An Updated Systematic Review of the Epidemiologic Evidence. Curr Diab Rep 13:831–849; doi:10.1007/s11892-013-0432-6.

Lauretta R, Sansone A, Sansone M, Romanelli F, Appetecchia M. 2019. Endocrine disrupting chemicals: Effects on endocrine glands. Front Endocrinol (Lausanne) 10:178; doi:10.3389/fendo.2019.00178.

Lin L, Wong H. 2017. Predicting oral drug absorption: Mini review on physiologically-based pharmacokinetic models. Pharmaceutics 9:41; doi:10.3390/pharmaceutics9040041.

Lin Z, Li M, Wang YS, Tell LA, Baynes RE, Davis JL, et al. 2020. Physiological parameter values for physiologically based pharmacokinetic models in food-producing animals. Part I: Cattle and swine. J Vet Pharmacol Ther 43:385–420; doi:10.1111/jvp.12861.

Malik MY, Jaiswal S, Sharma A, Shukla M, Lal J. 2016. Role of enterohepatic recirculation in drug disposition: cooperation and complications. Drug Metab Rev 48:281–327; doi:10.3109/03602532.2016.1157600.

Masjosthusmann S, Barenys M, El-Gamal M, Geerts L, Gerosa L, Gorreja A, et al. 2018. Literature review and appraisal on alternative neurotoxicity testing methods. EFSA Support Publ 15; doi:10.2903/sp.efsa.2018.EN-1410.

Masuo Y, Ishido M. 2011. Neurotoxicity of Endocrine Disruptors: Possible Involvement in Brain Development and Neurodegeneration. J Toxicol Environ Heal Part B 14:346–369; doi:10.1080/10937404.2011.578557.

Mayer P, Mayer B, Mayer G. 2012. Systems biology building a useful model from multiple markers and profiles. Nephrol Dial Transplant 27:3995–4002; doi:10.1093/ndt/gfs489.

McNamara PJ, Alcorn J. 2002. Protein binding predictions in infants. AAPS PharmSci 4:19–26; doi:10.1208/ps040104.

Meistelman C, Benhamou D, Barre J, Levron J-C, Mahe V, Mazoit X, et al. 1990. Effects of Age on Plasma Protein Binding of Sufentanil. Anesthesiology 72:470–473; doi:10.1097/00000542-199003000-00013.

Mršulja BB, Mršulja BJ, Fujimoto T, Klatzo I, Spatz M. 1976. Isolation of brain capillaries: a simplified technique. Brain Res 110:361–365; doi:10.1016/0006-8993(76)90408-X.

Neuhaus W. 2020. In Vitro Models of the Blood-Brain Barrier. In: (M. Schäfer-Korting, S. Stuchi Maria-Engler, and R. Landsiedel, eds). Springer International Publishing:Cham. 75–110.

Nicolotti O, Benfenati E, Carotti A, Gadaleta D, Gissi A, Mangiatordi GF, et al. 2014. REACH and in silico methods: an attractive opportunity for medicinal chemists. Drug Discov Today 19:1757–1768; doi:10.1016/j.drudis.2014.06.027.

Peyret T, Poulin P, Krishnan K. 2010. A unified algorithm for predicting partition coefficients for PBPK modeling of drugs and environmental chemicals. Toxicol Appl Pharmacol 249:197–207; doi:10.1016/j.taap.2010.09.010.

Poulin P, Krishnan K. 1996. A Mechanistic Algorithm for Predicting Blood:Air Partition Coefficients of Organic Chemicals with the Consideration of Reversible Binding in Hemoglobin. Toxicol Appl Pharmacol 136:131–137; doi:https://doi.org/10.1006/taap.1996.0016.

Poulin P, Krishnan K. 1995. An algorithm for predicting tissue : Blood partition coefficients of organic chemicals from n -octanol: Water partition coefficient data. J Toxicol Environ Health 46:117–129; doi:10.1080/15287399509532021.

Poulin P, Theil F. 2000. A Priori Prediction of Tissue:Plasma Partition Coefficients of Drugs to Facilitate the Use of Physiologically-Based Pharmacokinetic Models in Drug Discovery. J Pharm Sci 89:16–35; doi:10.1002/(SICI)1520-6017(200001)89:1<16::AID-JPS3>3.0.CO;2-E.

Rodgers T, Rowland M. 2006. Physiologically based pharmacokinetic modelling 2: Predicting the tissue distribution of acids, very weak bases, neutrals and zwitterions. J Pharm Sci 95:1238–1257; doi:10.1002/jps.20502.

Santaliz Casiano A, Lee A, Teteh D, Madak Erdogan Z, Treviño L. 2022. Endocrine-Disrupting Chemicals and Breast Cancer: Disparities in Exposure and Importance of Research Inclusivity. Endocrinol (United States) 163:bqac034; doi:10.1210/endocr/bqac034.

Sasidharakurup H, Diwakar S. 2020. Computational modelling of TNFα related pathways regulated by neuroinflammation, oxidative stress and insulin resistance in neurodegeneration. Appl Netw Sci 5:72; doi:10.1007/s41109-020-00307-w.

Schmitt W. 2008. General approach for the calculation of tissue to plasma partition coefficients. Toxicol Vitr 22:457–467; doi:10.1016/j.tiv.2007.09.010.

Sharma RP, Schuhmacher M, Kumar V. 2018. The development of a pregnancy PBPK Model for Bisphenol A and its evaluation with the available biomonitoring data. Sci Total Environ 624:55–

68; doi:10.1016/j.scitotenv.2017.12.023.

Sutton P, Woodruff TJ, Perron J, Stotland N, Conry JA, Miller MD, et al. 2012. Toxic environmental chemicals: the role of reproductive health professionals in preventing harmful exposures. Am J Obstet Gynecol 207:164–173; doi:10.1016/j.ajog.2012.01.034.

US EPA. 2016. Exploring ToxCast Data: Downloadable Data. Available: https://www.epa.gov/chemical-research/exploring-toxcast-data-downloadable-data.

Valentin J. 2002. Basic anatomical and physiological data for use in radiological protection: reference values. Ann ICRP 32:1–277; doi:10.1016/S0146-6453(03)00002-2.

Weksler BB, Subileau EA, Perrière N, Charneau P, Holloway K, Leveque M, et al. 2005. Blood-brain barrier-specific properties of a human adult brain endothelial cell line. FASEB J 19:1872–1874; doi:10.1096/fj.04-3458fje.

Wilhelm I, Fazakas C, Krizbai IA. 2011. In vitro models of the blood-brain barrier. Acta Neurobiol Exp (Wars) 71: 113–128.

Yim D-S, Choi S, Bae SH. 2020. Predicting human pharmacokinetics from preclinical data: absorption. Transl Clin Pharmacol 28:126; doi:10.12793/tcp.2020.28.e14.

Zoeller RT, Brown TR, Doan LL, Gore AC, Skakkebaek NE, Soto AM, et al. 2012. Endocrine-Disrupting Chemicals and Public Health Protection: A Statement of Principles from The Endocrine Society. Endocrinology 153:4097–4110; doi:10.1210/en.2012-1422.

Egeghy, Peter P et al. 2012. “The Exposure Data Landscape for Manufactured Chemicals.” *Science of The Total Environment* 414: 159–66. https://www.sciencedirect.com/science/article/pii/S0048969711012393.

Johnson, Andrew C., Xiaowei Jin, Norihide Nakada, and John P. Sumpter. 2020. “Learning from the Past and Considering the Future of Chemicals in the Environment.” *Science* 367(6476): 384–87. https://doi.org/10.1126/science.aay6637.

Kortenkamp, Andreas et al. 2022. “Combined Exposures to Bisphenols, Polychlorinated Dioxins, Paracetamol, and Phthalates as Drivers of Deteriorating Semen Quality.” *Environment International*: 107322. https://www.sciencedirect.com/science/article/pii/S0160412022002495.

UNIVERSITAT ROVIRA I VIRGILI
QUANTITATIVE SYSTEMS TOXICOLOGY MODELING FOR NEURONAL ADVERSE OUTCOME
Deepika

Annex for Chapter 1

Table 1: Combination of different search string for database search

Search String for Scopus	**Number of articles**
In vitro	
in vitro AND neurotoxicity AND flame retardants	67
In vitro AND neurotoxicity & fr	8
in vitro AND neurotoxicity AND pfos	7
in vitro AND neurotoxicity AND perfluorooctane sulfonic acid	5
in vitro AND neurotoxicity AND pfoa	5
in vitro AND neurotoxicity AND perfluorooctanoic acid	8
in vitro AND neurotoxicity AND pcb	41
In vitro AND neurotoxicity AND polychlorinated biphenyls	59
in vitro AND neurotoxicity AND bpa	17
in vitro AND neurotoxicity AND bisphenol a	24
in vitro AND neurotoxicity AND phthalates	14
In vivo	
in vivo AND neurotoxicity AND flame retardants	35
in vivo AND neurotoxicity AND fr	11
in vivo AND neurotoxicity AND pfos	7

in vivo AND neurotoxicity AND perfluorooctane sulfonic acid	5
in vivo AND neurotoxicity AND pfoa	4
in vivo AND neurotoxicity AND perfluorooctanoic acid	7
in vivo AND neurotoxicity AND pcb	26
in vivo AND neurotoxicity AND polychlorinated biphenyls	36
in vivo AND neurotoxicity AND bpa	8
in vivo AND neurotoxicity AND bisphenol a	12
in vivo AND neurotoxicity AND phthalates	9
Epidemiology	
epidemiology AND neurotoxicity AND FR	0
epidemiology AND neurotoxicity AND flame retardants	6
epidemiology AND neurotoxicity AND pfos	1
epidemiology AND neurotoxicity AND perfluorooctane sulfonic acid	1
epidemiology AND neurotoxicity AND pfoa	2
epidemiology AND neurotoxicity AND perfluorooctanoic acid	2
epidemiology AND neurotoxicity AND pcb	11
epidemiology AND neurotoxicity AND polychlorinated biphenyls	11
epidemiology AND neurotoxicity AND bpa	4
epidemiology AND neurotoxicity AND bisphenol a	5

epidemiology AND neurotoxicity AND phthalates	6
In silico	
in silico AND neurotoxicity AND fr	0
in silico AND neurotoxicity AND flame retardants	1
in silico AND neurotoxicity AND pfos	0
in silico AND neurotoxicity AND perfluorooctane sulfonic acid	0
in silico AND neurotoxicity AND pfoa	0
in silico AND neurotoxicity AND perfluorooctanoic acid	0
in silico AND neurotoxicity AND pcb	1
in silico AND neurotoxicity AND polychlorinated biphenyls	2
in silico AND neurotoxicity AND bpa	0
in silico AND neurotoxicity AND bisphenol a	0
in silico AND neurotoxicity AND phthalates	1
ivive AND neurotoxicity AND fr	0
ivive AND neurotoxicity AND flame retardants	0
ivive AND neurotoxicity AND pfos	0
ivive AND neurotoxicity AND perfluorooctane sulfonic acid	0
ivive AND neurotoxicity AND pfoa	0
ivive AND neurotoxicity AND perfluorooctanoic acid	0

ivive AND neurotoxicity AND pcb	0
ivive AND neurotoxicity AND polychlorinated biphenyls	0
ivive AND neurotoxicity AND bpa	0
ivive AND neurotoxicity AND bisphenol a	1
ivive AND neurotoxicity AND phthalates	0
qivive AND neurotoxicity AND fr	0
qivive AND neurotoxicity AND flame retardants	0
qivive AND neurotoxicity AND pfos	0
qivive AND neurotoxicity AND perfluorooctane sulfonic acid	0
qivive AND neurotoxicity AND pfoa	0
qivive AND neurotoxicity AND perfluorooctanoic acid	0
qivive AND neurotoxicity AND pcb	0
qivive AND neurotoxicity AND polychlorinated biphenyls	0
qivive AND neurotoxicity AND bpa	0
qivive AND neurotoxicity AND bisphenol a	0
qivive AND neurotoxicity AND phthalates	0
pbpk AND neurotoxicity AND fr	0
pbpk AND neurotoxicity AND flame retardants	1
pbpk AND neurotoxicity AND pfos	1

pbpk AND neurotoxicity AND perfluorooctane sulfonic acid	1
pbpk AND neurotoxicity AND pfoa	0
pbpk AND neurotoxicity AND perfluorooctanoic acid	0
pbpk AND neurotoxicity AND pcb	1
pbpk AND neurotoxicity AND polychlorinated biphenyls	1
pbpk AND neurotoxicity AND bpa	1
pbpk AND neurotoxicity AND bisphenol a	1
pbpk AND neurotoxicity AND phthalates	0
systems biology AND neurotoxicity AND fr	2
systems biology AND neurotoxicity AND flame retardants	5
systems biology AND neurotoxicity AND pfos	2
systems biology AND neurotoxicity AND perfluorooctane sulfonic acid	2
systems biology AND neurotoxicity AND pfoa	1
systems biology AND neurotoxicity AND perfluorooctanoic acid	1
systems biology AND neurotoxicity AND pcb	4
systems biology AND neurotoxicity AND polychlorinated biphenyls	6
systems biology AND neurotoxicity AND bpa	1
systems biology AND neurotoxicity AND bisphenol a	1
systems biology AND neurotoxicity AND phthalates	0

pk AND neurotoxicity AND fr	0
pk AND neurotoxicity AND flame retardants	0
pk AND neurotoxicity AND pfos	0
pk AND neurotoxicity AND perfluorooctane sulfonic acid	0
pk AND neurotoxicity AND pfoa	0
pk AND neurotoxicity AND perfluorooctanoic acid	0
pk AND neurotoxicity AND pcb	0
pk AND neurotoxicity AND polychlorinated biphenyls	1
pk AND neurotoxicity AND bpa	0
pk AND neurotoxicity AND bisphenol a	0
pk AND neurotoxicity AND phthalates	0
pd AND neurotoxicity AND fr	0
pd AND neurotoxicity AND flame retardants	2
pd AND neurotoxicity AND pfos	1
pd AND neurotoxicity AND perfluorooctane sulfonic acid	0
pd AND neurotoxicity AND pfoa	0
pd AND neurotoxicity AND perfluorooctanoic acid	0
pd AND neurotoxicity AND pcb	4
pd AND neurotoxicity AND polychlorinated biphenyls	7

pd AND neurotoxicity AND bpa	3
pd AND neurotoxicity AND bisphenol a	4
pd AND neurotoxicity AND phthalates	0
qsar AND neurotoxicity AND fr	0
qsar AND neurotoxicity AND flame retardants	1
qsar AND neurotoxicity AND pfos	0
qsar AND neurotoxicity AND perfluorooctane sulfonic acid	0
qsar AND neurotoxicity AND pfoa	0
qsar AND neurotoxicity AND perfluorooctanoic acid	0
qsar AND neurotoxicity AND pcb	5
qsar AND neurotoxicity AND polychlorinated biphenyls	5
qsar AND neurotoxicity AND bpa	0
qsar AND neurotoxicity AND bisphenol a	0
qsar AND neurotoxicity AND phthalates	1
gsmn AND neurotoxicity AND fr	0
gsmn AND neurotoxicity AND flame retardants	0
gsmn AND neurotoxicity AND pfos	0
gsmn AND neurotoxicity AND perfluorooctane sulfonic acid	0
gsmn AND neurotoxicity AND pfoa	0

gsmn AND neurotoxicity AND perfluorooctanoic acid	0
gsmn AND neurotoxicity AND pcb	0
gsmn AND neurotoxicity AND polychlorinated biphenyls	0
gsmn AND neurotoxicity AND bpa	0
gsmn AND neurotoxicity AND bisphenol a	0
Search String for PubMed	**Number of articles**
In vitro	
in vitro AND neurotoxicity AND flame retardants	45
In vitro AND neurotoxicity & fr	53
in vitro AND neurotoxicity AND pfos	5
in vitro AND neurotoxicity AND perfluorooctane sulfonic acid	4
in vitro AND neurotoxicity AND pfoa	1
in vitro AND neurotoxicity AND perfluorooctanoic acid	3
in vitro AND neurotoxicity AND pcb	36
In vitro AND neurotoxicity AND polychlorinated biphenyls	43
in vitro AND neurotoxicity AND bpa	12
in vitro AND neurotoxicity AND bisphenol a	12
in vitro AND neurotoxicity AND phthalates	1
In vivo	

in vivo AND neurotoxicity AND fr	44
in vivo AND neurotoxicity AND flame retardants	20
in vivo AND neurotoxicity AND pfos	5
in vivo AND neurotoxicity AND perfluorooctane sulfonic acid	3
in vivo AND neurotoxicity AND pfoa	1
in vivo AND neurotoxicity AND perfluorooctanoic acid	3
in vivo AND neurotoxicity AND pcb	20
in vivo AND neurotoxicity AND polychlorinated biphenyls	20
in vivo AND neurotoxicity AND bpa	3
in vivo AND neurotoxicity AND bisphenol a	4
in vivo AND neurotoxicity AND phthalates	1
Epidemiology	
epidemiology AND neurotoxicity AND fr	67
epidemiology AND neurotoxicity AND flame retardants	7
epidemiology AND neurotoxicity AND pfos	3
epidemiology AND neurotoxicity AND perfluorooctane sulfonic acid	1
epidemiology AND neurotoxicity AND pfoa	5
epidemiology AND neurotoxicity AND perfluorooctanoic acid	3
epidemiology AND neurotoxicity AND pcb	5

epidemiology AND neurotoxicity AND polychlorinated biphenyls	26
epidemiology AND neurotoxicity AND bpa	5
epidemiology AND neurotoxicity AND bisphenol a	4
epidemiology AND neurotoxicity AND phthalates	3
In silico	
in silico AND neurotoxicity AND fr	4
in silico AND neurotoxicity AND flame retardants	3
in silico AND neurotoxicity AND pfos	1
in silico AND neurotoxicity AND perfluorooctane sulfonic acid	1
in silico AND neurotoxicity AND pfoa	0
in silico AND neurotoxicity AND perfluorooctanoic acid	0
in silico AND neurotoxicity AND pcb	1
in silico AND neurotoxicity AND polychlorinated biphenyls	1
in silico AND neurotoxicity AND bpa	0
in silico AND neurotoxicity AND bisphenol a	0
in silico AND neurotoxicity AND phthalates	0
ivive AND neurotoxicity AND fr	0
ivive AND neurotoxicity AND flame retardants	0
ivive AND neurotoxicity AND pfos	0

ivive AND neurotoxicity AND perfluorooctane sulfonic acid	0
ivive AND neurotoxicity AND pfoa	0
ivive AND neurotoxicity AND perfluorooctanoic acid	0
ivive AND neurotoxicity AND pcb	0
ivive AND neurotoxicity AND polychlorinated biphenyls	0
ivive AND neurotoxicity AND bpa	0
ivive AND neurotoxicity AND bisphenol a	0
ivive AND neurotoxicity AND phthalates	0
qivive AND neurotoxicity AND fr	0
qivive AND neurotoxicity AND flame retardants	0
qivive AND neurotoxicity AND pfos	0
qivive AND neurotoxicity AND perfluorooctane sulfonic acid	0
qivive AND neurotoxicity AND pfoa	0
qivive AND neurotoxicity AND perfluorooctanoic acid	0
qivive AND neurotoxicity AND pcb	0
qivive AND neurotoxicity AND polychlorinated biphenyls	0
qivive AND neurotoxicity AND bpa	0
qivive AND neurotoxicity AND bisphenol a	0
qivive AND neurotoxicity AND phthalates	0

pbpk AND neurotoxicity AND fr	0
pbpk AND neurotoxicity AND flame retardants	0
pbpk AND neurotoxicity AND pfos	1
pbpk AND neurotoxicity AND perfluorooctane sulfonic acid	1
pbpk AND neurotoxicity AND pfoa	0
pbpk AND neurotoxicity AND perfluorooctanoic acid	0
pbpk AND neurotoxicity AND pcb	1
pbpk AND neurotoxicity AND polychlorinated biphenyls	1
pbpk AND neurotoxicity AND bpa	0
pbpk AND neurotoxicity AND bisphenol a	0
pbpk AND neurotoxicity AND phthalates	0
systems biology AND neurotoxicity AND fr	2
systems biology AND neurotoxicity AND flame retardants	2
systems biology AND neurotoxicity AND pfos	2
systems biology AND neurotoxicity AND perfluorooctane sulfonic acid	1
systems biology AND neurotoxicity AND pfoa	1
systems biology AND neurotoxicity AND perfluorooctanoic acid	1
systems biology AND neurotoxicity AND pcb	1
systems biology AND neurotoxicity AND polychlorinated biphenyls	0

systems biology AND neurotoxicity AND bpa	5
systems biology AND neurotoxicity AND bisphenol a	5
systems biology AND neurotoxicity AND phthalates	1
Pharmacokinetic model AND neurotoxicity AND fr	0
Pharmacokinetic model AND neurotoxicity AND flame retardants	0
Pharmacokinetic model AND neurotoxicity AND pfos	0
Pharmacokinetic model AND neurotoxicity AND perfluorooctane sulfonic acid	0
Pharmacokinetic model AND neurotoxicity AND pfoa	0
Pharmacokinetic model AND neurotoxicity AND perfluorooctanoic acid	0
Pharmacokinetic model AND neurotoxicity AND pcb	2
Pharmacokinetic model AND neurotoxicity AND polychlorinated biphenyls	2
Pharmacokinetic model AND neurotoxicity AND bpa	0
Pharmacokinetic model AND neurotoxicity AND bisphenol a	0
Pharmacokinetic model AND neurotoxicity AND phthalates	0
Pharmacodynamic model AND neurotoxicity AND fr	0
Pharmacodynamic model AND neurotoxicity AND flame retardants	0
Pharmacodynamic model AND neurotoxicity AND pfos	0
Pharmacodynamic model AND neurotoxicity AND perfluorooctane sulfonic acid	0
Pharmacodynamic model AND neurotoxicity AND pfoa	0

Pharmacodynamic model AND neurotoxicity AND perfluorooctanoic acid	0
Pharmacodynamic model AND neurotoxicity AND pcb	0
Pharmacodynamic model AND neurotoxicity AND polychlorinated biphenyls	0
Pharmacodynamic model AND neurotoxicity AND bpa	0
Pharmacodynamic model AND neurotoxicity AND bisphenol a	0
Pharmacodynamic model AND neurotoxicity AND phthalates	0
qsar AND neurotoxicity AND fr	0
qsar AND neurotoxicity AND flame retardants	0
qsar AND neurotoxicity AND pfos	0
qsar AND neurotoxicity AND perfluorooctane sulfonic acid	0
qsar AND neurotoxicity AND pfoa	0
qsar AND neurotoxicity AND perfluorooctanoic acid	0
qsar AND neurotoxicity AND pcb	6
qsar AND neurotoxicity AND polychlorinated biphenyls	6
qsar AND neurotoxicity AND bpa	0
qsar AND neurotoxicity AND bisphenol a	0
qsar AND neurotoxicity AND phthalates	0
gsmn AND neurotoxicity AND fr	0
gsmn AND neurotoxicity AND flame retardants	0

gsmn AND neurotoxicity AND pfos	0
gsmn AND neurotoxicity AND perfluorooctane sulfonic acid	0
gsmn AND neurotoxicity AND pfoa	0
gsmn AND neurotoxicity AND perfluorooctanoic acid	0
gsmn AND neurotoxicity AND pcb	0
gsmn AND neurotoxicity AND polychlorinated biphenyls	0
gsmn AND neurotoxicity AND bpa	0
gsmn AND neurotoxicity AND bisphenol a	0
gsmn AND neurotoxicity AND phthalates	0
gsmn AND neurotoxicity AND phthalates	0

Table 2: Input and translation for in vitro neurotoxicity assessment

Abbreviations: mRNA- Messenger RNA, RyR- Ryanodine Receptors, ATP- Adenosine Triphosphate, Ahr- Aryl hydrocarbon receptor, CYP1A1 - Cytochrome P4501A1, CYP1b1- Cytochrome P4501B1, GnRH1-Gonadotropin Releasing Hormone 1, Bdnf- Brain-Derived Neurotrophic Factor, Ntrk2- NTRK2 neurotrophic receptor tyrosine kinase 2, qRT-PCR-Quantitative real-time Polymerase Chain Reaction , RIPK1- RIPK3-MLKL-Receptor interacting protein kinase 1–receptor interacting protein kinase 3–mixed lineage kinase domain-like axis, ChIP- Chromatin immunoprecipitation, Ca2+- Calcium, ROS- Reactive Oxygen Species, NO-CGMP- Nitric Oxide Cyclic Guanosine Monophosphate, NMDA- N-methyl-D-aspartate, MTT- 3-(4,5-dimethylthiazol-2-yl)-2,5-diphenyl tetrazolium bromide, PC12- Pheochromocytoma Cells 12, EB- Embryoid body, AP- Alkaline phosphatase, qRT-PCR- , RyR, VM- , DA- Dopamine, DOPAC- 3,4-dihydroxyphenylacetic acid, HVA- homovanillic acid, VM-ventral mesencephalon, GABA -, RH123- 123-dihydrorhodamine, TH+-, DAT- Dopamine transporter , GAD- glutamic acid decarboxylase, LDH- , ROS, MDA, CAT, GSH/GSSSG-, ChAT- Choline acetyltransferase, TH- tyrosine hydroxylase.

S. No.	Title	Input	Translation	References
	Functional and Mechanistic Neurotoxicity Profiling Using Human iPSC-Derived Neural 3D Cultures	Human induced pluripotent stem cell (iPSC)	Calcium Oscillation, Cell viability, Mitochondrial integrity, Gene expression, Cell Assay	(Sirenko et al. 2019)
	The environmental pollutant BDE-209 regulates NO/cGMP signaling through activation of NMDA receptors in neurons	Rodent neurons	mRNA expression, NO cGMP levels	(Chen et al. 2018)
	TBBPA and Its Alternatives Disturb the Early Stages of Neural Development by Interfering with the NOTCH and WNT Pathways	J1 mESCs	cell viability, ROS, Calcium ion level, Embryoid Body (EB)-based neural progenitor cell (NPC) induction, ESC monolayer neural differentiation, Protein level for MAP2	(Yin et al. 2018a)
	Brominated and organophosphate flame retardants target different neurodevelopmental stages, characterized with embryonic neural stem cells and neuronotypic PC12 cells	Embryonic rat neural stem cells (NSCs) Rat neuronotypic PC12 cells	NSC assays, DNA measurements, Total protein, NSC viability	(Slotkin et al. 2017)
	The involvement of autophagy and cytoskeletal regulation in TDCIPP-induced SH-SY5Y cell differentiation	Human neuroblastoma SH-SY5Y cell line	Cytoskeletal components, Cell viability, Quantification of neurite-bearing cells and neurite outgrowths, Acidic vesicular organelles	(Li et al. 2017a)
	TBBPA causes neurotoxic and the apoptotic responses in cultured mouse hippocampal neurons in vitro	Primary hippocampal neuron cultures	Activity of caspase-3- Apoptosis, Apoptotic body formation, Cell death and cell lysis	(Szychowski and Wójtowicz 2016)
	Multiparameter toxicity assessment of novel DOPO-derived organophosphorus flame retardants	LUHMES cells Human pluripotent stem cell (hPSC) line H9	Skin sensitization, Neural crest cell (NCC) migration, Viability, Cell morphology	(Hirsch et al. 2017)

			Intracellular levels of ATP and glutathione (GSH)	
	A comparison of the in vitro cyto- and neurotoxicity of brominated and halogen-free flame retardants: prioritization in search for safe(r) alternatives	Rat PC12 pheochromocytoma cells Rat B35 neuroblastoma cells	Cell viability, ROS, Calcium homeostasis	(Hendriks et al. 2014)
	Changes in mitogen-activated protein kinase in cerebellar granule neurons by polybrominated diphenyl ethers and polychlorinated biphenyls	Cerebellar granule cell culture	Phosphorylated extracellular signal-regulated kinase (pERK)1/2, Western blot, Cytotoxicity	(Fan et al. 2010)
	Polybrominated Diphenyl Ethers Induce Developmental Neurotoxicity in a Human in Vitro Model: Evidence for Endocrine Disruption	Primary fetal human neural progenitor cells (hNPCs)	Viability assay, Proliferation analyses, Migration, Calcium imaging	(Götz et al. 2009)
	Neurotoxicity of a polybrominated diphenyl ether mixture (DE-71) in mouse neurons and astrocytes is modulated by intracellular glutathione levels	Cerebellar granule neurons Hippocampal neurons and cortical neurons	Cytotoxicity, Apoptosis by DNA fragmentation, GSH levels, ROS, Lipid peroxidation	(Giordano et al. 2008)
	Multiple Novel Modes of Action Involved in the In Vitro Neurotoxic Effects of Tetrabromobisphenol-A	B35 rat neuroblastoma cells, PC12 rat pheochromocytoma cells	Cell viability, ROS, Caspase activation, Calcium levels	(Hendriks et al. 2012)
	The role of the IRE1 pathway in PBDE-47-induced toxicity in human neuroblastoma SH-SY5Y cells in vitro	Human neuroblastoma SH-SY5Y cells	ROS, Apoptosis, Inositol-requiring enzyme 1 (IRE1), Western blotting	(Jiang et al. 2012)
	Some Commonly Used Brominated Flame Retardants Cause Ca2+ -ATPase Inhibition, Beta-Amyloid Peptide Release and Apoptosis in SH-SY5Y Neuronal Cells	SH-SY5Y Neuroblastoma cells	Cell Viability, Caspase activity, Cytochrome c Release, Measurement of Mitochondrial Membrane Potential, ROS, Calcium ATPase	(Al-Mousa and Michelangeli 2012)

	Synergistic neurotoxicity of oxygen-glucose deprivation and tetrabromobisphenolA in vitro: role of oxidative stress	Cell culture	Acute cytotoxicity, Calcium levels, Changes in mitochondrial membrane potential, ROS	(Ziemińska et al. 2012)
	Role of glutamate receptors in tetrabrominated diphenyl ether (BDE47) neurotoxicity in mouse cerebellar granule neurons	Cultures of cerebellar granule neurons (CGNs)	Cytotoxicity, Glutamate release, ROS, Lipid peroxidation, Calcium levels	(Costa et al. 2016)
	BDE-47 and BDE-49 Inhibit Axonal Growth in Primary Rat Hippocampal Neuron-Glia Co-Cultures via Ryanodine Receptor-Dependent Mechanisms	Neuronal-glial co-cultures Primary hippocampal cell cultures	Dendritic & axonal lengths, Cytotoxicity Analyses, Tau-1 levels, Immunocytochemical Localization of RyR	(Chen et al. 2017)
	Hexabromocyclododecane Inhibits Depolarization-Induced Increase in Intracellular Calcium Levels and Neurotransmitter Release in PC12 Cells	PC12 cell culture Rat pheochromocytoma (PC12) cells	Cell viability, Calcium levels, Vesicular catecholamine	(Dingemans et al. 2009)
	Evaluation of the early developmental neural toxicity of F-53B, as compared to PFOS, with an in vitro mouse stem cell differentiation model	J1 mouse embryonic stem cells (J1mESCs)	Embryoid body (EB) differentiation assay, Adherent monolayer neural differentiation, cell viability, ROS, Western blot	(Yin et al. 2018b)
	Possible mechanism of perfluorooctane sulfonate and perfluorooctanoate on the release of calcium ion from calcium stores in primary cultures of rat hippocampal neurons	Cultured neuron in rat hippocampus	ROS, Calcium ion content	(Liu et al. 2011)
	Developmental Neurotoxicity of Perfluorinated Chemicals Modeled in Vitro	PC 12 Cell culture	DNA synthesis, Lipid peroxidation, Viability, Enzyme activity	(Slotkin et al. 2008)

	Sensitive neurotoxicity assessment of bisphenol A using double immunocytochemistry of DCX and MAP2	Primary cultured neurons	Western blot, Cytotoxicity, ROS, Doublecortin (DCX) and microtubule-associated protein 2 (MAP2)	(Cho et al. 2018)
	High content imaging quantification of multiple in vitro human neurogenesis events after neurotoxin exposure	Cryopreserved hNP cells	Cell proliferation assay, Western blotting	(Wu et al. 2016)
	Bisphenol A promotes dendritic morphogenesis of hippocampal neurons through estrogen receptor-mediated ERK1/2 signal pathway	Hippocampal neurons primary culture	Time-lapse imaging of living neurons and quantification, Filopodia determination and density, Western blotting	(Xu et al. 2014)
	In vitro evaluation of gene expression changes for gonadotropin-releasing hormone 1, brain-derived neurotrophic factor and neurotrophic tyrosine kinase receptor type 2, in response to bisphenol A treatment	Embryonic mouse hypothalamus cell line N44.	GnRH1, Bdnf and Ntrk2 levels	(Warita et al. 2013)
	Bisphenol A is released from polycarbonate drinking bottles and mimics the neurotoxic actions of estrogen in developing cerebellar neurons	Primary cerebellar cultures	Cytotoxicity	(Le et al. 2008)
	Assessment of Bisphenol A (BPA) neurotoxicity in vitro with mouse embryonic stem cells	mESC differentiation into neural progenitor cells (NPCs)	Cytotoxicity, Embryoid body (EB) differentiation	(Yin et al. 2015)
	Estrogen receptor independent neurotoxic mechanism of bisphenol A, an environmental estrogen	Cell culture PC12 cells PC12/ER-α and PC12/ER-β cells	Cell viability, Apoptotic cells, Western blotting, Density of DNA binding bands	(Yoot et al. 2007)
	The Action of Di-(2-Ethylhexyl) Phthalate (DEHP) in Mouse Cerebral Cells Involves	Cultured mouse neurons and glial cells	ROS, Ahr, CYP1a1,and CYP1b1, Intracellular esterase activity, cell	(Wójtowicz et al. 2019)

	an Impairment in Aryl Hydrocarbon Receptor (AhR) Signaling		morphology, cell metabolic activity, cell viability	
	Classification of phthalates based on an in vitro neurosphere assay using rat mesencephalic neural stem cells	Rat mesencephalic neural stem cell	Neurosphere assay, Terminal deoxynucleotidyl transferase-mediated dUTP nick end-labelling (TUNEL)- cell migration, Cell proliferation, Apoptosis	(Ishido and Suzuki 2014)
	Primary neuronal-astrocytic co-culture platform for neurotoxicity assessment of di-(2-ethylhexyl) phthalate	Primary neuronal-astrocyte co-culture	ROS, Neuronal number, count and length	(Wu et al. 2014)
	Mono-(2-ethylhexyl) phthalate impairs neurodevelopment: Inhibition of proliferation and promotion of differentiation in PC12 cells	PC12 cells	Cell growth , Cell viability, DNA synthesis, Cellular DNA content, Oxidative stress, Total protein content, Neurite outgrowth, Subcellular proteins, Gene expression	(Chen et al. 2011)
	Insight into the neuroproteomics effects of the food-contaminant non-dioxin like polychlorinated biphenyls	Cerebellar neurons	Pre- and post-synaptic proteins, synaptic markers, Protein concentration, Total RNA, synaptic proteins- Cerebellum protein	(Fanelli et al. 2012)
	3,3′-Dichlorobiphenyl (PCB 11) promotes dendritic arborization in primary rat cortical neurons via a CREB-dependent mechanism	Primary rat cortical cell culture, Primary cortical neuron–glia co-cultures	Luciferase activity, Morphometric analyses of dendritic arborisation, Aryl hydrocarbon receptor, Thyroid hormone receptor (THR), cAMP response element-binding protein (CREB)	(Sethi et al. 2018)
	Species and Sex Differences in the Morphogenic Response of Primary Rodent Neurons to 3,30 -Dichlorobiphenyl (PCB 11)	Primary cortical and hippocampal neuron-glia co-cultures	Neuronal morphology, Total axonal length, Dendritic arborization , Dendritic Analyses, Axonal Outgrowth, Axonal lengths	(Sethi et al. 2017)

	The neurotoxicant PCB-95 by increasing the neuronal transcriptional repressor REST down-regulates caspase-8 and increases Ripk1, Ripk3 and MLKL expression determining necroptotic neuronal death	SH-SY5Y human neuroblastoma cells Cortical neurons (DIV 7–9) from rat embryos	Luciferase assay, qRT-PCR analysis, RIPK1- RIPK3-MLKL interactions, caspase-8 promoter, Transient transfection ChIP, cell death	(Canzoniero et al. 2017)
	Non–Dioxin-like Polychlorinated Biphenyls Interfere with Neuronal Differentiation of Embryonic Neural Stem Cells	Primary cultures of NSCs	Cell viability, Total cell number, Apoptotic cells, Cell cycle, total Notch, Ca2+ levels, Cell differentiation, Proliferation	(Tofighi et al. 2011)
	Differential Effects of 20 Non–Dioxin-Like PCBs on Basal and Depolarization-Evoked Intracellular Calcium Levels in PC12 Cells	Undifferentiated rat pheochromocytoma (PC12) cells	Changes in Free cytosolic & Basal Calcium	(Langeveld et al. 2012)
	Polychlorinated Biphenyls PCB 153 and PCB 126 Impair the Glutamate–Nitric Oxide–cGMP Pathway in Cerebellar Neurons in Culture by Different Mechanisms	Primary cultures of cerebellar neurons	Neuronal Viability, Basal cGMP, Glutamate–NO–cGMP Pathway, Soluble Guanylate Cyclase, NMDA, Calcium Concentration	(Rodrigo et al. 2009)
	An in vitro approach to assess the toxicity of certain food contaminants: Methylmercury and polychlorinated biphenyls	PC12 rat pheocromocytoma cells, SH-SY5Y human neuroblastoma cells, C6 rat glioma cells, 1321N1 human astrocytoma cells, NIH 3T3 mouse fibroblasts, PZ-HPV-7 human prostate cells, LNCaP human prostate carcinoma cells, TT human thyroid cells.	MTT reduction, Trypan blue exclusion, 3H-thymidine incorporation into DNA, Cell proliferation	(Costa et al. 2007)

		Cultures of primary cortical and hippocampal neurons Cerebellar neurons Cerebellar granule cells Cerebellar Purkinje cells Primary rat astrocytes		
	Neurotoxicity of the pentabrominated diphenyl ether mixture, DE-71, and hexabromocyclododecane (HBCD) in rat cerebellar granule cells in vitro	Cerebellar granule cells	ROS, Biotransforming enzyme systems, calcium measurement, Nuclear morphology, Caspase-3 activity	(Reistad et al. 2006)
	Mouse cerebellar astrocytes protect cerebellar granule neurons against toxicity of the polybrominated diphenyl ether (PBDE) mixture DE-71	Cultures of cerebellar granule neurons and cerebellar astrocytes, Co-cultures of neurons and astrocytes	GSH levels, cell viability, cytotoxicity assay, IC50	(Giordano et al. 2009)
	Assessment of Bisphenol A (BPA) neurotoxicity in vitro with mouse embryonic stem cells	mESCs	Cytotoxicity assay, AP staining (undifferentiated cells), EB differentiation assay, Adherent cell neuroectoderm differentiation, qRT-PCR analyses	(Yin et al. 2015)
	From the Cover: BDE-47 and BDE-49 Inhibit Axonal Growth in Primary Rat Hippocampal Neuron-Glia Co-Cultures via Ryanodine Receptor-Dependent Mechanisms	Rat Hippocampal Neuron-Glia Co-Cultures	Dendritic length, quantify axons, neuronal cell polarity, Cytotoxicity Analyses, Western Blot Analysis of Tau-1, Immunocytochemical Localization of RyR	(Chen et al. 2017)
	The environmental neurotoxicant PCB 95 promotes synaptogenesis via ryanodine receptor-dependent miR132 upregulation.	Hippocampal neurons culture	Dendritic spine imaging and quantification, RyR activity, synaptogenesis (mRFP-β-actin, synapsin1), CREB-miR132-p250GAP signaling	(Lesiak et al. 2014)

	Role of N-methyl-D-aspartate receptors in polychlorinated biphenyl mediated neurotoxicity	Human SH-SY5Y neuroblastoma cells	Cell viability, Caspase activation assay, NMDA receptor binding, Protein content	(Ndountse and Chan 2009)
	Polychlorinated Biphenyl-Induced Oxidative Stress in Organotypic Co-Cultures: Experimental Dopamine Depletion Prevents Reductions in Gaba	Organotypic co-cultures of VM and striatum	Levels of DA, DOPAC, HVA, VM &GABA, Glutathione Analysis	(Lyng and Seegal 2008)
	Polychlorinated Biphenyl–Induced Neurotoxicity in Organotypic Cocultures of Developing Rat Ventral Mesencephalon and Striatum	VM and striatum organotypic cocultures	Levels of DA, DOPAC, HVA, Neuronal cell death, protein levels	(Lyng et al. 2007)
	Evaluation of PFOS-mediated neurotoxicity in rat primary neurons and astrocytes cultured separately or in co-culture	Astrocyte–neurons co-cultures system	Cell viability, LDH cytotoxicity assay, ROS production, MDA content, SOD activity, CAT activity, GSH/GSSG dose, apoptotic cell damage, cell autophagy, mRNA expression, Glutamate and glutamine concentrations, Glutamine synthase activity, Neuronal degeneration	(Li et al. 2017b)
	BDE-47 and 6-OH-BDE-47 modulate calcium homeostasis in primary fetal human neural progenitor cells via ryanodine receptor-independent mechanisms	Normal hNPCs	Calcium imaging, Cell viability	(Gassmann et al. 2014)
	Is the PentaBDE Replacement, Tris (1,3-dichloro-2-propyl) Phosphate (TDCPP), a Developmental Neurotoxicant? Studies in PC12 Cells	PC12 cells	DNA and proteins, Oxidative stress (MDA content), Cell viability, Enzyme activities (ChAT, TH assay),	(Dishaw et al. 2011)

	A hydroxylated metabolite of flame-retardant PBDE-47 decreases the survival, proliferation, and neuronal differentiation of primary cultured adult neural stem cells and interferes with signaling of ERK5 MAP kinase and neurotrophin 3.	Primary aNSC cultures	Cell viability, Proliferation, Differentiation, Western blot analysis (EGF , bFGF & ERK5)	(Li et al. 2013)
	Low concentrations of the brominated flame retardants BDE-47 and BDE-99 induce synergistic oxidative stress-mediated neurotoxicity in human neuroblastoma cells.	Human neuroblastoma SK-N-MC cell line	Cytotoxicity assay (MTT), ROS formation, lipid peroxidation,	(Tagliaferri et al. 2010)

Table 3: Input and translation for *in vivo* neurotoxicity assessment

Abbreviations: DNA- Deoxyribonucleic Acid, RNA- Ribonucleic acid, qRT-PCR- Quantitative real-time polymerase chain reaction, ROS- Reactive Oxygen Species, TDCPP- Tris(1,3-dichloroisopropyl)phosphate, BDCPP- Bis (1,3-dichloro-2-propyl) Phosphate, GAP43- Growth Associated Protein 43, GFAP- Glial Fibrillary Acidic Protein, MBP- Myelin basic protein, synIIa- Synapsin IIa, LTP- Long-Term Potentiation, CaMK-II- Calcium/calmodulin-dependent protein kinase type II, GluR1- Glutamate receptor 1, PSD 95- Postsynaptic Density 95, f-EPSP- Field-excitatory postsynaptic potential, Ca2+ - Calcium, IL-10- Interleukin 10, mRNA- Messenger RNA, Cgmp- Cyclic guanosine monophosphate, GABA- Gamma-aminobutyric acid, APP- Amyloid precursor protein, AP-1- Activator protein 1, NF-Kb- nuclear factor kappa-light-chain-enhancer of activated B cells and CREB- cAMP response element-binding protein, DAT- Monoclonal anti-rat dopamine transporter, TH- polyclonal rabbit anti-tyrosine hydroxylase, COMT- anti-Catechol-O-Methyltransferase antibodies, NET- Antinorepinephrine transporter, VMAT2- anti-vesicular monoamine transporter 2, D1R- anti-dopamine D1 receptor, D2R- anti-dopamine D2 receptor, MAO-B- Monoamine oxidase B.

S.No.	**Title**	**Input**	**Translation**	**References**
	Neurological responses of embryo-larval zebrafish to short-term sediment exposure to decabromodiphenylethane	Adult zebrafish	Histopathology, Touch-escape response, Free swimming activity, Acetylcholinesterase activity, Gene expression, Apoptotic cell death	(Zhang et al. 2018)

	Profiling of Selected Functional Metabolites in the Central Nervous System of Marine Medaka (Oryziasmelastigma) for Environmental Neurotoxicological Assessments	Marine Medaka (Oryzaismelastigma)	Protein concentrations, Functional metabolites, Metabolic Pathway Analysis and Visualization	(Lei et al. 2017)
	Intranasal administration of tetrabromobisphenol A bis(2-hydroxyethyl ether) induces neurobehavioral changes in neonatal Sprague Dawley rats	Male neonatal rats	Histopathological study, Microarray analysis, Genomic DNA contamination, Physiological observation, Bioinformatics analysis of microarray data, Rotarod test, Open field test	(Liu et al. 2018)
	Tetrabromobisphenol A caused neurodevelopmental toxicity via disrupting thyroid hormones in zebrafish larvae	Zebrafish embryos	RNA, Thyroid hormone, Acetylcholinesterase activity, Locomotor activity, Gene transcription	(Zhu et al. 2018)
	Bioconcentration and transfer of the organophorous flame retardant 1,3-dichloro-2-propyl phosphate causes thyroid endocrine disruption and developmental neurotoxicity in zebrafish larvae	Adult zebrafish	Thyroid hormone, qRT-PCR, Protein extraction, Neurotransmitter measurements, Larval locomotor behavior, Larval acetylcholinesterase, ROS, Quantification of TDCPP and BDCPP, Protein Expression(MBP, GAP-43, synIIa, and GFAP)	(Wang et al. 2015)
	Effects of neonatal exposure to the flame retardant tetrabromobisphenol-A, aluminumdiethylphosphinate or zinc stannate on long-term potentiation and synaptic protein levels in mice	Male C57bl/6 mice	Ex vivo extracellular field recordings, Levels of postsynaptic proteins involved in LTP, Concentrations in brain, muscle and liver tissues, Synaptic transmission and activity-dependent plasticity, Slot-blot analysis for CaMK-II, GAP-43, GluR1, PSD 95 and synaptophysin protein expression, Internal dose analysis	(Lee et al. 2014)
	Neurotoxicological and thyroid evaluations of rats developmentally exposed to tris(1,3-dichloro-2-propyl)phosphate (TDCIPP) and tris(2-chloro-2-ethyl)phosphate (TCEP)	Pregnant Long Evans rats	Body weight, Righting reflex development, Brain weights, Motor activity, Behavioral testing, Standard locomotor activity, Elevated	(Moser et al. 2015)

			zero maze, Morris water maze, Thyroid hormone, Acetylcholinesterase	
	Neonatal Exposure to Brominated Flame Retardant BDE-47 Reduces Long-Term Potentiation and Postsynaptic Protein Levels in Mouse Hippocampus	C57Bl/6 mice	Postsynaptic proteins in LTP, Catecholamine, f-EPSP Proteins, Ca2+ levels	(Dingemans et al. 2007)
	Effects of Decabrominated Diphenyl Ether (PBDE 209) Exposure at Different Developmental Periods on Synaptic Plasticity in the Dentate Gyrus of Adult Rats In Vivo	Wistar rats	Input/output functions, Paired-pulse reactions, LTP Population spike amplitude, Hippocampus PBDE 209 determination	(Ruan et al. 2009)
	1 H-nuclear magnetic resonance metabolomics revealing the intrinsic relationships between neurochemical alterations and neurobehavioral and neuropathological abnormalities in rats exposed to tris(2-chloroethyl)phosphate	Female SD rats	Morris water maze, Histopathology, Metabolic pathways and enrichment analysis, Body weight	(Yang et al. 2018)
	Effects of perfluorooctane sulfonate and its alternatives on long-term potentiation in the hippocampus CA1 region of adult rats in vivo	Adult male SD rats	fEPSP, Input/output functions, Paired-pulse facilitations, LTP	(Zhang et al. 2016)
	Does developmental exposure to perflurooctanoic acid (PFOA) induce immunopathologies commonly observed in neurodevelopmental disorders?	Male and female C57BL/6N mice	Splenic Treg percentage, IL-10 production, Serum autoantibodies, T cell infiltration and myelin basic protein levels in cerebella	(Morris et al. 2012)
	Cognitive deficits and anxiety induced by diisononyl phthalate in mice and the neuroprotective effects of melatonin	Mice	Morris water maze, Open field test, Histopathological changes, Expression of caspase-3 and GFAP, ROS	(Ma et al. 2015)
	Phthalates Induce Neurotoxicity Affecting Locomotor and Thermotactic Behaviors and AFD Neurons through Oxidative Stress in Caenorhabditis elegans	Nematodes wild-type N2; DA1267, C. elegans, Escherichia coli OP50	Locomotor behaviors, Thermotacticbehaviors on AFD neurons, mRNA levels, ROS	(Tseng et al. 2013)

	Perinatal exposure to environmental polychlorinated biphenyls sensitizes hippocampus to excitotoxicity ex vivo	Time-mated rat dams	Field excitatory postsynaptic potentials (fEPSPs)	(Kim and Pessah 2011)
	Developmental Exposure To Polychlorinated Biphenyls 52, 138 Or 180 Affects Differentially Learning Or Motor Coordination In Adult Rats. Mechanisms Involved	Female rats	Y maze learning test, NO-CGMP, GABA and glutamate levels, Rotarod test	(Boix et al. 2010)
	Neurobehavioral assessment of rats exposed to low doses of PCB126 and methyl mercury during development	Female and male Wistar rats	Effects on pregnancy, body weight, Pre-weaning & Post-weaning tests, Open field test, Sudden silence test, Morris water maze test, Rotarod test, Novel object exploration test, Elevated plus maze test, Passive avoidance, Hg and PCB126 levels	(Vitalone et al. 2008)
	Polychlorinated biphenyls alter expression of αsynuclein, synaptophysin and parkin in the rat brain	Wistar rats	Brain weight, α-synuclein, parkin, synaptophysin and APP	(Malkiewicz et al. 2006)
	Ontogenetic alterations in prototypical transcription factors in the rat cerebellum and hippocampus following perinatal exposure to a commercial PCB mixture	Pregnant rats (Long Evans)	DNA-binding of various transcription factors (Sp1, AP-1, NF-kB and CREB), Nuclear transcription factors	(Basha et al. 2006)
	Polychlorinated biphenyls increase apoptosis in the developing rat brain	Rat pups	Apoptosis, Caspase-3 activity	(Yang and Lein 2010)
	Neurochemical changes following a single dose of polybrominated diphenyl ether 47 in mice	C57BL/6 mice	Monoamines concentration in Cortex, striatum and cerebellum	(Gee et al. 2011)
	Impairment in the mesohippocampal dopamine circuit following exposure to the brominated flame retardant, HBCDD	C57BL/6J mice	Western Blot Analysis (DAT, TH, VMAT2, D1R, D2R, NET, COMT, MAO-B, and β-actin) in hippocampus, Immunohistochemistry	(Pham-Lake et al. 2017)

Table 4: Input and translation for epidemiology neurotoxicity assessment

Abbreviations: WPPSI-Wechsler Preschool and Primary Scale of Intelligence, WISC- Wechsler Intelligence Scale for Children, BASC- Behavior Assessment System for Children, MDI- Major Depression Inventory, MSEL- Mullen Scales of Early Learning, ICCs-Intraclass correlation coefficients, BSID- Bayley Scales of Infant Development, BRIEF- Behavior Rating Inventory of Executive Function, VMWM- Virtual Water Maze Test, WASI- Wechsler Abbreviated Scale of Intelligence, WJ- Woodcock–Johnson Tests of Achievement, WRAT- Wide Range Achievement Test, LASSO-Least absolute shrinkage and selection operator test, ALS- Amyotrophic Lateral Sclerosis, BDI-II- Beck's depression inventory, SDQ-Strengths and Difficulties Questionnaire, CBCL/4-16- Child Behavior Checklist/4-16, SNAP-IV- Swanson, Nolan, and Pelham IV scale, CPT-II-Conners' continuous performance test–II, BRIEF-P- Behavior Rating Inventory of Executive Function–Preschool Version, WQS- Weighted Quantile Sum.

S.No.	Title	Input	Translation	Reference
	Prenatal environmental chemical exposures and longitudinal patterns of child neurobehavior	346 mother-child pairs	Urine analysis, Serum concentration, Neurobehavioral battery: BSID II, WPPSI III, WISC IV, MDI score and BASC-2, Linear mixed models, ICCs	(Braun et al. 2017)
	Brominated Flame Retardants in Breast Milk and Behavioural and Cognitive Development at 36 Months	304 mothers and their children	Breast milk concentration, BASC-2, MSEL, Multivariable robust regression	(Adgent et al. 2014)
	Prenatal exposure to perfluorinated chemicals and neurodevelopment in early infancy: The Hokkaido Study	514 mother infant pairs	BSID II, Maternal serum, Blood, Questionnaires and medical records, Spearman rank correlation coefficient, Mann–Whitney U-test, Kruskal–Wallis test, Multiple regression analysis, Hsu–Dunnet method	(Goudarzi et al. 2016)
	Childhood perfluoroalkyl substance exposure and executive function in children at 8 years	208 children	Serum sample, BRIEF, Multiple informant model, Multiple linear regression	(Vuong et al. 2018b)
	Prenatal phthalate, triclosan, and bisphenol A exposures and child visual-spatial abilities	198 mother-child dyads	VMWM, Urine sample, WASI, Linear mixed models, Linear regression, Pearson correlation coefficient	(Bellinger et al. 2016)

	Prenatal PBDE and PCB Exposures and Reading, Cognition, and Externalizing Behavior in Children	239 mother child pairs	Maternal serum, WJ-III, WRAT-4, WISC IV,BASC-2, Multiple linear regression, Trend test, LASSO	(Chen et al. 2016)
	Pesticides, polychlorinated biphenyls and polycyclic aromatic hydrocarbons in cerebrospinal fluid of amyotrophic lateral sclerosis patients: a case control study	38 ALS patients and 38 controls	Cerebrospinal fluid, Logistic regression model, Odds ratio	(Vinceti et al. 2017)
	Neurodevelopmental toxicity of prenatal polychlorinated biphenyls (PCBs) by chemical structure and activity: a birth cohort study	1134 Participants	Maternal and cord serum samples, Lipids measurement, BSID-II, Raven's Progressive Matrices, Bivariate analyses, Multiple linear regression models	(Park et al. 2010)
	Prenatal Phthalate Biomarker Concentrations and Performance on the Bayley Scales of Infant Development-II in a Population of Young Urban Children	479 participants	Phthalate metabolite concentrations Urine samples, BSID-II, Liner model	(Doherty et al. 2017)
	Polychlorinated biphenyls and depression: cross-sectional and longitudinal investigation of a dopamine-related Neurochemical path in the German HELPcB surveillance program	178 participants	Transmitter metabolites urine samples, BDI-II, multiple linear regression	(Gaum et al. 2017)
	Perfluoroalkyl substances, thyroid hormones, and neuropsychological status in older adults.	126 participants	Neuropsychological assessment, Serum chemical analysis, Thyroid function and lipid analysis, multivariable linear regressions	(Shrestha et al. 2017)
	Perfluoroalkyl substances in cord blood and attention deficit/hyperactivity disorder symptoms in seven-year-old children.	282 pairs	Questionares (SNAP-IV, CBCL/4-16, SDQ), cord blood levels, multivariable linear regression	(Lien et al. 2016)
	Perfluorinated Compound Levels in Cord Blood and Neurodevelopment at 2 Years of Age	239 mother–infant pairs	Cord blood, Comprehensive Developmental Inventory, linear and logistic regression	(Chen et al. 2013)

	Prenatal and childhood exposure to perfluoroalkyl substances (PFAS) and measures of attention, impulse control, and visual spatial abilities.	218 mother-child dyads	Maternal serum samples, CPT-II, VMWM, multiple informant models	(Vuong et al. 2018a)
	Polybrominated Diphenyl Ethers in Maternal Serum, Breast Milk, Umbilical Cord Serum, and House Dust in a South Korean Birth Panel of Mother-Neonate Pairs.	41 mother-neonate pairs	blood serum and breast milk samples, Umbilical Cord Serum, dust samples, Spearman's rank	(Shin et al. 2016)

Table 5: Input and translation for in silico neurotoxicity assessment

S. No.	Title	Input	Translation	References
	Developing integrated PBPK/PD coupled mechanistic pathway model (miRNA-BDNF): An approach towards system toxicology	In vitro data	PBPK,PD, Systems biology, IVIVE	(Sharma et al. 2017)
	Multivariate toxicity profiles and QSAR modeling of non-dioxin-like PCBs – An investigation of in vitro screening data from ultra-pure congeners	In vitro screening	QSAR, Principal component analysis (PCA), Multivariate analysis	(Stenberg et al. 2011)
	An Extended Structure–Activity Relationship of Nondioxin-Like PCBs Evaluates and Supports Modeling Predictions and Identifies Picomolar Potency of PCB 202 Towards Ryanodine Receptors	Male New Zealand White rabbits	QSAR, Pearson's correlation	(Holland et al. 2017)
	Evaluating the neurotoxic effects of lactational exposure to persistent organic pollutants (POPs) in Spanish children	1175 participants	PBPK model	(Gascon et al. 2013)
	Integrating data gap filling techniques: A case study predicting TEFs for neurotoxicity TEQs to facilitate the hazard assessment of polychlorinated biphenyls	In vitro data	QSAR	(Pradeep et al. 2019)

	Quantitative structure-activity relationship (QSAR) studies for predicting activation of the ryanodine receptor type 1 channel complex (RyR1) by polychlorinated biphenyl (PCB) congeners	In silico & Experimental	QSAR	(Rayne and Forest 2010)

Annex for Chapter 2a

Table 1: Physiological Parameters for the rat PBPK Model

Parameters	Values	Reference
Tissue Blood Flow (fraction of QC)		
Cardiac Output (L/h/kg)	18.7	(Emond et al. 2010) (Brown et al. 1997) (Sharma et al. 2020)
QCblood	0.131	
FQliver	0.174	
FQbrain	0.02	
FQfat	0.07	
FQKidney	0.141	
Tissue Volume (Fraction of BW)		
Gut	0.006	(Emond et al. 2010) (Brown et al. 1997) (Sharma et al. 2020)
Liver	0.034	
Brain	0.006	
Kidney	0.0073	
Fplasma	0.074	
Microsomal protein in liver (MPPGG)	60 (mg/g liver)	(Houston and Carlile 1997)

Equations used for developing PBPK Model

$$\frac{d}{dt}(Astomach) = -GE * Astomach + Input\ dose \qquad Eq.1$$

Astomach is amount of chemical in stomach, GE is gastric emptying rate constant, Input dose is the dose administered.

$$\frac{d}{dt}(Agut) = -kgut * Agut + GE * Astomach \qquad Eq.2$$

Agut is amount of chemical in gut, kgut is gut rate constant.

$$\frac{d}{dt}(Aliver) = \text{kgut} * \text{Agut} + \text{Qliver} * (\text{cplasma} * \text{fu} - \text{cliver} * (\frac{fu}{\text{k\_liver\_plasma}})) - \text{RAM} \qquad Eq.3$$

Aliver is amount of chemical in liver, Qliver is blood flow to the liver compartment from plasma and k_liver_plasma is partition coefficient of liver to plasma.

$$\frac{d}{dt}(Abrain) = \text{Qbrain} * (\text{cplasma} * \text{fu} - \text{cbrain} * (\frac{fu}{\text{k\_brain\_plasma}})) \qquad Eq.4$$

Abrain is amount of chemical in brain, Qbrain is blood flow to the brain compartment from plasma and k_brain_plasma is partition coefficient of brain to plasma.

$$\frac{d}{dt}(Akidney) = \text{Qkidney} * (\text{cplasma} * \text{fu} - \text{ckidney} * (\frac{fu}{\text{k\_kidney\_plasma}})) \quad Eq.5$$

Akidney is amount of chemical in kidney, Qkidney is blood flow to the kidney compartment from plasma and k_kidney_plasma is partition coefficient of kidney to plasma.

$$\frac{d}{dt}(Afat) = \text{Qfat} * (\text{cplasma} * \text{fu} - \text{cfat} * (\frac{fu}{\text{k\_fat\_plasma}})) \quad Eq.6$$

Afat is amount of chemical in fat, Qfat is blood flow to the fat compartment from plasma and k_fat_plasma is partition coefficient of fat to plasma.

$$\frac{d}{dt}(Arb) = \text{Qrb} * (\text{cplasma} * \text{fu} - \text{crb} * (\frac{fu}{\text{k\_rb\_plasma}})) \quad Eq.7$$

Arb is amount of chemical in rest of body, Qrb is blood flow to rest of body from plasma, k_rb_plasma is partition coefficient of rest body to plasma.

$$\frac{d}{dt}(Aplasma) = (\text{Qliver} * \text{cliver} * (\frac{fu}{\text{k\_liver\_plasma}})) + (\text{Qbrain} * \text{cbrain} * (\frac{fu}{\text{k\_brain\_plasma}})) + (\text{Qkidney} * \text{ckidney} * (\frac{fu}{\text{k\_kidney\_plasma}})) + (\text{Qfat} * \text{cfat} * (\frac{fu}{\text{k\_fat\_plasma}})) + (\text{Qrb} * \text{crb} * (\frac{fu}{\text{k\_rb\_plasma}})) - (QCplasma * cplasma * fu) \quad Eq.8$$

Aplasma is amount of chemical in plasma, QC plasma is cardiac output for plasma flow, cplasma is concentration in plasma.

$$RAM = \frac{Vmax_{met} * cliver * fu}{(cliver * fu) + Km_{met}} \quad Eq.9$$

RAM is the metabolism of OPFRs in their respective metabolite (BDCIPP, BCIPP and BCEP) in the microsomal fraction of liver. $Vmax_{met}$ is maximum reaction velocity at saturable

concentration, cliver is concentration in liver and Km_{met} is Michaels Menten constant (concentration at which reaction occurs at half-maximum rate).

PBPK Plots for TDCIPP

Scenario 2

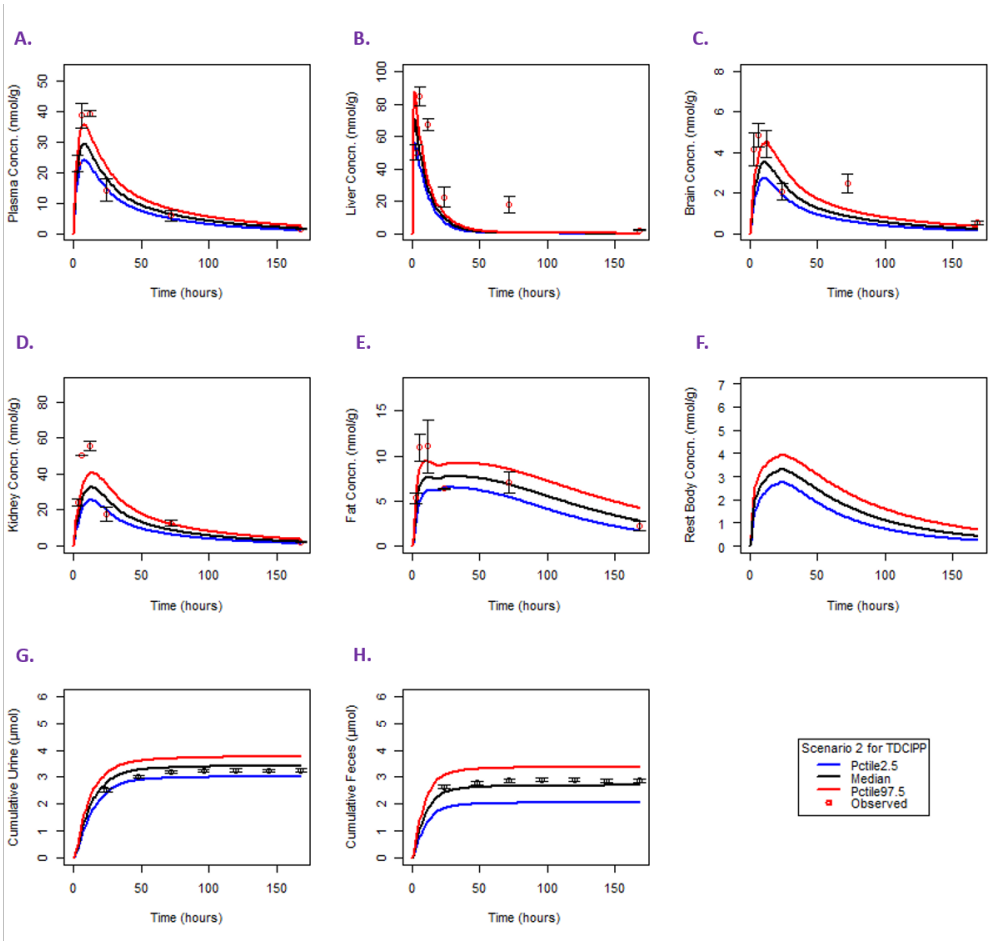

Figure 1: Concentration-time plot for TDCIPP in various organ for Scenario 2.

Scenario 3

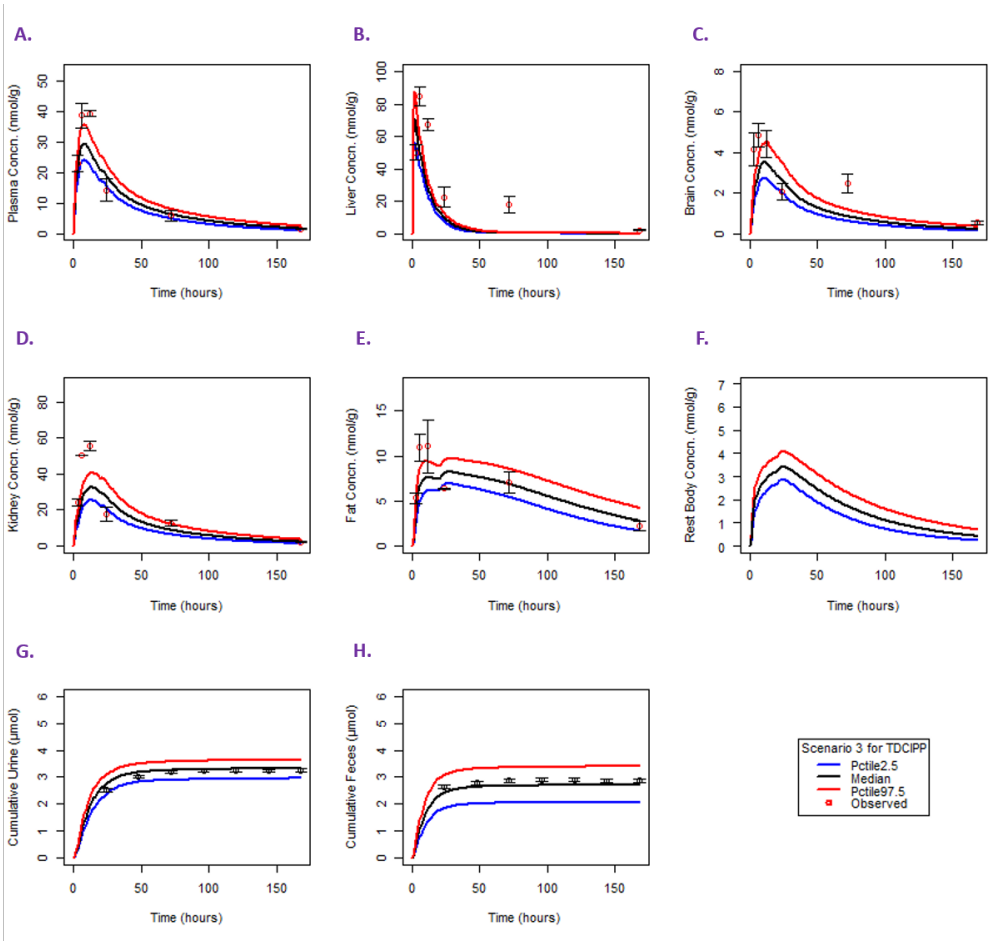

Figure 2: Concentration-time plot for TDCIPP in various organ for Scenario 3.

Scenario 4

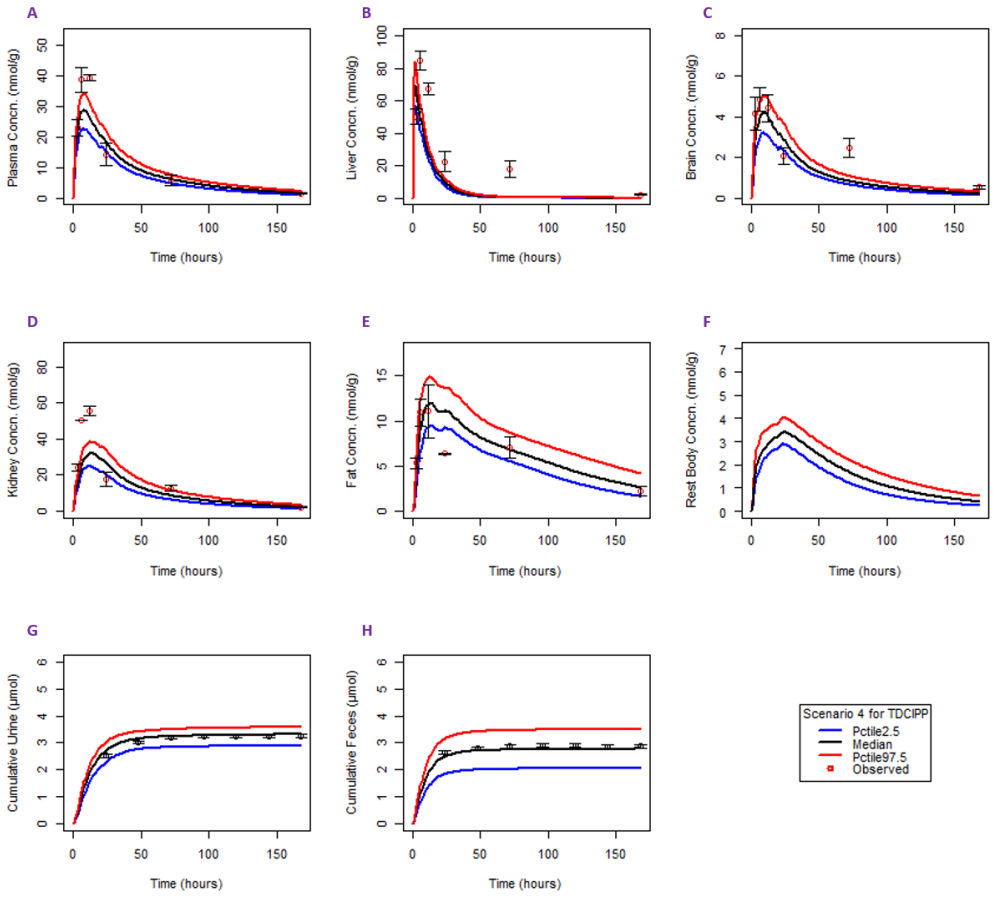

Figure 3: Concentration-time plot for TDCIPP in various organ for Scenario 4.

Plot for TDCIPP (Independent dataset)

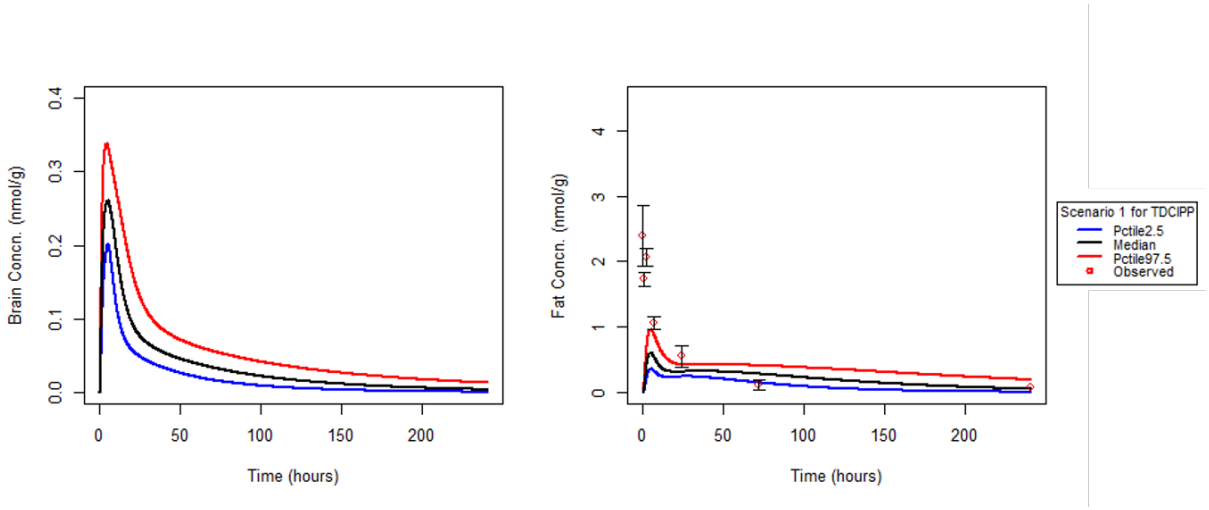

Figure 4: Concentration-time plot for brain and fat based on the experimental data from Noemi et al. for TDCIPP (Scenario 1) (Nomeir, Kato, and Matthews 1981).

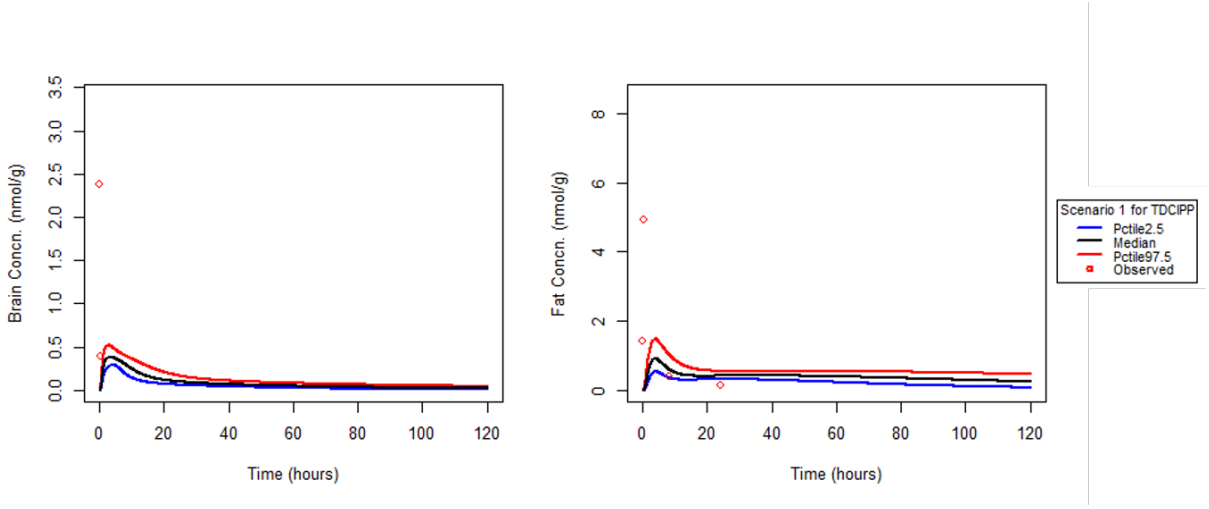

Figure 5: Concentration-time plot for brain and fat based on experimental data from Lynn et al. for TDCIPP (Scenario 1) (Lynn et al. 1981).

PBPK Plot for TCIPP

Scenario 1

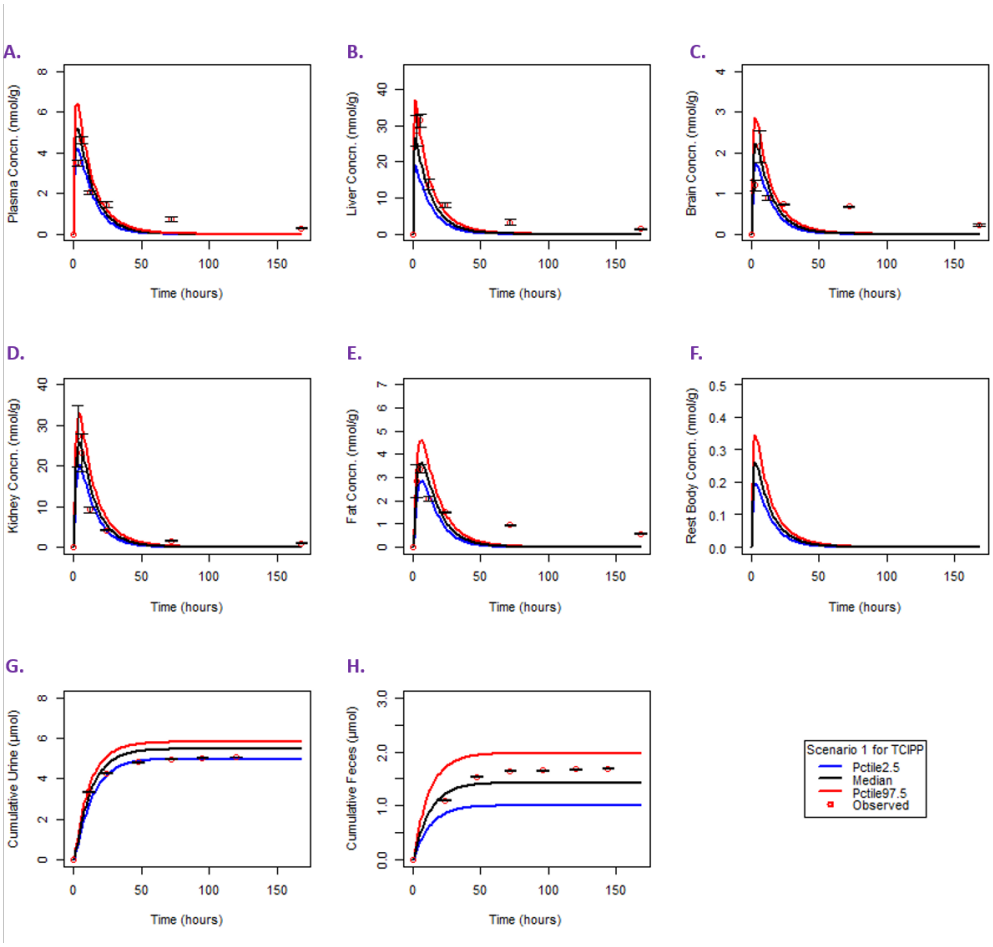

Figure 6: Concentration-time plot for TCIPP in various organ for Scenario 1.

Scenario 2

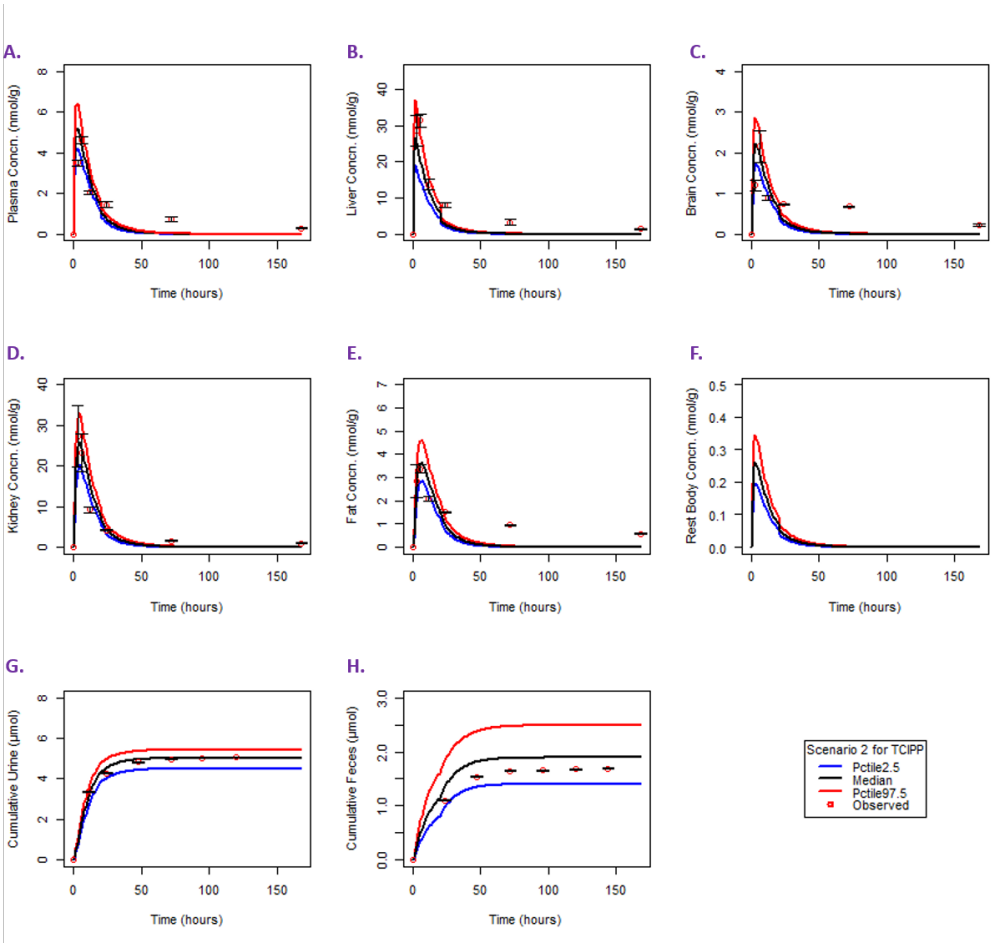

Figure 7: Concentration-time plot for TCIPP in various organ for Scenario 2.

Scenario 3

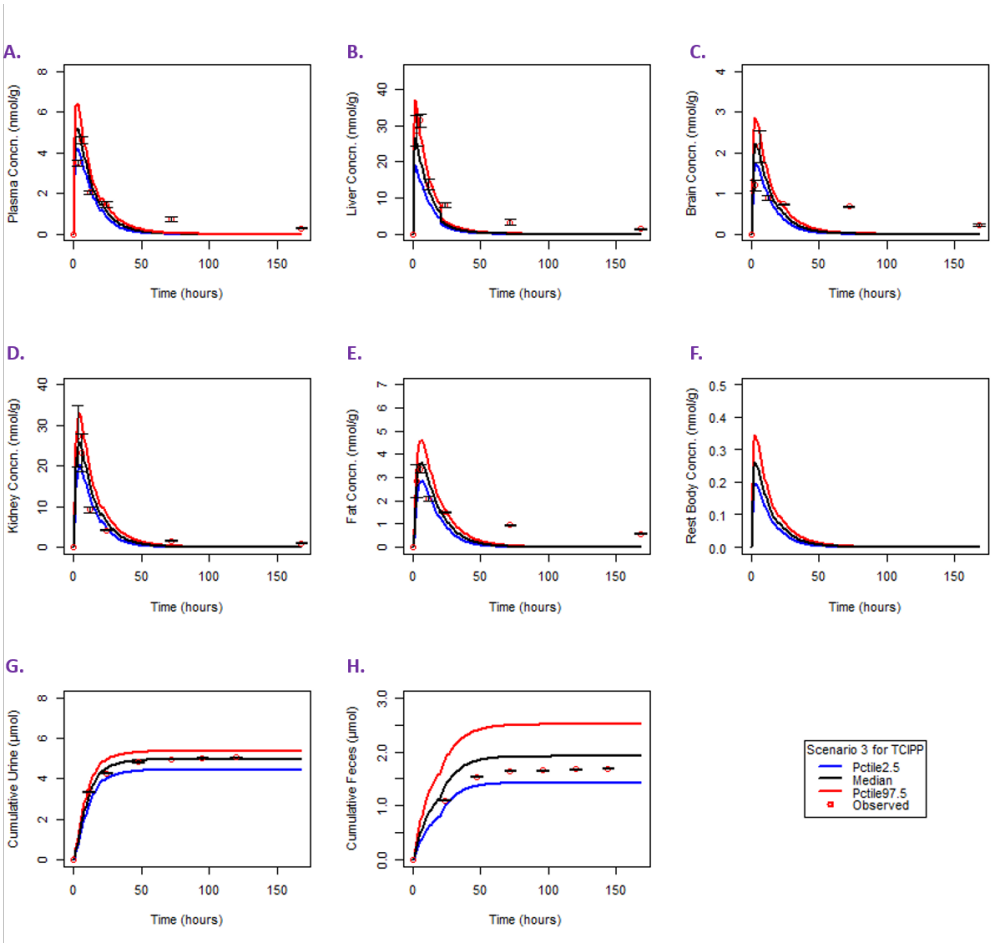

Figure 8: Concentration-time plot for TCIPP in various organ for Scenario 3.

PBPK Plot for TCEP

Scenario1

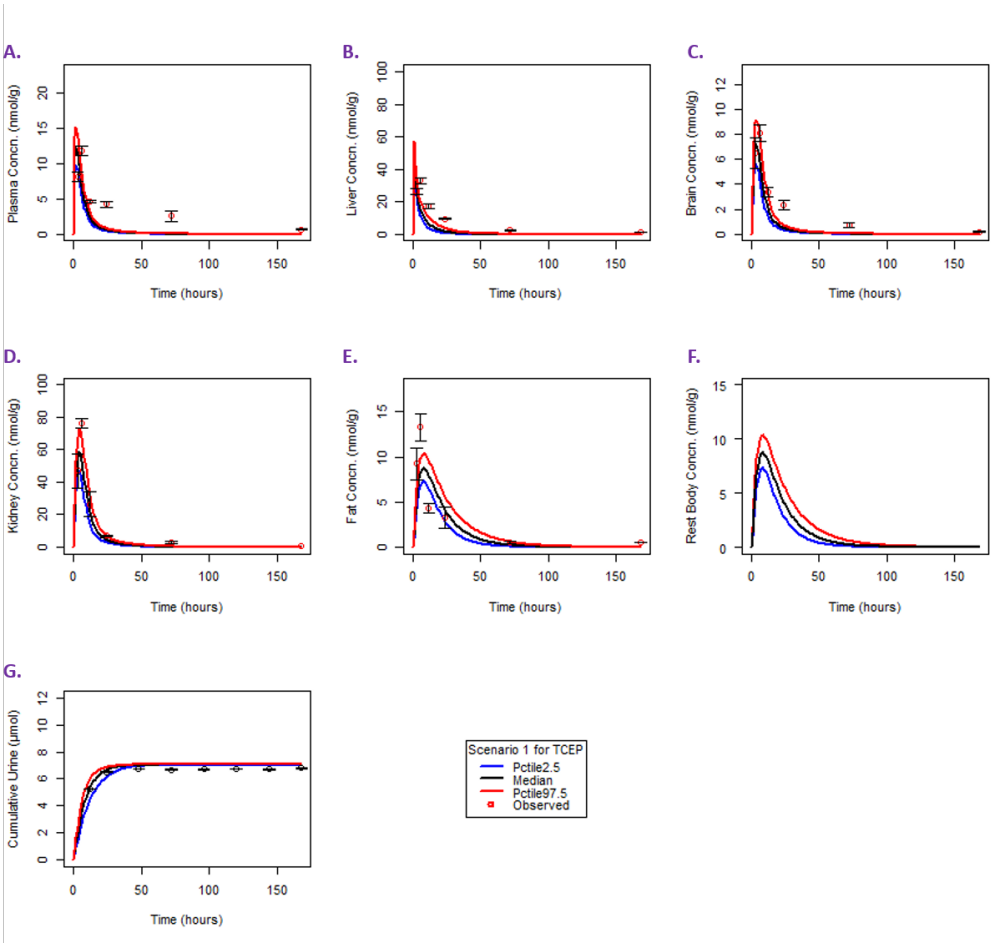

Figure 9: Concentration-time plot for TCEP in various organ for Scenario 1.

Scenario 2

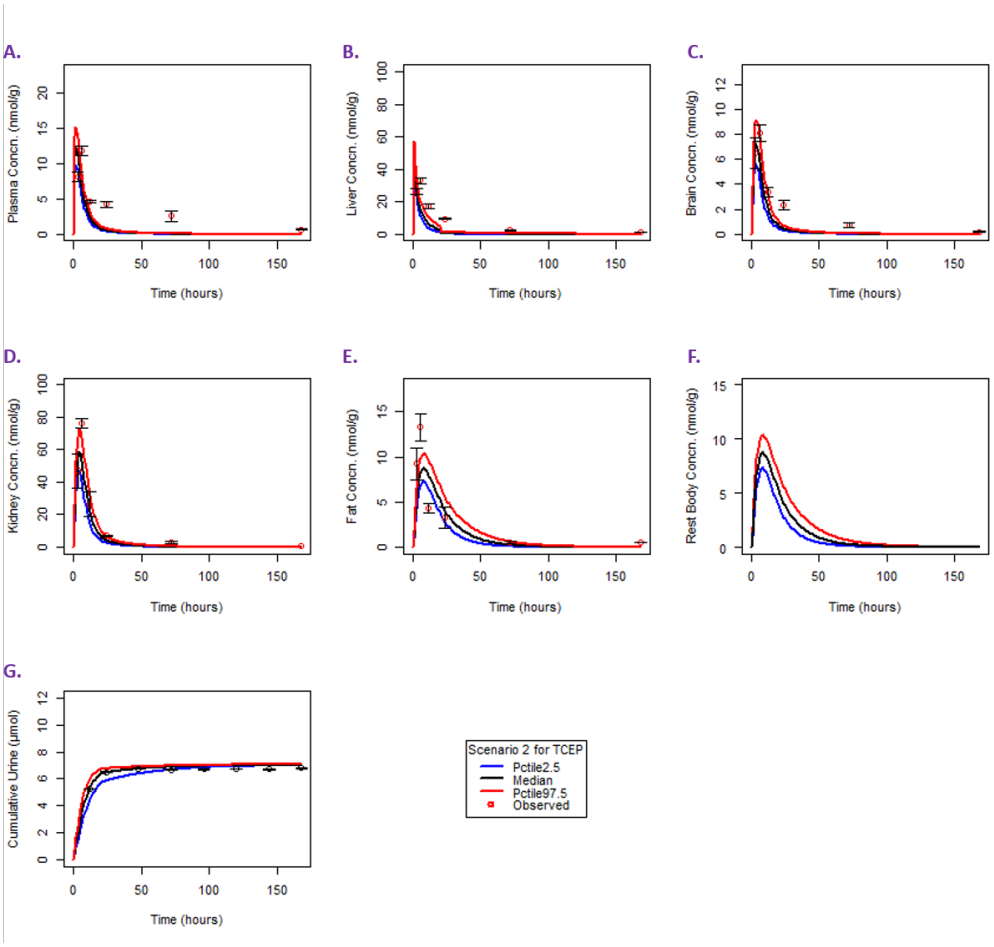

Figure 10: Concentration-time plot for TCEP in various organ for Scenario 2.

Scenario 3

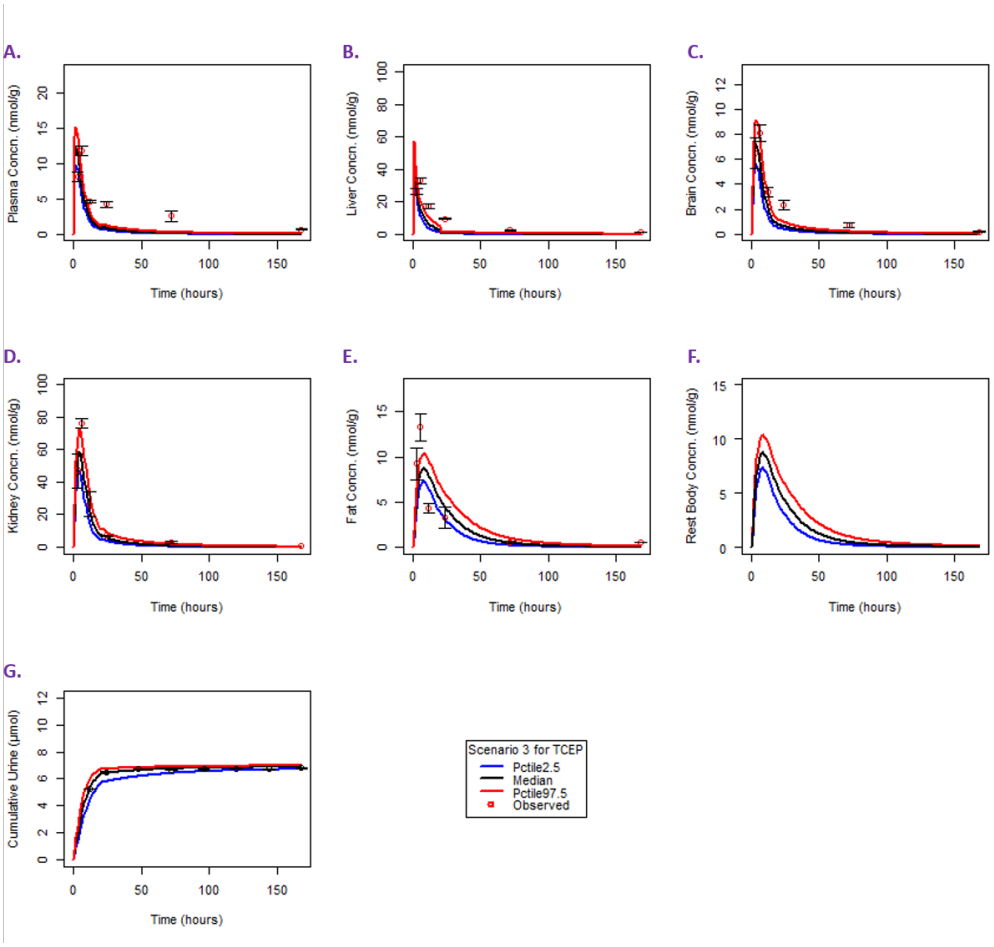

Figure 11: Concentration-time plot for TCEP in various organ for Scenario 3.

Goodness of fit plot for TDCIPP

Scenario 2

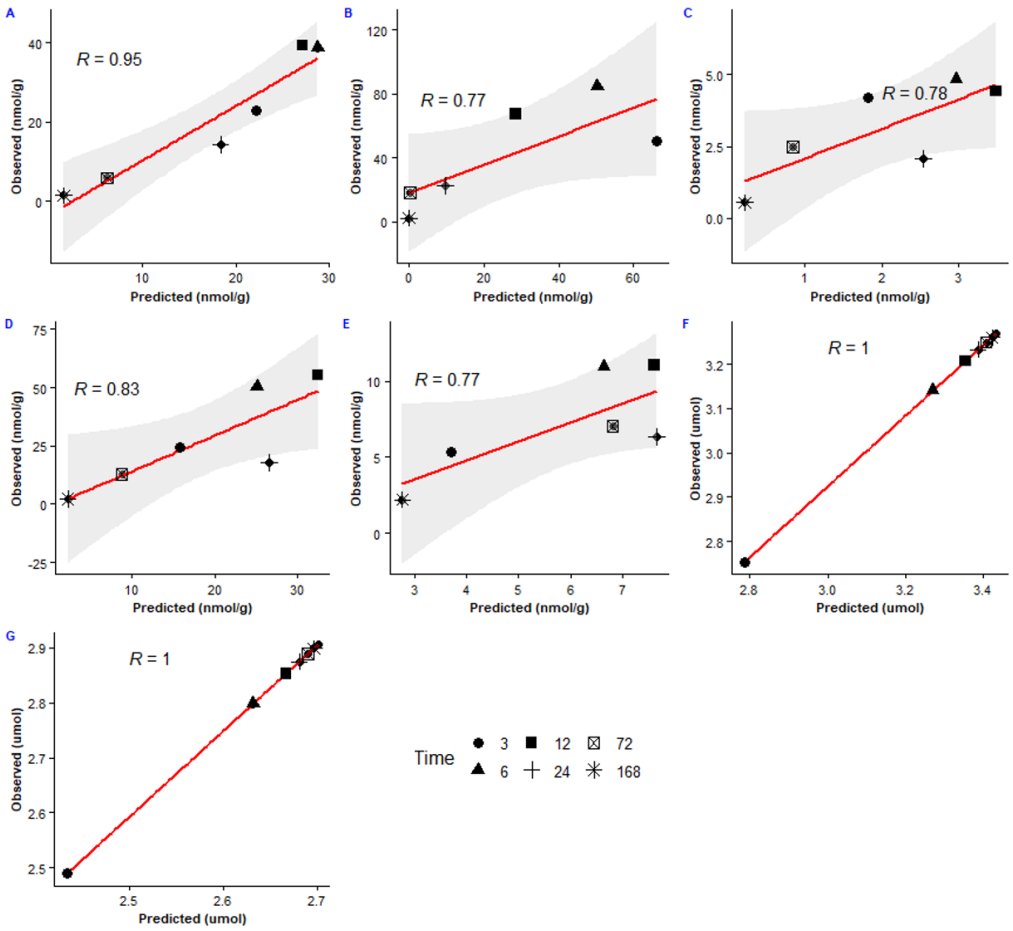

Figure 12: Goodness-of-fit plot for TDCIPP of several organs based on predicted and experimental data (Scenario 2).

Scenario 3

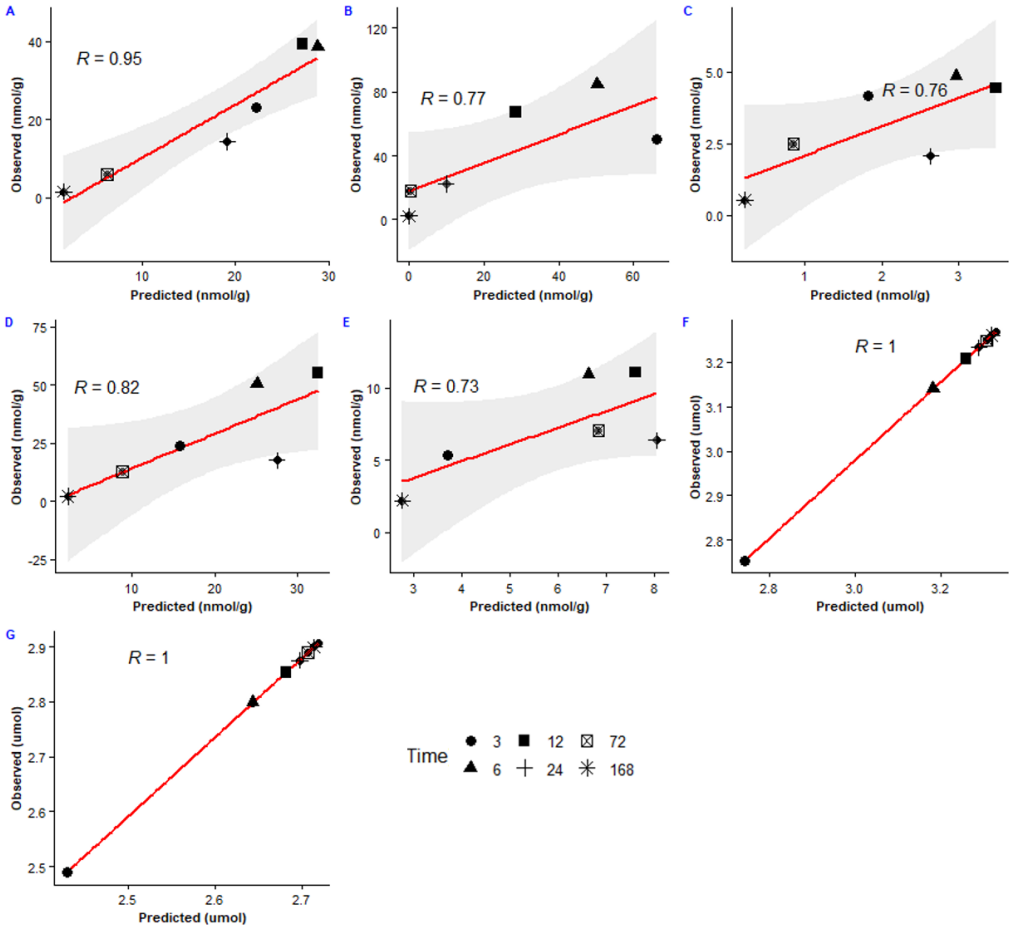

Figure 13: Goodness-of-fit plot for TDCIPP of several organs based on predicted and experimental data (Scenario 3).

Scenario 4

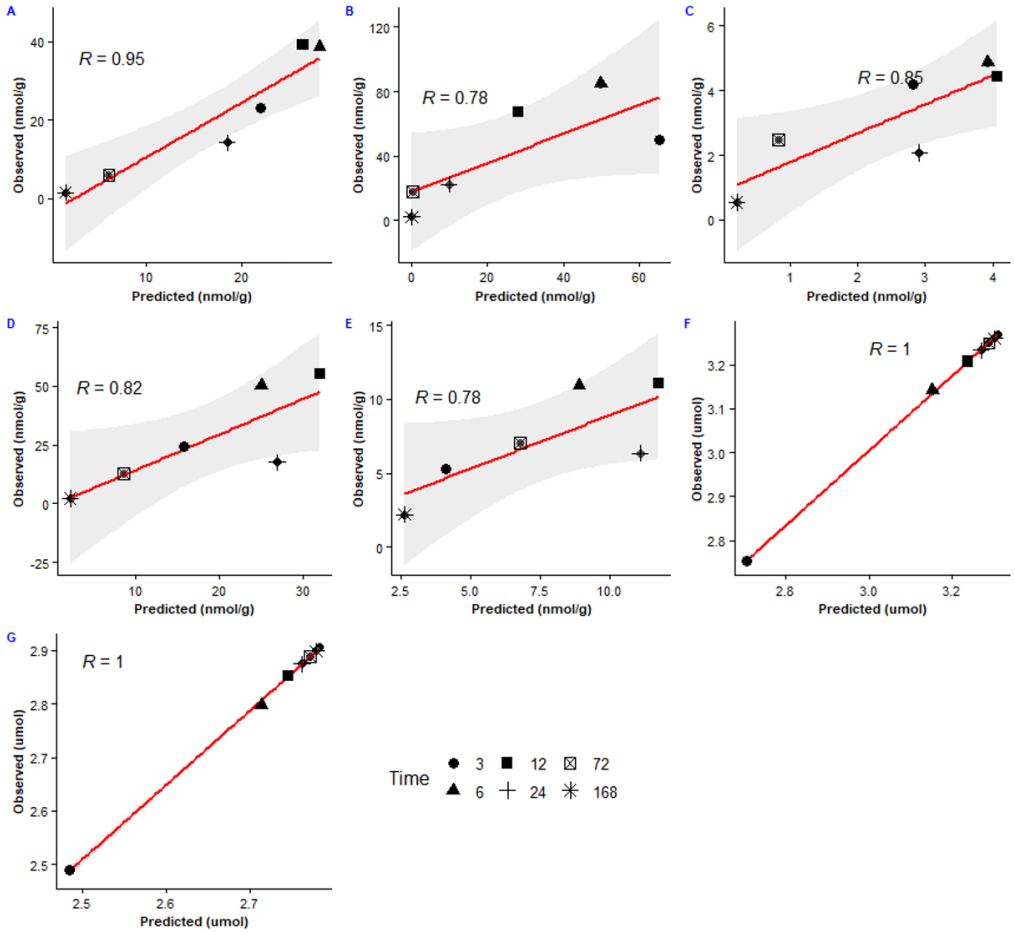

Figure 14: Goodness-of-fit plot for TDCIPP of several organs based on predicted and experimental data (Scenario 4).

Goodness-of-fit plot for TCIPP

Scenario 1

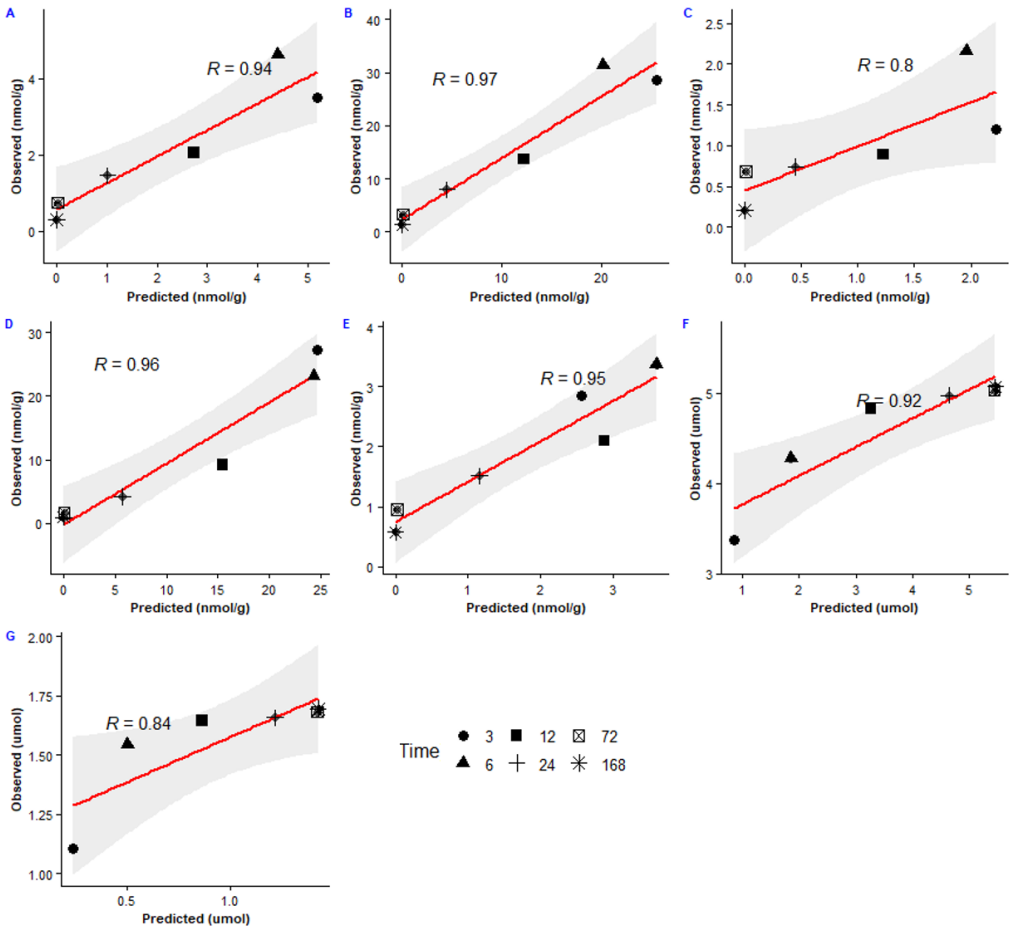

Figure 15: Goodness-of-fit plot for TCIPP of several organs based on predicted and experimental data (Scenario 1).

Scenario 2

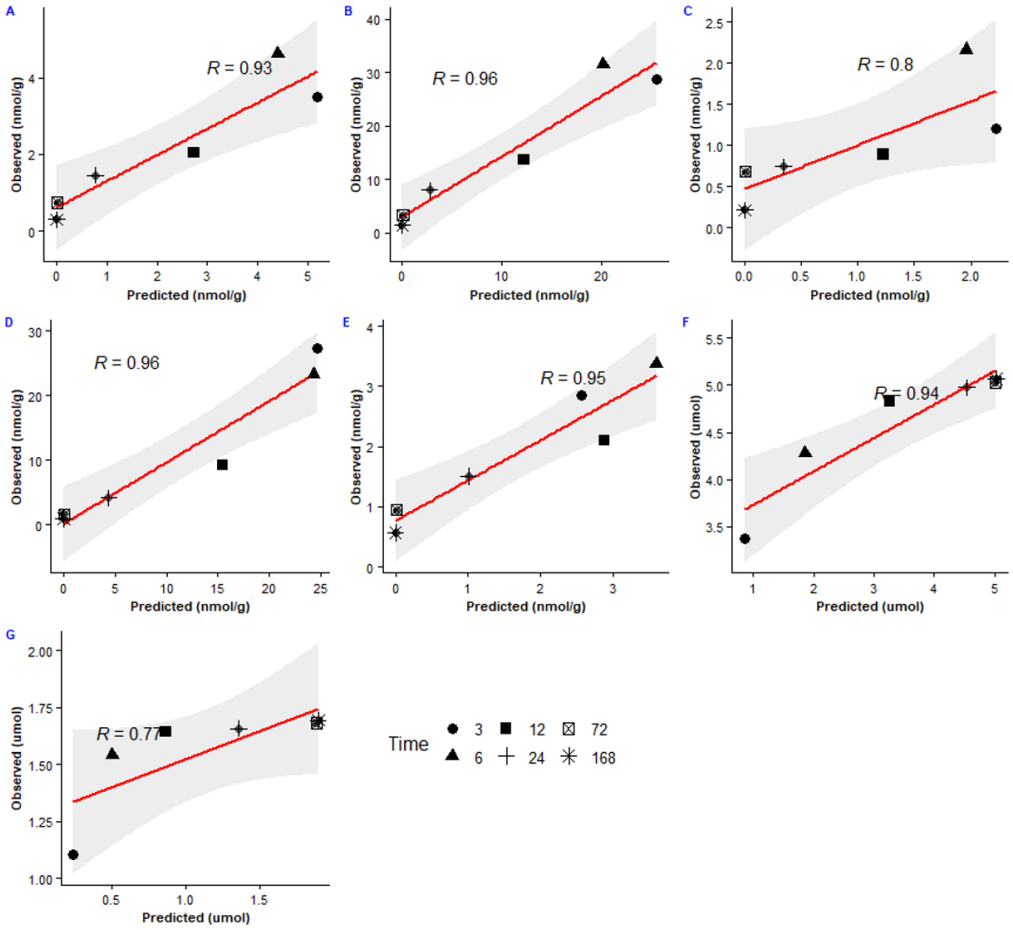

Figure 16: Goodness-of-fit plot for TCIPP of several organs based on predicted and experimental data (Scenario 2).

Scenario 3

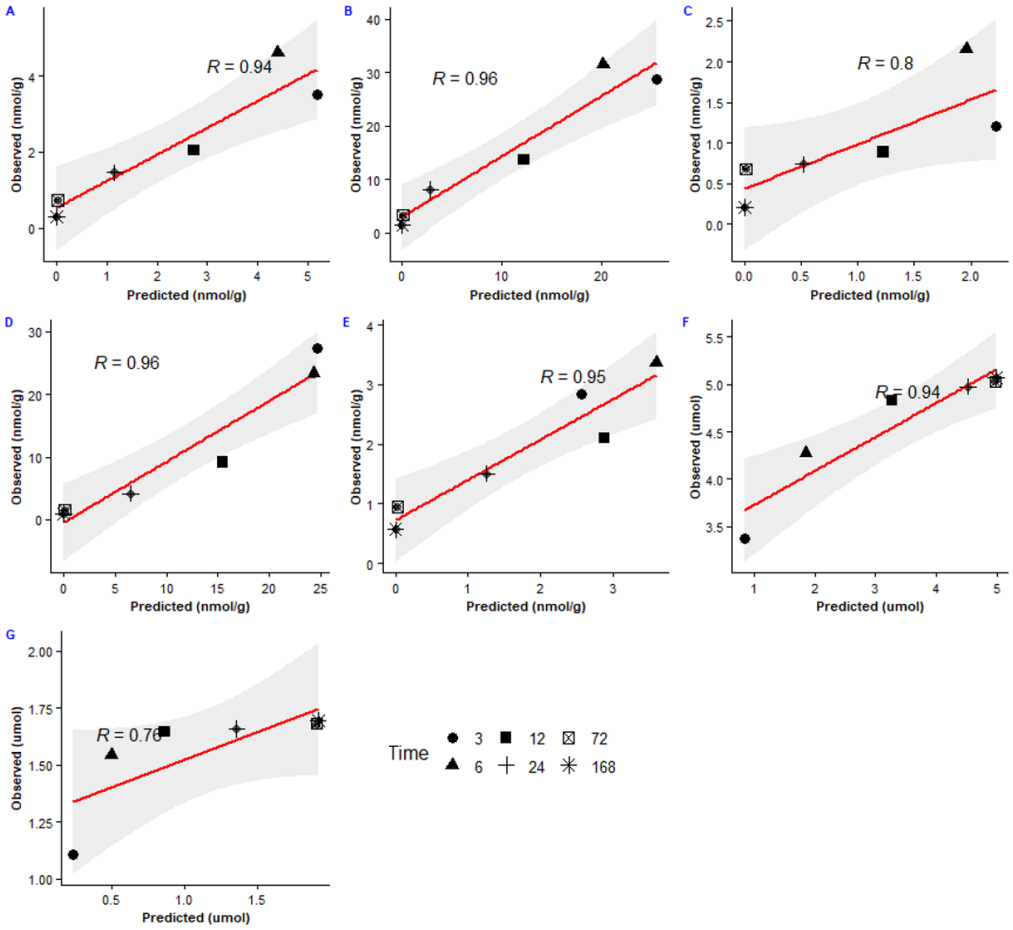

Figure 17: Goodness-of-fit plot for TCIPP of several organs based on predicted and experimental data (Scenario 3).

Goodness-of-fit plot for TCEP

Scenario 1

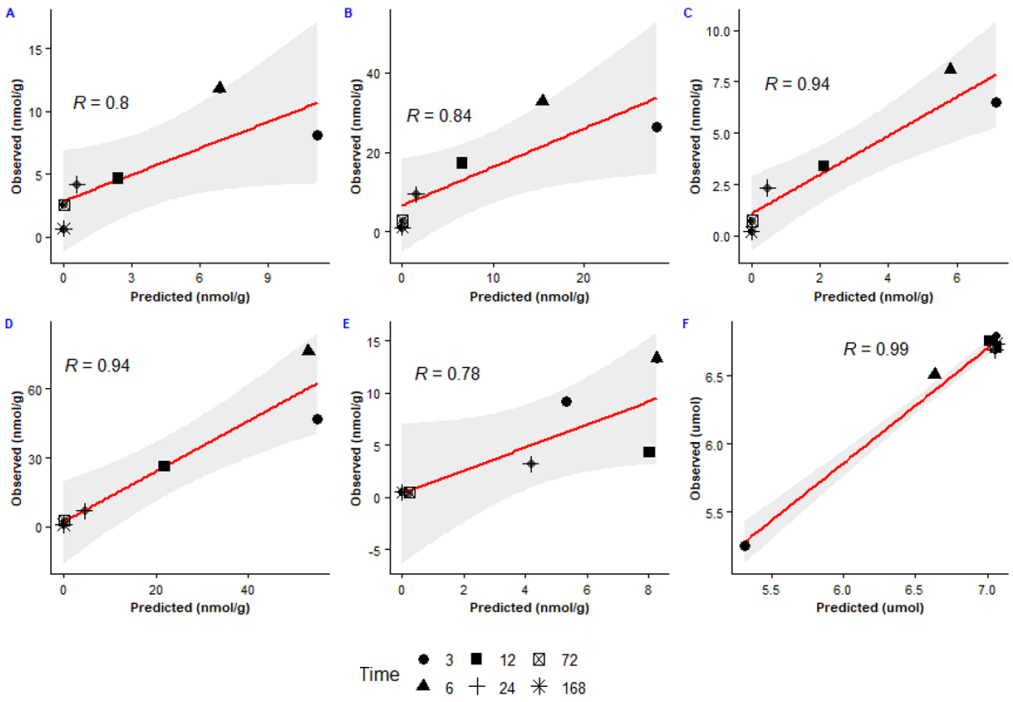

Figure 18: Goodness-of-fit plot for TCEP of several organs based on predicted and experimental data (Scenario 1).

Scenario 2

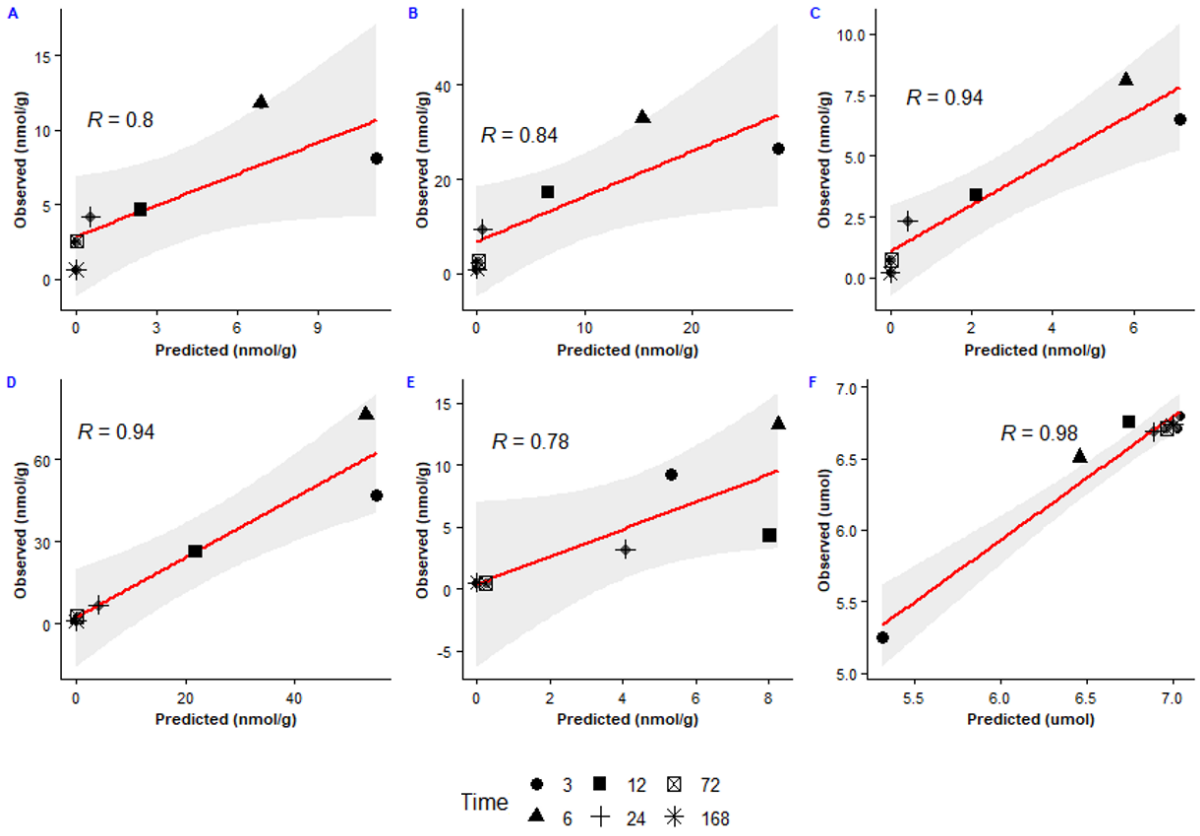

Figure 19: Goodness-of-fit plot for TCEP of several organs based on predicted and experimental data (Scenario 2).

Scenario 3

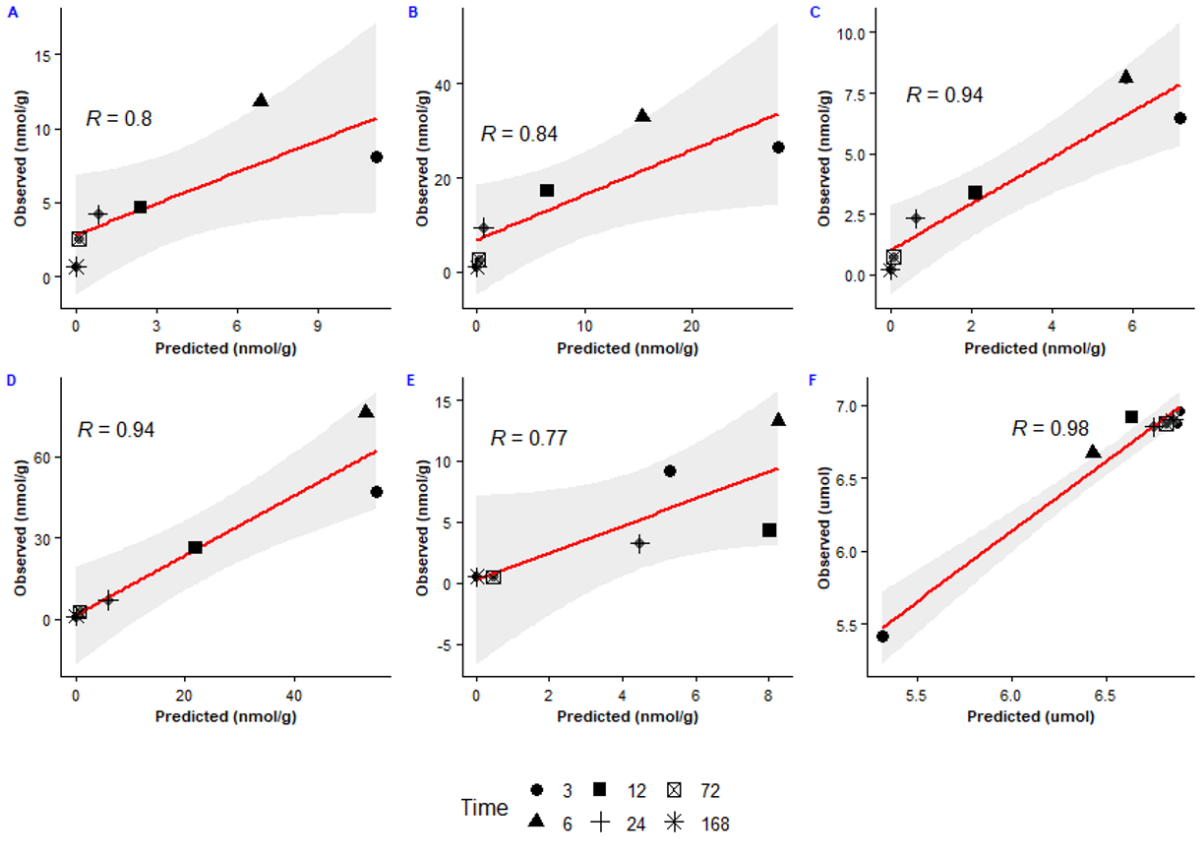

Figure 20: Goodness-of-fit plot for TCEP of several organs based on predicted and experimental data (Scenario 3).

AIC Scores

Table 3: AIC_c score for TDCIPP, TCIPP and TCEP (4 scenarios based on three last time points)

Model	**Plasma**	**Liver**	**Brain**	**Kidney**	**Fat**	**Urine**	**Feces**
TDCIPP							
Scenario 1	0.00	0	0.00	0.00	0.00	0.00	0.00
Scenario 2	0.45	0	0.02	0.06	0.72	0.00	0.00
Scenario 3	1.15	0	0.06	0.17	1.78	0.00	0.00
Scenario 4	1.20	0	0.19	0.20	5.27	0.00	0.00
TCIPP							
Scenario 1	0.02	0.00	0.18	0.05	1.16	0.04	0.00
Scenario 2	0.02	0.00	0.18	0.07	1.12	0.03	0.04
Scenario 3	0.02	0.00	0.18	0.05	1.11	0.05	0.04
Scenario 4	0.00	0.00	0.00	0.00	0.00	0.00	0.01
TCEP							
Scenario 1	1.67	7.56	6.51	2.23	0.00	0.00	-
Scenario 2	1.51	3.57	6.08	1.92	0.48	31.84	-
Scenario 3	0.64	0.00	3.38	0.02	3.45	30.96	-
Scenario 4	0.00	9.41	0.00	0.00	5.70	31.26	-

Annex for Chapter 2b

Physiological equations used in the model

All the equations used in the model for the boys and girls has been validated with the human biomointoring datasets. The equations has been previously published in the article (Deepika et al. 2021).

Equation for Boys and girls:

Height (HT)

$HT\_b = (5.869e+01)+(1.265e+01)*a-(4.665e-01)*a2+(7.198e-03)*a3-(3.224e-05)*a4-(2.512e-07)*a5+(2.071e-09)*a6$ Eq.1

$HT\_g = (5.373e+01)+(1.296e+01)*a-(5.506e-01)*a2)+(1.113e-02)*a3-(1.106e-04)*a4+(4.697e-07)*a5-(4.416e-10)*a6$ Eq. 2

Here a refers to age (years), ht (height in cm), HT_b refers to boys and HT_g refers to girls.

Body weight (BW in Kg)

$BW\_b=(3.382e+00)+(2.866e+00)*a+(1.694e-01)*a^2-(1.169e-02)*a^3+(2.577e-04)*a^4-(2.484e-06)*a^5+(8.891e-09)*a^6$ Eq. 3

$BW\_g= (2.354e+00)+(4.050e+00)*a-(3.240e-02)*a^2-(3.057e-03)*a^3+(9.353e-05)*a^4-(1.022e-06)*a5+(3.918e-09)*a^6$ Eq. 4

Surface Area (SA)

$SA=(0.007184* BW^{0.425}*HT^{0.725})$ Eq. 5

Volume of liver (Vliver)

$Vliver\_b=-0.0143744-0.0044728*a+0.0264591*BW$ Eq. 6

$Vliver\_g= 0.0017717-0.0030113*a+0.0253455*BW$ Eq. 7

Volume of brain (Vbrain)

$Vbrain\_b=0.218096-0.001590*a-0.003274*BW+0.008626*HT$ Eq. 8

$Vbrain\_g= 0.3757397-0.0003031*a-0.0021962*BW +0.0065721*HT$ Eq. 9

Volume of Kidney (Vkidney)

$Vkidney\_b=5.668e-02-4.962e-04*a+3.501e-03*BW$ Eq. 10

$Vkidney\_g= 0.0458676-0.0003957*a+0.0035115*BW$ Eq. 11

$Vfilterate = Ffilterate * BW;$ Eq. 12

Fraction of filtrate (Ffilterate) is considered as 10% of kidney volume.

Volume of fat (Vfat)

*Vfat_b=1.3054356+(0.3622685*a)-(0.0025165*a2)+(0.0906119*BW)+(0.0001731*BW2)*
Eq. 13

*Vfat_g= 6.132e-01+(8.475e-02*a)+(8.151e-05*a2) +(1.341e-01*BW)+(2.297e-03*BW2)*
Eq. 14

Volume of gonads (Vgonads)

*Vgonads=Fgondas*BW*
Eq. 15

Where Fgonads=0.027 (Sharma, Schuhmacher, and Kumar 2018)

Volume of skin (Vskin)

*Vskin_b=3.796e-01-(4.055e-02*a)+(2.564e-04*a2)+ (4.671e-02*BW)-(8.207e-05*BW2)*
Eq. 16

*Vskin_g=2.995e-01-(1.680e-02*a)+(7.151e-05*a2)+ (5.456e-02*BW)-(3.793e-04*BW2)*
Eq. 17

Volume of gut (Vgut)

*Vgut=Fgut*BW*
Eq. 18

Where Fgut=0.016 (Sharma, Schuhmacher, and Kumar 2018)

Volume of plasma (Vplasma)

*Vplasma=(1587*SA-304)/1000*
Eq. 19

Volume of rest body (Vrestbody)

*Vrestbody=0.84*BW-(Vliver- Vkidney - Vgut - Vplasma - Vfat- Vbrain -Vskin – Vgonads)*
Eq. 20

Blood flow in boys and girls

All the equations has been taken from the already published article by the same author (Deepika et al. 2021). Limited data on blood flow to organ makes it a challenging task to model these compartments for flow. In case of cardiac output, calculation was done based on body surface area. Body Surface area was calculated by Dubois formula shown in E5 (Du Bois and Du Bois 1989; Redlarski, Palkowski, and Krawczuk 2016). Variability was incorporated for cardiac output based on normal random distribution accounting for interindividual differences (E6 for female & E7 for male) (Mallick et al. 2019; Stader et al. 2019).

*QCblood_b=(6.48370-1.59948*a+214.68572*SA)* Eq. 21

*Qcblood_g= 5.528076-(2.834486*a)+(0.012591*a2)+(204.262351*SA)+(19.274290*SA2)* Eq. 22

*HCT_g=(0.00000112815*a3)-(0.000172362*a2)+(0.00851264*a)+0.327363)* Eq.23

For other organs, data from ICRP 89 and Stader et al. was used where they have collected the adult data and data from European population for age group 20 to 90 years. In the compartments where tissue blood flow has been rarely reported, adult blood flow was taken as standard for calculating relative blood flow and simulated data was validated with physiological values (Anatomical, Data, and Values n.d.; Stader et al. 2019).

*QCplasma =QCblood *(1-HCT)* Eq. 24

Qliver= FQliver QCplasma* Eq. 25

Qbrain = FQbrain QCplasma* Eq. 26

*Qkidney=FQkidney*QCplasma* Eq. 27

*Qfilterate=0.2*Qkidney* Eq. 28

*Qfat=FQfat*QCplasma* Eq. 29

*Qgonads = FQgonads*QCplasma* Eq. 30

Qskin = FQskin QCplasma* Eq. 31

Table 1: Physiological Parameters for blood flow for both boys and girls (Deepika et al. 2021)

Physiological Parameters	**Boys**	**Girls**
Fraction of blood flow to the organs		
Liver	0.257	0.141
Brain	0.117	0.0812
Kidney	0.177	0.0905
Fat	0.052	0.044
Gut	0.181	0.014
Skin	0.058	0.025
Gonads	0.0002	0.0002

Table 2: Biochemical Parameters used in the PBPK Model

Parameter	Values
k0C (Oral uptake from stomach into liver)	0
k1C (Oral uptake from small intestine to liver)	9
kGlin_BPAGC (Transportation of BPAG into liver from enterocytes)	50
vmaxgut_gluC (glucuronidation in gut)	22750
kmgut_glu	58400
RAMS_gutC (no data on sulfaion in gut)	0

Fbpagliver (fraction of bpag in liver to serum)[b]	0.9
Fbpasliver (fraction of bpas in liver to serum) [b]	1
vmaxliver_gluC (glucuronidation in liver)	707537[x] 452823.68[*] 199461.733[a]
kmliver_glu [b]	45800
vmaxliver_sulfC (sulfation in liver)	11657[x] 18301.49[*] 46764.493[a]
kmliver_sulf [b]	10100
EHRtime (time until EHR occurs) [b]	0.1
EHRrateC	0.2
Kde (reversible deconjugation and conjugation) [b]	0.35
Kde_BPAG (BPAG deconjugation) [b]	0.30
kurineC (Urinary elimination rate constant)	0.07

Most of the parameters were taken from article published by Sharma et al. (Sharma, Schuhmacher, and Kumar 2018). Only metabolic parameter was changed for boys and girls, rest other parameters were assumed similar. However, the difference might exist in the parameters as all the parameters have been scaled to body weight except those marked with [b], [x] for adults, [*] is for boys, [a] is for girls.

Ordinary differential equations (ODE) used in the PBPK Model

cgut = Agut/vgut;

cgut refers to concentration in gut (nM/L), Agut amount of chemical in gut (nM) and vgut refers to volume of gut (L) repectively.

cplasma = Aplasma/vplasma;

cliver = Aliver/vliver;

cbrain = Abrain/vbrain;

ckidney = Akidney/vkidney;

cfat = Afat/vfat;

cskin = Askin/vskin;

cgonads = Agonads/vgonads;

cfilterate = Afilterate/vfilterate;

crestbody = Arestbody/vrestbody;

RAM_gut refers to the gluuronidation in gut, RAMS1 refers to sulfation in liver.

RAM_gut = vmaxgut_glu*cgut/(cgut+kmgut_glu);

RAMS1 = vmaxliver_sulf*cliver*fu/(cliver*fu+kmliver_sulf);

RAM = vmaxliver_glu*cliver*fu/(cliver*fu+kmliver_glu);

dt(Agut) = GE*Astomach - RAM_gut - k1*Agut;

GE refers to gatric empyting and K1 is the rate constant (hr-1).

dt(Aliver) = Qliver*(cplasma*fu- cliver*(fu/k_liver_plasma)) + k1*Agut - RAM - RAMS1

fu refers to fraction unbound of chemical.

dt(Abrain) = Qbrain *(cplasma*fu - cbrain*(fu/k_brain_plasma))

dt(Afat) = Qfat *(cplasma*fu - cfat*(fu/k_fat_plasma))

dt(Akidney) = Qkidney *(cplasma*fu - ckidney*(fu/k_kidney_plasma))- kurine* ckidney

dt(Afilterate) = Qfilterate *(cplasma*fu - cfilterate*fu)

dt(Askin) = Qskin *(cplasma*fu - cskin*(fu/k_skin_plasma))

dt(Agonads) = Qgonads *(cplasma*fu - cgonads*(fu/k_gonads_plasma))

dt(Arestbody) = Qrestbody *(cplasma*fu - crestbody*(fu/k_restbody_plasma))

dt(Aurine)= kurine* ckidney;

dt(Aplasma) = (Qfat * cfat*(fu/k_fat_plasma) + Qliver*cliver*(fu/ k_liver_plasma) + (Qbrain *cbrain*(fu/k_brain_plasma))+(Qkidney *ckidney*(fu/k_kidney_plasma))+(Qrestbody *crestbody*(fu/k_restbody_plasma)) - (QCplasma* cplasma*fu) +(Qskin * cskin*(fu/k_skin_plasma)) + (Qgonads * cgonads*(fu/k_gonads_plasma))

dt(BPAG_gut) = RAM_gut - kGlin_BPAG*BPAG_gut;

dt(BPAG_prod_gut) = Fbpagliver *kGlin_BPAG*BPAG_gut;

dt(BPAG_prod_gut_delay) = Fbpagliver1*kGlin_BPAG*BPAG_gut;

dt(BPAG_prod_liver) =Fbpagliver * RAM;

dt(BPAG_prod_liver_delay) = Fbpagliver1*RAM ;

dt(BPAG_delay_in) = BPAG_delay*EHRrate;

dt(ABPAG) = (Fbpagliver * RAM + Fbpagliver *kGlin_BPAG*BPAG_gut + BPAG_delay*EHRrate-kurinebpag*CBPAG)

dt(BPAG_urine) = kurinebpag*CBPAG;

dt(BPAS_prod_liver) =Fbpasliver * RAMS1;

dt(ABPAS) = Fbpasliver*RAMS1 +Fbpasliver* RAMS_gut- kurinebpas * CBPAS;

dt(BPAS_urine) = kurinebpas * CBPAS;

dt(AUC)=cplasma;

dt(AUCBPAG)=CBPAG;

dt(AUCBPAS)=CBPAS;

dt(AUCliver)=cliver;

dt(AUCbrain)=cbrain;

dt(AUCfat)=cfat;

dt(AUCkidney)=ckidney;

dt(AUCskin)=cskin;

dt(AUCgonads)=cgonads;

dt(AUCrestbody)=crestbody;

Total BPA (conjugated + free) (nmole)

Auri_tBpa = BPAS_urine + BPAG_urine + Aurine;

Auri_tBpa refers to toal bpa in urine.

Auri_uBpa = Aurine;

Auri_Bpag = BPAG_urine;

Auri_Bpas = BPAS_urine;

Table 3: Twenty-four hour urinary creatinine excretion based on different height groups (Remer, Neubert, and Maser-Gluth 2002).

Sex	Creatinine (Mean, SD), mmol/d
Girls	5.01±0.92
Boys	4.47±0.92

Table 4: Prior distribution for the MCMC analysis for reconstructed exposure.

Parameter	Prior Distribution
Dosing	0.0001-2e+4

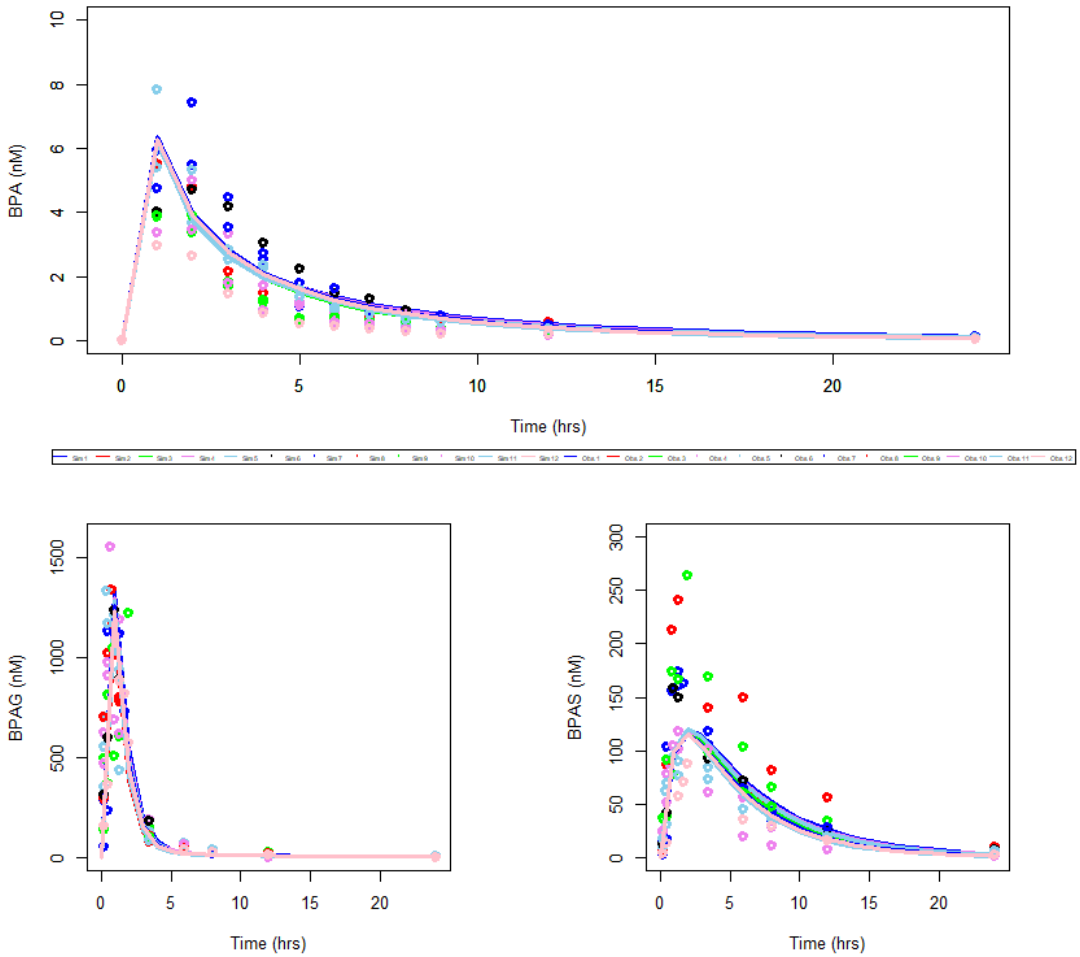

Figure 1: Plasma concentration vs time for adult population for 12 healthy volunteers. It includes free BPA and its metabolites (BPAG and BPAS) in 24 hour after single oral dose of 100 µg/Kg BW/day. Dot represents the observed data point (Thayer et al. 2015). Simulated individual is represented by different colored lines.

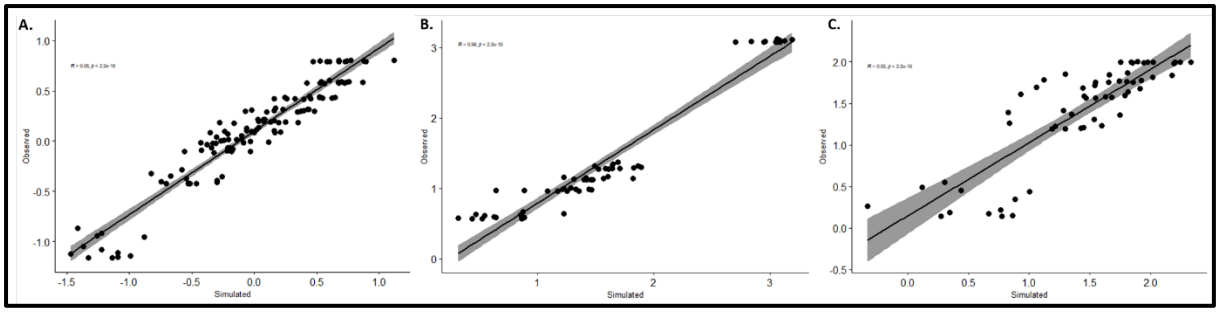

Figure 2: Correlation plot between simulated and observed concentration for BPA in plasma. A represents the logarithmic simulated and observed BPA concentration, B represents the glucuronide metabolite of BPA (BPAG) plasma concentration (logarithmic vale) in adults. All the simulations were performed individually and observed concentration were taken from Thayer et al. (2015).

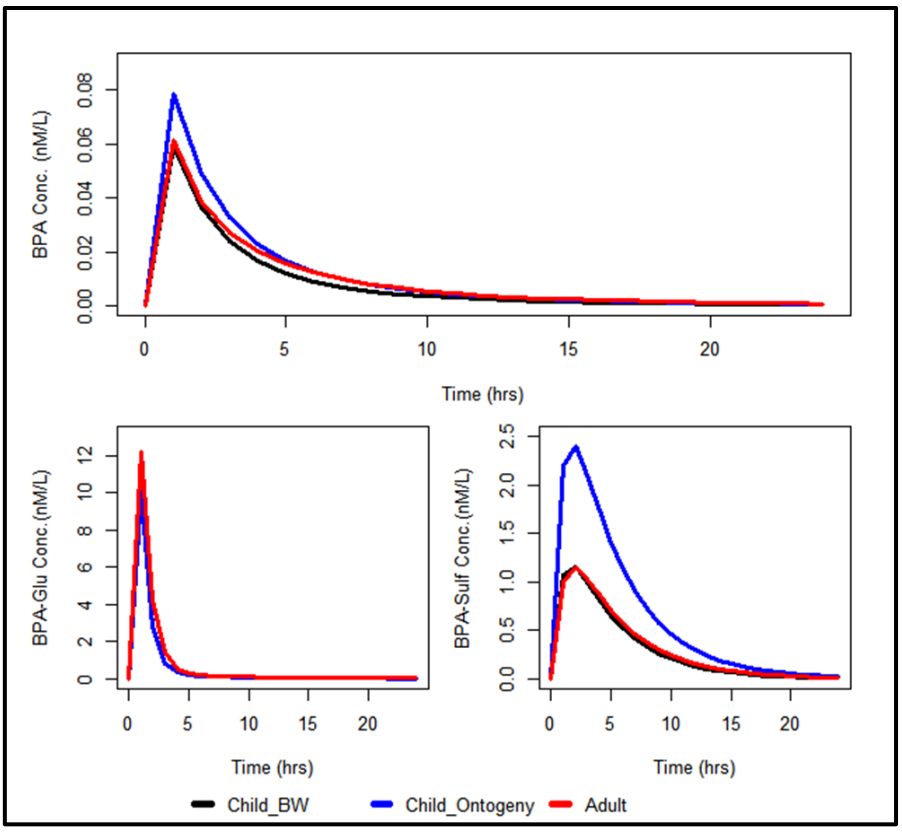

Figure 3: compares the glucuronidation and sulfation kinetics and BPA concentration in plasma in adults and children (median). The simulated concentration in ontogeny scaling was higher than adults for BPA at Cmax. Glucuronidation metabolism was higher in adults than children whereas sulfation in adult is slower than children.

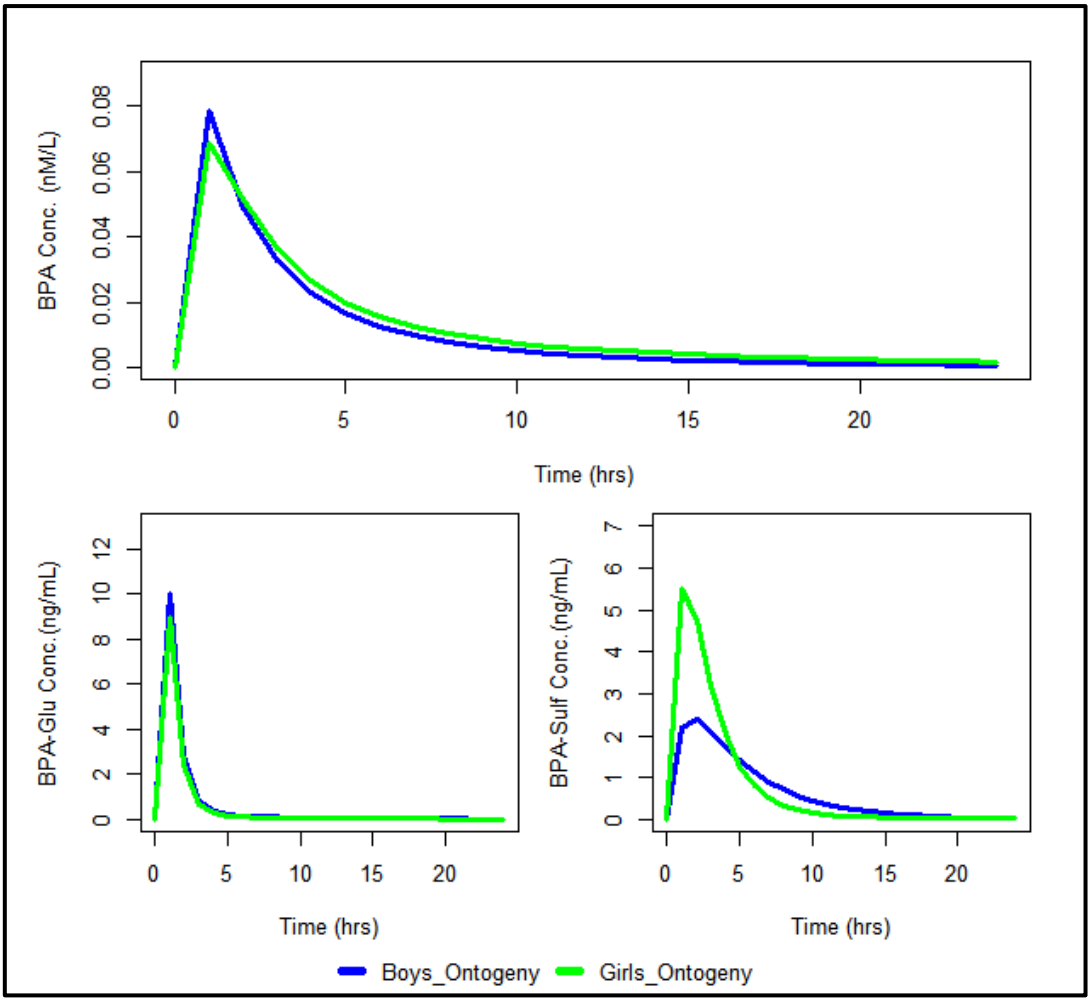

Figure 4: Concentration of BPAG and BPAS in plasma in boys and girls. Sulfation was higher in girls than boys and glucuronidation was similar in both based on ontogeny scaling.

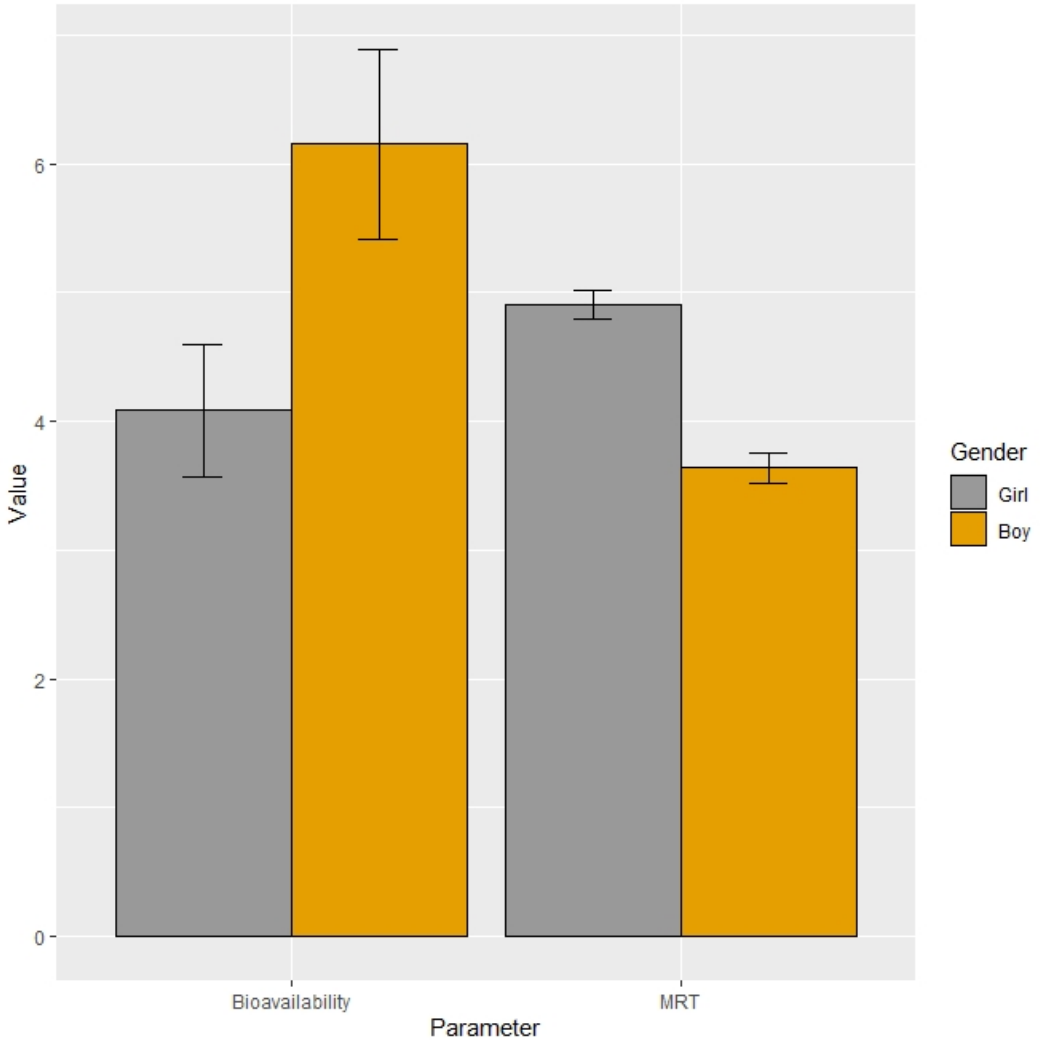

Figure 5: Bioavailability and MRT in both boys and girls based on ontogeny-based PBPK model.

Biomonitoring Data from Helix Cohort

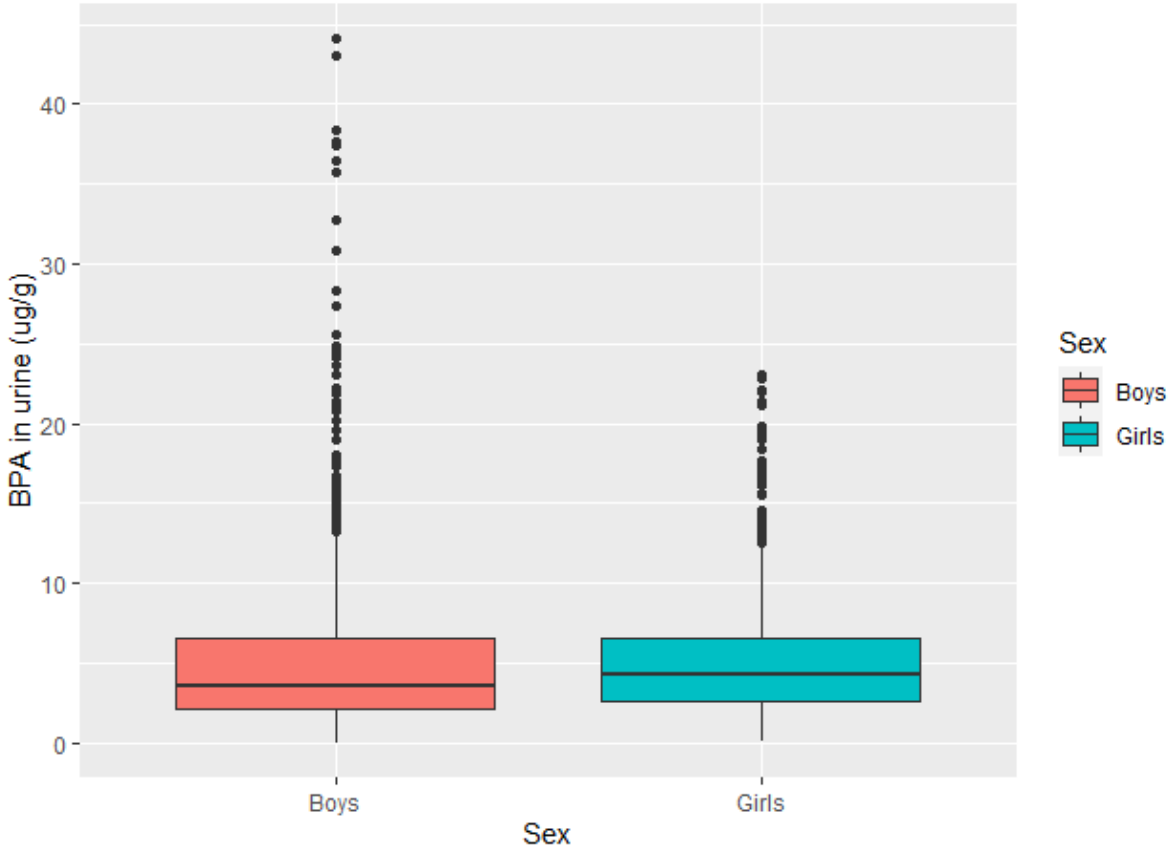

Figure 6: Biomonitoring data from Helix in boys and girls

Table 5: Statistics table for the response parameters in boys and girls. It includes mean, minimum (Min), maximum (max) and ranking.

Parameter	Mean	Min	Max	Rank
k_liver_plasma	-1.008	-1.087	0	1
kmliver_glu	0.851	0	0.92	2
vmaxliver_glu	-0.851	-0.92	0	3
kmgut_glu	0.737	0	0.784	4
k_fat_plasma	0.533	-0.136	2.019	5
k_restbody_plasma	0.54	-0.208	0.849	6
GE	-0.192	-0.704	1	7
vmaxliver_sulf	-0.156	-0.169	0	8
kmliver_sulf	0.156	0	0.169	9
k_skin_plasma	0.089	-0.053	0.132	10
k_brain_plasma	0.025	-0.05	0.042	11
kurine	-0.029	-0.039	0	12
k_kidney_plasma	-0.028	-0.037	0	13

k_gonads_plasma	0.001	-0.001	0.009	14
Fbpagliver	0	0	0	15
kurinebpag	0	0	0	16
EHRrate	0	0	0	17
Fbpasliver	0	0	0	19.5
kurinebpas	0	0	0	19.5
kde	0	0	0	19.5
kde_BPAG	0	0	0	19.5
k_liver_plasma	-0.955	-1	0	1
kmgut_glu	0.734	0	0.763	2
vmaxliver_sulf	-0.492	-0.508	0	3
kmliver_sulf	0.492	0	0.508	4
vmaxliver_glu	-0.462	-0.478	0	5
kmliver_glu	0.462	0	0.478	6
k_restbody_plasma	0.364	-0.301	0.826	7
k_fat_plasma	0.263	-0.219	1.33	8
GE	-0.155	-0.552	1	9
k_skin_plasma	0.129	-0.05	0.245	10
kurine	-0.034	-0.042	0	11
k_kidney_plasma	-0.033	-0.041	0	12
k_brain_plasma	0.026	-0.034	0.054	13
k_gonads_plasma	0.001	-0.001	0.006	14
Fbpagliver	0	0	0	15
kurinebpag	0	0	0	16
EHRrate	0	0	0	17
Fbpasliver	0	0	0	19.5
kurinebpas	0	0	0	19.5
kde	0	0	0	19.5
kde_BPAG	0	0	0	19.5

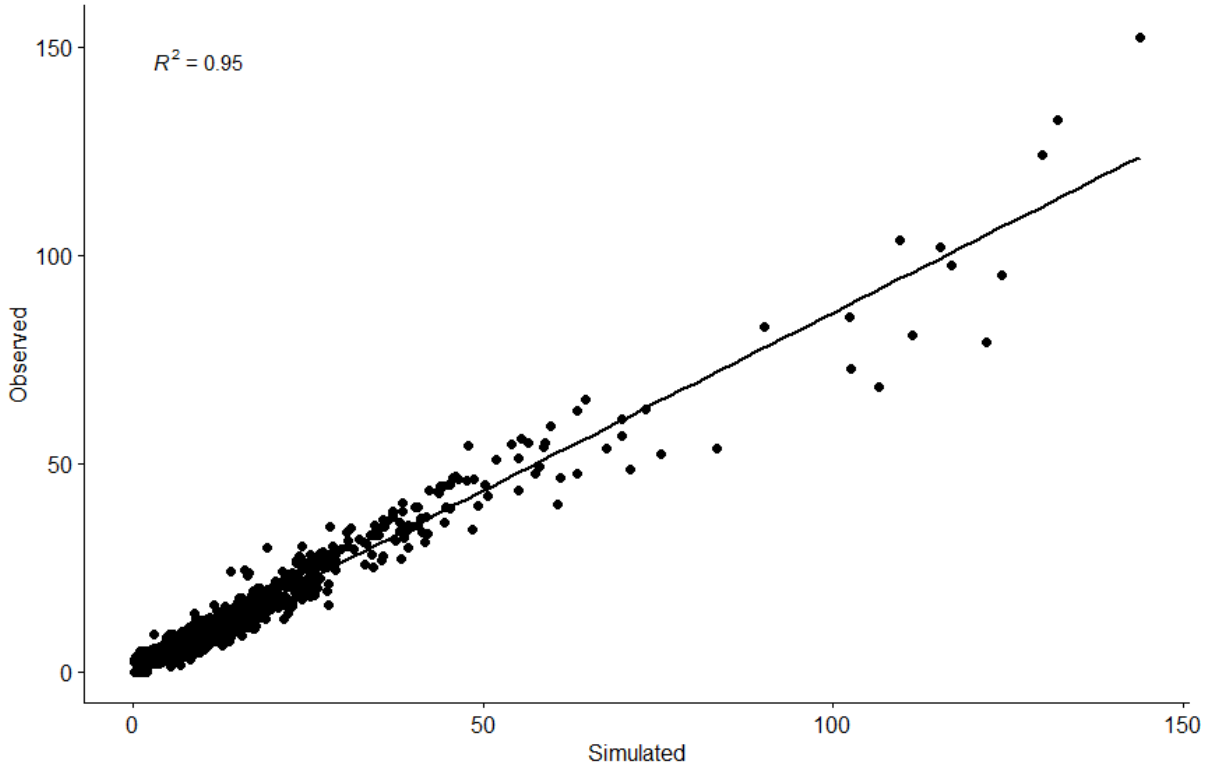

Figure 7: Correlation plot for simulated and observed total urine level for total BPA in pediatric population. Reconstructed exposure was used to forward calculate the urine level and compare it with the experimental data to check the prediction of model.

Annex for Chapter 3a

Biomonitoring data

Biomonitoring data was collected from three different countries (China, Norway and Australia) across different ages and used to evaluate the dynamic age dependent PBPK model (Haug et al. 2009; Kärrman et al. 2006; Zhang et al. 2010).

Table S1: Biomonitoring data of PFOS (ng/ml) with serum and plasma samples in three different countries (China, Norway and Australia)

Age group	PFOS concentration (ng/ml)	Description	Reference
China Data[a]			
Infants (n=14)	2.68 (4.20)	Median (mean)	(Zhang et al. 2010)
Toddlers (n=85)	2.52 (3.79)	Median (mean)	(Zhang et al. 2010)
Children (n=85)	5.55 (7.05)	Median (mean)	(Zhang et al. 2010)
Adolescents (n=19)	4.36 (6.79)	Median (mean)	(Zhang et al. 2010)
Adults (n=42)	8.07 (15.5)	Median (mean)	(Zhang et al. 2010)
Norway Data[b]			
0-4 years	1.8	Mean (1976 year)	(Haug et al. 2009)
5-14 years	19	Mean (1987 year)	(Haug et al. 2009)
15-24 years	24	Mean (1998 year)	(Haug et al. 2009)
25-59 years	10	Mean (2007 years)	(Haug et al. 2009)
Australia Data[c]			
<16 years	18.0	Rural (pool 1)	(Kärrman et al. 2006)
16-30 years	17.9	Rural (pool 1)	(Kärrman et al. 2006)
31-45 years	103[d]	Rural (pool 1)	(Kärrman et al. 2006)
46-60 years	26.2	Rural (pool 1)	(Kärrman et al. 2006)
>60 years	28.2	Rural (pool 1)	(Kärrman et al. 2006)
<16 years	20.5	Rural (pool 2)	(Kärrman et al. 2006)
16-30 years	17.2	Rural (pool 2)	(Kärrman et al. 2006)
31-45 years	22.3	Rural (pool 2)	(Kärrman et al. 2006)
46-60 years	25.6	Rural (pool 2)	(Kärrman et al. 2006)
>60 years	27.0	Rural (pool 2)	(Kärrman et al. 2006)
<16 years	19.9	Urban (pool 1)	(Kärrman et al. 2006)
16-30 years	19.8	Urban (pool 1)	(Kärrman et al. 2006)
31-45 years	22.2	Urban (pool 1)	(Kärrman et al. 2006)
46-60 years	28.9	Urban (pool 1)	(Kärrman et al. 2006)
>60 years	25.4	Urban (pool 1)	(Kärrman et al. 2006)
<16 years	23.6	Urban (pool 2)	(Kärrman et al. 2006)
16-30 years	21.5	Urban (pool 2)	(Kärrman et al. 2006)

31-45 years	23.4	Urban (pool 2)	(Kärrman et al. 2006)
46-60 years	20.8	Urban (pool 2)	(Kärrman et al. 2006)
>60 years	23.8	Urban (pool 2)	(Kärrman et al. 2006)

a China data with concentration in blood from infants (0-1 years), toddlers (1-5 years), children (5-10 years), adolescents (10-18 years) and adults (18-90 years). b Concentration in pooled serum samples from different age group in Norway. c Australian data with serum samples in age and different region. d PFOS with concentration from 103 ng/ml (age 31-45 years) was omitted for calculation due to extreme value in rural region and pool 1.

Sensitivity analysis

Global sensitivity analysis (GSA) was performed across the age using pksensi package through MCSIM and R (Bois 2009; Hsieh et al. 2018a, 2018b). The age groups include 0-5 years (2.5), 5-10 years (7.5), 10-18 (14) years, 18-55 (25) years, 55-70 (60) years and 70-90 (80) years. The sensitivity of partition coefficient (Figure 1) physiological parameters (Figure 2) and pharmacokinetic parameters (Figure 3) was analysed with respect to the output variables. Sensitive organs like bone marrow, liver, adipose tissue, kidney and plasma (output variables) where PFOS accumulates or are prone to damage was chosen to analyse the influential parameters.

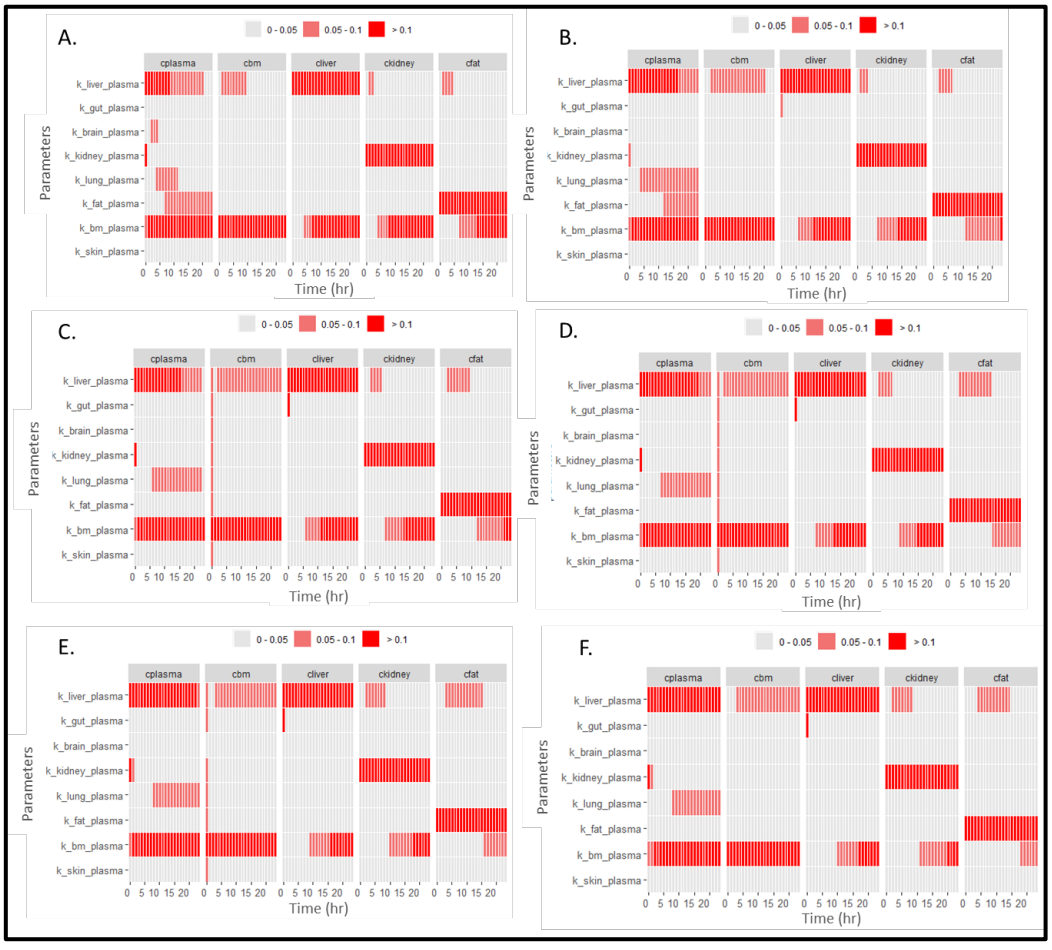

Figure S1: Heat map for sensitivity of partition coefficient to the plasma, bone marrow, liver, kidney and adipose tissue at different ages (A. 2.5 years, B. 7.5 years, C. 14 years, D. 25 years, E. 60 years and F. 80 years). Here, cplasma refers to concentration in plasma, cbm refers to concentration in bone marrow, cliver refers to concentration in liver, ckidney to concentration in kidney and cfat to concentration in adipose tissue.

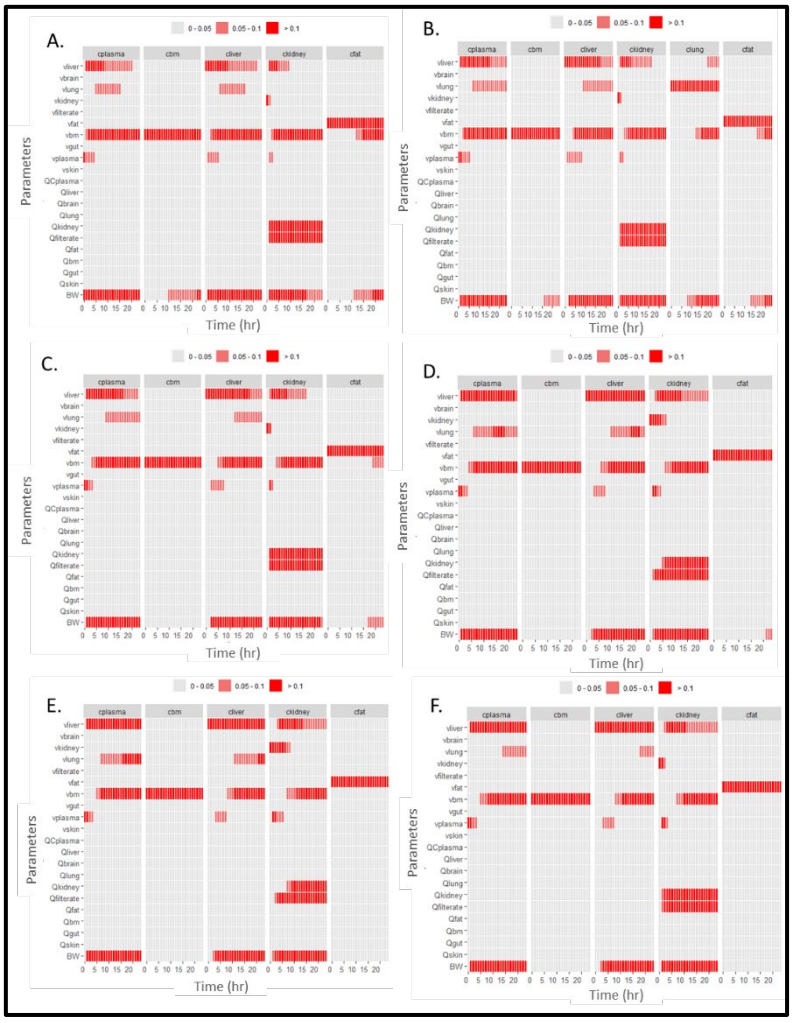

Figure S2: Heat map representing sensitive physiological parameters to the different body organs at different ages (A. 2.5 years, B. 7.5 years, C. 14 years, D. 25 years, E. 60 years and F. 80 years). Here, cplasma refers to concentration in plasma, cbm refers to concentration in bone marrow, cliver refers to concentration in liver, ckidney to concentration in kidney and cfat to concentration in adipose tissue, Kt refers to affinity constant, Tm for reabsorption, fu is fraction unbound and kurine for urine elimination constant.

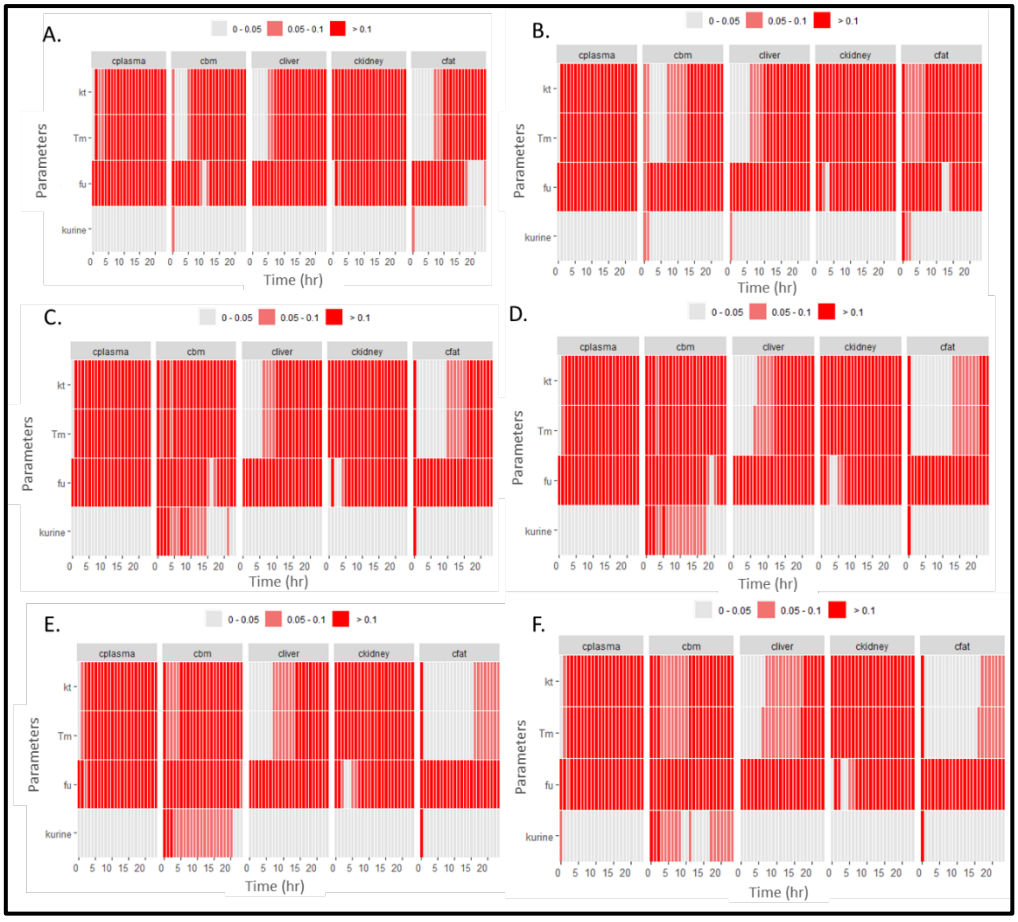

Figure S3: Heat map for sensitivity of pharmacokinetic parameters to the plasma, bone marrow, liver, kidney and adipose tissue at different ages (A. 2.5 years, B. 7.5 years, C. 14 years, D. 25 years, E. 60 years and F. 80 years). Here, cplasma refers to concentration in plasma, cbm refers to concentration in bone marrow, cliver refers to concentration in liver, ckidney to concentration in kidney and cfat to concentration in adipose tissue, Kt refers to affinity constant, Tm for reabsorption, fu is fraction unbound and kurine for urine elimination constant.

Organ Volume

Data from ICRP 89 and relationship with age, BW and height was used to derive equation for the weight of specific compartment in the general population (Anatomical et al.; Johnson et al. 2005; Ogiu et al. 1997; Price et al. 2003; Stader et al. 2019). Models for predicting weight of particular organ was done by performing linear regression with data obtained from already available equation and biomonitoring data with combination of different variables based on fit. For example, in case of liver, age and body weight were good fit whereas for brain, body weight and height lead to good fit. In similar way relationship was measured between other compartments and volume of different body tissues. As none of the equation in literature was able to cover the age group till 90 years, separate equation was able to simulate the weight and same was validated with available biomonitoring data as shown in figure. In the model, constant density of 1g/l was assumed so that mass in Kg is equal to volume in L.

In all the equation, variability was introduced based on age and Monte Carlo simulation was run for 1000 virtual population at each year. Lower (2.5), middle and higher percentile (97.5) was calculated at respective time to distribute the organ of volume in a range. Results were validated with physiological data (Anatomical et al.; Brown et al. 1962; Johnson et al. 2005; Ogiu et al. 1997; Price et al. 2003; Stader et al. 2019; Valentin and Streffer 2002).

Table S2: Equations describing the change in organ volume with age

Organs	**Male Equation**	**Female Equation**
Liver	-0.0143744-0.0044728*age+0.0264591*BW	0.0017717-0.0030113*age+0.0253455*BW
Brain	0.218096-0.001590*age-0.003274*BW+0.008626*HT	0.3757397-0.0003031*age-0.0021962*BW +0.0065721*HT
Kidney	5.668e-02-4.962e-04*age+3.501e-03*BW	0.0458676-0.0003957*age+0.0035115*BW
Lungs	-1.454e-02+7.269e-04*age+9.329e-06*age^2+6.430e-03*BW+3.083e-05*BW^2	5.042e-02-5.954e-03*age+7.035e-05*age+1.405e-05*BW+1.337e-04*BW^2
Adipose tissue	1.3054356+0.3622685*age-0.0025165*age^2 +0.0906119*BW+0.0001731*BW^2	6.132e-01+8.475e-02*age+8.151e-05*age^2 +1.341e-01*BW+2.297e-03*BW^2

Growth related equations

For males and females, body weight equation was taken from Price et al for 0 to 18 years (Price et al. 2003) and another equation used was from Stader et al. (Stader et al. 2019), where they have used the anthropometric data of 106,698 Caucasians to develop equation from year 20 to 90. Considering their equation and variability, regression equation was formed from 0 to 90 years, where equation 1 refers to male body weight and equation 2 denotes female body weight respectively. For validating the equation ICRP 89 dataset (Valentin and Streffer 2002) and another data from Stader et al was used where they have collected the data from 106,698 Caucasians. Similarly, equation for body height was made with introduced variability (E3 for male & E4 for female) (Hermanussen et al. 2012).

$$BW=3.382e+00+2.866e+00*a+(1.694e-01)*a^2-(1.169e-02)*a^3+(2.577e-04)*a^4-(2.484e-06)*a^5+(8.891e-09)*a^6 \quad (E1)$$

$$BW=2.354+4.050*a-(3.240e-02)*a^2-(3.057e-03)*a^3+(9.353e-05)*a^4-(1.022e-06)*a^5+(3.918e-09)*a^6 \quad (E2)$$

$$HT=(5.869e+01)+(1.265e+01)*a-(4.665e-01)*a^2+(7.198e-03)*a^3-(3.224e-05)*a^4-(2.512e-07)*a^5+(2.071e-09)*a^6 \quad (E3)$$

$$HT=(5.373e+01)+(1.296e+01)*a-(5.506e-01)*a^2+(1.113e-02)*a^3-(1.106e-04)*a^4+(4.697e-07)*a^5-(4.416e-10)*a^6 \quad (E4)$$

Blood flow to organs

Limited data on blood flow to organ makes it a challenging task to model these compartments for flow. In case of cardiac output, calculation was done based on body surface area. Body Surface area was calculated by Dubois formula shown in E5 (Du Bois and Du Bois 1989; Redlarski et al. 2016). Variability was incorporated for cardiac output based on normal random distribution accounting for interindividual differences (E6 for female & E7 for male) (Mallick et al. 2019; Stader et al. 2019).

$$SA= 0.007184*(BW^{0.425}) *(HT^{0.725}) \quad (E5)$$

$$QCC=5.528076-(2.834486*age) + (0.012591* age^2) + (204.262351*SA) + (19.274290*SA^2) \quad (E6)$$

$$QCC=6.48370-1.59948*age+214.68572*SA \quad (E7)$$

For other organs, data from ICRP 89 and Stader et al. was used where they have collected the adult data and data from European population for age group 20 to 90 years. In the compartments where tissue blood flow has been rarely reported, adult blood flow was taken as standard for calculating relative blood flow and simulated data was validated with physiological values (Anatomical et al.; Stader et al. 2019)

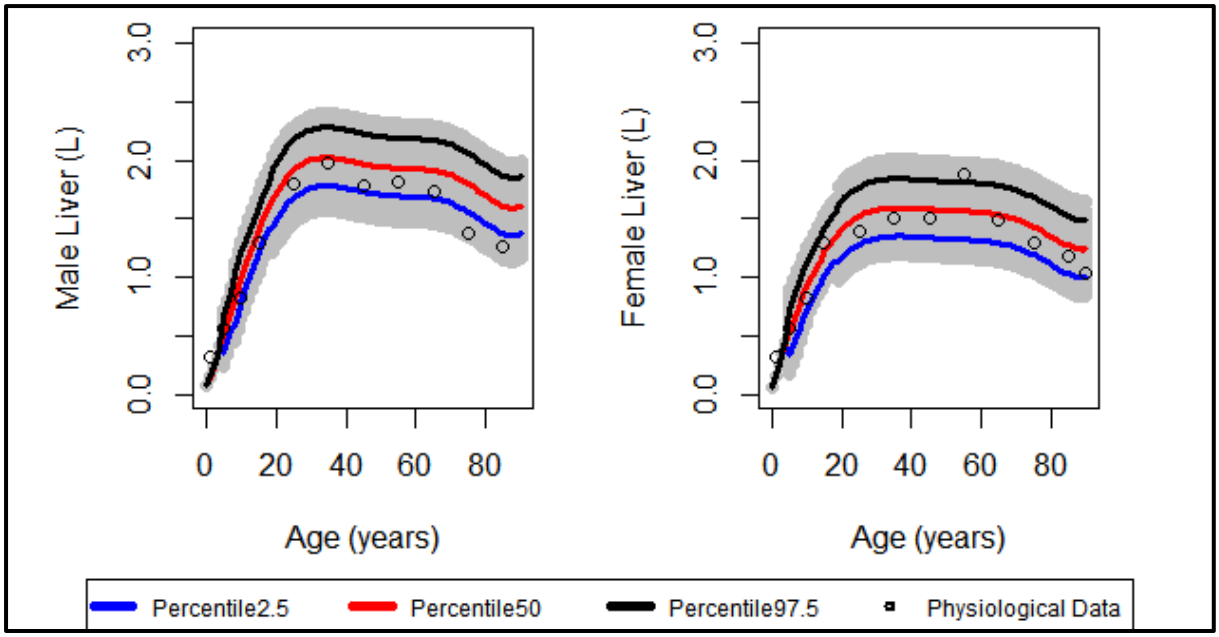

Figure S4: Liver volume (L) in male and female with age from 0 to 90 years

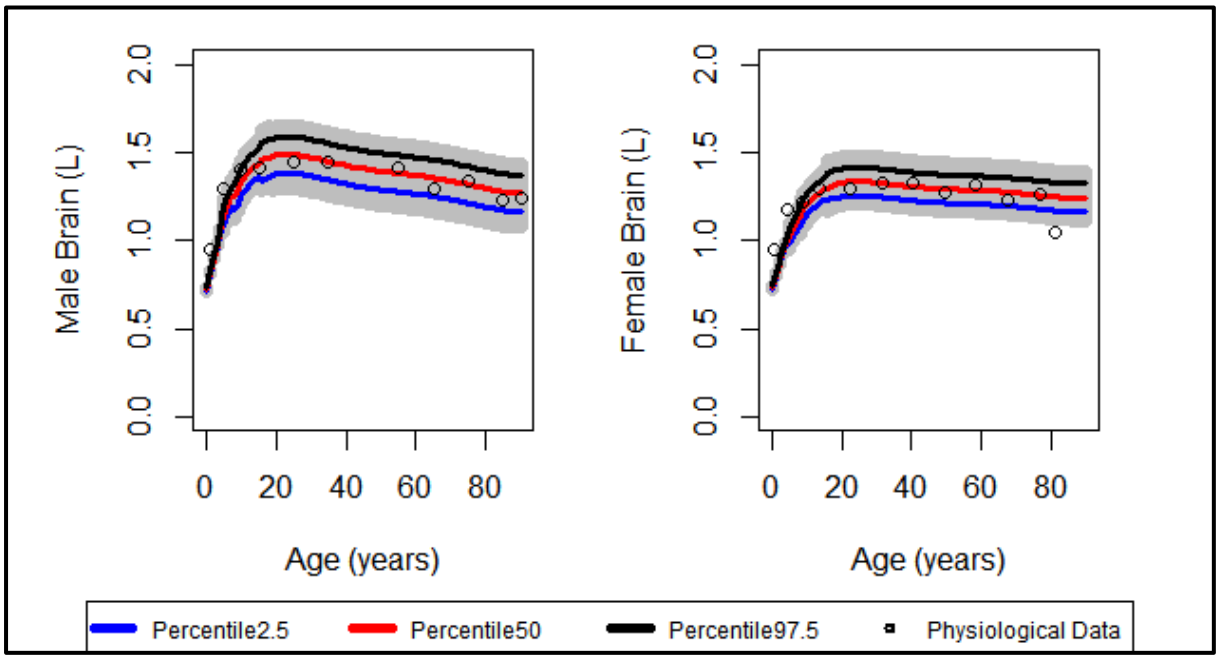

Figure S5: Brain volume (L) in male and female from 0 to 90 years

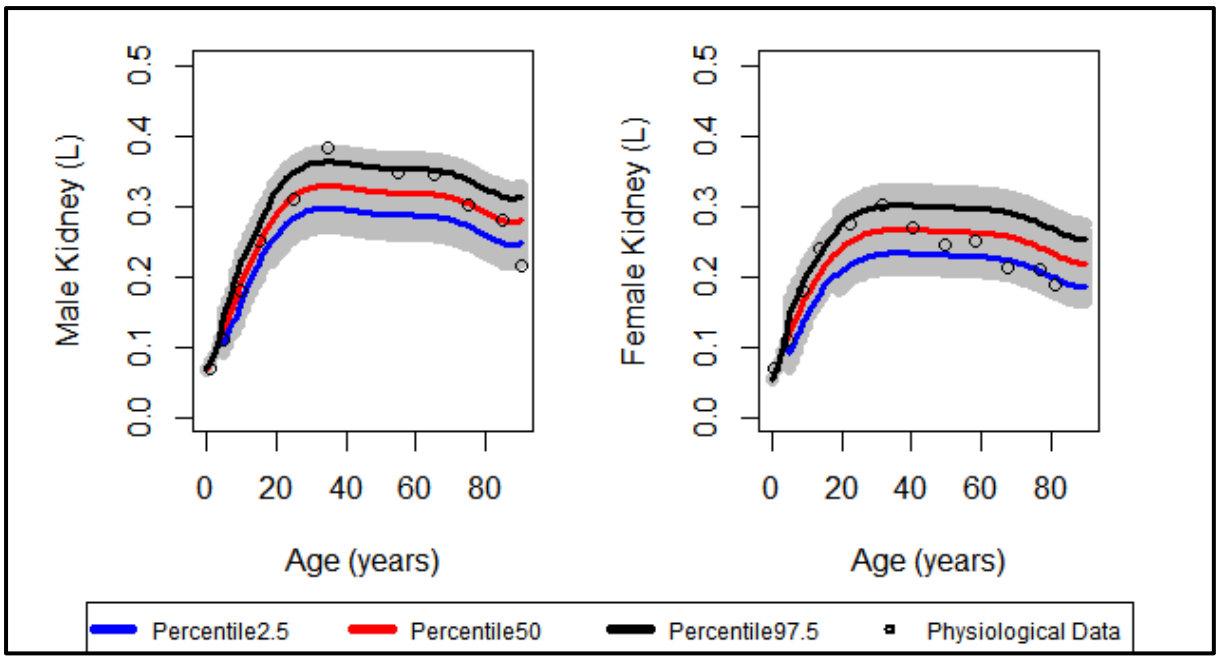

Figure S6: Kidney volume (L) in male and female from 0 to 90 years

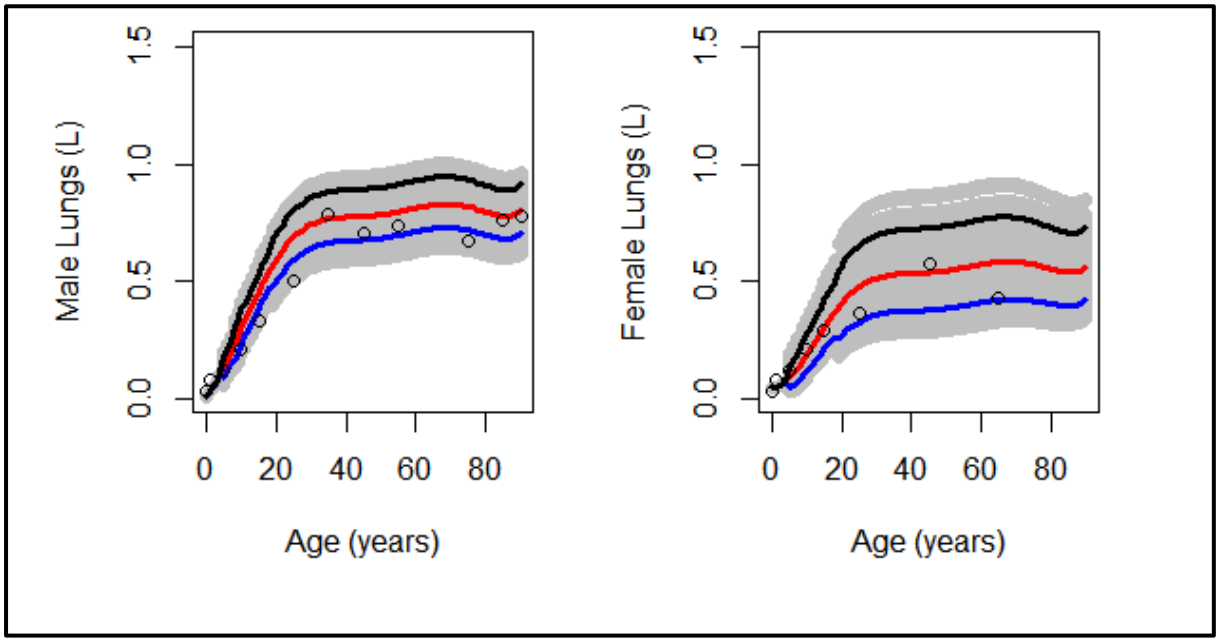

Figure S7: Lungs volume (L) in male and female from 0 to 90 years

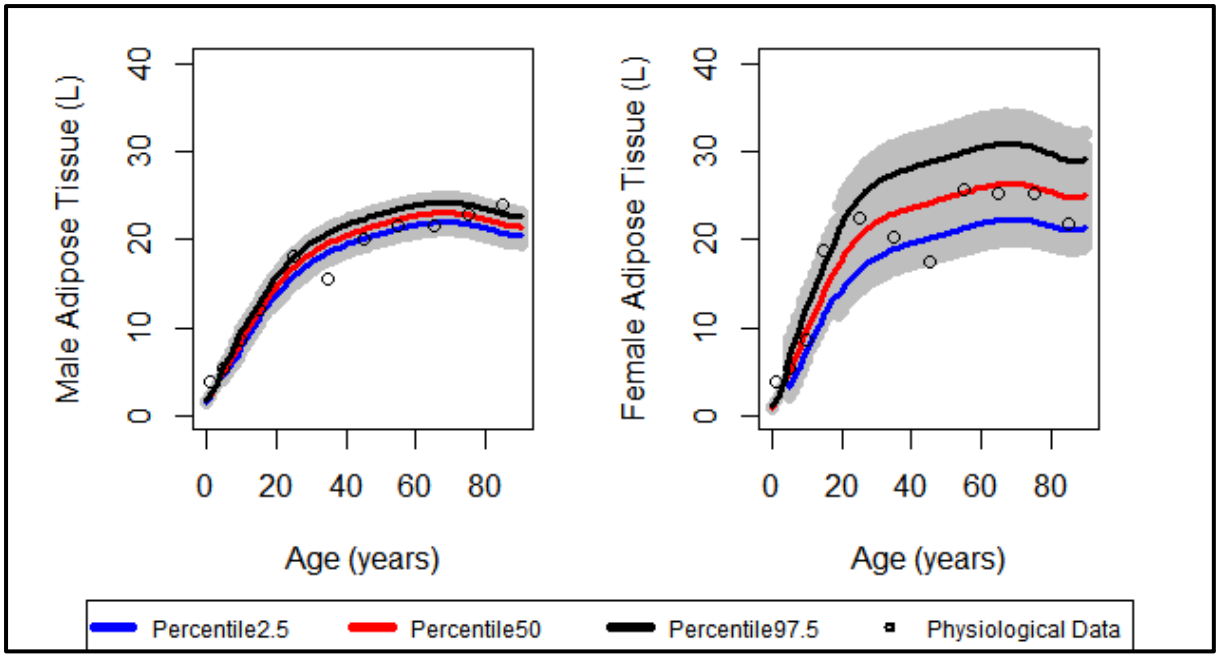

Figure S8: Adipose tissue volume (L) in male and female from 0 to 90 years

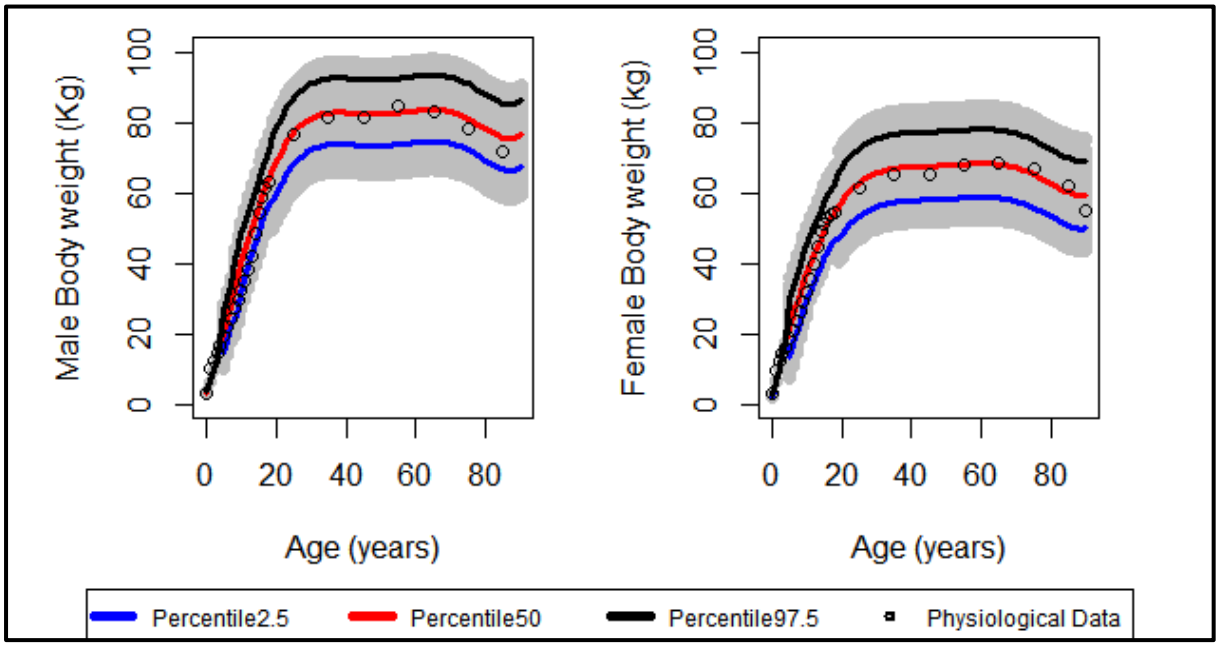

Figure S9: Body weight of the male and female in Kg from 0 to 90 years

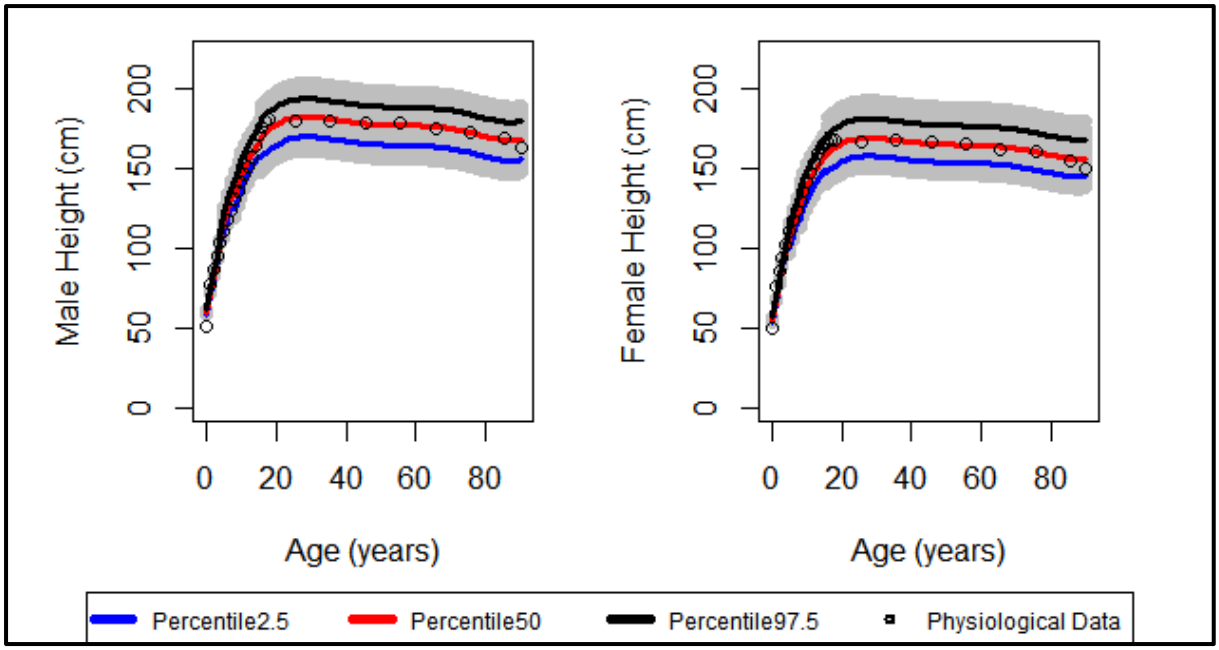

Figure S10: Height of the male and female in cm from 0 to 90 years

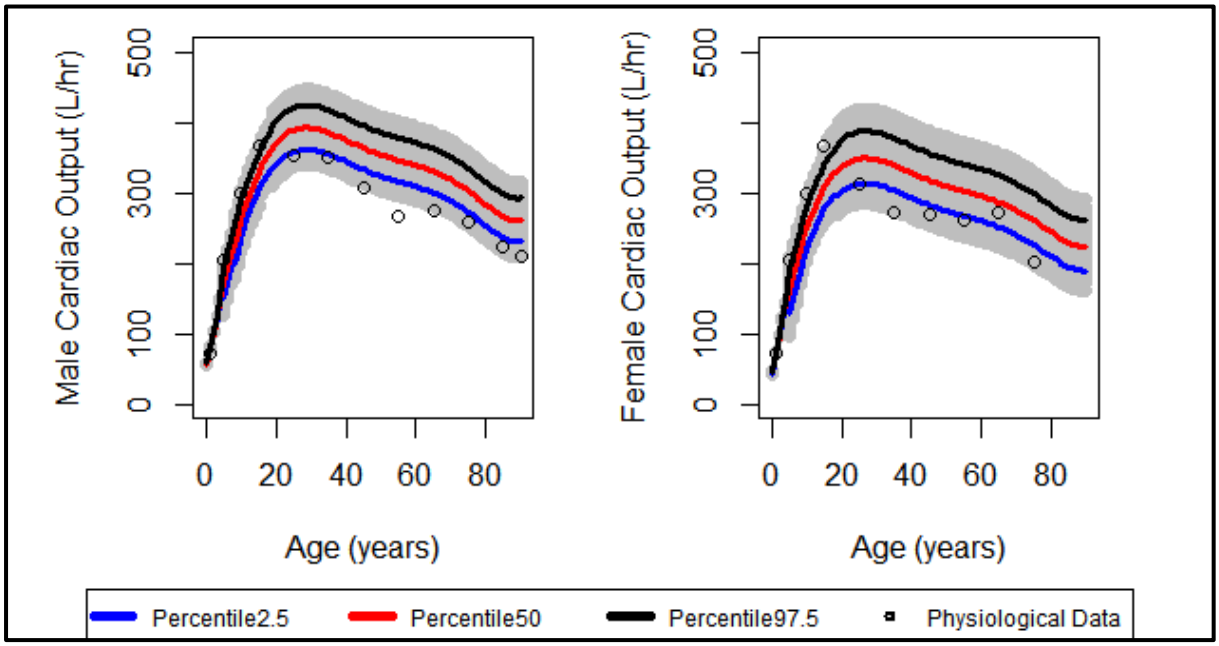

Figure S11: Cardiac output for male and female for 0 to 90 years

Reconstructed Exposure

The dynamic age dependent PBPK model was used to calculate reconstructed exposure for different age groups.

Table S3: Reconstructed exposure from different biomonitoring studies across age groups using dynamic age dependent PBPK model.

Cohort	Age group (years)	Reconstructed exposure* (Mean), (Min,Max)
(Zhang et al. 2010)	0-1	6.8e-5

	1-5	3.4e-5 (2.9e-5,3.9e-5)
	5-10	4.6e-5 (3.4e-5,5.4e-5)
	10-18	2.5e-5 (2e-5,3.1e-5)
	18-90	2.1e-5 (1.2e-5,3e-5)
(Haug et al. 2009)	0-4	1.8e-5 (1.7e-5,1.9e-5)
	5-14	8.0e-5 (6.1e-5,1.01e-4)
	15-24	4.9e-5 (4.6e-5,5.6e-5)
	25-59	1.4e-5 (1.1e-5,1.8e-5)
(Kärrman et al. 2006)	0-16©	6.7e-5 (4.9e-5,9.1e-5)
	16-30	3.8e-5 (2.8e-5,5.1e-5)
	46-60	3.6e-5 (2.9e-5,4.4e-5)
	61-80	3.2e-5 (2.8e-5,4.0e-5)
	0-16©	7.4e-5 (5.0e-5, 1.09e-4)
	16-30	3.7e-5 (2.7e-5, 5.1e-5)
	31-45	3.6e-5 (3.0e-5, 4.2e-5)
	46-60	3.5e-5 (3.0e-5, 4.1e-5)
	61-80	3.0e-5 (2.5e-5, 4.1e-5)
	0-16©	9.0e-5 (7.0e-5, 1.25e-4)
	16-30	4.7e-5 (3.9e-5, 5.7e-5)
	31-45	3.8e-5 (2.8e-5, 4.8e-5)
	46-60	2.7e-5 (2.5e-5, 3.0e-5)
	61-80	2.5e-5 (2.1e-5, 3.2e-5)
	0-16©	4.6e-5 (3.3e-5, 6.4e-5)

	16-30	3.1e-5 (2.5e-5, 3.5e-5)
	31-45	3.1e-5 (2.4e-5, 3.6e-5)
	46-60	2.4e-5 (2.1e-5, 3.0e-5)
	61-80	2.4e-5 (1.9e-5, 3.2e-5)

*Reconstructed exposure is in µg/g body weight per day for each age group.

©Data from Karrman et al. was of 4 pools, data from individual pools for reconstructed exposure was noted down in sequence from pool 1 to pool 4. Reconstructed exposure from pool 1 in 31-45 years was not included as (Kärrman et al. 2006) has not included that data for being an outlier. In this case the exposure value was assumed to be equal to previous exposure.

Adult Model Evaluation

Figure 12 represents the correlation in plasma from dynamic model with the published adult model from Fabrega et al. (Fàbrega et al. 2014, 2016a).

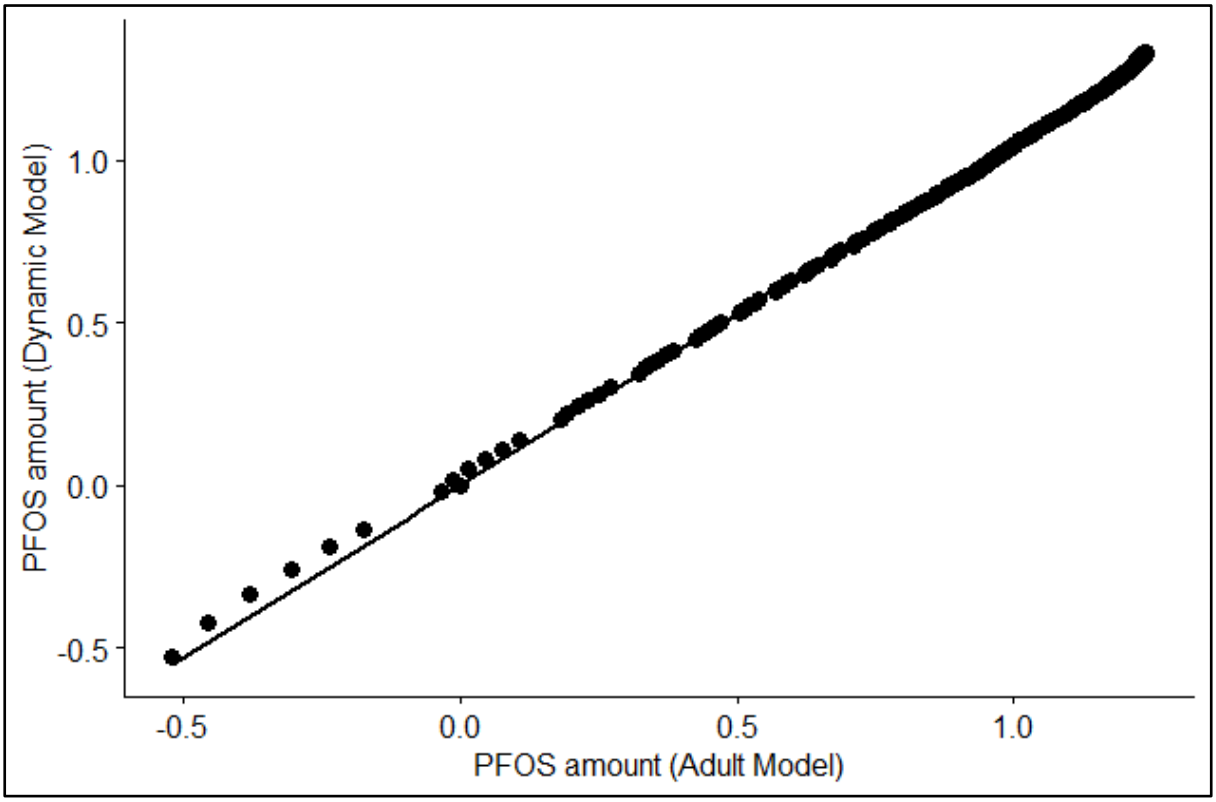

Figure S12: Correlation plot for simulation results from dynamic age dependent and published adult model (Fàbrega et al. 2016b). It represents the scatter plot in a logarithmic scale where output of model simulations from published adult model was compared against the simulations from the current dynamic model through Pearson correlation coefficient test.

Annex for Chapter 3b

Table 1: Summary table of Animal Studies

Animal used	**Exposure Dosage**	**Significant endpoint**	**Plasma/Organ Concentration**	**Level of Evidence**	**Reference**
Male and Female Sprague Dawley Rats	PFOS (0, 0.5, 2, 5 and 20 ug/g for 104 weeks	Statistically significant increase in hepatocellular adenoma at 20 ppm.	Reported	Moderate to high level of evidence for toxicity at higher dose.	(Butenhoff et al. 2012)
Pregnant C57BL/6 mice Bone marrow stromal cells	PFOA (0.3 mg/kg/day for mother) In-vitro (0,0.1,1,10,100 and 200 uM)	Increased body weight at 13 & 17 months. Higher PFOA accumulation in bones (tibia and femurs)	Reported	Moderate level of evidence for PFOA accumulation in bones.	(Koskela et al. 2016)
Pregnant CD1 Mice and Sprague-Dawley rats	PFOA (1, 3, 5, 10, 20, 40 mg/kg)	Increased weight gain in mice. Decrease in postnatal survival at 10 and 20 mg/kg. Significant delay in eye-opening (5mg/kg & more) Fast sexual growth in male offsprings	Reported	Moderate to high level of evidence for PFOA toxicity in relation to pregnancy and fetal growth.	(Lau et al. 2006)
Male CRL:CD BR Rats	PFOS (0, 1, 10, 30 and 100 ppm)	Reduction in weight gain at 100 ppm. Level of hormones unchanged. Reversible change in liver weight, PCoAO activity and hepatocyte hypertrophy	Reported	Moderate to high level of evidence for PFOA effect at doses of 10 ppm and higher with reversible liver changes.	(Perkins et al. 2004)

Male and female rats	PFOS (0, 0.1, 0.4, 1.6, 3.2 mg/kg/day)	Neonatal toxicity in 1.6 and 3.2 mg/kg. Reduction in body weight gain at 0.4 and higher dose. Effect on reproductive outcome at 3.2 mg/kg in F0 dams. Developmental delays in F1 at 0.4 & 1.6 mg/kg in F1 pups.	Reported	Moderate level of evidence for PFOS effect on developmental toxicity.	(Luebker et al. 2005)

Table 2: Summary table of Human Study

Chemical Studies and type	**Type of study**	**Outcome**	**Significant endpoint**	**Plasma/ Organ Concn.**	**Level of evidence for health effects or other outcome measured.**	**Reference**
PFOA, PFOS, PFBS, PFHxS, PFHxA, PFNA, PFDA, PFDoDA, ADONA	Cross-sectional study	Vaccine antibody against Hemophilus Type B, Tetanus, Diphtheria	Significant association between PFOA and vaccine antibody.	Reported	Moderate to High Level of evidence	(Abraham et al. 2020)
PFOA		Serum concentration. PFOA level in water.	Residential drinking water: PFOA contamination source responsible for human exposure	Reported	Moderate to high level of evidence.	(Emmett et al. 2006)
PFOS, PFOA, PFHxS, PFNA, PFDA PCB	Birth Cohort	Diphtheria and tetanus antibody concentration Serum concentration	PFOS exposure associated with decreased vaccine antibody concentration in children.	Reported	Moderate level of evidence.	(Grandjean et al. 2012)
PFOS, PFOA, PFHS	Occupational exposure worker	Serum concentration	Calculation of serum elimination half-life	Reported	Moderate level of evidence for the calculated half-life of PFAS.	(Olsen et al. 2007)

Appendix 2

Assessment Criteria used for systematic analysis

Methodology Protocol

- Administered dose/exposure level Randomized
- Concealing of study group allocation
- Appropriate comparison group
- Analysis of confounding
- Identical experimental conditions
- Blinding of research personnel
- Confident in exposure characterization and outcome assessment
- Measured outcomes reported
- No threats to internal validity

Statistical Protocol

- Statistical method appropriate (t-test, ANOVA, reporting homogeneity of variance)
- Adhering to study protocol (reporting exclusion of animals)
- Considering confounding or modifying variables in statistical analysis (un-intended or co-exposure of chemicals).

Exposure and Outcome Assessment

- Controlled Exposure
- Exposure occurred prior to development of outcome
- Outcome assessed on individual levels
- Appropriate comparison group
- Risk of bias based on trend key question
- Unexplained inconsistency
- Indirectness or population with less relevance
- Ability to distinguish treatment and control
- Publication Bias
- Magnitude of response
- Dose response
- Residual confounding
- Consistency across species/population
- Primary effects measured

Overall Rating: High risk, moderate risk, low risk or very low risk

Overall level of Health evidence based on methodology, exposure and outcome

High level of evidence
Moderate level of evidence
Low level of evidence
Inadequate level of evidence
No health effects

Calculating risk of bias and confidence level: Out of all the questions mentioned in the table 5, more than 80% are with low risk reported then overall low risk of bias was considered. Similar approach was used for calculating confidence level.

Table 3: Methodology and outcome used for Systematic Analysis

No.	Question	Risk Detected
	Methodology	
1	Administered dose or exposure level adequately randomized?	

2	Allocation to study groups adequately concealed?	Probably Low, Definitely low, Probably High, Definitely High risk of bias
3	Study participants selection resulted in the appropriate comparison groups?	
4	Study design or analysis account for important confounding and modifying variables?	
5	Identical experimental conditions across study groups?	
6	Blinding of research personnel to the study group during the study?	
7	Outcome data complete without attrition or exclusion from analysis?	
8	Confidence in the exposure characterization?	
9	Confidence in the outcome assessment	
10	All measured outcomes reported	
11	Any potential threat to internal validity	
Statistical Analysis		
12	Appropriateness of statistical methods?	Probably Low, Definitely low, Probably High, Definitely High risk of bias
13	Researchers adhere to the study protocol?	
14	Study design or analysis account for important confounding and modifying variables (including unintended co-exposures) in experimental studies?	

Table 4: Systematic Analysis protocol for synthesizing evidence and rate of confidence

No.	Question	
1	The exposure to the substance is experimentally controlled	High (all 4 yes), Moderate (3), Low (2) Very low (1) confidence

2	The exposure assessment demonstrates that exposures occurred prior to the development of the outcome	
3	The outcome is assessed on the individual level (i.e., not through population aggregate data)	
4	An appropriate comparison group is included in the study	
Initial confidence rating (Cohort Studies)		
5	In observational study, controlled exposure	High (all 4 likely), Low to moderate (2 likely, 1 unliley, 1 may or may not), Low (2 likely 2 unlikely) Very low to low (1 likely, 2 unliekly, 1 may or may not)
6	Exposure Prior to Outcome	
7	Individual Outcome Data	
8	Comparison Group Used	
Confidence Rating based on evidence		
9	"Was there risk of bias: trend, key questions, issues Serious or not serious"	High", "Moderate", "Low", "very low" confidence based on evidence
10	"Is there any unexplained consistency: results in terms of consistency, explain apparent inconsistency (if it can be explained) Serious or not serious"	
11	Indirectness: the use of upstream indicators or populations with less relevance Serious or not serious	
12	Imprecision: the ability to distinguish treatment from control. Confidence interval Serious or not serious	
13	Publication Bias: Discuss factors that might indicate publication bias (e.g., funding, lag) Detected or undetected	

14	"Magnitude: Describe magnitude of response, Large or not large"	
15	"Dose Response: Outline evidence for or against dose response Yes or no"	
16	"Residual Confounding: whether there is evidence that confounding would bias toward null Yes or no"	
17	"Consistency Across Species/ Model: cross species, model, or population consistency Yes or no "	
18	"Primary effects measured: ex. For carcinogenicity: checking tumor in organs Yes or no"	

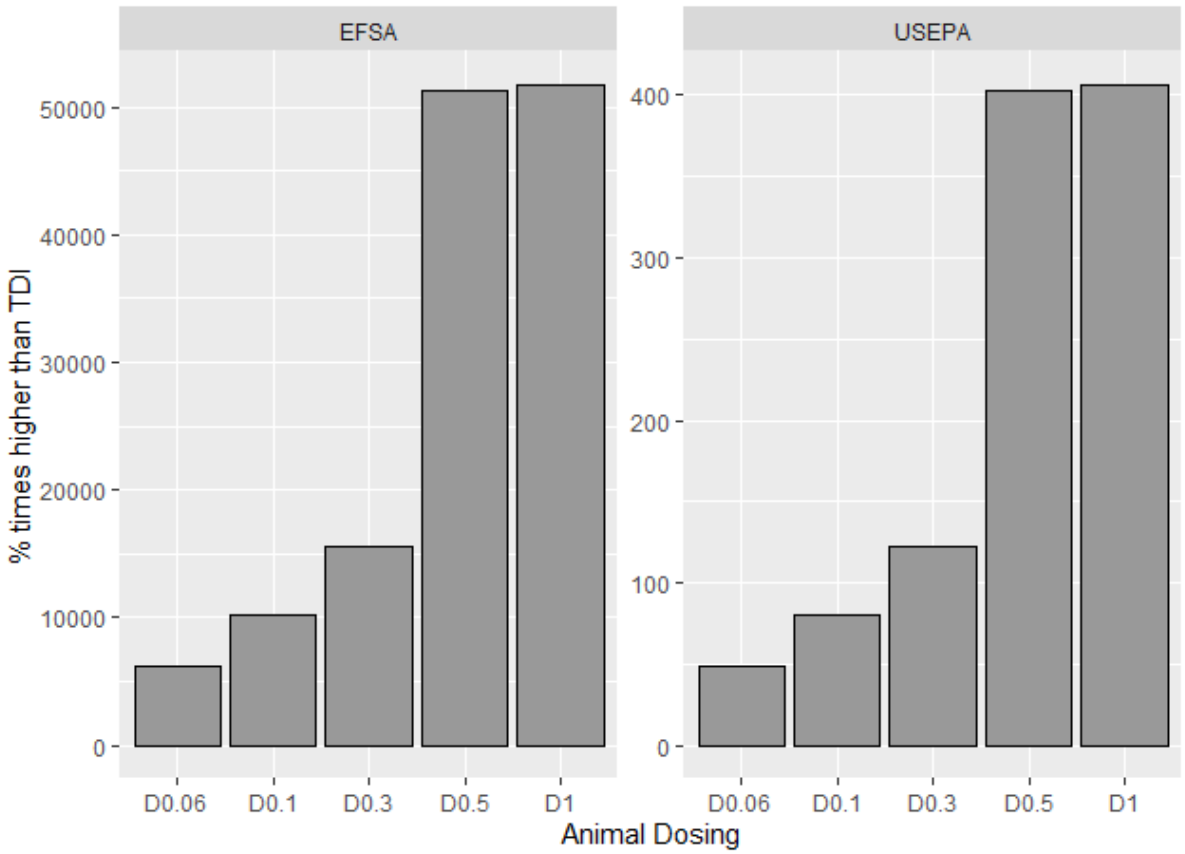

Figure 1: Inter-species extrapolation from animals to humans and comparison of the human equivalent dose with the TDI/RfD set by regulatory agencies.

Table 5: Parameters for PBPK Model for PFOS

Parameters	**Values**
Molecular weight (g/mol)	500.13
Unbound fraction in plasma (fu, age<=3)	0.031
Unbound fraction in plasma (fu, age<=10)	0.027
Unbound fraction in plasma (fu, age<=71)	0.025
Unbound fraction in plasma (fu, age<=89)	0.026
Unbound fraction in plasma (fu, age>=90)	0.028
Tmc*	3.5-5.5
Tissue: Plasma partition coefficient	
Liver	2.56
Gut	0.05

Brain	0.35
Kidney	1.21
Adipose Tissue	0.32
Lung	8.70
Bone marrow	17.94
Skin	0.11

Table 6: Parameters for PBPK Model for PFOA

Parameters	**Values**
Molecular weight (g/mol)	414.07
Unbound fraction in plasma	0.03
Tmc*	3-6
Tissue: Plasma partition coefficient	
Liver	4.231
Gut	0.05
Brain	0.37
Kidney	0.622
Adipose Tissue	0.467
Lung	9.08
Bone marrow	16.72
Skin	0.1

*Tmc refers to resorption maximum constant (ug/h/kg0.75)

Annex for Chapter 4

Resistance

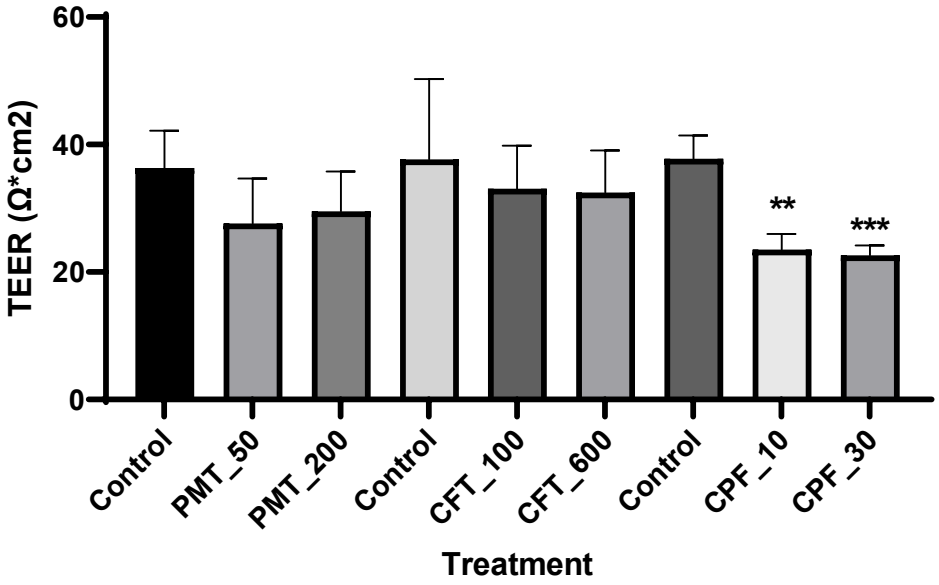

Figure 1: TEER ($\Omega*cm^2$) after treating the cell with chemical. After chemical exposure at 300 min, TEER was measured and compared with the control. Control was the TEER which was measured before starting the experiment.

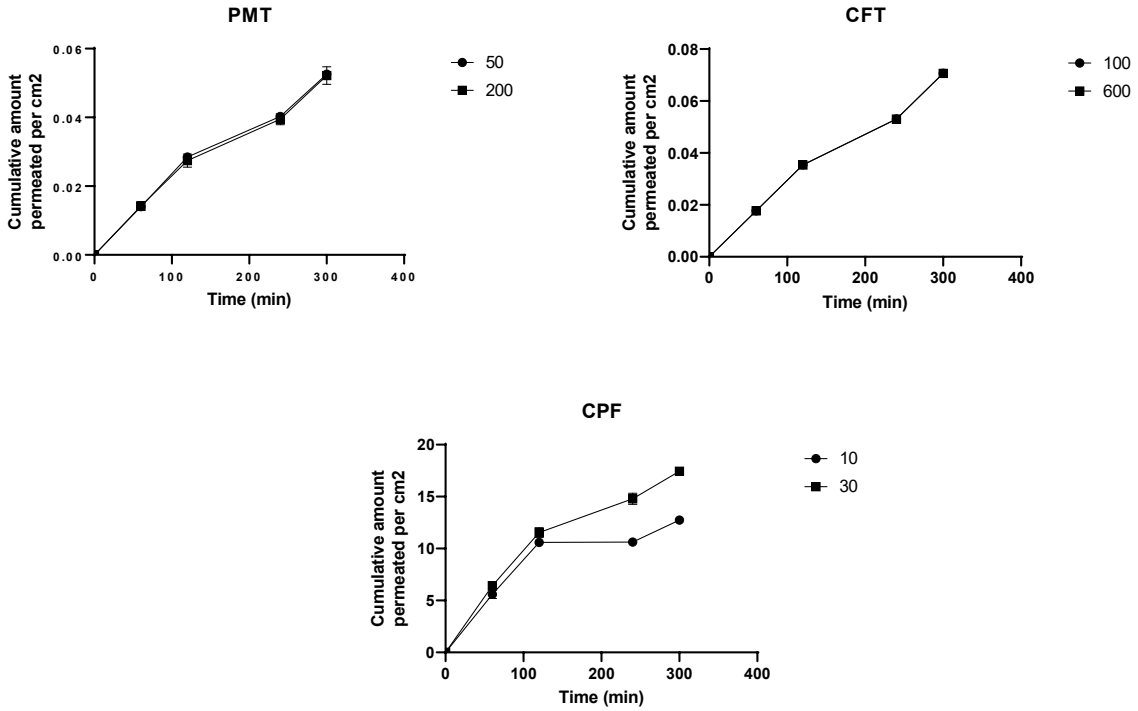

Figure 2: Cumulative amount (µg) permeated per cm^2 with two different concentration for three different chemicals. In case of PMT and CFT, there was no difference in permeation with respect to concentration. But for CPF, there was a little difference. Cumulative amount permeated for CPF was very high than other two concentrations.

Additional Analysis Curve for GC_ECD

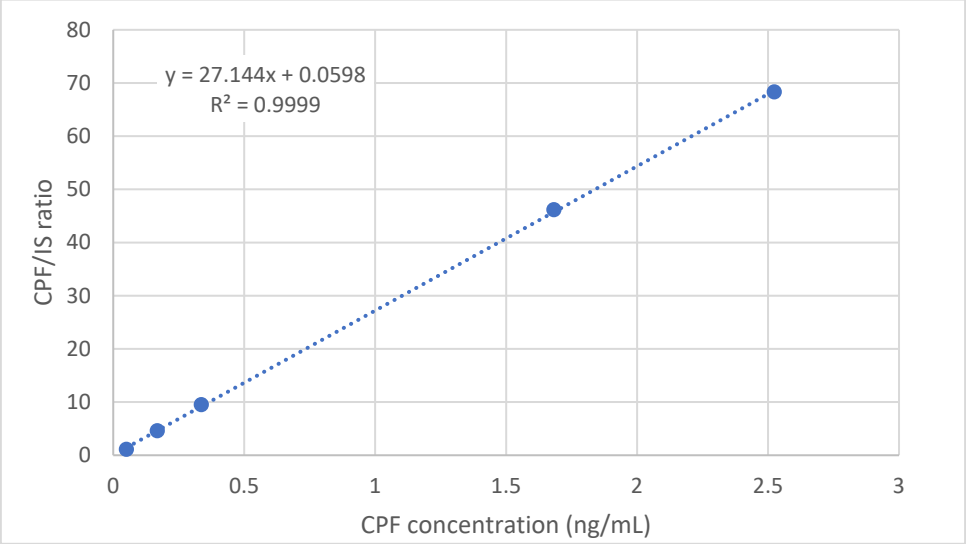

Figure 3: Calibration curve for CPF

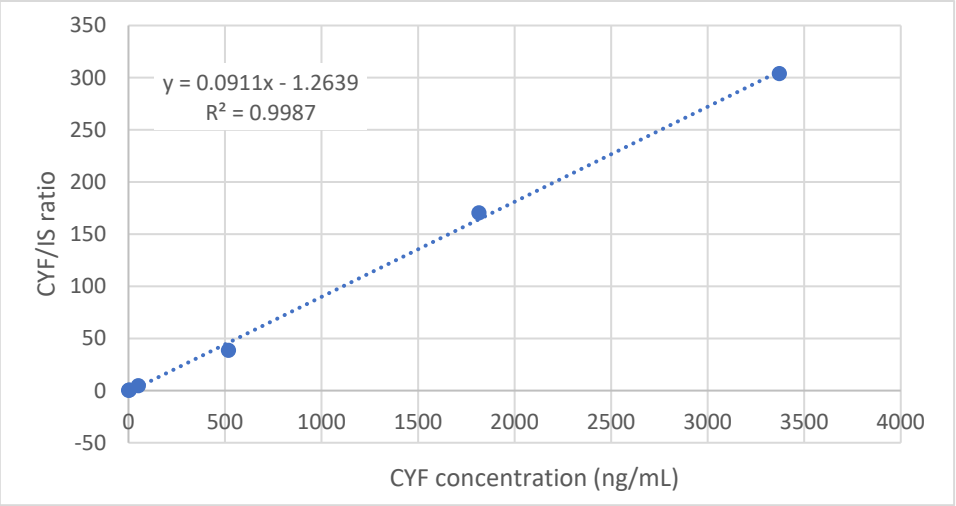

Figure 4: Calibration curve for CFT

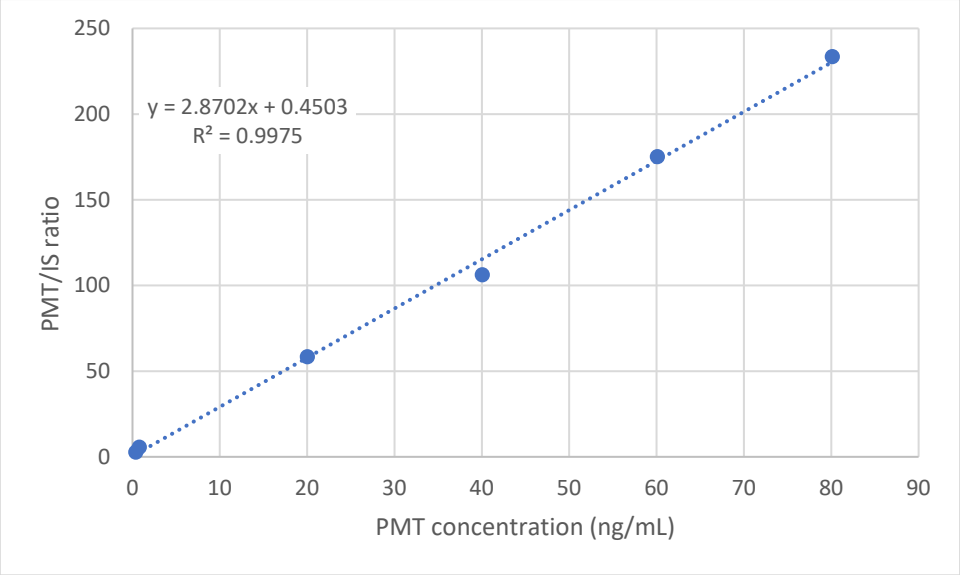

Figure 5: Calibration curve for PMT

Annex for Chapter 5a

Equations for brain PBPK Model

dt(Abrain) =Qbrain*(cplasma*fu-cbrain*fu_br)+(PSbt_bb*cbt*fu_bt - PSbb_bt*cbrain*fu_pl) + (Cl_bout*cbt*fu_bt - Cl_bin*cbrain*fu_pl)+ (QCsink*ccsf*fu_csf)+ (PShc_bb*chc*fu_hipp - PSbb_hc*cbrain*fu_pl)+(PSfc_bb*cfc*fu_fc - PSbb_fc*cbrain*fu_pl) eq. 1

Brain subcompartments

dt(Ahc)=(PSbb_hc*cbrain*fu_pl - PShc_bb*chc*fu_hipp)- Qhipp_csf*chc*fu_hipp + (PShc_bt*cbrain*fu_pl - PSbt_hc*chc*fu_hipp) eq. 2

dt(Afc)=(PSbb_fc*cbrain*fu_pl - PSfc_bb*cfc*fu_fc) - Qfc_csf*cfc*fu_fc + (PSbt_fc*cbt*fu_bt - PSfc_bt*cfc*fu_fc) eq. 3

dt(Abt)= (PSbb_bt*cbrain*fu_pl - PSbt_bb*cbt*fu_bt) -Qbt_csf*cbt*fu_bt + Cl_bin*cbrain*fu_pl - Cl_bout*cbt*fu_bt + (PSfc_bt*cfc*fu_fc - PSbt_fc*cbt*fu_bt)+ (PShc_bt*chc*fu_hipp - PSbt_hc*cbt*fu_bt); eq. 4

dt(Acsf)= Qbt_csf*cbt*fu_bt + Qfc_csf*cfc*fu_fc + Qhipp_csf*chc*fu_hipp - QCsink*ccsf*fu_csf; eq. 5

#chemical can pass from brain to csf following bulk flow and with Qsink it can return to plasma.

Plasma

dt(Aplasma) = Qfat * cfat*(fu/k_fat_plasma) + (Qliver +Qgut)*cliver*(fu/ k_liver_plasma) + (Qbrain*cbrain*fu_br) + (Qkidney *ckidney*(fu/k_kidney_plasma))+ (Qrestbody *crestbody*(fu/k_restbody_plasma)) - (QCplasma* cplasma*fu) + (Qlung * clung*(fu/k_lung_plasma)) + (Qbm * cbm*(fu/k_bm_plasma)) eq. 6

Annex for Chapter 5b

Table 1: Parameters related to ROS Model

Parameters	**Comp**	**Original Value (Initial), nmol/L**
KEAP1	Cyt	22.61606661
KEAP1 (Ros-modified)	Cyt	8.448488903
VDAC1	Cyt	121.9651581
PARK2	Cyt	49.2276025
S	Cyt	1
H2O	Cyt	5.55e+10
ATP	Cyt	3816809.278
O2_1/5th	Cyt	50000
ADP	Cyt	2733190.722
RE_4/5th	Cyt	4000000
Antioxidants Prot	Cyt	129.5240114
NRF2cyt	Cyt	68.6233417
PARK7act	Cyt	54.67269149
PARK7 inact (DJ-1)	Cyt	129.8893253
Uncoupprotprot	Cyt	43.53675209
PINK1	Cyt	40.88191764
Mit-Healthy	Cyt	1.402546261
Mit-Damaged	Cyt	0.6681925373
AP	Cyt	0.2856069966
p62im	Cyt	1.222546284
Alpha-synuclein	Cyt	3
p62cyt	Cyt	239.5682054
ROS	Cyt	0.4109175108
KEAP1:p62	Cyt	54.18087942
PINK1:PARK2	Cyt	12.78714699
Mtotal	Cyt	2.07074
VDAC1ub	Cyt	15.60806055

VDAC:p62	Cyt	37.39195057
KEAP1:NRF2cyt	Cyt	0.2000177766
NRF2cytUB	Cyt	0.09998627533
IKK	Cyt	1
NFKBsignal	Cyt	5.273363457
Bclxl	Cyt	10.54672691
CytC	Cyt	6612.188427
H202	Cyt	0
H202internal	Cyt	0
AO_mRNA_relative	Cyt	1
P62_mRNA_relative	Cyt	1
Bclxl_relative	Cyt	1
NFKB_relative	Cyt	1
ATP_relative	Cyt	1
ROS_relative	Cyt	1
deg	Cyt	0
Menandione	Cyt	0
Menandione_internal	Cyt	0
species	Cyt	1
Ncells	Cyt	100
ATP_measured	Cyt	1
Damage	Cyt	4.722694659e-19
Antioxidant Inact gene	nuc	0.000991325207 5207
Antioxidantact gene	nuc	0.000712674793
Antioxidant mRNA	nuc	0.06478861754
p62 mRNA	nuc	0.02573561684
P62act gene	nuc	0.0005147123373
P62inact gene	nuc	0.001185287663
Uncoupprot act gene	nuc	0.0003628062674
Uncoupprot RNA	nuc	0.02267539171
Uncoupprot inact gene	nuc	0.001327193733
Snuc	nuc	1
NRF2 nuc	nuc	68.6233417

UNIVERSITAT ROVIRA I VIRGILI
QUANTITATIVE SYSTEMS TOXICOLOGY MODELING FOR NEURONAL ADVERSE OUTCOME
Deepika

UNIVERSITAT ROVIRA I VIRGILI
QUANTITATIVE SYSTEMS TOXICOLOGY MODELING FOR NEURONAL ADVERSE OUTCOME
Deepika

UNIVERSITAT ROVIRA I VIRGILI
QUANTITATIVE SYSTEMS TOXICOLOGY MODELING FOR NEURONAL ADVERSE OUTCOME
Deepika

UNIVERSITAT ROVIRA I VIRGILI
QUANTITATIVE SYSTEMS TOXICOLOGY MODELING FOR NEURONAL ADVERSE OUTCOME
Deepika

UNIVERSITAT ROVIRA I VIRGILI
QUANTITATIVE SYSTEMS TOXICOLOGY MODELING FOR NEURONAL ADVERSE OUTCOME
Deepika

UNIVERSITAT ROVIRA I VIRGILI
QUANTITATIVE SYSTEMS TOXICOLOGY MODELING FOR NEURONAL ADVERSE OUTCOME
Deepika

UNIVERSITAT
ROVIRA i VIRGILI